NUSANTARA BIOSCIENCE

ISEA JOURNAL OF BIOLOGICAL SCIENCES

| Nusantara Biosci | vol. 16 | no. 1 | pp. 1-147 | May 2024 |
| ISSN 2087-3948 | E-ISSN 2087-3956|

Neurothemis ramburii (Kaup in Brauer, 1866) photo by Welson Xiong

Society for
Indonesian Biodiversity

Sebelas Maret University
Surakarta

ISSN 2087-3948 E-ISSN 2087-3956

Published semiannually

PRINTED IN INDONESIA

NUSANTARA
BIOSCIENCE
ISEAJournal of Biological Sciences
| Nusantara Biosci | vol. 16 | no. 1 | pp. 1-147 |May 2024 |
|ISSN 2087-3948| E-ISSN 2087-3956|

PUBLISHER: Smujo International

ASSOCIATION: Society for Indonesian Biodiversity

INSTITUTION: School of Graduates, Sebelas Maret University, Surakarta

FIRST PUBLISHED: 2009

ADDRESS:
Bioscience Program, School of Graduates, Sebelas Maret University
Jl. Ir. Sutami 36A Surakarta 57126, Indonesia. Tel. & Fax.: +62-271-663375, email: editors@smujo.id

ONLINE: smujo.id/nb

List of reviewers: https://smujo.id/nb/reviewers

Society for Indonesian Biodiversity **Sebelas Maret University Surakarta**

Published by Smujo International for The Society for Indonesian Biodiversity and Sebelas Maret University Surakarta

GUIDANCE FOR AUTHORS

Aims and Scope ***Nusantara Bioscience*** (Nusantara Biosci) encourages submission of manuscripts dealing with all aspects of biological sciences that emphasize issues germane to biological and nature conservation; especially for the research conducted in the Islands of the Southeast Asian reign or Nusantara, but also from around the world.

Article types The journal seeks original full-length: (i) **Research papers**, (ii) **Reviews**, and (iii) **Short communications**. Original research manuscripts are limited to 8,000 words (including tables and figures) or proportional to articles in this publication number. Review articles are also limited to 8,000 words, while Short communications should be less than 2,500 words, except for pre-study.

Submission: The journal only accepts online submissions through the open journal system **(https://smujo.id/nb/about/submissions)** or, for login problems, email the editors at unsjournals@gmail.com (or editors@smujo.id). Submitted manuscripts should be the original works of the author(s). Please ensure that the manuscript is submitted using the template, which can be found at (https://biodiversitas.mipa.uns.ac.id/D/template.doc). The manuscript must be accompanied by a cover letter containing the article title, the first name and last name of all the authors, and a paragraph describing the claimed novelty of the findings versus current knowledge. Please also provide a list of five potential reviewers in your cover letter. They should come from outside your institution and better from three different countries. Submission of a manuscript implies the submitted work has not been published (except as part of a thesis or report, or abstract) and is not being considered for publication elsewhere. When a group writes a manuscript, all authors should read and approve the final version of the submitted manuscript and its revision; and agree on the submission of manuscripts for this journal. All authors should have made substantial contributions to the concept and design of the research, acquisition of the data and its analysis, drafting the manuscript, and correcting the revision. All authors must be responsible for the work's quality, accuracy, and ethics.

Ethics Author(s) must be obedient to the law and/or ethics in treating the object of research and pay attention to the legality of material sources and intellectual property rights.

Copyright If the manuscript is accepted for publication, the author(s) still hold the copyright and retain publishing rights without restrictions. For the new invention, authors must manage its patent before publication.

Open Access The journal is committed to free-open access that does not charge readers or their institutions for access. Readers are entitled to read, download, copy, distribute, print, search, or link to the full texts of articles, as long as not for commercial purposes. The license type is CC-BY-NC-SA.

Acceptance Only articles written in US English are accepted for publication. Manuscripts will be reviewed by editors and invited reviewers (double-blind review) according to their disciplines. Authors will generally be notified of acceptance, rejection, or need for revision within 1 to 2 months of receipt. Manuscripts will be rejected if the content does not align with the journal scope, does not meet the standard quality, is in an inappropriate format, or contains complicated grammar, dishonesty (i.e., plagiarism, duplicate publications, fabrication of data, citations manipulation, etc.), or ignoring correspondence in three months. The primary criteria for publication are scientific quality and significance. **Uncorrected proofs** will be sent to the corresponding author by system or email as .doc or .docx files for checking and correcting typographical errors. The corrected proofs should be returned in 7 days to avoid publication delays. The accepted papers will be published online in chronological order at any time but printed at the end of each month.

Charges Publishing costs waiver is granted to foreign (non-Indonesian) authors who first publish the manuscript in this journal. However, other authors are charged USD 150 (IDR 2,100,000). **Reprint** Authors or other parties may freely download and distribute. However, a printed request will be charged, especially regarding postal charges.

Manuscript preparation Manuscript is typed on A4 (210x297 mm^2) paper size, in a single column, single space, 10-point (10 pt) Times New Roman font. The margin text is 3 cm from the top, 2 cm from the bottom, and 1.8 cm from the left and right. Smaller lettering sizes can be applied in presenting tables and figures (9 pt). Word processing program or additional software can be used; however, it must be PC compatible, use the template, and be Microsoft Word based (.doc or .rtf; not .docx). **Scientific names** of species (incl. subspecies, variety, etc.) should be written in italics, except in italicized sentences. Scientific names (genus, species, author) and cultivar or strain should be mentioned completely for the first time mentioning it in the body text, especially for taxonomic manuscripts. The genus name can be shortened after the first mention, except in early sentences, or where this may generate confusion; name of the author can be eliminated after the first mention. For example, *Rhizopus oryzae* L. UICC 524 can be written hereinafter as *R. oryzae* UICC 524. Using trivial names should be avoided. **Biochemical and chemical nomenclature** should follow the order of the IUPAC-IUB. For DNA sequences, it is better to use Courier New font. Standard chemical abbreviations can be applied for common and clear used, for example, completely written butilic hydroxyl toluene (BHT) to be BHT hereinafter. **Metric measurements** should use IS denominations, and other systems should use equivalent values with the denomination of IS mentioned first. A dot should not follow abbreviations like g, mg, mL, etc. Minus index (m^{-2}, L^{-1}, h^{-1}) suggested being used, except in things like "per-plant" or "per-plot." **Mathematical equations** can be written down in one column with text; in that case, they can be written separately. **Numbers** one to ten are written in words, except if it relates to measurement, while values above them are written in number, except in early sentences. The fraction should be expressed in decimal. In the text, it should be used "%" rather than "percent." Avoid expressing ideas with complicated sentences and verbiage/phrasing, and use efficient and effective sentences.

The title of the article should be written in compact, clear, and informative sentence, preferably not more than 20 words. Name of author(s) should be completely written, especially for the first and the last name. **Name and institution** address should also be completely written with street name and number (location), postal code, telephone number, facsimile number, and email address. We choose local names in Bahasa Indonesia for universities in Indonesia. The mention of "strata" program, should be avoided. Manuscript written by a group, author for correspondence along with address is required (marked with "♥"). **The title page** (first page) should include title of the article, full name(s), institution(s) and address(es) of the author(s); the corresponding authors detailed postage and e-mail addresses (P), and phone (O) and fax numbers (O).

Abstract A concise abstract is required (about 200 words). The abstract should be informative and state briefly the aim of the research, the principal results and major conclusions. An abstract is often presented separately from the article, thus it must be able to stand alone (completely self-explanatory). References should not be cited, but if essential, then cite the author(s) and year(s). Abbreviations should be avoided, but if essential, they must be defined at their first mention. **Keywords** are about five words, covering scientific and local name (if any), research themes, and special methods used; and sorted from A to Z. **Abbreviations** (if any): All important abbreviations must be defined at their first mention there. **Running title** is about five words.

Introduction is about 600 words, covering the aims of the research and provide an adequate background, avoiding a detailed literature survey or a summary of the results. **Materials and Methods** should emphasize on the procedures and data analysis. **Results and Discussion** should be written as a series of connecting sentences, however, for a manuscript with long discussion should be divided into subtitles. Thorough discussion represents the causal effect mainly explains why and how the results of the research were taken place, and do not only re-express the mentioned results in the form of sentences. **Concluding** sentence should be given at the end of the discussion. **Acknowledgements** are expressed in a brief; all sources of institutional, private and corporate financial support for the work must be fully acknowledged, and any potential conflicts of interest are noted.

Figures and Tables of a maximum of three pages should be clearly presented. The title of a picture is written down below the picture, while the title of a table is written above the table. Colored figures can only be accepted if the information in the manuscript can lose without those images; the chart is preferred to use black and white images. The author could consign any picture or photo for the front cover, although it does not print in the manuscript. All images property of others should be mentioned the source. Author is suggested referring to Wikipedia for international boundaries and Google Earth for satellite imagery. If not specifically mentioned, it is assumed to refer to these sources. **There is no appendix**, all data or data analysis is incorporated into Results and Discussions. For broad data, it can be displayed on the website as a supplement.

References Preferably 80% of it comes from scientific journals published in the last 10 years. In the text, give the author names followed by the year of publication and arrange from oldest to newest and from A to Z; in citing an article written by two authors, both of them should be mentioned; however, for three and more authors only the first author is mentioned followed by et al. For example, Saharjo and Nurhayati (2006) or (Boonkerd 2003a, b, c; Sugiyarto 2004; El-Bana and Nijs 2005; Balagadde et al. 2008; Webb et al. 2008). Extent citation should be avoided, as shown with the word "cit." Reference to unpublished data and personal communication should not appear in the list but should be cited in the text only (e.g., Rifai MA 2007, pers. com. (personal communication); Setyawan AD 2007, unpublished data). In the reference list, the references should be listed in alphabetical order. Names of journals should be abbreviated. Always use the standard abbreviation of a journal's name according to the **ISSN List of Title Word Abbreviations** (www.issn.org/2-22661-LTWA-online.php). Please include DOI links for journal papers. The following examples are for guidance.

Journal:

Saharjo BH, Nurhayati AD. 2006. Domination and composition structure change at hemic peat natural regeneration following burning; a case study in Pelalawan, Riau Province. Biodiversitas 7: 154-158. DOI: 10.13057/biodiv/d070213.

The usage of "et al." in long author lists will also be accepted:

Smith J, Jones M Jr, Houghton L et al. 1999. Future of health insurance. N Engl J Med 965: 325-329. DOI: 10.10007/s002149800025.

Book:

Rai MK, Carpinella C. 2006. Naturally Occurring Bioactive Compounds. Elsevier, Amsterdam.

Chapter in the book:

Webb CO, Cannon CH, Davies SJ. 2008. Ecological organization, biogeography, and the phylogenetic structure of rainforest tree communities. In: Carson W, Schnitzer S (eds.). Tropical Forest Community Ecology. Wiley-Blackwell, New York.

Abstract:

Assaeed AM. 2007. Seed production and dispersal of *Rhazya stricta*. 50th annual symposium of the International Association for Vegetation Science, Swansea, UK, 23-27 July 2007.

Proceeding:

Alikodra HS. 2000. Biodiversity for development of local autonomous government. In: Setyawan AD, Sutarno (eds.). Toward Mount Lawu National Park; Proceeding of National Seminary and Workshop on Biodiversity Conservation to Protect and Save Germplasm in Java Island. Universitas Sebelas Maret, Surakarta, 17-20 July 2000. [Indonesian]

Thesis, Dissertation:

Sugiyarto. 2004. Soil Macro-invertebrates Diversity and Inter-Cropping Plants Productivity in Agroforestry System based on Sengon. [Dissertation]. Universitas Brawijaya, Malang. [Indonesian]

Information from the internet:

Balagadde FK, Song H, Ozaki J, Collins CH, Barnet M, Arnold FH, Quake SR, You L. 2008. A synthetic *Escherichia coli* predator-prey ecosystem. Mol Syst Biol 4: 187. DOI: 10.1038/msb.2008.24. www.molecularsystembiology.com.

NUSANTARA
BIOSCIENCE
| Nusantara Biosci | vol. 16 | no. 1 | pp. 1-147 | May 2024|
| ISSN 2087-3948 | E-ISSN 2087-3956|
ISEAJournal of Biological Sciences

THIS PAGE INTENTIONALLY LEFT BLANK

NUSANTARA BIOSCIENCE
Vol. 16, No. 1, pp. 1-12
May 2024

ISSN: 2087-3948
E-ISSN: 2087-3956
DOI: 10.13057/nusbiosci/n160101

Geometric morphometric divergence of five populations of *Pampus argenteus* (Euphrasen, 1788) from Malaysian waters

SUZYELAWATI MOHD SHUKRI[1], KHALED BINASHIKHBUBKR[1,2], AHMAD DWI SETYAWAN[3], DARLINA MD NAIM[1,♥]

[1]School of Biological Sciences, Universiti Sains Malaysia. 11800 Pulau Pinang, Malaysia. Tel.+60-46534056, ♥email: darlinamdn@usm.my
[2]Department of Biology, Faculty of Science, Hadhramout University. Mukalla, Yemen
[3]Department of Environmental Science, Faculty of Mathematics and Natural Sciences, Universitas Sebelas Maret. Jl. Ir. Sutami 36A, Surakarta 57126, Central Java, Indonesia

Manuscript received: 13 November 2023. Revision accepted: 11 December 2023.

Abstract. *Shukri SM, Binashikhbubkr K, Setyawan AD, Md Naim D. 2024. Geometric morphometric divergence of five populations of* Pampus argenteus *(Euphrasen, 1788) from Malaysian waters. Nusantara Bioscience 16: 1-12.* Phenotypic variation in fish may indicate different environmental conditions that affect species' growth and maturation rates and result from genetic factors that allow fish to adapt to different environments. Understanding population structure and dynamics is extremely important for establishing sustainable fisheries. Silver pomfret, *Pampus argenteus* (Euphrasen, 1788), is an economically important fish species with extensive geographical distribution from the East China Sea to Southeast Asia, Indian Ocean, Arabian Gulf, and the North Sea. It may represent morphologically distinct populations across their range. The main aim of this study is to use geometric morphometric analysis based on physical characteristics to look into the phenotypic diversity of the species across five different populations in Malaysia. Digital images of 260 mature specimens were captured for further analysis. Principle Component Analysis (PCA) and Multivariate analysis (MANOVA) were used in the intra-population analysis based on the transformed distance. At the same time, the Canonical Variance Analysis (CVA) and the Procrustes ANOVA were utilized to determine the inter-population analysis of *P. argenteus*. The Unweighted Pair Group with Arithmetic Mean (UPGMA) method used to support the analysis has shown that the population is clearly grouped according to homologous body shape. The results show that South, West, and North Coast specimens were grouped while the East Coast and Borneo Island shared in another group. The variations in the body shape of *P. argenteus* occurred in body depth, caudal region, and head orientation. The findings separated the populations into two main groups representing the marine region to which they belong. This present study is the first report on phenotypic variations of *P. argenteus* from Malaysian waters utilizing the geometric morphometric method.

Keywords: Geometric morphometric, *Pampus argenteus*, shape variation, species identification

INTRODUCTION

The preservation of species is imperative to maintain sustainable population levels for each species, thereby securing the persistence of biodiversity for future generations. This becomes especially vital considering the severity of the present circumstances. The preservation of biodiversity resources, particularly commercially valuable fish species that play a crucial role in providing protein for human consumption, necessitates the maintenance of a robust and sustainable ecosystem.

Therefore, to ensure the efficient conservation and management of fisheries resources, it is imperative to possess a comprehensive understanding of the stock structure. This knowledge is crucial as it necessitates the separate management of each stock to maximize the overall yield (Lorenzen et al. 2016). Failure to accurately identify and effectively manage distinct population units results in excessive fishing activities, which can ultimately lead to a significant decline in population numbers (Cooke et al. 2016). To effectively address this and reduce the ongoing decline of fish populations, more sophisticated and effective species identification methodologies have been devised and effectively used to ascertain and differentiate the stock structure of various marine fish species (Chen et al. 2018).

Malaysia has recorded 1,951 species of freshwater and marine fishes belonging to 704 genera and 186 families (Chong et al. 2010). Almost half (48%) are currently threatened to some level, while nearly one-third (27%), mostly from the marine and coral habitats, require urgent scientific studies to evaluate their status (Chong et al. 2010; Binashikhbubkr et al. 2023). The endangerment of fish species in Malaysia, encompassing both freshwater and marine environments, is progressively escalating due to several significant factors. These factors include habitat loss or modification, accounting for 76% of the threat, as well as overfishing and bycatch, contributing to the rest of the issue (Chong et al. 2010).

Silver pomfret, *Pampus argenteus* (Euphrasen, 1788), from family Stromateidae, is Malaysia's economically important fish species. The *P. argenteus* is mostly marine and pelagic and has an extensive geographical distribution from the East China Sea to Southeast Asia, Indian Ocean, Arabian Gulf, and the North Sea (Mohitha 2016). The species is significant in Malaysian fishery sectors and has great value and demand as a protein source. However, Malaysia's *P. argenteus* fishery resource has declined

recently, with the total catch in 2019 being only 839 Metric Tons (MT), compared to 1,041 MT in 2018 (LKIM 2019). Furthermore, the fish caught are generally small, implying that better regular fishing and systematic resource management are required (LKIM 2020).

Environmental or habitat variations affect a species' phenotypic characteristics, including behavior, morphology, and physiology (Idaszkin et al. 2013). Specifically, natural selection and gene mutations affect phenotypic variation in inter and intra-populations, generating new morphotypes to maintain greater adaptation in new environments (Trevisan et al. 2016). As a result, the geographical distribution of a species is clearly represented in the shape variation and phenotypic variance of populations (Franssen et al. 2013). Most previous studies on *P. argenteus* relied on typical and traditional morphometric techniques; for example, Zhang et al. (2017) used sagittal otolith morphology to identify five different *Pampus* species from the Chinese coast; Jawad (2014) conducted successful research on the deformations of *P. argenteus* from the Oman coast of the Arabian Gulf, which is based on the conventional morphology of the fish's caudal fin; Iqbal et al. (2015) investigated the morphometrics of *P. argenteus* in Quetta, Pakistan, and discovered that morphometric features are useful for classifying fish and distinguishing sexual and phenotypic variations among species. In general, Geometric Morphometrics (GM) is the newest method focusing on biological shape analysis, which has changed recently. The creation and adoption of techniques for analyzing the Cartesian coordinates of anatomical landmarks are largely responsible for this shift. GM techniques emphasize keeping geometric information consistent throughout a study and offer effective, statistically potent analyses that easily connect abstract, multivariate findings to the physical structure of the original specimens (MacLeod 2018). GM is a powerful and widely used technique nowadays because the data includes information about spatial relationships and relationships between landmarks and organisms (Trevisan et al. 2012; Idaszkin et al. 2013).

Based on our current understanding, there is a lack of published research examining the morphological distinctions among *P. argenteus* populations in Malaysian waters. Thus, the present study aimed to examine GM's efficacy in distinguishing between five populations of *P. argenteus* found in Malaysian waters by analyzing body size and shape variations.

MATERIAL AND METHODS

Sampling

A total of 260 *P. argenteus* individuals were collected from 13 fish landing sites throughout Malaysia to achieve the optimal sample size (Table 1; Figure 1). All mature *P. argenteus* specimens measuring between 18-28 cm in length were acquired. As shown in Table 1, 11 locations from Peninsular Malaysia representing the East Coast (EC), West Coast (WC), North Coast (NC), and South Coast (SC), and two locations from Sabah and Sarawak representing the Borneo Island (BI) were selected in this study. Sampling activities were carried out between March and December 2019 in several locations identified as follows:1. Batu Maung, Penang, 2. Kuala Muda, Kedah, 3. Kuala Perlis, Perlis, 4. Tok Bali, Kelantan, 5. Kuala Kemaman, Terengganu, 6. Kuala Rompin, Pahang, 7. Kuala Benut, Johor, 8. Kuala Sungai Baru, Melaka, 9. Kuala Lukut, Negeri Sembilan, 10. Sg. Yu, Selangor 11. Teluk Melintang, Perak, 12. Sandakan, Sabah and 13. Bintulu, Sarawak (Table 1; Figure 1).

All samples were promptly subjected to morphological identification and verification upon collection, following the methodology outlined by Loy et al. (2000). The identified and confirmed samples were then put in a cold box before being transferred to the School of Biological Sciences, Universiti Sains Malaysia. Then, all samples were washed with running water, tapped, dried, and placed on the left side of a flat surface with a white background for maximum visibility. All fins are set up with pins to ensure correct insertion and origin. Morphometric characteristics were measured using a digital caliper (Figure 2).

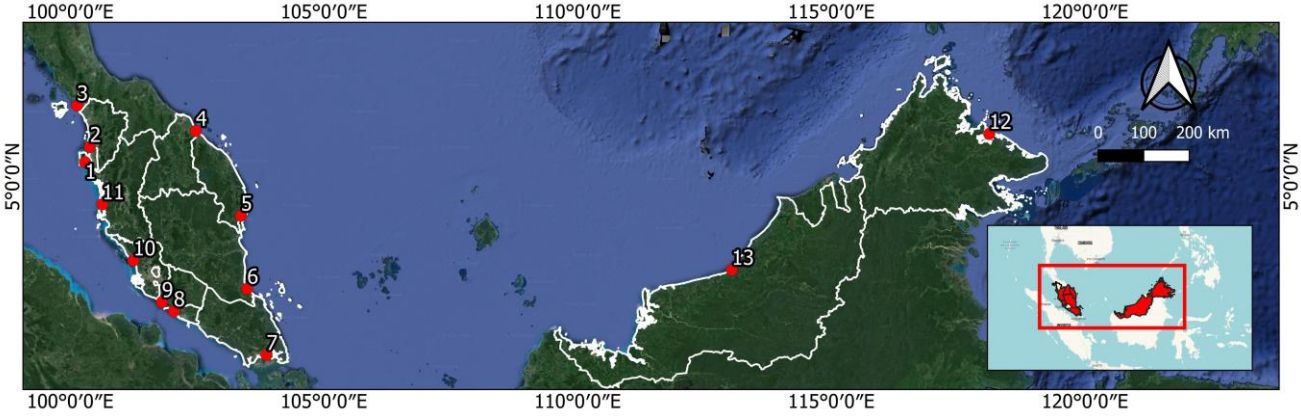

Figure 1. Sampling location of *Pampus argenteus* around Malaysian waters. 1. Batu Maung, Penang, 2. Kuala Muda, Kedah 3. Kuala Perlis, Perlis 4. Tok Bali, Kelantan 5. Kuala Kemaman, Terengganu 6. Kuala Rompin, Pahang 7. Kuala Benut, Johor 8. Kuala Sungai Baru, Melaka 9. Kuala Lukut Port Dickson, Negeri Sembilan 10. Sg. Yu Kuala Selangor, Selangor 11. Teluk Melintang (Teluk Intan), Perak 12. Sandakan, Sabah 13. Bintulu, Sarawak

Table 1. Description of sampling locations and sample size for each locality

Sampling site	Geographical location	Marine region	Coordinate Latitude; Longitude	Sample size (n)
Batu Maung, Penang (PNG)	NC	SM	5°17'5.0994"N; 100°17'14.9"E	20
Kuala Muda, Kedah (KD)	NC	SM	5°34'59.99"N; 100°22'59.99"E	20
Kuala Perlis, Perlis (PS)	NC	SM	6°23'52.44"N; 100°7'50.52"E	20
Tok Bali, Kelantan (K)	EC	SCS	5°53'51.36"N; 102°28'26.4"E	20
Kuala Kemaman, Terengganu (T)	EC	SCS	4°14'1.68"N; 103°21'49.6"E	20
Kuala Rompin, Pahang (P)	EC	SCS	2°48'2.16"N; 103°29'9.96"E	20
Kuala Benut, Johor (J)	SC	SM	1°30'1.03"N; 103°52'2.08"E	20
Kuala Sungai Baru, Melaka (M)	WC	SM	2°21'25.92"N; 102°2'21.12"E	20
Kuala Lukut Port Dickson, Negeri Sembilan (N9)	WC	SM	2°32'13.85"N; 101°48'20.56"E	20
Sg. Yu Kuala Selangor, Selangor (S)	WC	SM	3°21'17.29"N; 101°14'30.4"E	20
Teluk Melintang (Teluk Intan), Perak (PK)	NC	SM	4°27'20.52"N; 100°37'43.68"E	20
Sandakan, Sabah (SB)	BI	SS	5°50'21.84"N; 118°7'1.92"E	20
Bintulu, Sarawak (SR)	BI	SCS	3°10'16.68"N; 113°2'30.84"E	20

Note: North Coast of Peninsular Malaysia (NC), East Coast of Peninsular Malaysia (EC), South Coast of Peninsular Malaysia (SC), West Coast of Peninsular Malaysia (WC), Borneo Island (BI), South China Sea (SCS), Straits of Malacca (SM), Sulu Sea (SS), n = sample size

Geometric morphometric analyses

All samples were labeled and photographed with a digital camera (Olympus Tough TG-5) with a 12-megapixel BSI-CMOS 12.3 resolution. Images of each sample were taken on the left side only, using the same digital caliper throughout the measurement process to collect true scale information. The Tps_Utility (tpsUtil; https://life2.bio.sunysb.edu/ee/rohlf/software.html) application was used to generate an input file that the Tps_Digitise (tpsDig; https://life2.bio.sunysb.edu/ee/rohlf/software.html) data acquisition program could read. The x and y coordinates of the landmarks were captured on the digital pictures utilized as baseline data for subsequent analysis using the tpsDig2 program (ver. 2.31) (Rohlf 2017). MorphoJ (ver. 1.07) (Klingenberg 2011) reduces discrepancies in shape dimensions owing to changes in angle in digitizing images by configuring landmarks into Procrustes superimposition and generating a consensus configuration as explained by Savriama (2018).

Moreover, 13 homologous landmarks (corresponding to 13 X and 13 Y Cartesian coordinates) (Loy et al. 2000; Cantabaco et al. 2015) were chosen on digitized images of all samples such that the landmarks configurations (X, Y coordinate) on all images represent the same position (Figure 2). The centroid size is the total of all configured landmark distances from the body's center, and it is used to plot landmarks in Kendall's space shape (that is, the use of geometrical information of shape without impacts on location, scale, and rotation) (Kendall et al. 2005). A wireframe was constructed by linking landmarks with each other, measuring, and recording to analyze the shape variations.

Principal Component Analysis (PCA) was conducted to determine the maximum amount of variations in body shape to estimate species differentiation using MorphoJ Software (ver1.07) (Klingenberg 2011). Individual analyses were performed, and average values were used to analyze key variables for each individual. The significant eigenvalues from various PCAs addressed the number of variations. A Multivariate Analysis of Variance (MANOVA) was performed on Procrustes coordinates to determine the number of differences in mean body shape. Procrustes coordinates were utilized to generate Wilk's Lambda and F-ratio values, which were then employed to explain the observed variation. Resampling was performed using 1000 bootstrap iterations.

The Canonical Variate Analysis (CVA) on centroid size was used to explain differences between inter and intra-populations and performed using the MorphoJ software (ver. 1.07) (Klingenberg 2011). Procrustes ANOVA was used to test the size and shape differences significance between all populations. The CVA results were further validated by the Unweighted Pair Group Method (UPGMA), which was created on the Procrustes distance by superimposing it to infer phylogenetic signal (if any) from the occurred shape changes. The phylogenetic tree was constructed using Paleontology Statistic Software (PAST) version 4.03 (Hammer et al. 2001).

RESULTS AND DISCUSSION

Sampling data

Approximately 260 *P. argenteus* specimens were successfully collected from five different populations, namely WC, EC, NC, SC, and BI (Figure 1; Table 1).

Body size and shape variances in *P. argenteus*

A total of 22 variables were generated from 13 homologous landmarks and used to distinguish taxa based on variation in body shape among all *P. argenteus* specimens obtained. The homologous landmarks were chosen along the entire fish length to record the maximum variation in this species (Figure 2).

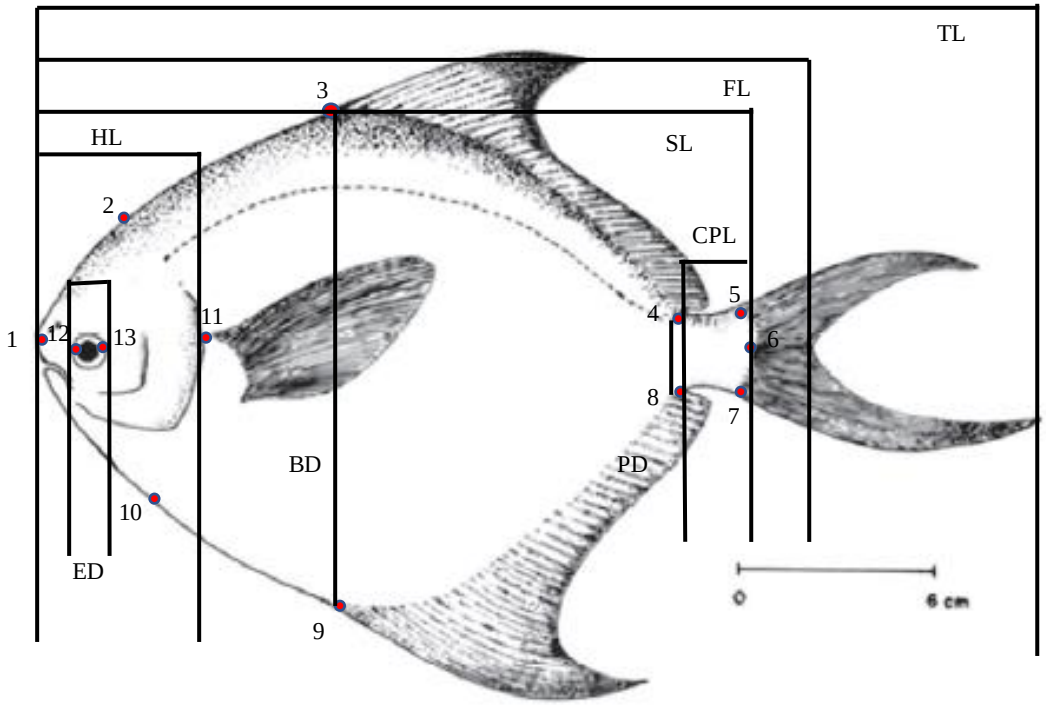

Figure 2. Locations of 13 landmarks with a description of 22 variables of *Pampus argenteus*. TL; total Length, FL; Fork Length, SL; Standard Length, BD; Body Depth, CPL; Caudal Peduncle Length, PD; Peduncle Depth, HL; Head Length. LM 1-2: Anterior tip of snout to posterior edge of the neurocranium, LM 2-3: Posterior edge of the neurocranium to anterior insertion of the dorsal fin, LM 3-4: Anterior insertion of the dorsal fin to posterior insertion of the dorsal fin, LM 4-5: Posterior insertion of the dorsal fin to point of maximum curvature of the peduncle, LM 5-6: Point of maximum curvature of the peduncle to posterior body extremity, LM 6-7: Posterior body extremity to point of maximum curvature of the peduncle, LM 7-8: Point of maximum curvature of the peduncle to posterior insertion of anal fin, LM 8-9: Posterior insertion of anal fin to anterior insertion of anal fin, LM 9-10: Anterior insertion of anal fin to insertion of the operculum on the lateral profile, LM 10-1: Insertion of the operculum on the lateral profile to anterior tip of snout, LM 13-11: Posterior margin through midline of orbit to superior insertion of the pectoral fin, LM 12-13: Anterior margin through midline of orbit to posterior margin through midline of orbit, LM 1-6: Standard length (Loy et al. 2000)

Principal Component Analysis (PCA)

The PCA of 260 *P. argenteus* specimens indicated 22 components utilized to elucidate body shape and size variations in two dimensions (x and y-axis). The first component (PC1) has the highest variance of 24.58% and eigenvalue of 0.0003, suggesting low significance [(an eigenvalue greater than 0.3 is considered significant) (Shrestha 2021)]. The first four Principal Components (PCs) are as follows: PC1 (variation in body size, body depth) with 24.58% (eigenvalue 0.0003), PC2 (variation in body depth and caudal region) with 16.6% (eigenvalue 0.0002), PC3 (variation in head region) with 12.32% (eigenvalue 0.0002) and PC4 (variation in head region and body depth) with 9.61% (eigenvalue 0.0001), respectively with a combined of all variances of approximately 63.11% (Figures 3, 4 and 5).

Based on the result in Figure 3, PC1, representing the sample's body depth and body size, showed the highest variable for overall body shape among all PCs. The second highest PCs was PC2, which appears to indicate perceptual variance in the location of the anterior insertion of the dorsal and anal fin (generally known as body depth; landmarks 3 and 9) and caudal region (landmarks 4, 5, 6, 7 and 8). A similar variation pattern is also visible in PC3, which displays variation in the location of the mouth and eye and the body depth, where the position of landmarks L1, L10, L12, and L13 are closely related. Furthermore, PC4 depicts the change in operculum insertion on the lateral profile due to landmark position transformation (landmark 10). The changes in body shape may also be seen in average specimen wireframes, as shown in Figure 4.

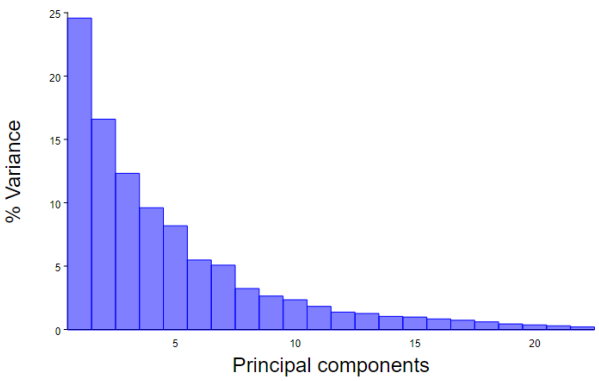

Figure 3. Values of all PCs plotted against the percentage of total variation for all samples (260 individuals) of *Pampus argenteus*

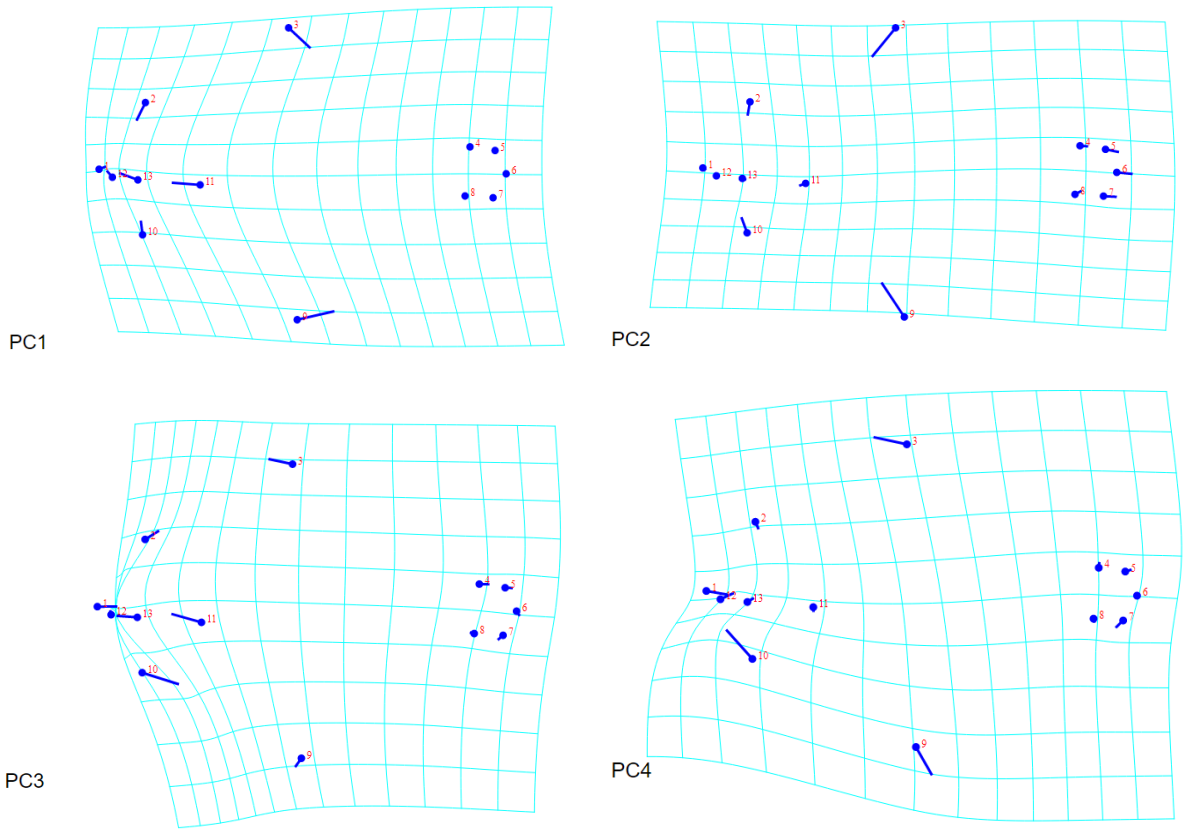

Figure 4. Visualization of shape variations from PC1 to PC4 using a wireframe to explain shape differences. PC1 demonstrates the changes in body size and depth, PC2 depicts the changes in body depth and caudal region, PC3 demonstrates changes in the mouth and eye regions (head region), and PC4 including the operculum, and it is the same as PC3

The overlapping patterns in the scatter plot of PC1 against PC2 (Figure 5) indicate that there is minimal variation in the body morphology of *P. argenteus*, with very low eigenvalues (less than 0.3) that are not significant in distinguishing individuals classified as *P. argenteus* based on the common body shape. Therefore, the averange values of all centroid size of *P. argenteus* (circle in Figure 5) from all populations (SC, NC, EC, WC, and BI) was used to get a clearer picture of the relationship between all the populations studied. The results show little segregation between all those populations considering the non-overlapping of averange value of centroid sizes (Figure 5). Figure 5 shows each sample's scatter point (centroid size) in the scatter plot of PC1 versus PC2. The circle in the scatter plots explained the averange values of all centroid size (x and y axis) of each population, which are [NC; (0.01762, -0.0099), WC; (0.004907, 0.008402), EC; (-0.01286, -0.01099), SC; (0.011098, 0.007792), and BI; (-0.01505, 0.00519)].

MANOVA was conducted to examine the disparities in mean body shape. The analysis results indicated significant variation in all examined aspects ($p < 0.0001$), and both tests yielded consistent findings. Among all currently studied samples, results revealed a significant variation ($F = 5.447$, Wilk's Lambda = 0.193, $p < 0.0001$) (Table 2). Based on the findings, the mean body shape disparities among all populations are highly significant if the F-ratio value is high. Furthermore, lower Wilks' lambda values show a better discriminating ability of body shape throughout the population. The Wilks' Lambda scale range is 0 to 1, with 0 representing total discrimination and 1 representing no discrimination (Teodoro et al. 2016). Based on the results obtained, Wilks' Lambda = 0.193, indicating discrimination among the studied population. The results obtained from MANOVA clearly show that a very significant difference is present among the *P. argenteus* population. At the same time, there is no significant difference within the population (Wilk's Lambda = 0.901, $F = 1.167$, p-value = 0.279 (Table 2). It is noteworthy that there existed statistically significant variations among the samples collected from the East Coast and North Coast ($p = 0.000$), East Coast and South Coast ($p = 0.000$), and East Coast and West Coast populations ($p = 0.001$), as indicated in Table 3. In contrast, EC and BI populations have no significant difference with p-value = 0.809. The results clearly showed populations from NC, EC, and SC, representing SM, were separated from EC and BI populations, representing SCS. The findings of this study provide clear evidence that the average body shape of *P. argenteus* exhibits significant variation, which is contingent upon their respective habitat and marine location.

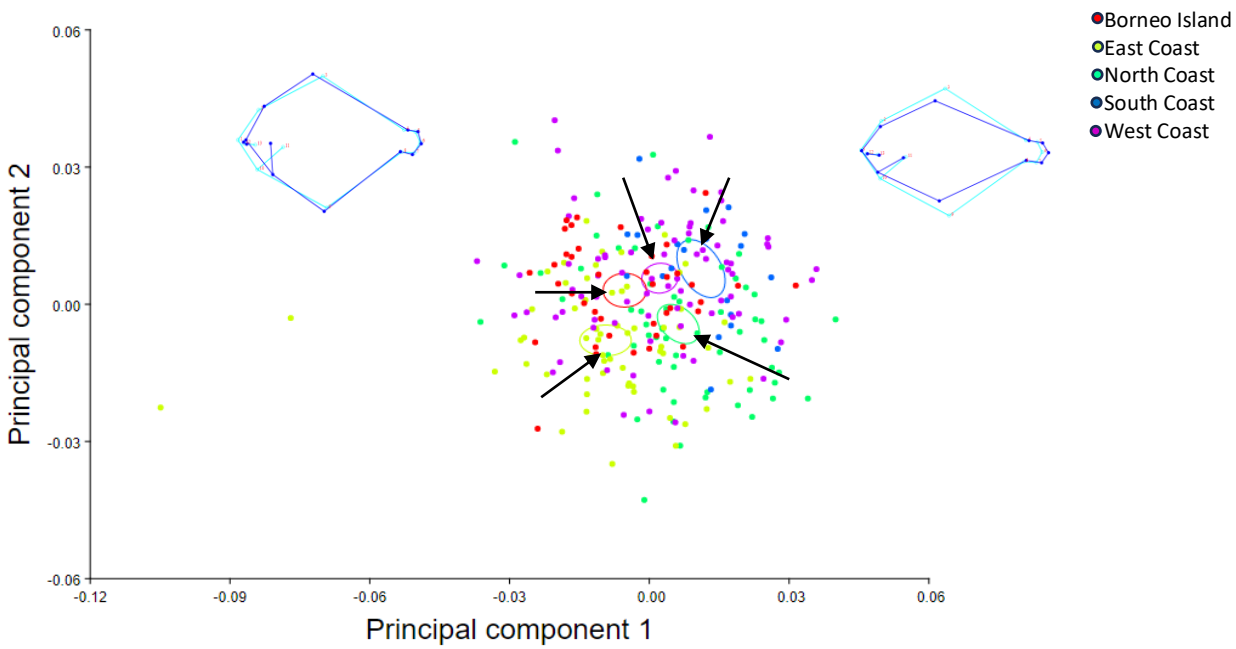

Figure 5. Principal component analysis of all *Pampus argenteus* specimens classified by region

Canonical Variate Analysis (CVA)

CVA was performed and applied to the current data of *P. argenteus* to validate the shape differences and prior group discrimination revealed by PCA analysis. CVA used new variables to minimize the within-group variation while maximizing the between-group variation. The analysis was performed on all specimens to get clear discrimination among populations by choosing 1000 permutation rounds that generated four CVs (Table 4; Figures 6 and 7). Table 4 describes the first three functions that show significant body shape differences. The maximum variation in function 1 (CV1; variation in body depth and head region) is 42.97% with a high eigenvalue of 0.92; function 2 (CV2; variation in body depth, caudal region, and head region) explains only 30.98% of body shape variations with eigenvalue of 0.66 while function 3 (CV3), 15.876% variance with eigenvalue 0.34. All four CVs had eigenvalue < 1 and 100% share the cumulative variation. The method produced identical findings as PCA but with higher support for differentiation based on eigenvalues.

Procrustes ANOVA calculated significant size and shape differences between all populations. The negative value in the x-axis of the graph explains that the population with deep body depth clusters together while the population with shallow body depth groups towards the positive zone (x-axis) of CV (Figure 7). In detail, the population of the SC, WC, and NC regions tends towards the positive zone (positive CV1 value, x-axis graph). In contrast, the population of the EC and BI tends towards the negative zone (negative CV1 value, x-axis graph). Several variations are formed based on the analysis of body shape variations from the CVA partial wrap score. CV1 describes the variation in body depth and head size region. CV2 and CV4 explain some variation in head region, caudal region, and body depth, while CV3 shows no variation among all samples (Figure 6). Procrustes ANOVA that runs on the CVA results indicates that morphological differences between all populations are highly significant ($p < 0.0001$) (Table 5). The results obtained from CVA show morphological differences between all populations of *P. argenteus* from Malaysian waters. However, the findings separated the populations into two main groups representing the marine region they belong to (Figure 7).

Table 2. Multivariate regression analysis of partial warp score and uniform centroid size of all *Pampus argenteus* specimens from all sampling sites

	F	Wilk's Lambda	p - value	df	N
Intra-population	1.167	0.901	0.279	234.000	260
Inter-population	5.447	0.193	< 0.0000	927.000	260

Note: significant p-value < 0.0001, N: Total number of samples and df: Degree of freedom.

Table 3. Multiple comparisons of samples from all populations studied

Population	NC	WC	SC	EC
NC	-			
WC	0.718	-		
SC	0.844	0.302	-	
EC	0.000*	0.001*	0.000*	-
BI	0.016*	0.208	0.008*	0.809

Note: *The mean difference is significant at p-value <0.05

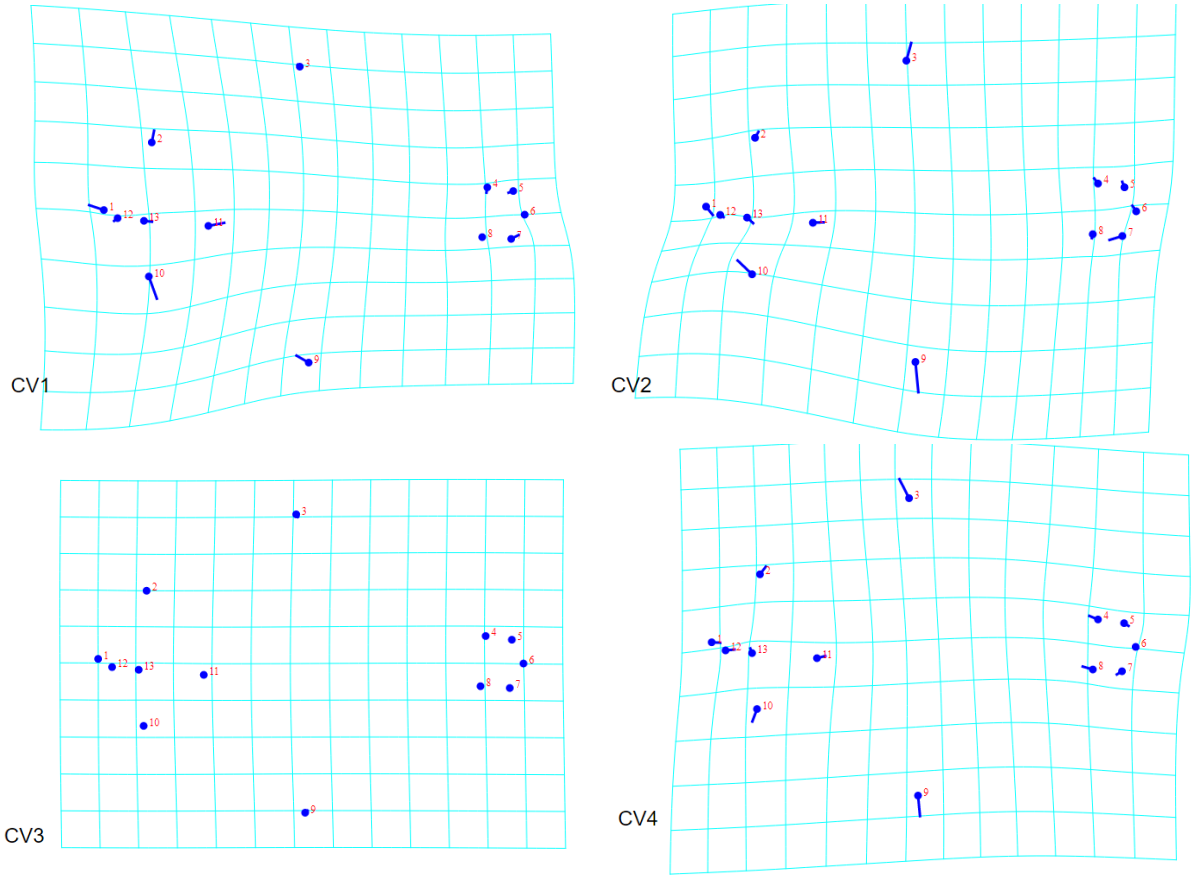

Figure 6. Visualization of shape variation along CV1 to CV4 by partial wraps along wireframe showing average shape variations. CV1 describes the variation in head size region. CV2 and CV4 explain some variation in head area and body depth, while CV3 shows no variation among all samples

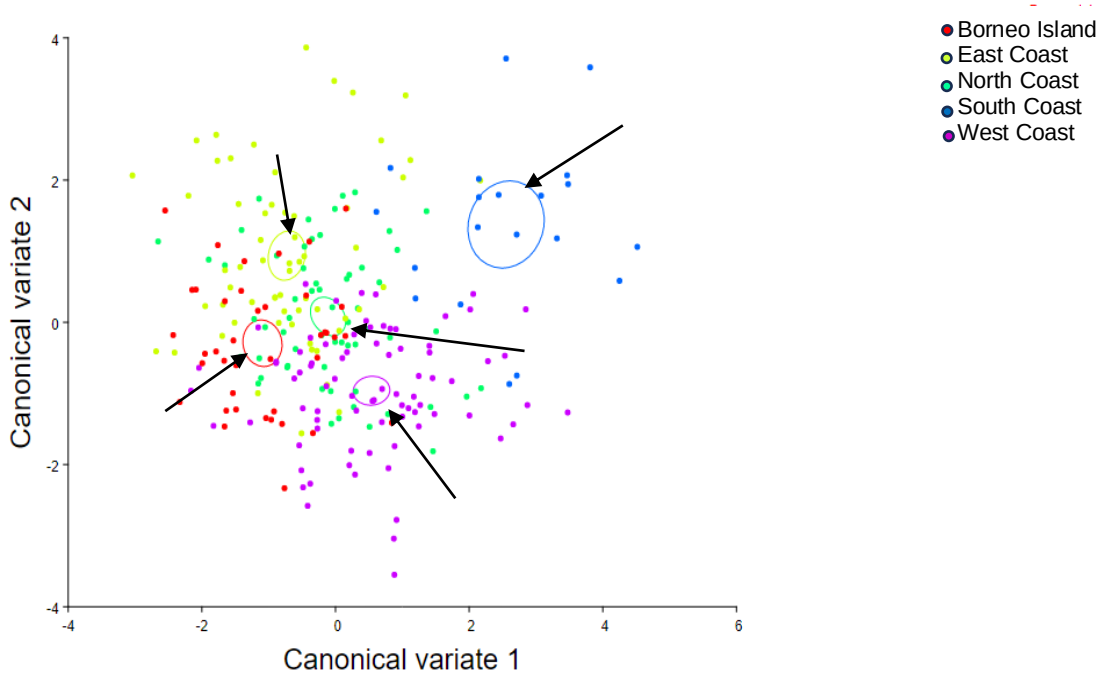

Figure 7. Canonical Variate Analysis (CVA) of five populations of *Pampus argenteus* from Malaysian waters

Pairwise differences among population

The SC was the most distinct in this research compared to all other groups (Table 6). The maximum Procrustes distance between the SC and BI is 0.0326. In contrast, a minimal distance value of 0.0129 was recorded between WC and NC, indicating that both populations had relatively similar body shapes. The p-value for all distances is 0.0001, indicating that the results are significant.

Reconstruction of evolutionary changes in *P. argenteus*

Based on the UPGMA method from the results of the CVA permutation test on the CVs, it was found that all the studied populations are closely related through their body shape and evolved in separate groups (Figure 8). The population on the SC is more diverse among the five populations studied and covers the maximum space in the canonical component. Populations from BI and EC were clustered together, explaining that they have similar morphological characteristics, while NC and WC populations clustered in another group (Figure 8). The topographic shape of the phylogenetic tree clearly shows that each group represents a different geographical sea region, namely, BI and EC represent the SCS, while the NC and WC represent the SM.

Discussion

Body shape and body size in GM are important approaches for recording morphological variations, particularly shape and size variation, as well as assessing relationships between taxa and populations of the same species based on changes in body shape (Openshaw and Keogh 2014; Imtiaz and Naim 2018). GM possesses the capacity to elucidate the underlying pattern of shape variation, which can be further correlated with additional variables, such as landmark coordinates, through the application of Procrustes superimposition (Adams and Otárola-Castillo 2013). Furthermore, GM is a powerful technique that may distinguish individuals even amongst closely related species, particularly in body structure (Cooke and Terhune 2015). The current study investigated whether GM data may be utilized to differentiate populations of *P. argenteus* in Malaysian water based on their body shape.

The GM results of this study were evident and sufficient for classifying the *P. argenteus* population into various groups based on differences in body form concerning various habitat settings. Five populations of *P. argenteus* in Malaysian waters demonstrated they were significantly different. However, the results of the PCA, CVA, and UPGMA indicated that all the samples grouped were from the same body of marine water. The findings of this study showed that populations from NC (PNG, KD, and PS) and WC (PK, S, N9, and M) were morphometrically homogeneous. This is because NC and WC belong to the SM marine region. Additionally, there was morphometric homogeneity between the populations of BI (SB and SR) and the EC (K, P, and T), both belong to the SCS maritime zone. However, individuals from SC (J) split apart from other individuals and formed a different group (Figures 5 and 7). PCA results of the GM data revealed a statistically significant outcome. However, it is worth noting that all the samples exhibited considerable overlap. This implies minimal variations in body morphology across the entire population (Figure 5). Nevertheless, CVA results (Figure 7) improved the visual representation of populations with close morphological characteristics (inter-population). Additionally, the results of PCA and CVA are further supported by the implementation of the UPGMA; this method utilizes the CVA Procrustes distance to summarise the clusters of populations effectively. This approach divides the populations into distinct groups based on their shared morphological characteristics (Figure 8).

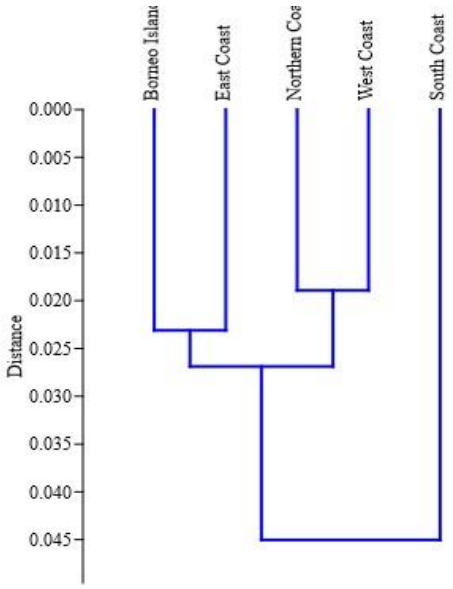

Figure 8. Reconstruction of evolutionary changes using CVA Procrustes distance of the body shape of *Pampus argenteus*

Table 4. Lists eigenvalues, variances, and cumulative based on Canonical Variate Analysis (CVA)

	Eigenvalues	Variance %	Cumulative %
CV1	0.91731592**	42.970	42.970
CV2	0.66135844**	30.980	73.950
CV3	0.33891808*	15.876	89.826
CV4	0.21718882	10.174	100.000

Note: * Eigenvalue > 0.3 showed significance; ** Eigenvalue > 0.5 were considered highly significant.

Table 6. CVA Procrustes distances among population groups of *Pampus argenteus* species

	EC	NC	SC	WC
NC	0.0179*			
SC	0.0319*	0.0232*		
WC	0.0196*	0.0129*	0.0237*	
BI	0.0158*	0.0185*	0.0326*	0.0138*

Note: * P < 0.0001 is highly significant

Table 5. Procrustes ANOVA of *Pampus argenteus* collected from Malaysian waters

Effect	SS	MS	df	F	P- value
Size					
Individual x region	1289641.213103	322410.303276	4	2.16	0.0738
Measurement error	38034737.141366	149155.831927	255	-	-
Shape					
Individual x region	0.03631603	0.0004126821	88	8.37	<.0001*
Measurement error	0.27647310	0.0000492822	5610	-	-

Note: *(P < 0.0001) highly significant; SS is the sum of squares; MS is the mean sum of squares; df is degrees of freedom, and F is the F ratio

Moreover, using the maximum number of landmarks enhances the accuracy of the data, allowing any minor variations in the body shape of the samples to be captured over the whole length of the specimens (Imtiaz and Naim 2018). In this study, 13 landmark values were computed into 22 variables. These landmark variables could fully discriminate between all individuals of the *P. argenteus* specimens in the morpho-space of PCA. Based on the presented findings, it can be observed that the initial four PCs collectively account for 63.107% of the overall body shape variation within the dataset. The study's findings comprehensively analyze the first four PCs, revealing variations in body depth, head area, and caudal region (Figures 3, 4, and 5), all of which are associated with the principal objective of adapting to environmental pressures. The locomotion, food acquisition, and fish activities vary following different environmental conditions (Imtiaz and Naim 2018). Furthermore, the study is consistent with the research conducted by Moreira et al. (2020), which examined the morphological variability of blue jack mackerel (*Trachurus picturatus* Bowdich, 1825) in the North East Atlantic and reported that there is phenotypic heterogeneity among populations, particularly in terms of body depth and caudal peduncle. Besides environmental factors, the phenotypic heterogeneity observed within species is influenced by individual genetic background (Westneat et al. 2015), culturing conditions such as temperature, hydrodynamics, and food availability (Moreira et al. 2020), as well as ecological niches that impact body shape adaptations for habitat utilization (Valladares et al. 2014). Generally, geographical differences contribute to all the aforementioned factors, thereby automatically influencing the morphological features of a species (Sajina et al. 2011). Specifically, it has been determined that the Malay Peninsular acts as a shared terrestrial barrier for many species, such as fish, whose geographical range relies on ocean currents (Binashikhbubkr et al. 2023).

The PCA results were confirmed by MANOVA analysis, which revealed that body shape had relative regional ordination. The results of the MANOVA analysis indicated significant differences in shape variation among populations (Wilk's Lambda = 0.193; F = 5.447; p < 0.000) (Table 2). However, no significant differences were observed within populations (Wilk's Lambda = 0.901; F = 1.167, p = 0.279) (Table 2). These findings also highlight that the phenotypic heterogeneity observed within *P. argenteus* in Malaysian waters is attributed to population separation, specifically geographical separation.

The positive side (positive value in PC1) of the x-axis of the graph classified individuals with extensive body depth and short caudal region. In contrast, the negative side (negative value in PC1) of the x-axis of the graph classified samples with shallow body depth and longer caudal region. Many species' morphology is well proven to be connected to their environment (Villéger et al. 2017; Fišer et al. 2018). Based on morphological investigations of *P. argenteus* populations, they are classified into five distinct populations, grouped into two main clusters representing marine regions. The SM is represented by SC, NC, and WC, which explains the clustering of individuals with similar body shape features (deep body depth and short caudal area). In contrast, the SCS is represented by BI and EC, which explains the clustering of individuals with similar body form traits (shallow body depth and longer caudal region). This demonstrates that the marine environment changes the species' physical traits based on their adaptation to the specific habitat. This statement is supported by a GM study conducted by Ismail (2018) on the Red Sea hermit crab (*Clibanarius signatus* Heller, 1861). The study found a large variation in the shape of the species' shield, which is influenced by geographical location. Likewise, Trevisan et al. (2016) have reported their work on applying GM to the carapace morphology of tiger crabs (*Aegla schmitti* Hobbs Iii, 1979*)*. Their approach successfully revealed considerable variations among all seven populations tested.

The results of this study are comparable to those reported by Moreira et al. (2020), who researched the morphology of the Ibis (*Ambassis interrupta* Bleeker, 1853) fish population. They discovered that the first four PCs showed 61.192% shape variance, which mean they had some body and head depth variations. Besides that, Binashikhbubkr et al. (2022) conducted research on the population of Kawakawa (*Eutynnus affinis* Cantor, 1849) in Peninsular Malaysia and indicated that the first four PCs accounted for 65.69% of the observed variation in body depth, head morphology, dorsal fin, anal fin, caudal fin characteristics, and overall body size. Moreover, Geiger et al. (2016) studied the morphological characteristics of barbels belonging to *Barbus* spp. Their study across different geographical areas indicated that the initial four PCs accounted for 81.3% of the body shape variation, specifically elucidating body depth alterations.

The distribution of individuals in the morpho-space represents the differences in body shape, and the clustering of the individuals into specific populations has explained that they are separated according to different body shapes (body depth, head region, and caudal region). In this study, the population's clustering pattern represents two main population groups: samples with deep body depth and shorter caudal region clusters in one group and vice versa. Based on the current study, the population from BI and EC cluster together in the morpho-space [negative-valued taxon in morpho-space- (x-axis of the graph)] and have homologous body features, such as deep body depth and a shorter caudal region. On the other hand, the population from the SC, NC, and WC cluster together in the morpho-space [positive-valued taxon in morpho-space (x-axis of the graph)] and exhibit homologous body features, including shallow body depth and a longer caudal region. Positive and negative sites in morpho-space separate the population into two major marine regions: the SCS and the SM. The changes in fish body shape are the basis for habitat diversity and ecological adaptation (Claverie and Wainwright 2014).

This study demonstrates that the body shape of the investigated *P. argenteus* can be classified into specific groups, each characterized by distinct body features. This result is most likely related to seasonal monsoons, especially in December-February and June-August. According to Liu et al. (2011), the SCS is heavily impacted by the monsoonal system, which has oceanic cyclonic circulation from December to February and anticyclonic circulation from June to August. The sampling of the *P. argenteus* for this study was done in December 2018, which was highly impacted by the monsoonal system. The theory has also been supported by Daryabor et al. (2016), who investigated the dynamics of water circulation and seasonal transport in the SCS and discovered that monsoon wind stress influences seasonal water circulation, influencing water flow. The EC water circulation patterns are mainly controlled by geostrophic currents known as ocean currents, where the Coriolis effect balances the pressure gradient force (Daryabor et al. 2016). Furthermore, the SC and SM regions are subject to wind pressure (Daryabor et al. 2016). Furthermore, water mass distribution in SM were affected by two monsoon seasons which is occurs in March and August (Mansor et al. 2023). Based on this occurrence, the wind, particularly during the monsoon, will impact the seascape and fish habitat. It is intriguing to consider the possibility that this phenomenon has indirectly influenced the morphometrics of *P. argenteus* in Malaysian waters.

Indeed, the presence of certain specimens in this study exhibiting minor differences in body size, head size, and caudal area, despite belonging to the intra-population, may elicit curiosity. This observation could potentially be associated with the gender variability exhibited by the specimen, encompassing both male and female characteristics. The present study's findings indicate that the variation in individual size was not considered, and the results demonstrate that there is no statistically significant difference ($p = 0.0738$) among all populations (Table 5). The findings of Cantabaco et al. (2015) support this observation, as they reported that females exhibited larger body sizes and higher body weights than males. These factors do not have an impact on the GM analysis. The present study's results indicate that there is a statistically significant difference ($p < 0.0001$) in the variation of individual shape across all populations (Table 5). The observed variations in the head, axial, and caudal regions of the fish examined in this study may contribute to their equilibrium and locomotion, influencing their ability to navigate water environments (Cantabaco et al. 2015). This discovery was further validated by Reece and Mehta (2013), who proposed that three regions, the head, body, and caudal area, are critical determinants in determining the variety of fish forms. Marine habitats are divided into zones based on ecological factors such as sunshine penetration, food availability, and water velocity (Mitra and Zaman 2016). The *P. argenteus* has a bilateral body that is highly compressed and oval to support its presence on muddy bottoms, brackish water, and estuaries. The variation in *P. argenteus* head shape detected in the PC zone of the wireframe explains how they adapt to different environments and habitats based on their eating habits. The species has a wide range of prey such as small crustaceans' zooplankton (copepods), algae, and semi-digested pulp that are very important in their diet (Gupta 2020). Liu et al. (2014) have reported that salps, hydromedusae, amphipods, shrimps, and other small fish groups are present in the diet of *P. argenteus* species from Kuwait water and that zooplankton and phytoplankton are the most popular food items. This statement elucidates that *P. argenteus* exhibits variations in diet based on the specific habitats they inhabit, which is influenced by ecological factors that are also reflected in their morphological characteristics. The finding mentioned above is also corroborated by Skoglund et al. (2015), whose research focused on the morphological characteristics of the head of the Arctic charr (*Salvelinus alpinus* Linnaeus, 1758). Their study revealed morphological variation following the Arctic charr's dietary preferences. In addition, Nautiyal (2018) described the influence of altered environments and dietary patterns on the catfish species' body, head, and jaw elongation (*Rita rita* Hamilton, 1822). The body shape variations observed among species are typically influenced by multiple factors, compelling them to adapt to the specific environmental conditions of their respective habitats.

The combination of morphometric data and a phylogenetic tree constructed using the UPGMA method is highly effective for presenting research findings. Numerous studies have provided evidence for the effectiveness of GM data in elucidating phylogenetic relationships. The present study has demonstrated the evolutionary patterns of *P. argenteus*, which have been represented in a phylogenetic tree (Figure 8). Interestingly, the results of the current investigation revealed that all samples could be divided into five populations and form three distinct clusters. These three different population clusters belong to geographical marine regions (SCS and SM) (Figure 8). The morphometric variability among stocks is expected due to the geographical segregation of stocks and the presence of

distinct ancestral origins. Furthermore, it has been indicated that morphological characteristics are influenced by hereditary factors, environmental factors, and their interactions (Aminan et al. 2020). The findings of this study are quite similar to those of Ramler et al. (2017), who studied Minnows (*Phoxinus*) from two different populations (Northern Italy and the Danube basin). In addition, Pauers and McMillan (2015) successfully constructed a phylogenetic tree using ecological distinctions among Cichlid fish. In addition, Killen et al. (2016) conducted a study on the morphological characteristics of Lake Trout (*Salvelinus namaycush* Walbaum, 1792). They found evidence of evolutionary relationships influenced by variations in body shape, which in turn are influenced by ecological diversity.

Morphometric variation within a fish species may arise due to various factors, including individual genetic background, culturing conditions, ecological niches, migration patterns, isolation events, environmental stressors, local adaptation, or a combination thereof. The morphological characteristics of individuals from intra-populations undergo modifications in response to their adaptive strategies, enabling their survival in novel environmental conditions. Taxonomic identification is crucial in differentiating species or populations within diverse ecological contexts. The utilization of GM proves to be a robust method for discerning the variations in body shape exhibited by *P. argenteus* within Malaysian waters. This work represents the preliminary initiative to employ a GM methodology on the *P. argenteus* species within Malaysian waters. PCA and CVA effectively demonstrated the notable differences in body morphology across the five studied populations of *P. argenteus*. Moreover, *P. argenteus* exhibits morphological heterogeneity, which can be categorized into three distinct groups based on their body shape and the marine regions they inhabit.

ACKNOWLEDGEMENTS

The authors would like to express their sincere gratitude to Universiti Sains Malaysia (USM) and the School of Biological Sciences (SBS) for providing opportunities and research facilities for this study. This work was funded by the Ministry of Higher Education Malaysia for Fundamental Research Grant Scheme (FRGS Fasa 1/2020), with project code: FRGS/1/2020/WAB11/USM/02/1.

REFERENCES

Adams DC, Otárola-Castillo E. 2013. Geomorph: An R package for the collection and analysis of geometric morphometric shape data. Method Ecol Evol 4 (4): 393-399. DOI: 10.1111/2041-210X.12035.

Aminan AW, Kit LLW, Hui CH, Sulaiman B. 2020. Morphometric analysis and genetic relationship of *Rasbora* spp. in Sarawak, Malaysia. Trop Life Sci Res 31 (2): 33-49. DOI: 10.21315/tlsr2020.31.2.3.

Binashikhbubkr K, Malik AA, Al-Misned F, Mahboob S, Naim DM. 2022. Geometric morphometric discrimination between seven populations of Kawakawa *Euthynnus affinis* (Cantor, 1849) from Peninsular Malaysia. J King Saud Univ Sci 34 (3): 101863. DOI: 10.1016/j.jksus.2022.101863.

Binashikhbubkr K, Setyawan AD, Naim DM. 2023. Population genetic structure of Kawakawa (*Euthynnus affinis* Cantor, 1849) in Malaysian waters based on COI gene. Nusantara Biosci 15 (2): 258-268. DOI: 10.13057/nusbiosci/n150213.

Cantabaco JKO, Celedio SF, Gubalani CMB, Sialana RJ, Torres MAJ, Requieron EA, Martin TTB. 2015. Determining sexual dimorphism in Bigtooth Pomfret, *Brama orcini*, in Tuka Bay, Kiamba, Sarangani Province. AACL Bioflux 8: 1009-1018.

Chen X, Wang JJ, Ai WM, Chen H, Lin HD. 2018. Phylogeography and genetic population structure of the spadenose shark (*Scoliodon macrorhynchos*) from the Chinese coast. Mitochondrial DNA Part A 29 (7): 1100-1107. DOI: 10.1080/24701394.2017.1413363.

Chong V, Lee P, Chai Ming L. 2010. Diversity, extinction risk and conservation of Malaysian fishes. J Fish Biol 76: 2009-2066. DOI: 10.1111/j.1095-8649.2010.02685.x.

Claverie T, Wainwright PC. 2014. A morphospace for reef fishes: Elongation is the dominant axis of body shape evolution. PLoS One 9 (11): e112732. DOI: 10.1371/journal.pone.0112732.

Cooke SB, Terhune CE. 2015. Form, function, and geometric morphometrics. Anat Rec 298 (1): 5-28. DOI:10.1002/ar.23065.

Cooke SJ, Martins EG, Struthers DP, Gutowsky LFG, Power M, Doka SE, Krueger CC. 2016. A moving target-incorporating knowledge of the spatial ecology of fish into the assessment and management of freshwater fish populations. Environ Monit Assess 188 (4): 239. DOI: 10.1007/s10661-016-5228-0.

Daryabor F, Ooi SH, Samah AA, Akbari A. 2016. Dynamics of the water circulations in the southern South China Sea and its seasonal transports. PLoS One 11 (7): e0158415. DOI: 10.1371/journal.pone.0158415.

Euphrasen. 1788. *Pampus argenteus*. https://www.fishbase.se/summary/491.

Fišer C, Robinson CT, Malard F. 2018. Cryptic species as a window into the paradigm shift of the species concept. Mol Ecol 27 (3): 613-635. DOI: 10.1111/mec.14486.

Franssen NR, Harris J, Clark SR, Schaefer JF, Stewart LK. 2013. Shared and unique morphological responses of stream fishes to anthropogenic habitat alteration. Proc Royal Soc B: Biol Sci 280 (1752): 20122715. DOI: 10.1098/rspb.2012.2715.

Geiger M, Schreiner C, Delmastro G, Herder F. 2016. Combining geometric morphometrics with molecular genetics to investigate a putative hybrid complex: a case study with barbels *Barbus* spp. (Teleostei: Cyprinidae). J Fish Biol 88 (3): 1038-1055. DOI: 10.1111/jfb.12871.

Gupta S. 2020. Reviews on the biology and culture of Silver Pomfret, *Pampus argenteus* (Euphrasen, 1788). Intl J Aquat Biol 8 (4): 228-245.

Hammer Ø, Harper DA, Ryan P. 2001. Paleontological statistics software package for education and data analysis. Paleontol Electron 4 (1): 1-9.

Idaszkin YL, Marquez F, Nocera A. 2013. Habitat-specific shape variation in the carapace of the crab *Cyrtograpsus angulatus*. J Zool 290 (2): 117-126. DOI: 10.1111/jzo.12019.

Imtiaz A, Naim DM. 2018. Geometric morphometrics species discrimination within the Genus Nemipterus from Malaysia and its surrounding seas. Biodiversitas 19 (6): 2316-2322. DOI: 10.13057/biodiv/d190640.

Iqbal F, Masood Z, Razzaq W, Rafique N, Din N, Zahid H, Bano N. 2015. Morphometric characteristics of silver pomfret, *Pampus argenteus* of Family Stromateidae collected from fish market of Quetta City of Pakistan. Glob Vet 15 (4): 394-396. DOI: 10.5829/idosi.gv.2015.15.04.96186.

Ismail TG. 2018. Effect of geographic location and sexual dimorphism on shield shape of the Red Sea hermit crab *Clibanarius signatus* using the geometric morphometric approach. Can J Zool 96 (7): 667-679. DOI: 10.1139/cjz-2017-0050.

Jawad LA. 2014. Caudal fin deformity in the wild silver pomfret *Pampus argenteus* collected from the Arabian Gulf coasts of Oman. Intl J Mar Sci 4 (38): 1-4. DOI: 10.5376/ijms.2014.04.0038.

Kendall FP, McCreary EK, Provance PG. 2005. Muscles: Testing and Function with Posture and Pain, ed 5 (with Primal Anatomy CD-ROM). Phys Ther 86 (2): 304-305. DOI: 10.1093/ptj/86.2.304.

Killen SS, Glazier DS, Rezende EL, Clark TD, Atkinson D, Willener AS, Halsey LG. 2016. Ecological influences and morphological correlates of resting and maximal metabolic rates across teleost fish species. Am Nat 187 (5): 592-606. DOI: 10.1086/685893.

Klingenberg CP. 2011. MorphoJ: an integrated software package for geometric morphometrics. Mol Ecol Resour 11 (2): 353-357. DOI: 10.1111/j.1755-0998.2010.02924.x.

Liu C, Zhuang Z, Chen S, Shi Z, Yan J, Liu C. 2014. Medusa consumption and prey selection of silver pomfret *Pampus argenteus* juveniles. Chin J Oceanol Limnol 32: 71-80. DOI:10.1007/s00343-014-3034-5.

Liu Q, Feng M, Wang D. 2011. ENSO-induced interannual variability in the southeastern South China Sea. J Oceanogr 67 (1): 127-133. DOI: 10.1007/s10872-011-0002-y.

LKIM. 2019. Laporan Risikan Pasaran 2019. http://portal.myagro.moa.gov.my/ms/mi/Laporan/Buku-Laporan-Risikan-Pasaran-2019.pdf

LKIM. 2020. Laporan Tahunan 2020. https://lkim.gov.my/wp-content/uploads/2022/04/LAPORAN-TAHUNAN-LKIM-2020.pdf

Lorenzen K, Cowx IG, Entsua-Mensah R, Lester NP, Koehn J, Randall R, Venturelli P. 2016. Stock assessment in inland fisheries: A foundation for sustainable use and conservation. Rev Fish Biol Fish 26: 405-440. DOI: 10.1007/s11160-016-9435-0.

Loy A, Busilacchi S, Costa C, Ferlin L, Cataudella S. 2000. Comparing geometric morphometrics and outline fitting methods to monitor fish shape variability of *Diplodus puntazzo* (Teleostea: Sparidae). Aquacult Eng 21: 271-283. DOI: 10.1016/S0144-8609(99)00035-7.

MacLeod N. 2018. The quantitative assessment of archaeological artifact groups: Beyond geometric morphometrics. Quat Sci Rev 201: 319-348. DOI: 10.1016/j.quascirev.2018.08.024.

Mansor KNAAK, Roseli NH, Ali FSM, Akhir MFM. 2023. Physical properties of seawater in Malacca Strait (Southeast Asia) during monsoon seasons. J Coast Res 39 (5): 921-932. DOI: 10.2112/JCOASTRES-D-22-00084.1.

Mitra A, Zaman S. 2016. Basics of Marine and Estuarine Ecology. Springer, New Delhi, India. DOI: 10.1007/978-81-322-2707-6.

Mohitha C. 2016. Population Genetic Structure of Silver Pomfret (*Pampus argenteus*) Along Indian Coast. ICAR-Central Marine Fisheries Research Institute. [Dissertation]. Cochin University of Science and Technology Cochin, Kerala. [India]

Moreira C, Froufe E, Vaz-Pires P, Triay-Portella R, Correia AT. 2020. Landmark-based geometric morphometrics analysis of body shape variation among populations of the blue jack mackerel, *Trachurus picturatus*, from the North-East Atlantic. J Sea Res 163: 101926. DOI: 10.1016/j.seares.2020.101926.

Nautiyal P. 2018. Diet components, dietary habits, resource and its use in the coexisting catfish species. J Inland Fish Soc India 50: 9-20.

Openshaw G, Keogh JS. 2014. Head shape evolution in monitor lizards (*Varanus*): Interactions between extreme size disparity, phylogeny and ecology. J Evol Biol 27 (2): 363-373. DOI: 10.1111/jeb.12299.

Pauers MJ, McMillan SA. 2015. Geometric morphometrics reveals surprising diversity in the Lake Malawi cichlid genus *Labeotropheus*. Hydrobiologia 748 (1): 145-160. DOI: 10.1007/s10750-014-1941-2.

Ramler D, Palandačić A, Delmastro GB, Wanzenböck J, Ahnelt H. 2017. Morphological divergence of lake and stream *Phoxinus* of Northern Italy and the Danube basin based on geometric morphometric analysis. Ecol Evol 7 (2): 572-584. DOI: 10.1002/ece3.2648.

Reece JS, Mehta RS. 2013. Evolutionary history of elongation and maximum body length in moray eels (Anguilliformes: Muraenidae). Biol J Linn Soc 109 (4): 861-875. DOI: 10.1111/bij.12098.

Rohlf FJ. 2017. TpsDig, Digitize Landmarks and Outlines (Version 2.31). Stony Brook, New York.

Sajina A, Chakraborty S, Jaiswar A, Pazhayamadam D, Sudheesan D. 2011. Stock structure analysis of *Megalaspis cordyla* (Linnaeus, 1758) along the Indian coast based on truss network analysis. Fish Res 108 (1): 100-105. DOI: 10.1016/j.fishres.2010.12.006.

Savriama Y. 2018. A step-by-step guide for geometric morphometrics of floral symmetry. Front Plant Sci 9: 1433. DOI:10.3389/fpls.2018.01433.

Shrestha N. 2021. Factor analysis as a tool for survey analysis. Am J Appl Math Stat 9 (1): 4-11. DOI: 10.12691/ajams-9-1-2.

Skoglund S, Siwertsson A, Amundsen PA, Knudsen R. 2015. Morphological divergence between three Arctic charr morphs–the significance of the deep-water environment. Ecol Evol 5 (15): 3114-3129. DOI: 10.1002/ece3.1573.

Teodoro S, Terossi M, Mantelatto F, Costa R. 2016. Discordance in the identification of juvenile pink shrimp (*Farfantepenaeus brasiliensis* and *F. paulensis*: Family Penaeidae): an integrative approach using morphology, morphometry and barcoding. Fish Res 183: 244-253. DOI: 10.1016/j.fishres.2016.06.009.

Trevisan A, Marochi MZ, Costa M, Santos S, Masunari S. 2012. Sexual dimorphism in *Aegla marginata* (Decapoda: Anomura). Nauplius 20: 75-86. DOI: 10.1590/S0104-64972012000100008.

Trevisan A, Marochi MZ, Costa M, Santos S, Masunari S. 2016. Effects of the evolution of the Serra do Mar mountains on the shape of the geographically isolated populations of *Aegla schmitti* Hobbs III, 1979 (Decapoda: Anomura). Acta Zool 97 (1): 34-41. DOI: 10.1111/azo.12102.

Valladares F, Matesanz S, Guilhaumon F, Araújo MB, Balaguer L, Benito-Garzón M, Naya DE, Nicotra AB, Poorter H, Zavala MA. 2014. The effects of phenotypic plasticity and local adaptation on forecasts of species range shifts under climate change. Ecol Lett 17 (11): 1351-1364. DOI: 10.1111/ele.12348.

Villéger S, Brosse S, Mouchet M, Mouillot D, Vanni MJ. 2017. Functional ecology of fish: Current approaches and future challenges. Aquat Sci 79: 783-801. DOI: 10.1007/s00027-017-0546-z.

Westneat DF, Wright J, Dingemanse NJ. 2015. The biology hidden inside residual within-individual phenotypic variation. Biol Rev Camb Philos Soc 90 (3): 729-743. DOI: 10.1111/brv.12131.

Zhang C, Fan Y, Ye Z, Li Z, Yu H. 2017. Identification of five *Pampus* species from the coast of China based on sagittal otolith morphology analysis. Acta Oceanol Sin 36 (2): 51-56. DOI: 10.1007/s13131-017-0982-6.

NUSANTARA BIOSCIENCE
Vol. 16, No. 1, pp. 13-22
May 2024

ISSN: 2087-3948
E-ISSN: 2087-3956
DOI: 10.13057/nusbiosci/n160102

Metal concentrations in Silver pomfret *Pampus argenteus* (Euphrasen, 1788) and its risk assessment in Malaysia

SUZYELAWATI MOHD SHUKRI[1], AHMAD DWI SETYAWAN[2], DARLINA MD NAIM[1,♥]

[1]School of Biological Sciences, Universiti Sains Malaysia. 11800 Pulau Pinang, Malaysia. Tel.: +60-46534056, ♥email: darlinamdn@usm.my
[2]Department of Environmental Sciences, Faculty of Mathematics and Natural Sciences, Universitas Sebelas Maret. Jl. Ir. Sutami 36A, Surakarta 57126, Central Java, Indonesia

Manuscript received: 8 November 2023. Revision accepted: 11 May 2024

Abstract. *Shukri SM, Setyawan AD, MD Naim D. 2024. Metal concentrations in Silver pomfret* Pampus argenteus *(Euphrasen, 1788) and its risk assessment in Malaysia. Nusantara Bioscience 16: 13-22.* Fish consumption is one of the most important sources of protein in Malaysia. Nevertheless, anthropogenic sources release contaminants, such as metals, which have the potential to accumulate within marine organisms via the food chain. Hence, ingesting fish polluted with metals can be potentially hazardous to human health. This study aimed to ascertain the levels of metal concentrations in the edible tissues of *Pampus argenteus* (Euphrasen, 1788) inhabiting Malaysian waters to evaluate potential health hazards associated with their use. This study examines the levels of three metals, specifically Cd, Ni, and Pb, in *P. argenteus*. The samples underwent microwave digestion in a closed vessel to extract metals, which were subsequently analyzed using ICP-OES. The study revealed that the quantities of metals in *P. argenteus* were primarily Pb, with Ni and Cd following suit. These values ranged from 0.651 mg/kg to 0.001 mg/kg when measured on a dry weight basis. Notably, the samples collected from the Straits of Malacca exhibit a greater concentration of metals than those obtained from the South China Sea region. The tolerable daily intake of *P. argenteus* from all populations in this study was below the FAO/WHO oral reference dose. The risk assessment results showed that all populations' target hazard quotient was below 1.0. The results indicate that exposure to the metals studied poses a low non-carcinogenic risk and is considered safe for human consumption. This research offers baseline data for evaluating food safety and developing risk management recommendations concerning *P. argenteus*.

Keywords: ICP-OES, metals, *Pampus argenteus*, Reference Dose (RfD), target hazard quotient

INTRODUCTION

Nutritionists widely recognize marine fish and shellfish as significant contributors to high-quality protein, constituting approximately 17% of animal protein intake and accounting for approximately 6% of human dietary intake (Iimtiaz and Naim 2018; Salam et al. 2019). These aquatic organisms also contain essential minerals and fatty acids, particularly omega-3. However, despite the numerous health benefits associated with seafood consumption, it is imperative to consider the potential health hazards that arise from the prevalence of metals in marine fish and seafood. This is particularly relevant for seafood consumers (Rajeshkumar et al. 2018).

Metals refer to a toxic element that can lead to toxicity in the human body, generating harmful species and potentially causing damage and chronic illnesses. Based on the research conducted by (Sankhla et al. 2016; Rehman et al. 2018), it is evident that consuming toxic metals poses numerous health hazards to humans. These risks encompass a range of conditions, including dermatological diseases, skin cancer, and various internal cancers, such as those affecting the liver, kidney, lung, and bladder. Additionally, the ingestion of toxic metals has been related to the expansion of cardiovascular disorders, diabetes, and anemia. Furthermore, these metals can also adversely impact the human body's reproductive, developmental, immunological, and neurological processes.

The escalating demand for fish stocks has caused increased pollution of the local environment, a substantial rise in trawling and culturing activities in the South China Sea, and the intensified human presence in the vicinity of marine culture (Amirah et al. 2013; Zhu et al. 2014). Consequently, this phenomenon poses a direct threat to marine organisms. Fish serve as reliable indicators of metal contaminations in water ecosystems caused by their ability to occupy various trophic levels and exhibit diverse sizes and ages (Cordeli et al. 2023). Fish can accumulate metals within their tissues via absorption mechanisms, which poses a potential risk to humans exposed to these metals through the food chain. The ingestion of contaminated fish has immediate and long-term impacts on human health. For example, high exposure to Ni intake by humans can cause some side effects such as nausea, vomiting, diarrhea, giddiness, lassitude, headache, cough and shortness of breath, lung fibrosis and respiratory tract cancer are some of the conditions/diseases related to the respiratory system (O'Neal and Zheng 2015). Cd is considered to be another carcinogenic hazardous element that can cause hypertension, renal tubular damage or Acute Tubular Necrosis (ATN), and pancreatic, breast, and prostate cancers (Schwartz and Reis 2000; Tamele and Vázquez 2020). Elevated Pb contamination can cause neurological damage (cognition, decreased IQ), kidney disease, an endocrine disorder, elevated blood pressure, decreased total sperm count, increased abnormal sperm frequencies, and

cancer (Kumar et al. 2020).

The establishment of a Provisional Tolerable Weekly Intake (PTWI) by the Joint Expert Committee on Food Additives (JECFA 2004) of the Food and Agriculture Organisation of the United Nations and the World Health Organisation (FAO/WHO) aims to safeguard consumers from the toxicological effects related with the ingestion of metals via fish consumption. The PTWI refers to the established threshold for the maximum daily exposure to a contaminant that an individual can sustain over their lifetime without incurring any adverse health effects related to food consumption. This definition is supported by the FAO/WHO and the research conducted by Peycheva et al. (2016). These limits may vary across species, as the metal accumulation process is subject to variations in developmental rates and metabolism among different organisms (Zaza et al. 2015). The United States Environmental Protection Agency (USEPA 2000) has established the Reference Dose (RfD) to assess the potential health risk associated with exposure to the contaminant. The RfD is a quantitative assessment of the daily oral intake of a contaminant that is expected to pose negligible risks of adverse effects on human health over a lifetime (USEPA 2000). Hence, it is of utmost significance to precisely quantify the levels of heavy metals in silver pomfret fish (*Pampus argenteus* ((Euphrasen, 1788)). This is imperative to ascertain its current and future safety for consumption while also serving as an indicator to alert Malaysian society if the metal concentrations surpass the established thresholds.

The *P. argenteus* primarily inhabits marine and pelagic environments ranging from 1 m to 100 m. Its widespread distribution spans the East China Sea to Southeast Asia, the Indian Ocean, the Arabian Gulf, and the North Sea (Mohitha 2016). The species is significant in Malaysian fishery sectors and has great value and demand as a protein source. Many inquiries undertaken in Malaysia have unequivocally recorded the existence of metals within fish (Kamaruzzaman et al. 2011; Alipour et al. 2021). However, the majority of these studies have primarily concentrated on examining the precise geographical areas where specific metals are present, as well as the particular fish species that are affected. Therefore, the current research was conducted to determine the concentrations of metals in consumable tissues of *P. argenteus* in Malaysia and the waters encircling it, as well as to assess the health risks associated with such substances.

MATERIALS AND METHODS

Sites and samples' description

Samples of *P. argenteus* were obtained from 13 landing sites around Malaysian waters (Figure 1). A total of 20 individuals were sampled from each sampling site. The samples were appropriately labeled to represent each respective sampling area, as indicated in Table 1, and the sampling period spanned from March to December 2018. All mature *P. argenteus* ranging from 18 to 28 cm long were collected. The specimens were examined to discover metal concentrations present in this species within the region of Malaysia.

All specimens were delivered to the School of Biological Science, Universiti Sains Malaysia, using a cool box and appropriate measures for the remaining transit process. Upon arriving at the laboratory, the samples underwent a running water cleaning process. Subsequently, the muscle tissue of the samples was excised using a sterile knife and kept separately in a designated icebox. All specimens were appropriately labeled and identified (Table 1).

Preparation of samples

Drying process

The drying procedure followed the approach outlined by Radojevic et al. (1999) and Feldsine et al. (2002), with slight adjustments to the procedural steps. The samples were homogenized and divided into two equal portions to facilitate the duplicate procedure. Subsequently, the samples underwent oven drying at 105°C. The dried samples were pulverized into fine powder and promptly placed into appropriately labeled containers for digestion.

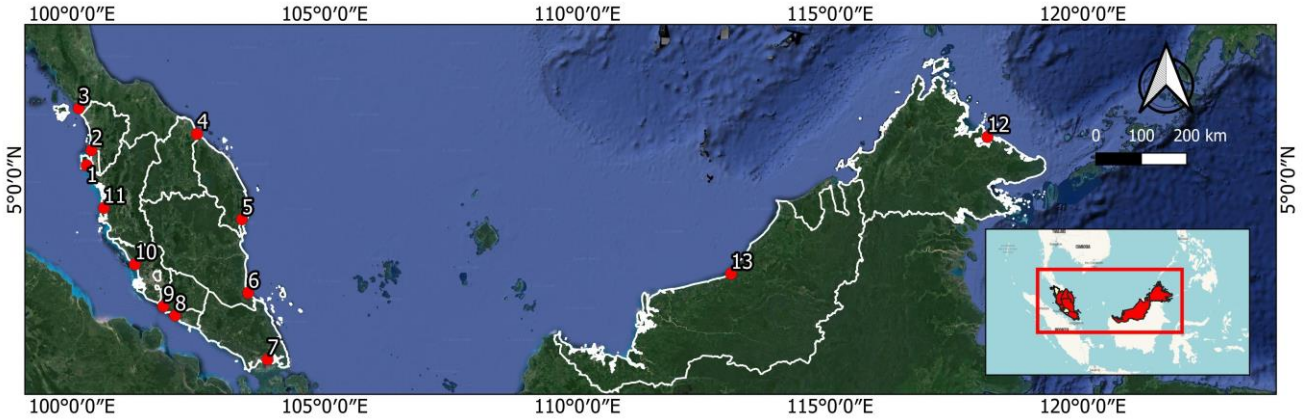

Figure 1. Sampling location of *P. argenteus* around Malaysian waters. 1. Batu Maung, Penang, 2. Kuala Muda, Kedah 3. Kuala Perlis, Perlis 4. Tok Bali, Kelantan 5. Kuala Kemaman, Terengganu 6. Kuala Rompin, Pahang 7. Kuala Benut, Johor 8. Kuala Sungai Baru, Melaka 9. Kuala Lukut Port Dickson, Negeri Sembilan 10. Sg. Yu Kuala Selangor, Selangor 11. Teluk Melintang (Teluk Intan), Perak 12. Sandakan, Sabah 13. Bintulu, Sarawak

Table 1. Description of sampling locations and sample size for each locality

Sampling Site	Geographical Location	Marine Region	Coordinate Latitude; Longitude	Sample Size (n)
Batu Maung, Penang (PNG)	NC	SM	5°17'5.0994"N, 100°17'14.9"E	20
Kuala Muda, Kedah (KD)	NC	SM	5°34'59.99"N, 100°22'59.99"E	20
Kuala Perlis, Perlis (PS)	NC	SM	6°23'52.44"N, 100°7'50.52"E	20
Tok Bali, Kelantan (K)	EC	SCS	5°53'51.36"N, 102°28'26.4"E	20
Kuala Kemaman, Terengganu (T)	EC	SCS	4°14'1.68"N, 103°21'49.6"E	20
Kuala Rompin, Pahang (P)	EC	SCS	2°48'2.16"N, 103°29'9.96"E	20
Kuala Benut, Johor (J)	SC	SM	1°30'1.03"N, 103°52'2.08"E	20
Kuala Sungai Baru, Melaka (M)	WC	SM	2°21'25.92"N, 102°2'21.12"E	20
Kuala Lukut Port Dickson, Negeri Sembilan (N9)	WC	SM	2°32'13.85"N, 101°48'20.56"E	20
Sg. Yu Kuala Selangor, Selangor (S)	WC	SM	3°21'17.29"N, 101°14'30.4"E	20
Teluk Melintang (Teluk Intan), Perak (PK)	NC	SM	4°27'20.52"N, 100°37'43.68"E	20
Sandakan, Sabah (SB)	BI	SS	5°50'21.84"N, 118°7'1.92"E	20
Bintulu, Sarawak (SR)	BI	SCS	3°10'16.68"N, 113°2'30.84"E	20
Total				260

Note: North Coast of Peninsular Malaysia (NC), East Coast of Peninsular Malaysia (EC), South Coast of Peninsular Malaysia (SC), West Coast of Peninsular Malaysia (WC), Borneo Island (BI), South China Sea (SCS), Straits of Malacca (SM), Sulu Sea (SS), n: sample size

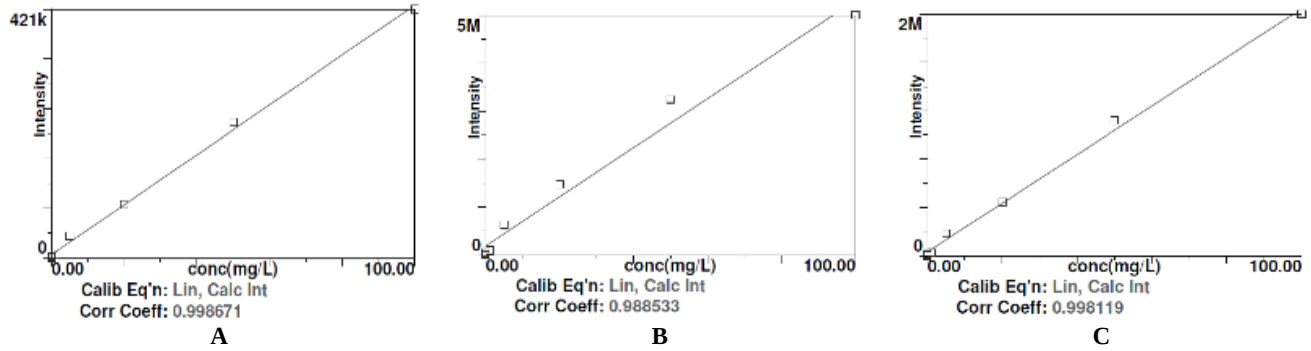

Figure 2. Calibration curve for standard used in the current study. A. Pb, B. Cd, C. Ni

Digestion process

The digestion process is a fundamental requirement technique for transforming the solid sample into a liquid state. This study employed the microwave digestion technique due to its recognized efficacy as a sample preparation method across various sample matrices. The evaluation of analytical quality was carried out by utilizing certified reference materials (CRM-DORM4) obtained from the National Research Council Canada. The dogfish muscle samples were used as a reference in CRM to confirm that all elements were within the designated range, as described by Willie et al. (2012). The observed recoveries of all elements in DORM4 were determined to vary between 80% and 130% of the declared value.

Next, 0.5g of dried samples and DORM4 were added to a Teflon vessel containing 10 ml of 70% nitric acid (HNO_3). The samples underwent digestion using a closed-vessel microwave digestion system (Milestone model Start D, Italy). The samples were filtered for future analysis.

Analysis of metals

Metals were determined on an ICP–OES model Optima 5300 DV (Perkin Elmer, USA). Certificate Recovery Material (CRM) - DORM4 standards were added to the samples to test the reliability of the approach, and their recovery rates were calculated. The results of the element recovery tests are presented in Table 2. The calibration curves were generated by graphing the absorbance readings against the corresponding concentrations using optimized instrument conditions. The calibration curve for each metal is depicted in Figure 2, demonstrating a high degree of correlation (R_2 = 0.999) between absorbance and concentration, indicating that the instrument yielded dependable outcomes.

Recovery tests

The recoveries of Pb, Ni, and Cd were found to be 88%, 90%, and 82.5%, respectively, thus fell within the acceptable range of 80 to 130%, as outlined in a previous study by Buhari and Ismail (2016), indicating a high level of accuracy (Table 2). The recovery values of the metals were determined using ICP-OES, as described in Equation 1. This finding provides initial validation for the calibration techniques employed in the ICP-OES instrument.

Equation 1: Recovery (%) = Observed concentration (mg/kg) / Published concentration (mg/kg) X 100

Table 2. Measured and certified values of metal concentrations (mg/kg DW) utilizing ICP-OES

Elements detected	Obtained conc.	CRM – Dorm4 (published conc. value) (Willie et al. 2012)	Percentage (%) recovery
Cd	0.26	0.299±0.018	88
Ni	1.29	1.34±0.14	90
Pb	0.33	0.404±0.062	82.5

Determination and calculation of metals concentration

The concentration of Pb, Ni, and Cd in triplicate was resolved by utilizing regression equations derived from a plot of absorbance readings of standards against their respective concentrations. This was performed based on the ICP-OES analysis results obtained, utilizing Equation 2.

Equation 2: Actual concentration (mg/kg) = Digested concentration (mg/L) x Volume digested (L) / Weight of dried sample digested (kg)

The metal concentrations that were acquired were then compared to the Estimated Daily Intake (EDI) for human consumption as established by the Malaysian Food Act (MFA) (1983), USEPA (2000), and FAO/WHO (2014).

Statistical analysis

A one-way analysis of variance (ANOVA) was conducted on the experimental data, and the means were compared using Tukey's test with SPSS software (version 22). This analysis aimed to determine if there were significant differences in the concentrations of metals among various sampling sites ($P < 0.05$).

Health risk assessment

To determine the human health risk associated with metal contaminations of *P. argenteus* inhabited in Malaysian waters, the Target Hazard Quotient (THQ) and allowable daily consumption (CR_{lim}) were calculated.

Target Hazard Quotient (THQ)

The Target Hazard Method (TH) is a measurement tool to assess the potential risk to human health from metal exposure (Taweel et al. 2013). The TH can be measured as Target Hazard Quotient (THQ) = (EF x ED x FIR x C/RFD x WAB x TA) x 10^{-3}, where EF = exposure frequency (from 52 days/year for people who eat *P. argenteus* once a week to 365 days/year for people who eat *P. argenteus* seven times a week); ED = exposure duration (70 years) equivalent to the average of a lifetime; FIR = fish ingestion rate (fish: 160 g/day/person) (Idriss and Ahmad 2015); C = element concentration in the muscle (edible part of fish) (mg/kg); RfD = oral reference dose (USEPA 2000; FAO/WHO 2014); WAB = average body weight (64 kg; the references weight were derived from numerous local Malaysian studies (Ismail al. 2018); and TA = average exposure time for non-carcinogens (365 days/year x ED). If the Hazard Quotient >1.00, there is potential risk related to study metals (Khan et al. 2008).

According to USEPA (2000) and FAO/WHO (2014), RfD for Cd = 0.5 mg/kg body wt./day, Pb = 2 mg/kg body wt./day, and Ni = 0.4 mg/kg body wt./day. Therefore, including the metals (Pb, Ni, and Cd) in assessing health risks associated with the consumption of *P. argenteus* is imperative in providing supplementary information on the potential health implications of consuming this fish.

Calculation of the allowable daily consumption (CR_{lim})

The equation presented herein was employed to compute the permissible daily fish consumption of *P. argenteus*. The daily permissible quantity of fish was quantified in kilograms per day (kg/day). This assumption posited that the diet exclusively consists of fish, with no other Cd, Ni, or Pb sources. Maximum safe daily intake is CR_{lim} = RfD x (BW / C_m) x 10^{-3}, where CR_{lim} = maximum safe daily consumption rate of *P. argenteus* (kg/day) (Moreau et al. 2007); RfD = oral reference dose for each metal concentrations (mg/kg/d) (USEPA 2000; FAO/WHO 2014); BW = average consumers body weight (kg); C_m = measured concentration of DW in fish (edible part) (mg/kg). USEPA determines RfD and estimates a safe amount, expecting no adverse effect on human health (USEPA 2000).

RESULTS AND DISCUSSION

The metal concentrations in fish

This study encompassed 13 sampling sites across five distinct regions with varying activities and pollution elements. Table 3 presents the recorded concentrations of metals within *P. argenteus* across various geographical locations. The concentrations of metals provided are expressed in terms of DW. Furthermore, regarding mean concentration, the sequence of metals in *P. argenteus* muscle was as follows: Pb > Ni > Cd. The concentration of Ni at the sampling site in S was observed to be the highest, with a value of 0.369 mg/kg, followed by SR, with a concentration of 0.322 mg/kg. Conversely, the remaining sites exhibited concentrations below 0.3 mg/kg. The sample obtained from T exhibited the lowest recorded concentration of Ni, measuring at 0.126 mg/kg. The sampling site of PNG exhibits the highest concentration of Cd at 0.181 mg/kg, surpassing K at 0.069 mg/kg and T at 0.048 mg/kg. The concentration of Cd observed at the other sampling sites was less than 0.04 mg/kg.

In addition, it is noteworthy that the Pb concentration (mg/kg) exhibited the highest value in the sample obtained from J, measuring at 0.651 mg/kg. Subsequently, the sample from T displayed a slightly lower concentration of 0.572 mg/kg, followed by the K sample exhibited a lower concentration of 0.532 mg/kg. The concentrations of Pb at the remaining sampling sites were found to be less than 0.4 mg/kg. Samples collected from M exhibited the lowest concentration of Pb, measuring 0.141 mg/kg.

Analysis of Variance (ANOVA) across sampling sites

Significant variations were observed in Pb, Cd, and Ni concentrations across all sampling locations. ANOVA test

reveals statistically significant variations in the concentrations of Cd among all samples obtained. The findings also indicate no statistically significant variations in the levels of Pb among the samples collected from PNG, KD, PK, PS, and S. However, notable distinctions were observed in the samples obtained from the remaining locations. The ANOVA test further reveals no statistically significant variation in the Ni content across the samples obtained from Peninsular Malaysia. Nevertheless, it is noteworthy to mention that significant differences in Ni content were observed exclusively among the samples collected from BI, with a p-value less than 0.005.

Health risk assessment

Target Hazard Quotient (THQ)

The calculation of the health risk from the consumption of *P. argenteus* for all the metals in this study is shown in Table 4. Pb, Ni, and Cd exhibit THQ values for individuals consuming *P. argenteus* weekly in various regions, ranging from 0.06 to 0.25, 0.29 to 0.4, and 0 to 0.06, respectively. Based on the data, the consumption of *P. argenteus* from all sampling sites at a frequency of five times per week is associated with an elevated health risk. However, it is important to note that this risk remains below the established threshold of risk, which is less than 1.0 (Biswas et al. 2023).

Allowable daily consumption (CR_{lim})

CR_{lim} was calculated and compared with RfD for all regions (Table 5). RfD for Cd, Ni, and Pb are 0.5, 0.4, and 2 mg/kg, respectively (FAO/WHO 2014; USEPA 2000). This study found that Cd exhibited the highest values of CR_{lim} of fish (kg/d) across various regions, including the NC, WC, SC, EC, and BI. Specifically, the calculated values for Cd were 0.744, 1.600, 10.667, 0.627, and 0 kg/d, respectively, surpassing those of the other metals investigated. Table 5 displays the association of Ni with the lowest CR_{lim} of *P. argenteus* across various regions, including the NC, WC, SC, EC, and BI. The CR_{lim} for these regions were recorded as 0.131, 0.126, 0.129, 0.106, and 0.086 kg/d, respectively.

Table 3. Metals (mg/kg DW) accumulation based on different sampling sites (mean value ± SD) (n = 20)

Sampling Site	Cd	Ni	Pb	Sig.
PNG	0.181±0.013	0.202±0.004	0.317±0.063	0.000
KD	0.024±0.009	0.206±0.019	0.331±0.037	0.000
PS	0.001±0.002	0.180±0.009	0.277±0.049	0.000
K	0.069±0.029	0.204±0.000	0.532±0.000	0.000
T	0.048±0.005	0.126±0.012	0.572±0.027	0.000
P	0.011±0.003	0.222±0.008	0.231±0.046	0.000
J	0.003±0.020	0.204±0.013	0.651±0.007	0.000
M	0.015±0.01	0.155±0.015	0.141±0.491	0.013
N9	Nd	0.157±0.067	0.221±0.017	0.000
S	Nd	0.369±0.006	0.248±0.025	0.000
PK	0.006±0.000	0.227±0.021	0.239±0.023	0.000
SB	Nd	0.289±0.003	0.243±0.020	0.000
SR	Nd	0.322±0.011	0.245±0.018	0.000

Note: n is the number of samples. Nd: Not detected due to small amount. Values are significantly different at $p < 0.05$. The RfD (Oral reference Dose) for Cd: 0.5, Ni: 0.4, and Pb: 2 mg/kg/day (USEPA 2000; FAO/WHO 2014)

Table 5. Allowable daily consumption (CR_{lim}) (kg/day) for the metals studied from *P. argenteus* muscle (edible part)

Metal	Location	Metal Concentration (mg/kg)	RfD (mg/kg/d)	Allowable Daily Consumption (CR_{lim})(kg/d)
Cd	NC	0.043	0.5	0.744
	WC	0.020		1.600
	SC	0.003		10.667
	EC	0.051		0.627
	BI	0		0
Ni	NC	0.195	0.4	0.131
	WC	0.203		0.126
	SC	0.199		0.129
	EC	0.241		0.106
	BI	0.299		0.086
Pb	NC	0.328	2	0.390
	WC	0.203		0.631
	SC	0.498		0.257
	EC	0.407		0.314
	BI	0.218		0.587

Table 4. Health risk estimates for Pb, Ni, and Cd ingestion from *P. argenteus* from five different regions in Malaysia

Sampling Region	Level of Exposure (DW)	Cd	THQ	Ni	THQ	Pb	THQ
NC	1	0.043±0.069	0.05	0.195±0.018	0.29	0.328±0.574	0.16
WC	1	0.020±0.003	0.02	0.203±0.088	0.3	0.203±0.656	0.06
SC	1	0.003±0.020	0.003	0.199±0.001	0.29	0.498±0.216	0.25
EC	1	0.051±0.051	0.06	0.241±0.136	0.3	0.407±0.155	0.2
BI	1	0	0	0.299±0.017	0.4	0.218±0.030	0.11

Note: The RfD (Oral reference Dose) for Cd: 0.5, Ni: 0.4, and Pb: 2 mg/kg/day (USEPA 2000; FAO/WHO 2014)

Discussion

This research indicates that the average amount of Cd, Ni, and Pb in *P. argenteus* is below the upper limit set by FAO/WHO and health authorities (Table 3). Generally, the average concentration patterns in the muscle of *P. argenteus* are as follows: Pb, Ni, and Cd. This indicates that the species has the potential to function as a bioindicator for monitoring Pb, Ni, and Cd pollution in Malaysian waters. In general, the metal concentrations identified in *P. argenteus* through this investigation were comparatively lower than those documented in studies carried out in China by Han et al. (2021), Pb (0.06 mg/kg) and Cd (0.02 mg/kg); in India by Bepari et al. (2021), Pb (8.45-13.02 mg/kg); and in Iran by Modheji et al. (2023), Ni (0.42 mg/kg) and Cd (0.14 mg/kg).

According to Yousif et al. (2021), various factors contribute to the accumulation of metals in fish tissues, including metal bioavailability, the ability of fish to absorb and remove pollutants, and variation in trophic structure. Malaysia's advanced industrial sector and rapid economic growth and development have increased the coastal water pollution risk. Therefore, when pollutants enter water, they cause significant changes that can affect the ecological balance of the environment either directly or indirectly (Matta et al. 1999). Additionally, due to their high toxicity and cumulative behavior, pollutants have adverse effects on the life and activity of aquatic organisms and can even cause mass death.

Analysis of metal concentrations based on sampling regions shows that the metal levels in the WC, NC, and SC of Peninsular Malaysia representing the SM tend to increase comparatively compared to other geographical areas (EC and BI). Interestingly, BI is moderately polluted with various metals, but the concentration is lower than in Peninsular Malaysia. Specimens collected from PNG show higher concentrations of Cd (0.181±0.013), S shows higher concentrations of Ni (0.369±0.006), and J shows higher concentrations of Pb (0.651±0.007) (Table 3).

Based on the findings of Buhari and Ismail (2016), the Prai industrial area in Penang is home to numerous industries that are supposed to be partly responsible for metal pollution in the marine environment. They revealed a significant contamination of Cd in Prai, Penang. It is important to note that various activities, including households, agriculture, and fishing, may also contribute to the elevated metal concentration levels observed in this area (Ong et al. 2016). These activities have released their waste products into the adjacent sea. The average Cd value obtained in this study (0.001±0.002 - 0.181±0.013 mg/kg) was lower than the findings by Rosli et al. (2018). Their research reported that Cd concentrations in fishes in the T site were 0.39±0.26 mg/kg. Generally, the accumulation of Cd in this research was lower than observed in fishes of Langkawi Island, Malaysia (0.20 to 0.90) (Octavianti and Jaswir 2017); North East Coast of India (0.41 mg/kg) (Kumar et al. 2012) and Miri coast, Sarawak, Borneo (0.41 mg/kg) (Anandkumar et al. 2018).

Additionally, Salam et al. (2021), who studied *P. argenteus* in K and S, discovered that the Cd levels ranged from 0.03 to 0.16 mg/kg. This signifies that the findings of this current study were lower than those of the prior ones. USEPA (2000) and FAO/WHO (2014) have established a regulatory threshold for Cd concentration in fish at 0.5 mg/kg; similarly, MFA (1983) has set a maximum allowable Cd content in fish at 1 mg/kg. The Cd accumulation in this research remains below the upper limit accumulations recommended by MFA (1983) and FAO/WHO (2014).

Besides that, Cd concentration from K (0.069±0.029) and T (0.048±0.005) showed moderately high. The results were substantiated by research conducted by Azmi et al. (2019), which indicated that the Kuantan region, situated on the EC, exhibited a greater concentration of Cd. The study revealed that it is possible to deduce that the EC of Peninsular Malaysia experienced contamination of metals that originated from a singular point source. This contamination occurred despite the area's relatively low levels of human activity. The main anthropogenic sources of Cd include metallurgical industries, municipal effluents, sewage sludge, mine wastes, fossil fuels, and fertilizers (Yao et al. 2015).

The concentrations of metals varied across different sampling sites or regions, potentially attributed to factors such as untreated sewage, industrial effluents, and variations in geological conditions (Pobi et al. 2019). Moreover, the regions on the EC experience significant impacts from industrial effluents due to the swift expansion of various industries, including chemical, oil and gas, and domestic sectors (Ahmad 2014). Environmental discharge of toxic elements is caused by various factors, including crop and commercial waste, mineral deposits, manufacturing and mining operations, atmospheric dissolution, and unregulated solid waste management (Atamaleki et al. 2019). Furthermore, the EC region is characterized by its urban environment and proximity to petrochemical industries, potentially serving as sources of Cd pollution in the coastal vicinity (Sujaul et al. 2013). This statement is further corroborated by Afshan et al. (2014), who observed that the combustion of fossil fuels and municipal waste is widely acknowledged as a significant factor in releasing Cd emissions into the environment.

Another metal that holds significance for living organisms is Ni. The bioavailability of Ni in the human body is considerable, although it can be substantially diminished when consumed alongside certain foods, such as orange juice, tea, coffee, and milk (Schrenk et al. 2020). The mean Ni values obtained in the present study (0.126±0.012 - 0.369±0.006 mg/kg) were found to be comparatively lower than the similar research conducted on *P. argenteus* from Hara Reserve, Iran (1.42 mg/kg) (Mohammadnabizadeh et al. 2014). Similarly, the results obtained from the metals analysis exhibited that the mean Ni concentration in the muscle tissue of various types of marine fish was as high as that recorded on the southwest coast of India (6.06-13.92 mg/kg) (Rejomon et al. 2010); Iran (49.4054.10 mg/kg) (Hosseini et al. 2015); and Miri, Sarawak, Malaysia (0.85-4.10 mg/kg) (Anandkumar et al. 2018). The southern region of Iran exhibits a higher concentration of Ni (49.40-54.10 mg/kg) due to the major

presence of an oil industry. As the petrochemical manufacturing and hydrocarbon industries are significant contributors to the accumulation of metals in the local environment, including Ni, the region's high Ni concentration is not unexpected (Abdolahpur et al. 2013). Based on a report by USEPA (2000), the limit set is 0.4 mg/kg for Ni concentration in fish, which is higher than the Ni concentration obtained in this study.

Pb is a substance that can accumulate in the body over time and has toxic properties. Despite the low bioavailability of Pb in the marine ecosystem, the ongoing bioaccumulation of this element by aquatic organisms, particularly fish, potentially poses a significant risk to human health if consumed (Kamaruzzaman et al. 2011). The accumulation of Pb in this research varied between 0.141 and 0.651 mg/kg in *P. argenteus.* SC showed the greatest accumulation of Pb compared to other locations. The findings were corroborated by Kamaruzzaman et al. (2011), who conducted a study on *P. argenteus* in the SC. Their research indicated that the fish from J exhibited the highest concentration of Pb (0.17±0.087 mg/kg). However, the average concentration of Pb on *P. argenteus* from the J population observed in this study (0.651±0.007 mg/kg) was significantly higher than the values reported by Kamaruzzaman et al. (2011). However, such values were found to be lower compared to findings by Rosli et al. (2018) (0.90±0.10 - 1.00±0.25 mg/kg).

The permissible Pb concentration threshold for fish is 0.5 mg/kg (FAO/WHO 2014). Conversely, USEPA (2000) has stipulated a maximum allowable Pb content of 2 mg/kg. The introduction of Pb into the water ecosystem can be attributed to various factors, including natural activities such as soil erosion, as well as anthropogenic sources like rapid industrialization, the use of fertilizers and pesticides, and agricultural disposal (Agah et al. 2009; Hamada et al. 2018; Shokr et al. 2019). Hence, it is unsurprising that the level of Pb concentration in the SC surpasses that of other regions since it correlates with population density and the prevalence of agricultural practices in the area (Jaji et al. 2018). Using fertilizers and pesticides has resulted in the discharge of waste from rivers into the ocean (Khan et al. 2018).

The most likely explanation for this is that the WC, NC, and SC, particularly the SM, exhibit a significant level of rapid development and are characterized by a significant concentration of human activity (Minhat et al. 2020). However, many additional factors play a role in the pollution of water bodies due to metals. Various natural processes, including soil erosion, geological weathering, atmospheric deposition, and human activities such as household and industrial waste disposal, fertilizer and pesticide use, and agricultural practices, have contributed to the entry of metals into aquatic ecosystems, further affecting the concentration of accumulated metals in the marine environment (Basim and Khoshnood 2016).

However, several factors have affected marine pollution in BI, including domestic waste disposal, tourism and recreational pressure, waste pollution and sedimentation problems due to two oil and gas companies located in Labuan, Sabah (Mokhtar et al. 2012). In addition, several palm oil production, wood processing, and car workshop enterprises have grown in Sarawak's coastal areas (Anandkumar et al. 2018) and ship-building industries in Miri (Nagarajan et al. 2014). The Analysis of Variance (ANOVA) conducted at a 95% confidence level reveals a statistically significant amount of variation across all sampling locations.

Fish consumption poses a potential hazard due to the presence of contaminants, which may result in negative effects on human health. Metals analysis revealed that the concentration of *P. argenteus* posed the least potential health risk to individuals who consumed fish from all sites once a week. This means that *P. argenteus* can be listed among humans' safest fish for ingestion and carries no known hazards. Muscle, the consumable portion of the fish, exhibited lower levels of metals than other fish components such as the gills and liver (Taweel et al. 2013).

Metals can undergo reactions with diffusing ligands, such as iron or molecules, as well as macromolecules. These reactions can result in biomagnification and bioaccumulation within the marine food chain. Consequently, these elements can persist in the environment and induce metabolic anomalies in the consumed organisms.

Anthropogenic sources include mining, refining, and coal-based industries, potentially introducing contaminants into the aquatic environment and reaching the sea through direct deposition (CCREM 2014). Pb contamination of marine species can be attributed to several processes, such as petroleum combustion, wastewater, sludge, metal processing and manufacturing, Pb mineralization, and atmospheric deposition (Singh et al. 2022). Meanwhile, weathering and sediment erosion, non-ferrous metal mining, non-ferrous metal ore smelting, and phosphate fertilizer manufacturing are all possible sources of Cd in the maritime environment (FAO/WHO 2014).

Calculating the THQ is a major method for evaluating long-term risk. According to the results of a risk analysis of *P. argenteus* ingestion, which incorporated an evaluation of multiple metals, the computed THQ value appears to be less than 1 (<1). This indicates that individuals who consume *P. argenteus* from the studied regions do not present a health risk. In contrast, if the THQ value surpasses 1.0, it signifies a potential risk of adverse health effects (Biswas et al. 2023). Recent research by Salam et al. (2021) indicates that *P. argenteus* exhibited a moderate health risk in KD and S and suggests that the consumption of *P. argenteus* acquired from Malaysian waters remains safe for consumers while consumed within the recommended daily intake. Based on these reasons, it is worth noting that *P. argenteus* found in Malaysian waters can still be considered part of an unpolluted ecosystem.

The allowable daily consumption (CR_{lim}) possesses a specific numerical value, and a proposed threshold has been suggested to mitigate potential health hazards for individuals who consume it (Table 5). Human consumption of *P. argenteus* may result in the ingestion of metals, potentially harming individuals' health. Consequently, the daily intake rates for each metal examined were denoted as consumption limits; the consumption limit (kg/d) has been

established for certain metals that hold significance for human health. The risk estimation related to the consumption limit of certain metals involved determining the maximum daily intake of contaminated fish that would not harm human health (USEPA 2000). The determination of the daily consumption limit was conducted by employing the aforementioned published formulae, and the calculation was predicated on the concentration of metals found in the edible portion (muscle) of *P. argenteus*.

Moreover, Table 5 revealed that all the metals were within daily permissible consumption value. Similar studies were also described by Singh et al. 2010; Salam et al. 2019 and Salam et al. 2021. The CR_{lim} of *P. argenteus* (kg/d) across various regions is 0.26-0.59 kg/d for Pb, 0.09-0.13 kg/d for Ni and 0-10.67 kg/d for Cd ranges (Table 5). The mean CRlim and THQ were generally lower than the thresholds associated with adverse health effects. This suggests that consuming *P. argenteus* in Malaysian waters does not pose significant health risks concerning the three metals examined.

Understanding the concentrations of metals in fish, particularly in *P. argenteus*, holds significant importance in regulating fish consumption. The *P. argenteus* had Pb's highest mean metal content, followed by Ni and Cd. Furthermore, it has been observed that the specimens collected from the marine region of the SM exhibit elevated accumulation of Ni and Pb in comparison to the specimens obtained from the marine region of the SCS (South China Sea). Furthermore, this current investigation unequivocally demonstrated the reduced toxicity of various metal concentrations in *P. argenteus* inhabiting Malaysian water bodies. All metal concentrations examined are below the maximum recommended concentrations established by MFA (1983) and FAO/WHO (2014). The *P. argenteus* obtained from Malaysian waters is unlikely to induce acute toxicity in humans upon consumption. Therefore, concerning human health, the THQ value suggests that daily consumption of *P. argenteus* does not pose any risk. Besides that, it is critical to consider all data because the absence of some facts would disrupt some crucial concerns and weaken the contents/analyses. This research offers baseline data for evaluating food safety and developing risk management recommendations about *P. argenteus*. Hence, this research offers an assessment of consumer vulnerability and recommendations for local consumers regarding their susceptibility to chronic or acute exposure to metals.

ACKNOWLEDGEMENTS

The authors would like to express their sincere gratitude to Universiti Sains Malaysia (USM) and the School of Biological Sciences (SBS), Malaysia for providing opportunities and research facilities for this study. This work was funded by the Fundamental Research Grant Scheme (FRGS Fasa 1/2020), Ministry of Higher Education Malaysia.

REFERENCES

Abdolahpur MF, Safahieh A, Savari A, Doraghi A. 2013. Heavy metal concentration in sediment, benthic, benthopelagic, and pelagic fish species from Musa Estuary (Persian Gulf). Environ Monit Assess 185 (1): 215-222. DOI: 10.1007/s10661-012-2545-9.

Afshan S, Ali S, Ameen US, Farid M, Bharwana SA, Hannan F, Ahmad R. 2014. Effect of different heavy metal pollution on fish. Res J Chem Environ Sci 2 (1): 74-79.

Agah H, Leermakers M, Elskens M, Fatemi SMR, Baeyens W. 2009. Accumulation of trace metals in the muscle and liver tissues of five fish species from the Persian Gulf. Environ Monit Assess 157: 499-514. DOI: 10.1007/s10661-008-0551-8.

Ahmad E. 2014. Siakap mati kerugian RM 400,000. http://m.utusan.com.my/berita/nasional/siakap-mati-kerugian-rm400-000-1.28887

Alipour M, Sarafraz M, Chavoshi H, Bay A, Nematollahi A, Sadani M, Fakhri Y, Vasseghian Y, Khaneghah AM. 2021. The concentration and probabilistic risk assessment of potentially toxic elements in fillets of silver pomfret (*Pampus argenteus*): A global systematic review and meta-analysis. J Environ Sci 100: 167-180. DOI: 10.1016/j.jes.2020.07.014.

Amirah M, Afiza A, Faiza, W, Nurliyana M, Laili S. 2013. Human health risk assessment of metal contamination through consumption of fish. J Environ Pollut Hum Health 1 (1): 1-5. DOI: 10.12691/jephh-1-1-1.

Anandkumar A, Nagarajan R, Prabakaran K, Bing CH, Rajaram R. 2018. Human health risk assessment and bioaccumulation of trace metals in fish species collected from the Miri coast, Sarawak, Borneo. Mar Pollut Bull 133: 655-663. DOI: 10.1016/j.marpolbul.2018.06.033.

Atamaleki A, Yazdanbakhsh A, Fakhri Y, Mahdipour F, Khodakarim S, Khaneghah AM. 2019. The concentration of potentially toxic elements (PTEs) in the onion and tomato irrigated by wastewater: A systematic review; meta-analysis and health risk assessment. Food Res Intl 125: 108518. DOI: 10.1016/j.foodres.2019.108518.

Azmi WNFW, Ahmad NI, Mahiyuddin WRW. 2019. Heavy metal levels and risk assessment from consumption of marine fish in Peninsular Malaysia. J Environ Prot 10 (11): 1450. DOI: 10.4236/jep.2019.1011086.

Basim Y, Khoshnood Z. 2016. Target hazard quotient evaluation of cadmium and lead in fish from Caspian Sea. Toxicol Ind Health 32 (2): 215-220. DOI: 10.1177/0748233713498451.

Bepari SP, Pramanick P, Zaman S, Mitra A. 2021. Comparative study of heavy metals in the muscle of two edible finfish species in and around Indian Sundarbans. J Mech Continua Math Sci 16 (10): 9-18. DOI: 10.26782/jmcms.2021.10.00002.

Biswas A, Kanon KF, Rahman MA, Alam MS, Ghosh S, Farid MA. 2023. Assessment of human health hazard associated with heavy metal accumulation in popular freshwater, coastal and marine fishes from southwest region, Bangladesh. Heliyon 9 (10): e20514. DOI: 10.1016/j.heliyon.2023.e20514.

Buhari TRI, Ismail A. 2016. Heavy metals pollution and ecological risk assessment in surface sediments of west coast of Peninsular Malaysia. Intl J Environ Sci Dev 7 (10): 750-756. DOI: 10.18178/ijesd.2016.7.10.874.

Canadian Council of Resource and Environment Ministers (CCREM). 2014. Canadian water quality guidelines. Task Force on Water Quality Guidelines. Canadian Council of Ministers of the Environment, Ottawa, Canada. https://www2.gov.bc.ca/assets/gov/environment/air-land-water/water/waterquality/water-quality-guidelines/approved-wqgs/bc_moe_se_wqg.pdf

Cordeli AN, Oprea L, Crețu M, Dediu L, Coadă MT, Mînzală DN. 2023. Bioaccumulation of metals in some fish species from the Romanian Danube River: A review. Fishes 8 (8): 387. DOI: 10.3390/fishes8080387.

FAO/WHO. 2014. Joint FAO/WHO Food Standards Programme Codex Alimentarius Commission. Rome, Italy.

Feldsine P, Abeyta C, Andrews WH. 2002. AOAC international methods committee guidelines for validation of qualitative and quantitative food microbiological official methods of analysis. J AOAC Intl 85 (5): 1187-1200. DOI: 10.1093/jaoac/85.5.1187.

Hamada MG, Elbayoumi ZH, Khader RA, M Elbagory AR. 2018. Assessment of heavy metal concentration in fish meat of wild and farmed Nile Tilapia (*Oreochromis Niloticus*), Egypt. Alex J Vet Sci 57 (1): 30. DOI: 10.5455/ajvs.295019.

Han JL, Pan XD, Chen Q, Huang BF. 2021. Health risk assessment of heavy metals in marine fish to the population in Zhejiang, China. Sci Rep 11 (1): 1-9. DOI: 10.1038/s41598-021-90665-x.

Hosseini M, Nabavi SMB, Nabavi SN, Pour NA. 2015. Heavy metals (Cd, Co, Cu, Ni, Pb, Fe, and Hg) content in four fish commonly consumed in Iran: Risk assessment for the consumers. Environ Monit Assess 187: 237. DOI: 10.1007/s10661-015-4464-z.

Idriss A, Ahmad A. 2015. Heavy metal concentrations in fishes from Juru River, estimation of the health risk. Bull Environ Contam Toxicol 94: 204-208. DOI: 10.4236/jep.2019.1011086.

Iimtiaz A, Naim DM. 2018. Geometric morphometrics species discrimination within the Genus *Nemipterus* from Malaysia and its surrounding seas. Biodiversitas 19 (6): 2316-2322. DOI: 10.13057/biodiv/d190640.

Ismail SN, Abd HM, Mansor M. 2018. Ecological correlation between aquatic vegetation and freshwater fish populations in Perak River, Malaysia. Biodiversitas 19 (1): 279-284. DOI: 10.13057/biodiv/d190138.

Jaji K, Man N, Nawi NM. 2018. Factors affecting pineapple market supply in Johor, Malaysia. Intl Food Res J 25 (1): 366-375.

Joint Expert Committee on Food Additives (JECFA). 2004. Evaluation of Certain Food Additives and Contaminants: Sixty-first Report of the Joint FAO/WHO Expert Committee on Food Additives. World Health Organization, Geneva.

Kamaruzzaman B, Rina Z, John BA, Jalal K. 2011. Heavy metal accumulation in commercially important fishes of South West Malaysian coast. Res J Environ Sci 5 (6): 595-602. DOI: 10.3923/rjes.2011.595.602.

Khan M, Mobin M, Abbas Z, Alamri S. 2018. Fertilizers and their contaminants in soils, surface and groundwater. Encycl Anthropocene 5: 225-240. DOI: 10.1016/B978-0-12-409548-9.09888-2.

Khan S, Cao Q, Zheng Y, Huang Y, Zhu Y. 2008. Health risks of heavy metals in contaminated soils and food crops irrigated with wastewater in Beijing, China. Environ Pollut 152 (3): 686-692. DOI: 10.1016/j.envpol.2007.06.056.

Kumar A, Kumar A, MMS CP, Chaturvedi AK, Shabnam AA, Subrahmanyam G, Kumar SS. 2020. Lead toxicity: Health hazards, influence on food chain, and sustainable remediation approaches. Intl J Environ Res Public Health 17 (7): 2179. DOI: 10.3390/ijerph17072179.

Kumar B, Sajwan, K, Mukherjee D. 2012. Distribution of heavy metals in valuable coastal fishes from north east coast of India. Turk J Fish Aquat Sci 12 (1): 81-88. DOI: 10.4194/1303-2712-v12_1_10.

Malaysian Food Act (MFA). 1983. Malaysian Food and Drug. MDC Publishers Printer Sdn. Bhd, Kuala Lumpur. http://fsq.moh.gov.my/v6/xs/page.php?id=72

Matta J, Milad M, Manger R, Tosteson T. 1999. Heavy metals, lipid peroxidation, and ciguatera toxicity in the liver of the Caribbean barracuda (*Sphyraena barracuda*). Biol Trace Elem Res 70 (1): 69-79. DOI: 10.1007/BF02783850.

Minhat FI, Shaari H, Razak NSA, Satyanarayana B, Saelan WNW, Yusoff NM, Husain ML. 2020. Evaluating performance of foraminifera stress index as tropical-water monitoring tool in Strait of Malacca. Ecol Indic 111: 106032. DOI: 10.1016/j.ecolind.2019.106032.

Modheji A, Nikppour Ghanavati Y, Larki A, Buazar F. 2023. Measurement of heavy metals (Pb, Cd, Ni, Fe, Zn and Cu) concentration in Snappers, *Pampus argenteus*, Tonguefishes, Tigertooth croaker, *Euryglossa orientalis* and Shrimp *Metapenaeus affinis*. J Mar Sci Technol 22 (3): 27-39. DOI: 10.22113/jmst.2020.152864.2218.

Mohammadnabizadeh S, Pourkhabbaz A, Afshari R. 2014. Analysis and determination of trace metals (nickel, cadmium, chromium, and lead) in tissues of *Pampus argenteus* and *Platycephalus indicus* in the Hara Reserve, Iran. J Toxicol 6: 576496. DOI: 10.1155/2014/576496.

Mohitha C. 2016. Population Genetic Structure of Silver Pomfret (*Pampus argenteus*) along Indian Coast. [Dissertation]. ICAR-Central Marine Fisheries Research Institute. Cochin University of Science and Technology Cochin, Kerala.

Mokhtar MB, Praveena SM, Aris AZ, Yong OC, Lim AP. 2012. Trace metal (Cd, Cu, Fe, Mn, Ni and Zn) accumulation in Scleractinian corals: A record for Sabah, Borneo. Mar Pollut Bull 64 (11): 2556-2563. DOI: 10.1016/j.marpolbul.2012.07.030.

Nagarajan R, Jonathan M, Roy PD, Prasanna MV, Elayaraja A. 2014. Enrichment pattern of leachable trace metals in roadside soils of Miri City, Eastern Malaysia. Environ Earth Sci 72: 1765-1773. DOI: 10.1007/s12665-014-3080-5.

O'Neal SL, Zheng W. 2015. Manganese toxicity upon overexposure: A decade in review. Curr Environ Health Rep 2: 315-328. DOI: 10.1007/s40572-015-0056-x.

Octavianti F, Jaswir I. 2017. Metal toxicity and environmental effects on health: A study report on mineral and heavy metal contents of different Malaysian fish species. Intl Food Res J 24: 544-551.

Ong M, Fok F, Sultan K, Joseph B. 2016. Distribution of heavy metals and rare earth elements in the surface sediments of Penang River estuary, Malaysia. Open J Mar Sci 6: 79-92. DOI: 10.4236/ojms.2016.61008.

Peycheva K, Panayotova V, Stancheva M. 2016. Assessment of human health risk for copper, arsenic, zinc, nickel, and mercury in marine fish species collected from Bulgarian Black Sea Coast. Intl J Fish Aquat Stud 4 (5): 41-46.

Pobi K, Satpati S, Dutta S, Nayek S, Saha R, Gupta S. 2019. Sources evaluation and ecological risk assessment of heavy metals accumulated within a natural stream of Durgapur industrial zone, India, by using multivariate analysis and pollution indices. Appl Water Sci 9 (3): 58. DOI: 10.1007/s13201-019-0946-4.

Radojevic M, Bashkin V, Bashkin VN. 1999. Practical Environmental Analysis. The Royal Society of Chemistry, Cambridge. DOI: 10.1039/9781847551740.

Rajeshkumar S, Liu Y, Zhang X, Ravikumar B, Bai G, Li X. 2018. Studies on seasonal pollution of heavy metals in water, sediment, fish and oyster from the Meiliang Bay of Taihu Lake in China. Chemosphere 191: 626-638. DOI: 10.1016/j.chemosphere.2017.10.078.

Rehman K, Fatima F, Waheed I, Akash MSH. 2018. Prevalence of exposure of heavy metals and their impact on health consequences. J Cell Biochem 119 (1): 157-184. DOI: 10.1002/jcb.26234.

Rejomon G, Nair M, Joseph T. 2010. Trace metal dynamics in fishes from the Southwest Coast of India. Environ Monit Assess 167: 243-255. DOI: 10.1007/s10661-009-1046-y.

Rosli MNR, Samat SB, Yasi MS, Yusof MFM. 2018. Analysis of heavy metal accumulation in fish at Terengganu Coastal Area, Malaysia. Sains Malays 47 (6): 1277-1283. DOI: 10.17576/jsm-2018-4706-24.

Salam MA, Dayal SR, Siddiqua SA, Muhib M, Bhowmik S, Kabir MM, Srzednicki G. 2021. Risk assessment of heavy metals in marine fish and seafood from Kedah and Selangor coastal regions of Malaysia: A high-risk health concern for consumers. Environ Sci Pollut Res 28 (39): 55166-55175. DOI: 10.1007/s11356-021-14701-z.

Salam MA, Paul S, Noor S, Siddiqua S, Aka T, Wahab R, Aweng E. 2019. Contamination profile of heavy metals in marine fish and shellfish. Glob J Environ Sci Manag 5 (2): 225-236. DOI: 10.22034/gjesm.2019.02.08.

Sankhla MS, Kumari M, Nandan M, Kumar R, Agrawal P. 2016. Heavy metals contamination in water and their hazardous effect on human health-a review. Intl J Curr Microbiol Appl Sci 5 (10): 759-766. DOI: 10.20546/ijcmas.2016.510.082.

Schrenk D, Bignami M, Bodin L, Chipman JK, Del Mazo J, Leblanc JC. 2020. Update of the risk assessment of nickel in food and drinking water. EFSA J 18 (11): e06268. DOI: 10.2903/j.efsa.2020.6268.

Schwartz GG, Reis IM. 2000. Is cadmium a cause of human pancreatic cancer? Cancer Epidemiol Biomar Prev 9 (2): 139-145.

Singh A, Sharma A, Verma RK, Chopade RL, Pandit PP, Nagar V, Aseri V, Choudhary SK, Awasthi G, Awasthi KK, Sankhla MS. 2022. Heavy metal contamination of water and their toxic effect on living organisms. In: Dorta DJ, de Oliveira DP (eds). The Toxicity of Environmental Pollutants. IntechOpen, London. DOI: 10.5772/intechopen.105075.

Singh A, Sharma RK, Agrawal M, Marshall FM. 2010. Health risk assessment of heavy metals via dietary intake of foodstuffs from the wastewater irrigated site of a dry tropical area of India. Food Chem Toxicol 48 (2): 611-619. DOI: 10.1016/j.fct.2009.11.041.

Shokr LA, Hassan MA, Elbahy EF. 2019. Heavy metals residues (mercury and lead) contaminating nile and marine fishes. Benha Vet Med J 36 (2): 40-48. DOI: 10.21608/bvmj.2019.12543.1007.

Sujaul IM, Hossain MA, Nasly MA, Sobahan MA. 2013. Effect of industrial pollution on the spatial variation of surface water quality. Am J Environ Sci 9 (2): 120-129. DOI: 10.3844/ajessp.2013.120.129.

Tamele IJ, Vázquez LP. 2020. Lead, mercury and cadmium in fish and shellfish from the Indian Ocean and Red Sea (African Countries): Public health challenges. J Mar Sci Eng 8 (5): 344. DOI: 10.3390/jmse8050344.

Taweel A, Shuhaimi-Othman M, Ahmad AK. 2013. Assessment of heavy metals in tilapia fish (*Oreochromis niloticus*) from the Langat River and Engineering Lake in Bangi, Malaysia, and evaluation of the health risk from tilapia consumption. Ecotoxicol Environ Saf 93: 45-51. DOI: 10.1016/j.ecoenv.2013.03.031.

United States Environmental Protection Agency [USEPA]. 2000. Guidance for Assessing Chemical Contaminant Data for Use in Fish Advisories. Volume 1: Fish Sampling and Analysis, 3rd Edition. United States Environmental Protection Agency (USEPA) 823-B-00-007, Office of Water (4305), Washington DC.

Willie S, Brophy C, Clancy V, Lam J, Sturgeon R, Yang L. 2012. DORM-4: Fish Protein Certified Reference Material for Trace Metals. National Research Council Canada, Ottawa. DOI: 10.4224/crm.2012.dorm-4.

Yao Q, Wang X, Jian H, Chen H, Yu Z. 2015. Characterization of the particle size fraction associated with heavy metals in suspended sediments of the Yellow River. Intl J Environ Res Public Health 12 (6): 6725-6744. DOI: 10.3390/ijerph120606725.

Yousif R, Choudhary MI, Ahmed S, Ahmed Q. 2021. Bioaccumulation of heavy metals in fish and other aquatic organisms from Karachi Coast, Pakistan. Nusantara Biosci 13 (1): 73-84. DOI: 10.13057/nusbiosci/n130111.

Zaza S, de Balogh K, Palmery M, Pastorelli AA, Stacchini P. 2015. Human exposure in Italy to lead, cadmium and mercury through fish and seafood product consumption from eastern central Atlantic fishing area. J Food Compost Anal 40: 148-153. DOI: 10.1016/j.jfca.2015.01.007.

Zhu CQ, Qin Y, Meng QS, Wang XZ, Wang R. 2014. Formation and sedimentary evolution characteristics of Yongshu Atoll in the South China Sea Islands. Ocean Eng 84: 61-66. DOI: 10.1016/j.oceaneng.2014.03.035.

NUSANTARA BIOSCIENCE
Vol. 16, No. 1, pp. 23-28
May 2024

ISSN: 2087-3948
E-ISSN: 2087-3956
DOI: 10.13057/nusbiosci/n160103

Seed viability assessment of *Campolay* fruits (*Lucuma campechiana*) across varying weights and storage periods

AULIA HASAN WIDJAYA[1,2,♥], DIAN LATIFAH[1], ENGGAL PRIMANANDA[1], RIZMOON NURUL ZULKARNAEN[1,3], ARIFAH RAHAYU[2]

[1]Research Center for Plant Conservation, Botanic Gardens and Forestry, National Research and Innovation Agency. Jl. Raya Jakarta-Bogor Km. 46, Cibinong, Bogor 16911, West Java, Indonesia. Tel.: +62-21-87907604, ♥email: auli001@brin.go.id; aulia.widjaya05@gmail.com
[2]Department of Agrotechnology, Faculty of Agriculture, Universitas Djuanda. Jl. Tol Ciawi 1, Bogor 16720, West Java, Indonesia
[3]Faculty of Science, University Brunei Darussalam. Jl. Tungku link, Jalan Tungku Link, Gadong BE1410, Brunei Darussalam

Manuscript received: 30 September 2023. Revision accepted: 13 May 2024.

Abstract. *Widjaya AH, Latifah D, Primananda E, Zulkarnaen RN, Rahayu A. 2024. Seed viability assessment of* Campolay *fruits (*Lucuma campechiana*) across varying weights and storage periods. Nusantara Bioscience 16: 23-28. Campolay* (*Lucuma campechiana* Kunth), a locally cultivated fruit in West Java, Indonesia, has become popular in gardens and yards, although its trading activity remains relatively limited. The methods used for propagating this fruit include seeds, grafting, and layering. However, hard and impermeable seed coats present a challenge in germination. This research aims to investigate the impact of seed weight and storage duration on the viability of *Campolay* seeds. This will be done by employing a factorial, completely randomized design. The study will examine various variables related to germination, including total germination, germination rate, simultaneity, time to achieve 50% germination, time to first germination, and time to final germination. Although these factors do not significantly affect total germination, it was observed that seeds stored for longer periods, up to 6 weeks, exhibited higher germination rates and faster germination times. Interestingly, the seeds' weight did not impact germination, and there was no interaction between the duration of storage and the seed weight. The overall capacity for seed germination ranged from 92% to 97%. These findings indicate that storing *Campolay* seeds in moist sawdust under dark conditions can delay germination, which ensures a more consistent and uniform sprouting process. Moreover, this approach can also aid in the transportation of the seeds and support programs aimed at conserving plant germplasm.

Keywords: *Campolay*, germination, seed viability, seed weight, storage periods

Abbreviations: BBG: Bogor Botanical Gardens; DAS: Day After Sowing; DMRT: Duncan Multiple Range Test; GT: Germination Total; ISTA: International Seed Testing Association; MC: Moisture Content; P: Periode; P50: The number of day required for 50% of the seed to germinate after sowing; RHS: Royal Horticultural Society; RH: Relative Humidity; STAR: Statistical Tool for Agricultural Research; W: Weight

INTRODUCTION

Campolay (*Lucuma campechiana* Kunth) is a tropical fruit that traces its roots back to the Sapotaceae family (POWO 2023). *Campolay* is a plant originating from Mexico. This exotic fruit reached the Philippines in 1915, later making its mark across Southeast Asian countries, including Indonesia. In the archipelago, it goes by many names, such as *Sawo Mentega, Sawo Ubi, Alkesa, Kanistel*, and *Sawo Belanda*. Across the seas in Taiwan, locals fondly refer to it as *Xiantao*, a poetic moniker translating to the "peach of the immortals". The nomenclature "*Campolay*" itself pays homage to the Mexican city of Campeche, and in English-speaking regions, it is recognized as canistel, egg fruit, or yellow sapote (Amalia et al. 2021; Pertiwi et al. 2022).

The allure of *Campolay* lies not only in its diverse nomenclature but also in its nutritional richness. This tropical gem is laden with high carbohydrates and calories, making it a substantial dietary component, as *Vatica venulosa* Blume contains 42.5% carbohydrates (Widjaya et al. 2021a). Further analysis reveals its mineral composition, boasting notable amounts of iron (Fe), vitamin B3 (niacin), and carotene (pro-vitamin A), which imparts the fruit its striking yellow hue. Beyond being savored as a standalone delicacy, *Campolay* finds its way into culinary creativity, contributing to snack noodles when combined with ingredients such as guar gum and mocaf (Lim 2013; Karsinah and Rebin 2013).

The scientific community has delved into unraveling the intricacies of *Campolay*, exploring its nutritional content, taxonomy, and processed products. Studies have unveiled a treasure trove of essential elements within the fruit, including vitamin C, total carotene, total sugar content, and an array of minerals, including calcium (Ca), magnesium (Mg), potassium (K), and sodium (Na) (Pertiwi et al. 2022; Do et al. 2023). These findings highlight Campolay's gastronomic appeal and its potential as a health-enhancing dietary component (Elsayed et al. 2016; Pai and Shenoy 2020).

Campolay's propagation, a vital aspect of its cultivation, predominantly relies on seeds. These seeds, with taproots that fortify adult plants, contribute to the plant's resilience, even though its fruiting age is relatively prolonged, spanning 3-6 years. However, the journey from seed to plant is not without challenges. The seeds are endowed

with hard, impermeable seed coats, endowing them with dormancy properties. Breaking this dormancy is essential for the germination process. Without the requisite treatment, germination may be delayed, occurring 2-3 months after planting (Crane and Carlos 2013). These seeds, classified as recalcitrant, exhibit short viability, with storage at room temperature (20°C) maintaining their viability for up to six months (Hong et al. 1996; Malavert et al. 2017).

Cultivating *Campolay* is not without its hurdles. The germination stage, marked by dormancy properties and variations in seed weight, presents challenges (Crane and Carlos 2013). The hard seed coats, impermeable to water, require specialized treatment for dormancy breaking (Zulkarnaen et al. 2015; Latifah et al. 2020). Moreover, disparities in seed weight can influence the overall viability and vigor of *Campolay* seeds. These challenges underscore the need for a nuanced understanding of the interplay between seed weight and viability, particularly in germination and seedling health (Baskin and Baskin 2014; Bian et al. 2018).

This directs attention to the principal objective of the contemporary research initiative: a systematic inquiry into the correlation between seed weight and the viability of *Campolay* seeds. This entails a comprehensive scrutiny encompassing germination rates and the overall vigor of ensuing seedlings. Concurrently, the study attempts to elucidate the recalcitrant attributes of *Campolay* seeds across diverse storage durations. This factor is important for seed banking initiatives and long-term cultivation planning (Zulkarnaen et al. 2020; Mueller et al. 2021). The study aspires to offer practical solutions for *Campolay* growers, aiding them in optimizing seed weight for enhanced viability and robust seedling health. In addition, the insights gained into the recalcitrant nature of *Campolay* seeds will contribute valuable data to the broader understanding of tropical fruit propagation and horticultural practices (Pertiwi et al. 2020).

Therefore, In the current global context, marked by a growing interest in diverse and exotic fruits, it is essential to invest in research to understand and improve *Campolay* cultivation. Such research not only benefits *Campolay* growers but also contributes significantly to our knowledge of tropical fruit cultivation, promoting sustainable agricultural practices and playing a key role in biodiversity conservation within scholarly discourse.

MATERIALS AND METHODS

Study area

Campolay fruit comes from the Bogor Botanical Gardens (BBG) in Indonesia, with the catalog number Vak IV.D. 182-182a (Figure 1) (Ariati et al. 2019). It was originally from Cuba and was planted in the gardens on March 12, 1990. The fruit was harvested on December 11, 2014, when its skin turned yellowish, which typically happens 60 to 90 days after the flowers bloom. We used tools like digital calipers and scales to study the fruit and its seeds. We also matched the colors we observed with a color chart from the Royal Horticultural Society (RHS 2007).

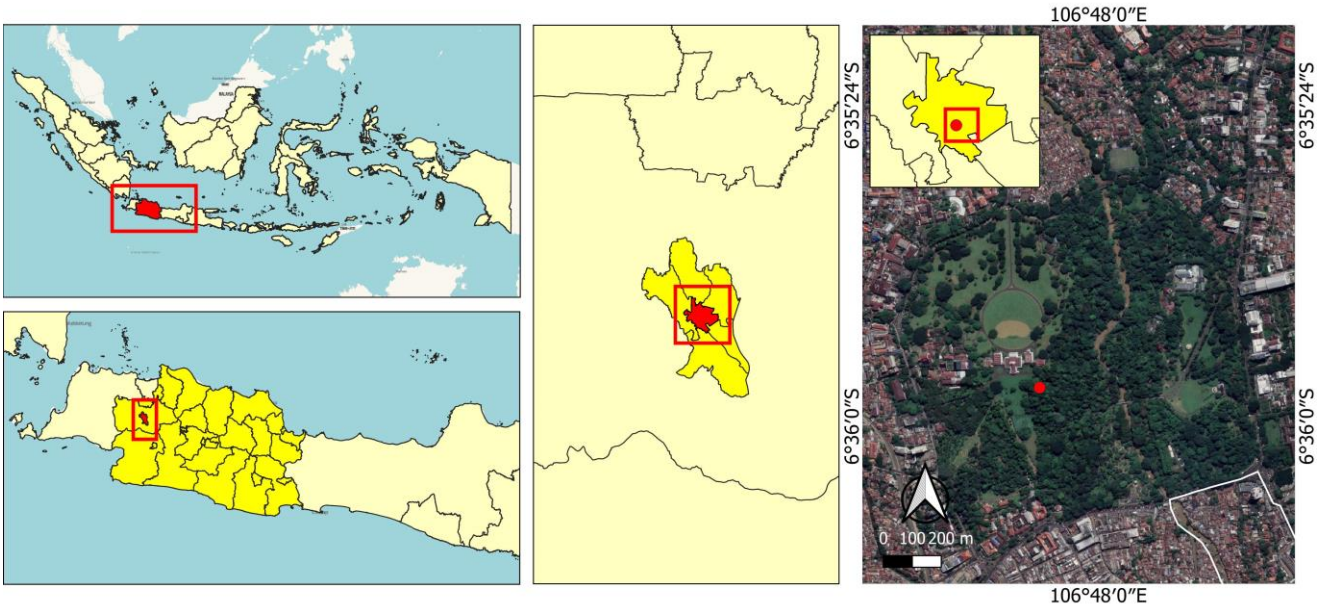

Figure 1. Map of research location in the Bogor Botanic Garden, West Java, Indonesia

Procedures

Seed weight class and seed Moisture Content (MC)

Classification of seeds based on the seed weight with analytical balance, directly separated between heavy seeds (>11.01 g), medium (9.01-11.00 g), and lightweight seeds (<9.00 g).

Seed moisture content was evaluated using a 105°C constant temperature oven for 17 hours (ISTA 2015), with the formula:

$$MC = \frac{(M2-M3)}{(M2-M1)} \times 100\%$$

M1 is the weight of the container used, M2 is the weight of the seed and the container before the oven, and M3 is the weight of the seed and the container after the oven. The initial moisture content of *Campolay* seeds was 46.66% (3 replicates, F8.11 = 0.12, p <0.05, coefficient of variations 3.43%).

During the 0-6 weeks storage period, the moisture content of seeds was maintained in the range of 45.98%-47.08%. The range of seed moisture content showed that *Campolay* seeds had recalcitrant characteristics.

Seed germination

Germination research was conducted at the Glasshouse and Seed Bank-BBG from December 2014 to June 2015. The materials used were sand, insecticides, fungicide, a polybag 25 cm x 35 cm, a storage box, sawdust, black plastic and 100°C hot water to sterilize media. The research design used was a factorial, completely randomized design, namely seed weight (W) and seed storage period time (P). The weight of the seeds to be tested in this study consisted of heavy (>11.01 g), medium (9.01-11.00 g), and lightweight (<9.00 g). seeds were tested at 0, 2, 4 and 6 weeks of storage. Thus, there were 12 treatment combinations with three replications of 36 experimental units (polybags). Each experimental unit consisted of 10 *Campolay* seeds, with 360 observation units. The linear design model used is:

$$Y_{ijk} = \mu \pm \alpha_i \pm \beta_j \pm (\alpha\beta)_{ij} \pm \varepsilon_{ijk}$$

Where: Yijk represents the response variable, μ stands for the overall mean, αi represents the effect of the first factor (i), βj represents the effect of the second factor (αβ)ij signifies the interaction between the first and second factors, and εijk denotes the random error. This formula is utilized in statistical analysis to describe the relationships between various factors in an experiment or study.

The germination medium used was sand in a glasshouse (microclimate conditions: average temperature 26.25±1.29°C, average humidity (RH) 78.39±4.67% and sunlight intensity 686.86±420.94 lux). The media was sterilized using hot water at 100°C, then sprinkled with about 2.5g/polybag of insecticide. *Campolay* seeds/polybags were planted after the media had cooled. Observations were made every two days, and the observed variables were

Germination total, calculated by the formula:

$$GT = \frac{n}{N} \times 100\%$$

Where: GT: Germination Total, n: seed germinated, N: seed sowing.

Germination rate, calculated by the formula:

$$x = \frac{\Sigma n}{\Sigma(txn)} \; x\, 100$$

Where: x: Germination rate, n: Seed germinated, t: The day when the seeds germinate

Simultaneity, calculated by the formula:

$$\frac{\Sigma n}{\Sigma\{(T-t)2\,x\,n)\}} \times 100 \; ; \; T = \frac{\Sigma(txn)}{\Sigma n}$$

Where: Σn: The total number of seeds to germinate, t x n: n seeds were germinated on day t

P50 is the number of days required for 50% of the seed to germinate Day After Sowing (DAS),

The initial germination assessment is calculated from the emergence of the first sprout following the sowing of the seeds (indicating the day on which the first seed begins to germinate).

The final germination assessment is calculated from the emergence of the last sprout after seed sowing (indicating the day on which the last seed germinates).

Seed storage

Seeds were stored in plastic boxes (box containers) containing moist sawdust covered with newsprint. The storage box was tightly closed using a container box lid and closed again using black plastic to stimulate dark storage conditions so that the recalcitrant seeds could survive without germination (Latifah et al. 2014). The boxes were Stored in a room with an AC temperature of 20±2°C and Relative Humidity (RH) of 50-60%.

Data analysis

STAR (Statistical Tool for Agricultural Research) software was used for data analysis. We Analyzed of Variance (ANOVA) with the F-test at a 5% significance level to determine if the treatments had significant effects. When significant effects were observed, we applied the Duncan Multiple Range Test (DMRT) at the same 5% level to identify which treatments differed significantly (Widjaya et al. 2021b).

RESULTS AND DISCUSSION

The germination performance of *Campolay* seeds was examined, considering various factors, including seed weight and storage duration. It was determined that there were no statistically significant variations in seed germination among different seed weights and storage periods. However, it is crucial to note that although germination rates remained consistent, there were notable differences in the coefficient of germination rate and concurrent seedling growth across various storage durations (Table 1).

The germination rates of *Campolay* seeds exhibited disparities depending on the duration of storage. Seeds stored for 4 and 6 weeks demonstrated considerably faster

germination than those stored for 0 and 2 weeks. This observation is particularly interesting as it suggests that the duration of storage has a noticeable impact on the germination of *Campolay* seeds. It is important to highlight that this variation was more pronounced in seeds with longer storage durations.

This difference in germination rates is attributed to the inherent properties of *Campolay* seeds, particularly the presence of a hard seed coat that renders them impermeable to water. The statistical analysis ($F24.35 = 55.04$, $p < 0.05$, coefficient of variation 12.43%) emphasizes the significance of this finding. Germination rate, a crucial parameter in evaluating seed vigor (Sadjad et al. 1999), reflects the seed's ability to germinate rapidly under different conditions. Seeds with higher vigor demonstrate a faster germination rate, and this characteristic is essential for the consistent and uniform emergence of seedlings, especially under diverse field conditions (Schmidt 2000).

The germination coefficient of *Campolay* seeds exhibited notable distinctions compared to a storage period of 6 weeks ($F24.35 = 6.16$, $p < 0.05$, coefficient of variance 100.01%; data not transformed). However, no significant differences were observed at storage durations of 0, 2, and 4 weeks, nor were there significant variations concerning different seed weights, as outlined in Table 1. After 6 weeks of storage, the seed coat may soften, allowing the seeds to absorb water and promoting germination.

The observed variations in germination coefficient at different storage durations, particularly the significant change at the 6-week mark, provide insights into the dynamic nature of *Campolay* seed dormancy and germination, contributing valuable knowledge to seed physiology and agricultural science. These findings emphasize the complex interaction between the seed coat's properties, the storage duration, and the potential for germination of *Campolay* seeds (Baskin and Baskin 2014).

Other studies have also investigated the effect of storage duration on seed germination. Nguyen et al. (2015) studied the variability in light, gibberellin, and nitrate requirement of *Arabidopsis thaliana* (L.) Heynh. seeds due to harvest time and dry storage conditions. Yilmaz and Tonguc (2013) investigated the effects of temperature on the germination of *Fraxinus ornus* subsp. *cilicica* (Lingelsh.) Yalt. seeds. Guo et al. (2020) studied the effect of temperature, light, and storage time on the seed germination of *Pinus bungeana* Zucc. ex Endl. Another study by Koutsika-Sotiriou et al. (2022) investigated the seed germination of *Silybum marianum* (L.) Gaertn. populations of Greek origin and the effects of temperature, duration, and storage conditions. For *Campolay* seeds, the observed faster germination rate after longer storage periods may reflect increased seed vigor. This could be essential for uniform and consistent seedling emergence, especially in variable field conditions. The findings emphasize the complex interaction between the properties of the seed coat, the duration of storage, and the potential for germination of seeds.

Seed size is an essential factor in seed biology, with its implications reaching the concept of seed vigor. Vigour is a critical measure of a seed's potential to thrive in unfavorable conditions, making it an essential attribute in agricultural and ecological contexts. Seeds with high vigor not only have the potential to develop into normal and healthy plants under less-than-optimal environmental conditions but also exhibit enhanced performance in ideal settings, leading to robust and productive plants. Moreover, seeds possessing vigor can endure extended periods of storage under less-than-ideal conditions while maintaining their ability to germinate and flourish when provided with favorable conditions. This is evidenced by the practices at the Royal Botanic Gardens, Kew, and the Millennium Seed Bank, where seeds are carefully dried and frozen to extend their viability, exemplifying the crucial role of seed vigor and proper storage in seed longevity (Pagano et al. 2023). Seed longevity is acquired during late maturation, accompanied by the degreening and de-differentiation of chloroplasts into non-photosynthetic plastids called eoplasts.

In contrast, seed weight is often considered a significant measurement associated with germination and viability. It provides valuable insights into a seed's capacity to initiate germination, with heavier seeds often showing more favorable germination traits. Besides, the weight of the seed functions as an indicator of the seed's long-term viability, demonstrating its potential to stay alive and maintain its germination capacity over prolonged periods (Schmidt 2000). The correlation between seed weight and these attributes is crucial in guiding seed selection, storage, and successful crop establishment, thus significantly impacting agricultural practices and ecological dynamics.

The study has revealed a strong correlation between the seed shelf life and the intricate dynamics of seed germination. Our research demonstrates a substantial increase in both the speed of germination ($F24.35 = 23.34$, $p < 0.05$, coefficient of variance 23.32%; data not transformed) and the earlier culmination of the germination process ($F24.35 = 27.38$, $p < 0.05$, coefficient of variance 14.02%; data not transformed) in seeds subjected to prolonged storage durations. This intriguing finding suggests that the longer seeds are stored, the quicker they germinate. An interesting observation is that this acceleration of germination appears to be independent of variations in seed weight (Table 2).

Moreover, the study highlights a substantial increase in the germination speed and the earlier culmination of the germination process in seeds subjected to prolonged storage durations. This effect, which significantly influences the timing of germination, remains consistent regardless of seed weight (Table 2). These findings carry significant implications for the practical implementation of seed management and conservation practices. It is suggested that the strategic use of *Campolay* seed storage can be beneficial when transporting seeds over long distances, from parent trees to production planting areas, which often takes several weeks.

The storage of *Campolay* seeds in a moist sawdust medium significantly influences the preservation of seed viability. This method plays a crucial role in maintaining the viability of the seeds (Table 2). The impact of this storage technique on shortening both the first and last day

of germination indicates its effectiveness in sustaining seed viability. This discovery validates the observed phenomenon of untreated *Campolay* seeds, which typically require a significantly longer period of 2-3 months to initiate germination (Crane and Carlos 2013).

Interestingly, the weight of *Campolay* seeds does not seem to have a substantial influence on their germination capacity. The duration these seeds are stored before being sown has a significant impact. *Campolay* seeds, when stored for extended periods of up to 6 weeks, tend to germinate more efficiently and with greater synchrony. Consequently, many seeds sprout simultaneously, typically denoting favorable plant development conditions.

Additionally, the seed achieves crucial germination milestones such as the P50 (the time required for 50% of seeds to germinate), the initial and final day of germination more quickly. *Campolay* seeds demonstrate a remarkably high success rate in germination, ranging from 92% to 97%. This indicates that one can securely store these seeds for up to 6 weeks without concern about their germination capacity diminishing. In certain cases, their germination performance may even improve under extended storage conditions.

Table 1. Germination total, germination rate, and simultaneity

	Germination total (%)	Germination rate (%/day)	Simultaneity (%/day)
Storage			
0 week	92.22	1.34 [d]	0.0168 [b]
2 week	97.78	1.61 [c]	0.0241 [b]
4 week	93.33	2.05 [b]	0.0379 [b]
6 week	92.22	2.70 [a]	0.0968 [a]
Seed weight			
Weight	95.84	1.92	0.0367
Medium	92.50	1.88	0.0350
Lightweight	93.33	1.98	0.0599

Note: The same letters in the same column showed no significant differences according to DMRT at the level of 5%

Table 2. The time when 50% germination occurred, the time to first germination and the time to final germination

	Time when 50% germination occurred (day)	Time to first germination (day)	Time to final germination (day)
Storage			
0 week	74.67[a]	47.89[a]	108.67[a]
2 week	61.00[b]	33.11[b]	93.44[b]
4 week	46.00[c]	26.78[bc]	79.00[c]
6 week	37.00[d]	19.79[c]	59.78[d]
Seed weight			
Weight	54.25	33.83	81.67
Medium	58.25	32.75	85.75
Lightweight	51.50	29.08	88.25

Note: The same letters in the same column showed no significant differences according to DMRT at the level of 5%

Moreover, the study discovered that the effects of storage time on germination remain consistent across seeds of varying weights. Therefore, regardless of whether the seeds are heavy or light, the impact of storage time on germination remains largely unchanged. These findings enhance our understanding of Campolay seed biology and provide valuable practical insights for conservation efforts and agricultural practices (Sukarya and Witono 2017; Latifah et al. 2020).

In conclusion, the study provides interesting insights into the viability and germination behavior of *Campolay* seeds. The influence of seed weight on germination capacity is not statistically significant, whereas the duration of seed storage emerges as a critical determinant. Prolonged storage periods of up to 6 weeks result in highly efficient and synchronized germination, characterized by significantly higher germination rates and accelerated attainment of key milestones. Indeed, the overall success of germination remains consistently high, ranging from 92% to 97%, even after extended storage, highlighting the resilience of *Campolay* seeds. Importantly, these advantages of prolonged storage are observed regardless of the weight of the seeds. Moreover, using a moist sawdust medium for storing *Campolay* seeds appears to be an efficacious approach for expediting germination and maintaining seed viability. These findings have practical implications for seed management, germplasm conservation, and agricultural practices, thereby contributing to our comprehension of the biology of *Campolay* seeds.

ACKNOWLEDGEMENTS

We thank the Head of the Center for Plant Conservation Botanical Gardens, Indonesia for kind and gracious permission, allowing the author to embark on this research journey. Additionally, we wish to express our deep appreciation to the esteemed members of the Family of Subfields Register Nurseries, specifically the dedicated Seed Bank staff, for their invaluable support and unwavering permission that has been instrumental in facilitating the successful execution of this research.

REFERENCES

Amalia L, Setiarto RHB, Fitrilia T, Masyrifah S. 2021. Effect of blanching on the physicochemical characteristics and microstructure of canistel seed flour (*Pouteria campechiana* (Kunth) Baehni). Afr J Food Agric Nutr Dev 20 (7): 17063-17080. DOI: 10.18697/ajfand.95.19520.

Ariati SR, Astuti RS, Supriyatna I, Yuswandi AY, Setiawan A, Saftaningsih D, Pribadi DO. 2019. An Alphabetical List of Plant Species Cultivated in The Bogor Botanic Gardens. Center for Plant Conservation and Botanic Gardens-LIPI, Bogor. DOI: 10.24823/Sibbaldia.2019.265.

Baskin CC, Baskin JM. 2014. Seeds: Ecology, Biogeography, and Evolution of Dormancy and Germination. Second Edition. Academic Press, San Diego. DOI: 10.1016/C2013-0-00597-X.

Bian F, Su J, Liu W, Li S. 2018. Dormancy release and germination of *Taxus yunnanensis* seeds during wet sand storage. Sci Rep 8 (1): 3205. DOI: 10.1038/s41598-018-21469-9.

Crane JH, Carlos FB. 2013. Canistel Gowing in The Florida Landscape. Horticultural Sciences Department, Florida Cooperative Extension Service, Institute of Food and Agicultural Sciences, University of Florida, Florida, USA. https://growables.com/information/TropicalFruit/documents/CanistelGrowingInTheFloridaHomeLandscape.pdf

Do TVT, Suhartini W, Phan CU, Zhang Z, Goksen G, Lorenzo JM. 2023. Nutritional value, phytochemistry, health benefits, and potential food applications of *Pouteria campechiana* (Kunth) Baehni: A comprehensive review. J Funct Foods 103: 105481. DOI: 10.1016/j.jff.2023.105481.

Elsayed AM, El-Tanbouly ND, Moustafa SF, Abdou RM, El Awdan SA. 2016. Chemical composition and biological activities of *Pouteria campechiana* (Kunth) Baehni. J Med Plants Res 10 (16): 209-215. DOI: 10.5897/JMPR2015.6031.

Guo C, Shen Y, Shi F. 2020. Effect of temperature, light, and storage time on the seed germination of *Pinus bungeana* Zucc. ex Endl.: The role of seed-covering layers and abscisic acid changes. Forests 11 (3): 300. DOI: 10.3390/f11030300.

Hong TD, Linington S, Ellis RH. 1996. Seed Storage Behaviour: A Compendium. Handbook for Genebank No. 4. International Plant Genetic Institute, Roma.

International Seed Testing Association (ISTA). 2015. International Rules for Seed Testing Vol. 215. The International Seed Testing Association, Bassersdorf.

Karsinah, Rebin. 2013. Tropical fruit with potential as an alternative source. Iptek Hortikultura 9: 1-15.

Koutsika-Sotiriou M, Koutsikos N, Tzortzakis N. 2022. Seed germination of three milk thistle (*Silybum marianum* (L.) Gaertn.) populations of greek origin: Temperature, duration, and storage conditions effects. Plants 12 (5): 1025. DOI: 10.3390/plants12051025.

Latifah D**,** Congdon RA, Holtum JA. 2014. A physiological approach to conservation of four palm species: *Arenga australasica*, *Calamus australis*, *Hydriastele wendlandiana* and *Licuala ramsayi*. Reinwardtia 14 (1): 237-247. DOI: 10.55981/reinwardtia.2014.421.

Latifah D, Wardani FF, Zulkarnaen RN. 2020. Seed germination, seedling survival and storage behavior of *Koompassia excelsa* (Leguminosae). Nusantara Biosci 12 (1): 46-49. DOI: 10.13057/nusbiosci/n120108.

Lim TK. 2013. *Pouteria campechiana*. In: Lim TK (eds). Edible Medicinal and Non-Medicinal Plants. Springer, Dordrecht. DOI: 10.1007/978-94-007-5628-1_23.

Malavert C, Batlla D, Benech-Arnold RL. 2017. Temperature-dependent regulation of induction into secondary dormancy of *Polygonum aviculare* L. seeds: A quantitative analysis. Ecol Model 352: 128-138. DOI: 10.1016/j.ecolmodel.2017.03.008.

Mueller P, Mendivil E, Jonas J, Kline A, Gornish ES. 2021. Seedball design to optimize germination. Cooperative Extension, University of Arizona, Arizona. https://extension.arizona.edu/sites/extension.arizona.edu/files/pubs/az1937-2021.pdf

Nguyen TP, Cueff G, Hegedus DD, Rajjou L, Bentsink L. 2015. A role for seed storage proteins in *Arabidopsis* seed longevity. J Exp Bot 66 (20): 6399-6413. DOI: 10.1093/jxb/erv348.

Pagano A, Kunz L, Dittmann A, Araújo SDS, Macovei A, Shridhar Gaonkar S, Sincinelli F, Wazeer H, Balestrazzi A. 2023. Changes in *Medicago truncatula* seed proteome along the rehydration-dehydration cycle highlight new players in the genotoxic stress response. Front Plant Sci 14: 1188546. DOI: 10.3389/fpls.2023.1188546.

Pai A, Shenoy C. 2020. Physicochemical, phytochemical, and GC–MS analysis of leaf and fruit of *Pouteria campechiana* (Kunth) Baehni. J Appl Biol Biotechnol 8 (4): 90-97. DOI: 10.7324/JABB.2020.80414.

Pertiwi SR, Nurhalimah S, Aminullah A. 2020. Optimization on process of ripe canistel (*Pouteria campechiana*) fruit flour based on several quality characteristics. Braz J Food Technol 23: e2019056. DOI: 10.1590/1981-6723.05619.

Pertiwi SRR, Novidahlia N, Aminullah A, Rohmayanti T, Siwi K. 2022. Sensory properties of snack noodles made from canistel flour and mocaf with addition of guar gum. IOP Conf Ser: Earth Environ Sci 1097 (1): 012005. DOI: 10.1088/1755-1315/1097/1/012005.

POWO. 2023. *Lucuma campechiana* Kunth. https://powo.science.kew.org/taxon/urn:lsid:ipni.org:names:787237-1

Royal Horticultural Society (RHS). 2007. The Royal Horticultural Society's Colour Chart, 59-200. Fifth Edition. The Royal Horticultural Society, London.

Sadjad S, Muniarti E, Ilyas S. 1999. Parameter Pengujian Vigor Benih: Dari Komparatif ke Simulatif. PT. Grasindo, Jakarta. [Indonesian]

Schmidt L. 2000. Guidelines for Handling Tropical and Subtropical Forest Plant Seeds. Danida Forest Seed Centre, Humlebaek.

Sukarya DG, Witono JR. 2017. Bogor Botanic Gardens: Two Centuries of Sowing the Earth's Plant Diversity in Indonesia. Sukarya Press, Jakarta.

Widjaya AH, Latifah D, Hardwick KA, Suhartanto MR, Palupi ER. 2021. Reproductive biology of *Vatica venulosa* Blume (Dipterocarpaceae). Biodiversitas 22 (10): 4327-4337. DOI: 10.13057/biodiv/d221025.

Widjaya AH, Suhartanto MR, Palupi ER, Latifah D. 2021. Physical and physiological characteristics of *Vatica venulosa* Blume (Dipterocarpaceae) seed and its conservation methods. J For Res Nat Conserv 18 (2): 167-181. DOI: 10.20886/jphka.2021.18.2.167-181.

Yilmaz M, Tonguç F. 2013. Effects of temperature on the germination of *Fraxinus ornus* subsp. *cilicica* seeds. Dendrobiology 69: 111-115. DOI: 10.12657/denbio.069.012.

Zulkarnaen RN, Nisyawati N, Witono JR. 2020. The growth and distribution pattern of endemic Java palm (*Pinanga javana* Blume) in Mt. Slamet, Central Java, Indonesia. AIP Conf Proc 2231 (1): 040056. DOI: 10.1063/5.0002814.

Zulkarnaen RN, Wardani FF, Rivai RR. 2015. Seedling characteristics of *Anchomanes difformis*. Pros Sem Nasl Masy Biodiv Indon 1: 824-827. DOI: 10.13057/psnmbi/m010427.

NUSANTARA BIOSCIENCE
Vol. 16, No. 1, pp. 29-36
May 2024

ISSN: 2087-3948
E-ISSN: 2087-3956
DOI: 10.13057/nusbiosci/n160104

Comparative study of root characteristics revealed distinctive responses between Moroberekan and MR297 rice varieties subjected to drought stress

MOHD FAUZIHAN KARIM[1,2,♥], NUR HAMIZATUN NABILAH TAJUDIN[2], SITI AISAH SALMIN[2], NUR FARAH SUHADA MOHD ROSELY[2], NUR NAZIFAH SAIMI[2], CHE NURUL AINI CHE AMRI[1,2]

[1]Sustainable Agriculture and Green Technology Research Group (AG-TECH), Kulliyyah of Science, International Islamic University Malaysia. Jl. Sultan Ahmad Shah, 25200 Pahang, Malaysia. Tel/Fax.: +60-09-5705150, ♥email: mfauzihan@iium.edu.my

[2]Department of Plant Science, Kulliyyah of Science, International Islamic University Malaysia. Jl. Sultan Ahmad Shah, 25200 Pahang, Malaysia

Manuscript received: 2 October 2023. Revision accepted: 2 January 2024.

Abstract. *Karim MF, Tajudin NHN, Salmin SA, Rosely NFSM, Saimi NN, Amri CNAC. 2024. Comparative study of root characteristics revealed distinctive responses between Moroberekan and MR297 rice varieties subjected to drought stress. Nusantara Bioscience 16: 29-36.* In light of the growing concern over climate change, it is crucial to comprehend how the rice plant, *Oryza sativa* L., responds to various environmental stress, particularly prolonged drought. This study investigated the morphological and anatomical characteristics of the roots of rice plants following a continuous drought on two selected varieties: MR297, known to produce a high yield but is highly sensitive to low water potential, and Moroberekan, known to be drought tolerant. The drought treatment was initiated on day 24 after sowing and continued for seven days or until any plant exhibited curled leaves. There was no significant difference in root length between the two varieties, but MR297 had substantially lower fresh and root dry weights (32.5% and 40%, respectively) than Moroberekan under drought stress. Drought also significantly affected root electrolyte leakage and MDA content, especially in MR297 compared to Moroberekan. Meanwhile, root anatomy studies have revealed differences between the control and drought treatments. While the root diameter of the control plants was greater, their aerenchyma cells were less developed than those of the drought-induced plants, which had a higher ratio of aerenchyma cells per sectioned area. The number of metaxylem was reduced by drought, but the effect was more pronounced in MR297 than in Moroberekan. This study provides evidence of the impact of drought on both Moroberekan and MR297, as observed through their root morpho-physiology and anatomical structure.

Keywords: Aerenchyma cells, MDA, metaxylem cells, *Oryza sativa*, root anatomy

INTRODUCTION

Rice, scientifically known as *Oryza sativa* L., is an essential staple crop that serves as a primary food source for more than half of the world's population. The majority of the production, accounting for almost 90%, is concentrated in the Asian region (Ali et al. 2017; Landi et al. 2017). Rice is known to be the most susceptible to drought among cereal crops (Panda et al. 2021). Water availability has been one of the most devastating abiotic stresses that have shaped the evolution of plants in general and rice in particular. According to Sandhu et al. (2012), 15% of Asia's 75 million acres of irrigated rice crop could face water shortages by 2025.

Drought has been one of the most significant stresses on rice growth over the past two decades, reducing global rice production by 25.4% (Zhang et al. 2018). According to Nahar et al. (2018), drought reduces crop yield and inhibits plant growth and development, resulting in more severe conditions and plant death. Numerous studies have examined plants' morphological, physiological, and biochemical responses in a drought environment to identify rice varieties with enhanced drought tolerance (Singh et al. 2017, 2018; Swapna and Shylaraj 2017). Several adverse effects can be caused by prolonged exposure to drought stress, including a shorter plant height, plant wilting, leaf rolling, leaf senescence, stomatal closure, reduced leaf elongation, and decreased dry matter production (Singh et al. 2017; Swapna and Shylaraj 2017; Karim et al. 2021). However, it is still challenging to determine whether they are drought-resistant or vulnerable based merely on their agronomic properties, even though the effects of drought can vary depending on the rice variety (Singh et al. 2017; Swapna and Shylaraj 2017).

The architecture of the root system, which is appropriately referred to as the "hidden half", has a significant impact on crop production, as the roots are principally responsible for adaptation and responses to varied stress circumstances through complex gene interactions. Knowledge about plant roots' growth and structure presents opportunities for leveraging and controlling root traits to enhance crop productivity and maximize agricultural land use efficiency (Den Herder et al. 2010). The root system architecture is depicted by a range of root traits such as root type, elongation rate, root thickness, growth duration, root density, root surface area, root volume, root gravitropism, and longevity (Schneider and Lynch 2020; Shamsuddin et al. 2021; Tajima 2021). These root behaviors provide insights into optimizing water acquisition and plant adaptation to various environmental

conditions (Kadam et al. 2015). Plants utilize their root plasticity to survive while producing stable yields even under adverse external factors (Suseela et al. 2020). Phenotypic selection based on root plasticity could be a potential target for extracting genetic variation for breeding stress-tolerant programs (Schneider and Lynch 2020).

Nevertheless, the interaction between root plasticity and a dynamic environment is intricate and varies depending on the genotype and the type and severity of environmental stress. Concerning water scarcity, recent evidence of Southeast Asian rice has shown that the highest grain yield was attained by higher root numbers and smaller stele diameters (Siangliw et al. 2022). Similarly, the drought-stressed root of maize alters the morphological traits by multiplying the fine roots to optimize water absorption (Yan et al. 2022). This phenotypic plasticity differs in response to adverse external factors. Fluctuation of Na^+ accumulation in soil resulted in the anatomical plasticity of apoplastic barriers (Shelden and Munns 2023). The rapid formation of suberin lamellae and Casparian bands as apoplastic barriers in barley and rice plants alleviate salt accumulation, thus promoting salt tolerance (Mehmet 2016; Chen et al. 2018; Ho et al. 2020).

Meanwhile, root architecture patterns during heat stress displayed compact, consistent, and longer roots to enhance the deeper root in the soil horizon (Yadav et al. 2022). Such deeper roots enable soil moisture uptake, resulting in transpirational cooling and mitigating the impact of heat stress. Thus, the dynamic of root plasticity provides advantageous insights for developing stress-tolerant cultivars. Therefore, from an anatomical perspective, it is crucial to support a comprehensive investigation into how the root systems contribute to mechanisms that make rice plants more resistant to drought stress.

This study has employed a morphological and anatomical method to investigate the adaptive strategies of rice roots under drought-stress conditions. The main objective of this study is to assess the phenotypic and morphological changes in the roots of rice plants as they are exposed to prolonged periods of drought.

MATERIALS AND METHODS

Experimental design

The experiment was conducted at the Glasshouse & Nursery Complex (GNC) of the International Islamic University of Malaysia in Kuantan, Pahang, Malaysia. Two different rice genotypes, Moroberekan (an upland rice variety) and MR297 (domestically cultivated and drought-susceptible) were subjected to two irrigation conditions: well-watered and drought stress. Seeds were pretreated by soaking in distilled water overnight before germinating on wet tissues. After a week, seedlings were transferred into 6 cm × 9 cm polybags with 100% topsoil. The standing water of about 3±1 cm was maintained above the soil surface in each tray during the planting period. The fertilizers were applied once every two weeks.

Drought stress treatment

Drought stress treatment was exposed by removing the standing water from the soil surface when rice seedlings reached the end of the pre-tillering stage. The pre-tillering stage can be defined as the period from the development of the first leave to the fourth leave stage (Hardke 2013). Rice plants typically enter the tillering stage between 15 and 25 days after seedling emergence. In this study, drought stress treatments were applied after 21 Days After Sowing (DAS). The standing water was maintained approximately 3±1 cm above the soil surface for control treatment throughout the study period.

Root morphology and physiology

The root was harvested on day 29 DAS after a few plants showed signs of rolled leaves. Root systems were cleaned thoroughly to remove excessive soil and dirt to determine their fresh weight. The length of the roots was measured from the plant's base to the top of the longest root branch. Then, root samples were oven-dried at 72°C for 3 days to get the constant weight.

Root leakage was assessed through the Root Electrolyte Leakage (REL) method (Radoglou et al. 2007). The root system was cut and washed in cold tap water to remove soil. Then, the root was rinsed in distilled water to remove adsorbed ions. The root sample was made certain to have as little soil contamination in the root as possible. Fresh samples were selected from a portion of the root system between 100 to 500 mg weights. The samples were then submerged in 28 mL universal glass bottles of distilled water. The bottles were capped, shaken, and left at room temperature for 24 hours. Next, the bathing solution's first conductivity (C1) was measured using a conductivity probe with a built-in temperature compensation system. The samples were then autoclaved at 110°C for 10 minutes. The samples were cooled to room temperature, and a second conductivity (C_2) was measured. REL was expressed as:

$$REL = (C_1/C_2) \times 100$$

Meanwhile, malondialdehyde (MDA) content was measured following the method by Hodges et al. (1999). 0.25-0.50g of root samples were homogenized in 3 mL of 0.1% (w/v) trichloroacetic acid (TCA) before being centrifuged at 10,000 g for 10 minutes. Then a 750 µl aliquot was pipetted and mixed with the same volume of either (a) a +thiobarbituric acid (TBA) solution containing 20% (w/v) TCA and 0.5% (w/v) TBA or (b) -TBA containing only 20% (w/v) TCA in a 2-ml capped microcentrifuge tube. All samples were then heated in a water bath for 25 minutes at 95°C before being brought to room temperature. After a centrifugation for 10 minutes at 10,000 g, the absorbances were recorded at 440, 532, and 600 nm.

Root anatomy

Root samples were cut 5cm from the root tip for root anatomy. Anatomical specimens were prepared with a sliding microtome, and the thickness was adjusted to 100 µm. As rice roots were very small and fragile, the clearing process was unnecessary. The root sections were stained immediately in Methylene Blue for 30 seconds after

sectioning. All the sections were observed under a light microscope LEICA ICC50 HD and captured by Leica LAS EZ Software.

RESULTS AND DISCUSSION

Effect of drought on root morphology and physiology

Shoot-related morpho-physiological assessments have been established in numerous research conducted on rice. Nevertheless, root architecture has traditionally been largely ignored by plant breeders in terms of potential yield increases and was not a major selection criterion as part of the crop development programs because of the absence of simple and effective techniques for investigating root systems in soil (Den Herder et al. 2010). This bias is extremely unfortunate, as the dearth of discoveries in root phenes could limit our understanding and ability to predict how crops and their surrounding environments respond to climate change-induced abiotic stress, particularly frequent drought. The present study subjected rice seedlings to normal water levels before drought treatments. No discernible difference in root growth was observed between the Moroberekan and MR297 varieties under control conditions (Figure 1.A).

Nevertheless, the root system in both varieties experienced significant impairment when the seedlings were exposed to drought-induced stress. The occurrence of drought stress resulted in a notable decrease in root length, with Moroberekan and MR297 exhibiting reductions of 33.3% and 36.2%, respectively, in comparison to MR297 plants that were subjected to regular watering (Figure 1.B). A longer root length was associated with drought resistance in plants. Soil exploration during drought necessitates a longer root system for water and nutrient search, resulting in a greater allocation of carbohydrates to root growth (Djanaguiraman et al. 2019). Although early studies have shown that drought-treated plants have longer roots than those with normal irrigation, the severity of the drought exposure and growth stage also affect the outcome (Karim et al. 2021). In this study, rice plants were exposed to drought stress at an early stage of tillering, which could be crucial for growth and development, resulting in the opposite result.

The root system is a crucial plant organ responsible for the absorption of water and nutrients, significantly influencing plant growth and yield productivity (Azmi et al. 2020; Cochavi et al. 2020). Drought impairs root development, particularly root branching, essential for increasing the root system's surface area. Furthermore, the reduced root length under drought stress also limits the enhanced access to subsoil water, resulting in lower grain yield when water is limited (Bodner and Robles 2017). In the control, no significant difference was seen in root fresh weight across all plants (Figure 2.A). On the other hand, drought stress resulted in a notable decrease in the fresh weight of plant roots compared to plants cultivated under controlled water conditions. Moroberekan and MR297 exhibited reductions of 47.5% and 67.3%, respectively, when exposed to drought, compared to the control.

Similarly, while root dry weight under normal watering showed no difference, drought substantially impacted the root biomass of all plants, with a more notable effect detected in MR297. The MR297 exhibited a significant decrease of 40% compared to the Moroberekan under drought stress and nearly 81% compared to its performance on the control. This observation implies that MR297 demonstrated a higher vulnerability to drought stress (Figure 2.B). The continuation of root growth in dry weight was important in yield determination and positively correlated with grain filling in rice (Chen et al. 2021).

Under drought, the roots can grow with sufficient sugars from the leaves. Miller et al. (2017) stated that this necessitates a dynamic acclimation within the leaf proteome, specifically photosynthetic-related proteins, to overcome the challenges. The decrease in plant dry weight, including root biomass, observed in response to drought stress can be attributed to a decline in photosynthetic activity. The impact of drought on the physiological metabolism of photosynthesis has been reported, leading to disruptions in the electron transport chain and reduced assimilation of carbon dioxide (Wang et al. 2018).

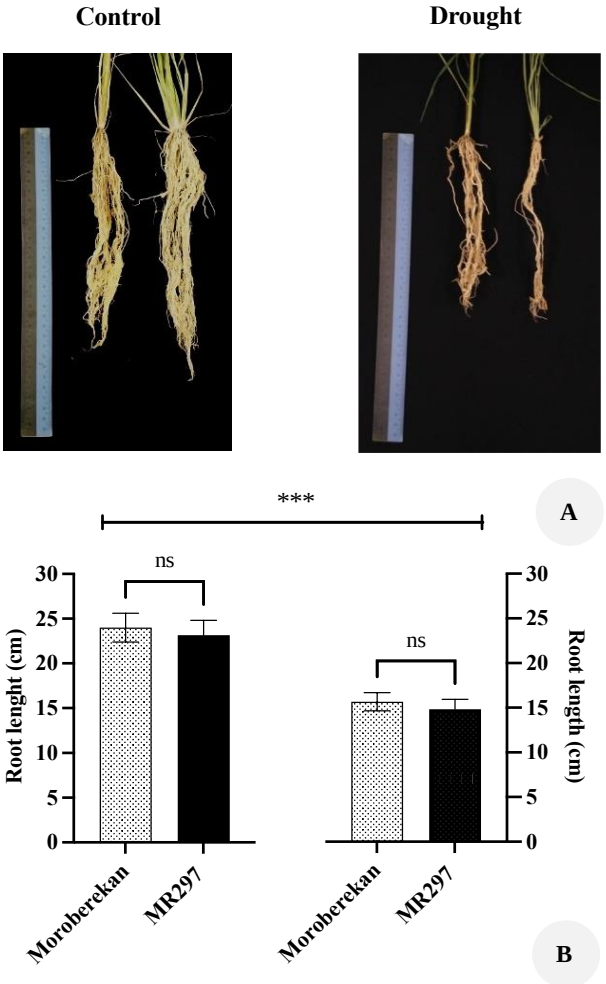

Figure 1. A. Root system and B. length of Moroberekan and MR297 rice seedlings subjected to normal irrigation and drought stress. Data was analyzed using a t-test to assess the significance level between means ($p \leq 0.05$). Values represent the mean ± SE of n = 3. *** indicates the significant level of drought treatment based on a two-way ANOVA

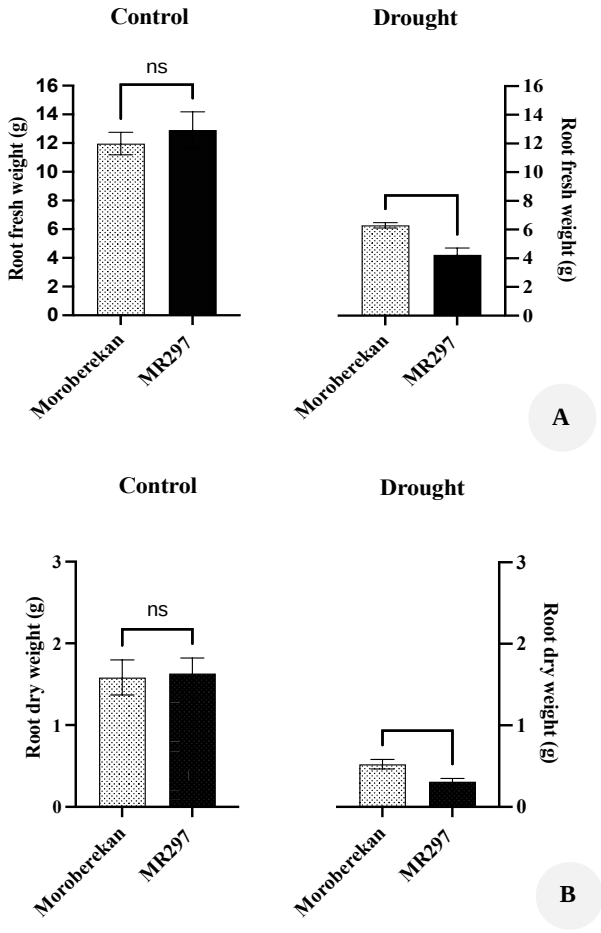

Figure 2. A. Root fresh weight and B. dry weight of Moroberekan and MR297 rice seedlings subjected to normal irrigation and drought stress. Data was analyzed using a t-test to assess the significance level between means ($p \leq 0.05$). Values represent the mean ± SE of n = 3

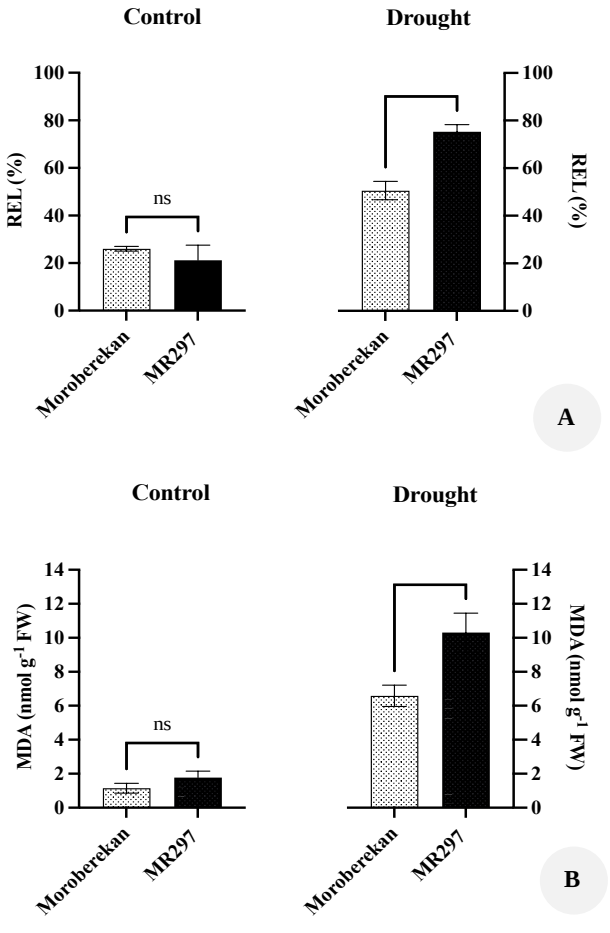

Figure 3. A. REL and B. MDA content of Moroberekan and MR297 rice seedlings subjected to normal irrigation and drought stress. Data was analyzed using a t-test to assess the significance level between means ($p \leq 0.05$). Values represent the mean ± SE of n = 3

The interruption of the electron transport chain can impede the synthesis of ATP by ATP synthase, potentially impacting the Calvin cycle's metabolic processes (Simkin et al. 2019). All of these processes depend on the acclimation capacity of plant species and cultivars in response to drought, which may explain why Moroberekan still recorded a significantly higher value than MR297 despite a lower root biomass under drought.

Evaluating root electrolyte leakage can provide insights into the resistance of root systems to drought-induced stress. Cells normally lose their membrane integrity; thus, electrolytes, such as K^+ ions, leak out of the cell, indicating the extent of cell death in the tissue, especially under abiotic stresses (Demidchik et al. 2014). Moroberekan and MR297 show no difference in the control, with an average REL value of 21-25%. However, a significant increase was observed in those plants exposed to drought ($p \leq 0.05$), with the effect being greater in MR297 compared to Moroberekan ($p \leq 0.01$) (Figure 3.A). According to Assaha et al. (2016), drought stress induces the overproduction of reactive oxygen species, which damage cellular membranes and can increase electrolyte leakage. The REL results correspond to the MDA level in roots where drought significantly increased lipid peroxidation compared to control (Figure 3.B). The oxidative stress was known to cause a higher accumulation of MDA (Karim and Johnson 2021). The production of MDA was more pronounced in MR297, with a significant 1.6-fold higher than that of Moroberekan. Hence, considering the root physiology, it can be inferred that Moroberekan exhibits higher drought resistance than MR297, indicating that the response to drought may differ depending on the specific variety and ecotype.

Effect of drought on root anatomy

The present study examines root anatomy to determine whether there were any alterations in root structure between two rice varieties, an upland rice variety (Moroberekan) and a domestically grown rice variety (MR297). In the absence of stress exposure, it was shown that Moroberekan naturally exhibited a larger root diameter than MR297, with an average difference of 16% (Figure 4). However, the exposure to drought resulted in a substantial

decrease in the root diameter of the MR297 and Moroberekan varieties. Specifically, the root diameter of MR297 was reduced by 50.1%, while Moroberekan had a loss of 33.4% when compared to their respective control. Analysis of rice roots under drought stress revealed that Moroberekan had more root hairs surrounding its epidermis cells than MR297. According to Hernández et al. (2010), certain plant species have been reported to decrease their root diameter but with longer root systems for subsoil water exploration.

Nevertheless, the present study did not observe such an outcome, as both diameter and root length were impacted by drought, which aligns with the findings reported by Boguszewska-Mańkowska et al. (2020). A separate study observed that drought environments resulted in a reduction in root length and an increase in root diameter (Zhou et al. 2018). In contrast, another study found no significant alterations in fine root morphology (Mrak et al. 2019).

Rice has special tissue that allows it to live in a root submergence environment called aerenchyma. Aerenchyma cells in rice roots are formed by cell lysis and cell deflation to provide air channels that allow gas diffusion from above-part to below-part organs to maintain aerobic respiration in submerged conditions. This study observed aerenchyma formation in rice roots regardless of treatments. While the control plants exhibited greater root diameter, the aerenchyma cells in these plants were not fully developed compared to the drought-induced plants, which displayed a higher ratio of the number of aerenchyma cells present per sectioned area. This indicates that the formation of aerenchyma cells continues despite the prolonged exposure of the root system to drought. According to Schneider et al. (2023), the development of cortical aerenchyma formation is predominantly regulated by a root cortex-expressed gene-encoding transcription factor bHLH121.

Meanwhile, in a study conducted by Ni et al. (2019), it was observed that the presence of ethylene and reactive oxygen species facilitated the process. The transformation of live cortical cell tissue into a porous structure can decrease respiration activity and, hence, lower the metabolic expenditure associated with soil exploration during drought (Schneider et al. 2023). This is because root exploration in the soil is metabolically costing, sometimes surpassing 50% of the daily photosynthetic activity (Lynch et al. 2021).

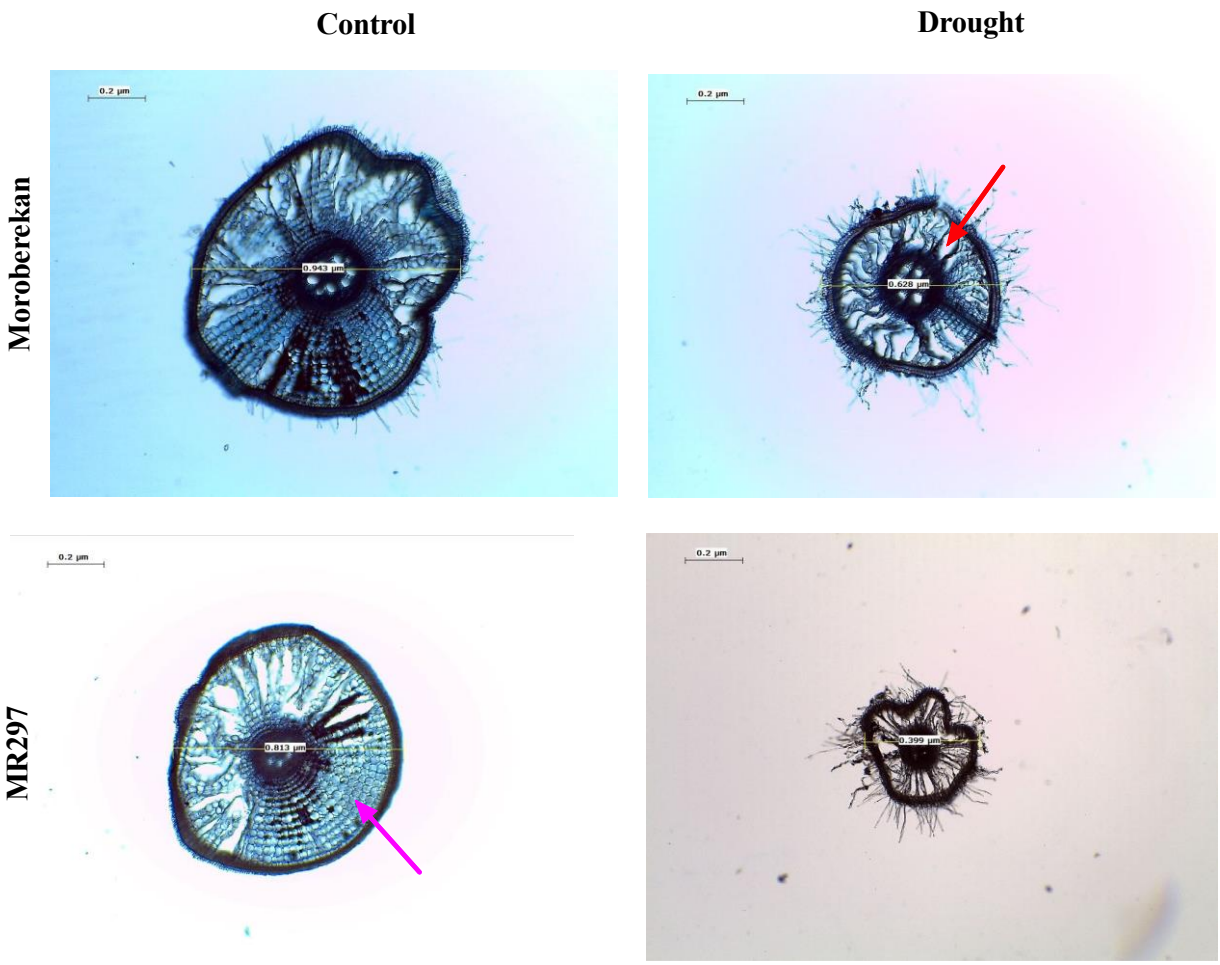

Figure 4. Cross-sectioned roots of Moroberekan and MR297 were subjected to control and drought conditions. The samples were obtained approximately 5 cm from the root tip and observed under a compound microscope, 4x magnificent with scale bar = 0.2 µm. The red and magenta arrows indicate specific anatomical structures: Aerenchyma and undeveloped aerenchyma cells

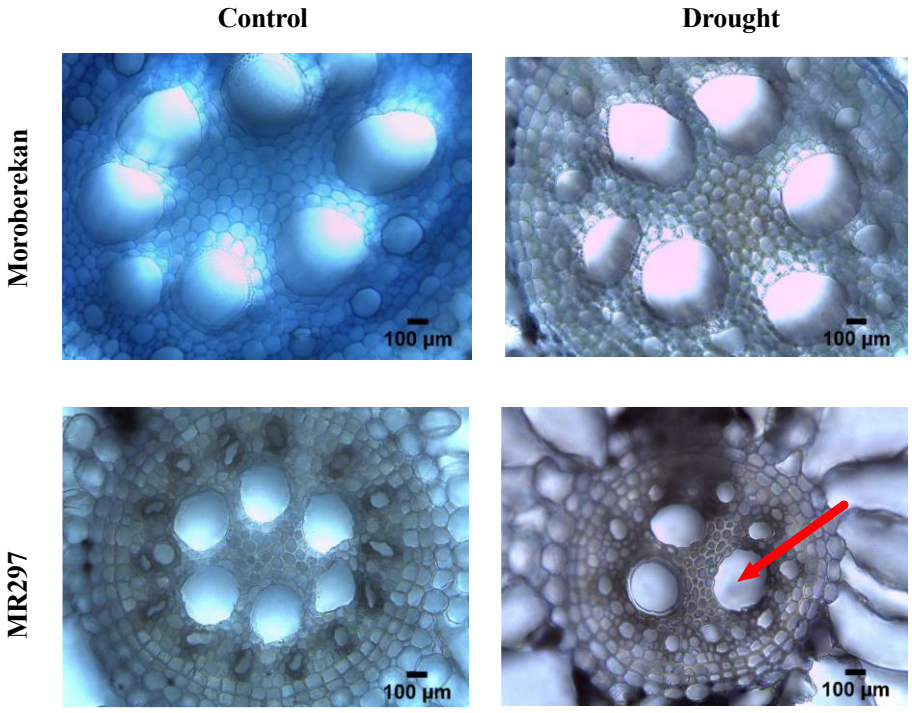

Figure 5. Anatomical analysis of metaxylem cells in Moroberekan and MR297 under control and drought treatment, respectively. The sections were obtained 5 cm from the root tip and observed under a compound microscope, 4x magnificent with scale bar = 100 µm. The red arrow indicates a specific anatomical structure: metaxylem cells

In addition, the drought resistance features in rice have also been assessed on the root xylem. Metaxylem cells originate from primary xylem tissue, formed during the primary growth phase. The current study examined metaxylem cells and the number in rice roots, revealing different responses under normal and stress conditions (Figure 5). The results of the study showed that there were variations in the number of metaxylem cells in both varieties. MR297 showed a decrease in metaxylem numbers, in contrast to Moroberekan, which showed only a slight decrease in response to drought conditions relative to control. The average number of metaxylem cells in MR297 under drought conditions ranged from 3 to 4, which was lower than its performance in the control, where the average number was 6 to 7.

In contrast, Moroberekan developed 5 to 6 metaxylem cells, a count nearly equivalent to the amount observed under normal water level. The studies conducted by Prince et al. (2017) and Cornelis and Hazak (2022) have demonstrated a positive correlation between increased xylem number and diameter and enhanced drought tolerance. Root metaxylem traits were found to have different outcomes in previous research. While there are reports that the smaller metaxylem vessel and number benefit the plants reduced hydraulic conductance per root and lower risk of cavitation and collapse (Klein et al. 2020; Reeger et al. 2021), the greater diameter and number of metaxylem vessels were typically found in upland rice, where it could be the phenotype of tolerance in upland rice varieties (Gowda et al. 2011). This observation may account for the greater drought tolerance exhibited by Moroberekan in comparison to MR297. It suggests that further research on drought tolerance traits based on root phenes could be expanded to include upland rice varieties commonly cultivated in areas with limited water resources.

In conclusion, the availability of water is crucial for facilitating the normal growth and development of plants. Even a minor decrease in soil moisture levels can significantly impact the physiological processes of less resilient plant species. Hence, identifying appropriate candidates with superior root traits that can withstand adverse conditions is crucial in breeding programs, particularly in challenging climate uncertainty. The present study revealed that the root morpho-physiology of the MR297 and Moroberekan was impacted by drought stress. This includes the significantly lower root fresh and dry weight, maximal root length, and % of REL and MDA accumulation compared to the plants maintained in the control condition. However, the impact was more pronounced in MR297 in all the mentioned parameters except for the maximal root length. Similarly, the root anatomical study results indicate that drought stress had reduced root diameter and metaxylem number compared to the control, but not the aerenchyma formation. Furthermore, it was demonstrated that Moroberekan exhibited better root structure than MR297 when subjected to drought stress.

ACKNOWLEDGEMENTS

This work was supported by the Malaysian Fundamental Research Grant Scheme (FRGS) (grant number FRGS/1/2019/WAB01/UIAM/02/2).

REFERENCES

Ali S, Liu Y, Ishaq M, Shah T, Abdullah, Ilyas A, Din IU. 2017. Climate change and its impact on the yield of major food crops: Evidence from Pakistan. Foods 6: 39. DOI: 10.3390/foods6060039.

Assaha DV, Liu L, Ueda A, Nagaoka T, Saneoka H. 2016. Effect of drought stress on growth, solute accumulation and membrane stability of leafy vegetable, huckleberry (*Solanum scabrum* Mill.). J Environ Biol 37: 107-114.

Azmi FA, Tajudin NS, Shahari R, Aini CN. 2020. Early growth response and nutrients quality of fig (*Ficus carica* L.) planted on bris soil effected by chicken manure amendments. J Clean WAS 4: 61-65. DOI: 10.26480/jcleanwas.02.2020.61.65.

Bodner GS, Robles MD. 2017. Enduring a decade of drought: Patterns and drivers of vegetation change in a semi-arid grassland. J Arid Environ 136: 1-14. DOI: 10.1016/j.jaridenv.2016.09.002.

Boguszewska-Mańkowska D, Zarzyńska K, Nosalewicz A. 2020. Drought differentially affects root system size and architecture of potato cultivars with differing drought tolerance. Am J Potato Res 97: 54-62. DOI: 10.1007/s12230-019-09755-2.

Chen M, Yang Z, Liu J, Zhu T, Wei X, Fan H, Wang B. 2018. Adaptation mechanism of salt excluders under saline conditions and its applications. Intl J Mol Sci 19: 3668. DOI: 10.3390/ijms19113668.

Chen X, Zhu Y, Ding Y, Pan R, Shen W, Yu X, Xiong F. 2021. The relationship between characteristics of root morphology and grain filling in wheat under drought stress. PeerJ 9: e12015. DOI: 10.7717/peerj.12015.

Cochavi A, Cohen IH, Rachmilevitch S. 2020. The role of different root orders in nutrient uptake. Environ Exp Bot 179: 104212. DOI: 10.1016/j.envexpbot.2020.104212.

Cornelis S, Hazak O. 2022. Understanding the root xylem plasticity for designing resilient crops. Plant Cell Environ 45: 664-676. DOI: 10.1111/pce.14245.

Demidchik V, Straltsova D, Medvedev SS, Pozhvanov GA, Sokolik A, Yurin V. 2014. Stress-induced electrolyte leakage: The role of K^+-permeable channels and involvement in programmed cell death and metabolic adjustment. J Exp Bot 65: 1259-1270. DOI: 10.1093/jxb/eru004.

Den Herder G, Van Isterdael G, Beeckman T, De Smet I. 2010. The roots of a new green revolution. Trends Plant Sci 15: 600-607. DOI: 10.1016/j.tplants.2010.08.009.

Djanaguiraman M, Prasad PVV, Kumari J, Rengel Z. 2019. Root length and root lipid composition contribute to drought tolerance of winter and spring wheat. Plant Soil 439: 57-73. DOI: 10.1007/s11104-018-3794-3.

Gowda VRP, Henry A, Yamauchi A, Shashidhar HE, Seeraj R. 2011. Root biology and genetic improvement for drought avoidance in rice. Field Crops Res 122: 1-13. DOI: 10.1016/j.fcr.2011.03.001.

Hardke JT. 2013. Arkansas Rice Production Handbook. University of Arkansas Division of Agriculture Cooperative Extension Service MP192, Little Rock.

Hernández E, Vilagrosa A, Pausas J, Bellot J. 2010. Morphological traits and water use strategies in seedlings of Mediterranean coexisting species. Plant Ecol 207: 233-244. DOI: 10.1007/s11258-009-9668-2.

Ho WWH, Hill CB, Doblin MS, Shelden MC, van DMA, Rupasinghe T, Bacic A, Roessner U. 2020. Integrative multi-omics analyses of barley rootzones under salinity stress reveal two distinctive salt tolerance mechanisms. Plant Commun 1: 100031. DOI: 10.1016/j.xplc.2020.100031.

Hodges D, DeLong J, Forney C, Prange RK. 1999. Improving the thiobarbituric acid-reactive-substances assay for estimating lipid peroxidation in plant tissues containing anthocyanin and other interfering compounds. Planta 207: 604-611. DOI: 10.1007/s004250050524.

Kadam NN, Yin X, Bindraban PS, Struik PC, Jagadish KS. 2015. Does morphological and anatomical plasticity during the vegetative stage make wheat more tolerant of water deficit stress than rice? Plant Physiol 167: 1389-1401. DOI: 10.1104/pp.114.253328.

Karim MF, Johnson GN. 2021. Acclimation of photosynthesis to changes in the environment results in decreases of oxidative stress in *Arabidopsis thaliana*. Front Plant Sci 12: 683986. DOI: 10.3389/fpls.2021.683986.

Karim MF, Rosely NFSM, Kamil NAM, Amri CNAC. 2021. Morpho-physiological and anatomical assessment of different rice varieties subjected to drought stress at early vegetative stage. Malays Appl Biol 50: 55-64. DOI: 10.55230/mabjournal.v50i1.12.

Klein SP, Schneider HM, Perkins AC, Brown KM, Lynch JP. 2020. Multiple integrated root phenotypes are associated with improved drought tolerance. Plant Physiol 183: 1011-1025. DOI: 10.1104/pp.20.00211.

Landi S, Hausman JF, Guerriero G, Esposito S. 2017. Poaceae vs. Abiotic stress: Focus on drought and salt stress, recent insights and perspectives. Front Plant Sci 8: 1214. DOI: 10.3389/fpls.2017.01214.

Lynch JP, Strock CF, Schneider HM, Sindhu JS, Ajmera I, Galindo-Castañeda T, Klein SP, Hanlon MT. 2021. Root anatomy and soil resource capture. Plant Soil 466: 21-63. DOI: 10.1007/s11104-021-05010-y.

Mehmet A. 2016. Root anatomical plasticity in response to salt stress under real and full-season field conditions and determination of new anatomic selection characters for breeding salt-resistant rice (*Oryza sativa* L.). Trakya Univ J Nat Sci 17: 87-104.

Miller MAE, O'Cualain R, Selley J, Knight D, Karim MF, Hubbard SJ, Johnson GN. 2017. Dynamic acclimation to high light in *Arabidopsis thaliana* involves widespread reengineering of the leaf proteome. Front Plant Sci 8: 1239. DOI: 10.3389/fpls.2017.01239.

Mrak T, Štraus I, Grebenc T, Gricar J, Hoshika Y, Carriero G, Paoletti E, Kraigher H. 2019. Different belowground responses to elevated ozone and soil water deficit in three European oak species (*Quercus ilex*, *Q. pubescens* and *Q. robur*). Sci Total Environ 651: 1310-1320. DOI: 1016/j.scitotenv.2018.09.246.

Nahar S, Sahoo L, Tanti B. 2018. Screening of drought tolerant rice through morpho-physiological and biochemical approaches. Biocatal Agric Biotechnol 15: 150-159. DOI: 10.1016/j.bcab.2018.06.002.

Ni XL, Gui MY, Tan LL, Zhu Q, Liu WZ, Li CX. 2019. Programmed cell death and aerenchyma formation in water-logged sunflower stems and its promotion by ethylene and ROS. Front Plant Sci 9: 1928. DOI: 10.3389/fpls.2018.01928.

Panda D, Mishra SS, Behera PK. 2021. Drought tolerance in rice: Focus on recent mechanisms and approaches. Rice Sci 28: 119-132. DOI: 10.1016/j.rsci.2021.01.002.

Prince SJ, Murphy M, Mutava RN, Durnell LA, Valliyodan B, Shannon JG, Nguyen HT. 2017. Root xylem plasticity to improve water use and yield in water-stressed soybean. J Exp Bot 68: 2027-2036. DOI: 10.1093/jxb/3rw472.

Radoglou K, Cabral R, Repo T, Sutinen ML. 2007. Appraisal of root leakage as a method for estimation of root viability. Plant Biosyst 141: 443-459. DOI: 10.1080/11263500701626143.

Reeger JE, Wheatley M, Yang Y, Brown KM. 2021. Targeted mutation of transcription factor genes alters metaxylem vessel size and number in rice roots. Plant Direct 5: e00328. DOI: 10.1002/pld3.328.

Sandhu N, Jain S, Battan KR, Jain RK. 2012. Aerobic rice genotypes displayed greater adaptation to water-limited cultivation and tolerance to polyethyleneglycol-6000 induced stress. Physiol Mol Biol Plants 18: 33-43. DOI: 10.1007/s12298-011-0094-2.

Schneider HM, Lor VS, Zhang X, Saengwilai P, Hanlon MT, Klein SP, Davis JL, Borkar AN, Depew CL, Bennett MJ, Kaeppler SM, Brown KM, Bhosale R, Lynch JP. 2023. Transcription factor bHLH121 regulates root cortical aerenchyma formation in maize. Proc Natl Acad Sci USA 120: e2219668120. DOI: 10.1073/pnas.2219668120.

Schneider HM, Lynch JP. 2020. Should root plasticity be a crop breeding target? Front Plant Sci 11: 546. DOI: 10.3389/fpls.2020.00546.

Shamsuddin MS, Shahari R, Amri CNAC, Tajudin NS, Mispan MR, Salleh MS. 2021. Early development of Fig (*Ficus carica* L.) root and shoot using different propagation medium and cutting types. Trop Life Sci Res 32: 83-90. DOI: 10.21315/tlsr2021.32.1.5.

Shelden MC, Munns R. 2023. Crop root system plasticity for improved yields in saline soils. Front Plant Sci 14: 1120583. DOI: 10.3389/fpls.2023.1120583.

Siangliw JL, Thunnom B, Natividad MA, Quintana MR, Chebotarov D, McNally KL, Lynch JP, Brown KM, Henry A. 2022. Response of Southeast Asian rice root architecture and anatomy phenotypes to drought stress. Front Plant Sci 13: 1008954. DOI: 10.3389/fpls.2022.1008954.

Simkin AJ, López CPE, Raines CA. 2019. Feeding the world: improving photosynthetic efficiency for sustainable crop production. J Exp Bot 70: 1119-1140. DOI: 10.1093/jxb/ery445.

Singh B, Reddy KR, Redoña ED, Walker T. 2017. Screening of rice cultivars for morpho-physiological responses to early-season soil moisture stress. Rice Sci 24: 322-335. DOI: 10.1016/j.rsci.2017.10.001.

Singh S, Prasad S, Yadav V, Kumar A, Jaiswal B, Kumar A, Kumar A, Dwivedi DK. 2018. Effect of drought stress on yield and yield components of rice (*Oryza sativa* L.) genotypes. Intl J Curr Microbiol Appl Sci 7: 2752-2759. DOI: 10.5455/faa.277118.

Suseela V, Tharayil N, Orr G, Hu D. 2020. Chemical plasticity in the fine root construct of *Quercus* spp. varies with root order and drought. New Phytol 228: 1835-1851. DOI: 10.1111/nph.16841.

Swapna S, Shylaraj KS. 2017. Screening for osmotic stress responses in rice varieties under drought condition. Rice Sci 24: 253-263. DOI: 10.1016/j.rsci.2017.04.004.

Tajima R. 2021. Importance of individual root traits to understand crop root system in agronomic and environmental contexts. Breed Sci 71: 13-19. DOI: 10.1270/jsbbs.20095.

Wang Z, Li G, Sun H, Ma L, Guo Y, Zhao Z, Gao H, Mei L. 2018. Effects of drought stress on photosynthesis and photosynthetic electron transport chain in young apple tree leaves. Biol Open 7: bio035279. DOI: 10.1242/bio.035279.

Yadav MR, Choudhary M, Singh J, Lal MK, Jha PK, Udawat P, Gupta NK, Rajput VD, Garg NK, Maheshwari C, Hasan M, Gupta S, Jatwa TK, Kumar R, Yadav AK, Prasad PVV. 2022. Impacts, tolerance, adaptation, and mitigation of heat stress on wheat under changing climates. Intl J Mol Sci 23: 2838. DOI: 10.3390/ijms23052838.

Yan S, Weng B, Jing L, Bi W, Yan D. 2022. Adaptive pathway of summer maize under drought stress: Transformation of root morphology and water absorption law. Front Earth Sci 10: 1020553. DOI: 10.3389/feart.2022.1020553.

Zhang J, Zhang S, Cheng M, Jiang H, Zhang X, Peng, Lu X, Zhang M, Jin J. 2018. Effect of drought on agronomic traits of rice and wheat: A meta-analysis. Intl J Environ Res Public Health 15: 839. DOI: 10.3390/ijerph15050839.

Zhou G, Zhou X, Nie Y, Bai SH, Zhou L, Shao J, Cheng W, Wang J, Hu F, Fu Y. 2018. Drought-induced changes in root biomass largely result from altered root morphological traits: Evidence from a synthesis of global field trials. Plant Cell Environ 41: 2589-2599. DOI:10.1111/pce.13356.

NUSANTARA BIOSCIENCE
Vol. 16, No. 1, pp. 37-42
May 2024

ISSN: 2087-3948
E-ISSN: 2087-3956
DOI: 10.13057/nusbiosci/n160105

Chemical composition with different drying methods and ruminant methane gas production of *Palisada perforata*

NUR HIDAYAH[1,2], CUK TRI NOVIANDI[3], ANDRIYANI ASTUTI[3], KUSTANTINAH[3,♥]

[1]Graduate School of Animal Science, Universitas Gadjah Mada. Jl. Fauna No. 3 Bulaksumur, Sleman 55281, Yogyakarta, Indonesia
[2]Department of Animal Science, Faculty of Agriculture, Universitas Tidar. Jl. Kapten Suparman No. 39, Magelang 56116, Central Java, Indonesia
[3]Faculty of Animal Science, Universitas Gadjah Mada. Jl. Fauna No. 3 Bulaksumur, Sleman 55281, Yogyakarta, Indonesia. Tel.: +62-274-513363, ♥email: kustantinah.ugm.ac.id
[4]Center for Environmental Studies, Universitas Gadjah Mada. Jl. Kuningan Caturtunggal, Sleman, Yogyakarta 55281, Indonesia

Manuscript received: 28 November 2023. Revision accepted: 3 January 2024.

Abstract. *Hidayah N, Noviandi CT, Astuti A, Kustantinah. 2024. Chemical composition with different drying methods and ruminant methane gas production of* Palisada perforata*. Nusantara Bioscience 16: 37-42.* Indonesia is a tropical country with a large diversity of seaweed, but a few studies analyzed it as an ingredient or supplement for ruminant feed. Evaluation of the nutrient content and phenolic compound with different drying methods (freeze-drying and shade-drying) and ruminant gas production from *Palisada perforata* (Bory) K.W.Nam to know about the potential for ruminant feed and methane mitigation were the goals of this investigation. The nutrient content, kinetic, and methane gas production were analyzed descriptively; meanwhile, the phenolic compound was analyzed with T-tests for the differences among treatments, using 4 replications. The result showed that the nutrient content of *P. perforata* had higher Organic Matter (OM), Crude Protein (CP), and Nitrogen-Free Extract (NFE) with the freeze-drying method (83.47 vs. 52.85%DM, 19.33 vs. 16.05%DM, and 54.16 vs 26.80%DM, respectively) and the mineral content was higher with shade-drying method (16.53 vs 47.15%DM). The shade-drying method decreased almost 50% of the phenolic compound compared to the freeze-drying method. The kinetic gas production of *P. perforata* had easily degraded, potentially degraded, and total degraded and fermented fractions at 5.88, 24.91, and 30.80 mL/200 mgDM, respectively; the methane gas production in 24 and 48 hours incubation at 1.80 and 3.01 mL/gDM. The study concluded that the freeze-drying method is better than the shade-drying method to dry *P. perforata* and this species' potential as ruminant feed and methane mitigation.

Keywords: Nutrient content, *Palisada perforata*, phenolic compound, ruminant methane gas production

INTRODUCTION

Recent research on improving feed management is interested in using seaweed as a feed ingredient or additional feed for ruminant livestock (Roque et al. 2019; Min et al. 2021). Min et al. (2021) stated that seaweed is rich in polysaccharides, amino acids, vitamins, secondary metabolites, and minerals, which are important for livestock metabolic functions. Therefore, using seaweed can increase feed conversion efficiency, growth rate, health, and productivity of ruminants (Belanche et al. 2016; Pirian et al. 2017; Gaillard et al. 2018; Roque et al. 2019). Seaweed is also very efficient in reducing CH_4 emissions in ruminant livestock (Kinley et al. 2016, 2020; Machado et al. 2016; Li et al. 2017; Roque et al. 2019; Choi et al. 2021; Min et al. 2021; Mihaila et al. 2022) because it contains metabolite compounds; there is halogen (such as bromoform) and phlorotannin compounds which are not present in terrestrial plants, phenolic compound, and others. Hagaggi and Abdul-Raouf (2022) reported that *Cystoseira myrica* (S.G.Gmelin) C.Agardh was extracted with methanol and ethyl acetate for *Catenococcus thiocycli* Sorokin, 1994 had the highest quantities of flavonoids (2,164.7 and 1,418.4 µg quercetin equivalent/mg extract), respectively. A notable quantity of saponins and tannins (778 µg diosgenin equivalent/mg extract and 606 µg catechol equivalent/mg extract, respectively) were present in the *C. myrica* extracted with ethyl acetate.

Studies on using various seaweed species as feed ingredients or additional feed for ruminants and their effectiveness in reducing enteric CH_4 from subtropical seaweed species are still minimal. The genus of *Asparagopsis* is the most vigorous additive in decreasing enteric CH4 production (40-98%) with low levels (0.2-2% Organic Matter (OM)) (Machado et al. 2016; Li et al. 2017; Kinley et al. 2020; Mihaila et al. 2022). Indonesia is one of the tropical countries that produces the largest seaweed in the world (38.7%) after China (47.9%) (FAO 2018), with a fresh seaweed harvest of almost 10 million metric tons in 2019 (van der Heijden et al. 2022). Erniati et al. (2016) stated that seaweed diversity in Indonesia is the largest than in other countries. Waters et al. (2019) stated that Indonesia is a good place to grow different kinds of seaweed because it has a tropical climate, 64,000,000 km^2 of ocean area, and 110,000 km of coastline.

Seaweed in Indonesia has been used as food raw material, especially *Eucheuma cottonii* Weber Bosse, 1913 and *Gracilaria* Greville, 1830 for carrageenan and agar-agar, respectively, which are used in the production of various food items, including crackers, drinks, noodles, jellies, sweets, etc. (van der Heijden et al. 2022). However, until now, the seaweed used and commercialized is still

very limited to the *Eucheuma* spp. and *Gracilaria* spp. So, there are still many seaweed species that have not been explored. Haryatfrehni et al. (2015) stated that Gunungkidul, Yogyakarta, Indonesia, has several beaches with the potential for high diversity and availability of natural seaweed sources. *Palisada perforata* (Bory) K.W.Nam is one of the seaweed species abundant in Gunungkidul coastal areas, with the potential to evaluate the chemical composition (nutrient content and phenolic compound) as an alternative feed ingredient or additional feed for ruminant livestock (Figure 1).

However, it is crucial to investigate the different drying methods to evaluate the chemical composition of *P. perforata* because seaweeds are high in water content. Kustantinah et al. (2022) reported that some tropical seaweed species had water content higher than 70% and even up to 85%, depending on the species, as Badmus et al. (2019) stated. Hence, the drying process is very important to investigate. Moreira et al. (2015) found that the total polyphenol content and antioxidant activity decreased as the drying temperature increased. So, this study aims to evaluate the effect of different drying methods (low temperature: freeze drying and high temperature: shade drying) on the chemical composition of *P. perforate.* This study also investigates ruminant gas production from the best drying method to observe seaweed degradation in the rumen and potential methane mitigation.

MATERIALS AND METHODS

The *P. perforata* collection and drying method

This sample was collected by hand picking in October 2022 from Gunungkidul, Yogyakarta, Indonesia, and identified with the morphological method in the Plant Systematics Laboratory, Biology Faculty, Universitas Gadjah Mada, Yogyakarta, Indonesia. After water rinsing to remove any remaining sand or grit, the seaweed samples were dried using a freeze drier (Buchi, Lyovapor, L-200) for the freeze-drying method (-20°C for 3 days). The sample was spread on the bamboo shelf and left to dry under the roof, which was indirectly exposed to the sunlight for the shade drying method (25-30°C for 4 days). The dry samples were pulverized in a hammer mill to a fine powder (80-100 mesh) and placed in sealed plastic bags in a freezer for further analysis.

Chemical composition analysis

Powder samples, comprising nutritional content and phenolic component analysis, were employed for the chemical composition examination.

Nutrient content analysis

Dry Matter (DM), ash, Organic Matter (OM), Crude Protein (CP), Ether Extract (EE), Crude Fiber (CF), and Nitrogen-Free Extract (NFE) were the components of the nutrient content analysis, which was conducted following AOAC (2005). After the sample was dried at 105°C to determine the DM concentration, the residue was burned at 550°C to the analyzed ash concentration. The amount of OM as [100-ash], following N analysis using the Kjeldahl method, CP values were determined as N × 6.25. After the material was extracted using the Soxhlet technique and dried at 105°C, the amount of ether extract was determined. In the meantime, the CF was assessed using the boiling sample in a solution of sulfuric acid (H_2SO_4), and it was further boiled for 30 minutes at 300°C using a solution of sodium hydroxide (NaOH) before being dried at 105°C. The formula for calculating NFE was [100-(ash+CP+EE+CF)].

Phenolic component analysis

Flavonoids, phenol, and tannin were among the phenolic compounds analyzed. The procedure was followed by Abdulrazak and Fujihara (1999), who specified methanol as the solvent in preparing the extracts. In summary, during the extraction process, 200 mg of dried seaweed powder was dissolved in 10 mL of methanol solvent and incubated for 90 min at 130 rpm and 30°C in a platform incubator shaker series (Innova 42, New Brunswick, Eppendorf AG, DE).

Figure 1. *Palisada perforata* (Bory) K.W.Nam

Next, for phenolic analysis, the mixture was centrifuged at 3000 rpm for 20 minutes at 4°C, and the supernatant was moved to another tube as much as possible without disturbing the residue. The phenol and tannin were assessed using the Folin-Ciocalteau method (Makkar 2003); we utilized solutions of tannic acid (20-100 µg/mL) from Sigma–Aldrich as a standard with the curve (y= 0.0108x+0.0102, r^2= 0.99). The absorbance was measured at a wavelength of 725 nm. Next, Arvouet-Grand et al. (1994) adopted the Dowd method for measuring flavonoid concentration. The absorbance was measured at 415 nm using quercetin (Sigma-Aldrich) solutions in the 20-100 µg/mL range for the standard curve (y= 0.002934x-0.032, r^2= 0.99).

In vitro gas production evaluation

A Bali bull and cow (350 and 290 kg body weight and 5 years old) were employed as donors of ruminal fluid for the in vitro incubations, and this provided the rumen fluid for in vitro feeding. The feed was in the 60:40%DM fresh Napier grass and beef cattle concentrate ratio. Clean water was constantly accessible, and feed was offered twice, between 8 a.m. and 5 p.m. The National Research Council (NRC) guidelines for feeding cattle based on maintenance needs are followed. Rumen fluid was taken before morning feeding, then filtered and added to the media, according to Menke and Steingass (1988). All the experimental procedures were approved by the Animal Care Committee at the Faculty of Veterinary Medicine Universitas Gadjah Mada, Indonesia (Approval number: 052/EC-FKH/Eks./2022).

The powdered seaweed samples were used as substrate and put into 100 mL glass syringes (Haberle Labortechnik, Lonsee, Germany) with 200 mgDM. They were mixed with 30 mL of rumen liquor-buffer solution (1:2 ratio vol/vol) and incubated for 72 hours at 39°C under anaerobic conditions. Next, to adjust the gas production values for gas release from endogenous substrates, a total of 12 glass syringes were used in the in vitro incubation runs: 4 glass syringes for the samples, 4 glass syringes for blanks (without substrate) to correct the gas production values for gas release from endogenous substrates, and 4 glass syringes for standard (the seaweed substrate replaced with Pangola grass) as an indicator in vitro incubation process; the gas production was determined at 2, 4, 8, 12, 24, 48, and 72 hours. The Neway program (Chen 1994) was used to calculate the gas production using the formula $Y= a+b(1-e^{-ct})$, where Y is the total gas produced in time t, a and b are the easily degraded and potentially degraded fractions, c is the rate at which the b fraction is producing gas, and the total fraction fermented and degraded (a+b fraction) is the total fraction; the Fievez et al. (2005) method measured methane emissions from gas samples. After a 24-hour incubation period, 10 mL samples were collected from the aliquot and placed in a vacuum tube to analyze methane gas production (Kang Jian, China). Gas chromatography (GC 14B, Shimadzu Crop., Kyoto, Japan) with a Paropak column (50 m × 0.2 mm × 0.3 µm) and an FID detector were used to measure the methane emissions from gas samples.

Research design and statistical analysis

The nutrient content and phenolic compound, kinetic, and methane gas production were analyzed descriptively using a Completely Randomized Design with 4 replications and T-tests for the differences among treatments. Analysis of statistics was executed using IBM SPSS Statistics (26 versions).

RESULTS AND DISCUSSION

Nutrient content

The nutrient content of *P. perforata* had higher Organic Matter (OM), Crude Protein (CP), and Nitrogen-Free Extract (NFE) with the freeze drying method (83.47 vs. 52.85% DM, 19.33 vs 16.05% DM, and 54.16 vs 26.80% DM respectively) than the shade drying method. Meanwhile, the mineral content was higher with the shade-drying method than the freeze-drying method (16.53 vs 47.15% DM) (Figure 2).

The lower CP in the shade drying method might be due to the high drying temperature that caused protein degradation. Ullah et al. (2023) stated that the protein may become more denaturized due to the high-temperature drying processes, which could make the protein less extractable. Hamid et al. (2018) also reported that the nutrients in seaweed are decreased when dried at high temperatures. Meanwhile, as a low heat-drying treatment, the freeze-drying method will not break down the protein formation, so it is lower in the Maillard reaction process than high heat-drying (Boateng and Yang 2021). The same result was reported by Regal et al. (2020); the CP content of *Asparagopsis taxiformis* (Delile) Trevis. with oven-drying (high temperature at 60°C for 72 h) was lower than freeze-drying (low temperature at -40°C and 4 × 10-4 mbar for 48 h). One possible reason for the reduced protein in oven-dried *A. taxiformis* could be that there was dripping during the 72 hours in the oven (while the water is freeze-dried, making this dripping impossible).

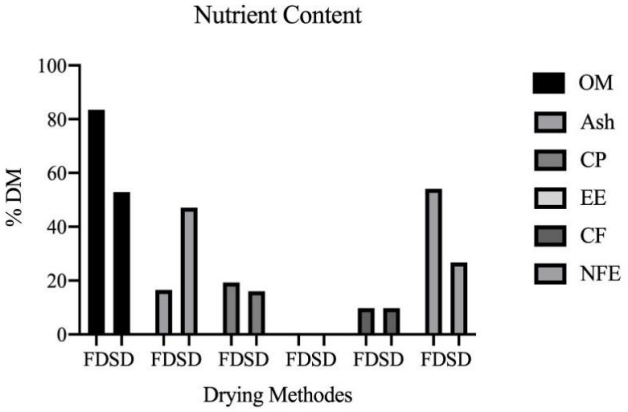

Figure 2. Nutrient content of *P. perforata* with different drying methods. FD: Freeze Drying, SD: Shade Drying, OM: Organic Matter, CP: Crude Protein, EE: Ether Extract, CF: Crude Fiber, NFE: Nitrogen-Free Extract

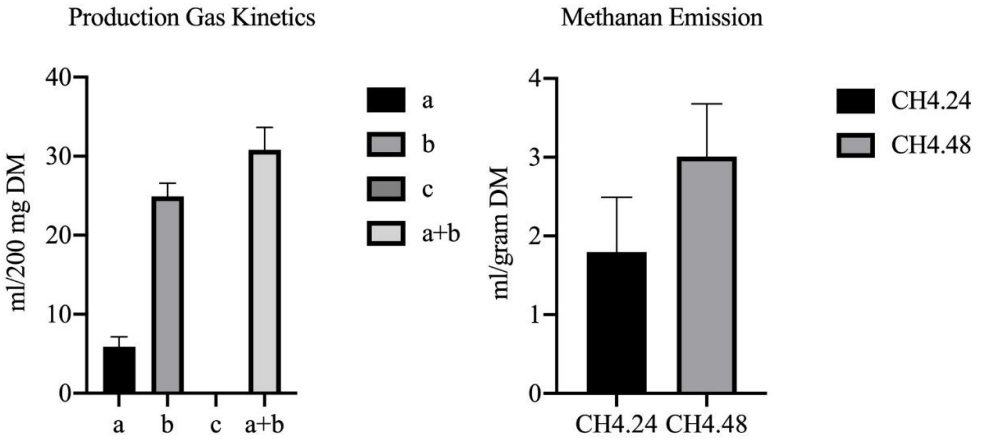

Figure 3. Kinetic and methane gas production of *P. perforata* dried with freeze-drying method. a: Easily degraded fraction, b: potentially degraded fraction, and a+b: Degraded and fermented fractions, CH4.24: Methane gas production that incubated 24 hours, CH4.48: Methane gas production that incubated 48 hours

Table 1. The phenolic compound of *P. perforata* with different drying methods (mg/g DM)

Drying methods	Phenol	Tannin	Flavonoid
Freeze drying	0.80^{b}±0.11	0.76^{b}±0.12	4.26^{b}±0.13
Shade drying	0.45^{a}±0.03	0.42^{a}±0.04	3.70^{a}±0.34
P- Value	0.00	0.00	0.00

However, the freeze-drying method had lower mineral content than the shade-drying method. This condition might be due to the high temperature not affecting the mineral content of *P. perforata*. Uribe et al. (2018) reported the same result: the ash content in dried *Ulva* spp. Linnaeus, 1753 was higher with the high temperature (Solar Drying (SD) and Convective Drying (CD), with the average ash content of 19.65 g/100 mg DM) than with low temperature (Freeze Drying (FD) and Vacuum Drying (VD) that average ash of 17.69 g/100 mg DM). Paga et al. (2021) explained that *Sargassum* sp. C.Agardh, 1820 that dried with the sun-drying method (high temperature) had a higher mineral content (P <0.01) than the freeze-drying methods (low temperature) based on macro minerals like cobalt (30.62 vs. 22.98 ppm) and micro minerals like calcium (38.48 vs 20.98 g/kgDM) and magnesium (13.20 vs 11.10 g/kgDM). Therefore, the sun-drying method (high temperature) can optimally preserve the fresh *Sargassum* sp. without compromising the mineral composition.

Phenolic compound

The shade-drying method decreased (P <0.01) almost 50% of the phenol and tannin compound and 13.15% of the flavonoid content of *P. perforata* than the freeze-drying method. The phenolic compound from the freeze-drying method at 0.80 mg tannic acid per g of dry matter for phenol, 0.76 mg tannic acid per g of dry matter for tannin, and 4.26 mg quercetin per g of dry matter for flavonoid. Meanwhile, the shade drying method at 0.45 mg tannic acid per g of dry matter for phenol, 0.042 mg tannic acid per g of dry matter for tannin, and 3.70 mg quercetin per g of dry matter for flavonoid (Table 1).

Kamiloglu et al. (2016) stated that the drying process directly exposed to the sun had the lowest phenol content. This could be because the sample was exposed to the atmosphere for a longer period, which caused the phenolic compounds to oxidize and cause degradation. In comparison, the low-temperature drying methods had higher retention of bioactive compounds and better antioxidant activities (Meng et al. 2018). The same result reported by Paga et al. (2021) reported that the phenolic compound (phenol, tannin, and flavonoid) of *Sargassum* sp. was higher with freeze dry than with sun dry method (9.43 vs. 6.61%, 1.22 vs. 0.89%, and 7233.03 vs 2393 mg/kg respectively). The same result reported by Neoh et al. (2021) that *Sargassum polycystum* C.Ag. extracted with cold water had total phenol and flavonoid compound, with freeze dry method (25.33 mg PGE/gDE and 12.12 mg RE/gDE) higher than sun dry method (22.76 mg PGE/gDE and 7.30 mg RE/gDE).

Kinetic gas production and methane emission

The dried *P. perforata* methods had different results for nutrient and phenolic compounds. The freeze-drying method had a higher nutrient content and phenolic compound than the shade-drying method. So, the freeze-drying sample was used for the in vitro gas production evaluation to know about the rumen degradability of *P. perforata*. The result showed that the kinetic gas production of *P. perforata* had easily degraded, potentially degraded, and degraded and fermented fractions at 5.88, 24.91, and 30.80 mL/200 mgDM, respectively, and methane gas production in 24 and 48 hours incubation at 1.80 and 3.01 mL/gDM (Figure 3). This result on the several compounds is higher than the result reported by Hidayah et al. (2023), the *Gracilaria* sp. collected from Kalapa beach, Tuban, East Java, Indonesia at 2.02, 27.60, 29.62 mL/200 mgDM and high methane gas production in 24 hours incubation at 9.81 mL/gDM. The result indicated

that *P. perforata* for single feed was easily degraded by rumen microbes and produced low gas methane production.

In comparison with the previous research by Hidayah et al. (2023), kinetic gas production of *P. perforata* had a higher easily degraded fraction (a) but a lower potentially degraded (b) and degraded and fermented fraction (a+b) than *Laminaria* sp. J.V.F.Lamouroux, 1813, *Padina australis* Hauck, *Gracilaria* sp., and *E. cottonii*. This condition might be affected by the CP and NFE of *P. perforata, which are higher than those of* these seaweeds. Jayanegara et al. (2009) reported that gas production ($P < 0.05$) had a positive correlation ($r = 0.81$) with crude protein. This is because protein is an easily degraded component in the rumen, except for proteins protected using certain compounds. Meanwhile, the methane gas production incubated for 24 hours was less than that of all these seaweed species. This condition might be due to the higher phenolic compound of P. perforata than all these seaweed species. Lee-Rangel et al. (2022) explained many studies showing that seaweed secondary metabolites can reduce rumen CH_4 production during enteric fermentation. Gemeda and Hassen (2015) also reported that there was a significant ($p < 0.001$) negative correlation between methane production at 24 hours of incubation with phenolic compounds (total phenol, total tannin, condensed tannin, and hydrolyzable tannin). The study concluded that the freeze-drying method is better than the shade-drying method for chemical composition to dry *P. perforata*. This seaweed species is easily degraded by rumen microbial and low gas methane production, so the seaweed species has potential as ruminant feed and methane mitigation.

ACKNOWLEDGEMENTS

We want to thank and highly appreciate the Center for Environmental Studies, Universitas Gadjah Mada, Indonesia, for supporting this publication through the "*Program Hibah Publikasi Mahasiswa*" 2023, letter of assignment number: 725-32/UN1/PSLH/TU/PT/2023.

REFERENCES

Abdulrazak SA, Fujihara T. 1999. Animal Nutrition: A Laboratory Manual. Laboratory of Animal Science, Faculty of Life and Environmental Science, Shimane University, Shimane.

AOAC. 2005. Official Methods of Analysis. 18th ed. AOAC International, Arlington.

Arvouet-Grand A, Vennat B, Pourrat A, Legret PJJB. 1994. Standardization of a propolis extract and identification of the main constituents. J Pharm Belg 49: 462-468.

Badmus UO, Taggart MA, Boyd KG. 2019. The effect of different drying methods on certain nutritionally important chemical constituents in edible brown seaweeds. J Appl Phycol 31: 3883-3897. DOI: 10.1007/s10811-019-01846-1.

Belanche A, Pinloche E, Preskett D, Newbold CJ. 2016. Effects and mode of action of chitosan and ivy fruit saponins on the microbiome, fermentation and methanogenesis in the rumen simulation technique. FEMS Microbiol Ecol 92: fiv160. DOI: 10.1093/femsec/fiv160.

Boateng ID, Yang XM. 2021. Thermal and non-thermal processing affect Maillard reaction products, flavor, and phytochemical profiles of *Ginkgo biloba* seed. Food Biosci 41: 101044. DOI: 10.1016/j.fbio.2021.101044.

Chen X. 1994. Neway Program International Feed Resources Unit. Backburn, Rowett Research Institute, Aberdeen.

Choi Y, Lee SJ, Kim HS, Eom JS, Jo SU, Guan LL, Seo J, Kim H, Lee SS, Lee SS. 2021. Effects of seaweed extracts on in vitro rumen fermentation characteristics, methane production, and microbial abundance. Sci Rep 11: 24092. DOI: 10.1038/s41598-021-03356-y.

Erniati E, Zakaria FR, Prangdimurti E, Adawiyah DR. 2016. Potensi rumput laut: Kajian komponen bioaktif dan pemanfaatannya sebagai pangan fungsional. Acta Aquatic 3: 12-17. DOI: 10.29103/aa.v3i1.332. [Indonesian]

FAO. 2018. The Global Status of Seaweed Production, Trade and Utilization. Food and Agriculture Organization of the United Nations, Rome.

Fievez V, Babayemi O, Demeyer D. 2005. Estimation of direct and indirect gas production in syringes: A tool to estimate short chain fatty acid production that requires minimal laboratory facilities. Anim Feed Sci Technol 123-124: 197-210. DOI: 10.1016/j.anifeedsci.2005.05.001.

Gaillard C, Bhatti HS, Novoa-Garrido M, Lind V, Roleda MY, Weisbjerg MR. 2018. Amino acid profiles of nine seaweed species and their in situ degradability in dairy cows. Anim Feed Sci Technol 241: 210-222. DOI: 10.1016/j.anifeedsci.2018.05.003.

Gemeda BS, Hassen A. 2015. Effect of tannin and species variation on in vitro digestibility, gas, and methane production of tropical browse plants. Asian Australas J Anim Sci 28: 188-199. DOI: 10.5713/ajas.14.0325.

Hagaggi NSA, Abdul-Raouf UM. 2022. Macroalga-associated bacterial endophyte bioactive secondary metabolites twinning: *Cystoseira myrica* and its associated *Catenococcus thiocycli* QCm as a model. World J Microbiol Biotechnol 38: 205. DOI: 10.1007/s11274-022-03394-2.

Hamid SS, Wakayama M, Soga T, Tomita M. 2018. Drying and extraction effects on three edible brown seaweeds for metabolomics. J Appl Phycol 30: 3335-3350. DOI: 10.1007/s10811-018-1614-z.

Haryatfrehni R, Dewi SC, Meilianda A, Rahmawati S, Sari IZR. 2015. Preliminary study the potency of macroalgae in Yogyakarta: Extraction and analysis of algal pigments from common Gunungkidul seaweeds. Proc Chem 14: 373-380. DOI: 10.1016/j.proche.2015.03.051.

Hidayah N, Kustantinah K, Noviandi CT, Astuti A, Hanim C, Suwignyo B. 2023. Evaluation of rumen in vitro gas production and fermentation characteristics of four tropical seaweed species. Vet Integr Sci 21: 229-238. DOI: 10.12982/vis.2023.018.

Jayanegara A, Sofyan A, Makkar H, Becker K. 2009. Kinetika produksi gas, kecernaan bahan organik dan produksi gas metana *in vitro* pada hay dan jerami yang disuplementasi hijauan mengandung tanin. Med Pet 32: 120-129. [Indonesian]

Kamiloglu S, Toydemir G, Boyacioglu D, Beekwilder J, Hall RD, Capanoglu E. 2016. A review on the effect of drying on antioxidant potential of fruits and vegetables. Crit Rev Food Sci Nutr 56 (sup1): S110-S129. DOI: 10.1080/10408398. 2015.1045969.

Kinley RD, Martinez-Fernandez G, Matthews M K, de Nys R, Magnusson M, Tomkins NW. 2020. Mitigating the carbon footprint and improving productivity of ruminant livestock agriculture using a red seaweed. J Clean Prod 259: 120836. DOI: 10.1016/j.jclepro.2020.120836.

Kinley RD, Vucko MJ, Machado L, Tomkins NW. 2016. Evaluation of the antimethanogenic potency and effects on fermentation of individual and combinations of marine macroalgae. Am J Plant Sci 07: 2038-2054. DOI: 10.4236/ajps.2016.714184.

Kustantinah, Hidayah N, Noviandi CT, Astuti A, Paradhipta DHV. 2022. Nutrients content of four tropical seaweed species from Kelapa Beach, Tuban, Indonesia and their potential as ruminant feed. Biodiversitas 23: 6191-6197. DOI: 10.13057/biodiv/d231213.

Lee-Rangel HA, Roque-Jiménez JA, Cifuentes-López RO, Álvarez-Fuentes G, Cruz-Gómez ADI, Martínez-García JA, Arévalo-Villalobos JI, Chay-Canul AJ. 2022. Evaluation of three marine algae on degradability, in vitro gas production, and CH_4 and CO_2 emissions by ruminants. Fermentation 8: 511. DOI: 10.3390/fermentation8100511.

Li Y, Fu X, Duan D, Liu X, Xu J, Gao X. 2017. Extraction and identification of phlorotannins from the brown alga, *Sargassum fusiforme* (Harvey) Setchell. Mar Drugs 15: 49. DOI: 10.3390/md15020049.

Machado L, Magnusson M, Paul NA, Kinley R, de Nys R, Tomkins N. 2016. Identification of bioactives from the red seaweed *Asparagopsis*

taxiformis that promote antimethanogenic activity in vitro. J Appl Phycol 28: 3117-3126. DOI: 10.1007/s10811-016-0830-7.

Makkar HPS. 2003. Quantification of Tannins in Tree and Shrub Foliage: A Laboratory Manual. Springer Science & Business Media, Berlin. DOI: 10.1007/978-94-017-0273-7.

Meng Q, Fan H, Li Y, Zhang L. 2018. Effect of drying methods on physico-chemical properties and antioxidant activity of *Dendrobium officinale*. J Food Meas Charact 12: 1-10. DOI: 10.1007/s11694-017-9611-5.

Menke KH, Steingass H. 1988. Estimation of the energetic feed value obtained from chemical analysis and *in vitro* gas production using rumen fluid. J Anim Res 28: 7-55.

Mihaila AA, Glasson CRK, Lawton R, Muetzel S, Molano G, Magnusson M. 2022. New temperate seaweed targets for mitigation of ruminant methane emissions: An in vitro assessment. Appl Phycol 3: 274-284. DOI: 10.1080/26388081.2022.2059700.

Min BR, Parker D, Brauer D, Waldrip H, Lockard C, Hales K, Akbay A, Augyte S. 2021. The role of seaweed as a potential dietary supplementation for enteric methane mitigation in ruminants: Challenges and opportunities. Anim Nutr 7: 1371-1387. DOI: 10.1016/j.aninu.2021.10.003.

Moreira R, Chenlo F, Sineiro J, Arufe S, Sexto S. 2015. Drying temperature effect on powder physical properties and aqueous extract characteristics of *Fucus vesiculosus*. J Appl Phycol 28: 2485-2494. DOI: 10.1007/s10811-015-0744-9.

Neoh YY, Matanjun P, Lee JS. 2021. Effects of various drying processes on Malaysian brown seaweed, *Sargassum polycystum* pertaining to antioxidants content and activity. Trans Sci Technol 8: 25-37.

Paga A, Agus A, Kustantinah, Budisatria IGS. 2021. Effect of drying methods on the mineral content of seaweed *Sargasum* sp. Livest Res Rural Dev 33 (3): 35.

Pirian K, Jeliani ZZ, Sohrabipour J, Arman M, Faghihi MM, Yousefzadi M. 2017. Nutritional and bioactivity evaluation of common seaweed species from the Persian Gulf. Iran J Sci Technol Trans A Sci 42: 1795-1804. DOI: 10.1007/s40995-017-0383-x.

Regal AL, Alves V, Gomes R, Matos J, Bandarra NM, Afonso C, Cardoso C. 2020. Drying process, storage conditions, and time alter the biochemical composition and bioactivity of the anti-greenhouse seaweed *Asparagopsis taxiformis*. Eur Food Res Technol 246: 781-793. DOI: 10.1007/s00217-020-03445-8.

Roque BM, Salwen JK, Kinley R, Kebreab E. 2019. Inclusion of *Asparagopsis armata* in lactating dairy cows diet reduces enteric methane emission by over 50 percent. J Clean Prod 234: 132-138. DOI: 10.1016/j.jclepro.2019.06.193.

Ullah MR, Akhter M, Khan ABS, Yasmin F, Hasan MM, Bosu A, Haque MA, Islam M, Mahmud Y. 2023. Comparative estimation of nutritionally important chemical constituents of red seaweed, *Gracilariopsis longissima*, affected by different drying methods. J Food Qual 2023: 6623247. DOI: 10.1155/2023/6623247.

Uribe E, Vega-Gálvez A, García V, Pastén A, López J, Goñi G. 2018. Effect of different drying methods on phytochemical content and amino acid and fatty acid profiles of the green seaweed, *Ulva* spp. J Appl Phycol 31: 1967-1979. DOI: 10.1007/s10811-018-1686-9.

van der Heijden PG, Lansbergen R, Axmann H, Soethoudt H, Tacken G, van den Puttelaar J, Rukminasari N. 2022. Seaweed in Indonesia: Farming, Utilization and Research. Wageningen Centre for Development Innovation, Wageningen. DOI: 10.18174/578007.

Waters TJ, Lionata H, Prasetyo Wibowo T, Jones R, Theuerkauf S, Usman S, Amin I, Ilman M. 2019. Coastal Conservation and Sustainable Livelihoods through Seaweed Aquaculture In Indonesia: A Guide for Buyers, Conservation Practitioners, and Farmers, Version 1. The Nature Conservancy, Arlington VA and Jakarta.

NUSANTARA BIOSCIENCE
Vol. 16, No. 1, pp. 43-53
May 2024

ISSN: 2087-3948
E-ISSN: 2087-3956
DOI: 10.13057/nusbiosci/n160106

Notes on Gerridae (Hemiptera: Heteroptera: Gerromorpha) from the Eastern Ghats of Telangana and Northern Andhra Pradesh, India

DEEPA JAISWAL, SOMESH BANERJEE♥
Freshwater Biology Regional Center, Zoological Survey of India. Hyderabad, 500048, Telangana, India. Tel.: +91-33-24008595,
♥email: banerjeesomesh49@gmail.com

Manuscript received: 6 October 2023. Revision accepted: 6 January 2024.

Abstract. *Jaiswal D, Banerjee S. 2024. Notes on Gerridae (Hemiptera: Heteroptera: Gerromorpha) from the Eastern Ghats of Telangana and Northern Andhra Pradesh, India. Nusantara Bioscience 16: 43-53.* Gerridae is the family of semi-aquatic bugs found in both the lentic and lotic freshwater bodies. The present study focused on the Gerridae from the Eastern Ghats of Telangana and Northern Andhra Pradesh, India. This study documented a total number of 16 species belonging to 13 genera and 7 subfamilies under the family Gerridae. *Tenagogonus nicobarensis* Andersen, 1964, was earlier described from Andaman and Nicober islands and also known to be endemic to that particular geographical area. We are recording this species for the first time from the mainland of the Indian subcontinent. *Ventidius aquarius* Distant, 1910 was also recorded for the first time during this present study from the Eastern Ghats, an endemic species to peninsular India. Another species, *Naboandelus signatus* Distant, 1910 is also recorded from the Eastern Ghats of Andhra Pradesh as well as an addition to the state fauna of Andhra Pradesh. It is a widespread species and reported from both central and northeastern India. In southern India, it was reported from the two states and present record will be the additional third state to its distribution. In addition to taxonomic details, the article covers the geographic distribution of the 16 species. This study has also led to the addition of nine species of Gerridae to the state fauna of Andhra Pradesh.

Keywords: Distributions, Eastern Ghats, India, new records, semi-aquatic bugs

INTRODUCTION

The Eastern Ghats, also known as Kizhakku thodarchi malaigal, Prva Gha, or toorpu kanumalu in the south, are a discontinuous series of mountains along India's eastern coast. It spans five states, including Odisha, Andhra Pradesh, Telangana, Karnataka, and Tamil Nadu, and is located between 76° 50' E and 86° 30' E Longitudes and 11° 30' N and 22° 0' N Latitudes. It is substantially older than the Western Ghats and has a complex geologic history related to the formation and dissolution of the ancient supercontinent of Rodinia and the formation of the Gondwana supercontinent (ENVIS 2023). It is divided into three regions: the northern area from Odisha to Guntur, the central section from Guntur to the Tamil Nadu border, and the southern section wholly in Tamil Nadu (Legris and Meher 1982). The Eastern Ghats are a mix up of various ecoregions that run from south to north along India's east coast. Eastern Highlands wet deciduous forests, East Deccan dry evergreen forests, Deccan thorn scrub forests, shrub lands, and South Deccan Plateau dry deciduous forests are the most important ecoregions (ENVIS 2023).

The term "aquatic bugs" refers to freshwater hemipterans, which are mostly adapted to aquatic environments. Based on their preferred habitats and niches, the water bugs, members of the suborder Heteroptera (known as true bugs), are classified into three infraorders: Nepomorpha, Gerromorpha, and Leptopodomorpha. As predators, scavengers, or collectors, they are essential to freshwater environments and have a significant impact on the food web. Compared to Nepomorpha, the Gerromorphan has a smaller fossil record. The Nepomorphan has a vast fossil record. Nepomorpha and Leptopodomorpha are members of the sister group of the Panheteroptera, known as Gerromorpha (Schuh and Slater 1995).

The world's aquatic insect biota is largely composed of aquatic and semi-aquatic Heteroptera, or water bugs. Heteroptera suborder (Insecta, Hemiptera) members are found all over the world and inhabit a diverse range of environments (Schuh and Slater 1995; Gullan and Cranston 2017). The Heteroptera infraorders Gerromorpha, Leptopodomorpha, and Nepomorpha are associated with water bodies (Nieser and Melo 1997; Panizzi and Grazia 2015). Small to medium-sized, semiaquatic insects belong to the infraorder Gerromorpha and are typically found near the edges or on the surface of freshwater bodies (Andersen 1982; Dias-Silva et al. 2009, 2013).

Currently, eight families and about 160 genera comprise the more than 2,100 species of Gerromorpha that are known to exist globally (Polhemus and Polhemus 2008). The Infraorder Gerromorpha is a group of semi-aquatic insects that can be recognized by long, conspicuous antennae that are placed in front of the eyes and longer than the head. Except the coldest and driest regions, they are found throughout all climatic zones (Thirumalai 2002). Eight families make up this infraorder: Hermatobatidae, Veliidae, Paraphrynoveliidae, Mesoveliidae, Hebridae, and Gerridae (Andersen 1964). Of the eight families mentioned above, there are currently no records of Paraphrynoveliidae, Macroveliidae, or Hermatobatidae from India

(Subramanian and Basu 2017).

The family Gerridae commonly known as water striders belonging to the superfamily Gerroidea, predatory water bugs, which suck body fluids of live and partly dead insects (Jehamalar and Chandra 2013a,b). They occur in diverse habitats both in lentic (lakes, ponds, pools, reservoirs, agricultural fields and temporary waters) and lotic ecosystems (streams, seepage, springs, rivers and irrigation canals). According to Polhemus and Polhemus (2008), there are more than 751 species belonging to 67 genera belonging to the family Gerridae known from the world. Whereas from the oriental region, more than 287 Gerridae species are documented so far, which is around 38% of the total reported species in this family. Thirumalai (2002) documented 77 species belonging to 27 genera under 7 subfamilies belonging to the family Gerridae from India. Later, Subramanian and Basu (2017) did study on aquatic and semi-aquatic Hemiptera from India and documented 93 species of family Gerridae belonging to 26 genera. After several studies done on this family, around 109 species were recorded from India (Basu et al. 2018a,b,c; Jehamalar et al. 2018a,b, 2023; Chandra et al. 2020, 2022; Jehamalar and Chandra 2020; Jehamalar and Dash 2021; Lyngdoh et al. 2021). Bal (2007) made a taxonomic account of the aquatic and semi-aquatic bugs from Andhra Pradesh and recorded 31 species belonging to 16 genera and 8 families, where he mentioned 8 species under 5 genera and 3 subfamilies belonging to the family Gerridae, whereas, only 8 species and 6 genera were documented under this family from Telangana after the bifurcation from Andhra Pradesh (Chandra et al. 2021). This study made an attempt to assess the Gerridae species, their status of diversity and their distribution from freshwater bodies of parts of the Eastern Ghats of Telangana and northern Andhra Pradesh.

MATERIALS AND METHODS

Study area

Throughout the past years, aquatic and semi-aquatic Hemiptera were studied from different parts from India, mainly from central, eastern parts and some southern, north and north eastern parts. At the same time these bugs were documented from parts of Western Ghats also. Eastern Ghats are left from extensive studies. Semi-aquatic bugs were collected from 46 sampling locations from the Eastern Ghats of Telangana and northern Andhra Pradesh (Table 1). There has been an extensive study carried out in those said localities between July 2021 and January 2023 (Figure 1).

Collection and preservation

Long-handled round nylon water nets with long handles were used for collecting the specimens. The specimens were preserved in 70% ethyl alcohol and stored in glass vials of 50 ml. For better results, aquatic and semi-aquatic bugs are collected using both qualitative and quantitative methods. A qualitative strategy was used to obtain a greater number of species from various collection locations. All collecting sites were swept three times for quantitative analysis, and the materials were preserved in glass vials for future research. After arriving at the laboratory, all specimens were identified to the species level, and each species was numbered from each collection locality for quantification. The species abundance, richness, and diversity indices were calculated using the statistical software PAST 4.03.

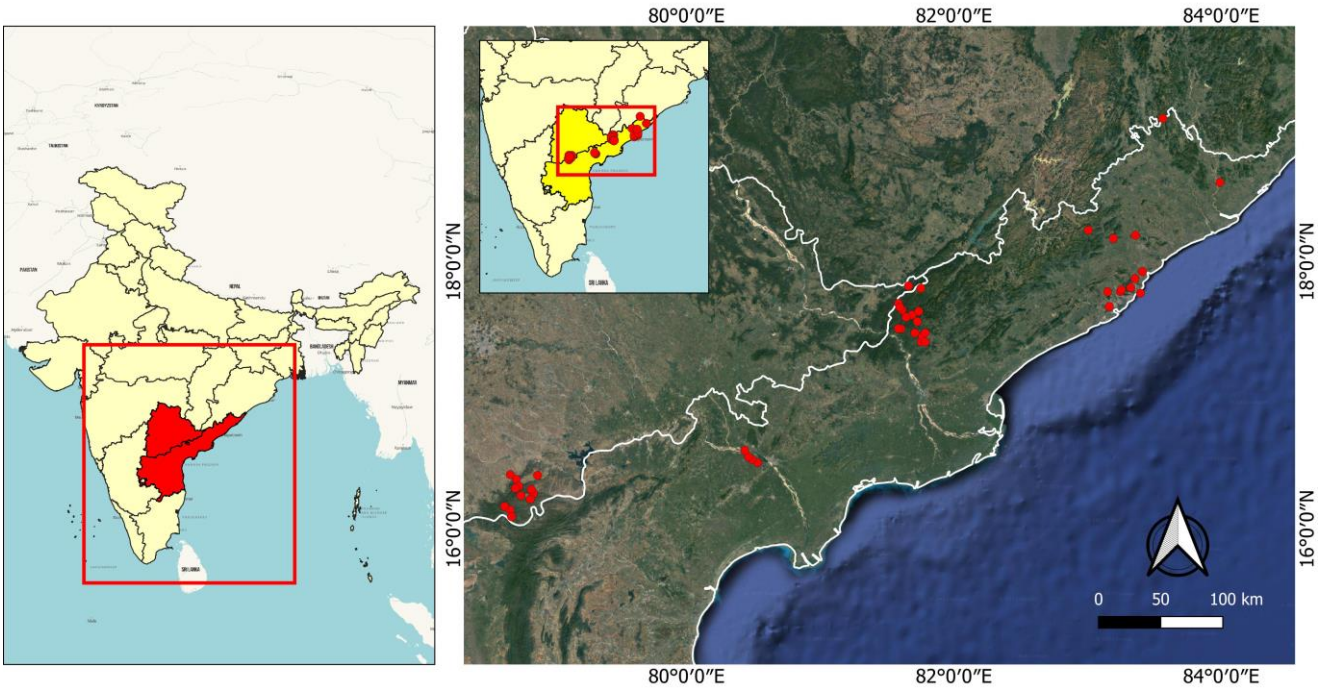

Figure 1. Survey locations in Andhra Pradesh and Telangana of India and points indicating the survey localities throughout the Eastern Ghats of both states

Table 1. Collection locations throughout the Eastern Ghats of Telangana and northern Andhra Pradesh, India

Locations	District	State	Coordinates	Elevation (m)
Mallela Theertham waterfalls	Nagarkurnool	Telangana	16°16’02.0” N, 78°51’21.9” E	673
Bairampally	Nagarkurnool	Telangana	16°8'33.72" N, 78°40'52.68" E	756
Bolghatpally	Nagarkurnool	Telangana	16°24'7.92" N, 78°53'9.96" E	592
Nadimpally	Nagarkurnool	Telangana	16°24'25.2" N, 78°40'55.92' E	463
Octopus view point	Nagarkurnool	Telangana	16°13’22.5” N, 78°49’53.9” E	801
Mannanur	Nagarkurnool	Telangana	16°19’12” N, 78°44’44” E	791
Pichakuntla Cheruvu	Nagarkurnool	Telangana	16°5’31.8” N, 78°41’29.5” E	514
Saleshwarama	Nagarkurnool	Telangana	16°10’11.09” N, 78°38’21.69” E	725
Maisamma loddi	Nagarkurnool	Telangana	16°18’18” N, 78°43’14” E	730
Ramapenta	Nagarkurnool	Telangana	16°17’45” N, 78°50’21” E	586
Umamaheshwarama	Nagarkurnool	Telangana	16°22’21” N, 78°43’38” E	544
Mulliguda	Alluri Sitharama Raju	Andhra Pradesh	19°4'18.84" N, 83°33'48.96" E	337
Barangi village	Alluri Sitharama Raju	Andhra Pradesh	17°24'1.44" N, 81°45'19.8" E	149
Bhupathipalem reservoir	Alluri Sitharama Raju	Andhra Pradesh	17°26'40.56" N, 81°45'54.36" E	214
Koyalagudam	Alluri Sitharama Raju	Andhra Pradesh	17°29'54.6" N, 81°36'15.48" E	410
Anampalli	Alluri Sitharama Raju	Andhra Pradesh	17°28'1.56" N, 81°42'30.24" E	307
Kintukuru base camp	Alluri Sitharama Raju	Andhra Pradesh	17°29'58.56" N, 81°35'5.28" E	116
Stream near Kintukuru base camp	Alluri Sitharama Raju	Andhra Pradesh	17°28'1.2" N, 81°42'29.88" E	305
Near Coffee plantation	Alluri Sitharama Raju	Andhra Pradesh	17°36'5.04" N, 81°41'16.44" E	502
GM Vallasa	Alluri Sitharama Raju	Andhra Pradesh	17°35'5.64" N, 81°38'33" E	468
Maredumilli	Alluri Sitharama Raju	Andhra Pradesh	17°33'6.48" N, 81°43'38.28" E	520
Pamulamaredi	Alluri Sitharama Raju	Andhra Pradesh	17°48'5.4" N, 81°45'14.4" E	1045
Thatipudi reservoir	Alluri Sitharama Raju	Andhra Pradesh	18°10'28.92" N, 83°11'36.24" E	114
Jala Tharangini waterfalls	Alluri Sitharama Raju	Andhra Pradesh	17°49'8.04" N, 81°39'39.96" E	277
Amrutadhara waterfalls	Alluri Sitharama Raju	Andhra Pradesh	17°38'21.48" N, 81°36'47.16" E	629
Near Tiger club	Alluri Sitharama Raju	Andhra Pradesh	17°41'16.08" N, 81°35'8.16" E	484
Ijjaluru	Alluri Sitharama Raju	Andhra Pradesh	17°39'32.76" N, 81°35'47.4" E	614
Sivalingapuram	Visakhapatnam	Andhra Pradesh	18°14'7.0794" N, 83°0'25.2" E	990
Relli Lake	Visakhapatnam	Andhra Pradesh	17°48'22.68" N, 83°19'24.9594" E	135
Mudasarlova reservoir	Visakhapatnam	Andhra Pradesh	17°45'50.75" N, 83°23'46.3194" E	12
Gambheeram gadda reservoir	Visakhapatnam	Andhra Pradesh	17°52'25.67" N, 83°21'18.01" E	55
KB reservoir	Visakhapatnam	Andhra Pradesh	17°39'52.91" N, 83°9'47.88" E	285
Koneru	Visakhapatnam	Andhra Pradesh	17°46'36.48" N, 83°14'47.76" E	74
Adidavaram cheruvu	Visakhapatnam	Andhra Pradesh	17°47'23.27" N, 83°15'14.7594" E	199
Meghadri gadda reservoir	Visakhapatnam	Andhra Pradesh	17°46'28.91" N, 83°9'3.9594" E	53
Gosthani river	Visakhapatnam	Andhra Pradesh	17°55'36.83" N, 83°24'41.04" E	36
Kakru Nelivada roadside	Alluri Sitharama Raju	Andhra Pradesh	18°11'51.72" N, 83°21'29.5194" E	99
Near AP Secretariate	Guntur	Andhra Pradesh	16°29'51.71" N, 80°31'56.28" E	45
Near AP High Court	Guntur	Andhra Pradesh	16°31'13.43" N, 80°29'22.2" E	47
Thullur	Guntur	Andhra Pradesh	16°32'26.52" N, 80°27'50.76" E	47
Guntivada	Alluri Sitharama Raju	Andhra Pradesh	18°35'34.73" N, 83°59'27.30" E	104
Kondavada	Alluri Sitharama Raju	Andhra Pradesh	17°37'43.81" N, 81°44'15.64" E	494
Ananthavaram	Guntur	Andhra Pradesh	16°35'19.31" N, 80°26'10.31" E	45
Vatavarlapally pond	Nagarkurnool	Telangana	16°15'01.17" N, 78°45'45.61"E	825
Rampa waterfalls	Alluri Sitharama Raju	Andhra Pradesh	17°28'02.87" N, 81°47'09.59" E	276
Pala Kalwa	Alluri Sitharama Raju	Andhra Pradesh	17°23'58.88" N, 81°47'9.72" E	141

Identification

Each individual was examined under a stereo-zoom binocular microscope, Olympus SZX10 and photographed under Leica M205A. Identification was done following standard literature by Gupta (1981), Chen and Zettel (1999), Thirumalai (1986, 1999, 2002), Bal and Basu (1994), Jehamalar and Chandra (2013a,b, 2016), Subramanian and Basu (2017), Basu et al. (2018a,b,c). All the identified specimens were registered and deposited in the National Zoological Collections of Zoological Survey of India, Freshwater Biology Regional Centre, Hyderabad.

RESULTS AND DISCUSSION

We examined semi-aquatic bugs of the family Gerridae from the Eastern Ghats in the Telangana districts of Nagarkurnool and Nalgonda, as well as the Andhra Pradesh districts of Alluri Sitharama Raju, Guntur, and Visakhapatnam. During the collection periods, all of the collection locations cover freshwater bodies, small ponds, reservoirs, and rocky streams. There were 16 species identified from 46 sites surveyed, representing 13 genera and 7 subfamilies. These locations were located in both protected and non-protected areas of both states. Collection location wise species distribution was discussed in Table 2.

Table 2. Location wise species distribution

Locations/species	*C. Productus*	*A. Kumari*	*O. Rhexenor*	*A. Adelaidis*	*G. Nepalensis*	*N. Parvulus*	*L. Fossarum fossarum*	*L. Nitidus*	*L. Fluviorum*	*T. Nicobarensis*	*M. Communis*	*M. Communoides*	*V. Aquarius*	*P. Agriodes*	*R. Kraepelini*	*N. Signatus*
Mallelatheertham waterfalls	+	+						+	+		+			+		
Bairampally							+	+								
Bolghatpally							+									
Nadimpally							+	+								
Octopus view point							+	+								
Mannanur							+									
Pichakuntla Cheruvu								+			+					
Saleshwarama									+		+			+		
Maisamma loddi									+							
Ramapenta											+					
Umamaheshwarama												+				
Mulliguda									+		+			+		
Barangi village	+															
Bhupathipalem reservoir	+							+								
Koyalagudam														+		
Anampalli	+													+		
Kintukuru base camp	+	+							+	+	+		+	+		
Stream near Kintukuru base camp	+												+			
Near Coffee plantation	+												+			
GM Vallasa	+									+	+					
Maredumilli	+															
Pamulamaredi														+		
Thatipudi reservoir	+				+						+			+		+
Jala Tharangini waterfalls														+		
Amrutadhara waterfalls														+		
Near Tiger club	+													+		
Ijjaluru														+		
Sivalingapuram														+		
Relli Lake				+												
Mudasarlova reservoir									+							
Gambheeram gadda reservoir							+	+								
KB reservoir				+												
Koneru				+												
Adidavaram cheruvu			+	+	+		+		+							
Meghadri gadda reservoir							+	+								
Gosthani river							+									
Kakru Nelivada roadside										+						
Near AP Secretariate							+	+								
Near AP High Court							+									
Thullur							+	+								
Guntivada	+					+		+					+			
Kondavada	+										+		+			
Ananthavaram															+	
Vatavarlapally pond															+	
Rampa waterfalls							+	+						+		
Pala Kalwa								+						+		

Nine species were documented as new records from the Andhra Pradesh state fauna, out of the 16 species that were found in this study. Among the six subfamilies, Gerrinae dominated with seven species, followed by Halobatinae with three and Eotrechinae with two species. *Ptilomera agriodes* Schmidt, 1926 was the most abundant species (Figure 2), according to all survey locations, followed by *Metrocoris communis* Distant, 1910 and *Limnogonus fossarum fossarum* Fabricius 1775). Two species were collected from a single location, *Naboandelus signatus* Distant, 1910 from the subfamily Trapobatinae and *Metrocoris communoides* Chen & Nieser, 1993 of subfamily Halobatinae. These two species are very rare to be collected and *M. Communoides* is often overlooked with misidentification with *M. Communis* as there is very little difference in the paramere structure between them.

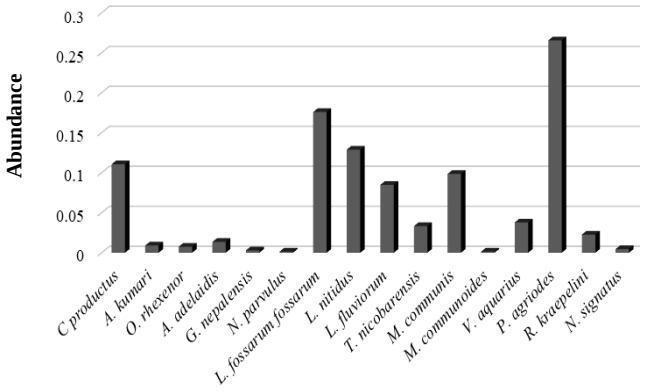

Figure 2. Illustration of species abundance from the study sites.

Another species *N. Signatus* also collected from single location in Andhra Pradesh with only two individuals along with the *M. Communis*. It was observed that *N. Signatus* was restricted to a single site within Andhra Pradesh's Papikonda National Park (Table 2). One specimen each of the two species, *M. Communoides* and *N. Parvulus*, has been collected from a single collection location.

Systematic account

Order Hemiptera Linnaeus, 1758

Family Gerridae Leach, 1815

Subfamily Cylindrostethinae Matsuda, 1960

Cylindrostethus productus (Spinola, 1840) (Figure 3.A)

Gerris productus Spinola, 1840, 2: 184, Syntype ♂. – Museum of Natural History, London.

Material examined: 4♂, 5♀, 24.xii.2021, Mallelatheertham waterfalls; 5♂, 5♀, 16.vii.2021, Bhupathipalem reservoir; 3♂, 6♀, 18.vii.2021, Tiger club; 1♂, 3♀, 17.vii.2021, Barangi village; 1♂, 5.xii.2021, Kondavada; 1♂, 2♀, 20.i.2022, Guntivada; 4♂, 5♀, 7.xii.2021, Anampalli; 1♂, 7.xii.2021, 4♂, 3♀, 30.vii.2022, Kintukuru base camp; 2♂, 3♀, 7.xii.2021, Stream near Kintukuru base camp; 1♀, 31.vii.2022, Coffee plantation; 2♂, 3♀, 31.vii.2022, Gm Vallasa; 2♂, 31.vii.2022, Maredumilli; 2♂, 5♀, 27.vii.2022, Thatipudi reservoir, Coll. Dr. Deepa and Somesh.

Distribution: India: Andhra Pradesh (New record), Chhattisgarh, Karnataka, Kerala, Madhya Pradesh, Maharashtra, Odisha, Punjab, Tamil Nadu (Jehamalar and Chandra 2016); Telangana (Chandra et al. 2021); Uttarakhand, Uttar Pradesh and West Bengal (Jehamalar and Chandra 2016). **Elsewhere:** Nepal and Sri Lanka (Jehamalar and Chandra 2016).

Subfamily Eotrechinae Matsuda, 1960

Amemboa* (*Amemboa*) *kumari (Distant, 1910) (Figure 3.B)

Onychotrechus kumari Distant, 1910, 5: 145, Holotype ♂. – Travancore, Kerala.

Material examined: 2♂, 3♀, 24.xii.2021, Mallelatheertham waterfalls; 1♂, 7.xii.2021. Kintukuru base camp, Coll. Dr. Deepa and Somesh.

Distribution: India: Andhra Pradesh (New record), Chhattisgarh, Karnataka, Kerala, Madhya Pradesh, Odisha, Tamil Nadu (Chandra et al. 2020); Telangana and West Bengal (Chandra et al. 2020).

Remark: It is an endemic species of the Indian subcontinent with wide distribution in Peninsular India.

Onychotrechus rhexenor Kirkaldy, 1903 (Figure 3.C)

Onychotrechus rhexenor Kirkaldy, 1903, 44: 108, Holotype ♂. – Museum of Natural History, London.

Material examined: 2♂, 3♀, 24.vii.2022, Adidavaram Cheruvu, Coll. Dr. Deepa and Somesh.

Distribution: India: Andhra Pradesh (New record), Chhattisgarh, Karnataka, Kerala, Maharashtra, Rajasthan, Tamil Nadu (Chandra et al. 2020) and Telangana. **Elsewhere:** Socotra Island (Chandra et al. 2020).

Subfamily Gerrinae Bianchi, 1896

Aquarius adelaidis **(**Dohrn, 1860) (Figure 3.D)

Gerris adelaidis Dohrn, 1860, 21: 408, Holotype ♂. – Natural History Museum, Leipzig

Material examined: 2♂, 20.viii.2022, Relli lake; 1♂, 2♀, 24.vii.2022, Koneru; 1♂, 19.vii.2022, KB reservoir; 3♂, 2♀, 24.viii.2022, Adidavaram Cheruvu, Coll. Dr. Deepa and Somesh.

Distribution: India: Andhra Pradesh, Bihar, Chhattisgarh, Karnataka, Kerala, Madhya Pradesh, Maharashtra, Manipur, Meghalaya, Mizoram, Odisha, Punjab, Rajasthan, Sikkim, Tamil Nadu, Telangana, Uttarakhand, Uttar Pradesh and West Bengal (Chandra et al. 2021). **Elsewhere:** Bangladesh, China, Indonesia, Laos, Malaysia, Myanmar, Nepal, Pakistan, Singapore, Sri Lanka, Thailand and Vietnam (Chandra et al. 2020).

Gerris* (*Gerris*) *nepalensis Distant, 1910 (Figure 3.K)

Gerris nepalensis Distant, 1910, 5 (8): 142, Holotype ♂. – Kathmandu, Nepal.

Material examined: 1♂, 27.vii.2022, Thatipudi reservoir; 1♂, 24.vii.2022, Adidavaram Cheruvu, Coll. Dr. Deepa and Somesh.

Distribution: India: Andhra Pradesh (New record), Arunachal Pradesh, Jammu and Kashmir, Madhya Pradesh, Sikkim, and Uttar Pradesh (Chandra et al. 2020). **Elsewhere:** Bangladesh, China, Japan, Myanmar, Nepal, North Korea, Russia, South Korea, Taiwan, Thailand and Vietnam (Chandra et al. 2020).

Neogerris parvulus (Stål, 1859) (Figure 3.E)

Gerris parvula Stål, 1859, 265: 107, Holotype ♂. – Naturhistoriska Riksmuseet.

Material examined: 1♂, 5.xii.2021, Guntivada, Coll. Dr. Deepa and Somesh.

Distribution: India: Andhra Pradesh, Bihar, Chhattisgarh, Karnataka, Kerala, Madhya Pradesh, Arunachal Pradesh, Assam, Odisha, Pondicherry, Tamil Nadu, Telangana, Uttar Pradesh and West Bengal (Chandra et al. 2020). **Elsewhere:** Bangladesh, China, Iran, Japan, Java, Malay Peninsula, Myanmar, New Guinea, Oman, Philippines, Pakistan, Singapore, Sri Lanka, Solomon Islands, Taiwan and Vietnam (Chandra et al. 2020).

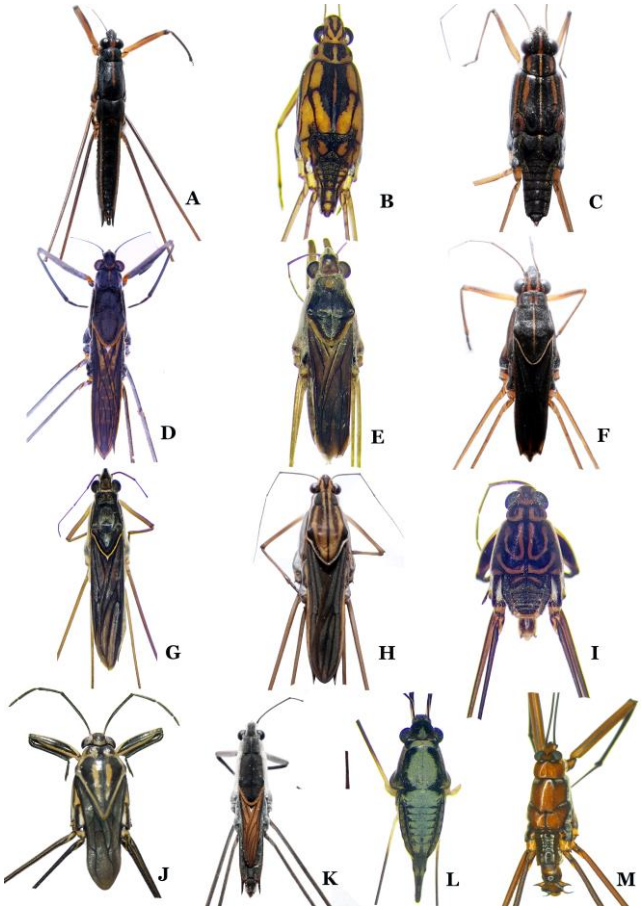

Figure 3. A. *C. Productus* (Spinola, 1840); B. *A. Kumari* (Distant, 1910); C. *O. Rhexenor* Kirkaldy, 1903; D. *A. Adelaidis* (Dohrn, 1860); E. *N. Parvulus* (Stal, 1859); F. *L. Fossarum fossarum* (Fabricius, 1775); G. *L. Nitidus* (Mayr, 1865); H. *L. Fluviorum* (Fabricius, 1798); I. *M. Communis* Distant, 1910; J. *M. Communoides* Chen & Nieser 1993; K. *Gerris nepalensis* Distant, 1910; L. *R. Kraepelini* Breddin, 1905; M. *P. Agriodes* Schmidt, 1926.

Limnogonus (Limnogonus) fossarum* subsp. *Fossarum (Fabricius, 1775) (Figure 3.F)

Cimex fossarum Fabricius, 1775, 727: 105, Holotype ♂. – Zoological Museum, University of Copenhagen.

Material examined: 1♀, 22.xii.2021, Bairampally; 2♂, 20.xii.2021, Bolghatpally; 15♂, 21♀, 21.xii.2021, Nadimpally; 1♀, 3.x.2020, Octopus view point; 1♂, 3♀, 15.vii.2021, Rampa waterfalls; 6♂, 3♀, 3.x.2020, Mannanur; 18♂, 11♀, 31.xii.2020, pond near AP Secretariat; 4♂, 3♀, 25.ii.2023, Thullur; 1♂, 25.ii.2023, pond near AP High Court; 2♂, 3♀, 22.xii.2020, Gambheeram gadda reservoir; 1♀, 12.xii.2020, Pushkar ghat; 6♂, 3♀, 19.vii.2022, Meghadri gadda reservoir; 5♂, 4♀, 24.vii.2022, Adidavaram Cheruvu; 1♂, 1♀, 21.ii.2023, Gosthani River, Coll. Dr. Deepa and Somesh.

Distribution: India: Andaman & Nicobar Islands, Andhra Pradesh, Arunachal Pradesh, Assam, Bihar, Chandigarh, Chhattisgarh, Delhi, Goa, Haryana, Himachal Pradesh, Jammu & Kashmir, Karnataka, Kerala, Madhya Pradesh, Maharashtra, Manipur, Odisha, Pondicherry, Punjab, Rajasthan, Tamil Nadu, Telangana and West Bengal (Chandra et al. 2020). **Elsewhere:** Bangladesh, China, Hong Kong, Indonesia, Japan, Malay Peninsula, Myanmar, Philippines, Singapore, Sri Lanka, Taiwan, Thailand and Vietnam (Chandra et al. 2020).

Limnogonus* (*Limnogonus*) *nitidus (Mayr, 1865) (Figure 3.G)

Hydrometra nitida Mayr, 1865, 443: 105, Holotype ♂. – Narurhistorisches Museum Wien.

Material examined: 2♂, 1♀, 31.xii.2020, pond near AP Secretariat; 6♂, 3♀, 15.xi.2021, Ananthavaram; 1♀, 15.xi.2021, Thullur; 2♀, 15.xi.2021, pond near AP high Court; 2♂, 2♀, 4.xii.2021, Bhupathipalem reservoir; 9♂, 4.xii.20221, Pala Kalwa; 4♂, 9♀, 5.xii.2021, Guntivada; 2♂, 22.xii.2020, Gambheeram gadda reservoir; 2♂, 1♀, 19.vii.2022, Meghadri gadda reservoir; 4♂, 21.xii.2021, Pichakuntla Cheruvu; 5♂, 3♀, 22.xii.2021, Bairampally; 3♀, 21.xii.2021, Nadimpally; 2♂, 1♀, 24.xii.2021, Mallelatheertham waterfalls; 2♂, 3.x.2020, Octopus view point; 8♂, 11♀, 15.vii.2021, Rampa waterfalls, Coll. Dr. Deepa and Somesh.

Distribution: India: Andaman & Nicobar Islands, Andhra Pradesh, Arunachal Pradesh, Assam, Bihar, Chandigarh, Chhattisgarh, Delhi, Himachal Pradesh, Karnataka, Kerala, Madhya Pradesh, Maharashtra, Manipur, Meghalaya, Mizoram, Odisha, Rajasthan, Sikkim, Tamil Nadu, Tripura, Uttarakhand, Uttar Pradesh, Telangana and West Bengal (Chandra et al. 2020). **Elsewhere:** Bangladesh, Bhutan, China, Indonesia, Laos, Maldives, Malaysia, Myanmar, Nepal, Singapore, Sri Lanka, Thailand and Vietnam (Chandra et al. 2020).

Limnometra fluviorum (Fabricius, 1798) (Figure 3.H)

Cimex fluviorum Fabricius, 1798, 2: 177, Lectype ♂. – Museum of Natural History, London.

Material examined: 2♂, 3♀, 14.ii.2020, 7♂, 9♀, 24.xii.2021, Mallelatheertham waterfalls; 7♂, 5♀, 12.ii.2020, 3♀, 10.viii.2021, Saleshwaram; 1♂, 1♀, 22.ix.2020, Maisamma loddi; 3♂, 3♀, 5.xii.2021, Guntivada; 1♂, 1♀, Mulliguda; 1♀, 30.vii.2022, Kintukuru base camp; 3♂, 3♀, 24.vii.2022, Adidavaram Churuvu; 3♀, 19.vii.2022, Mudasarlova reservoir, Coll. Dr. Deepa and Somesh.

Distribution: India: Andhra Pradesh, Chhattisgarh, Karnataka, Kerala, Madhya Pradesh, Maharashtra, Odisha, Puducherry, Tamil Nadu, Telangana and West Bengal (Chandra et al. 2020). **Elsewhere:** Reunion Islands, Sri Lanka (Chandra et al. 2020).

Tenagogonus nicobarensis Andersen, 1964 (Figure 4.A-D)

Tenagogonus nicobarensis Andersen, 1964, 32: 321–334, Holotype ♂. – Andaman Islands, India.

Material examined: 1♂, 15.xi.2019, Stream near Kakru Nelivada Road, Vijianagram, 18°11'51.72"N, 83°21'29.52"E, Coll. Dr. Boni AL; 7♂, 5♀, 30.vii.2022, Kintukuru Base camp, 17°29'58.56"N, 81°35'5.28"E; 4♂, 5♀, 31.vii.2022, GM Vallasa, 17°35'5.64"N, 81°38'33"E, Alluri Sitharama Raju, Andhra Pradesh, Coll. Dr. Deepa and Somesh.

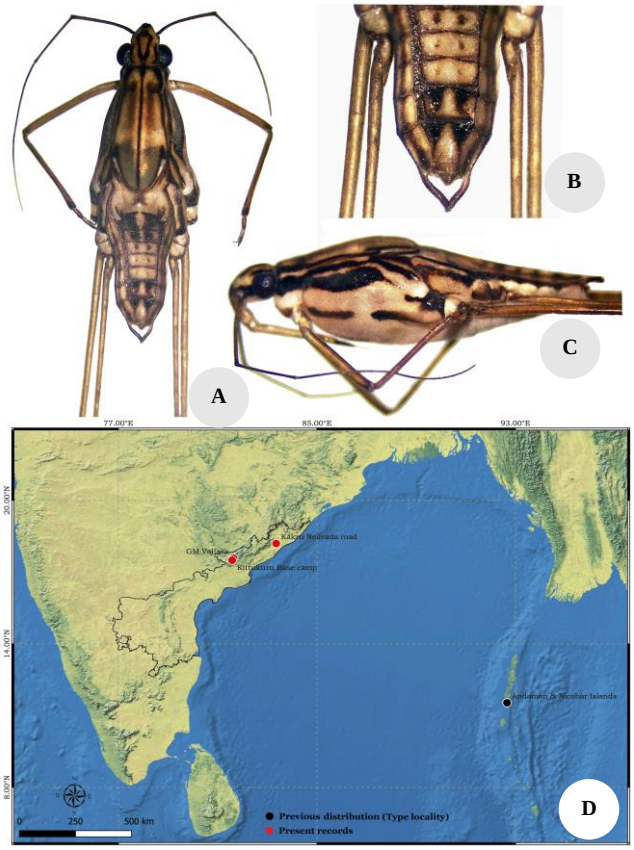

Figure 4. A-C. *Tenagogonus nicobarensis* Andersen, 1964; A. Male (habitus), dorsal view, B. Terminal abdominal segment of female, dorsal view, C. Male (habitus), lateral view; D. Global distribution with present record

Diagnosis: Average male body length in apterous form 6.67 mm, and female 7.14 mm. Body colour creamy white on the ventral and yellowish brown on the dorsal side (Figure 4.A). Head with four black stripes. Mesopleuron with two stripes, the outer one being wider. The black band on the lateral area of mesosternum. Male devoid of lateral processes of seventh sternum (connexival spines) and females with long connexival processes (Figure 4.B). A male ninth sternum has two sheath-like structures on its anterior surface below a broad longitudinal depression.

Distribution: India: Andaman & Nicobar Islands (Jehamalar and Chandra 2013a), Andhra Pradesh (New record).

Remark: In previous studies, *T. Nicobarensis* was only reported from its type locality on the Andaman Islands and a few Nicobar groups of Islands and later on, it was further reported from South Andaman Island but lacks its distribution in the Great Nicobar Islands (Jehamalar and Chandra 2013a, 2020). We have collected this species from the fast-flowing rocky streams along with another species group, *L. Fluviorum* Fabricius, 1798. They were scattered together in the stream near the base camp at Kintukuru and on the roadside of a small stream at Kakru Nelivada road. This species is endemic to the Indian subcontinent, as previously reported only from the Andaman and Nicobar Islands, however its range is now being expanded to the Indian mainland as well.

Subfamily Halobatinae Matsuda, 1960

Metrocoris communis **(**Distant, 1910) (Figure 3.I)

Euodus communis Distant, 1910, 151: 112, Holotype ♂. – Museum of Natural History, London.

Material examined: 3♂, 1♀, 21.xii.2021, Pichakuntla Cheruvu; 7♂, 8♀, 24.xii.2021, Mallelatheertham waterfalls; 2♀, 18.iii.2019, Ramanapenta; 1♂, 25.i.2018, Saleshwaram; 1♂, 5.xii.2021, Kondavada; 8♂, 11♀, 7.xii.2021, 3♂, 2♀, 30.vii.2022, Kintukuru base camp; 4♂, 3♀, 5.xii.2021, Guntivada; 2♂, 28.vii.2022, Mulliguda; 1♀, 31.vii.2022, GM Vallasa; 5♂, 3♀, 27.vii.2022, Thatipudi reservoir, Coll. Dr. Deepa and Somesh.

Distribution: India: Andhra Pradesh (New record), Chhattisgarh, Karnataka, Madhya Pradesh, Maharashtra, Rajasthan, Tamil Nadu, Telangana and Uttar Pradesh (Chandra et al. 2020). **Elsewhere:** Afghanistan, Iran, Iraq and Oman (Chandra et al.2020).

Metrocoris communoides Chen and Nieser, 1993 (Figure 3.J)

Metrocoris communoides Chen & Nieser, 1993, 19 (2): 51, Holotype ♂. – Tamil Nadu, India.

Material examined: 1♂, 20.xii.2021, Umamaheshwaram temple, Coll. Dr. Deepa and Somesh.

Distribution: India: Himachal Pradesh, Odisha, Tamil Nadu (Basu et al. 2015), Madhya Pradesh (Chandra et al. 2020) and Telangana (Chandra et al. 2021).

Remark: It is an endemic species to the Indian subcontinent, described from Tamil Nadu and distributed mainly in Deccan peninsular region.

Ventidius **(*Ventidius*)** ***aquarius*** Distant, 1910 (Figure 5.A-C)

Ventidius aquarius Distant, 1910, 156-158, Holotype ♂. – Travancore, Kerala.

Material examined: 3♂, 31.vii.2021, Coffee plantation, 17°35'21.84"N, 81°40'37.92"E; 1♂, 30.vii.2022, Kintukuru Base camp, 17°29'58.56"N, 81°35'5.28"E; 4♂, 3♀, 05.xii.2021, Stream near Guntivada, 17°39'11.88"N, 81°42'50.4"E; 2♂, 3♀, 05.xii.2021, Stream near Kondavada, 17°31'29.37"N, 81°39'18.71"E; 4♂, 5♀, 07.xii.2021, stream near Kittukuru base camp, 17°29'58.56"N, 81°35'17.16"E; Alluri Sitharama Raju, Andhra Pradesh, Coll. Dr. Deepa and Somesh.

Diagnosis: The average male body length 3.45 mm and for females its 3.66 mm. The entire body is conspicuously bright yellowish or light greenish, with prominent dark stripes. Brown to blackish eyes with a brown inner rim. Pronotum is likewise yellowish, with dark lateral lines on the anterior and posterior margins. A single black, tiny rod-shaped structure formed just before the fifth abdominal segment, and the dorsal section of the body was covered with black patterns at the margin. In macropterous form, the dorsal half of the body has a black "T"-shaped structure. The intersegmental morphology between the meso and metanotum is distinct, and the mesonotum is inflated. Parameres are small, symmetrical, cucumber-shaped, and with a blunt apex.

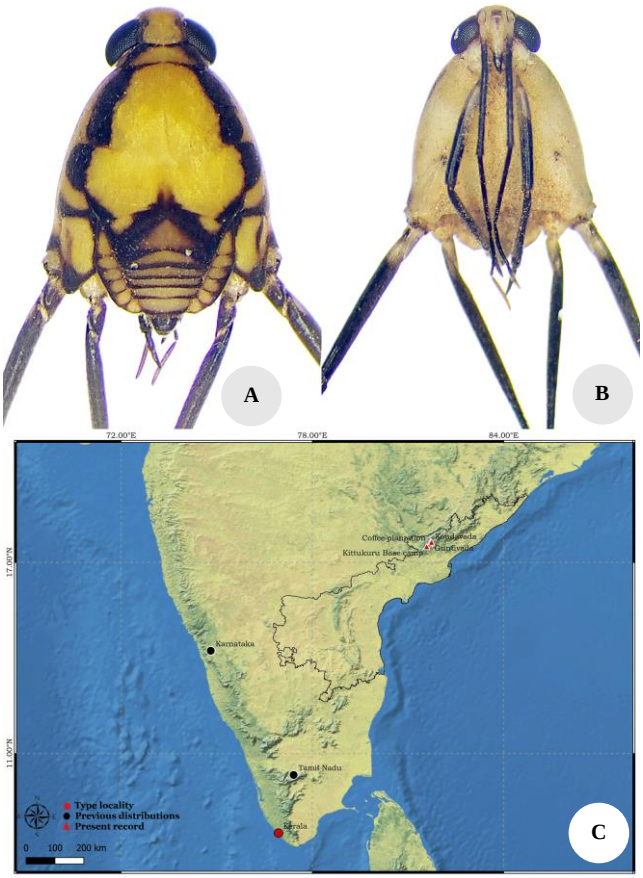

Figure 5. A-B. *Ventidius aquarius* Distant, 1910; Male habitus (A. Dorsal view, B. Ventral view); C. Distribution throughout India.

Distribution: India: Andhra Pradesh (New record); Karnataka, Kerala and Tamil Nadu (Thirumalai 2002). **Elsewhere:** Sri Lanka (Thirumalai 2002).

Remark: This species was collected from a moderately flowing rocky stream inside the Papikonda National Park. At three locations, i.e. Kittukuru base camp, a small stream near Guntivada, and stream near Kondavada, we have collected this species along with *M. Communis*. All of the collection sites were small, rocky streams with ankle-deep or less water in the month of December and knee-high or higher water in the month of July. But in July, we found this species in an area with very shallow water.

Subfamily Ptilomerinae Bianchi, 1896

Ptilomera* (*Ptilomera*) *agriodes Schmidt, 1926 (Figure 3.M)

Ptilomera agriodes Schmidt, 1926, 15 (1): 63, Holoype ♂. – Tiruchirappali, India.

Material examined: 9♂, 7♀, 14.ii.2020, Mallelatheertham waterfalls; 9♂, 10♀, 10viii.2021, Saleshwaram; 2♀, 15.vii.2021, Rampa waterfalls; 4♂, 3♀, 1.viii.2022, 9♂, 4.xii.20221, Pala Kalwa; Jala Tharangini waterfalls; 1♂, 19.vii.2021, Pamulamaredi; 4♂, 2♀, 18.vii.2021, Ijjaluru; 2♀, 18.vii.2021, Tiger club; 11♂, 14♀, 5.xii.2021, Guntivada; 4♂, 7.xii.2021, Anampally; 2♂, 2♀, 7.xii.2021, Koyalagudam; 2♂, 5♀, 30.vii.2022, Kintukuru base camp; 1♂, 5.xii.2021, Mulliguda; 18♂, 15♀, 28.vii.2022, Sivalingapuram; 10♂, 8♀; 1.viii.2022, Amrutadhara waterfalls; 11♂, 15♀, 27.vii.2022, Thatipudi reservoir, Coll. Dr. Deepa and Somesh.

Distribution: India: Andhra Pradesh (New record), Chhattisgarh, Jharkhand, Karnataka, Kerala, Madhya Pradesh, Maharashtra, Odisha, Rajasthan, Tamil Nadu and Telangana (Chandra et al. 2020).

Remark: This is an endemic species to the Indian subcontinent with wide distribution throughout India.

Subfamily Rhagadotarsinae Lundblad, 1933

Rhagadotarsus (Rhagadotarsus) kraepelini Breddin, 1905 (Figure 3.L)

Rhagadotarsus kraepelini Breddin, 1905, 137: 97, Holotype ♂. – Zoologisches Museum, Universität Hamburg.

Material examined: 2♂, 15.xi.2021, Ananthavaram; 2♂, 4♀; 13.viii.2021, 3♂, 4♀, 23.xii.2021, Vatavarlapally, Coll. Dr. Deepa and Somesh.

Distribution: India: Andhra Pradesh, Arunachal Pradesh, Karnataka, Kerala, Madhya Pradesh, Puducherry, Tamil Nadu, Telangana and West Bengal (Chandra et al. 2020). **Elsewhere:** South China, Palau, Papua New Guinea, Philippines, Indonesia, Malaysia, Myanmar, Singapore, Sri Lanka, Taiwan, Thailand and Vietnam (Chandra et al. 2020).

Subfamily Trepobatinae Polhemus & Polhemus, 1994

Naboandelus signatus Distant, 1910 (Figure 6.A-C)

Naboandelus signatus Distant, 1910, 5 (8): 150, Holotype ♂, ♀. – Indian Museum, Kolkata.

Material examined: 2♂, 1♀, 27.vii.2022, Thatipudi reservoir, 18°10'35.4"N, 83°11'52.08"E, Alluri Sitharama Raju, Andhra Pradesh, Coll. Dr. Deepa and Somesh.

Diagnosis: First antennal segment longer than head; female abdomen about as long as pronotum and mesonotum together, slightly longer in males; middle legs much longer than hind legs; lateral margins of head ochraceous or stramineous; pronotum short and transverse with a large central yellow spot; anterior margin truncate but posterior margin moderately convex; apex of pronotum convex.

Distribution: India: Andhra Pradesh (New record); Chandigarh, Karnataka, Madhya Pradesh, Pondicherry, Tamil Nadu, Tripura, Uttar Pradesh and West Bengal (Chandra et al. 2020). **Elsewhere:** Myanmar and Vietnam (Chandra et al. 2020).

Remark: This species was collected along with two other Gerridae i.e. *C. Productus* Spinola, 1840 and *M. Communis* Distant, 1910 skating over the surface of the lake. The collection site is located at the foothills of the Ananthagiri Hill ranges of Andhra Pradesh at a distance of nearly 70 km from Visakhapatnam city.

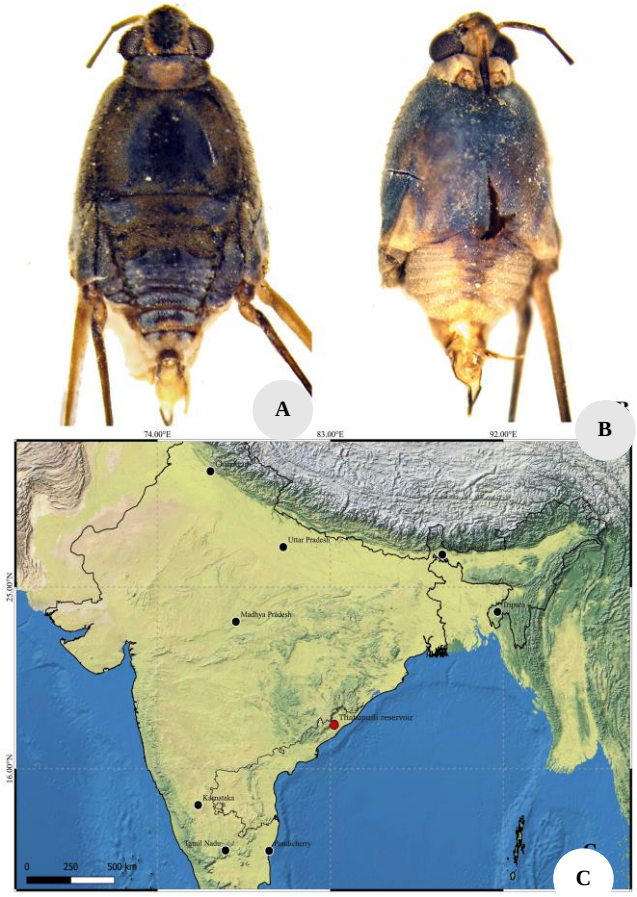

Figure 6. A-B. *Naboandelus signatus* Distant, 1910; Male habitus (A. Dorsal view, B. Ventral view); C. Distribution throughout India

Discussion

The family Gerridae, comprising semi-aquatic beetles commonly known as water striders, has been studied in the Eastern Ghats of Telangana and northern Andhra Pradesh. A total of 659 specimens have been collected from the aforementioned collection locations, and during this study, a total of sixteen species from the thirteen genera and seven subfamilies of the family Gerridae were identified. Moreover, nine species will be added to the state fauna of Andhra Pradesh: *O. Rhexenor*, *C. Productus*, *G. Nepalensis*, *N. Signatus*, *A. Kumari*, *P. Agriodes*, *M. Communis*, *V. Aquarius*, and *T. Nicobarensis*. The *P. Agriodes* was the most abundant species compared to the other 15 species that were identified, with *L. Fossarum fossarum* and *M. Communis* coming in second and third, respectively (Figure 3) (Karuthapandi and Jaiswal 2021). There have been specimens of these three species found at almost every collection site. The least common species from Andhra Pradesh were *N. Signatus* and *N. Parvulus*, only collected each of these species from one location in Andhra Pradesh. Another species *M. Communoides* had been collected from a single collection location as Mallelatheertham waterfalls in Telangana. Species list according to the all collection locations have been discussed in Table 2. *M. Communoides* is an endemic species reported from Tamil Nadu, India, and latter extended its distributional range to Madhya Pradesh, Odisha and Telangana (Chandra et al. 2020). There was a greater species diversity in collections locations that were undisturbed by humans or any other nuisance as opposed to disturbed locations like lakes or waterfalls where disturbance was more due to tourism.

The *T. Nicobarensis* was first described from the Andaman Islands, by Andersen (Andersen 1964). Jehamalar and Chandra (2013a,b) reviewed this genus from India and documented three species, in which *T. Nicobarensis* is restricted to the Andaman Islands. Earlier studies by Jehalamar and Chandra (2020) suggested the reported 5 species from India, *T. Nicobarensis* and *T. Venkataramani* Jehamalar and Chandra, 2013 are exclusively distributed in the Andaman and Nicobar Islands, *T. Ceylonensis* Hungerford and Matsuda, 1962 distributed in the southern India and *T. Kuiterti* Hungerford and Matsuda, 1958 and *T. Aruli* Jehamalar and Chandra, 2020 exclusively from Meghalaya. Additionally, we are expanding *T. Nicobarensis* range into Eastern Ghats of the state of Andhra Pradesh. This species was only found in an isolated region in Papikonda National Park, in a swiftly moving rocky stream with water that fluctuates in temperature from 17 to 22 degree Celsius, depending on the season. From the previous records, it is clear about the preferred habitat of this species (Jehamalar and Chandra 2013, 2020), in mainly hilly small rocky streams at an altitude of 12 meters to 1045 meters above sea level.

The *V. Aquarius* was described by Distant in the year 1910 from Travancore in the Trivandrum district of Kerala. Later, the same species was reported from the original site by Thirumalai and also extended its distribution range in the Western Ghats of Tamil Nadu (Thirumalai 1986, 1999). The taxonomic revision of the oriental genus *Ventidius* was then undertaken by Chen and Zettel (1999), and also extended the distribution of *V. Aquarius* at Jog falls in the state of Karnataka as well as its type locality (Jehamalar and Chandra 2020). The *V. Aquarius* is the only species among the reported four species of this genus that has been documented from southern India (Thirumalai 2002), and we are expanding its range to include the Eastern Ghats. Prior to this study, this species was reported only from the three states of Kerala, Karnataka and Tamil Nadu, though many studies have been undertaken in the parts of Indian region (Thirumalai 1999, 2002, Thirumalai and Sharma 2008; Jehamalar and Chandra 2013a, 2013b, 2016, 2020), but there had been no record of this species from all of the study localities.

During the survey period, *N. Signatus*, a species that is rarely collected, was also found and collected from a single location in Andhra Pradesh. There are extremely few records from past research on the status of this species. According to earlier records, it is thought to have a rare distribution range that includes Pondicherry, one union territory, and four states: Karnataka, Tamil Nadu, Uttar Pradesh, and West Bengal (Bal and Basu 1994; Thirumalai 1999, 2002). The distribution of this species was only mentioned in Kolkata, West Bengal, and Burma (now Myanmar) by Bal and Basu (1994). Later, Thirumalai

(2002) worked on the Gerridae family and expanded this species range to include four more states mentioned above. Following that, Chandra et al. 2012 added another distribution from a single location in Sehore District of Madhya Pradesh. The *N. Signatus* is the only species from India that has been identified till date in this genus. We are expanding its distribution to include the Eastern Ghats even though it was previously documented from the Southern Indian region's Western Ghats (Thirumalai 2002).

The family Gerridae from the Eastern Ghats in northern Andhra Pradesh and Telangana has been evaluated for the first time in this publication. Comprehensive faunal research with a focus on this group, related with freshwater bodies, is necessary to highlight the real richness of aquatic and semi-aquatic Hemipterans throughout the Eastern Ghats and to aid in the protection of their natural habitat resources.

ACKNOWLEDGEMENTS

The authors are thankful to Dr. Dhriti Banerjee, Director, and Dr. C. Raghunathan, Additional-Director, Zoological Survey of India, Kolkata, for the facilities and encouragement. The authors convey special thanks to Dr. Swetapadma Dash and Dr. E.E. Jehamalar, Hemiptera section, Zoological Survey of India, Kolkata, for confirming the species as well as other identification support provided. It is also with great gratitude that the authors acknowledge Dr. Karuthapandi M. And Dr. S.S. Jadhav for their valuable input and continuous support.

REFERENCES

Andersen NM. 1964. The genus *Tenagogonus* Stål in the collections of the Zoological Museum of Copenhagen (Hemiptera: Gerridae). Entomologiske Meddelelser 32: 321-334.

Andersen NM. 1982. The Semi-Aquatic Bugs (Hemiptera, Gerromorpha). Phylogeny, Adaptation, Biogeography, and Classification. Series Entomonograph Vol. 3. Brill Publisher, Leiden. DOI: 10.1163/9789004631267.

Bal A,Basu RC. 1994. Insecta: Hemiptera: Mesoveliidae, Hydrometridae: Veliidae and Gerridae; Belostomatidae; Nepidae: Notonectidae and Pleidae. Fauna of West Bengal. State Fauna Series. Rec Zool Surv India, Kolkata 3 (5): 535-558.

Bal A. 2007. Fauna of Andhra Pradesh. State Fauna Series. Rec Zool Surv India, Kolkata 5 (3): 347-374.

Basu S, Chandra K, Subramanian KA, Saha GK. 2018a. Water bugs (Insecta: Hemiptera: Heteroptera) of Himalayan and sub-Himalayan regions of West Bengal, India. J Threat Taxa 10: 12619-12714. DOI: 10.11609/jott.3060.10.12.12619-12714.

Basu S, Chandra K, Venkatesan T. 2018b. *Metrocoris sikkimensis* sp. Nov. (Hemiptera: Heteroptera: Gerridae) from northeastern India, with a key to species of the compare group occurring in India. Zootaxa 4471: 369-374. DOI: 10.11646/zootaxa.4471.2.9.

Basu S, Chandra K, Venkatesan T. 2018c. Morphological and molecular characterization of predatory aquatic and semi-aquatic bugs of India. J Biol Control 32: 75-80. DOI: 10.18311/jbc/2018/16342.

Basu S, Thirumalai G, Subramanian KA, Saha GK. 2015. New records of aquatic and semi-aquatic Heteroptera (Insecta: Hemiptera) from West Bengal and Odisha. Rec Zool Surv India 115 (2): 191-201. DOI: 10.26515/rzsi/v115/i2/2015/120725.

Chandra K, Deepa J, Raghunathan C, Jadhav SS, Karuthapandi M. 2021. Current Status of Faunal Diversity in Telangana. Zoological Survey of India, M-Block, New Alipore, Kolkata, India.

Chandra K, Jehamalar EE, Thirumalai G. 2012. Four new records of Gerroidea (Hemiptera: Heteroptera) from Madhya Pradesh. Rec Zool Surv India Kolkata 112 (1): 71-74. DOI: 10.26515/rzsi/v112/i1/2012/122117.

Chandra K, Kushwaha S, Jehamalar EE. 2020. True Bugs of Central India (Chhattisgarh and Madhya Pradesh). Records of the Zoological Survey of India Occasional Papers Vol. 43. Zoological Survey of India, Kolkata.

Chandra K, Lyngdoh J, Basu S, Kushwaha S, Hassan M. 2022. Water bug of East Kolkata wetland. Zoological Survey of India, M-Block, New Alipore, Kolkata, India.

Chen PP, Zettel H. 1999. A taxonomic revision of the Oriental water strider genus *Ventidius* Distant (Hemiptera: Gerromorpha: Gerridae). Tijds voor Entom 137-208. DOI: 10.1163/22119434-99900010.

Dias-Silva K, Cabette HSR, Juen L, de Marco Jr P. 2009. The influence of habitat integrity and physical-chemical water variables on the structure of aquatic and semi-aquatic Heteroptera. Zoologia (Curitiba) 27: 918-930. DOI: 10.1590/S1984-46702010000600013.

Dias-Silva K, Moreira FFF, Giehl NFS, Nóbrega CC, Cabette HSR. 2013. Gerromorpha (Hemiptera: Heteroptera) of eastern Mato Grosso State, Brazil: checklist, new records, and species distribution modeling. Zootaxa 3736 (3): 201-235. DOI: 10.11646/zootaxa.3736.3.1.

ENVIS. 2023. ENVIS CENTRE ON ECO – TOURISM Hosted by Department of Science & Technology, Sikkim Sponsored by Ministry of Environment, Forests & Climate Change, Govt of India, Sikkim. Https://scstsenvis.nic.in/index3.aspx?Sslid=3261&subsublinkid=2487&langid=1&mid=1.

Gullan PJ, Cranston PS. 2017. Insetos. Fundamentos da entomologia. Guanabara Koogan, Rio de Janeiro, Brazil.

Gupta YC. 1981. A new species of *Ventidius* Distant (Hemiptera: Gerridae) from India. Oriental Insects 15: 97-102. DOI: 10.1080/00305316.1981.10434478.

Jehamalar EE, Chandra K, Basu S, Chellappa S. 2018a. Review of *Ptilomera* (*Ptilomera*) (Hemiptera: Heteroptera: Gerridae) from India, with description of a new species. Zootaxa 4370: 501-518. DOI: 10.11646/zootaxa.4370.5.3.

Jehamalar EE, Chandra K, Srinivasan G. 2018b. Water striders, the genus *Cylindrostethus* Mayr (Insecta: Heteroptera: Gerridae) from India with a new record. J Threat Taxa 10: 11665-11671. DOI: 10.11609/jott.3750.10.5.11665-11671.

Jehamalar EE, Chandra K. 2013a. On a collection of aquatic and semi-aquatic bugs (Hemiptera: Heteroptera) from Chhattisgarh, India. Rec Zool Surv India 113 (1): 183-195. DOI: 10.26515/rzsi/v113/i1/2013/121946.

Jehamalar EE, Chandra K. 2013b. On the genus *Tenagogonus* Stal (Hemiptera: Heteroptera: Gerridae) from India with description of a new species. Zootaxa 3616 (4): 378-374. DOI: 10.11646/zootaxa.3616.4.6.

Jehamalar EE, Chandra K. 2016. Additional records of aquatic and semi-aquatic Heteroptera (Insecta: Hemiptera) from Chhattisgarh, India. Rec Zool Surv India 116 (2): 99-109. DOI: 10.26515/rzsi/v116/i2/2016/117798.

Jehamalar EE, Chandra K. 2020. A new species of *Tenagogonus* Stål (Hemiptera: Heteroptera: Gerridae) and first records of eight species of aquatic and semi-aquatic Heteroptera from India. Zootaxa 4718 (1): 095-107. DOI: 10.11646/zootaxa.4718.1.8.

Jehamalar EE, Dash S, Chandra K, Raghunathan C. 2023. *Amemboa* Esaki (Hemiptera: Gerromorpha: Gerridae) of India, with descriptions of two new species and establishment of species groups of world species. Zootaxa 5239: 91-111. DOI: 10.11646/zootaxa.5239.1.4.

Jehamalar EE, Dash S. 2021. Three new species of *Metrocoris* Mayr, 1865 (Heteroptera: Gerridae) from India and establishment of species groups. Zootaxa 5082: 341-356. DOI: 10.11646/zootaxa.5082.4.3.

Karuthapandi M, Jaiswal D. 2021. Littoral zooplankton diversity in Himayat Sagar Reservoir, Telangana, India. Lakes Reserv: Sci Policy Manag Sustain Use 26 (1): 42-51. DOI: 10.1111/lre.12349.

Legris P, Meher VMM. 1982. The Eastern Ghats: Vegetation and bioclimatic aspects. Proc Natl Semin Resou Dev Environ Eastern Ghats pp 1-17.

Lyngdoh J, Basu S, Chandra K, Kushwaha S. 2021. On a collection of Insecta: Hemiptera (aquatic and semi-aquatic) fauna of Rajasthan, India. J Natl Resour Dev 16 (1): 9-18.

Nieser N, Melo AL. 1997. Os heterópteros aquáticos de Minas Gerais. Guia introdutório com chave de identificação para as espécies de Nepomorpha e Gerromorpha. Universidade Federal de Minas Gerais, Belo Horizonte, Brazil.

Panizzi AR, Grazia J. 2015. True Bugs (Heteroptera) of the Neotropics. Springer Science plus Business Media, Dordrecht, the Netherlands. DOI: 10.1007/978-94-017-9861-7.

Polhemus JT, Polhemus DA. 2008. Global diversity of true bugs (Heteroptera; Insecta) in freshwater. Hydrobiologia 595 (1): 379-391. DOI: 10.1007/s10750-007-9033-1.

Schuh RT, Slater JA. 1995. True Bugs of the World (Hemiptera: Heteroptera). Classification and Natural History. Cornell University Press, Ithaca, USA.

Subramanian KA, Basu S. 2017. Insecta: Hemiptera (Aquatic Bugs). Rec Zool Surv India, Kolkata 23: 357-378.

Thirumalai G, Sharma RM. 2008. Faunal Diversity of Jabalpur District, Madhya Pradesh. Zoological Survey of India, Kolkata.

Thirumalai G. 1986. On Gerridae and Notonectidae (Heteroptera: Hemiptera: Insecta) from the Silent Valley, Kerala. Rec Zool Surv India 84: 9-33. DOI: 10.26515/rzsi/v84/i1-4/1986/161078.

Thirumalai G. 1999. A checklist of aquatic and semi-aquatic Hemiptera (Insecta) of Tamil Nadu. Zoos' Print J I-XIV (1-10): 132-135. DOI: 10.11609/jott.ZPJ.14.10.132-5.

Thirumalai G. 2002. A checklist of Gerromorpha (Hemiptera) from India. Rec Zool Surv India 100 (1-2): 55-97. DOI: 10.26515/rzsi/v100/i1-2/2002/159613.

NUSANTARA BIOSCIENCE
Vol. 16, No. 1, pp. 54-61
May 2024

ISSN: 2087-3948
E-ISSN: 2087-3956
DOI: 10.13057/nusbiosci/n160107

Antioxidant activity of invasive species *Solanum jamaicense*

NIA YULIANI[1], RIDWAN RACHMADI[1], ADE AYU OKSARI[1,♥], IRVAN FADLI WANDA[2]

[1]Department of Biology, Faculty of Mathematics and Natural Sciences, Universitas Nusa Bangsa. Jl. KH. Sholeh Iskandar KM 4, Bogor 16166, Indonesia. Tel.: +62-251-7533189, Fax.: +62-251-8340217, ♥email: adeayuoksari@gmail.com

[3]Research Center for Biosystematics and Evolution, National Research and Innovation Agency. Jl. Raya Jakarta-Bogor KM. 46 Cibinong, Bogor 16911, West Java, Indonesia

Manuscript received: 27 August 2023. Revision accepted: 15 January 2024.

Abstract. *Yuliani N, Rachmadi R, Oksari AA, Wanda IF. 2024. Antioxidant activity of invasive species* Solanum jamaicense. *Nusantara Bioscience 16: 54-61. Solanum jamaicense* Mill. belongs to the Solanaceae family and is categorized as an invasive species. The leaves of *S. jamaicense* own some of these compounds, which are known to contain several compounds, including phenolics, coumarins, and flavonoids, which have the potential to be a source of antioxidants. This study aims to determine the content of phytochemical compounds and antioxidant activity of the leaves of *S. jamaicense*. Phytochemical testing includes tests for alkaloids, flavonoids, saponins, tannins, steroids, and terpenoids. The total phenolic content was tested using tannic acid as a comparison by spectrophotometry. They tested the antioxidant activity of *S. jamaicense* leaf extract by using spectrophotometric method. The antioxidant activity of the extract is expressed in the value of 50% Inhibition Concentration (IC_{50}). Based on the results of the phytochemical test, the ethanol extract of *S. jamaicense* leaves contains alkaloids, flavonoids, tannins, saponins, and steroids. The research showed that the total phenolic content was 59.953 $mg.g^{-1}$ of the extract, and the antioxidant activity was intense, with an IC_{50} value of 10.41 $mg.L^{-1}$ (active). *S. jamaicense* leaves ethanol extract has the potential as a source of natural antioxidants.

Keywords: Antioxidant activity, phenolic, phytochemical, *Solanum jamaicense* leaves

INTRODUCTION

Invasive alien plant species grow and develop in certain areas outside their original range of distribution and harm native biodiversity, ecosystem services, and human well-being (IUCN 2021). The negative impact caused is due to the tendency of allelopathic content, including secondary metabolites such as terpenoids, alkaloids, steroids, polyacetylene, essential oils, phenolics, flavonoids, and saponins (Moses et al. 2014; Mushtaq and Siddiqui 2018). In addition, saponins, phenolics, and flavonoids have the potential as antioxidants (Khan et al. 2022). Utilizing the content of these compounds is expected to be one of the efforts in tackling the spread of invasive alien plant species.

Antioxidants can capture and neutralize free radicals that cause the cessation of oxidative stress to avoid cell damage. Thus, antioxidants can stop disease induction (Flieger et al. 2021). Researchers have studied using secondary metabolites found in invasive alien plant species as antioxidants within the Solanaceae family, namely *Solanum mauritanium* Scop. and *S. rostratum* Dunal are invasive alien plant species that cause severe environmental and agricultural impacts in Australian territory (Randall 2017). The *S. mauritanium* is known to produce several chemical compounds, including alkaloids, anthraquinone glycosides, steroids, tannins, saponins, phenols, and flavonoids, which have the potential as antioxidants (Jayakumar and Murugan 2015). Based on the research results of Chaitanya et al. (2015), *S. mauritanium* contains alkaloids, phenolic compounds, and flavonoid compounds that are potentially a source of antioxidants with a total saponin fraction showing an IC_{50} value of 101.68 $mg.L^{-1}$ (medium antioxidant activity). The results of research by Gutiérrez et al. (2014) showed that *S. rostratum* produced secondary metabolites, namely alkaloids α-, β-, γ-solanine, and α-, β-, γ-chaconne. In addition, the methanol extract of *S. rostratum* leaf has an inhibitory value of 86.76%, which is effective as an anti-free radical. In addition, other studies have shown that the ethanol extract from the leaves of the *Solanum* genus produces antioxidant activity. Species that are known to have antioxidant activity are invasive plant species, including *Physalis angulata* L. with an IC_{50} value of 59.73±0.24 ppm (intense antioxidant activity) and *S. torvum* Swartz of 107.42±0.43 ppm (moderate antioxidant activity) (Ozaslan et al. 2017; Musarella 2020). Another invasive alien plant species from the Solanaceae family with antioxidant activity is *Solanum jamaicense* Mill.

The *S. jamaicense* belongs to the Solanaceae family, is native to the Neotropics, and is an invasive alien plant species that grows in nature as an agricultural weed in Australia (Randall 2007; Diaz et al. 2008). In this research, The species was primarily found in the undergrowth at the location where it was discovered. According to Diaz et al. (2008), *S. jamaicense* is found mainly in wooded habitats, which can quickly become dominant in the understory. Still, it also occasionally grows in isolated patches in the open. The obtained information suggests that the leaves of *S. jamaicense* can be used as medicine. According to Schultes (1980), people use a warm leaf decoction to eliminate body parasites. *S jamaicense* leaves contain several compounds, including phenolics, coumarins, and flavonoids, which can be a source of antioxidants (Thiesen et al. 2018; Ramón-Valderrama and Galeano-García 2020;

Bouslamti et al. 2022). However, research on the antioxidant activity of *S. jamaicense* leaves is still limited. Differences in place and environments, such as altitude, rainfall, and temperature, will affect the content of secondary metabolites in plants (Yang et al. 2018). Therefore, researchers need to conduct further studies on the content of secondary metabolites and antioxidant activity in the leaves of *S. jamaicense*. This study aimed to determine the scope of phytochemical compounds and antioxidant activity of the plant *S. jamaicense* leaves.

MATERIALS AND METHODS

Materials

The materials used are the leaves of *S. jamaicense*. A sampling of *S. jamaicense* was carried out in Curug, Bojongsari Sub-district, Depok, West Java, Indonesia (6° 23' 51,5576" S and 106° 44' 13,5312" E). *S. jamaicense* was identified in Herbarium Bogoriense, Research Center for Biosystematic and Evolution, National Agency for Research and Innovation (BRIN), Bogor, Indonesia.

Procedures

Sample preparation

Mature leaves of *S. jamaicense* at the 5th to 10th positions were picked to ±3 kg, then wash the leaves with running water. After that, *S. jamaicense* was oven-dried at 40°C for 48 hours and blended until smooth. The *S. jamaicense* leaves blender results were sieved using a 40-mesh sieve (Suryani et al. 2016).

Determination of water content

Two bottles were oven-dried at 105ºC for 30 minutes and cooled in a desiccator for 15 minutes. The bottle is then measured in weight and is known as W. In the bottle, 2 g of *S. jamaicense* leaves powder was added and then measured in weight (known as W1). The leaf powder of *S. jamaicense* was then dried in an oven at 105°C for three hours. Then, the leaf powder of *S. jamaicense* Mill was put in a desiccator for 15 minutes and measured in weight (known as W2). The bottles with samples were oven-dried at 105°C for ±2 hours to obtain a constant weight (Suryani et al. 2016).

$$Water\ Content\ (\%\ bb) = \frac{(W1 - W2)}{(W1 - W)} \times 100$$

Extraction of the leaves of S. jamaicense

A sample of 50 grams was macerated with 250 mL of 96% ethanol solvent thrice in 24 hours. The mixture was filtered every 24 hours, and the filtrate obtained was collected in a closed container. The powder is added back with the same 96% ethanol solvent. The filtrate was combined and evaporated with a rotary evaporator at an 80°C temperature, 100 mBar pressure, and 100 rpm speed for 1 hour. The extract was then evaporated further with a water bath to obtain a thick extract of the leaves of the *S. jamaicense* (Julfitriyani et al. 2016).

Phytochemical test of the leaf of S. jamaicense

Phytochemical tests were carried out on alkaloids, flavonoids, terpenoids/steroids, tannins, and saponins based on the Sembiring et al. (2018) methods.

Alkaloid test

The *S. jamaicense* extract was put into a test tube and added with 10 mL of 0.05 N chloroform-ammonia. The test tube is shaken slowly and allowed to stand until it forms two layers. Then, the liquid on the top layer (chloroform) was dripped onto a drip plate. The liquid was added to Mayer's reagent, Wagner's reagent, and Dragendorff's. The formation of white precipitate indicated positive alkaloids in the extract with Mayer reagent, brown precipitate with Wagner reagent, and orange with Dragendorff reagent.

Flavonoid test

The *S. jamaicense* extract was put into a test tube, and ethanol was added. The solution is then added with magnesium tape and drops of concentrated HCl on the magnesium tape. The formation of red color indicates the presence of flavonoids.

Saponin test

S. jamaicense extract was added with 10 mL of hot water, cooled, and shaken vigorously for 10 seconds. Foam formed steadily for not less than 10 minutes as high as 1-10 cm indicates the presence of saponin compounds. The mixture added with 2N HCl solution will make the foam disappear.

Tannin test

The *S. jamaicense* extract was put into a test tube, soaked in hot water, and cooled. The extract was then added with 1 mL of 10% FeCl3 solution. The formation of dark blue, blue-black, or greenish-black color indicates the presence of tannins.

Steroid and triterpenoid test

The *S. jamaicense* extract was dissolved in 0.5 mL of chloroform and then added with 0.5 mL of acetic anhydride. This mixture is then dripped with 2 mL of concentrated H_2SO_4 through the tube wall. The formation of a green-blue color indicates the presence of steroids. A brownish or violet-colored ring that appears shows the presence of triterpenoid compounds.

Total phenolic content

The total phenolic content was determined using the Folin Ciocalteu method. A total of 1 mL of extract solution of 1,000 mg/L was put in a test tube, and then 1 mL of Folin Ciocalteu 50% reagent was added. The mixture was allowed to stand for 5 minutes, shaking with a vortex and 2 mL of 5% Na_2CO_3 solution. Then, the mixture was incubated in the dark for 1 hour. The absorbance was read at a wavelength of 725 nm with a spectrophotometer. Total phenol extract was expressed as milligram (mg) gallic acid equivalent per gram extract weight (TAE mg/g fruit extract). The total phenolic content was obtained by

entering the absorbance value of the sample in the standard curve equation for tannic acid (Aryal et al. 2019).

Antioxidant testing method 2,2-diphenyl-1-picrylhydrazyl (DPPH)

The *S. jamaicense* extract and quercetin (as positive control) were put into a test tube with 2 mL of 0.1 mg/LDPPH solution and shaken with a vortex until homogeneous (four replications). The change from purple to yellow indicates the efficiency of free radical scavengers. The absorbance on the spectrophotometer was measured at a wavelength of 515 nm after being incubated for 30 minutes. Free radical scavenging activity (% inhibition) was calculated as the percentage of DPPH color reduction (Aryal et al. 2019).

$$\%\ Inhibition = \frac{Absorbance\ of\ standard - Absorbance\ of\ crude\ extract}{Absorbance\ of\ standard} \times 100$$

RESULTS AND DISCUSSION

Water content and leaf extract of *Solanum jamaicense*

The weight of the fresh leaves of *S. jamaicense* is 2.275 g, and after the drying process, it is 554 g, so the water content of the leaves of *S. jamaicense* is 75.65%. The results are different from the water content of *Solanum jamaicense* Mill leaves powder obtained was 8.96%. The water content of a sample below 10% is good, so it is expected to last a long time in storage.

Phytochemical screening analysis of *S. jamaicense*

The phytochemical analysis shows that the compounds in the thick extract of *S. jamaicense* leaves included alkaloids, flavonoids, saponins, tannins, and steroids (Table 1).

Total phenolic of *S. jamaicense*

The content of phenolic compounds in plant extracts can be determined by quantitative testing, and testing the total phenolic content can be done by the Folin-Ciocalteu method. The total phenolic content is expressed in mg of Tannic Acid Equivalent (TAE). The standard curve of tannic acid can be seen in Figure 1.

Antioxidant activity of *S. jamaicense*

The solution concentration and the inhibition value obtained were then processed to obtain the curve. The curve obtained will produce the equation y = ax+b value, which is needed to determine the Inhibition Concentration (IC_{50}) value. The positive control used in this study was quercetin to compare the amount of antioxidant potential contained in the ethanol extract of *S. jamaicense* with a comparable antioxidant. The standard curve of quercetin and ethanol extract of *S. jamaicense* can be seen in Figure 2.

Table 1. Phytochemical test results of *Solanum jamaicense* leaf extract

Secondary Metabolites	Test Method	Results
Alkaloid	Mayer	+
	Wagner	+ +
	Dragendoff	+ +
Flavonoid	HCl	+ +
Saponin	Warmup	+ +
Tanin	$FeCl_3$	+ + +
Steroid	H_2SO_4	+ + +
Triterpenoid	H_2SO_4	-

Note: + + +: Very concentrated, + +: Concentrated, +: Not concentrated, -: Negative

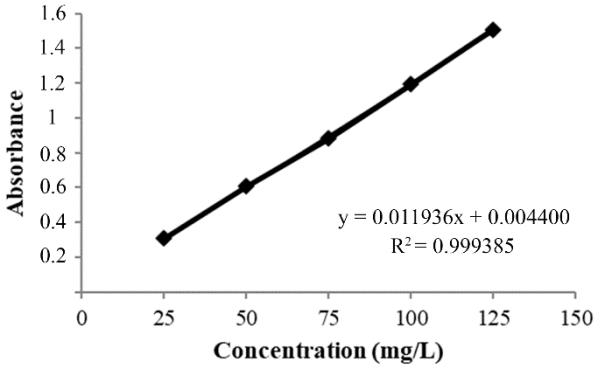

Figure 1. Standard curve of tannic acid

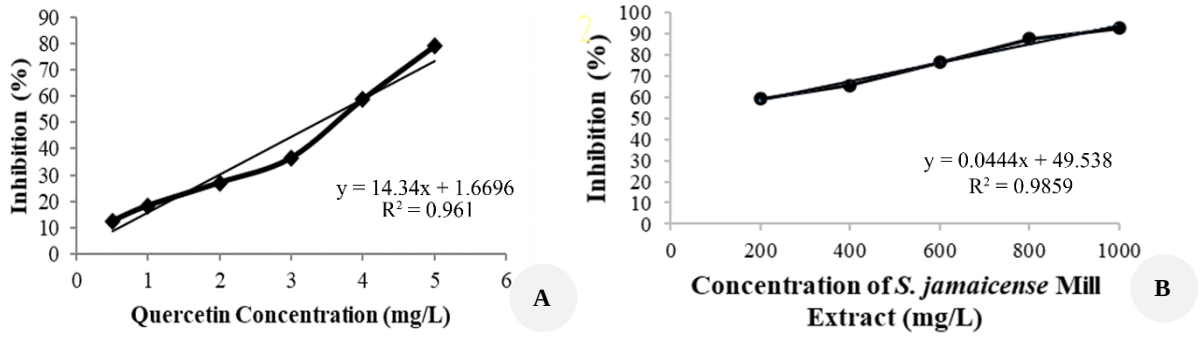

Figure 2. A. Standard curve of quercetin, B. Ethanol extract of *S. jamaicense* leaves

Discussion

Water content and leaf extract of Solanum jamaicense

The leaves' water content of *S. jamaicense* is probably influenced by the presence of fine hairs and spines on the surface of the leaves, which is a form of morphological adaptation in the face of drought stress. Nasruddin et al. (2019) state that the patchouli plant (*Pogostemon cablin* Benth) forms a thick layer of wax or hair that maintains water content.

The high water content in *S. jamaicense* leaves is probably related to the large number of stomata so that water from the environment is absorbed and fills the cavities in the leaves (Maylani et al. 2020). Leaves consist of several tissues, including sponge tissue that is not tightly packed, so many cavities exist. Water and nutrient minerals then fill the holes of leaf sponge tissue, a photosynthetic unit in plants (Ievinsh 2023).

Water content that is too large will trigger the growth of microorganisms in the sample, which can change the conformation of the chemical compounds in the sample (Hallsworth 2022). The moisture content of the leaf powder of *S. jamaicense* is possibly related to the leaf powder refining and sifting. The purpose of grinding and sifting leaf powder is to reduce the particle size to increase the surface contact between the sample and the solvent used in the extraction (Chaves et al. 2020).

The weight of the *S. jamaicense* leaf powder was 50 g, while the total weight of the *S. jamaicense* leaf extract obtained was 22.8537 g, so the yield value of the *S. jamaicense* extract was obtained by 45.71%. This yield is higher than the *S. nigrum* methanol extract value of 24% (Almoulah et al. 2017), probably due to the solvent's polarity and the substance's polarity to be extracted. Solvents with a polarity similar to the secondary metabolites in the sample will dissolve more of the secondary metabolite components in the material, which has implications for increasing the yield value of the extract obtained (Wakeel et al. 2019).

The polarity of flavonoid and alkaloid compounds is close to the polarity of the 96% ethanol solvent, which affects the extract yield, which is higher than other solvents such as acetone: water and ethyl acetate (Noviyanty et al. 2019). Niawanti et al. (2019) state that ethanol has a polar -OH group and a nonpolar CH_2CH_3 group, which allows it to extract both polar and nonpolar compounds. This high polarity of the ethanol solvent causes the extract yield to be higher than other solvents.

Therefore, using ethanol as a solvent is due to some of its properties. Ethanol is effective in obtaining more metabolite compounds, non-toxic, neutral extracts and has good absorption. Ethanol can mix with water in all ratios and has a boiling point that is not too high. Ethanol can dissolve alkaline, alkaloids, essential oils, glycosides, curcumin, coumarins, anrakinones, flavonoids, steroids, resins, and chlorophyll (Jacotet-Navarro et al. 2018).

Phytochemical screening analysis of S. jamaicense

In recent years, information on alternative therapeutic agent sources in dealing with synthetic drugs' side effects has been widely studied for their potential from several plants. The approach used in this study is a combination of traditional and advanced techniques (biological, ethnopharmacological, molecular, phytochemistry, and metabolic processes) (Chakraborty 2018; Süntar 2019). Therefore, we screened medicinal *S. jamaicense*, potential candidates for antioxidants, as part of a new drug discovery program using natural products.

Roy et al. (2022) state that secondary metabolites in natural plant extracts include alkaloids, saponins, terpenoids, polyphenols, flavonoids, and steroids. Secondary metabolites in *S. jamaicense* are related to non-protoplasmic components such as vacuoles, constituent parts of plant cells. The vacuole is filled with fluid and is lined by the tonoplast membrane, and the liquid in the vacuole stores secondary metabolite compounds such as alkaloids, terpenes, tannins, and flavonoids. Apart from that, vacuoles also store crystals, silica objects, and organic and inorganic materials such as salts and sugars, protein-forming amino acids, and phosphates (Tan et al. 2019).

The secondary metabolite contents stored in the vacuole come from the photosynthesis and cellular respiration results. The number of secondary metabolite compounds will increase with the plant's age, where the cell vacuoles will enlarge and dominate the cytoplasm (Tan et al. 2019).

The compounds included in this phytochemical test have the potential for medicinal, including antioxidants. Dalimunthe et al. (2018) and Sembiring et al. (2018) stated that compounds derived from the phenol, flavonoid, and alkaloid groups have many antioxidants, as well as Saponins and flavonoids also have antioxidants (Them et al. 2019). Tannins with -OH groups have antioxidant potential to reduce free radicals (Maisetta et al. 2019). In addition, flavonoids and tannins are included in natural phenolic compounds. Phenolic compounds are a group of compounds that act as natural antioxidants in plants (Pourreza 2013). The presence of the above compounds, especially the phenolic compounds in the leaf extract of *S. jamaicense*, makes this plant a potential source of antioxidants.

Total phenolic of S. jamaicense

Phenolics have a unique structure consisting of several hydroxyl groups, so one of these plant-derived substances is the leading free radical scavenger (Li et al. 2020). The significant phenolic substances have primary antioxidant activity or free radical scavengers. Therefore, the total amount of phenolic compounds in plant extracts is significant (Lou et al. 2014; Engida et al. 2015; Mursandi et al. 2022).

The standard curve for tannic acid is obtained by calculating the equation from linear regression between the concentration of tannic acid as the X value and the absorbance value of tannic acid as the Y value. The value of the regression equation obtained is $y = 0.011936x + 0.0044$ with $R^2 = 0.999385$. The equation value is used to calculate the total phenolic content of the sample. The determination of the total phenolic content of *S. jamaicense* ethanol extract was 59,953 mg TAE/g extract. The total phenolic content in the ethanol extract of *S. jamaicense* was much higher than that of the leaf extract of *Ipomoea*

batatas L belonging to the order Solanales of 2.57 mgTAE/g extract (Kuddus et al. 2020).

The high total phenolic content of *S. jamaicense* leaves is thought to be influenced by several factors, including the ability of the leaves to synthesize secondary metabolites and sunlight. The leaves of *S. jamaicense* used are matured (5^{th} to 10^{th} leaves from the shoot) and are dark green. Mature leaves can produce secondary metabolites in optimum quantities so that the content of these compounds is higher than that of young leaves; young leaves have not yet grown on large amounts of secondary metabolites, containing less (Anwar et al. 2017). The results supported by Kingne et al. (2019) stated that mature avocado leaves (*Persea americana* Mill.) produced higher total flavonoid and phenolic content than young leaves. In addition, sunlight also affects the production of secondary metabolites; sunlight exposure determines the number of secondary metabolite compounds produced, such as anthocyanins, flavonols, and carotenoids (Yang et al. 2018). Excessive sun exposure reduces the production of secondary metabolites such as flavonoids and phenolic compounds in the leaves of *Orthosiphon stimaneus* Benth. (Ibrahim and Jaafar 2012).

The ability of phenolic compounds to form stable phenoxy radicals in oxidation reactions causes these compounds to potentially act as a source of antioxidants (Nurhasnawati et al. 2019). The activity of antioxidants from phenolic compounds, because of their redox properties, plays a vital role in absorbing and neutralizing free radicals, reducing singlet and triplet oxygen, and peroxide decomposition (Ningsih et al. 2016). Nur et al. (2019) revealed that the total phenolic content in white teak leaves (*Gmelina arborea* Roxb.) had a correlation value of 0.567, which means the total phenolic content influenced 56.7% of antioxidant activity. The study indicates a positive correlation between the range of phenolic compounds in the extract and antioxidant activity. The scavenging activity of DPPH is caused by its ability to transfer hydrogen atoms or electrons. Phenolic compounds have one (phenol) or more (polyphenols) phenol rings, namely hydroxy groups which is attached to an aromatic ring, so it is easy oxidized by donating hydrogen atoms on free radicals. The ability of these phenolic compounds to donate hydrogen atoms causes the DPPH radical to be reduced to a more stable form. The amount and position of phenolic hydrogen in the molecule affect phenolic compounds' free radical scavenging activity. The number of hydroxyl groups possessed by phenolic compounds is directly proportional to the antioxidant activity produced (Tian et al. 2021).

Antioxidant activity of S. jamaicense

The research on the antioxidant potential of *S. jamaicense* used the DPPH assay; DPPH is commonly used for antioxidant assay because of its simple application with high sensitivity. The scavenging activity of DPPH is caused by its ability to transfer hydrogen atoms or electrons; mainly by phenolic compounds such as polyphenols or flavonoids (Hidayati et al. 2017; Tohma et al. 2017; Kusumah et al. 2020).

The standard curves of quercetin and ethanol extract of *S. jamaicense* have different equation values of y = ax+b. The ordinary regression equation for quercetin is y = 14.34x + 1.6696, so the IC_{50} value of quercetin is 3.37 $mg.L^{-1}$, which includes a potent antioxidant activity. In comparison, the extract regression equation is y = 0.0444x + 49.538, so the IC_{50} value of the ethanol extract of leaves *S. jamaicense* Mill of 10.41 $mg.L^{-1}$, which includes a potent antioxidant activity. The presence of secondary metabolites of phenolic and flavonoid groups is thought to produce antioxidant activity capable of carrying out the free radical scavenging biological activity. This ability is because the phenolic and flavonoid groups are rich in hydroxyl, so they are suspected of providing good free radical scavenging activity (Ningsih et al. 2016; Widiyantoro et al. 2022). These results follow research conducted by Ismanto et al. (2017) that Surian leaves (*Toona sureni* (Bl.) Merr.) have antioxidant activity because this plant contains flavonoid and phenolic compounds.

According to Takao et al. (2015), the IC_{50} value of the standard quercetin is smaller than the extract because it is a pure compound that can bind to the DPPH molecule effectively. The ethanol extract of *S. jamaicense* has an IC_{50} value more significant than the quercetin standard, presumably because the sample is still a crude extract and interfering compounds may dissolve. Disruptive compounds such as proteins and fats can interfere with scavenging free radicals by flavonoid compounds (Martemucci et al. 2022).

The IC_{50} value of the *S. jamaicense* extract of 10.41 $mg.L^{-1}$ (active), including the potent antioxidant activity, is related to compounds detected in phytochemical testing and phenolic compounds. According to Venkatesan et al. (2019), antioxidant activity in plants is related to polar solvents used, such as ethanol, to dissolve phenolic compounds. Phenolic compounds are known to influence the antioxidant activity of a plant.

The antioxidant activity of the ethanolic extract of there the IC50 value of the *S. jamaicense* extract (at 10.41 $mg.L^{-1}$) was lower than that of *S. incanum* (177.9 $mg.L^{-1}$); *S. schimperianum* (156.1 mg.L-1); *S. nigrum* (179.1 $mg.L^{-1}$); *Physalis lagascae* (199.0 mg.L-1); *Withania somnifera* (168.9 $mg.L^{-1}$) (Almoulah et al. 2017). The antioxidant activity of the ethanolic extract of *S. jamaicense* is presumably due to different solvents during the extraction process.

The phenolic content in the above species is lower because it uses methanol as a solvent, while *S. jamaicense* extraction uses ethanol. The research by Mahasuari et al. (2020) showed that 75% ethanol as a solvent in extracting *Pluchea indica* L. leaves resulted in a higher total phenolic content than methanol solvent. Polar solvents like ethanol generally dissolve phenol compounds better, so the extracted levels are higher (Noviyanty et al. 2019). In addition, the drying method also affects the antioxidant activity revealed. The antioxidant activity of *S. jamaicense* is also more substantial than that of *S. mauritanium* Scop, with an IC_{50} value of 101.68 $mg.L^{-1}$ (Chaitanya et al. 2015), which has moderate antioxidant activity. The leaves

of *S. jamaicense* were dried in an oven at 40°C for 48 hours, while the leaves of *S. mauritianum* were dried using indirect sunlight.

Adhamatika et al. (2021) revealed that the drying method in indirect sunlight with black cloth resulted in lower antioxidant activity than the oven drying method at 40°C on *Pandanus amaryllifolius* Roxb leaves. Damage to the material's antioxidant compounds, such as phenol, is due to the interaction between UV light and oxygen (Del Valle et al. 2020). Bernard et al. (2014) reported the effect of the drying method on total phenol, where the total phenol produced by the oven drying method was higher than that of drying in the sunlight and room temperature. This result is due to the faster inactivation of the enzyme. Therefore, the leaves of *S. jamaicense* can replace synthetic antioxidants and be used as potential sources of natural bioactive molecules. Antioxidants are one of the essential ingredients of today's therapy since they reduce in vivo oxidative damage. In addition, good natural antioxidants are found in many plants (Manurung et al. 2016).

This research concludes that the ethanolic extract of *S. jamaicense* leaves contains alkaloids, flavonoids, tannins, saponins, and steroids, a total phenolic content of 59.953 $mg.g^{-1}$ extract, and potent antioxidant activity with an IC_{50} value of 10.41 $mg.L^{-1}$. The search for plants with the potential as natural antioxidants and good medicinal value has attracted researchers, so they are expected to be substitutes for synthetic antioxidants. Further research is needed to determine the antioxidant activity of *S. jamaicense* using different types of solvents and extraction methods. In addition, its antioxidant activity can be compared with other plant parts of *S. Jamaicense*.

ACKNOWLEDGEMENTS

We want to thank the Rector of Nusa Bangsa University, Bogor, Indonesia and National Research and Innovation Agency (BRIN), Indonesia for supporting this research. We are also grateful for the lecturer from the Chemistry Department, Faculty of Mathematics and Natural Sciences (Devy Susanty; Nurlela), the generous assistance from all Biology and Chemistry Laboratory team members: Asep, Mona, and Hamza.

REFERENCES

Adhamatika A, Murtini ES, Sunarharum WB. 2021. The effect of leaf age and drying method on physico-chemical characteristics of Pandan (*Pandanus amaryllifolius* Roxb.) leaves powder. IOP Conf Ser: Earth Environ Sci 733 (1): 012073. DOI: 10.1088/1755-1315/733/1/012073.

Almoulah NF, Voynikov Y, Gevrenova R, Schohn H, Tzanova T, Yagi S, Thomas J, Mignard B, Ahmed AAA, El Siddig MA, Spina R, Laurain-Mattar D. 2017. Antibacterial, antiproliferative and antioxidant activity of leaf extracts of selected Solanaceae species. South Afr J Bot 112: 368-374. DOI: 10.1016/j.sajb.2017.06.016.

Anwar K, Rahmanto B, Triyasmono L, Rizki MI, Halwany W, Lestari F. 2017. The influence of leaf age on total phenolic, flavonoids, and free radical scavenging capacity of *Aquilaria beccariana*. Res J Pharm Biol Chem Sci 2017 (129): 129-133.

Aryal S, Baniya MK, Danekhu K, Kunwar P, Gurung R, Koirala N. 2019. Total phenolic content, flavonoid content, and antioxidant potential of wild vegetables from western Nepal. Plants 8 (4): 96. DOI: 10.3390/plants8040096.

Bernard D, Kwabena A, Osei O, Daniel G, Elom S, Sandra A. 2014. The effect of different drying methods on the phytochemicals and radical scavenging activity of Ceylon Cinnamon (*Cinnamomum zeylanicum*) plant parts. Eur J Med Plants 4 (11): 1324-1335. DOI: 10.9734/ejmp/2014/11990.

Bouslamti M, El Barnossi A, Kara M, Alotaibi BS, Al Kamaly O, Assouguem A, Lyoussi B, Benjelloun AS. 2022. Total polyphenols content, antioxidant and antimicrobial activities of leaves of *Solanum elaeagnifolium* Cav. from Morocco. Molecules 27 (13): 4322. DOI: 10.3390/molecules27134322.

Chaitanya M, Dhanabal SP, Pavithra N, Rama Satyanarayana Raju K, Jubie S. 2015. Phytochemical analysis and in-vitro antioxidant and cytotoxic activity of aerial parts of *Cestrum aurantiacum* and *Solanum mauritianum* (Solanaceae weeds of Niligiris). Helix 3: 683-687.

Chakraborty P. 2018. Herbal genomics as tools for dissecting new metabolic pathways of unexplored medicinal plants and drug discovery. Biochim Open 6: 9-16. DOI: 10.1016/j.biopen.2017.12.003.

Chaves JO, de Souza MC, da Silva LC, Lachos-Perez D, Torres-Mayanga PC, Machado AP. da F, Forster-Carneiro T, Vázquez-Espinosa M, González-de-Peredo AV, Barbero GF, Rostagno MA. 2020. Extraction of flavonoids from natural sources using modern techniques. Front Chem 8: 507887. DOI: 10.3389/fchem.2020.507887.

Dalimunthe A, Hasibuan PAZ, Silalahi J, Sinaga SF, Satria D. 2018. Antioxidant activity of alkaloid compounds from *Litsea cubeba* Lour. Orient J Chem 34 (2): 1149-1152. DOI: 10.13005/ojc/340270.

Del Valle JC, Buide ML, Whittall JB, Valladares F, Narbona E. 2020. UV radiation increases phenolic compound protection but decreases reproduction in *Silene littorea*. PLoS ONE 15 (6): e0231611. DOI: 10.1371/journal.pone.0231611.

Diaz R, Overholt WA, Langeland K. 2008. Jamaican nightshade (*Solanum jamaicense*): A threat to Florida's hammocks. Invasive Plant Sci Manag 1 (4): 422–425. DOI: 10.1614/ipsm-08-079.1.

Engida AM, Faika S, Nguyen-Thi BT, Ju YH. 2015. Analysis of major antioxidants from extracts of *Myrmecodia pendans* by UV/visible spectrophotometer, liquid chromatography/tandem mass spectrometry, and high-performance liquid chromatography/UV techniques. J Food Drug Anal 23 (2): 303-309. DOI: 10.1016/j.jfda.2014. 07.005.

Flieger J, Flieger W, Baj J, Maciejewski R. 2021. Antioxidants: Classification, natural sources, activity/capacity measurements, and usefulness for the synthesis of nanoparticles. Materials 14 (15): 4135. DOI: 10.3390/ma14154135.

Gutiérrez ADM, Bah M, Garduño R ML, Mendoza DSO, Serrano CV. 2014. Anti-inflammatory and antioxidant activities of methanol extracts and alkaloid fractions of four Mexican medicinal plants of Solanaceae. Afr J Tradit Complement Alternat Med 11 (3): 259-267. DOI: 10.4314/ajtcam.v11i3.36.

Hallsworth JE. 2022. Water is a preservative of microbes. Microb Biotechnol 15 (1): 191-214. DOI: 10.1111/1751-7915.13980.

Hidayati MD, Ersam T, Shimizu K, Fatmawati S. 2017. Antioxidant activity of *Syzygium polynthum* extracts. Indonesian J Chem 17 (1): 49-53. DOI: 10.22146/ijc.23545.

Ibrahim MH, Jaafar HZE. 2012. Primary, secondary metabolites, H_2O_2, malondialdehyde and photosynthetic responses of *Orthosiphon stimaneus* benth. to different irradiance levels. Molecules 17 (2): 1159-1176. DOI: 10.3390/molecules17021159.

Ievinsh G. 2023. Water content of plant tissues: So simple that almost forgotten? Plants 12 (6): 1238. DOI: 10.3390/plants12061238.

Ismanto SD, Anggraini T, Wahyu B. 2017. The effect of drying temperature to chemical components of Surian herbal tea leaves (*Toona sureni* (Blume) Merr.). J Pharm Biol Chem Sci 8 (1): 229-238.

IUCN. 2021. Invasive alien species and Climate Change. IUCN Issues Brief, Gland, Switzerland.

Jacotet-Navarro M, Laguerre M, Fabiano-Tixier AS, Tenon M, Feuillère N, Bily A, Chemat F. 2018. What is the best ethanol-water ratio for the extraction of antioxidants from rosemary? Impact of the solvent on yield, composition, and activity of the extracts. Electrophoresis 39 (15): 1946-1956. DOI: 10.1002/elps.201700397.

Jayakumar K, Murugan K. 2015. Pharmacological, micromorphological studies on *Solanum mauritianum* Scop. (Solanaceae): A search. Intl J Pharm Sci Rev Res 35 (2): 134-139.

Julfitriyani, Runtuwene M, Wewengkang D. 2016. Uji aktivitas antioksidan dan toksisitas ekstrak etanol daun Foki sabarati (*Solanum torvum*). Pharmacon 5 (3): 94-101. DOI: 10.35799/pha.5.2016.12942. [Indonesian]

Khan MI, Karima G, Khan MZ, Shin JH, Kim JD. 2022. Therapeutic effects of saponins for the prevention and treatment of cancer by ameliorating inflammation and angiogenesis and inducing antioxidant and apoptotic effects in human cells. Intl J Mol Sci 23 (18): 10665. DOI: 10.3390/ijms231810665.

Kingne FK, Djikeng FT, Tsafack HD, Karuna MSL, Womeni HM. 2019. Phenolic content and antioxidant activity of young and mature mango (*Mangifera indica*) and avocado (*Persea americana*) leave extracts. Intl J Phytomed 10 (4): 181. DOI: 10.5138/09750185.2289.

Kuddus MA, Miah MMA, Datta GC, Sarker AK, Alam MH, Khan MMH. 2020. Proximate and micronutrient analysis of orange fleshed sweet potato leaves grown in Sylhet regions of Bangladesh. Res Agric Livest Fish 7 (1): 43-50. DOI: 10.3329/ralf.v7i1.46830.

Kusumah RR, Arrisujaya D, Susanty D, Yuliani N. 2020. Phytochemicals, total flavonoid content and antioxidant activity of methanol extract of *Diospyros discolor* seeds. J Mater Environ Sci 2020 (4): 609-614.

Li Y, Kong D, Fu Y, Sussman MR, Wu H. 2020. The effect of developmental and environmental factors on secondary metabolites in medicinal plants. Plant Physiol Biochem 148: 80-89. DOI: 10.1016/j.plaphy.2020.01.006.

Lou SN, Hsu YS, Ho CT. 2014. Flavonoid compositions and antioxidant activity of calamondin extracts prepared using different solvents. J Food Drug Anal 22 (3): 290-295. DOI: 10.1016/j.jfda.2014.01.020.

Mahasuari NPS, Paramita NLPV, Yadnya PAGR. 2020. Effect of methanol concentration as a solvent on total phenolic and flavonoid content of beluntas leaf extract (*Pulchea indica* L.). J Pharm Sci Appl 2 (2): 77-84. DOI: 10.24843/jpsa.2020.v02.i02.p05.

Maisetta G, Batoni G, Caboni P, Esin S, Rinaldi AC, Zucca P. 2019. Tannin profile, antioxidant properties, and antimicrobial activity of extracts from two Mediterranean species of parasitic plant *Cytinus*. BMC Complement Alternat Med 19: 82. DOI: 10.1186/s12906-019-2487-7.

Manurung H, Kustiawan W, Kusuma IW, Marjenah. 2016. Total flavonoid content and antioxidant activity in leaves and stems extract of cultivated and wild tabat barito (*Ficus deltoidea* Jack). AIP Conf Proc 1813: 1-6. DOI: 10.1063/1.4975945.

Martemucci G, Costagliola C, Mariano M, D'andrea L, Napolitano P, D'Alessandro AG. 2022. Free radical properties, source and targets, antioxidant consumption and health. Oxygen 2 (2): 48-78. DOI: 10.3390/oxygen2020006.

Maylani ED, Yuniati R, Wardhana W. 2020. The effect of leaf surface character on the ability of water hyacinth, *Eichhornia crassipes* (Mart.) Solms. to transpire water. IOP Conf Ser: Mater Sci Eng 902 (1): 012070. DOI: 10.1088/1757-899X/902/1/012070.

Moses T, Papadopoulou KK, Osbourn A. 2014. Metabolic and functional diversity of saponins, biosynthetic intermediates and semi-synthetic derivatives. Crit Rev Biochem Mol Biol 49 (6): 439-462. DOI: 10.3109/10409238.2014.953628.

Mursandi H, Susanty D, Nurhayati L, Oksari AA. 2022. Short Communication: Antioxidant activity of ethanol extract of *Chlorella sorokiniana* cultured in tofu wastewater. Nusantara Biosci 14 (2): 155–159. DOI: 10.13057/nusbiosci/n140204.

Musarella CM. 2020. *Solanum torvum* Sw. (Solanaceae): A new alien species for Europe. Genet Resour Crop Evol 67: 515-522. DOI:. 10.1007/s10722-019-00822-5.

Mushtaq W, Siddiqui MB. 2018. Allelopathy in Solanaceae plants. J Plant Prot Res 58 (1): 1-7. DOI: 10.24425/119113.

Nasruddin N, Harahap EM, Hanum C, Siregar LA. 2019. The level of water supply and its effect on the growth of plants and yields patchouli (*Pogostemon cablin* Benth.). Proc 1st Workshop Multidiscip Appl Part 1 WMA-01 2018: 1-9. DOI: 10.4108/eai.20-1-2018.2282082.

Niawanti H, Lewar YS, Octavia NN. 2019. Effect of extraction time on *Averrhoa bilimbi* leaf ethanolic extracts using soxhlet apparatus. IOP Conf Ser: Mater Sci Eng 543 (1): 012018. DOI: 10.1088/1757-899X/543/1/012018.

Ningsih IY, Zulaikhah S, Hidayat MA, Kuswandi B. 2016. Antioxidant activity of various kenitu (*Chrysophyllum cainito* L.) leaves extracts from Jember, Indonesia. Agric Agric Sci Procedia 9: 378-385. DOI: 10.1016/j.aaspro.2016.02.153.

Noviyanty A. Salingkat C, Syamsiar S. 2019. Pengaruh jenis pelarut terhadap ekstraksi dari kulit buah naga merah (*Hylocereus polyrhizus*). KOVALEN: J Riset Kimia 5 (3): 271-279. DOI: 10.22487/kovalen.2019.v5.i3.14037. [Indonesian]

Nur S, Sami FJ, Awaluddin A, Afsari MIA. 2019. Korelasi antara kadar total flavonoid dan fenolik dari ekstrak dan fraksi daun Jati putih (*Gmelina arborea* Roxb.) terhadap aktivitas antioksidan. Jurnal Farmasi Galenika (Galenika J Pharm) (e-Journal) 5 (1): 33-42. DOI: 10.22487/j24428744.2019.v5.i1.12034. [Indonesian]

Nurhasnawati H, Sundu R, Sapri, Supriningrum R, Kuspradini H, Arung ET. 2019. Antioxidant activity, total phenolic and flavonoid content of several indigenous species of ferns in East Kalimantan, Indonesia. Biodiversitas 20 (2): 576-580. DOI: 10.13057/biodiv/d200238.

Ozaslan C, Farooq S, Onen H, Ozcan S, Bukun B, Gunal H. 2017. Germination biology of two invasive *Physalis* species and implications for their management in arid and semi-arid regions. Sci Rep 7 (1): 16960. DOI: 10.1038/s41598-017-17169-5.

Pourreza N. 2013. Phenolic compounds as potential antioxidant. Jundishapur J Nat Pharm Prod 8 (4): 149-150. DOI: 10.17795/jjnpp-15380.

Ramón-Valderrama JA, Galeano-García PL. 2020. Antioxidant and antimicrobial activities in leaf methanolic extracts from the plant genus *Solanum*. Inf Tecnol 21 (5): 33-42. DOI: 10.4067/S0718-07642020000500033.

Randall RP. 2007. The Introduced Flora of Australia and Its Weed Status. CRC for Australian Weed Management, Glen Osmond, Australia.

Randall RP. 2017. A Global Compendium of Weeds (3rd ed.). Weeds Society of Western Australia, Perth.

Roy A, Khan A, Ahmad I, Alghamdi S, Rajab BS, Babalghith AO, Alshahrani MY, Islam S, Islam MR. 2022. Flavonoids a bioactive compound from medicinal plants and its therapeutic applications. BioMed Re Intl 2022: 5445291. DOI: 10.1155/2022/5445291.

Schultes RE. 1980. Coca in the northwest Amazon. Bot Mus leaf Harv Univ 28 (1): 47-60. DOI: 10.5962/p.168640.

Sembiring E, Elya B, Sauriasari R. 2018. Phytochemical screening, total flavonoid and total phenolic content and antioxidant activity of different parts of *Caesalpinia bonduc* (L.) Roxb. Pharmacogn J 10 (1): 123-127. DOI: 10.1016/j.hermed.2014.01.002.

Süntar I. 2019. Importance of ethnopharmacological studies in drug discovery: Role of medicinal plants. Phytochem Rev 19: 1199-1209. DOI: 10.1007/s11101-019-09629-9.

Suryani N, Permana DG, Jambe AAGN. 2016. Pengaruh jenis pelarut terhadap kandungan total flavonoid dan aktivitas antioksidan ekstrak daun matoa (*Pometia pinnata*). Jurnal Ilmu Dan Teknologi Pangan 5 (1): 1-9. [Indonesian]

Takao LK, Imatomi M, Gualtieri SCJ. 2015. Antioxidant activity and phenolic content of leaf infusions of Myrtaceae species from Cerrado (Brazilian Savanna). Braz J Biol 75 (4): 948-952. DOI: 10.1590/1519-6984.03314.

Tan X, Li K, Wang Z, Zhu K, Tan X, Cao J. 2019. A review of plant vacuoles: Formation, located proteins, and functions. Plants 8 (9): 327. DOI: 10.3390/plants8090327.

Them LT, Tuong Nguyen Dung P, Thi Nhat Trinh P, Tong Hung Q, Tuong LN, Trong Tuan N, Duc Lam T, Thuy Nguyen V, Dung LT. 2019. Saponin, polyphenol, flavonoid content and α-glucosidase inhibitory activity, antioxidant potential of *Launaea sarmentosa* leaves grown in Ben Tre province, Vietnam. IOP Conf Ser: Mater Sci Eng 542 (1): 012036. DOI: 10.1088/1757-899X/542/1/012036.

Thiesen L de C, Colla IM, Silva GJ, Kubiak MG, Faria MGI, Gazim ZC, Linde GA, Colauto NB. 2018. Antioxidant and antimicrobial activity of *Brunfelsia uniflora* leaf extract. Arquivos de Ciências Veterinárias e Zoologia Da UNIPAR 21 (3): 93-97. DOI: 10.25110/arqvet.v21i3.2018.7203.

Tian C, Liu X, Chang Y, Wang R, Lv T, Cui C, Liu M. 2021. Investigation of the anti-inflammatory and antioxidant activities of luteolin, kaempferol, apigenin and quercetin. South Afri J Bot 137: 257-264. DOI: 10.1016/j.sajb.2020.10.022.

Tohma H, Gülçin İ, Bursal E, Gören AC, Alwasel SH, Köksal E. 2017. Antioxidant activity and phenolic compounds of ginger (*Zingiber officinale* Rosc.) determined by HPLC-MS/MS. J Food Meas Charact 11 (2): 556-566. DOI: 10.1007/s11694-016-9423-z.

Venkatesan T, Choi YW, Kim YK. 2019. Impact of different extraction solvents on phenolic content and antioxidant potential of *Pinus*

densiflora bark extract. BioMed Res Intl 2019: 3520675. DOI: 10.1155/2019/3520675.

Wakeel A, Jan SA, Ullah I, Shinwari ZK, Xu M. 2019. Solvent polarity mediates phytochemical yield and antioxidant capacity of *Isatis tinctoria*. PeerJ 7: e7857. DOI: 10.7717/peerj.7857.

Widiyantoro A, Wahdaningsih S, Luliana S. 2022. Antioxidant activity of young leaves extracts of *Lygodium microphyllum* on boiling variation. IOP Conf Ser: Earth Environ Sci 978: 012054. DOI: 10.1088/1755-1315/978/1/012054.

Yang L, Wen KS, Ruan X, Zhao YX, Wei F, Wang Q. 2018. Response of plant secondary metabolites to environmental factors. Molecules 23 (4): 762. DOI: 10.3390/molecules23040762.

NUSANTARA BIOSCIENCE
Vol. 16, No. 1, pp. 62-67
May 2024

ISSN: 2087-3948
E-ISSN: 2087-3956
DOI: 10.13057/nusbiosci/n160108

Determination of volatile oil compounds and antioxidant activities of some *Cirsium* taxa grown in Türkiye

ÖZLEM SARAL[1,♥], MUSTAFA KARAKÖSE[2]
[1]Department of Nutrition and Dietetic, Faculty of Health Science, Recep Tayyip Erdogan University. Rize 53100, Türkiye.
Tel.: +90-464-214-10-59, ♥email: ozlem.saral@erdogan.edu.tr
[2]Programme of Medicinal and Aromatic Plants, Espiye Vocational School, Giresun University. Giresun 28600, Türkiye

Manuscript received: 19 September 2023. Revision accepted: 17 January 2024.

Abstract. *Saral Ö, Karaköse M. 2024. Determination of volatile oil compounds and antioxidant activities of some* Cirsium *taxa grown in Türkiye. Nusantara Bioscience 16: 62-67.* Several *Cirsium* taxa are commonly used as a folk remedy or food in Anatolia and some countries. The study aims to determine the volatile oil profile and antioxidant activity of endemic *Cirsium trachylepis* Boiss., *Cirsium echinus* Hand.-Mazz., and *Cirsium osseticum* Petr. subsp. *osseticum*. The volatile oil compounds of three *Cirsium* species were analyzed by Gas Chromatography-Mass Spectrometry (GC-MS) using Solid Phase Microextraction (SPME). Additionally, total phenolic content was measured, and antioxidant activity capacity was determined by FRAP and DPPH• analyses in three *Cirsium* taxa methanolic extracts. A total of 32 (87.89%), 25 (88.69%), and 27 (80.68%) volatile compounds were identified from *C. trachylepis*, *C. osseticum* subsp. *osseticum*, and *C. echinus*, respectively. Pentadecanolide was the major volatile oil in three *Cirsium* species and was first reported in *Cirsium* taxa in this study. When the fatty acid content was examined, palmitic acid was determined as the common and main fatty acid for the three *Cirsium* species. A comparison of the antioxidant activity of three species showed that *C. echinus* had the highest antioxidant activity. The total phenolic content of *C. echinus* was found to be 250.84±0.46 mg GAE/100 g sample. While the FRAP value of *C. echinus* was 36.47±1.04 µmol Fe/g sample, the SC_{50} value was 1.89±0.05 mg/mL. This study may pave the way for the determination of volatile oils by SPME and the further development of research on *Cirsium* taxa.

Keywords: Antioxidant, *Cirsium trachylepis*, GC/MS, SPME, volatile oil

INTRODUCTION

Cirsium Mill., generally known as thistles, belongs to the Asteraceae family. It spreads worldwide, including Europe, North Africa, Siberia, Central Asia, West and East Africa, and Central America (Özcan et al. 2016). *Cirsium* taxa are known in Türkiye as "*körkenger, çakır dikeni,* and *eşek dikeni*" (Orhan et al. 2007). In Türkiye, this genus is represented by 73 taxa, and 28 taxa of these are found in North-east Anatolia. *Cirsium echinus* Hand.-Mazz. grows on rocky slopes, rarely on shores at 1,200-1,600 m asl (Özcan et al. 2008). *Cirsium trachylepis* Boiss. grows in woods at 500-1,760 m asl and is endemic (Özcan et al. 2008; Karaköse 2019). *Cirsium osseticum* Petr. subsp. *osseticum* grows at 700-1,132 m asl (Özcan 2017). Due to the uncontrolled proliferation of *Cirsium* taxa in Türkiye, it is considered a harmful weed in agricultural areas. In addition, local people use the root and stem of the genus *Cirsium* as a food and alternative medicinal plant (Demirtaş et al. 2017). Not only in Türkiye, but also in different world cultures, *Cirsium* taxa are used for medical purposes (Akbulut et al. 2022; Karaköse 2022a; Şen et al. 2022). *Cirsium* leaves are used to relieve abdominal pain and intestinal disorders in Italy (Guarrera 2005). Root or whole plant relieves bleeding, jaundice, and gastrointestinal disorders in China (He et al. 2014). *Cirsium* taxa are rich in silibinin and silymarin, which have biological activity. These two metabolites have a hepatoprotective effect (Yıldız et al. 2013; Ma et al. 2016). In addition, researchers have shown that *Cirsium* taxa have antioxidant (Sabudak et al. 2017), antifungal, antibacterial (Gulen et al. 2019), antidiabetic (Perez et al. 2001), and hepatoprotective effects (D'Andrea et al. 2005).

Although oxygen molecules are indispensable for the continuity of biological life, they also constitute the source of free radicals, which are highly reactive in the natural functioning of metabolism. These Reactive Oxygen Species (ROS) are a natural byproduct of metabolic functioning and are harmful substances (Chaudhary et al. 2023). Excessive ROS production in the body causes disorders such as DNA damage, lipid peroxidation, or cancer. Antioxidants protect cells by counteracting the damaging effects of the physiological process of oxidation (Kumar et al. 2017). Recently, we have witnessed increased interest in using natural substances from plant sources. Plants have valuable bioactive compounds such as phenolics, vitamins, carotenoids, and volatile oils. These compounds are responsible for significant antioxidant, anti-inflammatory, and antimicrobial activities (Pavela and Benelli 2016; Che and Zhang 2019).

Plant-based volatile oils are natural compounds with biological activity (Zeng et al. 2016). Therefore, volatile oils are used as additives in the food and cosmetics industry and pharmaceuticals, as well as their use in the field of health. The widespread use of volatile oils in different areas adds economic importance to the plant (Xing et al. 2019; Sadiq et al. 2021). The plant type and extraction method affect the composition and amount of volatile oils (Amiri et

al. 2018). The most widely used method to obtain volatile oil from plants is hydrodistillation. The use of the SPME (solid phase microextraction) method, which does not require solvent and is faster, has been increasing recently. SPME has been used in various fields, including determining volatile composition and screening flavors and taints (Kim et al. 2020).

There are many studies on volatile oil analysis by hydrodistillation in different *Cirsium* taxa (Özcan et al. 2016; Tüfekçi et al. 2018; Gulen et al. 2019; Kim et al. 2020), but the number of studies with SPME is limited in *Cirsium* species (Nazaruk et al. 2012; Amiri et al. 2018). For this reason, it was aimed to determine the volatile oil contents of *C. echinus*, and *C. osseticum* subsp. *osseticum*, and *C. trachylepis* (endemic to Türkiye) grown in Türkiye using the SPME method. In addition, the antioxidant activities of these plants were examined in the study.

MATERIALS AND METHODS

Plant material

The *C. echinus* and *C. trachylepis* were collected from Akpınar Village in Giresun (Türkiye) in July 2019. The *C. osseticum* subsp. *osseticum* was collected from Güllüce Village in Giresun (Türkiye) in July 2019 (Karaköse 2022b); Dr. Mustafa Karaköse identified these plants. Aerial parts of plants were dried at room temperature and powdered in an electric grinder (Waring Commercial, USA). The dry plant samples were divided into two. Five (5) g of the dry samples were weighed, and 25 mL methanol was added. Then, it was stirred at room temperature for 24 hours and filtered. Methanolic extracts were used for antioxidant activity assay. The remaining dry samples were used for volatile oil analysis. All the samples were stored at -20°C until analysis.

SPME procedure and GC/MS analysis

The dry plant (one gram) was placed in a vial of 10 mL, and then fiber coating was placed in the headspace. An SPME fiber (A polydimethylsiloxane/divinyl-benzene, Supelco, USA) was firstly conditioned for 5 min at 250°C in a gas chromatography (GC) injector. SPME analysis was done at 50°C with incubation time of 5 min, and extraction time of 10 min. Volatile oil analysis was performed on a Shimadzu QP2010 plus gas (connected to a Shimadzu QP2010 Ultra mass selector detector) chromatography using a TRB-5MS capillary column (30 mx 0.25 mm, film thickness, 0.25 µm). SPME fiber was inserted into the injection port of the GC-MS. The oven temperature was programmed to hold at 60°C for 2 min and then to increase to 240°C at 3°C/min, finally holding at 250°C for 4 min. The column flow rate was 1.0 mL/min, and transporter gas was utilized as Helium (99.999%). The MS was scanned from 40 m/z to 400 m/z at 70 eV. The volatile compounds were detected by comparing the mass spectra of the two libraries (FFNSC1.2 and W9N11) (Renda et al. 2016).

Total phenolic content analysis

The plant's Total Phenolic Content (TPC) was obtained using the Folin-Ciocalteu assessment (Slinkard and Singleton 1977). Initially, 400 µL Folin-Ciocalteu solution (0.5 N), 20 µL methanolic extract or standard (Gallic acid, 1-0.125 mg/mL), 680 µL of distilled water were added in a test tube, and the solution was vortexed. After 3 minutes of waiting, 400 µL of Na_2CO_3 (10%) was added, and the solution was vortexed again. After incubation for about 2 h, absorbance was measured at 760 nm. All measurements were made in triplicate.

Determination of antioxidant activity

The FRAP assay was made utilizing the technique of Benzie and Szeto (1999). The 100 µL of sample solution or standard ($FeSO_4$) and daily prepared 3 mL of FRAP solution (including TPTZ, iron (III) chloride, and acetate buffer) were added and vortexed. The absorbance on 593 nm was determined to be about 4 min at 25°C. All measurements were made in triplicate.

The scavenging capacity of DPPH• radical (2,2-diphenyl-1-picrylhydrazyl) of methanolic extraction was defined using the method of Molyneux (2004). 0.75 mL of methanolic extract or standard (various concentrations) and 0.75 ml of methanolic DPPH• solution (0.1mM) were added to the test tube, and the mixture was vortexed. Then, the mixture was left at room temperature for 50 min in the dark. Absorbance was monitored at 517 nm. Trolox was utilized as standard, and amounts were explained as SC_{50} (mg sample per mL). All measurements were made in triplicate.

RESULTS AND DISCUSSION

Volatile oils are a mixture of several bioactive chemical components, and their content varies from plant to plant, according to the growing season and environmental conditions (Zeng et al. 2016; Elshibani et al. 2020). SPME is one of the techniques for identifying volatile oil components and is based on the adsorption of these compounds on silica phase-coated fiber. It also determines the volatile oil composition of substances with different properties, such as fruit, vegetables, meat, or biological fluids (Bentivenga et al. 2004). SPME is a solvent-free, simple, inexpensive, rapid, and selective method for evaluating volatile compounds (Zhao et al. 2007; Renda et al. 2017). SPME fibers determine volatile oils based on their polarity and the thickness of the selected fibers (Pripdeevech et al. 2011).

GC-MS determined the volatile oil composition of Cirsium taxa with SPME. The volatile oil contents of the plant samples are given in Table 1. A total of 32 (87.89%), 25 (88.69%), and 27 (80.68%) constituents were identified from *C. trachylepis, C. osseticum* subsp. *osseticum,* and *C. echinus,* respectively. Of these, 14 volatile oils were the shared components, imparting the same aroma to all samples. While most of its volatile oil consists of

hydrocarbons and lactones, it contains small amounts of terpenes, esters, carboxylic acids, aldehydes, and ketones. As we all know, alcohols and aldehydes are the main aromatic substances.

Pentadecanolide was the major volatile oil in all samples, even though this was not reported previously in *Cirsium* taxa. Pentadecanolide, a macrocyclic lactone, is mostly used in the polymer, perfumery, and pharmaceutical industries (Emel'yanenko et al. 2011). 2-Hexenal, which has antimicrobial activity against food spoilage and pathogenic microbial species (Patrignani et al. 2008), was only detected in the *C. osseticum* subsp. *osseticum*. The lowest volatile l oil in it was found to be 2-ethyl hexanol. As far as we know, no study in the literature investigates the volatile content of *C. osseticum* subsp. *osseticum.* However, the fatty acid content of *C. osseticum* subsp. *osseticum* was investigated by hydrodistillation (Özcan et al. 2016). Linalool, ethyl propionate, and 2-phenylethanol were found only in *C. echinus*. In addition, 2-phenylethanol has the lowest percentage of volatile oil. This is the second study in which the volatile oil content of *C. echinus* was determined. In the first study, Rasulov et al. (1989) reported that β-sitosterol, stearic aldehyde, and triacontane were found in *C. echinus*. The *C. trachylepis* is endemic (Özcan 2017; Karaköse 2019), and only fatty acid content was investigated by hydrodistillation (Özcan et al. 2016). The volatile oil content of *C. trachylepis* was examined for the first time in this study. Among the three *Cirsium* samples, isobutyl angelate, heptanoic acid, undecylenic acid, and ethylene brassylate were found only in *C. trachylepis.*

There is limited research in the literature where volatile oil analysis in *Cirsium* has been performed using SPME. Zeng et al. (2016) compared the volatile oil content of *C. japonicum* Fisch. ex DC. and *C. setosum* (Willd.) Besser ex M.Bieb. obtained by hydrodistillation and SPME and found only 13 common components. It has been reported that 2,6,6-trimethyl-1-cyclohexene-1-carboxaldehyde, hexyl alcohol, 1-pentanol, 1-aziridineethanamine, and hexanal were detected in volatile oil analysis with SPME in *C. japonicum* and *C. setosum*. Notably, in the Zeng et al. (2016) study, 39 hydrocarbons were detected by hydrodistillation, while SPME detected 1 hydrocarbon. In the present study, 14 hydrocarbons were detected. These results indicate that volatile oil content varies depending on the extraction method and plant species. Kim et al. (2020) determined the volatile compounds in *C. setidens* (Dunn) Nakai in a study using four different SPME fibers (CWR/PDMS, DVB/PDMS, PDMS, PA). It was stated in the study that CWR/PDMS and DVB/PDMS coated SPME fibers had better results for *Cirsium* taxa. In the present study, DVB/PDMS-coated SPME fiber was used. They also reported that the main components were 2-pentylfuran, 1-methylcycloheptanol, 1-penten-3-ol, and 2,2,4,6,6,6-pentamethylheptane, regardless of SMPE fibers. However, benzaldehyde, β-ionone, and acetoin were detected, similar to our results. In another study, volatile oil analysis was examined by SPME in the fruits of *C. palustre* (L.) Scop. and *C. rivulare* (Jacq.) All.. Limonene was determined as the main component in both samples. In the same study, in which hexane extract was performed with Soxhlet apparatus, the main component was determined as β-sitosterol, but limonene could not be detected (Nazaruk et al. 2012). The present study found small amounts of limonene in *C. osseticum* subsp. *osseticum* and *C. echinus.*

As for the fatty acid content, palmitic acid stands out in all *Cirsium* samples. In addition, lower amounts of oleic and linoleic acids were detected compared to palmitic acid. However, unlike the literature, butyric acid was found in *C. osseticum* subsp. *osseticum.* Özcan et al. (2016) found that, unlike the present study, seeds of *C. trachylepis* contained high levels of linoleic and oleic acids, while palmitic acid levels were low. Similar to the previous study, Nazaruk et al. (2012) reported that linoleic and oleic acid were dominant in fruits of *C. palustre* and *C. rivulare*. Unlike the current study, extraction was performed with hexane in the Soxhlet apparatus in these studies. On the other hand, in previous studies on different *Cirsium* species, the main fatty acid was found as palmitic acid in *C. arvense* (L.) Scop. (Tüfekçi et al. 2018), *C. creticum* (Lam.) d'Urv. (Gulen et al. 2019), and *C. setidens* (Choi 2015). In addition, previous studies reported that it was detected in myristic acid, unlike other studies (Nazaruk et al. 2012; Zeng et al. 2016). It can be thought that factors such as the differences in the extraction method, plant species, and the plants' harvest time affect the results being so different.

Although oxygen molecules are indispensable for the continuity of biological life, they also constitute the source of free radicals, which are highly reactive in the natural functioning of metabolism (Kunwar and Priyadarsini 2011). Phenolics are also known to defend against free radicals due to their high antioxidant activity (Pietta et al. 2003). In this study, total phenolic content, FRAP, and DPPH$^{\bullet}$ analyses of methanolic extracts were performed to determine the antioxidant activities of the *Cirsium* samples. The results of total phenolic content and antioxidant activity are given in Table 2. In all analyses, *C. echinus* showed the highest antioxidant activity. The total phenolic content of *C. echinus* was 250.84±0.46 mg/100 g GAE sample. FRAP value was determined as 36.47±1.04 µmol Fe/g sample, and DPPH$^{\bullet}$ activities were determined as 1.89±0.05 mg/mL in *C. echinus*. There is a correlation between the total phenolic content and antioxidant activity. The FRAP value and DPPH$^{\bullet}$ scavenging activity of *C. echinus*, which has a high total phenolic content, was also high. To the best of our knowledge, our findings are the first results of antioxidant activity for *C. trachylepis*, *C. echinus*, and *C. osseticum* subsp. *osseticum*; previous studies in Türkiye and different countries have shown that other *Cirsium* taxa have antioxidant activity. While the total phenolic content in the methanolic extracts of *C. yildizianum* Arabaci & Dirmenci collected from Bingöl in Türkiye was found to be 37.10 mg GAE/g, the FRAP value was 89.95 mg TE/g, and the DPPH radical scavenging activity was found to be 40.76 mg TE/g (Llorent-Martínez et al. 2020). In another study, total phenolic of 61.21 ± 0.37µg catechol Eq/mg and SC_{50} of 0.22 mg/ml was determined in methanolic extracts of *C. vulgare* (Savi) Ten. (Thrace Region, Türkiye) (Sabudak et al. 2017). The total phenolic content was found to be 174.7±21.7 mg gallic

acid/g dw, and the DPPH· inhibition value was found to be 38.34±1.87% in the study in the methanolic extracts of the leaves of *C. palustren* in Poland (Malejko et al. 2014). It should be noted that the results of the antioxidant activity of plants could vary depending on the location, plant species, harvest time, and the extraction solvent or process.

Table 1. Volatile oil composition of *Cirsium trachylepis*, *C. osseticum* subsp. *osseticum* and *C. echinus*

Compound	**RI Exp.**[a]	**RI Lit.**[b]	***C. trachylepis* (%)**[c]	***C. osseticum* (%)**[c]	***C. echinus* (%)**[c]
Aldehydes					
Caproaldehyde	804	806	2.36	2.01	2.63
2-Hexenal	826	827	-	2.29	-
Benzaldehyde	950	962	1.48	2.64	1.68
Octanal	986	998	0.68	-	-
Nonanal	1109	1083	-	0.98	0.71
Phellandral	1250	1274	1.24	-	-
Cyclamal	1451	1459	-	4.10	-
Tridecanal	1490	1491	-	0.88	-
Ketone					
Acetoin	711	713	2.09	1.86	1.72
Hydrocarbons					
Hendecane	1065	1100	1.09	-	1.22
Dodecane	1207	1200	-	0.73	1.33
Tridecane	1291	1299	1.13	2.38	1.21
Tetradecane	1380	1399	3.63	9.44	4.55
Pentadecane	1507	1499	0.62	-	5.12
Hexadecane	1599	1600	1.43	-	-
Heptadecane	1705	1701	3.51	7.71	4.12
Octadecane	1792	1799	4.51	4.34	4.79
Nonadecane	1897	1899	-	1.61	0.56
Eicosane	1998	2000	3.28	3.09	-
Heneicosane	2093	2099	2.41	-	-
Docosane	2197	2200	1.01	-	-
Tetracosane	2397	2400	-	-	0.51
Pentacosane	2499	2500	1.30	-	0.56
Alcohols					
2-ethyl hexanol	1030	1030	-	0.75	0.53
2-Phenylethanol	1117	1114	-	-	0.48
Esters					
Ethyl propanoate	716	716	-	-	4.85
İsobutyl angelate	1053	1051	0.93	-	-
Lactones					
γ-Butyrolactone	916	915	2.76	2.32	2.36
γ-Hexalactone	1058	1047	0.45	-	-
Pentadecanolide	1841	1839	15.16	12.06	17.76
Ethylene brassylate	2017	2015	4.24	4.42	-
Terpens					
Limonene	1027	1029	-	1.81	1.17
Linalool	1165	1095	-	-	1.46
Isopulegol	1141	1145	0.65	-	-
Anethole	1281	1282	0.67	-	-
Anethofuran	1187	1186	0.67	-	-
β-ionone	1481	1487	2.55	3.62	2.89
Fatty Acids					
Butyric acid	804	808	-	3.24	-
Isovaleric acid	844	835	1.76	-	2.63
Valeric acid	887	882	3.86	3.58	3.75
Palmitic acid	1925	1921	7.52	7.07	6.25
Linoleic acid	2139	2133	6.02	3.65	2.98
Oleic acid	2144	2141	5.22	2.11	2.86
Carboxylic acids					
Heptanoic acid	1080	1076	1.55	-	-
Undecylenic acid	1453	1458	2.11	-	-
Total			87.89	88.69	80.68

Note: [a]: RI calculated from retention times relative to that of n-alkanes (C7-C30) on the nonpolar TRB-5MS column, [b]: RI lit. Literature value (Adams 2007), [c]:%Area obtained by FID peak-area normalization

Table 2. Results of TPC, FRAP and DPPH analyses

Samples	TPC (mg GAE /100 g sample)	FRAP (µmol Fe/g sample)	DPPH:SC50 (mg/mL)
C. osseticum	171.63±0.18	19.38±0.58	2.53±0.98
C. trachylepis	195.64±0.20	22.23±0.22	3.91±0.85
C. echinus	250.84±0.46	36.47±1.04	1.89±0.05
Trolox	-	-	0.02±0.00

In summary, this study aimed to determine the volatile oil content of endemic *C. trachylepis*, *C. echinus*, and *C. osseticum* subsp. *osseticum* grown in Türkiye by SPME with GC-MS. Pentadecanolide was found as the major volatile oil in all *Cirsium* species. Pentadecanolide was reported for the first time in *Cirsium* taxa in this study. Palmitic acid was detected as the main fatty acid in all samples. Additionally, in this study, the antioxidant activity of *Cirsium* species could be compared, and the highest activity was found in *C. echinus.* As far as we know, there is limited research in the literature in which volatile oil analysis has been performed in the *Cirsium* species using SPME (Nazaruk et al. 2012; Zeng et al. 2016; Kim et al. 2020). This is the first study to determine the volatile oil content of *C. trachylepis*, *C. echinus*, and *C. osseticum* subsp. *osseticum* using SPME. Fewer studies using SPME for volatile oil and fatty acid analysis in *Cirsium* taxa make it difficult to compare studies. Increasing the number of studies in which volatile oil contents are determined using SPME in different *Cirsium* taxa will allow comparisons between studies. The presence of various volatile oils of pharmaceutical or industrial importance can also be detected.

ACKNOWLEDGEMENTS

This research is funded by the Recep Tayyip Erdogan University, Türkiye of Scientific Research Projects Coordinator (Project No. FBA-2018-953).

REFERENCES

Adams RS 2007. Identification of Essential Oil Components by Gas Chromatography/Mass Spectrometry. 4th Edition Allured Publishing Corporation, Carol Stream.

Akbulut S, Karaköse M, Şen G 2022. Medicinal plants used in folk medicine of Akçaabat District (Turkey). Fresenius Environ Bull 31: 7160-7176.

Amiri N, Yadegari M, Hamedi B 2018. Essential oil composition of *Cirsium arvense* L. produced in different climate and soil properties. Rec Nat Prod 12: 251-262. DOI: 10.25135/rnp.27.17.06.043.

Bentivenga G, D'Auria M, Fedeli P, Mauriello G, Racioppi R. 2004. SPME-GC-MS analysis of volatile organic compounds in honey from Basilicata. Evidence for the presence of pollutants from anthropogenic activities. Intl J Food Sci Tech 39: 1079-1086. DOI: 10.1111/j.1365-2621.2004.00889.x.

Benzie IF, Szeto Y 1999. Total antioxidant capacity of teas by the ferric reducing/antioxidant power assay. J Agric Food Chem 47: 633-636. DOI: 10.1021/jf9807768.

Chaudhary P, Janmeda P, Docea AO, Yeskaliyeva B, Razis AFA, Modu B, Calina D, Sharifi-Rad J. 2023. Oxidative stress, free radicals and antioxidants: Potential crosstalk in the pathophysiology of human diseases. Front Chem 11: 1158198. DOI: 10.3389/fchem.2023.1158198.

Che C-T, Zhang H 2019. Plant natural products for human health. Intl J Mol Sci 20: 830. DOI: 10.3390/ijms20040830.

Choi H-S 2015. Chemical composition of the essential oil from *Cirsium setidens*, a Korean medicinal plant. Anal Chem Lett 5: 94-102. DOI: 10.1080/22297928.2015.1068132.

D'Andrea V, Pérez LM, Pozzi EJS 2005. Inhibition of rat liver UDP-glucuronosyltransferase by silymarin and the metabolite silibinin-glucuronide. Life Sci 77: 683-692. DOI: 10.1016/j.lfs.2005.01.011.

Demirtaş I, Tufekci AR, Yağlıoğlu AŞ, Elmastas M 2017. Studies on the antioxidant and antiproliferative potentials of *Cirsium arvense* subsp. *vestitum*. J Food Biochem 41: e12299. DOI: 10.1111/jfbc.12299.

Elshibani F, Alshalmani S, Mohammed HA 2020. *Pituranthos tortuosus* essential oil from Libya: Season effect on the composition and antioxidant activity. J Essent Oil-Bear Plants 23: 1095-1104. DOI: 10.1080/0972060X.2020.1843550.

Emel'yanenko VN, Verevkin SP, Stepurko EN, Roganov GN. 2011. The thermodynamic characteristics of 15-pentadecanolide and 16-hexadecanolide. Russ J Phys Chem 85: 348-356 DOI: 10.1134/S0036024411030083.

Guarrera PM 2005. Traditional phytotherapy in Central Italy (marche, abruzzo, and latium). Fitoterapia 76: 1-25. DOI: 10.1016/j.fitote.2004.09.006.

Gulen D, Sabudak T, Orak HH, Caliskan H, Ozer M. 2019. Bioactive compounds, antibacterial and antifungal activities of two *Cirsium* species. Acta Sci Pol Hortorum Cultus 18: 213-221. DOI: 10.24326/asphc.2019.5.21.

He XF,He ZW, Jin XJ, Pang XY, Gao JG, Yao XJ, Zhu Y. 2014. Caryolane-type sesquiterpenes from *Cirsium souliei*. Phytochem Lett 10: 80-85. DOI: 10.1016/j.phytol.2014.08.003.

Karaköse M 2019. Numerical classification and ordination of Esenli (Giresun) forest vegetation. Biologia 74: 1441-1453. DOI: 10.2478/s11756-019-00321-z.

Karaköse M 2022a. An ethnobotanical study of medicinal plants in Güce district, north-eastern Turkey. Plant Divers 44 (6): 577-597. DOI: 10.1016/j.pld.2022.03.005.

Karaköse M 2022b. Vascular Plant diversity of Esenli (Giresun) forest planning unit. Forestist 72: 156-164. DOI: 10.5152/forestist.2021.21014.

Kim SJ, Lee JY, Choi YS, Sung JM, Jang HW. 2020. Comparison of different types of SPME arrow sorbents to analyze volatile compounds in *Cirsium setidens* nakai. Foods 9: 785. DOI: 10.3390/foods9060785.

Kumar S, Sharma S, Vasudeva N 2017. Review on antioxidants and evaluation procedures. Chin J Integr Med 1-12. DOI: 10.1007/s11655-017-2414-z.

Kunwar A, Priyadarsini K 2011. Free radicals, oxidative stress and importance of antioxidants in human health. J Med Allied Sci 1: 53-60.

Llorent-Martínez EJ, Zengin G, Sinan KI, Polat R, Canlı D, Picot-Allain MCN, Mahomoodally MF. 2020. Impact of different extraction solvents and techniques on the biological activities of *Cirsium yildizianum* (Asteraceae: Cynareae). Ind Crops Prod 144: 112033. DOI: 10.1016/j.indcrop.2019.112033.

Ma Q, Wang LH, Jiang JG 2016. Hepatoprotective effect of flavonoids from *Cirsium japonicum* DC on hepatotoxicity in comparison with silymarin. Food Funct 7: 2179-2184. DOI: 10.1039/C6FO00068A.

Malejko J, Nalewajko-Sieliwoniuk E, Nazaruk J, Siniło J, Kojło A. 2014. Determination of the total polyphenolic content in *Cirsium palustre* (L.) leaves extracts with manganese (IV) chemiluminescence detection. Food Chem 152: 155-161. DOI: 10.1016/j.foodchem.2013.11.138.

Molyneux P 2004. The use of the stable free radical diphenylpicrylhydrazyl (DPPH) for estimating antioxidant activity. Songklanakarin J Sci Technol 26: 211-219.

Nazaruk J, Wajs-Bonikowska A, Bonikowski R. 2012. Components and antioxidant activity of fruits of *Cirsium palustre* and *C. rivulare*. Chem Nat Compd 48: 8-10. DOI: 10.1007/s10600-012-0147-y.

Orhan DD, Ergun F, Yeşilada E, Tsuchiya K, Takaishi Y, Kawazoe K. 2007. Antioxidant activity of two flavonol glycosides from *Cirsium hypoleucum* DC. through bioassay-guided fractionation. Turkish J Pharm Sci 4: 1-14.

Özcan M, Ayaz FA, Özoğul Y, Glew R, Ozogul F. 2016. Fatty acid composition of achenes of *Cirsium* taxa (Asteraceae, Carduoideae)

from Turkey. Z Naturforsch C J Biosci 71: 45-54. DOI: 10.1515/znc-2015-0128.

Özcan M. 2017. *Cypsela* micromorphology and anatomy in *Cirsium* sect. *Epitrachys* (Asteraceae, Carduoideae) and its taxonomic implications. Nord J Bot 35: 653-668. DOI: 10.1111/njb.01670.

Özcan M, Hayırlıoğlu-Ayaz S, İnceer H 2008. Chromosome counts of some *Cirsium* (Asteraceae, Cardueae) taxa from Turkey. Caryologia 61: 375-382. DOI: 10.1080/00087114.2008.10589649.

Patrignani F, Iucci L, Belletti N, Gardini F, Guerzoni ME, Lanciotti R. 2008. Effects of sub-lethal concentrations of hexanal and 2-(E)-hexenal on membrane fatty acid composition and volatile compounds of *Listeria monocytogenes*, *Staphylococcus aureus*, *Salmonella enteritidis* and *Escherichia coli*. Intl J Food Microbiol 123 (1-2): 1-8. DOI: 10.1016/j.ijfoodmicro.2007.09.009.

Pavela R, Benelli G 2016. Essential oils as ecofriendly biopesticides? Challenges and constraints. Trends Plant Sci 21: 1000-1007. DOI: 10.1016/j.tplants.2016.10.005.

Perez GR, Ramirez LME, Vargas SR 2001. Effect of *Cirsium* pascuarense on blood glucose levels of normoglycaemic and alloxan-diabetic mice. Phytother Res 15: 552-554. DOI: 10.1002/ptr.882.

Pietta P, Minoggio M, Bramati L 2003. Plant polyphenols: Structure, occurrence and bioactivity. Stud Nat Prod Chem 28: 257-312. DOI: 10.1016/S1572-5995(03)80143-6.

Pripdeevech P, Khummueng W, Park SK 2011. Identification of odor-active components of agarwood essential oils from Thailand by solid phase microextraction-GC/MS and GC-O. J Essent Oil Res 23: 46-53. DOI: 10.1080/10412905.2011.9700468.

Rasulov F, Serkerov S, Ismailov N, Novruzov E 1989. Chemical investigation of *Cirsium echinus*. Izv Akad Nauk Azerbaidzhnsk SSR Ser Biol Nauk 6: 14-16.

Renda G, Bektaş NY, Korkmaz B, Çelik G, Sevgi S, Yaylı N. 2017. Volatile constituents of three *Stachys* L. species from Turkey. Marmara Pharm J 21: 278-285. DOI: 10.12991/marupj.300353.

Renda G, Tosun G, Yaylı N 2016. SPME GC/MS analysis of three *Ornithogalum* L. species from Turkey. Rec Nat Prod 10: 497-502.

Sabudak T, Orak HH, Gulen D, Ozer M, Caliskan H, Bahrisefit I, Cabi E. 2017. Investigation of some antibacterial and antioxidant properties of wild *Cirsium vulgare* from Turkey. Indian J Pharm Educ Res 51: 363-367. DOI: 10.5530/ijper.51.3s.48.

Sadiq Y, Khan MMA, Khan AM 2021. Effect of physical and chemical strategies on extraction-recovery of lemongrass volatile oil. Rev Bras Farmacogn 31: 193-198. DOI: 10.1007/s43450-021-00142-9.

Slinkard K, Singleton VL 1977. Total phenol analysis: Automation and comparison with manual methods. J Enol Vitic 28: 49-55. DOI: 10.5344/ajev.1977.28.1.4.

Şen G, Akbulut S, Karaköse M 2022. Ethnopharmacological study of medicinal plants in Kastamonu province (Türkiye). Open Chem 20: 873-911. DOI: 10.1515/chem-2022-0204.

Tüfekçi AR, Akşit H, Gül F, Demirtaş İ 2018. Determination of phenolic profile of *Cirsium arvense* (L.) Scop. subsp. *vestitum* (Wimmer et Grab.) Petrak plant. Eurasian J Bio Chem Sci 1: 33–36.

Xing C, Qin C, Li X, Zhang F, Linhardt RJ, Sun P, Zhang A. 2019. Chemical composition and biological activities of essential oil isolated by HS-SPME and UAHD from fruits of bergamot. LWT-Food Sci Technol 104: 38-44. DOI: 10.1016/j.lwt.2019.01.020.

Yıldız O, Can Z, Saral Ö, Yuluğ E, Oztürk F, Aliyazıcıoğlu R, Canpolat S, Kolaylı S. 2013. Hepatoprotective potential of chestnut bee pollen on carbon tetrachloride-induced hepatic damages in rats. J Evid Based Complement Alternat Med 2013: 461478. DOI: 10.1155/2013/461478.

Zeng QH, Zhao JB, Wang JJ, Zhang XW, Jiang JG. 2016. Comparative extraction processes, volatile compounds analysis and antioxidant activities of essential oils from *Cirsium japonicum* Fisch. ex DC and *Cirsium setosum* (Willd.) M.Bieb. LWT-Food Sci Technol 68: 595-605. DOI: 10.1016/j.lwt.2016.01.017.

Zhao D, Tang J, Ding X 2007. Analysis of volatile components during potherb mustard (*Brassica juncea*, Coss.) pickle fermentation using SPME–GC-MS. LWT-Food Sci Technol 40: 439-447. DOI: 10.1016/j.lwt.2005.12.002.

NUSANTARA BIOSCIENCE
Vol. 16, No. 1, pp. 68-80
May 2024

ISSN: 2087-3948
E-ISSN: 2087-3956
DOI: 10.13057/nusbiosci/n160109

Botany, morphology, ecology, cultivation, traditional utilization and conservation of *andaliman* (*Zanthoxylum acanthopodium)* in North Sumatra, Indonesia

YATI NURLAENI[1,♥], DECKY INDRAWAN JUNAEDI[2], JOHAN ISKANDAR[3,4]

[1]Research Center for Applied Botany, National Research and Innovation Agency. Cibinong Science Center Jl. Raya Jakarta-Bogor Km. 46, Cibinong, Bogor 16911, West Java, Indonesia. Tel.: +62-21-87907604, ♥email: yatinurlaeni007@gmail.com

[2]Research Center for Ecology and Ethnobiology, National Research and Innovation Agency. Cibinong Science Center Jl. Raya Jakarta-Bogor Km. 46, Cibinong, Bogor 16911, West Java, Indonesia

[3]Department of Biology, Faculty of Mathematics and Natural Sciences, Universitas Padjajaran. Jl. Raya Bandung-Sumedang Km. 21 Jatinangor, Sumedang 45363, West Java, Indonesia

[4]Center for Environment and Sustainability Science, Universitas Padjadjaran. Jl. Sekeloa Selatan 1, Bandung 40134, West Java, Indonesia

Manuscript received: 13 November 2023. Revision accepted: 19 January 2024.

Abstract. *Nurlaeni Y, Junaedi DI, Iskandar J. 2024. Botany, morphology, ecology, cultivation, traditional utilization and conservation of* andaliman *(*Zanthoxylum acanthopodium*) in North Sumatra, Indonesia*. *Nusantara Bioscience 16: 68-80*. This study examines the botany, ecology, cultivation, utilization, and traditional conservation of *andaliman* (*Zanthoxylum acanthopodium* DC.) in North Sumatra, Indonesia. This information were collected through in-depth interviews. The collected data consisted of primary and secondary data. Primary data were obtained in the field through in-depth interviews, participatory observation, and documentation. Meanwhile, to strengthen the results of the interviews, a literature study was conducted, which was obtained from academic sources that can be scientifically accounted for it grows naturally in relatively cool forests, foothills, and cultivated areas. *Z. acanthopodium* is distributed around Lake Toba at 800-1,300 masl (meters above sea level), a temperature 17-22°C, and a 5-40% slope. In North Sumatra, there are nine varieties: Siholpu, Siganjangpat, Sihalus, Sihorbo, Simanuk, and Sirangkak, and three varieties that have not been named yet. *Z. acanthopodium* is planted by maintaining wild plants, burning the land to be planted, collecting dead or old parts of the plant then burned, and collecting mature seeds as material for seeding then burned. The plant does not require fertilization and pesticides. The preservation of *Z. acanthopodium* in North Sumatra is based on local communities' traditional agricultural and ecological management.

Keywords: *Andaliman*, conservation, cultivation, ecology, morphology

INTRODUCTION

Plants of the genus *Zanthoxylum*, family Rutaceae, are of economic importance. The genus is widely distributed in tropical and subtropical regions, including China, Japan, Korea, India, and others. The genus *Zanthoxylum* to date, more than 250 species have been identified worldwide. The genus has high economic value as spices, oils, medicinal plants, and culinary applications (Chen et al. 2022; Zhang et al. 2023). The biodiversity of North Sumatra, Indonesia contains specific and endemic species. A unique spice plant considered a primary commodity in North Sumatra is *Andaliman* (*Zanthoxylum acanthopodium* DC.). Hartley (1966) reported the distribution of *Z. acanthopodium* in India, Nepal, Sikkim, East Pakistan, Myanmar, Thailand, China, and Sumatra (Indonesia). In Indonesia, this plant is naturally distributed in the provinces of North Sumatra and Aceh. *Z. acanthopodium* fruit is often used by the Batak tribe in North Sumatra as a seasoning for traditional dishes such as *sambal, arsik* (the fish is cooked with a mixture of *Z. acanthopodium*, kecombrang, galangal and lemongrass. The spices are mashed and then coated on the fish, cooked in a little oil, on low heat until slightly dry), *na tinombur* (grilled fish served with a thick sauce full of spices that has a distinctive *Z. acanthopodium* flavour), *dengke mas na niura* (fresh raw fish without cooking but not fishy. The fish is given acid and spices, one of which is *Z. acanthopodium*, allowed to stand for about 3-5 hours, after the fermentation process it is ready to eat), *saksang* (meat that is chopped into small pieces and seasoned with spices such as *Z. acanthopodium*, cooked with blood from the slaughtered animal or regular spices without blood), *manuk napinadar* (the chicken is grilled and then doused with chicken blood, mixed with *Z. acanthopodium* and garlic powder and cooked. The mixture of spices with chicken blood makes the soup thicker and more savoury), *mie gomak* (large stick noodles are boiled using a traditional stove and topped with a sauce containing *Z. acanthopodium* spices and sambal). As spices, *Z. acanthopodium* can add delicious flavor and distinctive aroma to food, increase appetite, and increase endurance. This spice plant is only known in Batak cuisine and is considered as Batak pepper. The name of *andaliman* itself varies in each region such as in Simalungun District calls it tuba; in South Tapanuli District, it has the name of *sinyarnyar*; in Karo District, it is called *itir-itir;* and usually, the Toba people call it *tuba* or *andaliman.*

Z. acanthopodium is a wild plant that grows in forests and fields and is useful as a spice. In traditional Batak cuisine, *Z. acanthopodium* is one of the spices that must be

present. It is a habit that every traditional Batak cuisine uses it as a spice. Batak cuisine feels bland if it doesn't use *Z. acanthopodium*. In meat-based dishes, it is used as a fishy odor reducer in meat and fish, so the dish has a distinctive taste. The shape of the fruit is small and clustered, large like a green pepper. *Z. acanthopodium* has a fresh, citrus-like taste when eaten, with a distinctive sharp, pungent smell and a biting taste on the tongue, with a distinctive tartness. The sensation produced when consuming *Z. acanthopodium* feels tart on the tongue due to the content of hydroxy alpha sanshool compounds. This plant has a delicate citrus-like aroma that increases appetite.

Zanthoxylum acanthopodium has high medical benefits and economic value and has been widely studied in many researchs. Several studies have been conducted including as a producer of carminative and anthelmintic (Gupta and Mandi 2013), essential oils (He et al. 2018; Diep et al. 2023), a source of traditional medicine (Kholibrina and Aswandi 2021), improving the human immune system (Yonzone and Rai 2016), improving the livestock immune system (Faradillah et al. 2020), antimicrobial (Julistiono et al. 2018; Muzafri et al. 2018; Susanti et al. 2020; Diep et al. 2023), antioxidant (Wijaya et al. 2019; Napitupulu et al. 2020), anticancer (Rosidah et al. 2019; Arsita et al. 2019; Panggabean et al. 2020; Sibero et al. 2020; Simanullang et al. 2022; Situmorang et al. 2022; Ilyas et al. 2022; MCF-7, dan HepG2), anti-inflammatory (Yanti 2016; Natasutedja et al. 2020; Susanti et al. 2020; Diep et al. 2023), anti-aging and anti-acne (Hanum and Laila 2018; Anggraini et al. 2022; Kintamani et al. 2023), antifertility (Batubara et al. 2020), pesticides (He et al. 2018), insecticides, an insect repellentas, larvicidal activity (Gupta and Mandi 2013; He et al. 2018), antipreeclampsia (Situmorang et al. 2021), wound healing activity (Pasaribu et al. 2020; Manurung 2021). The fruit and seeds are also prescribed for treating rheumatism, dysentery, and stomach ache. Seeds and barks are also aromatic and tonic in fever, dyspepsia, and cholera (Gupta and Mandi 2013).

The demand for *Z. acanthopodium* is increasing due to the dependence of the people of North Sumatra, which is used as a spice in typical Batak cuisine. *Z. acanthopodium* is used as a spice when holding Batak rituals such as weddings, births, entering a new house, deaths, and other events. The price of *Z. acanthopodium* in April to July is usually low, then rises in August, and the highest price in December to January. Based on interviews with *Z. acanthopodium* farmers and traders in traditional markets located in Samosir, Simalungun, Dairi, and Karo The selling price of *Z. acanthopodium* fruit fluctuates greatly from IDR 20,000 to IDR 200,000, sometimes lower or higher than this range. The *Z. acanthopodium* cultivation is traditionally done; the plant is not cultivated widely or specifically in large areas. Generally, farmers cultivate this plant by raising wild seedlings in their fields, as the seeds are difficult to germinate. Most farmers collect its seedlings that grow wild around existing *Z. acanthopodium* plants, collecting seedlings that grow from burnt land with some remnants of old plants and collected at the edge of the land. This is one of the obstacles for most farmers to propagate and cultivate the plant en masse (Nurlaeni et al. 2021; Siregar 2022).

The distribution of *Z. acanthopodium* is especially in North Sumatra and a small part of Aceh. People in the area have local wisdom to maintain the existence of *Z. acanthopodium*. Some community farming techniques to date have maintained the existence of *Z. acanthopodium* and the environment properly. Not many people know what *Z. acanthopodium* is, the shape of the plant, and other related issues. Moreover, no research has thoroughly explored the botany, morphology, ecology, cultivation, utilization, and traditional conservation in North Sumatra. This study aims to explore the botany, morphology, ecology, cultivation, utilization, and traditional conservation in North Sumatra.

MATERIALS AND METHODS

Study area

The study was conducted in Samosir (Tanjungan Village, Simanindo Sub-district; Salaon Dolok Village, Ronggur Nihuta Sub-district), Simalungun (Sibaganding Village, Girsang Sipangan Bolon Sub-district; Sipangan Bolon Village, Girsang Sipangan Bolon Sub-district), Toba Samosir (North Lumban Rang Sionggang Village, Lumban Julu Sub-district), Dairi (Tanjung Beringin Village, Sumbul Sub-district), and Karo (Berastagi Market on Jalan Penghasilan Tambak Law Mulgap II, Berastagi District, Tanah Karo), North Sumatra, Indonesia (Figure 1).

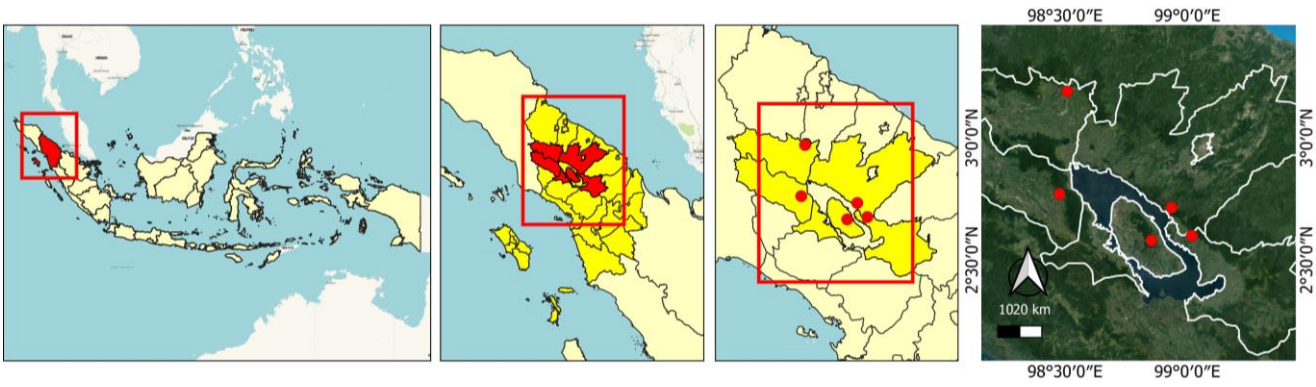

Figure 1. Map of the study area in Samosir, Simalungun, Toba Samosir, Dairi, and Karo, North Sumatra, Indonesia

Observation at the *Z. acanthopodium* planting area

This research was conducted in 2018 and 2019 at Samosir, Simalungun, Toba Samosir, Dairi, and Karo, North Sumatra, Indonesia. The research studied botany, morphology, ecology, cultivation, utilization, and traditional conservation of *Z. acanthopodium* in forests, forest margins, fields, agricultural land, and surrounding community settlements. In addition, interviews were also conducted with landowners and farmers. We also visited two traditional markets in North Sumatra and observed directly the traders who traded *Z. acanthopodium*. During the COVID-19 pandemic, the research was stopped until it was resumed in 2020-2022. Throughout 2020-2022, indirect activities were carried out by conducting interview activities that were carried out by telephone or video call to respondents.

In-depth interviews

Information on the botany, ecology, cultivation, utilization, and traditional conservation of *Z. acanthopodium* was collected by in-depth interviews with selected key informants. Data were collected using qualitative methods that consisted of primary and secondary data. Primary data was obtained in the field through in-depth interviews, participatory observation, and documentation. Participatory observation was conducted by observing the condition of the research sites and participating in the botany, ecology, cultivation, utilization, and traditional conservation of *Z. acanthopodium*. The interview guideline contained topics explored by discussing them in depth with informants via interview processes. An informant is someone who has a great deal of knowledge about an aspect of the local culture (Martin 1955). Interviews with informants were selected based on the snowball method. The interviews were qualitative, also called semi-structured interviews, with informants using interview guidelines. Informants were selected by purposive sampling based on their competence from the population and snowball sampling, considering diversity (triangulation) based on existing categorization. There were a total of 73 respondents interviewed. The informants in this study included 10 farmers in Samosir, 5 farmers in Simalungun, 5 farmers in Dairi, 5 farmers in Humbang Hasundutan, 5 farmers in Toba Samosir, 5 farmers in Toba, an observer in Tobasa, 6 entrepreneurs in Samosir, 2 entrepreneurs in Tobasa, 6 entrepreneurs in Simalungun, three traders in Medan City, a farmer and a trader in Takengon-Aceh District, 2 researchers who have conducted *Z. acanthopodium* research in North Sumatra, 10 spice traders in traditional markets selling *Z. acanthopodium* and 10 samples of household consumers. Interviews were conducted from June to December 2022.

The qualitative data from observations and semi-structured interviews with informants were analyzed by cross-checking, summarizing, synthesizing, and then narrated in a descriptive analysis. Qualitative data analysis is carried out by analyzing the consistency of two perspectives, namely the perspective of the informant (emic) and the researcher's analysis (etic) (Newing 2010; Partasasmita et al. 2016); during the data collection, researchers must always check the validity of the data. This is done by cross-checking by triangulating or comparing data from several informants to obtain their objectivity and reliability or comparing informants with the results of direct research observations. Then, summarizing is done to select the data needed to be combined into a narrative (synthesizing).

Literature review

Meanwhile, to add to the comprehensiveness of the interview results, a literature study was conducted, obtained from scientifically accounted-for sources. Information on the botany, ecology, cultivation, utilization, and traditional conservation of *Z. acanthopodium* was searched through digital reference using keywords: "botany, ecology, cultivation, utilization and traditional conservation of *Z. acanthopodium*." The relevant articles obtained from these keywords were taken from national and international journal articles until September 2023. The articles' language was limited to English and Bahasa Indonesia, and the information on the potential of *Z. acanthopodium* was manually extracted from the collected articles. This research was conducted from January 2018 to September 2023.

RESULTS AND DISCUSSION

Botany of *Z. acanthopodium*

Based on observations at the research site, *Z. acanthopodium* plants have a low-branched shrub habitus with a height of up to 5 meters and have thorns on stems, branching, and twigs. The stem is woody, the shape of the stem is round, there are spines on the surface of the stem, and it is covered with blackish-red or brownish dark green hair. Some varieties have spines on their stems, and some have no spines. On stems with spines, the spines are usually pointed triangles or hook-like. The stem also has branches. The branching appears on the main stem or away from the main stem. The surface of the bark is gray-green or light gray-brown. The leaves are green with serrations on the edges. The leaves are odd-numbered compound leaves characterized by of leaflets at the ends of the main leaf bones. Gasal-pinnate compound leaves or, also called triple leaves, leaf length ranges from 2-25 cm with 3-7 leaflets, overgrown by spines, ovate to obovate-lanceolate, measuring 1-12×0.5-4.5 cm, blunt base, flat or wrinkled glandular edges, pointed or tapered tip. The leaf shape is lanceolate, with serrated leaf margins, dark green leaf color, and leathery leaf surface. The shape of the thorns they are very concave with a brown thorn color, 3-membered compound leaves, dorsiventral, containing oil glands, the leaf seating arrangement is scattered, stalked, leaf length and width 5-20×3-15 cm (Figure 2).

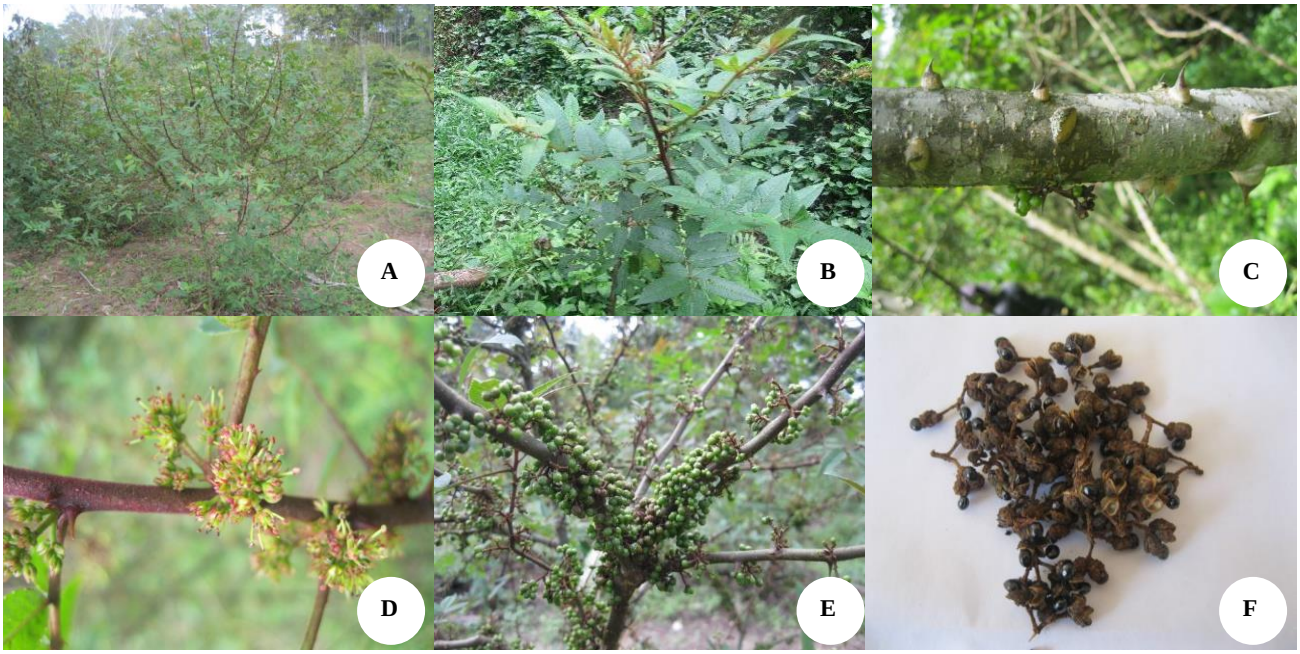

Figure 2. A. *Zanthoxylum acanthopodium* tree, B. Leaves, C. Steam, D. Flower, E. Fruit, F. Ripe fruit with visible seeds

Flowers grow in the leaf axils or on the stem. Flowers are bisexual and pale yellow, including limited compound flowers. The petals are slightly yellowish-green or slightly reddish-green. There are about 5-7 petals on each flower. The fruit is shaped like a pepper and is green when unripe, reddish when ripe, and black when dry. Each fruit has only one seed. Ripe fruits are protected by hard skin and are round, 2-3 mm in size; each fruit has 1 seed: round seed shape, hard skin, shiny black seed surface, smooth surface; young seeds are white while old seeds are black. The fruit gives off a distinctive aroma in the form of a tart taste on the tongue and a citrus-like aroma. The fruit is utilized as a cooking ingredient and traditional medicine. Seeds have a skin with a very hard structure that can inhibit water imbibition and gas exchange during the germination process. Therefore, the germination and regeneration capacity of *Z. acanthopodium* is low.

The root system in *Z. acanthopodium* is a taproot, an institutional root that will continue to grow into a main root that branches out eventually into smaller roots with fine hairs all over its surface. Generally, farmers are very careful when clearing weeds in the area around the roots. Some farmers even argue that the area around the root does not need to be cleaned; it is intended to keep the roots from being damaged by the tools used when cleaning the land, resulting in the plant dying.

Morphology and characteristics of *Z. acanthopodium* varieties

Based on the field observations, it is known that the name *Z. acanthopodium* itself is different in each region in North Sumatra. *Andaliman* in Simalungun is called "*tuba*," in South Tapanuli, it has the name "*sinyarnyar*," in Tanah Karo, it is called "*itir-itir*," and usually the Toba Batak people call it "*tuba*" or "*Andaliman*." In Dairi, it is better known as "*tuba*." In general, the people of North Sumatra recognize three kinds of *Andaliman* cultivars: Simanuk, Sihorbo, and Sitanga (Figure 3). Simanuk is derived from the word '*manuk*' in the Batak language, meaning chicken; it has smaller fruit characters, a stronger aroma than the Sihorbo cultivar, and higher fruit production, while Sihorbo is derived from the word '*horbo*' in the Batak language meaning buffalo; it has larger fruit but less aromatic aroma and lower fruit production compared to Simanuk. Sitanga is derived from the word '*tanga*' in the Batak language, which means ladybug. Sitanga has a very sharp aroma fruit characteristic that resembles the smell of a ladybug, high production but less favored by the public because of its aroma similarity with the smell of a ladybug.

The *Z. acanthopodium* cultivars reported in publications are Simanuk, Sihorbo, Siparjolo, and Sitanga. Batak people in the Toba Samosir area recognize different cultivars: Siramping, Silokot, and Sikoreng. There are two varieties, i.e.: tuba sihorbo and tuba siparjolo, in Dairi, and three varieties: Simanuk, Sihorbo, and Sitanga, around Lake Toba. Raja and Hartana (2017) found that there are four *Z. acanthopodium* cultivars: Simanuk, Sihorbo, Silokot, and Sikoreng, spread across Toba Samosir, Simalungun, Dairi, and North Tapanuli. Meanwhile, according to Simbolon et al. (2018), there are two *Z. acanthopodium* varieties: Simanuk and Sihorbo in Dairi, Toba Samosir, and Simalungun. Moreover, Kintamani et al. (2019) stated in North Sumatra, there are nine varieties of *Z. acanthopodium*: Siholpu, Siganjangpat, Sihalus, Sihorbo, Simanuk, Sirangkak, and three unnamed varieties. Each variety grows at a different altitude and has its morphological characteristics. Kintamani et al. (2019) suggested further research on the essential oil content of each *Z. acanthopodium* variety and its ecological conditions should be studied.

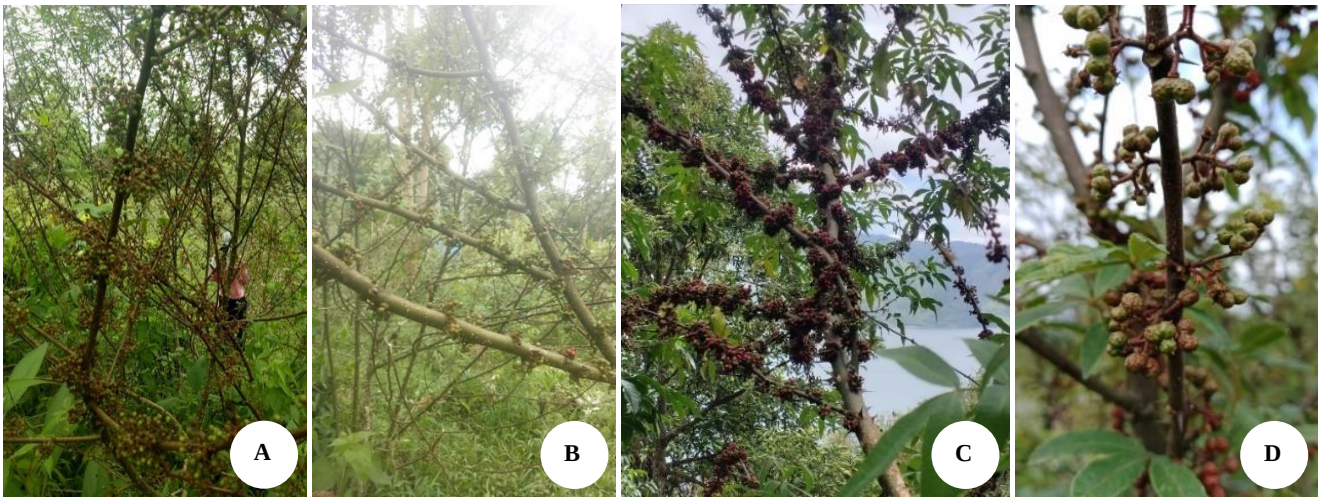

Figure 3. *Zanthoxylum acanthopodium* habits and fruits. A. Simanuk, B. Sihorbo, C. fruit of the simanuk variety, D. fruit of the Sihorbo variety

Siholpu variety has greener leaves, smaller leaf size, more prickles in the middle of the leaf, and short petioles. The fruit has a smaller size and a greener color, and the stalks are short and swarming, with more fruit production than the Siganjangpat variety, fruiting throughout the year; the local community prefers the fruit due to more spiciest taste and the most fragrant. The stem is brown and smaller; the stem prickles and leaves are longer and harder. The siganjangpat variety has yellowish leaves, bigger leaf size, leaves have fewer prickles, and long petioles. Larger-sized fruits, fewer green fruits, longer fruit stalks, less fruit production (only bear fruit twice a year), fruit has a less spicy taste and less fragrant. The stem has a lighter color and bigger size; there are less prickles on the stems and the leaves. The sihalus variety has a smaller leaf size, tight spacing between leaves, and long petioles. The fruit is smaller and more durable to store and produces more fruit; the fruit has the same taste and aroma as the Sihorbo variety. The stem has a smaller size and slightly prickles. The Sihorbo variety has long and large leaf sizes; the fruit has a large size, green and clumps like kaffir lime with the highest fruit production; the fruit has a less spicy taste and is less fragrant; the stem is light green and is very tight prickles. The sirangkak variety has green and red leaves, with more fruit production; the fruit has a spicy taste and is fragrant, and the stem is gray. There are many prickles (Kintamani et al. 2019).

Variety 1 has green-reddish leaves, bigger and longer size. The fruit has a bigger size, less fruit production, and a spicy and fragrant taste. The stem is reddish, and there are many prickles. Variety 2 has small leaves, green and short in size, with smaller fruit and less fruit production; fruit tastes spicy and fragrant. The stem is gray and has short prickles. Variety 3 has greener leaves, moderate and smaller prickles in the middle of the leaf, and a short petiole. The fruit has a smaller size, greener fruit color, short fruit stalk, and the highest fruit production comparable to Siholpu and Siganjangpat varieties; the fruit has a spicy taste and fragrant, and the stem size is bigger and higher than Siholpu and Siganjangpat varieties; has medium prickles, fewer prickles than Siholpu variety but more prickles than Siganjangpat variety (Kintamani et al. 2019).

Ecology of *Z. acanthopodium*

Generally, the study site is at an altitude of 800-1300 masl with a temperature of 17-22°C and a 5-40% slope. *Z. acanthopodium* grows wild in the forest, on forest margins, and some are cultivated along with other crops in farmlands. *Z. acanthopodium* in North Sumatra were harvested from several planting condition types. They are: grow naturally in the forests, as agroforestry planted under pine trees, planted on areas with fairly steep slopes, and planted in the valleys.

***Zanthoxylum acanthopodium* grows wild in the forest.** *Z. acanthopodium* is a wild plant commonly found in North Sumatra's forests (Figure 4.A). Naturally, it will grow after the forest area is burned. Based on information from the community and some farmers, *Z. acanthopodium* is a wild plant that has grown in the forest for decades. The community initially searched for this plant in the forest during certain events, for example, during traditional events, celebrations of holidays involving the entire village population, and family events.

Using an agroforestry system planted under pine trees. *Z. acanthopodium* is planted under pine trees with a spacing of 5x5 meters to 10x10 meters (Figure 4.B). In addition, pine is a type of tree that is large and tall and has a wide crown so that it functions to shade the plants. It is a type of wild plant that cannot tolerate direct sunlight.

Planting *Z. acanthopodium* on areas with fairly steep slopes. *Z. acanthopodium* is found to be planted in areas with a slope of 40% to 50% (Figure 4.C). Generally, these areas were previously vacant, farmers utilize these areas to plant *Z. acanthopodium*.

Planting in the valley. Some farmers utilize the valley area as a location for planting *Z. acanthopodium* (Figure 4.D). This is a wild plant type that cannot tolerate direct sunlight, and the valley area is suitable for the growth.

Particularly for *Z. acanthopodium* that were planted alongside other crops or trees, several cultivation systems are observed in this study. These are the following:

***Zanthoxylum acanthopodium* is planted interspersed with annual crops such as corn, chili, and tomatoes.** Using this planting pattern has many advantages, namely that farmers continue farming crop activities and can continue to harvest the other alternately according to the commodities planted (Figure 4.E). When the price of one commodity decreases, they can rely on other commodities whose prices are stable or even increased.

Using an agroforestry system planted alongside coffee plants. North Sumatra is one of Indonesia's largest Arabica coffee production regions and Arabica coffee is one of the Indonesian main export commodities. *Z. acanthopodium* is usually planted between coffee plants or on the side of coffee plants (Figure 4.F). This is often used as a border plant in the garden to protect coffee plants from pests such as bats, mongooses, and civets. The thorns on the stem become a barrier from these pests attacking.

***Zanthoxylum acanthopodium* is planted next to other crops such as corn fields, upland rice plants, and vegetable fields.** After planting annual crops, some farmers burn the land before starting farming activities again, and *Z. acanthopodium* will grow within one to two months (Figure 4.G). They was then allowed to grow, nurtured, and moved to adjust the planting distance. Therefore, an *Z. acanthopodium* field is formed. The location of this field is usually next to a field that has been planted with annual crops.

***Zanthoxylum acanthopodium* is planted on land not used to cultivate crops in an empty area.** Farmers use land that is still empty for *Z. acanthopodium* planting areas, and they burn the land before starting farming activities and it will grow within one to two months (Figure 4.H). *Z. acanthopodium* is allowed to grow, then nurtured and sorted to adjust the planting distance.

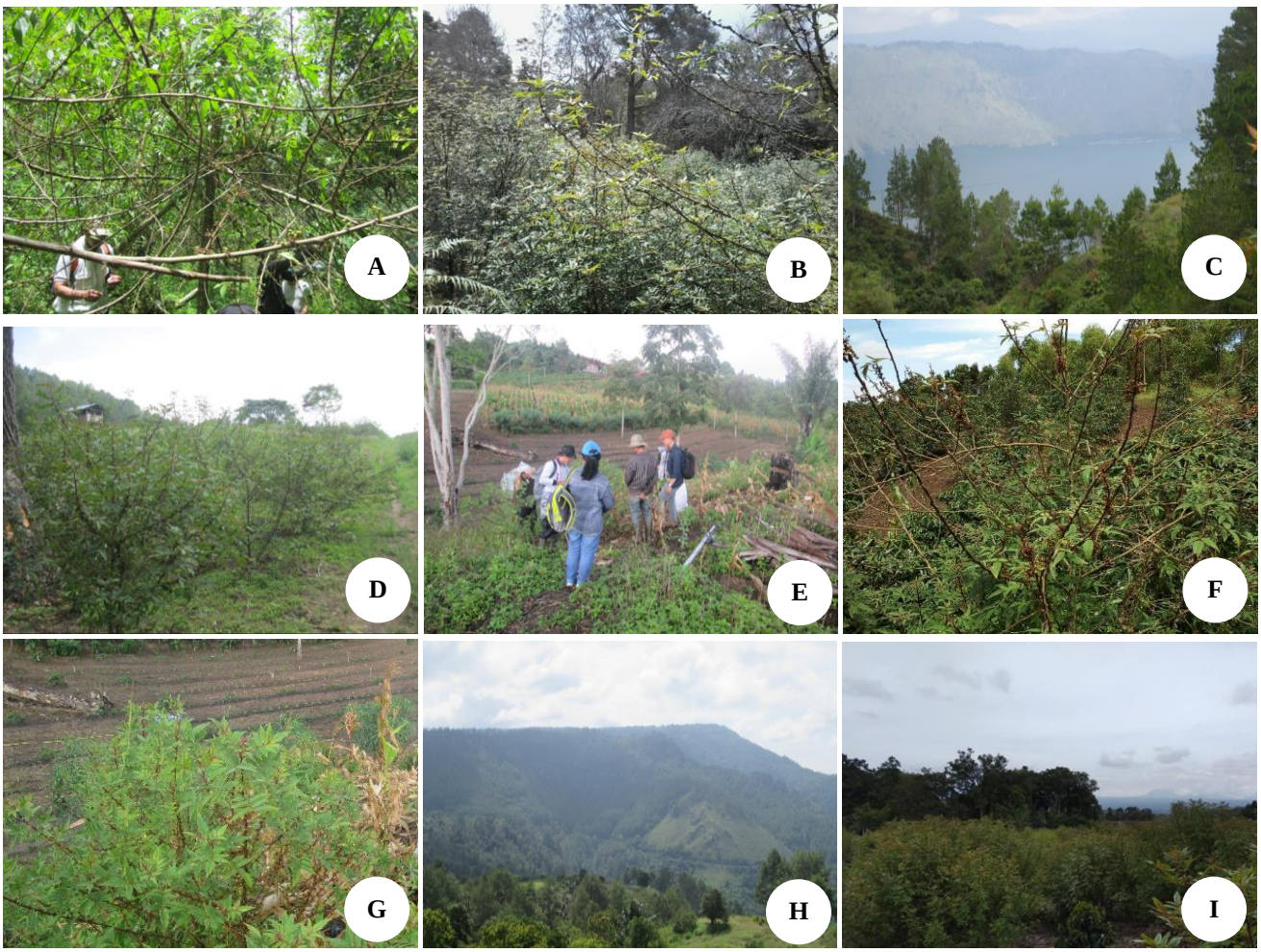

Figure 4. *Zanthoxylum acanthopodium* growth and cultivation. A. Grows wild in the forest. B**.** Planted under pine trees. C**.** On areas with fairly steep slopes. D**.** Valley area as a location for planting. E**.** Planted with chilies, tomatoes, and sweet corn. F. Using an agroforestry system planted alongside coffee plants. G. *Andaliman* is planted next to other crops, such as corn fields. H. *Andaliman* is planted on land that is not used for cultivation of other crops in the form of an empty area. I. *Andaliman* planted in the field by planting *Andaliman* only

***Zanthoxylum acanthopodium* planted in the field by planting this one only.** Some farmers have consistently only planted *Z. acanthopodium* in one large land expanse. Generally, this type of planting is done by farmers with a large land area of 5 to 10 hectares (Figure 4.I). The planted *Z. acanthopodium* can reach 500 and even thousands of stems. Some *Z. acanthopodium* are planted regularly with consistent spacing, and some are irregular. With so many *Z. acanthopodium* planted, farmers can alternately and sustainably harvest fruit. If the price is high, it can be very profitable. Due to the large number of *Andaliman* planted in one large area, many seedlings are also growing around it.

Cultivation of *Z. acanthopodium*

There have been many studies related to the germination of *Z. acanthopodium* seeds. The problem faced in efforts to propagate them generatively is the low germination rate of the seeds. The seeds without treatment had a germination percentage of 30% at 100 days after planting. The hard seed coat structure causes low germination and a relatively long germination age because the hard structure can cause barriers in the water imbibition and gas exchange process. Several studies revealed these low germination and varying germination ages. Shofyani and Sujarwati (2020) scarified *Z. acanthopodium* seeds in H_2SO_4 soaking at concentrations of 0%, 25%, 75%, and 100% with soaking times of 15 minutes, 30 minutes, 45 minutes, and 60 minutes, resulting in a germination percentage of 6.67% at 7th day. Pardosi (2021) also soaked *Z. acanthopodium* seeds with coconut water at concentrations of 0%, 25%, 75%, and 100% with a soaking time of 6 hours, 12 hours, and 60 minutes. Soaking time of 6 hours, 12 hours, 18 hours, 24 hours, and 30 hours resulted in a germination percentage of 0.16% on the 16th day.

Pasaribu (2021) and Pardosi (2021) observed the splitting of the seeds to confirm the presence or absence of endosperm and embryo in the seeds. Based on the observations of Pasaribu (2021), some of the seeds used did not have endosperm and embryos, with a percentage of seeds of 58%, and the results of Pardosi (2021) showed some *Z. acanthopodium* seeds did not have endosperm and embryos with a percentage of seeds 59%. Seeds that do not contain endosperm and embryos are obtained from physiologically mature fruits and have passed seed selection by water immersion due to the thick skin of seeds. These results indicate that seed selection by water immersion is unsuitable for the seeds. Other methods are needed to distinguish seeds that contain endosperm and embryos from those that do not contain endosperm and embryos. Fransiska and Sujarwati (2023) also studied by treatment of seed wounding and soaking with coconut water, revealed the method cannot break the dormancy of seeds; no seeds germinated until the 45th day; the study results on the condition of the seeds on 45th was 76-88% intact, 4-16% slimy, and 4-16% moldy. In addition, seeds are harvested in large quantities when the seed coat is still green; this stage is the best, widely used as a spice. Therefore, the low seed germination potential is largely due to the high number of immature seeds in the panicles and seed fertility due to inadequate pollination caused by excessive humidity and temperature during flowering (Jacob et al. 2023). Based on the results of field surveys and interviews with respondents, it was found that *Z. acanthopodium* is generally planted by maintaining wild plants because the seeds are difficult to germinate (Figure 5.A). Farmers also still use wild seeds taken from their gardens or by asking from other gardeners. Some farmers germinate by burning the area to be planted with *Z. acanthopodium*. Some farmers have planted *Z. acanthopodium* by collecting dead or old ones on the edge of the field by piling them up. After the pile is already high, the pile is burned before the rainy season, and then within one to two months, it will grow. The plant is allowed to grow, then maintained and sorted to adjust the planting distance.

Some farmers germinate by collecting old *Z. acanthopodium* seeds as material to be germinated. Farmers make a 1 x 1 m area of land. The land is dug approximately 2 cm deep. When it has rained 2 to 3 times, the seeds are sown into the excavated soil, and the seeds are sprinkled until the seeds are not visible about 1 cm. Next, apply litter in the form of dry leaves on top, and then burn it. Wait until one to two months for the seedlings to grow. After the seedlings have grown 2 leaves, they can be transferred to polybags. Finally, after about 1 month in the polybag, the seedlings are ready to be planted in the field (Figure 5.D-G).

The interview revealed that this plant does not require fertilization. Farmers only rely on forest litter or apply some litter near the roots; the falling and decomposed litter are important factors contributing to soil quality. Nutrient inputs from litter play an important role in maintaining soil fertility.

The *Z. acanthopodium* farmers have their way, which is the local wisdom of the locals in cultivating them. Their intervention, as well as their skills, are crucial to maintain their farm most sustainably. The farmers often cultivated *Z. acanthopodium* in the agroforestry farm by utilizing land previously overgrown with other plants, such as frankincense, coffee, and other annual crops. The cultivation system was not carried out by cultivating the land areas by regular spacing as in conventional farming, but they planted the seeds found in the forest or around the plants in vacant areas on their agroforestry land, irregularly.

Just before the rainy season, the farmers collect the remaining *Z. acanthopodium* plants and prune the old plants, which are then piled on the edge of the farmland to be burned. After the farmland is exposed to rain for 2 to 4 weeks, the seedlings usually grow and may reach 20 cm before being planted on the dedicated land (Figure 5.B). Techniques for propagating them are done by soaking seeds in hot water for 30 minutes. Next, the seeds are spread on the ground, covered with thin litter, and burned. After that, the seeds are left until they grow into seedlings naturally.

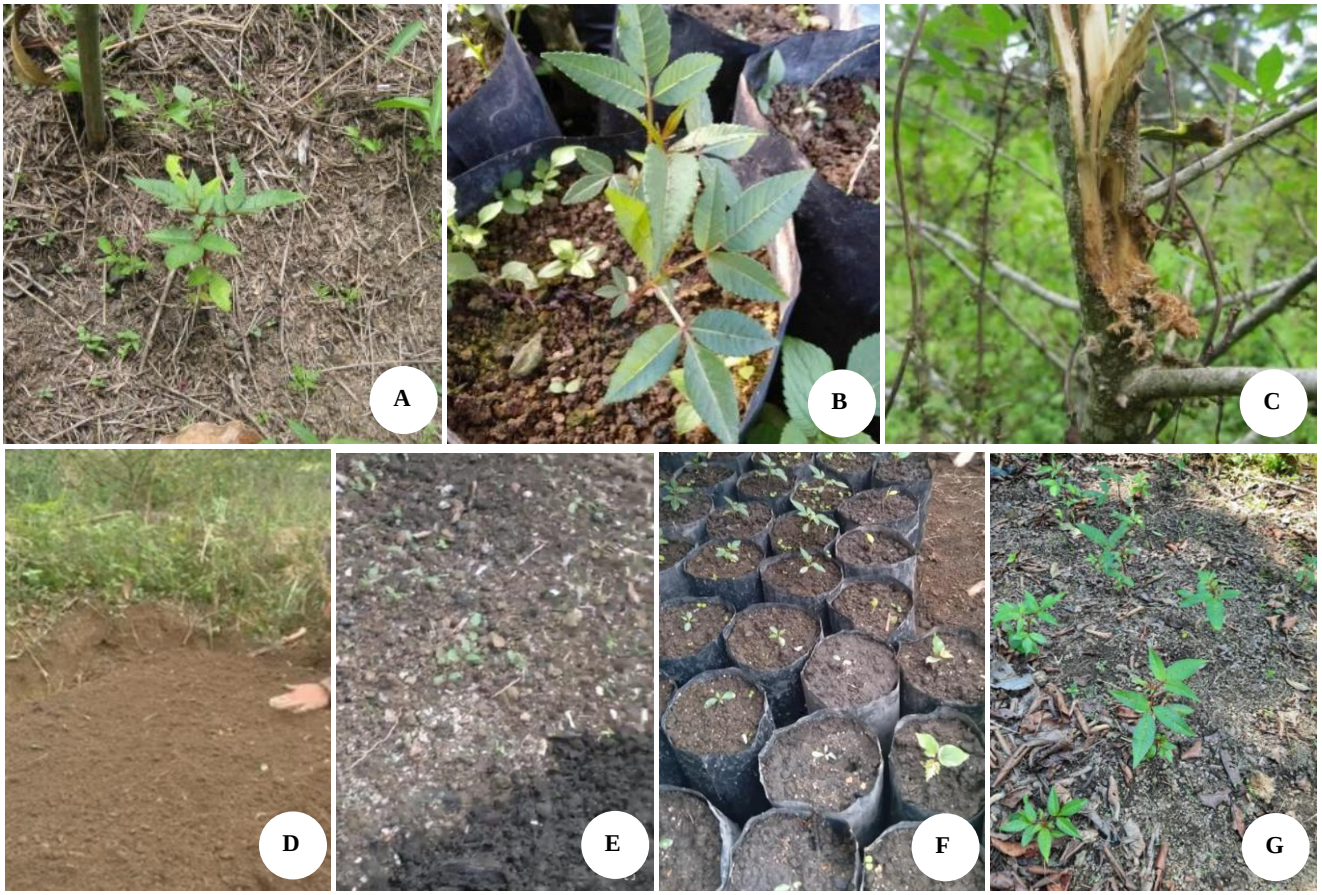

Figure 5. 14. Cultivation of *Z. Acanthopodium.* A. Wild seedlings in the *Andaliman* planting area. B. Symptoms of stem borer attack. C. Seedlings that have reached a height of 20 cm are ready to be planted. D. Making a place for *Andaliman* nursery, E. One to two months later, seedlings will grow, F. After the *Andaliman* seedlings have grown 2 leaves, they can be transferred to polybags, G. After about 1 month in the polybag, the seedlings are ready to be planted in the field

Based on the farmer's information, seed propagation is done by breaking the seeds' dormancy with high-temperature treatment (soaking in hot water and burning). *Z. acanthopodium* seedlings are then put in planting holes and covered with soil and organic litter around the roots to maintain the soil moisture. Then, the seedlings are covered with large leaves to keep the moisture in the soil and to cover the seedlings from direct sunlight exposure. The planting is usually carried out during the rainy season to reduce the mortality rate of the planted seedlings. Local farmers usually use bamboo to mark the planting spot for *Z. acanthopodium* seedlings. The activity of planting the seedlings is not conducted simultaneously but depends on the situation and condition of the land and the age of existing trees. If the farmers have a lot of spare land, the farmers usually multiply planting. Also, if many trees are old and considered unproductive, the plants will be replaced, and planting will be carried out again.

Based on the results of surveys in *Z. acanthopodium* planting locations such as in Simalungun and Dairi, it shows that some *Z. acanthopodium* plants are attacked by stem borers. The symptoms of the attack are that the tip of the twig dries up and there are burrow holes, the larvae burrow into the stem under the skin layer with a burrow diameter of 0.5-1 cm, on the surface of the burrow hole there is sawdust, the larvae burrow into the stem, the depth of the burrow is 1.5-2 cm and the length is 5-15 cm, the affected stem will rot so that it accelerates the death of the plant, and finally the upper end of the branch will die (Figure 5.C).

Traditional utilization

The interview revealed, generally, *Z. acanthopodium* fruit is widely used as a seasoning for traditional Batak dishes, such as in *arsik* carp (carp curry without coconut milk) (Figure 6.A), *natinombur* (grilled fish with *Z. acanthopodium* chili sauce), *saksang* (meat cooked with *Z. acanthopodium* spices), *manuk napinadar* (chicken roasted and mixed with chicken blood) (Figure 6.B), *dengke mas na niura* (raw fish fermented with spices), *gota* chicken (Figure 6.C), *gomak* noodles (Figure 6.D), *tanggo tanggo*, and *Z. acanthopodium* chili sauce (Figure 6.E).

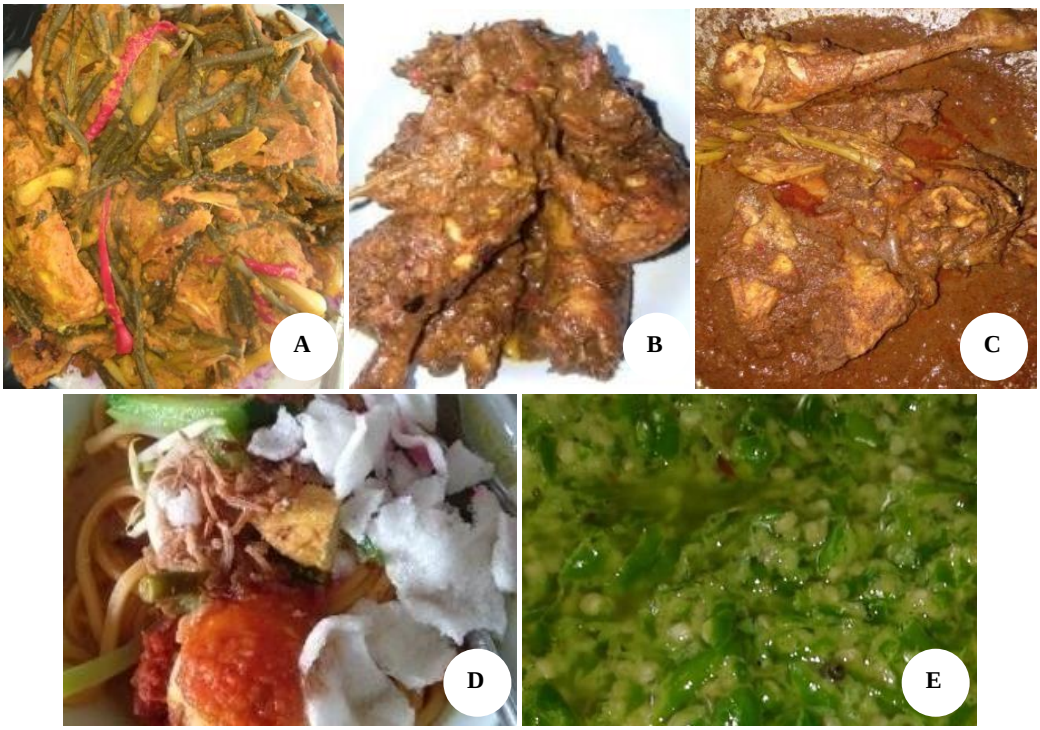

Figure 6. A.*Arsik* carp. B. *Manuk napinadar*. C. *Gota* chicken. D. *Gomak* noodles. E. Chili sauce

The *Z. acanthopodium* fruit as a spice is favored for its distinctive flavor with a citrus, spicy, and bitter aroma, making it flavorful. Apart from being processed with fish or meat, this spice is also consumed as a chili sauce, especially as a complement to food processed by grilling or frying. In processed fish or meat, *Z. acanthopodium* serves as a fishy odor reducer. Since ancient times, the fruit has also been mixed in processed foods for preservation. This is done considering that the technique of extending the expiration time of processed foods by salting is limited due to the lack of salt sources in the highland areas of North Sumatra. Apart from being a spice, various *Z. acanthopodium*-derived products have also been developed in North Sumatra, such as powder, *bandrek*, tea, flavored chips, flavored candy, instant *arsik* seasoning, noodles, meatballs, and pizza.

Zanthoxylum acanthopodium fruits have been one of the main ingredients of various typical cuisines of Bataknese communities in Lake Toba for centuries. This herb is preferred considering the distinctive taste with citrus aroma, bitter spicy and flavorful taste. In these local people, besides being processed with fish or meat, the fruit is also consumed as pickles or chili sauce, especially as a complement to processed foods by grilling or frying. In the past, mixing the fruits in processed food was also applied as a food preservative.

Zanthoxylum acanthopodium conservation

The *Z. acanthopodium* conservation in North Sumatra is based on local communities' traditional agricultural and ecological management. People love and respect them as a plant that can only grow well in their ancestral lands; the existence of *Z. acanthopodium* brings blessings to the people of North Sumatra. There are so many advantages and benefits derived from the existence of *Z. acanthopodium*. Tradition is local wisdom in the form of culture from generation to generation. Based on years of farming experience, farmers state that forests are very suitable for planting locations. The community believes that the forest provides life for the surrounding community economically and spiritually. As part of the environment, the forest must be well preserved. The community manages the forest to protect and fulfill life needs, social integration, education, belief, and self-actualization. Forest resource management based on traditional ecological knowledge encourages the creation of sustainable forest resources. Local knowledge of management and cultivation can contribute to developing cultivation practices that will support farmers' economic growth due to the commercialization as a spice commodity for domestic and export needs. However, the commercialization of *Z. acanthopodium* must still pay attention to environmental sustainability. Due to their distinctiveness and many benefits obtained from *Z. acanthopodium*, people increasingly believe that this plant must be preserved.

Discussion

Moreover, most *Zanthoxylum* species' isolated geographical environments and different climates usually lead to consolidated differences between taxa. *Z. acanthopodium* was classified as a *Zanthoxylum* species and mostly exhibits apomixis, where differences between cultivars may be negligible. Therefore, we hypothesized that the genetic diversity of *Zanthoxylum* species is low on

the cultivar level because of their apomixis and stable genotypes, although they have many different names and are distributed in several different areas (Fei et al. 2021a, b). Unfortunately, the published literature on the genetic diversity of *Zanthoxylum* species and the relationship between their morphological traits and genetic diversity is lacking (Deng et al. 2023).

Aside from the common method of *Z. acanthopodium* farming in farmland, local communities also cultivate this plant as part of the agroforestry system planted under pine trees in Samosir Forest. The farmers planted the seedlings under the shade of large trees such as pine (*Pinus merkusii*), *kayu putih* (*Melaleuca* spp.), *attarasa* (*Litsea cubeba*), and other large trees. *Z. acanthopodium* is usually planted in the forest or on the edge of the forest with a specific habitat profile, namely areas with a steep slope and slightly shaded (Nurlaeni et al. 2021).

Field surveys in these sites show that *Z. acanthopodium* distributed around the Lake Toba Districts, such as in Simalungun, Dairi, Humbang Hasudutan, Samosir, Toba Samosir, Karo, North Tapanuli, and South Tapanuli. The data obtained from field explorations shows 169 distribution points across 8 districts, following Suriani et al. (2019) stated that *Z. acanthopodium* is widely distributed in the Lake Toba region. Habitat characteristics of *Z. acanthopodium* are at an elevation of 854-2,676 masl with rainfall of 1,500-4,000 mm/annual, suitable on 7 land cover types (dryland, agriculture, rice fields, secondary dryland forests, shrubs, industrial plantations, and settlements), 4 soil types (Humic Acrisols, Orthic Acrisols, Humic Cambisols, and Orthic Ferralsols), and 4 critical land types (critical, rather critical, critical potential, and very critical). Environmental variable data used in the analysis. Soil Type, Land Soil type data, FAO, 1979. Soil Map of the World. Rainfall, Sumatra Island rainfall data, ESRI shape rain observation station source files (BMKG, PU, Private) 1970-2004 with a 0.01 degree resolution or 1.11 km. Critical Land, Sumatran Island critical land data, Directorate General of Forestry Planning, Ministry of Forestry Indonesian Repoblic of Indonesia, KML format. Elevation, Sumatera island elevation data, DIVA-GIS shapefile source SRTM30 data set, CGIAR-SRTM data with resolution of 30 arc sec. Land Cover, Land Cover map data, Directorate General of Forestry Planning, Ministry of Forestry Indonesian Republic of Indonesia, KML format.

Research conducted by Junaedi (2019) on the ecology of *Z. acanthopodium* showed that land slope is an important factor in *Z. acanthopodium* abiotic habitat preferences. The SLA measurements showed values that varied between 29.38-88.55 mm^2/mg with a mean SLA value of 54.05 mm^2/mg. Statistical analyses to compare the SLA data of *Z. acanthopodium* differentiated by habitat land use (i.e., natural area versus cultivated area) and habitat slope (high slope versus low slope) showed that they were not statistically different. This was indicated by the p-value of the t-test statistic of 0.073 for different habitat land uses and 0.075 for different habitat slopes. The SLA value between cultivated and growing wild of *Z. acanthopodium* in the forest is not significantly different. In contrast, the SLA value between *Z. acanthopodium* on low and high slopes is relatively different. SLA can capture differences in the habitat conditions. *Z. acanthopodium* that grows naturally requires shade to support its life. The results of this study indicate that fully open habitats with full sun exposure during the day are not suitable for *Z. acanthopodium*. Therefore, to cultivate *Z. acanthopodium*, shade plants are required to a limited extent (especially when it is still a seedling) until it can grow stably. Thus, it can be grown inter-cropped with tall trees that shade the cultivation area.

In this traditional farming, *Z. acanthopodium* growth depends on soil fertility and sufficient rainfall (Nurlaeni and Junaedi 2018; Nurlaeni et al. 2021). Farmers also do not carry out regular maintenance to control weeds and irrigation; watering only relies on rainfall. Furthermore, pesticides for pests and diseases are never used because, according to farmers, the plants are rarely attacked by pests and diseases; for example, the common pests include leaf caterpillars, stem borers, and ants. Generally, farmers collect pests manually because the number of pests can still be controlled without pesticides. *Z. acanthopodium* cultivation growth did not use chemical fertilizers or fungicides, and the control treatment was carried out by clearing the land around the plants (Pane et al. 2022). However, a common disease is root rot, making the plant wither over time, dry up, and die. Usually, farmers will immediately remove the affected part of the plant and then burn it. Local varieties of cultivated crops originate from ancient times, have unique characteristics and have not undergone changes, usually have high genetic diversity, are more adaptable to the local environment, and are closely related to the traditions and cultivation systems that exist in local communities (Feng et al. 2020; Yan et al. 2023).

Some *Zanthoxylum* species are traditional dual-use plants as medicine (Yan et al. 2023). Apart from being a source of healthy nutrition, this spice is also processed and applied in traditional medicine. Ripe fruit can be eaten separately or mixed with other foodstuffs to treat dyspepsia, such as nausea, fullness-feeling (bloating), ulcers, and other stomachache symptoms. Both dried and fresh fruits are crushed into a paste and then rubbed on the gums to reduce the pain of tooth inflammation. In cold weather conditions, especially in higher and mountainous regions, *Z. acanthopodium* fruit is often chewed to warm the body and overcome colds. The roots are also boiled to cure toothache. For topical application, the fruit is crushed into a lotion to treat scabies, and the bark is boiled and used to cure fever, colds, and worm medicine. The essential oil derived from dried and fresh fruit is used for the inflammation of toothaches and to warm the body (Kholibrina and Aswandi 2021). The *Zanthoxylum* genus has become very valuable for discovering and utilizing medicinal and agrochemical natural products (Chen et al. 2022).

Zanthoxylum acanthopodium is also an analgesic that can reduce or eliminate pain. The high iron content in the fruit helps the formation of hemoglobin, a protein in red blood cells responsible for carrying oxygen to all organs and tissues. This condition will facilitate the circulatory system in the body (Natasutedja et al. 2020; Susanti et al.

2020). In addition to the Batak people in the Lake Toba highlands, the people of the Himalayas, Tibet, and the surrounding areas also use them as an aromatic, tonic, appetite generator, and stomach pain medicine (Yonzone et al. 2012; Yonzone and Rai 2016). The successful experience of traditional utilization shows that *Z. acanthopodium* has great prospects as an herbal medicinal ingredient (Bhatt et al. 2018; Muzafri 2019).

Therefore, many steps are needed to protect *Zanthoxylum* biodiversity, including ex-situ conservation. In addition, efforts are needed to strengthen the management of local commodity protection in an area and reduce the disturbance of excessive human activities and exploitation. Genetic diversity and wild *Zanthoxylum* germplasm must be protected immediately, and the community's local wisdom to preserve the environment must be maintained. *Z. acanthopodium*, a typical spice plant that only exists in North Sumatra and part of Aceh, characterizes itself, and we must preserve its existence. Hopefully this article will be a useful reference material as an effort to introduce and preserve it.

ACKNOWLEDGEMENTS

The authors acknowledge the facilities, scientific and technical support from Cibodas Botanical Gardens, Research Center for Plant Conservation, Botanic Gardens and Forestry, the National Research and Innovation Agency, The Head of the Plantation Division of the Samosir District Agriculture Office, Indonesia and staff who have allowed and helped collect research data; the people of North Sumatra, Indonesia who have allowed and helped facilitate research data collection.

REFERENCES

Anggraini DR, Ilyas S, Hasibuan PAZ, Machrina Y, Purba A, Munir D, Putra IB. 2022. Anti-aging activity of *Andaliman* (*Zanthoxylum acanthopodium* DC) fruit ethanol extract on brain weight and p16INK4a expression of hippocampus in aging model rats. Acta Inform Med 30 (4): 283-286. DOI: 10.5455/aim.2022.30.283-286.

Arsita EV, Saragih DE, Aldrin K. 2019. Anticancer potential from ethanol extract of *Zanthoxylum acanthopodium* DC. seed to against MCF-7 cell line. IOP Conf Ser: Earth Environ Sci 293 (1): 12016. DOI: 10.1088/1755-1315/293/1/012016.

Batubara MS, Ginting N, Safri I, Tua S, Umar K. 2020. Osmoregulation and toxicity test ethanolic extracts of *Andaliman* leaves (*Zanthoxylum acanthopodium* DC) against physiological of goldfish (*Cyprinus carpio* L.). J Phys: Conf Ser 1477 (7): 72012. DOI: 10.1088/1742-6596/1477/7/072012.

Bhatt V, Kumar N, Sharma U, Singh B. 2018. Comprehensive metabolic profiling of *Zanthoxylum armatum* and *Zanthoxylum acanthopodium* leaves, bark, flowers and fruits using ultra high performance liquid chromatography. Separation Sci Plus 1 (5): 311-324. DOI: 10.1002/sscp.201800004.

Chen X, Tian L, Tian J, Wang G, Gong X, Feng S, Wei A. 2022. Extensive sampling provides new insights into phylogenetic relationships between wild and domesticated *Zanthoxylum* species in China. Horticulturae 8 (5): 440. DOI: 10.3390/horticulturae8050440.

Deng Y, He Z, Li Y, Ye M, Xiang L. 2023. Six express sequence tag–simple sequence repeat primers reveal genetic diversity in the cultivars of three *Zanthoxylum* species. Curr Issues Mol Biol 45 (9): 7183-7196. DOI: 10.3390/cimb45090454.

Diep TT, Dung LV, Trung PV, Hoai NT, Thao DT, Uyen NTT, Linh TTH, Ha THN, Truc HT. 2023. Chemical composition, antimicrobial, nitric oxide inhibition and cytotoxic activity of essential oils from *Zanthoxylum acanthopodium* DC. leaves and stems from Vietnam. Chem Biodivers 20 (8): e202300649. DOI: 10.1002/cbdv.202300649.

Faradillah F, Santi MA, Sipahutar LW, Nurmi A, Mahmud A. 2020. Effects of *Andaliman* (*Zantoxylum achantopodium*, DC) supplementation on broiler immunity. J Phys: Conf Ser 1477 (7): 72009. DOI: 10.1088/1742-6596/1477/7/072009.

Fei X, Lei Y, Qi Y, Wang S, Hu H, Wei A. 2021a. Small RNA sequencing provides candidate miRNA-target pairs for revealing the mechanism of apomixis in *Zanthoxylum bungeanum*. BMC Plant Biol 21: 178. DOI: 10.1186/s12870-021-02935-5.

Fei X, Shi Q, Qi Y, Wang S, Lei Y, Hu H, Liu Y, Yang T, Wei A. 2021b. ZbAGL11, a class D MADS-box transcription factor of *Zanthoxylum bungeanum*, is involved in sporophytic apomixis. Horticult Res 8 (1): 23. DOI: 10.1038/s41438-020-00459-x.

Feng S, Liu Z, Hu Y, Tian J, Yang T, Wei A. 2020. Genomic analysis reveals the genetic diversity, population structure, evolutionary history and relationships of Chinese pepper. Horticult Res 7: 158. DOI: 10.1038/s41438-020-00376-z.

Fransiska W, Sujarwati S. 2023. Analisis upaya pematahan dormansi biji *Andaliman* (*Zanthoxylum acanthopodium* DC.) dengan pelukaan dan perendaman air kelapa. JOSTECH J Sci Technol 3 (1): 13-22. DOI: 10.15548/jostech.v3i1.4969. [Indonesian]

Gupta DD, Mandi SS. 2013. Species specific AFLP markers for authentication of *Zanthoxylum acanthopodium* & *Zanthoxylum oxyphyllum*. J Med Plants 1 (6): 1-9.

Hanum TI, Laila L. 2018. Physical evaluation of anti-aging and anti-acne peel off gel mask containing *Andaliman* (*Zanthoxylum acanthopodium* DC.) ethanolic extract peel off gel mask. Der Pharm Chem 8 (23): 6-10.

Hartley TG. 1966. A revision of the Malesian species of *Zanthoxylum* (Rutaceae). J Arnold Arboretum 47 (3): 171-221. DOI: 10.5962/p.33416.

He Q, Wang W, Zhu L. 2018. Larvicidal activity of *Zanthoxylum acanthopodium* essential oil against the malaria mosquitoes, *Anopheles anthropophagus* and *Anopheles sinensis*. Malar J 17: 194. DOI: 10.1186/s12936-018-2341-2.

Ilyas S, Simanullang RH, Hutahaean S, Rosidah R. 2022. Suppression of Wnt expression by increasing PI3K in rats cervical carcinoma by *Andaliman* (*Zanthoxylum acanthopodium*). Pak J Biol Sci 25 (1): 29-36. DOI: 10.3923/pjbs.2022.29.36.

Jacob SR, Mishra A, John JK, Gupta V. 2023. Rapid viability test—A tool to aid conservation efforts in *Zanthoxylum rhetsa*. J Trop For Sci 35 (1): 77-81. DOI: 10.26525/jtfs2023.35.1.77.

Julistiono H, Lestari FG, Iryanto R, Lotulung PD. 2018. Antimycobacterial activity of fruit of *Zanthoxylum acanthopodium* DC against *Mycobacterium smegmatis*. Avicenna J Phytomed 8 (5): 432-438.

Junaedi DI. 2019. Ecology of *Zanthoxylum acanthopodium*: Specific leaf area and habitat characteristics. Biodiversitas 20 (3): 732-737. DOI: 10.13057/biodiv/d200317.

Kholibrina CR, Aswandi A. 2021. The ethnobotany and ethnomedicine of *Zanthoxylum acanthopodium* in Lake Toba, North Sumatra, Indonesia. Jurnal Lahan Suboptimal 10 (1): 78-90. DOI: 10.36706/JLSO.10.1.2021.526.

Kintamani E, Batubara I, Kusmana C, Tiryana T, Mirmanto E, Asoka SF. 2023. Essential oil compounds of *Andaliman* (*Zanthoxylum acanthopodium* DC.) fruit varieties and their utilization as skin anti-aging using molecular docking. Life 13 (3): 754. DOI: 10.3390/life13030754.

Kintamani E, Kusmana C, Tiryana T, Batubara I, Mirmanto E. 2019. Wild *Andaliman* (Zanthoxylum acanthopodium DC.) varieties as an aromatic plant from North Sumatera. Proceedings of the 2nd International Conference of Essential Oil. DOI: 10.5220/0009958201400146.

Manurung RD. 2021. Diabetic wound healing in FGF expression by nano herbal of *Rhodomyrtus tomentosa* L. and *Zanthoxylum acanthopodium* fruits. Pak J Biol Sci 24 (3): 401-408. DOI: 10.3923/pjbs.2021.401.408.

Martin AR. 1955. A further study of the statistical composition of the end-plate potential. J Physiol 130 (1): 114-122. DOI: 10.1113/jphysiol.1955.sp005397.

Muzafri A. 2019. Uji aktivitas antimikroba ekstrak *Andaliman* (*Zanthoxylum acanthopodium* DC.) pada *Staphylococus aureus*. Jurnal Sungkai 7 (1): 122-126. [Indonesian]

Muzafri A, Julianti E, Rusmarilin H. 2018. The extraction of antimicrobials component of *Andaliman* (*Zanthoxylum acanthopodium* DC.) and its application on catfish (*Pangasius sutchi*) fillet. IOP Conf Ser: Earth Environ Sci 122: 012089. DOI: 10.1088/1755-1315/122/1/012089.

Napitupulu FIR, Wijaya CH, Prangdimurti E, Akyla C, Yakhin LA, Indriyani S. 2020. Comparison of several processing methods in preserving the flavor properties of *Andaliman* (*Zanthoxylum acanthopodium* DC.) fruit. J Eng Technol Sci 52 (3): 399-412. DOI: 10.5614/j.eng.technol.sci.2020.52.3.7.

Natasutedja AO, Lumbantobing E, Josephine E, Carol L, Junaedi DI, Normasiwi S, Putra ABN. 2020. Botanical aspects, phytochemicals and health benefits of *Andaliman* (*Zanthoxylum acanthopodium*). Indonesian J Life Sci 2 (1): 8-15. DOI: 10.54250/ijls.v2i1.32.

Newing H. 2010. Conducting Research in Conservation: Social Science Methods and Practice. Routledge, New York. DOI: 10.4324/9780203846452.

Nurlaeni Y, Iskandar J, Junaedi DI. 2021. Ethnoecology of *Zanthoxylum acanthopodium* by local communities around Lake Toba, North Sumatra, Indonesia. Biodiversitas 22 (4): 1806-1818. DOI: 10.13057/biodiv/d220426.

Nurlaeni Y, Junaedi DI. 2018. Studi ekologi habitat, teknik perbanyakan dan pengoleksian dalam rangka konservasi ex-situ *Andaliman* (*Zanthoxyllum acanthopodium* DC.). Bioma 14 (2): 79-88. DOI: 10.21009/Bioma14(2).4. [Indonesian]

Pane TC, Rumaijuk BT, Jufri M, Khaliqi M. 2022. Farm business analysis and marketing channels for *Andaliman* agroforestry in Humbang Hasundutan District. IOP Conf Ser: Earth Environ Sci 977 (1): 12048. DOI: 10.1088/1755-1315/977/1/012048.

Panggabean L, Nurhamidah N, Handayani D. 2020. Profil fitokimia dan uji sitotoksik ekstrak etanol tumbuhan *Zanthoxylum acanthopodium* DC (*Andaliman*) menggunakan metode BSLT. ALOTROP 4 (1): 59-68. DOI: 10.33369/atp.v4i1.13711. [Indonesian]

Pardosi JF. 2021. Upaya Pematahan Dormansi Biji *Andaliman* (*Zanthoxylum acanthopodium* DC.) dengan Perendaman Air Kelapa [Skripsi]. Fakultas Matematika dan Ilmu Pengetahuan Alam, Universitas Riau, Pekanbaru. [Indonesian]

Partasasmita R, Iskandar J, Malone N. 2016. Karangwangi people's (South Cianjur, West Java, Indonesia) local knowledge of species, forest utilization and wildlife conservation. Biodiversitas 17: 154-161. DOI: 10.13057/biodiv/d170123.

Pasaribu KM, Gea S, Ilyas S, Tamrin T, Sarumaha AA, Sembiring A, Radecka I. 2020. Fabrication and in-vivo study of micro-colloidal *Zanthoxylum acanthopodium*-loaded bacterial cellulose as a burn wound dressing. Polymers 12 (7): 1436. DOI: 10.3390/polym12071436.

Raja RNL, Hartana A. 2017. Variasi morfologi *Andaliman* (*Zanthoxylum acanthopodium*) di Sumatra Utara. Floribunda 5 (7): 258-266.. [Indonesian]

Rosidah R, Hasibuan PAZ, Haro G, Satria D. 2019. Cytotoxicity activity of ethanol extract of *Andaliman* fruits (*Zanthoxylum acanthopodium* DC.) towards 4T1 breast cancer cells. Indonesian J Pharm Clin Res 2 (2): 31-35. DOI: 10.32734/idjpcr.v2i2.3220.

Shofyani E, Sujarwati S. 2020. Efforts to increase the power seed germinantion of *Andaliman* (*Zanthoxylum acanthopodium* DC) with cemical scarification using sulfuric acid (H_2SO_4). Jurnal Natur Indonesia 18 (2): 82-91. DOI: 10.31258/jnat.18.2.82-91. [Indonesian]

Sibero MT, Siswanto AP, Murwani R, Frederick EH, Wijaya AP, Syafitri E, Farabi K, Saito S, Igarashi Y. 2020. Antibacterial, cytotoxicity and metabolite profiling of crude methanolic extract from *Andaliman* (*Zanthoxylum acanthopodium*) fruit. Biodiversitas 21 (9): 4147-4154. DOI: 10.13057/biodiv/d210928.

Simanullang RH, Situmorang PC, Herlina M, Silalahi B, Manurung SS. 2022. Histological changes of cervical tumours following *Zanthoxylum acanthopodium* DC treatment, and its impact on cytokine expression. Saudi J Biol Sci 29 (4): 2706-2718. DOI: 10.1016/j.sjbs.2021.12.065.

Simbolon WI, Kardhinata EH, Bangun MK, Simatupang S. 2018. Identifikasi karakter morfologis *Andaliman* (*Zanthoxylum acanthopodium* DC.) di beberapa kabupaten di Sumatera Utara. Jurnal Online Agroekoteknologi 6 (4): 745-756. DOI: 10.32734/joa.v6i4.2437. [Indonesian]

Siregar BL. 2022. Budidaya tanaman *Andaliman* (*Zanthoxylum acanthopodium* DC.) di Desa Linggaraja II, Kabupaten Dairi. Jurnal Methodagro 8 (1): 126-136. [Indonesian]

Situmorang C, Herlina M, Silalahi B. 2022. Cytochrome c expression by *Andaliman* (*Zanthoxylum acanthopodium*) on cervical cancer histology. Pak J Biol Sci 25 (1): 49-55. DOI: 10.3923/pjbs.2022.49.55.

Situmorang T, Hasairin A, Gani ARF. 2021. Ragam jenis makanan Etnis Batak Toba dan pengaruh *Andaliman* (*Zanthoxylum Acanthopodium* DC) terhadap makanan Batak Toba. Prosiding Webinar Nasional VII Biologi dan Pembelajarannya 6: 319-329. [Indonesian]

Suriani C, Prasetya E, Harsono T, Handayani D. 2019. Habitat characteristics of *Andaliman* (*Zanthoxylum acanthopodium* DC) in North Sumatra using a GIS (Geographical Information System) approach. J Phys: Conf Ser 1317: 021097. DOI: 10.1088/1742-6596/1317/1/012097.

Susanti N, Situmorang E, Fitri W. 2020. Effectiveness of the antibacterial activity of n-hexane *Andaliman* (*Zanthoxylum acanthopodium* DC) extract against *Bacillus subtilis*, *Salmonella typhi*, and *Staphylococcus aureus*. J Phys: Conf Ser 1462 (1): 12072. DOI: 10.1088/1742-6596/1462/1/012072.

Wijaya CH, Napitupulu FI, Karnady V, Indariani S. 2019. A review of the bioactivity and flavor properties of the exotic spice "*Andaliman*" (*Zanthoxylum acanthopodium* DC.). Food Rev Intl DOI: 10.1080/87559129.2018.1438470.

Yan S, Zhao J, Li X, Zhao C, Huang D, Hu Z, Diao Y. 2023. Genetic variation and population genetic structure of *Zanthoxylum armatum* in China. Genet Resour Crop Evol 70: 2425-2437. DOI: 10.1007/s10722-023-01571-2.

Yanti Y. 2016. Active fractions from *Zanthoxylum acanthopodium* fruit modulate inflammatory biomarkers in lipopolysaccharide-induced macrophages in vitro. Intl J Infect Dis 45: 289. DOI: 10.1016/j.ijid.2016.02.639.

Yonzone R, Bhujel RB, Rai S. 2012. Medicinal wealth of darjeeling hills used against various ailments. Adv Plant Sci 25 (2): 603-607. DOI: 10.1016/S2221-1691(12)60203-2.

Yonzone R, Rai S. 2016. *Zanthoxylum acanthopodium* DC.(Rutaceae)—A favourable ethnomedicinal fruit for the local inhabitants of Darjeeling Himalaya of West Bengal, India. J Complement Med Alternat Healthcare 1: 555554. DOI: 10.19080/JCMAH.2016.01.555554.

Zhang J, Yu L, Han N, Wang D. 2023. Characterization of phenolic chemotypes, anatomy, and histochemistry of *Zanthoxylum bungeanum* Maxim. Ind Crops Prod 193: 116149. DOI: 10.1016/j.indcrop.2022.116149.

THIS PAGE INTENTIONALLY LEFT BLANK

NUSANTARA BIOSCIENCE
Vol. 16, No. 1, pp. 81-88
May 2024

ISSN: 2087-3948
E-ISSN: 2087-3956
DOI: 10.13057/nusbiosci/n160110

Mammal diversity in the geothermal power plants, West Java, Indonesia

TEGUH HUSODO[1,2,3,♥], ERRI NOVIAR MEGANTARA[1,2,3], INDRI WULANDARI[1,2,3], IRINA ANINDYA MUSTIKASARI[1,2,3], PUPUT FEBRIANTO[3], MUHAMMAD PAHLA PUJIANTO[3], NUGRAHA PUTRA MAULANA[3], YUANSAH[4]

[1]Department of Biology, Faculty of Mathematics and Natural Sciences, Universitas Padjadjaran. Jl. Raya Bandung-Sumedang KM 21, Jatinangor, Sumedang 45363, West Java, Indonesia. Tel.: +62-22-7796412, Fax.: +62-22-7794545, ♥email: teguhhusodo2@gmail.com
[2]Program in Environmental Science, School of Graduates, Universitas Padjadjaran. Jl. Sekeloa, Coblong, Bandung 40134, West Java, Indonesia
[3]Centre of Environment and Sustainable Science, Directorate of Research, Community Services and Innovation, Universitas Padjadjaran. Jl. Sekeloa, Coblong, Bandung 40134, West Java, Indonesia
[4]PT PLN Indonesia Power Kamojang Power Generation and O&M Service Unit Komplek PLTP Kamojang. Laksana Village, Ibun, Bandung 40384, West Java, Indonesia

Manuscript received: 22 November 2023. Revision accepted: 2 February 2024.

Abstract. *Husodo T, Megantara EN, Wulandari I, Mustikasari IA, Febrianto P, Pujianto MP, Maulana NP, Yuansah. 2024. Mammal diversity in the geothermal power plants, West Java, Indonesia. Nusantara Bioscience 16: 81-88.* Geothermal energy is a critical renewable resource to address global energy demands. West Java, Indonesia, in particular, stands out with six geothermal power plants, including Kamojang, Gunung Salak, and Darajat Geothermal Power Plants. However, developing geothermal potential in biodiverse highland ecosystems raises concerns about its negative impact on biodiversity, especially mammals, making it essential to monitor and manage these areas for environmental sustainability. In 2019, a comprehensive study on mammal species was conducted in three geothermal power plants: Kamojang, Darajat, and Gunung Salak, all located in West Java, Indonesia. These geothermal power plants are located within diverse natural landscapes. The study employed various methods such as direct encounters, sign surveys, collapsible trapping, camera traps, and interviews with local communities. The mammal diversity study around the Kamojang, Darajat, and Gunung Salak Geothermal Power Plant areas revealed 32 mammal species from 18 families. Gunung Salak had the highest diversity with 22 species, primarily Sciuridae, primates, and some Carnivora species. Conversely, Kamojang had 20 species dominated by Muridae, and Darajat had 19 species with a similar dominance of Muridae, highlighting different characteristics among these geothermal power plant locations. Conservation status analysis identified species of high conservation concern, emphasizing the importance of preserving these habitats for biodiversity conservation.

Keywords: Darajat, Halimun-Salak National Park, Kamojang, mammals

Abbreviations: PLTP: Geothermal Power Plant

INTRODUCTION

The geothermal energy is one of the renewable resources that provides an alternative solution to meet the growing global energy demand. Indonesia is the largest geothermal producer worldwide, having 29.5 Gigawatt electrical potential (Pambudi and Ulfa 2023). West Java has the largest geothermal potency than other provinces, with six geothermal power plants in Indonesia (Setiawan et al. 2018). The top three geothermal power plants with more than 200 MWe capacity are Kamojang, Gunung Salak, and Darajat Geothermal (Setiawan et al. 2018).

Geothermal systems are associated with volcanic structures situated in subduction zones along the edges of continental plates. Most geothermal heat sources are higher along the volcanic belt (Pambudi and Ulfa 2023). Many of these locations are still covered by forests and are integrated into Indonesia's protected area network for conservation purposes. Furthermore, 57% of the geothermal areas are located in forest areas, 22% in conservation forest areas, and others in protection and production forest areas (Meijaard et al. 2019).

In contrast to the high potential of geothermal as a renewable energy source, the increasing development of geothermal potential negatively impacts habitats and species in the geothermal potential location. The decline in biodiversity will significantly impact the environment (Rehbein et al. 2020). The expansion of operational areas for geothermal power plants significantly impacts mammal populations by diminishing the available comfortable and suitable habitats. Therefore, the increased operational footprint disrupts the natural habitat of mammals, potentially leading to ecological imbalances, altered species dynamics, and challenges sustaining a healthy and diverse mammal population. The effects of geothermal activity in forested regions are manifested through expected consequences like fragmentation, disturbance to wildlife and their distribution, poaching, and illegal logging (Meijaard et al. 2019). Geothermal operations contribute to ecosystem disruptions, posing biodiversity and wildlife behavior challenges. The biological characteristics of an ecosystem are usually seen in its biodiversity, as well as the

existence of important fauna and flora (endemic, rare, and endangered), such as mammals. Mammals are considered bioindicators within terrestrial ecosystems due to their role in conserving other species and upholding ecosystem balance (Udy et al. 2021). The mammal species' roles include the dispersal of vegetation seeds, playing a significant role in maintaining the balance of the rainforest ecosystem (Lacher et al. 2019).

The various impacts generated by geothermal power plants must be managed to preserve forests and biodiversity and their ecological functions. The geothermal power plant developments aim to provide clean and green electrical energy. The company is responsible for protecting natural resource balance and preventing environmental damage based on state regulation Number 5 of 1984 about industrial. Therefore, it strives to provide the latest information about biotic environmental components, such as mammal diversity. Then, the information will be used as a reference in managing biodiversity in the future.

A previous study showed that 54 species of mammals are distributed from lowland to highland in several sites of West Java (Husodo et al. 2019). Some high-risk conservation species were recorded in West Java, such as the Javan leopard (*Panthera pardus* subsp. *Melas* Cuvier, 1809), Javan gibbon (*Hylobates moloch* Audebert, 1798), Javan pangolin (*Manis javanica* Desmarest, 1822), Javan slow loris (*Nycticebus javanicus* E. Geoffroy, 1812), lesser mouse-deer (*Tragulus javanicus* Osbeck, 1765), and small-clawed otter (*Aonyx cinereus* Illiger, 1815) (Husodo et al. 2019). This research aims to determine the latest condition of mammal diversity, including its conservation in the geothermal power plants in West Java, Indonesia, i.e., Kamojang, Gunung Salak, and Darajat Geothermal Power Plants.

MATERIALS AND METHODS

Study area

The study was conducted in the Kamojang (April 2019), Gunung Salak (June 2019), and Darajat (September 2019) Geothermal Power Plant area, West Java, Indonesia (Figure 1). Administratively, Kamojang-Darajat Geothermal Power Plants covered 45,380 ha in Bandung and Garut Districts, while Gunung Salak is in the western of Gunung Salak, Bogor and Sukabumi Districts, West Java. The Gunung Salak Geothermal area is an area of 10,000 ha, including 228 ha of Perhutani Land (Meijaard et al. 2019). In Kamojang, the study area covered with production forests, shrubs, secondary forests, mixed gardens, riparian, swamps, and artificial parks. In Darajat, the study area covered with built-up area (Indonesia Power Office), craters, riparian, secondary forests, and lake. In Gunung Salak, the study area covered with secondary forests, riparian, tea plantation, and built-up areas.

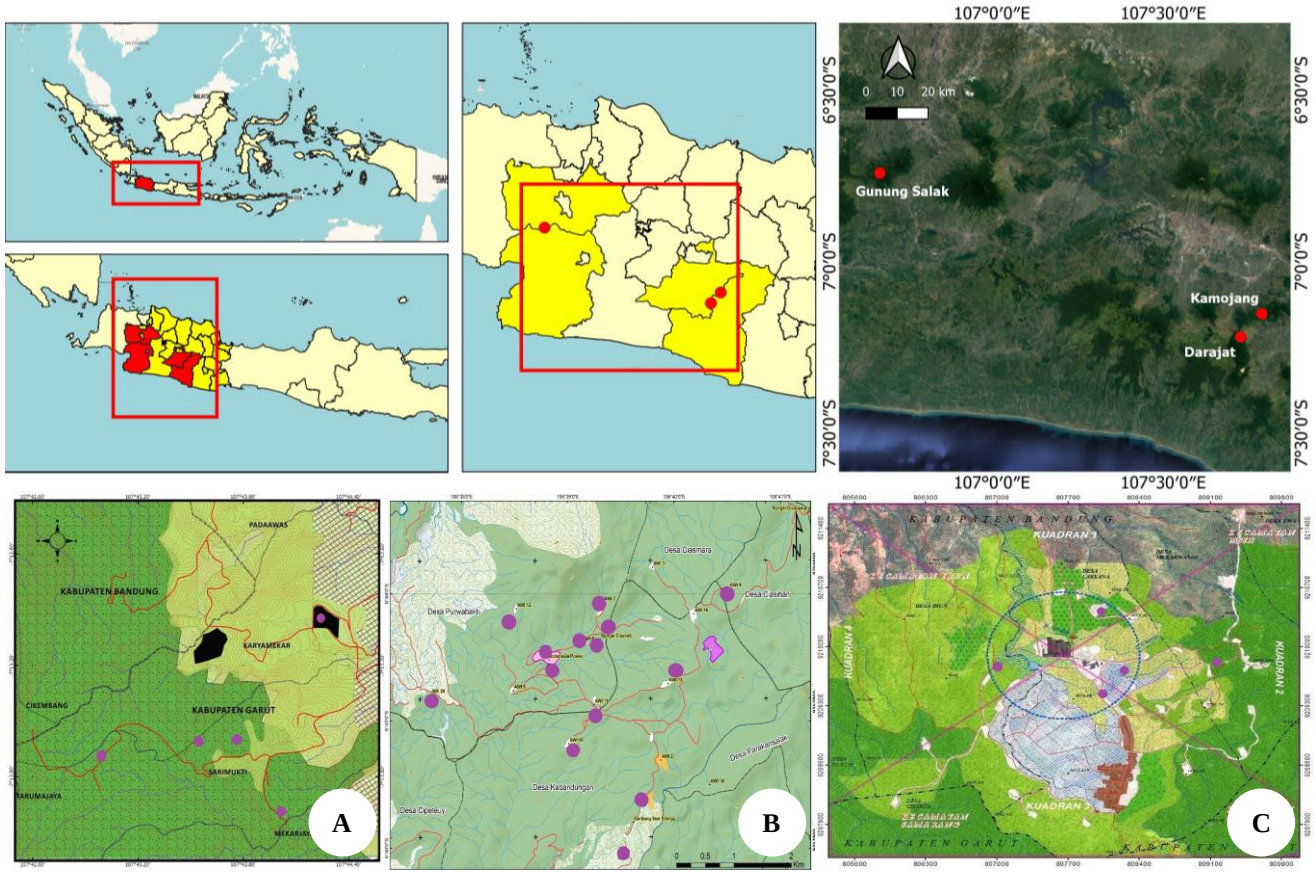

Figure 1. Study areas at Geothermal Power Plants in West Java, Indonesia. A. Darajat Geothermal Power Plant (48 M, 800811.68 m E 9200549.76 m S); B. Gunung Salak Geothermal Power Plant (48 M, 683756.00 m E 9255797.00 m S); and C. Kamojang Geothermal Power Plant (48 M, 808381.73 m E 9209763.04 m S) (●: Sample areas)

Procedures

The data were collected through a qualitative approach by combining several methods, such as unstructured interviews, sign surveys, direct observation, camera trapping, and collapsible traps. Each site was studied for five days.

Unstructured interviews

The interviews were conducted to identify potential habitats and the presence of mammal species. The interview was conducted with guidelines made previously and could be developed during the interview. The informants were patrol workers, security officers, and local people. Those informants were encountered during observation. We assume that those informants had experiences in mammal discovery during day and night. The species recorded were those discovered by the informants in the last six months.

Sign surveys

Sign surveys were conducted to encounter the mammal tracks, such as feces, footprints, scratches on the ground or trees, hairs, and leftovers. Two observers survey in the sampled areas (Figure 1) at 06.00 a.m. - 11.00 a.m. and 03.00 p.m. - 05.00 p.m. Indirect evidence is beneficial for surveying mammals, such as carnivores, that are elusive, rare, found in low densities, and challenging to capture repeatedly. The presence of medium and large mammals was also precisely indicated using indirect evidence, such as sounds, spines, burrows, and feces (Campos et al. 2013; Borges et al. 2014; Dereje et al. 2015). References of mammals track used a guidebook of van Strien (1983).

Direct observation

Observations were conducted on mammals, except bats. Surveys in the sample areas (Figure 1) were performed three times a day: 06.00 a.m. - 11.00 a.m. and 03.00 p.m. - 05.00 p.m., when most mammals were more active in the study area (Meseret and Solomon 2014; Dereje et al. 2015), and at night (07.00 p.m. - 10.00 p.m.). During data collection, an observer walks on foot along each transect and directly counts all the individuals sighted with their respective species using unaided eyes and binoculars. Information like species, the number of individuals, location, habitat type, sex, and age were recorded (Campos et al. 2013). Signs of the mammal's existence that need to be considered included the movement of tree branches and branches and sounds.

Camera trapping

Camera traps are widely used in Southeast Asia for conservation and research, particularly for the inventory of ground-dwelling mammals within conservation landscapes (Moo et al. 2017). Camera trap installation is used to optimize the sampling time for 24 hours. Five camera traps were installed in 6-7 days using hybrid mode (one unit) and photo mode (four units). The camera trap installation determination was based on the local people's recommendations, the mammal tracks, and previous research (Husodo et al. 2019). Cameras were placed between 30 and 50 cm above and perpendicular to the ground. All photographs were checked manually, and encounters were identified to species by the author (Gray 2018). According to Sollmann et al. (2013), the primary survey area's camera traps were set along active or abandoned logging roads, but the others were set randomly within the forest. We recorded each camera's installation period and retrieval and calculated the total trap days (Debata and Kedar 2018).

Collapsible trap

The traps used are the Collapsible Sherman Trap and Collapsible Wire Trap. The Sherman Trap measured 30 cm × 10 cm × 12 cm, and the Wire Trap measured 30 cm × 20 cm × 15 cm. The number of traps set was ten each, placed on the ground at a distance of 5 m each. Trap installation was carried out for one day at each predetermined sampling location. In this monitoring, the bait used to capture small mammals was oatmeal flavored with peanut butter (Hoffmann et al. 2010). This collapsible trap is set in several hotspots for overnight. Traps should be set as late in the afternoon as possible (around sunset) and opened as early as possible (sunrise) (Machtinger and Williams 2020). The bait used was a mix of peanut butter and oats wrapped in gauze (Hoffmann et al. 2010; Husodo et al. 2019).

Data analysis

The data obtained by unstructured interviews, camera trapping, collapsible trapping, and sign surveys were entried using Ms. Excel. Each species encountered was recorded based on conservation status, referring to the Environment and Forestry Ministry of the Republic of Indonesia Regulation No. P 106 of 2018 concerning the protected plant and animal species, IUCN (International Union for Conservation of Nature) Red List, and CITES (Convention on International Trade of Endangered Species).

RESULTS AND DISCUSSION

A total of 32 species of 18 families (Table 1; Figure 2) were encountered in the geothermal power plants and its surroundings. Almost 78% of mammals were found directly with direct encounter and collapsible trap methods, and the others were discovered indirectly with sign surveys, camera traps, or local people interviews. Gunung Salak Geothermal Power Plant was found the most with 22 species; about 68% of species are found directly, especially the Sciuridae family, Primate family, and some species of Carnivore orders. Twenty species was encountered in the Kamojang Geothermal Power Plant following the Gunung Salak Geothermal Power Plant. 80% of species of mammals are encountered directly, and the most commonly found species are from the Muridae family. And lastly, Darajat Geothermal Power Plant has 19 species, with 74% encountered directly. This location has the exact most commonly found species, the Muridae family.

Table 1. Mammals diversity in the geothermal power plants, West Java, Indonesia

Ordo | Family | Species	Common Name	Study Areas			Conservation Status		
		KMJ	DRJ	GS	P106	IUCN	CITES
Artiodactyla							
Cervidae							
Muntiacus muntjak (Zimmermann, 1780)	Southern Red Muntjak		S,I	S, I	✓	LC	
Suidae							
Sus scrofa (Linnaeus, 1786)	Wildboar	S,I	S	S		LC	
Tragulidae							
Tragulus javanicus (Osbeck, 1765)	Lesser Mouse-Deer			S	✓	DD	
Carnivore							
Felidae							
Panthera pardus melas (Cuvier, 1809)	Javan Leopard	I	S	S, I	✓	CR	I
Prionailurus bengalensis (Kerr, 1782)	Leopard Cat	S, I	S, CT	I	✓	LC	II
Herpestidae							
Herpestes javanicus (E. Geoffroy Saint-Hilaire, 1818)	Javan Mongoose	I	S	DE		LC	III
Mephitidae							
Mydaus javanensis (Desmarest, 1820)	Sunda Stink Badger			DE		LC	
Mustelidae							
Melogale orientalis (Horsfield, 1821)	Javan Ferret-badger		DE			LC	
Prionodontidae							
Prionodon linsang (Hardwicke, 1821)	Banded Linsang			S, I	✓	LC	II
Viverridae							
Paradoxurus hermaphroditus (Pallas, 1777)	Asian Palm Civet	DE	DE	DE		LC	III
Chiroptera							
Pteropodidae							
Rousettus amplexicaudatus (E. Geoffroy Saint-Hilaire, 1810)	Geoffroy's Rousette			DE		LC	
Eulipotyphla							
Soricidae							
Suncus murinus (Linnaeus, 1758)	Asian House Shrew	T				LC	
Pholidota							
Manidae							
Manis javanica (Desmarest, 1822)	Sunda Pangolin			S, I	✓	CR	I
Primate							
Cercopithecidae							
Macaca fascicularis (Raffles, 1821)	Long-tailed Macaque			DE		EN	II
Presbytis comata (Desmaret, 1822)	Grizzled Leaf Monkey	DE	DE	DE	✓	VU	II
Trachypithecus auratus (E. Geoffroy, 1822)	Javan Langur	DE	DE	DE	✓	VU	II
Hylobatidae							
Hylobates moloch (Audebert, 1798)	Silvery Gibbon			DE	✓	EN	I
Lorisidae							
Nycticebus javanicus (E. Geoffroy, 1812)	Javan Slow Loris	DE		DE	✓	CR	I
Rodentia							
Sciuridae							
Callosciurus nigrovittatus (Horsfield, 1823)	Black-striped Squirrel	DE	DE	DE		NT	
Callosciurus notatus (Boddaert, 1785)	Plantain Squirrel			DE		LC	
Petaurista petaurista (Pallas, 1766)	Red Giant Flying Squirrel	DE	DE	DE		LC	
Ratufa bicolor (Sparman, 1778)	Black Giant Squirrel			DE		NT	II
Muridae							
Chiropodomys gliroides (Blyth, 1856)	Pencil-tailed Tree Mouse	T	T			LC	
Hylomys suillus (Muller, 1840)	Short-tailed Gymnure	T	T			LC	
Maxomys surifer (Miller, 1900)	Red Spiny Rat	T	T			LC	
Rattus exulans (Peale, 1848)	Polynesian Rat	T	T			LC	
Rattus tiomanicus jalorensis (Bonhote, 1903)	Malayan Field Rat	T	T			LC	
Rattus norvegicus (Berkenhout, 1769)	Brown Rat		T			LC	
Rattus rattus (Linnaeus, 1758)	House Rat	T				LC	
Rattus tiomanicus sabae (Miller, 1900)	Malayan Wood Rat	T	T	T		LC	
Scandentia							
Tupaiidae							
Tupaia glis (Diard & Duvaucel, 1820)	Common Tree Shrew	DE				LC	II
Tupaia javanica (Horsfield, 1822)	Javan Tree Shrew	DE	DE	DE		LC	II

Note: Primary Data (2019); KMJ: Kamojang; DRJ: Darajat; and GS: Gunung Salak. Data Types = DE: Direct Encounter, I: Interview, T: Collapsible Trap, S: Sign, CT: Camera Trap; P106: Regulation of the Minister of Environment and Forestry of the Republic of Indonesia No. P 106 of 2018 on species of Protected Plants and Animals; IUCN = CR: Critically Endangered; EN: Endangered; VU: Vulnerable; NT: Near Threatened; DD: Data Deficient, CITES = I: Appendix I; Appendix II; Appendix III

Figure 2. Mammal species in Geothermal Power Plant, West Java, Indonesia. A. *Melogale orientalis*, B. *Trachypithecus auratus*, C. *Presbytis comata*, D. *Nycticebus javanicus*, E. *Hylobates moloch*, F. *Callosciurus notatus*, G. *Paradoxurus hermaphroditus*, H. *Rousettus amplexicaudatus*, I. *Petaurista petaurista*, J. *Panthera pardus* subsp. *melas*, K. *Prionailurus bengalensis*, L. *Sus scrofa*

Although these three sites are in the highlands, every site has different characteristics. Gunung Salak Geothermal Power Plant has the most diverse characteristics. In this location, the Sciuridae family has the highest number of species; this may indicate that no species dominates the presence. From 2018, there was no significant change in this family of black giant squirrels, which previously could not be found directly (Husodo et al. 2019); in June 2019, while monitoring, it was found directly. In this study, the family Muridae is rarely seen. It was only found in a disturbing forest community dominated by existing buildings. Family Muridae can adapt to highly damaged habitats; these rats could be found in highly damaged habitats, such as around settlements or urban areas (Amni et al. 2019). It was also recorded by Husodo et al. (2019) that only Malayan wood rat (*Rattus tiomanicus sabae* (Miller, 1900)) was found in the Gunung Salak Power Plant. Gunung Salak Power Plant has some species that are only found in this power plant, such as lesser mouse-deer (*T. javanicus*), Sunda stink badger (*Mydaus javanensis* (Desmarest, 1820)), banded linsang (*Prionodon linsang* (Hardwicke, 1821)), geoffroy's rousette (*Rousettus amplexicaudatus* (E. Geoffroy Saint-Hilaire, 1810)), long-tailed macaque (*Macaca fascicularis* (Raffles, 1821)), Sunda pangolin (*M. javanica*), and silvery gibbon (*H. moloch*).

The *T. javanicus*, *M. javanensis*, *P. linsang*, and *R. amplexicaudatus* are lack information because their status conservation is still of the Least Concern and Data Deficient (IUCN 2023). In 2014, the previous study recorded that *T. javanicus*, *M. javanensis*, and *P. linsang* was encountered in Java by Rode-Margono et al. (2014). Moreover, that study explains there is no direct encounter or camera trap record of *M. javanensis* (Desmarest, 1820). In addition, *M. fascicularis*, *M. javanica*, and *H. moloch* are rare species also found in this location. As one of the

potential locations of mammals' habitat, the Gunung Salak Power Plant is located at the hill of Gunung Salak, so it is possible to find diverse mammals (Megantara et al. 2019). The *M. fascicularis* population is believed to have decreased by around 40% (42 years) over the last three generations (IUCN 2023). It makes the status conservation of *M. fascicularis* change, being Endangered (IUCN 2023). This species is observed to be abundant, especially in Java and the density of this species is around eight ind/ha (Hansen et al. 2020a). This species is in danger due to various threats, so it is necessary to study the population and range across Southeast Asia (Hansen et al. 2021).

Meanwhile, Kamojang-Darajat, as an adjoining location, also has the same characteristics. In Kamojang-Darajat, small mammals from the Muridae family are the most dominating species because they are found in all monitoring locations. The genus *Rattus* dominates the Indonesia Power office area. The malayan field rat (*Rattus tiomanicus jalorensis* (Bonhote, 1903)) is the most common species in three sites. Rodents can be found in many land environment types, including farmland and local housing areas; the fields with high crop density could increase the density of rodents (Fischer et al. 2017). The condition of these four monitoring locations, which are adjacent to horticultural gardens and shrubs at specific points, is a supporting factor for the continued existence of rodent species, such as rats; as an individual rodent's ability to move around, its tolerance to different environmental conditions, and how it interacts with other species. Rodents play a crucial role in utilizing resources in their surroundings, especially in predation, competition, and environmental stress, which can hinder their access to essential resources (Royer et al. 2016).

Moreover, 11 species were found in all sites, such as wildboar (*Sus scrofa* (Linnaeus, 1786)), Javan leopard (*P. pardus* subsp. *melas*), leopard cats (*Prionailurus bengalensis* (Kerr, 1782)), Javan mongoose (*Herpestes javanicus* (E. Geoffroy Saint-Hilaire, 1818)), Asian palm civet (*Paradoxurus hermaphroditus* (Pallas, 1777)), grizzled leaf monkey (*Presbytis comata* (Desmaret, 1822)), Javan langur (*Trachypithecus auratus* (E. Geoffroy, 1822)), Black-striped squirrel (*Callosciurus nigrovittatus* (Horsfield, 1823)), red giant flying squirrel (*Petaurista petaurista* (Pallas, 1766)), malayan wood rat (*Rattus tiommanicus sabae* (Miller, 1900)), and Javan tree shrew (*Tupaia javanica* (Horsfield, 1822)). All those species were also encountered in the previous study by Husodo et al. (2019).

Javan leopard (*P. pardus* subsp. *melas*) and its population across various fragmented landscapes in Java land are more isolated than previously hypothesized. The three sites of the Geothermal power plants are identified as suitable for *P. pardus* subsp. *melas* habitat on the Indonesian island of Java (Wibisono et al. 2018). Only two primates exist in the Kamojang-Darajat location, including *P. comata* and *T. auratus.* The *P. comata* has an adaptive ability in a disturbed forest area with the availability of food and shelter, and it is recorded as nine meters away from the settlement and three meters from the road (Supartono et al. 2016). The *T. auratus* also exhibits adaptability by thriving in various habitats, including dry habitats with disturbance without human conflict (Hansen et al. 2020b).

Conservation status

Based on the Environment and Forestry Ministry Regulation P.106 of 2018, 10 out of 32 species are protected by the Kamojang-Darajat and Gunung Salak Geothermal Power Plants. Furthermore, 7 out of 10 species of mammals protected by the Minister Regulation have a high risk of extinction based on the IUCN. These species include *T. auratus*, *P. pardus* subsp. *melas, P. comata*, *H. moloch*, *M. javanica*, and Javan slow loris (*N. javanicus*). The other four species are southern red muntjak (*Muntiacus muntjak* (Zimmermann, 1780)), *P. bengalensis*, *P. linsang*, and *T. javanicus*. These four species are categorized as low risk of extinction, although in Indonesia, it is quite challenging to find them directly in nature. The rest is classified as low risk of extinction and also commonly easy to find.

Species considered the most traded internationally by CITES, so they are strictly prohibited for commercial use (AP. I) are *P. pardus* subsp. *melas*, *H. moloch*, *M. javanica*, and *N. javanicus*. Two of these four species are difficult to find directly at the monitoring site, such as *P. pardus melas* and *M. javanica.* The *N. javanicus* was found in the Kamojang and Gunung Salak sites, with only one individual on each site. As for the Javan gibbon species, up to three groups were observed. The Javan gibbon is challenging due to its high sensitivity to human disturbance and was only found in the Gunung Salak site.

The findings of mammals in the Geothermal Power Plants show that habitat conditions are still maintained. Some mammals have been found to have a significant role in biodiversity conservation efforts. The *H. moloch* is generally categorized as an umbrella species; the leopard is charismatic, and the Javan slow loris are both flagship species. Flagship species are defined as memorable and iconic species in conservation efforts. Researchers define umbrella species as those with a wide home range and requiring special habitat conditions, which generally provide habitat protection for many other species. Charismatic species have several different definitions, especially in the standards set by researchers. A requirement for a species to be considered charismatic is potential information that can be investigated from the species. An alternative or complementary method for prioritizing conservation efforts may be necessary when dealing with range-limit species or those requiring specialized conservation measures to mitigate threats to their survival (Runge et al. 2019).

The flagship species in the mammal class and classified as a primate is the *N. javanicus*; this species was detected in the natural forest area around Kamojang and Gunung Salak sites. The number of individuals caught was only one, considering lorises are good hiding animals. Because they are nocturnal or primarily nocturnal, the possibility of direct encounters is also limited at night. The *N. javanicus* is also not a primate grouped in large numbers, such as langurs or monkeys. Although information circulating in

the community says lorises are slow primates, they can occasionally move quickly.

The umbrella species of mammals found in the Gunung Salak area is *H. moloch*, which belongs to the Hylobatidae family and is the only species of lesser apes found on the island of Java (endemic to Java). It inhabits lowland tropical rainforests to hills up to 1,500 meters above sea level. Gunung Halimun Salak National Park is classified as a highly suitable habitat for the Javan gibbon (Oktaviani et al. 2023). The study revealed that from three different locations in geothermal power plants, the Gunung Salak site has distinctive characteristics with pristine forest conditions characterized by the diversity of species from the Sciuridae family. In contrast, the Kamojang-Darajat site, dominated by the Muridae family, indicates high anthropogenic activities such as plantations and settlements. Based on the area's conservation status, the Gunung Salak is the national park. Meanwhile, Kamojang-Darajat has the status of a nature tourism park conservation area.

As stipulated in Law No. 5 of 1990, based on its utilization, the national park area is more protected because of the government's legal zoning system. The utilization of the area is restricted for the community, unlike Natural Tourist Parks, which, in its utilization, will have a high anthropogenic impact that affects the presence of various species of animals. This conservation helps maintain the mammals diversity because the existence of this conservation area can increase public awareness to preserve natural resources in this area (Anggraini and Gunawan 2021).

In conclusion, the mammal diversity study around the Kamojang, Darajat, and Gunung Salak Geothermal Power Plant areas revealed 32 mammal species from 18 families. Gunung Salak had the highest diversity with 22 species, primarily Sciuridae, primates, and some Carnivora species. Conversely, Kamojang had 20 species dominated by Muridae, and Darajat had 19 species with a similar dominance of Muridae, highlighting different characteristics among these geothermal power plant locations. Conservation status analysis identified species of high conservation concern, emphasizing the importance of preserving these habitats for biodiversity conservation.

ACKNOWLEDGEMENTS

Acknowledgments were given to PT. Indonesia Power Kamojang Power Generation and O&M Services, PLTP Kamojang POMU Unit, PLTP Gunung Salak Unit, and Unit PLTP Darajat. We also thank to *Balai Konservasi Sumber Daya Alam* (BKSDA) Garut District, Gunung Halimun Salak National Park, Papandayan and Kamojang Natural Tourist Park. We also thank the *Pusat Unggulan IPTEK Perguruan Tinggi* Center of Environment and Sustainable Science (PUIPT CESS) Universitas Padjadjaran, Indonesia, the researcher team, the surveyor team, and the local community.

REFERENCES

Amni WN, Ravindran S, Saufi S, Hamid NH, Abidin CMRZ, Ahmad AH, Salim H. 2019. Commensal small mammal species and bait preferences in urban areas of Penang Island. Malays J Sci 38 (2): 18-30. DOI: 10.22452/mjs.vol38no2.2.

Anggraini RI, Gunawan B. 2021. Ecotourism development in National Parks: A new paradigm of forest management in Indonesia. E2S Web Conf 249: 03010. DOI: 10.1051/e3sconf/202124903010.

Borges HLM, Calouro AM, Botelho ALM, Silveira M. 2014. Diversity and habitat preference of medium and large sized mammals in an urban forest fragment of south western Amazon. Iheri Ser Zool 104 (2): 168-174. DOI: 10.1590/1678-476620141042168174.

Campos FS, Large ARB, Ribeirop PHP. 2013. Diversity of medium and large sized mammals in a Cerrado fragment of central Brazil. J Threat Taxa 5 (15): 4994-5001. DOI: 10.11609/JoTT.o3342.4994-5001.

Debata S, Kedar KS. 2018. Estimating mammalian diversity and relative abundance using camera traps in a tropical deciduous forest of Kuldiha Wildlife Sanctuary, eastern India. Mamm Stud 43: 45-53. DOI: 10.3106/ms2017-0078.

Dereje N, Tsegaye G, Tadese H. 2015. The diversity, distribution and relative abundance of medium and large-sized mammals in Baroye Controlled Hunting Area, Illubabor Zone, Southwest Ethiopia. Intl J Mol Evol Biodivers 5 (4): 1-9. DOI: 10.5376/ijmeb.2015.05.0004.

Fischer C, Gayer C, Kurucz K, Riesch F, Tscharntke T, Batáry P. 2017. Ecosystem services and disservices provided by small rodents in arable fields: Effects of local and landscape management. J Appl Ecol 55 (2): 548 - 558. DOI: 10.1111/1365-2664.13016.

Gray TNE. 2018. Monitoring tropical forst ungulates using camera-trap data. J Zool 305 (3): 173-179. DOI: 10.1111/jzo.12547.

Hansen MF, Ellegaard S, Moeller MM, van Beest FM. 2020a. Comparative home range size and habitat selection in provisioned and non-provisioned long-tailed macaques (*Macaca fascicularis*) in Baluran National Park, East Java, Indonesia. Contrib Zool 89: 1-19. DOI: 10.1163/18759866-bja10006.

Hansen MF, Gill M, Nawangsari VA, Sanchez KL, Cheyne SM, Nijman V, Fuentes A. 2021. Conservation of Long-tailed Macaques: Implications of the Update IUCN Status and the CoVID-19 Pandemic. Primate Conserv 35: 1-11.

Hansen MF, Nawangsari VA, van Beest FM, Schmidt NM, Stelvig M, Dabelsteen T, Nijman V. 2020b. Habitat suitability analysis reveals high ecological flexibility in a "strict" forest primate. Front Zool 17: 6. DOI: 10.1186/s12983-020-00352-2.

Hoffmann A, Jan Decher, Rovero F, Schaer J, Voigt C, Wibbelt G. 2010. Field methods and techniques for monitoring mammals. In: Eymann J, Degreef J, Häuser C, Monje JC, Samyn Y, van den Speigel D (eds). 2010. Manual on Field Recording Techniques and Protocols for All Taxa Biodiversity Inventories and Monitoring (Vol. 8). Abc Taxa, Belgium.

Husodo T, Shanida SS, Febrianto P, Pujianto MP, Megantara EN. 2019. Mammalian diversity in West Java, Indonesia. Biodiversitas 20 (7): 1846-1858. DOI: 10.13057/biodiv/d200709.

IUCN. 2023. The IUCN red list of threatened species. www.iucnredlist.org. Accessed on November 5, 2023.

Lacher T, Davidson A, Fleming TH, Gomez-Ruiz EP, McCracken GF, Owen-Smith N, Peres CA, Wall SBV. 2019. The functional roles of mammals in ecosystems. J Mammal 100 (3): 942-964. DOI: 10.1093/jmammal/gyy183.

Machtinger ET, Williams SC. 2020. Practical guide to trapping *Peromyscus leucopus* (Rodentia: Cricetidae) and *Peromyscus maniculatus* for vector and vector borne pathogen surveillance and ecology. J Insect Sci 20 (6): 5. DOI: 10.1093/jisesa/ieaa028.

Megantara EN, Shanida SS, Husodo T, Febrianto P, Pujianto MP, Hendrawan R. 2019. Habitat of mammals in West Java, Indonesia. Biodiversitas 20 (11): 3380-3390. DOI: 10.13057/biodiv/d201135.

Meijaard E, Dennis R, Saputro B. 2019. Rapid Environmental and Social Assessment of Geothermal Power Development in Conservation Forest Areas of Indonesia. PROFOR, Washington DC.

Meseret C, Solomon Y. 2014. Diversity of medium and large-sized mammals in Borena-Sayint National Park, South Wollo, Ethiopia. Intl J Sci Bas Appl Res 15 (1): 95-106.

Moo SSB, Froese, GZ, Gray TNE. 2017. First structured camera-trap surveys in Karen State, Myanmar, reveal high diversity of globally threatened mammals. Oryx 52 (3): 537-543. DOI: 10.1017/S003060531600113.

Oktaviani R, Borzée A, Cahyana AN, Lappan S, Mardiastuti A, Giri MS. 2023. Predicting suitable habitat for the endangered Javan gibbon in a submontane forest in Indonesia. JoTT 15(7): 23463-23471. DOI: 10.11609/jott.8291.15.7.23463-23471.

Pambudi NA, Ulfa DK. 2023. The geothermal energy landscape in Indonesia: A comprehensive 2023 update on power generation, policies, risks, phase and the role of education. Renew Sustain Energy Rev 189 (B): 114008. DOI:10.1016/j.rser.2023.114008.

Rehbein JA, James EMW, Joe LL, Laura JS, Oscar V, Scott CA, James RA. 2020. Renewable energy development threatens many globally important biodiversity areas. Glob Change Biol 26 (5): 3040-3051. DOI: 10.1111/gcb.15067.

Rode-Margono EJ, Voskamp A, Spaan D, Lehtinen JK, Roberts PD, Nijman V, Nekaris KAI. 2014. Records of small carnivores and of medium-sized nocturnal mammals on Java, Indonesia. Small Carniv Conserv 50: 1-11.

Royer A, Montuire S, Legendre S, Discamps E, Jeannet M, Lécuyer C. 2016. Investigating the influence of climate changes on rodent communities at a regional-scale (MIS 1-3, Southwestern France). PLoS One 11 (1): e0145600. DOI: 10.1371/journal.pone.0145600.

Runge CA, Withey J, Naugle DE, Fargione JE, Helmstedt KJ, Larsen AE, Martinuzzi S, Tack JD. 2019. Single species conservation as an umbrella for management of landscape threats. PLoS One 14 (1): e0209619. DOI: 10.1371/journal.pone.0209619.

Setiawan I, Indarto S, Sudarsono, Fauzi I, Yuliyanti A, Lintjewas L, Alkausar A, Jakah. 2018. Geothermal and volcanism in West Java. IOP Conf Ser Earth Environ Sci 118 (1): 012074. DOI: 10.1088/1755-1315/118/1/012074.

Sollmann R, Mohamed A, Samejima H, Wilting A. 2013. Risky business or simple solution - relative abundance indices from camera trapping. Biol Conserv 159: 405-412. DOI: 10.1016/j.biocon.2012.12.025.

Supartono T, Lilik BP, Agus H, Agus PK. 2016. Spatial distribution and habitat use of Javan langur (*Presbytis comata*): Case study in District of Kuningan. Procedia Environ Sci 33: 340-353. DOI: 10.1016/j.proenv.2016.03.085.

Udy K, Fritsch M, Meyer KM, Grass I, Hanß S, Hartig F, Kneib T, Kreft H, Kukunda CB, Pe'er G, Reininghaus H, Tietjen B, Tscharntke T, van Waveren CS, Wiegand K. 2021. Environmental heterogeneity predicts global species richness patterns better than area. Glob Ecol Biogeo 30 (4): 842-851. DOI:10.1111/geb.13261.

van Strien NJ. 1983. A Guide to the Tracks of the Mammals of Western Indonesia. School of Environmental Conservation Management, Bogor.

Wibisono HT, Wahyudi HA, Wilianto E, Pinondang IMR, Primajati M, Liswanto D, Linkie M. 2018. Identifying priority conservation landscapes and actions for the Critically Endangered Javan leopard in Indonesia: Conserving the last large carnivore in Java Island. PLoS ONE 13(6): e0198369. DOI: 10.1371/journal.pone.0198369.

NUSANTARA BIOSCIENCE
Vol. 16, No. 1, pp. 89-95
May 2024

ISSN: 2087-3948
E-ISSN: 2087-3956
DOI: 10.13057/nusbiosci/n160111

Floral nectar secretion dynamics of *Pavonia urens* (Malvaceae) and honey production potential

TURA BAREKE♥, ADMASSU ADDI
Oromia Agricultural Research Institute, Holeta Bee Research Center. P. O. Box 22 Holeta, Ethiopia.
Tel.: +251-112370023/0371, Fax.: +251-112372115, ♥email: tura_berake@iqqo.org

Manuscript received: 7 November 2023. Revision accepted: 4 February 2024.

Abstract. *Bareke T, Addi A. 2024. Floral nectar secretion dynamics of* Pavonia urens *(Malvaceae) and honey production potential. Nusantara Bioscience 16: 89-95.* The honey production potential of honey plant is estimated using the total floral nectar secretion potential of the plant foraged by honeybees within a given location. The current study aimed to determine the floral nectar secretion dynamics of *Pavonia urens* Cav. in addition to estimating the potential amount of honey that can be produced thereof. Nectar volume (using micropipette), nectar concentration (using digital refractometer), temperature, and humidity (using thermo hygrometer) were measured at 3 h intervals. Nectar volume and concentration differed significantly at different time points throughout the day. Also, nectar volume and concentration differed annually. There was a positive correlation between nectar volume and humidity as well as between temperature and nectar concentration. The mean nectar volume per 24 hours of *P. urens* was 7.23±0.43 µL. Individual flowers continuously secreted nectar for about 10 days throughout flower life. During each flowering season, an average of 823.5 mg g^{-1} of honey was generated per plant. Additionally, the average honey production capacity of *P. urens* was 35 kg ha^{-1}. This suggests that *P. urens* has the capacity to produce honey; therefore, for sustainable honey production, planting and in-situ conservation of this plant are recommended.

Keywords: Concentration, humidity, sugar, temperature, volume

INTRODUCTION

Ethiopia has favourable climatic conditions that encourage wide flora biodiversity which in turn favours beekeeping activities (Fichtl and Adi 1994). According to Addi et al. (2014), most of Ethiopia's flowering plants are foraged by bees for their flora nectar and pollen to satisfy their energy and protein requirement (Obeng-Darko et al. 2022, 2023). However, different plants produce varying nectar amounts hence, impacting the resultant honey obtained from different plants. Beekeeping promotes planting of trees, which indirectly addresses climate change by creating favourable microclimate (Bareke et al. 2022). The value chain of beekeeping is huge, thus it creates direct employment for the many unemployed in Ethiopia (Abro et al. 2022). According to Bareke and Addi (2019), bee plants are those plant species that produce floral nectar and/or pollen for honeybees. Nectar volume and concentration are indices used to evaluate the amount of honey that can be obtained from a potential bee plant species (Bareke et al. 2020a). Nectar is basically plant syrup produced by nectaries, specialized secreting structures beneath the flower surface (Galetto and Bernardello 2004). Nectar is chiefly composed of sucrose and hexoses with trace amounts of other constituents like amino acid, flavonoids, vitamins and other several organic compounds which may affect foraging ecology and the behaviour of foragers (Bertazzini and Forlani 2016).

Honeybee plant species' contributions to honey production are influenced by floral shape, flower anatomy, flowering phenology, and the quality and quantity of secreted nectar (Alqarni et al. 2015). The quality and quantity of nectar is affected by environmental variables (Adgaba et al. 2017). Since nectar is exposed to evaporation, temperature, humidity (Bareke et al. 2021a), wind speed, and sunlight (Dafni 1992), it is necessary to perform nectar measurement relative to these climatic variables (Dafni 1992).

Therefore, it is imperative to evaluate the honey production potential of flowering plant species to understand the relationship between the nectar production of flowering plants, and the carrying capacity of beehives per honeybee colony. Ultimately, such studies help to improve our understanding of forest and watershed management strategies within the environments (Bareke et al. 2022). Different plant species have different capacities for producing honey (Bareke et al. 2021b). There are only few major honey source plants in any region that provide high amount of nectar for honey production (Adgaba et al. 2017) to the world. Therefore, it is crucial to categorize them in accordance with their level of honey production capacity.

Different studies have investigated the nectar exudation and accumulation dynamics in some flowering plants (Búrquez and Corbet 1991; Obeng-Darko et al. 2022) and the capacity of various bee foraging plants to produce honey (Adgaba et al. 2017). Accordingly, the honey production capacity of *Acacia gerrardii* Benth. (Alqarni et al. 2015), *Otostegia fruticosa* (Forssk.) Schweinf. ex Penzig, *Ziziphus spina-christi* (L.) Desf. (Adgaba et al.

2017), *Schefflera abyssinica* (Hochst. ex A.Rich.) Harms (Bareke et al. 2020a), *Croton macrostachyus* Hochst. ex Delile (Bareke et al. 2020b), and *Coffea arabica* L. (Bareke et al. 2021b) were recognized.

The dynamics of nectar secretion and the potential for honey production in flowering plants remain mostly unknown to Ethiopians. Nectar secretion capability and its impact on honey production for significant numbers of bee forage plant species are not yet known. Among these plants, *Pavonia urens* Cav. (Inchinni) is one of the most significant melliferous species (Addi et al. 2014). It is a perennial herb that can reach a height of 2 m and is a member of the Malvaceae family. In addition to being common in Madagascar and tropical Africa, it also grows along edges, trails, and clearings in upland and riverine forests, secondary forest, scrub, abandoned cultivations, and up to 3000 m above sea level in the Ethiopian Highlands and Eritrea (Fichtl and Adi 1994). According to de Boer et al. (2005), *P. urens* is a medicinal plant that is used to cure stomachaches and pneumonia in addition to giving honeybees' nectar and pollen (Addi et al. 2014). However, studies to quantify the amount of honey that could be obtained from the flora nectar of *P. urens* are non-existent. The current work focused on determining the nectar secretion patterns and the potential amount of honey that can be sourced from the nectar of *P. urens*.

MATERIALS AND METHODS

Nectar volume was measured using micropipette. Nectar concentration was measured using a digital refractometer, while temperature and humidity were measured simultaneously using a thermo hygrometer.

Study area

Based on the accessibility and abundance of *P. urens*, study locations were chosen. *P. urens* was chosen because of its ecological adaption range, honeybee foraging intensity, and its honey production potential. The three-year experiment took place in Ethiopia's southwest Shewa Zone from 2018 to 2020.

Calculating the proportion of plants and flowers in a given region

To estimate the number of plants per area at each site, ten plots were randomly selected. Three plants per plot, each measuring 2 m by 2 m, were selected at random. The quantity of flowers on each plant was counted individually (Bareke and Addi 2022). Sixty plots were identified for the study and a total of 180 plants were selected. It is used to estimate the number of flowers per plant as well as flowers per area.

Determining the length of the nectar secretion

Nectar secretion and flower opening and ending times were recorded. To identify the length of the nectar secretion, five distinct flowers were measured every day from the starting to ending of nectar secretion repeatedly (Bareke et al. 2020a).

Measurement of the nectar's volume and nectar concentration

Insect nectar robbers were precluded by covering the inflorescences with fine mesh for 24 h before nectar harvest from each flower. Wyatt et al. (1992) labeled flowers from various inflorescence portions at random and nectar secretions within 24 h from 20 random flowers were harvested each day for three consecutive days at three hour interval (Esteves et al. 2014).

Determining dynamics of nectar secretion

Nectar volume, nectar concentration, temperature, and humidity were measured four times per day at intervals of 3 hours concurrently (Wyatt et al. 1992). The nectar volume was measured from an average of five separate flowers per plant and sampling period, which equates to 20 blooms per day (Esteves et al. 2014).

Calculating the amount of sugar in each flower's nectar

The amount of sugar present in the nectar was determined based on nectar volume, concentration, and sucrose density. The sucrose density was estimated from the nectar concentration using the Prys-Jones and Corbet (1991) equation as follows:

$$\rho = 0.003729/C + 0.0000178\ C^2 + 0.9988603$$

Where:
ρ: The estimate of sucrose density for a given value of C,
C: Nectar concentration (%) (Refractometer reading)

The equation from Dafni (1992) was used to determine the amount of sugar per flower as follows:

$$\text{Amount of sugar (A)} = \frac{\text{\% of sugar reading in the refractometer}}{100} \times \text{A volume (µl)} \times \frac{\text{Density of sucrose at the observed concentration}}{}$$

Estimation of sugar and Honey Production Potential (HPP)

The plants' potential for producing honey was assessed to be as follows: Average sugar content per ha = average number of flowers per ha (Minimum to maximum number of flowers per ha) * average sugar content per flower/flowering season (Dafni 1992; Masierowska 2003; Kim et al. 2017).

One kg of ripe honey is expected to have an average moisture content of 18% while the sugar content is 82%. Therefore, the honey per ha of *P. urens* plants= sugar content per ha of *P. urens* plants divided by 0.82 kg of sugar (Bareke et al. 2020a).

Data analysis

One-way ANOVA was used to evaluate the gathered data. For mean separation between the treatments, Tukey Test was utilized. Additionally, a linear regression model was generated using the R programming language to examine how temperature and humidity affect the volume and sugar concentration of nectar.

RESULTS AND DISCUSSION

Flowers per plant and hectare

The highest level of flowers per m^2 and flowers per plant were found in 2018, while the lowest was obtained in 2019 (Figure 1). This demonstrates that plant bloom counts fluctuated annually and was somewhat influenced by climatic factors. Due to differences in plant size and age as well as changes in environmental factors throughout time, the mean quantity of blooms per plant and per hectare of land fluctuated. Similar research on *C. macrostachyus* and *S. abyssinica* suggested that changes in the ecological distribution of these plants as well as environmental conditions like temperature, rainfall, and wind as well as habitat could explain variations in the number of flowers per plant (Bareke et al. 2020a,b).

Early in the morning, *P. urens* flowers opened, supplying nectar to honeybees. It was immediately visited by honeybees after being opened. Depending on the weather, it begins to close after 12:00, but areas with shade remain open until 15:00 (Figure 2). This is due to the nature of plants and might be physiological constraints that the plant performs to conserve water loss through evaporation. Depending on the local weather, the honeybees begin visiting the flower between 6:30 and 7:00 hours in the morning and continue until the flower closed. The length of time that nectar and pollen are released varies from plant species to plant species. For instance: For *Z. spina-christi* 6 h to 18 h (Adgaba et al. 2012); *Antigonon leptopus* Hook. & Arn. 6 h to 19 h (Adjaloo et al. 2015); *Lavandula dentata* L. and *Lavandula pubescens* Decne. 6 h to 18 h (Adgaba et al. 2015); and Pear cultivars 8 h to 19 h (Farkas and Orosz-Kovacs 2003). The entire plant's blossoms could remain in bloom for up to a month. The length of the floral period has a significant impact on reproductive ecology, affecting both the potential of the plants to produce honey and the total number of visits by bees and other pollinators (Adgaba et al. 2015).

Dynamic of nectar secretion

The nectar volume varied greatly during the day ($p= 0.01$), reaching its highest value at 6:00 h and its lowest at 15:00 h (Table 1). The highest volume of nectar was collected at 6^{th} hour in the morning when the humidity was at its peak. The nectar concentration was varied significantly ($p=0.000$) during the day depending on the time of day. The highest concentration was measured at 15:00 h whereas, the lowest concentration was detected 6:00 h (Table 1).

The amount of sugar varied significantly during the day ($p=0.03$), with the highest amount recorded at 6:00 and 15:00 h (Table 1). In general, the plants studied had their main nectar production occurring between 6:00 and 12:00, and in the open, the flower petals will be furled after this period (at where no shade plant). However, in the shade, the flower stayed opened to continuously offer nectar to the honeybees until 15:00 h. This is due to the physiological constraints. Microclimate influences pollinator behavior (time of activity, frequency, and duration of visits, as well as foraging behavior), patterns of daily and/or seasonal fluctuations, and the likelihood of changes in nectar volume and concentration (Dafni 1992). Due to climatic factors like air temperature and humidity, which can significantly affect the nectar secretion and concentration of sugars, nectar secretion varies throughout the flowering seasons (Denisow et al. 2018).

The amount of daily secreted nectar varies from plant species to plant species. For instance, *L. pubescens* and *L. dentata* both supply nectar every day for 12 hours each, as well as *A. leptopus* and *Thevetia peruviana* Thevetia peruviana for 14:00 h (Adgaba et al. 2015). For *P. urens*, the largest nectar volume was measured after 6:00 h, whereas the highest concentration was observed at 15:00 h. At the lowest temperature and maximum humidity, nectar volume and concentration were at their highest and lowest, respectively. This implies that temperature and humidity may have some relationships with nectar secretion. The highest sugar amount, however, was recorded during 15:00 h of the day. The weather was quite hot and dry during this time. This demonstrates that both temperature and humidity have an impact on the plant's ability to secrete nectar. In addition to environmental factors, nectar concentration can change based on the floral sexual stages and flower position (Antoń and Denisow 2014; Lu et al. 2015). Honeybee foraging can be significantly impacted by the concentration and quality of nectar (Bertazzini and Forlani 2016).

Among the different years of data collection, there are considerable variations in nectar volume and concentration. The value of nectar volume was the highest in 2020 whilst nectar concentration was lowest for the same year. This indicates that nectar concentration decreases with increasing nectar volume. The nectar volume was the lowest in 2019 while the greatest nectar concentration was recorded in this year (Figure 3.A). This is due to the windy and sunny weather that prevailed during the data collecting. However, compared to the other data collection years, nectar volume was substantially higher in 2020, and this year's concentration was at its lowest (Figure 3.B). This is a result of a brief period of rain during field data gathering.

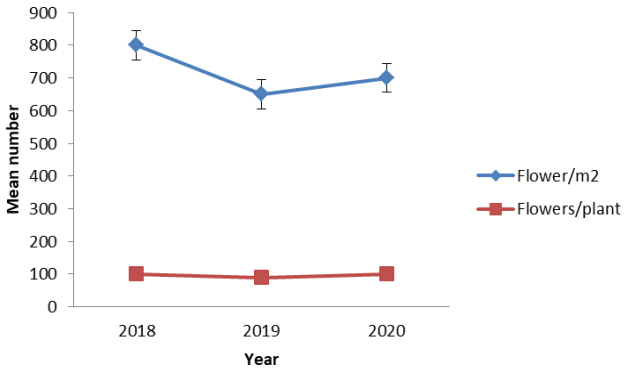

Figure 1. The average number of *Pavonia urens* flowers per plant and flowers per square meter from 2018 to 2020

Table 1. Mean nectar concentration (%), nectar volume (µl) and sugar amount (mg) /flower with ± (SE) in nectar per flower at 3 hours intervals of *Pavonia urens* with mean temperature (°C) and humidity (%) at 6:00 to 15:00 hours (h) in South west Shewa Zone, Ethiopia

Time (h)	Temp (°C)	Humidity (%)	Volume ± SE (µl)	Concentration (%) ± SE	Sugar (mg)/flower ± SE
6:00	14.3	60.6	5.79±0.39^{a}	16.89±1.1^{d}	8.33±0.60^{ab}
9:00	21.4	43.3	4.49±0.42^{ab}	22.28±1.14^{c}	7.12±0.5^{ab}
12:00	27.1	28.6	3.18±0.21^{bc}	29.38±1.16^{b}	6.66±0.26^{b}
15:00	27.7	22.7	2.24±0.21^{c}	38.63±0.94^{a}	8.93±0.83^{a}
Mean	22.6	38.8	4.3±0.2	24.43±0.85	7.5±0.3
Significance level			**	***	*
P-value			0.01	0.000	0.03

Note: Treatments with the same letter are not significantly different along column

Figure 2. A *Pavonia urens* flower with nectar and closed flowers in the late afternoon. A. Accumulated nectar, B. Nectar collection, C. Closed after 12:00 hour, D. Opened early in the morning

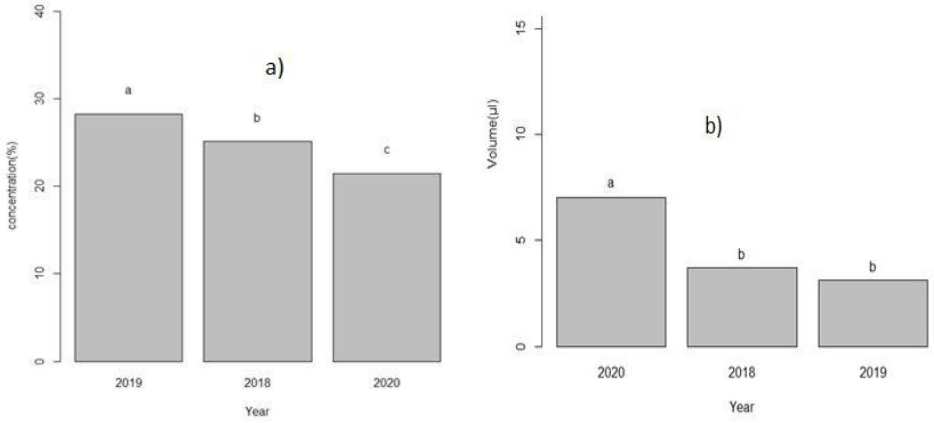

Figure 3. A. Nectar concentration and B. Volume of *Pavonia urens* from 2018-2020 years in South West Shewa Zone, Ethiopia

The nectar concentration of *P. urens* was directly correlated with temperature (°C). This indicates that the values of nectar concentration increased as the temperature rose. However, the concentration of nectar was less affected by temperature (Figure 4.A). The maximum nectar concentrations were obtained between 20 and 30°C. On the other hand, the volume of nectar was indirectly related to temperature. This suggests that the volume of nectar decreased with rising temperature. However, the amount of nectar secreted was not highly influenced (R^2= 32.84) by temperature. The highest amount of nectar was produced between 15 and 25°C (Figure 4.B).

Nectar volume and air humidity in the research area are directly correlated (Figure 5.A). Therefore, a rise in air humidity resulted in an increased nectar volume. The volume of nectar was influenced by air humidity by 30.94%. The largest nectar volume values were detected between 40 and 70% air humidity, whereas the lowest nectar volume were detected at less than 40% air humidity.

The nectar concentration produced by *P. urens* was inversely associated with the humidity of the air (Figure 5.B). This shows that the higher nectar concentration values were obtained at the lower air humidity values and vice versa. The parameters of nectar concentration were influenced by air humidity by 50.88%.

The amount of sugar in *P. urens* was not significantly impacted by the research area's temperature or air humidity (Figure 6). Based on the plant's nectar volume and concentration, sugar content was calculated. As shown before, there was a direct correlation between temperature and concentration as well as between humidity and nectar volume. However, there was indirect correlations between nectar volume and nectar concentration. Temperature and humidity had negligible effects on sugar content because their effects on nectar and volume are the reverse of one another.

Number of flower/plants, nectar secretion length, sugar and honey production capacity of *P. urens* per flower

The *P. urens*'s nectar secretion lasted an average of 10 days, ranging from 9 to 12 days (Table 2). However, the flower can stay alive for up to 15 days. In addition to this, the average number of flowers per plant was 90±8.47 with 15 and 217 as the minimum and maximum record per plant, respectively. This range of variation shows that extremely small to large plants with enormous flowers were included in the plants used to estimate the number of flowers per plant. The mean nectar volume per 24 h of *P. urens* was 7.23±0.43 µL (Table 2).

Table 2: Mean no. of plants/m^2 (N= 60 plots), mean no. plants/ha, mean no. of flowers/plant (N= 180 plants), mean no. of flowers/ha, mean nectar secretion length and mean sugar per flower/season for *Pavonia urens*

Parameters	Mean ± SE	Minimum	Maximum
No. of plants/m^2	4±0.37	1.00	10.00
No. of plant/ha	40000±3415.7	10000.00	100000.00
No. flowers/plant	90±8.47	17.00	198.00
No. of flowers/ha	3820250±485856	170000.00	11880000.00
Nectar volume (µl)/24 hours	7.23±0.43	1.30	20.00
Nectar secretion length	10±0.11	9.00	12.00
Sugar (mg)/flower	7.5±0.27	2.45	19.53
Honey (mg)/flower	9.15±0.33	2.99	23.83

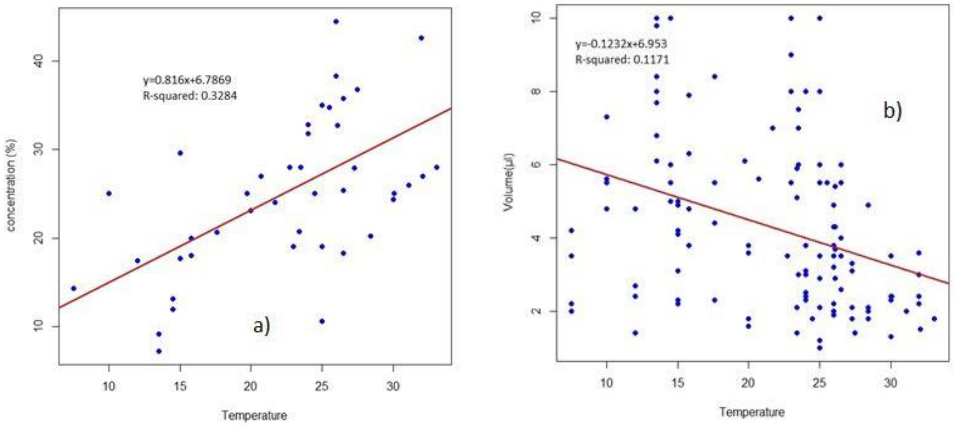

Figure 4. A. Effect of Temperature on nectar concentration and B. Volume of *Pavonia urens*

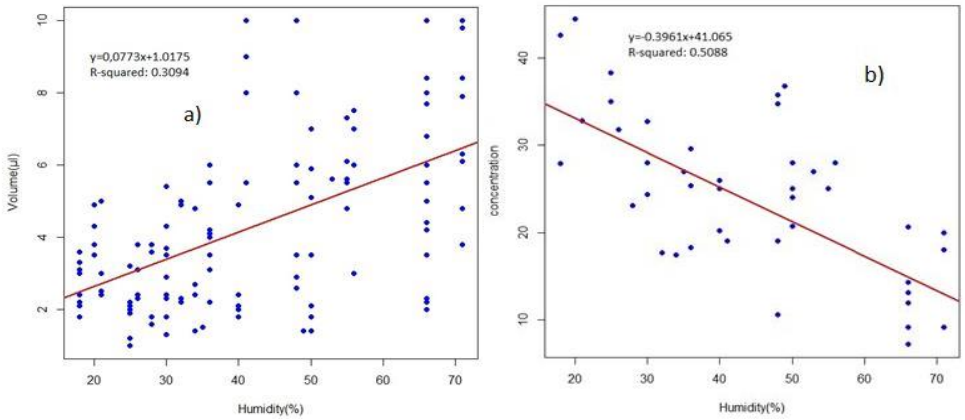

Figure 5. A.Effect of air humidity on nectar volume and B. Concentration of *Pavonia urens*

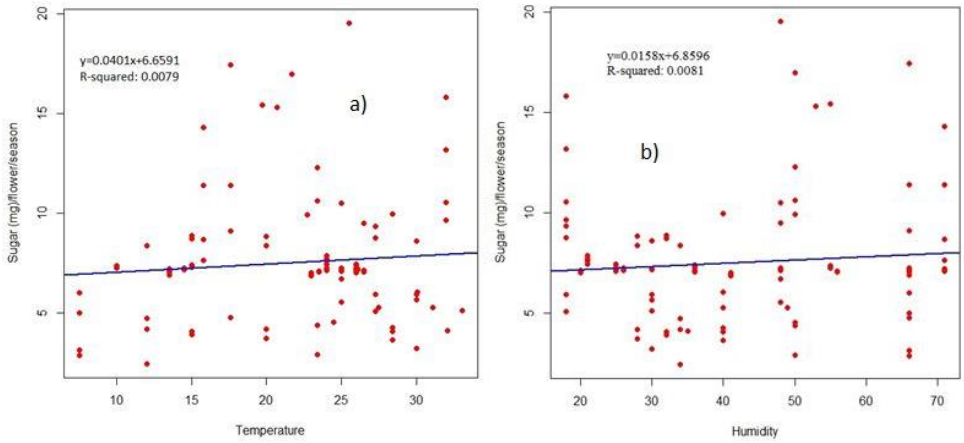

Figure 6. A. Effect of temperature and B. Air humidity on amount of sugar/flowers/season of *Pavonia urens*

There were about 170,000 to 11,880,000 flowers per hectare with a mean value of 3,820,250 flowers (Table 2). This was used to calculate the amount of sugar per hectare by multiplying it by the sugar per flower (Table 2). Accordingly, the average sugar per flower per flowering season was 7.5±0.27 mg (ranges from 2.45 to 19.53 mg) whilst the honey per flower was 9.15±0.33 mg (ranges from 2.99 to 23.83 mg).

Estimated honey production potential of *P. urens* plants per hectare of land

The average sugar per hectare of *P. urens* plants was estimated as follows: average number of flowers per ha (Minimum to maximum number of flowers per ha) * average sugar content per flower/flowering season. Hence, the average sugar content per ha was 3820250 (170,000 to 11,880,000) * 7.5 mg (Table 2) = 28651875 mg (ranges from 416,500 to 232,016,400 mg) or 28.65 kg (ranges from 0.42 kg to 232 kg) of sugar.

On the global market, 1 kg of honey has an average moisture content of 18% while the sugar content is 82%. Hence, Honey (kg) per ha of *P. urens* plants = sugar content per ha of *P. urens* plants divided by 0.82 kg of sugar. When sugar per hectare of *P. urens* plants was converted to honey per ha, it was an average of 35 kg (ranging from 0.5 kg to 283 kg from very small plant to big) per hectare of *P. urens* plants. This finding suggests that a plant's ability to produce honey is influenced by its flower density. The amount of honey that can actually be taken out of the hive is anticipated to be less than its potential. The ability of a plant to secrete nectar that honeybees use to make honey is referred to as the capacity of the plant for producing honey. It is anticipated that half of the potential of the plant will be collected via the bee colonies' honey. Merely 50% of the honey is used for nectar and pollen gathering, with the remaining 50% being stored. Study conducted by Al-Ghamdi et al. (2016) indicated that the honeybees use sugar as an energy source throughout their journey to collect nectar and pollen.

The ability of bee plants to produce honey varies from plant species to plant species. Accordingly, *L. pubescens* and *L. dentata* produce honey at rates of 51 kg per hectare and 24.1 kg per hectare per flowering season, respectively (Adgaba et al. 2015). The *C. arabica* produces 125 kg of honey per hectare (Bareke et al. 2021b); *S. abyssinica* produces 1791 kg per hectare per flowering season (Bareke et al. 2020a). Accordingly, the honey production potential of *Lavandula* species is somewhat similar with *P. urens*; because it is herb. However, the others are trees and shrubs which are bigger in size as compared to *P. urens.*

The amount of honeybee colonies needed to be installed in a chosen region depends heavily on the bee plant species' capacity to produce honey. A honeybee colony's effective foraging range can cover a 2 km radius, a 12.56 km^2 area. By addressing the issue of colony overstocking, supreme honey is produced by balancing several honeybee colonies with the available floral resource.

In conclusion, *P. urens* has a strong chance of producing nectar that greatly aids in the creation of honey. Local temperature and air humidity had an impact on *P. urens* nectar volume and concentration. The volume and concentration of the nectar varied greatly throughout the day. It offers nectar for anywhere between 6 and 15 hours, depending on the habitat. *P. urens* secret nectar only remains open for 12 hours under normal circumstances; in shade, it remains open until 15 hours. 35 kg of honey might be produced per season from a hectare of *P. urens* plants.

ACKNOWLEDGEMENTS

We acknowledge the Holeta Bee Research Center and Oromia Agricultural Research Institute, Ethiopia for providing required facilities and logistics. Our sincere thanks also extended to Tesfaye Abera, and our driver Bekele Gemechu for helping us during field data gathering.

REFERENCES

Abro Z, Kassie M, Tiku HA, Taye B, Ayele ZA, Ayalew W. 2022. The impact of beekeeping on household income: Evidence from north-

western Ethiopia. Heliyon 8 (5): e09492. DOI: 10.1016/j.heliyon.2022.e09492.

Addi A, Wakjira K, Kelbessa E, Bezabeh A. 2014. Honeybee Forages of Ethiopia. United Printers Ethiopia, Addis Ababa.

Adgaba N, Al-ghamdi A, Tadesse Y, Getachew A, Awad AM, Ansari MJ, Owayss AA, Mohammed SEA, Alqarni AS. 2017. Nectar secretion dynamics and honey production potentials of some major honey plants in Saudi Arabia. Saudi J Biol Sci 24 (1): 180-191. DOI: 10.1016/ j.sjbs.2016.05.002.

Adgaba N, Al-Ghamdi AA, Tena YT, Shenkut AG, Ansari MJ, Al-Maktary A. 2015. Floral Phenology, nectar secretion dynamics, and honey production potential, of two Lavender species (*Lavandula dentata*, and *L. pubescens*) in Southwestern Saudi Arabaia, J Apic Sci 59 (2): 135-144. DOI: 10.1515/JAS-2015-0028.

Adgaba N, Awad AM, Al-Ghamdi AA, Alqarni AS, Radloff SE. 2012. Nektar *Ziziphus spina-christi* (L.) Willd (Rhamnaceae): Dynamika Nektarowania I Wydajność Miodowa. J Apic Sci 56 (2): 49-59. DOI: 10.2478/v10289- 012-0023-9.

Adjaloo M, Ankomah A, Yeboah-Gyan K, Dzomeku B. 2015. Nectar production dynamics in two melliferous plant species. Genet Plant Physiol 5 (2): 145-161.

Al-Ghamdi A, Adgaba N, Getachew A, Tadesse Y. 2016. New approach for determination of an optimum honeybee colony's carrying capacity based on productivity and nectar secretion potential of bee forage species. Saudi J Biol Sci 23 (1): 92-100. DOI: 10.1016/j.sjbs.2014.09.020.

Alqarni AS, Awad A M, Owayss A A. 2015. Evaluation of *Acacia gerrardii* Benth. (Fabaceae: Mimosoideae) as a honey plant under extremely hot-dry conditions: Flowering phenology, nectar yield and honey potentiality. J Anim Plant Sci 25 (6): 1667-1674.

Antoń S, Denisow B. 2014. Nectar production and carbohydrate composition across floral sexual phases: Contrasting patterns in two protandrous *Aconitum* species (Delphinieae, Ranunculaceae). Flora 209 (9): 464-470. DOI: 10.1016/j.flora.2014.07.001.

Bareke T, Abera T, Addi A. 2021a. Nectar secretion of *Callistemon citrinus* (Curtis) Skeels, Myrtaceae: Potential for honey production. Plants Environ 3 (2): 30-36. DOI: 10.22271/2582-3744.2021.jun.30.

Bareke T, Addi A, Wakjira K, Kumsa T. 2021b. Dynamics of nectar secretion, honey production potential and colony carrying capacity of *Coffea arabica* L. (Rubiaceae). J Agric Environ Intl Dev 115 (1): 125-138. DOI: 10.12895/jaeid.20211.1556.

Bareke T, Addi A. 2019. Bee flora resources and honey production calendar of Gera Forest in Ethiopia. Asian J For 3 (2): 69-74. DOI: 10.13057/asianjfor/r030204.

Bareke T, Addi A. 2022. Quantifying nectar secretion potential of *Hygrophila auriculata* (Schum), Heine (Acanthaceae), and *Salvia leucantha* Cav. (Lamiaceae) for honey production. Adv Agric 2022: 8301903. DOI: 10.1155/2022/8301903.

Bareke T, Gemeda M, Kumsa T, Addi A, Endale W. 2022. Beekeeping as an incentive to catchment rehabilitation. Intl J Environ Stud 79: 613-623. DOI: 10.1080/00207233.2021.1940533.

Bareke T, Kumsa T, Addi A. 2020a. Nectar secretion and honey production potential of *Schefflera abyssinica* (Hochst. ex a. rich.) Harms, Araliaceae. Trop Agric 97 (3): 186-196.

Bareke T, Kumsa T, Roba K, Addi A. 2020b. Nectar secretion dynamics and honey production potential of *Croton macrostachyus* L., Euphorbiaceae. Bee World 97 (4): 123-127. DOI: 10.1080/0005772X.2020.1763086.

Bertazzini M, Forlani G. 2016. Intraspecific variability of floral nectar volume and composition in Rapeseed (*Brassica napus* L.var. oleifera). Front Plant Sci 7: 288. DOI: 10.3389/fpls.2016.00288.

Búrquez A, Corbet SA. 1991. Do flowers reabsorb nectar? Funct Ecol 5: 369-379. DOI: 10.2307/2389808.

Dafni A. 1992. Pollination Ecology. A practical Approach. Oxford University Press, Tokyo.

de Boer HJ, Kool A, Broberg A, Mziray WR, Hedberg L, Levenfors JJ. 2005. Anti-fungal and anti-bacterial activity of some herbal remedies from Tanzania. J Ethnopharmacol 96 (3): 461-469. DOI: 10.1016/j.jep.2004.09.035.

Denisow B, Strzalkowska-Abramek M, Wrzesien M. 2018. Nectar secretion and pollen production in protandrous flowers of *Campanula patula* L. (Campanulaceae). Acta Agrobot 71 (1): 1734. DOI: 10.5586/aa.1734.

Esteves RJP, Villadelrey MC, Rabajante JF. 2014. Determining the optimal distribution of bee colony locations to avoid overpopulation using mixed integer programming. J Nat Stud 9 (1): 79-82. DOI: 10.1080/00218839.2017.1357942.

Farkas Á, Orosz-Kovács Z. 2003. Nectar secretion dynamics of Hungarian local pear cultivars. Plant Syst Evol 238 (1): 57-67. DOI: 10.1007/s00606-003-0268-7.

Fichtl R, Adi A. 1994. Honeybee Flora of Ethiopia. Margraf Verlag, Weikersheim, Germany.

Galetto L, Bernardello G. 2004. Floral nectaries, nectar production dynamics and chemical composition in six *Ipomoea* species (Convolvulaceae) in relation to pollinators. Ann Bot 94: 269-280. DOI: 10.1093/aob/mch137.

Kim S H, Lee A, Kang D, Kwon H Y, Park Y, Kim M S. 2017. Análisis de características de néctar floral de espino blanco coreano y chino (*Crataegus pinnatifida* Bunge). J Apic Res 57 (1): 119-128. DOI: 10.1080/00218839.2017.1357942.

Lu NN, Li XH, Li L, Zhao ZG. 2015. Variation of nectar production in relation to plant characteristics in protandrous *Aconitum gymnandrum*. J Plant Ecol 8 (2): 122-129. DOI: 10.1093/jpe/rtv020.

Masierowska ML. 2003. Floral nectaries and nectar production in brown mustard (*Brassica juncea*) and white mustard (*Sinapis alba*) (Brassicaceae). Plant Syst Evol 238 (1): 97-107. DOI: 10.1007/s00606-002-0273-2.

Obeng-Darko SA, Brooks PR, Veneklaas EJ, Finnegan PM. 2022. Sugar and dihydroxyacetone ratios in floral nectar suggest continuous exudation and reabsorption in *Leptospermum polygalifolium* Salisb. Plant Sci 323: 111378. DOI: 10.1016/j.plantsci.2022.111378.

Obeng-Darko SA, Sloan J, Binks RM, Brooks PR, Veneklaas EJ, Finnegan PM. 2023. Dihydroxyacetone in the floral nectar of *Ericomyrtus serpyllifolia* (Turcz.) Rye (Myrtaceae) and *Verticordia chrysantha* Endl. (Myrtaceae) demonstrates that this precursor to bioactive honey is not restricted to the Genus *Leptospermum* (Myrtaceae). J Agric Food Chem 71 (20): 7703-7709. DOI: 10.1021/acs.jafc.3c00673.

Prys-Jones OE, Corbet SA. 1991. A Bumblebees. Naturalists' Handbooks 6. Pelagic Publishing, London, UK.

Wyatt R, Broyles SB, Derda GS. 1992. Environmental influences on nectar production in milkweeds (*Asclepias syriaca* and *A. exaltata*). Am J Bot 79 (6): 636-642. DOI: 10.1002/j.1537-2197.1992.tb14605.x.

NUSANTARA BIOSCIENCE
Vol. 16, No. 1, pp. 96-103
May 2024

ISSN: 2087-3948
E-ISSN: 2087-3956
DOI: 10.13057/nusbiosci/n160112

Foliar salicylic acid application to enhance the morphophysiology of *Basella alba* and *Basella alba* var. *cordifolia* under water deficit stress

ANNIS WATURROIDAH AYUNINGTIAS[1,♥], SOLICHATUN[2,♥♥], ARTINI PANGASTUTI[2]

[1]Graduate Program of Bioscience, Faculty of Mathematics and Natural Sciences, Universitas Sebelas Maret. Jl. Ir. Sutami 36A Surakarta 57126, Central Java, Indonesia. Tel./fax.: +62-271- 669376, ♥email: waturroidahannis@gmail.com

[2]Department of Biology, Faculty of Mathematics and Natural Sciences, Universitas Sebelas Maret. Jl. Ir. Sutami 36A Surakarta 57126, Central Java, Indonesia. Tel./fax.: +62-271-663375, ♥♥email: solichatun@staff.uns.ac.id

Manuscript received: 1 September 2023. Revision accepted: 6 February 2024.

Abstract. *Ayuningtias AW, Solichatun, Pangastuti A. 2024. Foliar salicylic acid application to enhance the morphophysiology of* Basella alba *and* Basella alba *var.* cordifolia *under water deficit stress. Nusantara Bioscience 16: 96-103.* Global climate change and increasing temperatures are becoming problems in the cultivation of medicinal plants such as *Basella alba* L. and *Basella alba* var. *cordifolia* (Lam.) M.R.Almeida. Foliar salicylic acid on leaves increases growth and productivity in medicinal cultivation. This study aims to determine the exogenous application of salicylic acid to increase the morphophysiology measurement in *B. alba* and *B. alba* var. *cordifolia* under water deficit stress. The study was carried out using a two-factor, completely randomized design consisting of salicylic acid concentration (0, 2, and 6 mM) and water deficit stress (100% (control), 75% field capacity (light stress), 50% wide field capacity (medium stress) and 25% field capacity (heavy stress). The observation results included morphophysiology. The best result on dry weight for *B. alba* was followed by SA 0mM+Medium stress with 5.45 g; in *B. alba* var. *cordifolia* was followed by SA 0mM+ Heavy stress with 3.09 g. Fresh weight for *B. alba* was followed by SA 4mM+ Heavy stress with 35.95 g, and *B. alba* var. *cordifolia* was followed by SA 0mM+ Heavy stress with 35.66 g. The shoot-to-root ratios in *B. alba* and *B. alba* var. *cordifolia* were followed by SA 2mM+Medium stress with 0.93 and 0.99, respectively. Quercetin in *B. alba* was followed by SA 4mM+ Heavy stress with 2.88% w/w, and *B. alba* var. *cordifolia* was followed by SA 6mM+Medium stress with 1.93% w/w. The gallic acid in *B. alba* and *B. alba* var. *cordifolia* was followed by SA 6mM+Medium stress with 10.21% w/w and 9.44% w/w. Prolin in *B. alba* and *B. alba* var. *cordifolia* was followed by SA 6mM+Medium stress with 8.74 and 9.73 µmol/gram wet weight. This study concluded that foliar salicylic acid application enhanced the morphophysiology, including growth, secondary metabolites, and proline accumulation of *B. alba* and *B. alba* var. *cordifolia* under water deficit stress.

Keywords: Basellaceae, climate change, medicinal, proline, secondary metabolites

INTRODUCTION

The environment controls medicinal plants' growth and output. Phytochemicals are also called anti-nutritional factors and are generally not essential for the body's normal functioning but have important therapeutic functions. Natural plant extracts can be used as a new source of antimicrobial agents with potential mechanisms of action. Plant extracts with antimicrobial properties can be used in therapeutic treatments (Ogbe et al. 2020).

Basellaceae is a family of plants used in the ancient Indian medical system known as Ayurvedic medicine. The plants *Basella alba* L. and *Basella alba* var. *cordifolia* (Lam.) M.R.Almeida are species from the Basellaceae family. The other names are Malabar spinach, white gondola (alba), red gondola (*B. alba* var. *cordifolia*), red Malabar spinach, and Ceylon spinach; only about 20 types of plants from this family are divided into five genera (Tjitrosoepomo 2007). *B. alba* has been used commercially in various products since ancient times. The phytochemical properties of *B. alba* are widely used for various purposes, especially in herbal medicine. This plant has been reported as androgenic, antiviral, antibacterial, antioxidant, antidiabetic, anti-inflammatory, antidepressant, antiulcer (because it heals canker sores), wound healing, nephron activity, and hepatoprotective (Deshmukh and Gaikwad 2014; Alakinde and Ojo 2018).

Global climate change and increasing temperatures are problems in the cultivation of medicinal plants. Water deficit stress is the most significant risk for global agricultural food security. If the temperature increases by about 2°C this century, one-fifth of the world's population will be severely affected by drought stress because of water deficit. Global warming is one of the biggest problems in agriculture worldwide and causes dryness. How plants deal with stress varies with different strategies, such as avoiding stress with a short life span, susceptibility to stress to death, and surviving by producing secondary metabolites. In recent decades, public interest in plant secondary metabolites has increased significantly due to their direct therapeutic effects or as precursors for drugs. Secondary metabolites in medicinal plants contain bioactive compounds but must be scaled up in large enough quantities for commercial needs because these compounds are not essential for plant growth (Salehi-Lisar and Bakhshayeshan-Agdam 2016; Ray et al. 2019; Sultan et al. 2019).

Salicylic Acid (SA) can increase growth measurements such as fresh weight, dry weight, root-to-shoot ratio, production of secondary metabolites, and proline accumulation for plants to defend themselves from stress by influencing physiological and biochemical aspects (Khalvandi et al. 2021). Serious water deficit stress conditions can change morphological, physiological, and biochemical. Morphological changes include dwarf plants, early maturity, and a high root-to-shoot ratio. Physiological changes are increased oxidative stress, high proline accumulation, and growth stops. Biochemical changes are ROS production, oxidative damage, antioxidant defense, and secondary metabolites (Seleiman et al. 2021). When exposed to stress, salicylic acid is involved in physiological processes such as photosynthesis, proline, nitrogen metabolism, glycine betaine production, and water-plant relations. It also protects plants. SA affects plant function in a dose-dependent (Khan et al. 2015). Spraying 140 mg l-1 SA, 4 g l-1 Zn, and 11.5 g l-1 GB increased photosynthesis and RWC, increased leaf gas exchange attributes, increased antioxidant enzyme activity, reduced MDA, H_20_2, and O_2 - in corn plants experiencing water deficit stress (Shemi et al. 2021). This study aims to determine the exogenous application of SA as a strong, cost-effective, environmentally friendly strategy to increase the growth measurements, synthesis, and accumulation of proline and secondary metabolites in *B. alba* and B. *alba* var. *cordifolia*.

MATERIALS AND METHODS

Experimental design

The *Basella* plants were grown in Assalaam Islamic Modern Boarding School greenhouse, Pabelan, Kartasura Sukoharjo Regency, Central Java, Indonesia (±114 meters above sea level). This study used a two-factor Completely Randomized Design (CRD) with 3 replications. The different concentrations of salicylic acid were 0 mM (control), 2 mM, 4 mM, and 6 mM; the water deficit stress treatment with 3 kg of planting medium was doused with water until the first drop came out. Pour 1 L of water as field capacity, then calculate soil water content with a 10 grams sample using the formula (Soil water content%) = (A-B)/A x 100%; A: Initial weight of soil sample before drying (g); B: Final soil weight after drying (g). Calculated watering concentrations of water Deficit Stress (DS) were 100% (control), 75% (light stress), 50% (medium stress), and 25% (heavy stress) based on field capacity. This treatment was carried out for 8 weeks after the seeds were planted in polybags at 8 weeks old.

Procedures

Plant materials

The *B. alba* and *B. alba* var. *cordifolia* seeds were obtained from traditional markets, "Ninu Farm," three seeds containing embryos were selected and planted in each polybag. The daily temperatures inside the greenhouse are about 23-31℃. The soil used is black with a sandy texture, has coarse grains, is not sticky, and has high porosity; the soil pH is 6.5. After the seeds were 8 weeks old, they were transferred to polybags with a diameter of 20 cm to be treated for 8 weeks. Salicylic acid with different concentrations, namely 2 mM, 4 mM, and 6 mM, was sprayed on the leaves every 2 days. Water deficit stress based on field capacity is provided every 3 days. Control plants were not given water deficit stress or salicylic acid treatment. Plant dry weight was calculated by weighing the total plant weight after drying for approximately 10 days by sun drying.

Growth measurements

Observational data are presented in grams (g) and measured using an analytical balance. The wet weight of the plants was weighed using an analytical balance at harvest time with the plants aged 4 months after planting. The wet weight of the plants was carried out by uprooting all the plants from the polybag, removing any soil that was still attached, and then weighing them using an analytical balance. The shoot-to-root ratio was obtained by comparing the root and shoot of dry weight.

Plant extraction

Plant extraction used all aerial parts: stems, leaves, and seeds. Extraction occurred after the plants were harvested or 88 days after planting. Next, dry all parts of the plant for 14 days at 50ºC, then finely grind the dried plant with a mortar. Extracts of *B. alba* and *B. alba* var. *cordifolia* were taken from each treatment as much as 0.3 grams sample and dissolved in absolute methanol sonicated at 50 Hz for 15 minutes and then centrifuged the extract at 5,000 rpm for 10 minutes. The centrifuged supernatant was transferred to the flacon bottle according to the treatment.

Secondary metabolites determination

Quercetin quantification by $AlCl_3$ method. 0.3 g of dry extracts of *B. alba* and *B. alba* var. *cordifolia* were dissolved in 10 mL of methanol each. The extract solution obtained was pipetted 1 mL plus 1 mL of 2% $AlCl_3$, and then 1 mL of 1M potassium acetate was added. The mixed solution was left for 1 hour at room temperature, and then a microplate reader (ELISA) was used to measure the absorption solution at a wave of 374 nm, repeated three times. Next, the wavelength was determined from the average absorption results. The quercetin standard series solutions preparation with 40 ppm, 60 ppm, 80 ppm, 100 ppm, and 120 ppm concentrations were obtained by diluting 1,000 ppm quercetin mother liquor. Then, 1 mL was added to 1 mL of 2% $AlCl_3$ and 1 mL of 1M potassium acetate. The standard solution that has been made is left for 1 hour at room temperature, and its absorbance is measured at a wavelength of 374 nm. Reading the concentration of flavonoids on the calibration line (μg/mL), the content of flavonoids in the extract is expressed in quercetin equivalents (mgQE/g extract). Quercetin levels are expressed in% w/w. The determination of gallic acid with the Folin ciocalteu method; a total of 0.3 g of dry extracts of *B. alba* and *B. alba* var. *cordifolia* were dissolved in 10 mL of methanol mixture each. The extract solution obtained was pipetted 1 mL plus the Folin-Ciocalteu

reagent, shaken, left for 3 minutes, added 1.2 mL of 7% Na_2CO_3 solution and left for 60 minutes at room temperature. The absorbance of the extract solution was measured with a Microplate reader (ELISA) at a wavelength of 725 nm and repeated 3 times. Then, the wavelength value was determined with the average absorbance value. Preparation of gallic acid standard series solutions at 40 ppm, 60 ppm, 80 ppm, 100 ppm, and 120 ppm concentrations were obtained by diluting 1,000 ppm gallic acid mother liquor. Then, 1 mL of Folin-Ciocalteu reagent was added, shaken, and left for three minutes. Added 1 mL of 20% Na_2CO_3 solution and then shake until homogeneous. Set aside one hour at room temperature and measure the absorbance at the maximum wavelength. A calibration curve was made for the relationship between gallic acid concentration (µg/mL) and absorbance (Supriningrum et al. 2020)

Calculation of proline accumulation

The accumulation of proline calculation begins by preparing a standard proline solution. Make a 2.5 µM stock solution diluted with 10 mL of 3% sulfosalicylic acid. Then, a proline standard was made with a concentration of 0.1 µM, 0.2 µM, 0.3 µM, and 0.4 µM. Next, each solution was mixed with ninhydrin acid and glacial acetic acid. Place the solution on a Microplate Reader (ELISA) to measure the absorption of the solution at a wave of 520 nm and repeat this three times, then determine the wavelength from the average absorption results. A standard proline curve was made by correlating the concentration of the standard solution with the absorbance results obtained from proline measurements of *B. alba* and *B. alba* var. *cordifolia* leaves. Y = ax+b, the absorbance value of the sample is entered as a Y value to obtain an X value (Bates 1973).

$$\text{proline} = \frac{\text{µmol proline/ml toluene}}{\text{Sample (g)}/5} = \frac{\text{µmol proline}}{\text{Fresh weight}}$$

Analysis of proline levels was carried out when the plants were 88 days after planting. The part used is the fresh leaves and the analysis of proline levels using the Bates method (1973). Samples of *B. alba* and *B. alba* var. *cordifolia* leaves were weighed as much as 2 g and then finely ground. Add 5 mL of 3% sulfosalicylic acid to the sample and filter using Whatman paper No. 1. Next, react 2 mL of filtrate with 2 mL of ninhydrin and 2 mL of glacial acetic acid. Next, it was heated in a water bath at 100°C for 1 hour, and the reaction was ended by placing the test tube in a glass beaker containing ice water. Next, 4 mL of the reaction mixture was extracted with 4 mL of toluene and shaken for 15-20 seconds. Toluene containing proline was pipetted using a micropipette and inserted into the microplate. The blank solution used is toluene. ELISA measured the absorbance of the solution on a Microplate reader (*Lab Geni*) at a wavelength of 520 nm.

Data analysis

Initial statistical analysis used normality and homogeneity tests, then continued with a two-way analysis of variance. After that, Duncan's multiple range test was continued at the 5% level to determine the real effect of each treatment. Data analysis using SPSS 26.0 software.

RESULT AND DISCUSSION

Analysis of growth characteristics of *B. alba* and *B. alba* var. *cordifolia* treated with salicylic acid under water deficit stress

Dry weight

The results are shown in Table 1; the highest value in dry weight was *B. alba* at treatment by SA 6mM+light stress with 5.45 g compared to control 1.42 g, while the lowest weight was treatment by SA 6mM+heavy stress 1.38 g. The highest value in *B. alba* var. *cordifolia* was in treatment SA 4mM+medium stress with a weight of 3.09 g compared to control 1.26 g, while the lowest weight was treated by SA 0mM+medium stress with 0.99 g. Dry weight indicates photosynthate assimilation results because the photosynthate is translocated from the roots to all parts of the plants, and there is an increase in protoplasmic addition due to the increased size and number of cells. So, dry weight also indicates the absorption of nutrients in a plant (Gardner et al. 1991).

Fresh weight

Table 1 shows the highest treatment in fresh weight study for *B. alba* was treatment by SA 4mM+heavy stress with 35.95 g compared to the control 25.81 gr while the lowest weight was treatment by SA 0mM+heavy stress with 18.68 g. The highest value in *B. alba* var. *cordifolia* was followed by SA 4mM+moderate with 35.66 g compared to the control 19.69 gr, while the lowest weight was treated by SA 0mM+medium stress with 18.51 g. Fresh plant weight shows the level of air absorption and nutrients plants absorb for metabolism (Noctor et al. 2018). In this study, the fresh weight of the initial plants had a uniform weight of ± 1.0-2.5 grams/plant. Treatment with water deficit stress (SA 0 mM) reduced the fresh weight of both *B. alba* and *B. alba* var. *cordifolia* plants, but salicylic acid increased the fresh weight.

Shoot-to-root ratio

The root ratio is a character that can be used to determine excess or lack of water. As shown in Table 1, the results showed that the highest shoot-to-root ratio in *B. alba* was in treatment SA 6mM+light stress with 0.93, while the lowest ratio in treatment SA 0mM+heavy stress with 0.21 or in the treatment with heavy stress. The best results for *B. alba* var. *cordifolia* were in treatment SA 6mM+light stress with 0.99, while the lowest ratio was followed by SA 0mM+heavy stress with 0.27 or in the treatment with severe water deficit stress.

Table 1. The growth characteristics of *B. alba* and *B. alba* var. *cordifolia* treated with salicylic acid under water deficit stress

Parameters	Species	Treatment														
		Control	SA 2mM + DS control	SA 4mM + DS control	SA 6mM + DS control	SA 0mM + Light stress	SA 2mM + Light stress	SA 4mM + Light stress	SA 6mM + Light stress	SA 0 mM + medium stress	SA 2mM + medium stress	SA 4mM + medium stress	SA 6mM + medium stress	SA 0mM + heavy stress	SA 2mM + heavy stress	SA 4mM + heavy stress	SA 6mM + heavy stress
Dry Weight	*B. alba*	1.42± 0.01Ac	2.07± 0.27Ac	1.85± 0.14Ab	1.71± 1.23Aa	1.71± 0.12Bc	2.29± 0.06Bc	2.33± 0.33Bb	5.45± 0.48Ba	1.86± 0.04Cc	3.80± 0.58Cc	2.70± 0.73Cc	1.44± 0.06Ca	1.44± 0.31Cc	1.99± 0.24Cc	1.43± 0.05Cb	1.38± 0.12Ca
	B. alba var. *cordifolia*	1.26± 0.35Ac	1.06± 0.02Ac	1.55± 0.02Ab	1.77± 0.02Aa	1.37± 0.03Bc	1.08± 0.01Bc	2.46± 0.01Bb	1.63± 0.06Ba	0.99± 0.02Cc	1.91± 0.01Cc	3.09± 0.04Cb	1.72± 0.0.01Cca	1.48± 0.07Cc	1.44± 0.03Cc	1.06± 0.00Cb	1.32± 0.02Ca
Fresh Weight	*B. alba*	25.81± 4.31Ba	25.65± 4.65Ba	26.74± 5.80Ba	23.57± 3.44Ba	28.75± 1.30Ba	23.79± 4.87Ba	30.95± 1.76Ba	23.14± 3.52Ba	23.45± 2.38ABa	25.08± 2.22ABa	31.80± 4.43ABa	19.39± 2.93ABa	18.68± 2.41Aa	28.16± 3.86Aa	35.95± 4.13Aa	26.19± 3.76Aa
	B. alba var. *cordifolia*	19.69± 1.95Aa	23.89± 0.69Ab	22.33± 4.11Ab	24.04± 2.90Ab	22.06± 3.69Cb	25.95± 3.32Cb	30.56± 0.92Cb	21.00± 2.58Cb	18.51± 1.81BCb	23.47± 2.13BCb	35.66± 3.32BCb	23.74± 3.83BCb	24.74± 3.48ABb	32.97± 1.49Abb	21.56± 1.03ABb	25.14± 0.97ABb
Shoot-to-root ratio	*B. alba*	0.40± 0.003Aa	0.37± 0.001Ac	0.36± 0.002Ab	0.55± 0.002Ab	0.42± 0.001Ca	0.90± 0.001Cc	0.92± 0.003Cb	0.93± 0.003Cb	0.42± 0.003Ba	0.64± 0.001Bc	0.60± 0.001Bb	0.62± 0.001Bb	0.21± 0.003Ca	0.43± 0.002Cc	0.49± 0.003Cb	0.58± 0.001Cb
	B. alba var. *cordifolia*	0.42± 0.002Aa	0.38± 0.004Ad	0.64± 0.002Ac	0.64± 0.002Ab	0.35± 0.005Da	0.90± 0.004Dd	0.97± 0.002Dc	0.99± 0.002Db	0.38± 0.003Ba	0.66± 0.224Bd	0.69± 0.993Bc	0.75± 0.002Bb	0.29± 0.001Ca	0.77± 0.304Cd	0.58± 0.003Cc	0.27± 0.001Cb

Note: The averages marked with capital letters differ significantly between SA levels within each water availability level (FC), and the averages marked with lowercase letters differ significantly between water availability levels (FC) within each SA level based on the DMRT test on level 5%

Table 2. Secondary metabolites of *B. alba* and *B. alba* var. *cordifolia* treated with salicylic acid under water deficit stress

Parameters	Species	Treatment														
		Control	SA 2mM + DS control	SA 4mM + DS control	SA 6mM + DS control	SA 0mM + Light stress	SA 2mM + Light stress	SA 4mM + Light stress	SA 6mM + Light stress	SA 0 mM + medium stress	SA 2mM + medium stress	SA 4mM + medium stress	SA 6mM + medium stress	SA 0mM + heavy stress	SA 2mM + heavy stress	SA 4mM + heavy stress	SA 6mM + heavy stress
Quercetin (% w/w)	*B. alba*	1.2± 0.30Aa	0.99± 0.04Ba	1.15± 0.04Ca	1.34± 0.03Ba	0.33± 0.015Aa	1.41± 0.017Ba	1.52± 0.05Ca	1.69± 0.12Ba	0.75± 0.15Ab	1.8± 0.20Ab	1.87± 0.015Bb	2.04± 0.03Cb	0.27± 0.23Ac	2.33± 0.09Ab	2.88± 0.14Bb	1.80± 0.12Cb
	B. alba var. *cordifolia*	0.78± 0.14Ac	0.73± 0.25Bc	1.17± 0.04Dc	1.43± 0.04Cc	0.12± 0.03Aa	0.42± 0.03Ba	0.26± 0.03Da	0.15± 0.03Ca	0.04± 0.01Ad	1.16± 0.06Bd	1.59± 0.04Dd	1.93± 0.08Cd	0.02± 0.005Ab	1.37± 0.16Bb	1.41± 0.11Db	1.61± 0.04Cb
Gallic acid (%w/w)	*B. alba*	2.15± 0.39Aa	1.83± 0.31Ba	3.08± 0.14Ca	3.95± 0.11Da	0.27± 0.13Ab	3.74± 0.25Bb	5.05± 0.05Cb	5.25± 0.38Db	0.13± 0.05Ad	6.01± 0.12Bd	6.37± 0.13Cd	10.21± 0.14Dd	0.16± 0.005Ac	3.32± 0.12Bc	7.25± 0.09Cc	4.44± 0.19Dc
	B. alba var. *cordifolia*	3.18± 0.13Aa	4.57± 0.22Ba	4.73± 0.20Ca	5.21± 0.06Ca	2.53± 0.22Ac	6.40± 0.25Bc	6.9± 0.1Cc	7.16± 0.08Cc	0.86± 0.44Ad	7.38± 0.14Bd	9.31± 0.67Cd	9.44± 0.77Cd	0.19± 0.17Ab	6.31± 0.1Bb	8.08± 0.26Cb	7.34± 0.8Cb

Note: The averages marked with capital letters differ significantly between SA levels within each water availability level (FC), and the averages marked with lowercase letters differ significantly between water availability levels (FC) within each SA level based on the DMRT test on level 5%

Table 3. Proline accumulation of *B. alba* and *B. alba* var. *cordifolia* treated with salicylic acid under water deficit stress

Parameters	Species	Treatment														
		Control	SA 2mM + DS control	SA 4mM + DS control	SA 6mM + DS control	SA 0mM + Light stress	SA 2mM + Light stress	SA 4mM + Light stress	SA 6mM + Light stress	SA 0 mM + medium stress	SA 2mM + medium stress	SA 4mM + medium stress	SA 6mM + medium stress	SA 0mM + heavy stress	SA 2mM + heavy stress	SA 4mM + heavy stress	SA 6mM + heavy stress
Proline accumulation (µmol/gram wet weight)	*B. alba*	1.90± 0.3Aa	2.49± 0.35Ba	3.38± 0.12Ca	3.84± 0.34Da	2.12± 0.11Ac	4.95± 0.19Bc	5.57± 0.15Cc	5.87± 0.08Dc	3.29± 0.18Ad	4.47± 0.58Bd	6.57± 0.15Cd	8.74± 0.16Dd	3.58± 0.03Ab	2.31± 0.30Bb	3.62± 0.08Cb	4.97± 0.27Db
	B. alba var. *cordifolia*	1.28± 0.17Aa	3.12± 0.007Ba	3.51± 0.21Da	4.02± 0.16Ca	2.95± 0.12Ab	5.03± 0.04Bb	5.59± 0.09Db	6.08± 0.18Cb	2.29± 0.11Ad	6.14± 0.06Bd	9.35± 0.06Dd	9.83± 0.06Cd	2.87± 0.46Ac	6.22± 0.17Bc	8.05± 0.07Dc	5.20± 0.16Cc

Note: The averages marked with capital letters differ significantly between SA levels within each water availability level (FC), and the averages marked with lowercase letters differ significantly between water availability levels (FC) within each SA level based on the DMRT test on level 5%

Analysis of secondary metabolites of *B. alba* and *B. alba* var. *cordifolia* treated with salicylic acid under water deficit stress

Quercetin level

Table 2 shows the best treatment in quercetin for *B. alba* was in treatment by SA 4mM+heavy stress) with 2.88% w/w, the lowest ratio followed by SA 0mM+light stress with 0.27% w/w or in the treatment with heavy stress. The best ratio for *B. alba* var. *cordifolia* was in treatment by SA 6mM+medium stress with 1.93% w/w, while the lowest ratio was followed by SA 0mM+heavy stress with 0.02% w/w or in the treatment with severe water deficit stress.

Gallic acid level

The DMRT test at a 5% level showed significant results on the gallic acid content of the *Basella* plant. As shown in Table 2, the best treatment in gallic acid for *B. alba* was in treatment by SA 6mM+medium stress with 10.21% w/w while the lowest ratio followed by SA 0mM+heavy stress with 0.13% w/w or in the treatment with heavy stress. The best results for *B. alba* var. *cordifolia* were in treatment by SA 6mM+medium stress with 9.44% w/w, while the lowest ratio was in treatment by SA 0mM+heavy stress with 0.19% w/w or in the treatment with heavy stress.

Analysis of proline accumulation of *B. alba* and *B. alba* var. *cordifolia* treated with salicylic acid under water deficit stress

Proline accumulation

The DMRT test at a 5% level (Table 3) showed significant results on the proline accumulation of the *Basella* plant. The results indicate that the highest proline in *B. alba* was in treatment by SA 6mM+medium stress with 8.74 µmol/gram wet weight while the lowest ratio was treatment by SA 0mM+light stress with 2.12% µmol/gram wet weight. The best ratio for *B. alba* var. *cordifolia* was in treatment by SA 6mM+medium stress with 9.83 µmol/gram wet weight, while the lowest ratio was in treatment by SA 0mM+medium stress with 2.29 µmol/gram wet weight.

Discussion

The foliar salicylic acid application enhances the growth of B. alba *and* B. alba *var.* cordifolia

Basella plants easily adapt to various types of soil and climate and are considered one of the tropical spinach plants grown annually. *Basella,* known as Malabar spinach, is also planted because of its very important nutritional content (Adhikari et al. 2012; Sharma et al. 2022). The growth measurements observed were root shoot ratio, fresh weight, and final dry weight on *B. alba* and *B. alba B. alba* var. *cordifolia*. On the growth parameter, *B. Alba* and *B. alba* var. *cordifolia* have better results; this result aligns with Alakinde's and Ojo's (2015) research on *Basella* Linn's anatomy, which significantly differs in stress adaptation. *B. rubra* has anatomical characteristics that are more adaptive in dealing with stress with several features, including a multi-series epidermis, which prevents water loss; also, the long vascular bundles with a larger diameter allow plants to absorb water from the soil and distribute the water more effectively. The closed areoles and the absence of vein endings ensure water conservation; the final feature is the differentiation of the leaf mesophyll (Alakinde and Ojo 2015).

Plant dry weight is an indicator of the results of photosynthate assimilation, which is translocated from the roots to all parts of the plant and produced from an increase in protoplasm, so the size and number of cells also increase. SA activates the plant's defense system and helps adjust water needs when exposed to water deficit stress. In addition, SA increases the activity of SOD, CAT, and POD enzymes, reduces lipid peroxidation, and helps maintain PSII (Noctor et al. 2018). Applying salicylic acid increases fresh weight, which causes an active shift in photosynthesis processes. Salicylic acid sprayed on leaves modulates important enzymatic components such as monodehydroascorbate reductase, MDHAR; dehydroascorbate reductase, DHAR; GR; GSH peroxidase, GPX) and non-enzymatic (including GSH) of the AsA-GSH pathway, as well as the glyoxalase system (Gly I and Gly II) and reduce oxidative stress in plants when exposed to drought stress (Alam et al. 2013; Sohag et al. 2020).

The ratio of shoots to roots is a characteristic that can determine excess or lack of water. Our research revealed that root growth is greater under water deficit stress than shoot growth. In water shortage conditions, plants allocate more photosynthate to the roots to absorb more nutrients. This causes root weight to increase while shoot weight decreases under water deficit stress conditions, making the ratio smaller (Table 1). Reduced shoot growth due to water deficit stress can be caused by loss of turgor, which causes limitations in cell enlargement and leaf expansion. Inhibition of leaf growth reduces photosynthesis due to stomata closing because it limits gas exchange. Disruption of photosynthesis also causes several enzymatic and hormonal changes (Tombesi et al. 2015; Xu et al. 2015; Furlan et al. 2017; Kou et al. 2022). Shoot-to-root ratio, fresh weight, and dry weight are closely related to photosynthesis. Salicylic acid sprayed on plants during drought accumulates more proline to maintain photosynthesis by stabilizing the Rubisco protein. SA also increases the activity of NR (nitrate reductase) and ATPS (ATP Sulfurylase) so that the metabolism of N (nitrogen) and S (sulfur) also increases. The increased N and S directly affect photosynthesis, so administering SA can control water deficit stress (Ashraf and Foolad 2007; Nazar et al. 2015).

The foliar salicylic acid application enhances the morphophysiology of B. alba *and* B. alba *var.* cordifolia

Proline production during long periods of water deficit stress increases because proline is synthesized in the leaves and transported to the roots to overcome water shortages. This study proved that salicylic acid in both *Basella* plants increased proline accumulation (Table 3). Several studies report that exogenously administered salicylic acid can reduce the adverse effects, increasing growth, photosynthesis, and proline accumulation in water deficit stress. Wang et al. (2022) stated that proline in the roots,

stems, and leaves of the germplasm of watermelon M08 strain Y34 was very significant when exposed to water deficit stress. Profiles and enzyme activity measurements revealed that the ClP5CS1 gene contributes primarily to leaf proline synthesis via the Glu pathway. Nazar et al. (2015) stated that proline production increased in *Brassica juncea* (L.) Czern. given 0.5 mM SA by increasing γ-glutamyl kinase (GK) and decreasing proline oxidase (PROX) activity. Salicylic acid significantly inhibits the activity of 1-aminocyclopropane carboxylic acid synthase (ACS) in *B. juncea* plants during water deficit stress. The increase in proline during water deficit stress regulates water balance as an osmoprotectant so that plants are protected from oxidative stress; thus, the photosynthesis process runs well. Exogenous application of SA increases proline content due to increased pyrroline-5-carboxylate reductase activity by converting pyrroline-5-carboxylate into proline so that proline synthesis increases. The study proves that SA can improve the antioxidant defense system of plants and increase the levels of osmotic regulatory substances to remove ROS. These results follow our observations that the levels of ROS and MDA were significantly reduced in plants after SA treatment (Sharma et al. 2023).

Currently, drought is the most critical abiotic stress and affects agriculture throughout the world. The main negative impact that occurs due to drought is oxidative damage. Flavonoids are a non-enzymatic antioxidant that increases plant defense against drought stress. During abiotic stress conditions, modifications to plant flavonoid biosynthesis occur for the defense system. Plants with higher concentrations of flavonoids cope better with oxidative stress. Flavonoids are synthesized in plants via the shikimate and phenylpropanoid pathways. Exogenously administered salicylic acid in appropriate doses activates several genes associated with cellular processes and responses to environmental stimuli or stress conditions. The expressed genes were directly and indirectly related to phenylpropanoid metabolism. Salicylic acid works on signaling pathways to increase plant tolerance to stress so that yields remain good. Apart from that, salicylic acid plays an important role in increasing physiological processes, stomatal conductance, photosynthesis rate, and chlorophyll content under stress conditions (Arbona et al. 2013; Li et al. 2013; Nazar et al. 2015; Shomali et al. 2022).

Quercetin can protect chloroplasts from singlet oxygen produced by visible light. An increase followed a rapid increase in PAL activity in quercetin levels. This is in line with research (Khalil et al. 2022), which states that salicylic acid has a positive impact on increasing secondary metabolites in *Eriocephalus africanus* L. Adegoke and Ojo (2017) stated that phenolic and flavonoid content in *B. alba* greater than in *B. alba* var. *cordifolia*. Salicylic acid influences receptor transcription to produce defense gene expression, increasing plant immunity. Prolonged drought stress increases excitation energy and ROS levels, but salicylic acid works the opposite, namely increasing the antioxidant system in plants experiencing stress (Badri et al. 2008; Gondor et al. 2016; Kumar et al. 2021; Peng et al. 2021).

Phenol content is a good indicator for assessing environmental stress and plant metabolism tolerance. It can scavenge free radicals such as ROS, reduce singlet oxygen, break down peroxides, and inhibit autooxidation of lipids and plant antioxidant compounds necessary to protect plants against proliferation and oxidative stress. The increase in phenol content is due to the induction of special defense mechanisms that protect the cytoplasm and chloroplasts from oxidative damage. Moreover, Salicylic acid has been shown to help the synthesis of phenolic compounds such as the PAL enzyme, which catalyzes the phenylpropanoid pathway to form trans-cinnamic acid, the main mediator of phenolic biosynthesis (Ksouri et al. 2008; Oh et al. 2009; Sharma et al. 2019; Moradbeygi et al. 2020; Shohani et al. 2023).

REFERENCES

Adegoke OG, Ojo OA. 2017. Phytochemical, antioxidant and antimicrobial activities in the leaf, stem and fruit fractions of *Basella alba* and *Basella rubra*. Plant 5 (5): 73-79. DOI: 10.11648/j.plant.20170505.11.

Adhikari R, Kumar HN, Shruti SD. 2012. A review on medicinal importance of *Basella alba* L. Intl J Pharm Sci Drug Res 4 (2): 110-114.

Alakinde TAA, Ojo FMA. 2015. Some anatomical features of *Basella*: Their adaptive significance to water stress. Res Plant Biol 5 (3): 2231-5101.

Alakinde TAA, Ojo FMA. 2018. Phytochemical and antioxidant properties of forms of *Basella*. Intl J Veg Sci 25 (5): 1-10. DOI: 10.1080/19315260.2018.1524808.

Alam MM, Hasanuzzaman M, Nahar K, Fujita M. 2013. Exogenous Salicylic acid ameliorates short-term water deficit stress in mustard (*Brassica juncea* L) seedlings by up-regulating the antioxidant defens and glyoxalase system. Aust J Crop Sci 7 (7): 1053-1063.

Arbona V, Manzi M, de Ollas C, Gómez-Cadenas A. 2013. Metabolomics as a tool to investigate abiotic stress tolerance in plants. Intl J Mol Sci 14 (3): 4885-4911. DOI: 10.3390/ijms14034885.

Ashraf M, Foolad M. 2007. Roles of glycine betaine and proline in improving plant abiotic stress resistance. Environ Exp Bot 59: 206-216. DOI: 10.1016/j.envexpbot.2005.12.006.

Badri DV, Loyola-Vargas VM, Du J, Stermitz FR, Broeckling CD, Iglesias-Andreau L, Vivanco JM. 2008. Transcriptome analysis of *Arabidopsis* roots treated with signaling compounds: A focus on signal transduction, metabolic regulation and secretion. New Phytol 179: 209-223. DOI: 10.1111/j.1469-8137.2008.02458.x.

Bates LS. 1973. Rapid determination of free proline for water stress studies. Plant Soil 39: 205-207. DOI: 10.1007/BF00018060.

Deshmukh SA, Gaikwad DK. 2014. A review of the taxonomy, ethnobotany, phytochemistry and pharmacology of *Basella alba* (Basellaceae). J Appl Pharm Sci 4 (1): 153-165. DOI: 10.7324/JAPS.2014.40125.

Furlan A, Bianucci, Castro S, Dietz KJ. 2017. Metabolic features involved in drought stress tolerance mechanisms in peanut nodules and their contribution to biological nitrogen fixation. Plant Sci 263: 12-22. DOI: 10.1016/j.plantsci.2017.06.009.

Gardner FP, Pearce RB, Mitchell RL. 1991. Physiology of Crop Plants. Universitas Indonesia Press, Jakarta.

Gondor OK, Janda T, Soós V, Pál M, Majláth I, Adak MK, Balázs E, Szalai G. 2016. Salicylic acid induction of flavonoid biosynthesis pathways in wheat varies with treatment. Front Plant Sci 7: 1447. DOI: 10.3389/fpls.2016.01447.

Khalil N, Elhady SS, Diri RM, Fekry MI, Bishr M, Salama O, El-Zalabani SM. 2022. Salicylic acid spraying affects secondary metabolites and radical scavenging capacity of drought-stressed *Eriocephalus africanus* L. Agronomy 12 (10): 2278. DOI: 10.3390/agronomy12102278.

Khalvandi M, Adel S, Ebrahim R, Sara K. 2021. Salicylic acid alleviated the effect of drought stress on photosynthesis characteristics and leaf protein pattern in winter wheat. Heliyon 7 (1): E05908. DOI: 10.1016/J.Heliyon.2021.

Khan MI, Fatma M, Per TS, Anjum NA, Khan NA. 2015. Salicylic acid-induced abiotic stress tolerance and underlying mechanisms in plants. Front Plant Sci 6: 462. DOI: 10.3389/fpls.2015.00462.

Kou X, Weihua H, Jian K. 2022. Responses of root system architecture to water stress at multiple levels: A meta-analysis of trials under controlled conditions. Front Plant Sci 13: 1085409. DOI: 10.3389/fpls.2022.1085409.

Ksouri R, Megdiche W, Falleh H, Trabelsi N, Boulaaba M, Smaoui A, Abdelly C. 2008. Influence of biological, environmental and technical factors on phenolic content and antioxidant activities of Tunisian halophytes. C R Biol 331 (11): 865-873. DOI: 10.1016/j.crvi.2008.07.024.

Kumar M, Patel MK, Kumar N, Bajpai AB, Siddique KHM. 2021. Metabolomics and molecular approaches reveal water deficit stress tolerance in plants. Intl J Mol Sci 22 (17): 9108. DOI: 10.3390/ijms22179108.

Li G, Peng X, Wei L, Kang G. 2013. Salicylic acid increases the contents of glutathione and ascorbate and temporally regulates the related gene expression in salt-stressed wheat seedlings. Gene 529 (2): 321-325. DOI: 10.1016/j.gene.2013.07.093.

Moradbeygi H, Jamei R, Heidari R, Darvishzadeh R. 2020. Investigating the enzymatic and non-enzymatic antioxidant defense by applying iron oxide nanoparticles in *Dracocephalum moldavica* L plant under salinity. Sci Hortic 272: 109537. DOI: 10.1016/j.scienta.2020.109537.

Nazar R, Umar S, Khan NA, Sareer O. 2015. Salicylic acid supplementation improves photosynthesis and growth in mustard through changes in proline accumulation and ethylene formation under water deficit stress. S Afr J Bot 98: 84-94. DOI: 10.1016/j.sajb.2015.02.005.

Noctor G, Reichheld JP, Foyer CH. 2018. ROS-related redox regulation and signaling in plants. Semin Cell Dev Biol 80: 3-12. DOI: 10.1016/j.semcdb.2017.07.013.

Ogbe AA, Finnie JF, Van Staden J. 2020. The role of endophytes in secondary metabolites accumulation in medicinal plants under abiotic stress. S Afr J Bot 134: 126-134. DOI: 10.1016/j.sajb.2020.06.023.

Oh MM, Carey EE, Rajashekar CB. 2009. Environmental stresses induce health-promoting phytochemicals in lettuce. Plant Physiol Biochem 47 (7): 578-583. DOI: 10.1016/j.plaphy.2009.02.008.

Peng Y, Jianfei Y, Xin L, Zhang Y. 2021. Salicylic acid: Biosynthesis and signalling. Ann Rev Plant Biol 72: 761-791. DOI: 10.1146/annurev-arplant-081320-092855.

Ray DK, West PC, Clark M, Gerber JS, Prishchepov AV, Chatterjee S. 2019. Climate change has likely already affected global food production. PLoS One 4 (5): e0217148. DOI: 10.1371/journal.pone.0217148.

Salehi-Lisar SY, Bakhshayeshan-Agdam H. 2016. Water deficit stress in plants: Causes, consequences, and tolerance. In: Hossain MA, Wani SH, Bhattacharjee S, Burritt DJ, Tran LSP (eds). Water Deficit Stress Tolerance in Plants Vol 1. Springer, Cham. DOI: 10.1007/978-3-319-28899-4_1.

Seleiman MF, Al-Suhaibani N, Ali N, Akmal M, Alotaibi M, Refay Y, Dindaroglu, Abdul-Wajid HH, Battaglia ML. 2021. Water deficit stress impacts on plants and different approaches to alleviate its adverse effects. Plants 10: 259. DOI: 10.3390/plants10020259.

Sharma A, Shahzad B, Rehman A, Bhardwaj R, Landi M, Zheng B. 2019. Response of phenylpropanoid pathway and the role of polyphenols in plants under abiotic stress. Molecules 24: 2452. DOI: 10.3390/molecules24132452.

Sharma A, Kohli S, Khanna K, Ramakrishnan M. 2023. Salicylic acid: A phenolic molecule with multiple roles in salt-stressed plants. J Plant Growth Regul 42 (8): 1-25. DOI: 10.1007/s00344-022-10902-z.

Sharma V, Kumar A, Chaudhary A, Mishra A, Rawat S, Basavaraj YB, Shami V, Kaushik P. 2022. Response of wheat genotypes to water deficit stress stimulated by PEG. Stresses 2 (1): 26-51. DOI: 10.3390/stresses2010003.

Shemi R, Wang R, Gheith ESMS, Hussain HA, Hussain S, Irfan M, Cholidah L, Zhang K, Zhang S, Wang L. 2021. Effects of salicylic acid, zink, and glycine betaine on morpho-physiological growth and yield of maize under water deficit stress. Sci Rep 11 (1): 3195. DOI: 10.1038/s41598-021-82264-7.

Sohag AAM, Tahjib-Ul-Arif M, Brestič M, Afrin S, Sakil MA, Hossain MT, Hossain MA, Hossain MA. 2020. Exogenous salicylic acid and hydrogen peroxide attenuate water deficit stress in rice. Plant Soil Environ 66 (1): 7-13. DOI: 10.17221/472/2019-PSE.

Shohani F, Fazeli A, Sarghein SH. 2023. The effect of silicon application and salicylic acid on enzymatic and non-enzymatic reactions of *Schophularia striata* L. under drought stress. Sci Hortic 319: 112143. DOI: 10.1016/j.scienta.2023.112143.

Shomali A, Das S, Arif N, Sarraf M, Zahra N, Yadav V, Aliniaeifard S, Chauhan DK, Hasanuzzaman M. 2022. Diverse physiological roles of flavonoids in plant environmental stress responses and tolerance. Plants 11 (22): 3158. DOI: 10.3390/plants11223158.

Sultan B, Defrance D, Iizumi T. 2019. Evidence of crop production losses in West Africa due to historical global warming in two crop models. Sci Rep 9 (1): 12834. DOI: 10.1038/s41598-019-49167-0.

Supriningrum R, Nurhasnawati H, Faisah S. 2020. Penetapan kadar fenolik total ekstrak etanol daun serunai (*Chromolaena odorata* l.) dengan metode spektrofotometri UV-VIS. Al Ulum Jurnal Sains dan Teknologi 5 (2): 54-57. DOI: 10.31602/ajst.v5i2.2802. [Indonesian]

Tombesi S, Nardini A, Frioni T, Soccolini M, Zadra C, Farinelli D, Poni S, Palliotti A. 2015. Stomatal closure is induced by hydraulic signals and maintained by ABA in drought-stressed grapevine. Sci Rep 5: 12449. DOI: 10.1038/srep12449.

Tjitrosoepomo G. 2007. Taksonomi Tumbuhan (Spermatophyta). Universitas Gadjah Mada Press, Yogyakarta. [Indonesian]

Wang Z, Yang Y, Yadav V, Zhao W, He Y, Zhang X, Wei C. 2022. Drought-induced proline is mainly synthesized in leaves and transported to roots in watermelon under water deficit. Hortic Plant J 8 (5): 615-626. DOI: 10.1016/j.hpj.2022.06.009.

Xu W, Cui K, Xu A, Nie L, Huang J, Peng S. 2015. Drought stress condition increases root to shoot ratio via alteration of carbohydrate partitioning and enzymatic activity in rice seedlings. Acta Physiol Plant 37: 9. DOI: 10.1007/s11738-014-1760-0.

NUSANTARA BIOSCIENCE
Vol. 16, No. 1, pp. 104-110
May 2024

ISSN: 2087-3948
E-ISSN: 2087-3956
DOI: 10.13057/nusbiosci/n160113

The difference between Bali cattle and Limousin-Bali (Limbal) crossed cattle concerning their qualitative characteristics in Lombok Tengah District, Indonesia

ADI TIYA WARMAN[1], PANJONO[1,♥], GALIH TRIE FADHILAH[1], BAYU ANDRI ATMOKO[2], SIGIT BINTARA[1], TRI SATYA MASTUTI WIDI[1], ENDANG BALIARTI[1], ZAENAB NURUL JANNAH[1]

[1]Faculty of Animal Science, Universitas Gadjah Mada. Jl. Fauna No. 3, Bulaksumur, Sleman 55281, Yogyakarta, Indonesia. Tel.: +62-274-513363, Fax.: +62-274-521578, ♥email: panjono@mail.ugm.ac.id

[2]Research Center for Animal Husbandry, National Research and Innovation Agency, Cibinong Science Center. Jl. Raya Jakarta-Bogor, Bogor 16915, West Java, Indonesia

Manuscript received: 29 December 2023. Revision accepted: 26 February 2024.

Abstract. *Warman AT, Panjono, Fadhilah GT, Atmoko BA, Bintara S, Widi TSM, Baliarti E, Jannah ZN. 2024. The difference between Bali cattle and Limousine-Bali (Limbal) crossed cattle concerning their qualitative characteristics in Lombok Tengah District, Indonesia. Nusantara Bioscience 16: 104-110.* Crossbreeding is a potential approach that farmers might employ to improve the productivity of Bali cattle (*Bos javanicus* d'Alton, 1823). Exotic cattle breeds, such as Limousin cattle (*Bos taurus* Linnaeus, 1758), are frequently used for crossbreeding. This study aimed to determine the qualitative characteristic differences between Bali cattle and Limousin-Bali (Limbal) crossed cattle in the Lombok Tengah District of West Nusa Tenggara Province, Indonesia. Data sampling was conducted in 2 sub-districts, namely Pringgarata and Jonggat Sub-districts. The research used 80 adult female cattle, consisting of 40 Bali and 40 Limbal cattle. The average age of cattle was 4.24 years, and the average body weight was 236.66 kg for Bali cattle and 367.88 kg for Limbal cattle. Local farmers kept cattle using the same intensive methods. Phenotypic characterization included color and physical characteristics according to the guidelines provided by the Food and Agriculture Organization (FAO) and the Indonesian Institute of Sciences (LIPI). The Data were presented descriptively, and differences across variables were assessed using the chi-square method. The research indicated no significant difference in tail-tip color ($P > 0.05$). The body and eyelid color showed a significant difference ($P < 0.05$). Furthermore, legs color, buttocks color, dorsal line color, vulva color, muzzle color, horn color, face profile, backline profile, horn orientation, and ear orientation differed significantly ($P < 0.01$). Thus, it can be concluded that crossbreeding caused changes in phenotypic characteristics in the next generation. Therefore, phenotypic characterization in the next generation of these crossbreeds must be conducted, and selection criteria must be established to achieve sustainable breeding goals.

Keywords: Characterization, crossing, native cattle, phenotypic

Abbreviations: Limbal: Limousin-Bali

INTRODUCTION

Indonesia is the second most biodiverse country in the world (Muhtadi et al. 2023). This is also reflected in the diversity of its livestock, as Indonesia has indigenous and local cattle (Widyas et al. 2022). Indonesia's indigenous cattle breed is Bali cattle. Bali cattle originated from the domestication of Banteng (*Bos javanicus* d'Alton, 1823) around 3500 years BC. Natural selection and climatic pressures in the wet tropics have adapted Bali cattle to low feed quality, parasites, and local diseases, giving rise to adaptive phenotypes (Mohamad et al. 2009; Sutarno and Setyawan 2015). These adaptive phenotypes include heat tolerance, resistance to tick-borne diseases, and survival in harsh environments with limited resources. The unique characteristics of Bali cattle make them well-suited for small-scale farming systems in Indonesia, where they are valued for their resilience and ability to thrive in challenging conditions.

Bali cattle have excellent adaptability and demonstrate high reproductive performance, capable of giving birth annually. The carcass percentage is high 54-55%, low-fat meat, and thin skin (Zulkharnaim et al. 2010; Tahuk et al. 2018). The existence of negative selection over a long period has caused Bali cattle a decrease in productivity. This can be observed in terms of body size, namely the shortened withers height, small body size, and decreased body weight, which cannot reach that of its ancestor, the Banteng. In addition to negative selection, existing Bali cattle have uncontrolled mating and even inbreeding (Sutarno and Setyawan 2015; Habaora et al. 2020).

The development of current mating technology provides breeders with the mechanism to increase productivity through artificial insemination. In this process, breeders can choose breeds for mating, whether for purification or crossbreeding. However, crossbreeding is favored among Bali cattle breeders to enhance productivity for its high economic value (Sumantri et al. 2022). Various exotic cattle breeds, such as Simmental and Limousin cattle, have been crossed with Bali cattle, as reported by Baliarti et al. (2023). One region where many Bali cattle have been crossbred with exotic cattle breeds is Lombok

Island, West Nusa Tenggara Province, as documented by Chusna et al. (2022).

These crossbreeds will undoubtedly change the genetic diversity that appears in the form of diverse phenotypic characteristics. Understanding livestock characteristics is necessary for managing genetic resources (Adinata et al. 2023). Phenotypic characterization is the initial stage in conserving cattle genetic resources (Bila et al. 2023); this in cattle breeds is the first concern to ensure unique genetic resources, becoming the basis for the formation of improvement strategies, conservation, selection criteria, and rational utilization (Heryani et al. 2016; King et al. 2022).

Phenotypic characterization of genetic resources generally refers to identifying populations of different breeds and describing them from external characteristics. Information on phenotypic characterization of livestock genetic resources can be used to measure and describe the genetic diversity of livestock to be understood further and utilized sustainably (FAO 2012). Characterization, inventory, and monitoring are critical in sustainable livestock genetic resource management. Information on breed characteristics is also important for effective planning to improve livestock genetic resources at the country level (Mekonnen and Meseret 2020).

Characterization is typically classified according to physical characteristics such as color, size, shape, and genetic history (Bhinchhar et al. 2017). Various studies on phenotypic characterization have been conducted on several cattle breeds in Indonesia, such as Jabres, Ongole Grade, Madura, Pasundan, Kebumen Ongole Grade, and Rambon cattle (Adinata et al. 2023). However, information on the phenotypic characterization of crossbreeds of Bali cattle with exotic cattle in Indonesia still needs to be improved because the crossbreeds have higher economic value than its Bali cattle. Based on these considerations, it is important to research the differences in phenotypic characteristics between Bali cattle and Limousin-Bali crossed cattle kept by smallholder farmers in Indonesia. This study intends to compare the phenotypic characteristics of Bali cattle and Limousin-Bali crossbred cattle in Lombok.

MATERIALS AND METHODS

Ethical clearance

The Research Ethics Commission of the Faculty of Veterinary Medicine at Universitas Gadjah Mada, Yogyakarta, Indonesia, approved the research under Number 00018/EC-FKH/Eks/2021, as it adhered to the ethical standards for animal research.

Research region

The research was conducted in Jonggat and Pringgarata, two sub-districts in the Lombok Tengah District of West Nusa Tenggara, Indonesia. This region is located between 8° 24' to 8° 57' South latitude, and 116° 05' to 116° 24' East longitude in the middle part of Indonesia. The region has a tropical climate with an average yearly temperature of 26.5°C, average humidity of 85.1%, and annual rainfall of 160.7 mm. The two sub-districts are 100-340 meters above sea level (BPS 2023).

Procedures

The sampling technique employed was purposive sampling. The research location was purposefully selected after consulted with the Department of Agriculture on Lombok Tengah District, as the area is known to be a source of Bali cattle and their crosses. The cattle breeds were determined based on the cattle's physical appearance and mating records provided by farmers and inseminators.

The 80 studied cattle consisted of 40 Bali and 40 Limousin-Bali (Limbal) cattle, selected using purposive sampling. The cattle used were adult females with an average age of 4.24 years, determined by interviewing the farmer and observing the incisor growth. The estimated average body weight of cattle based on the Lambourne formula between Bali vs Limbal cattle is 236.66 vs 367.88 kg. The cattle were kept by 63 smallholder farmers utilizing the same intensive-rearing system. The feed was native grass, rice straw, *Pennisetum purpureum*, *P. purpureum* cv. *Mott*, and *Sesbania grandiflora*. Drinking water was provided from wells and storage ponds. The cattle are tethered in enclosures throughout the day.

Assessments were conducted by the first author during daylight hours in the enclosure, with each of the cattle in a standing position to avoid bias refers to Traoré et al. (2015). Qualitative characteristics observed were color (body, legs, buttocks, tail tip, dorsal line, muzzle, horn, eyelid, and vulva) and physical (horn and ear orientation, face and backline profile). The phenotypic characteristics used refer to the FAO (2012) entitled "Phenotypic Characterization of Animal Genetic Resources" and the Indonesian Institute of Sciences (LIPI) (2015) Physical Appearance Filling Instructions.

Data analysis

The data were presented descriptively, and differences across variables were assessed using the chi-square test. This statistical analysis identified significant differences between the breeds, providing insights into their distinct qualitative characteristics. Additionally, the chi-square test helped determine whether these variations were statistically significant or simply due to chance. Software of Statistical Package for the Social Sciences (SPSS) version 25 (IBM USA) was employed to analyze the variations in qualitative characteristics.

RESULTS AND DISCUSSION

Color characteristics

The number and percentage of nine variables of body part color characteristics in Bali and Limbal cattle are presented in Table 1. It was found that muzzle color, horn color, legs color, buttocks color, dorsal line color, and vulva color were significantly different with significance ($P < 0.01$). Additionally, there were significant differences in body and eyelid color ($P < 0.05$). In contrast, no significant difference was observed in the color of the tail tip between

the two groups (P >0.05). Based on phenotypic appearance, the body colors of Bali vs. Limbal cattle are dark red (52.50% vs. 42.50%), dark brown (5.00% vs. 17.50%), light brown (35.00% vs. 15.00%), and fawn (7.50% vs. 25.00%), respectively. The difference between Bali cattle and Limbal cattle is also in the muzzle color. The muzzle color in Bali cattle is black (pigmented) (100.00%), while Limbal cattle have black (pigmented) (82.50%) and light brown (unpigmented) (17.50%) (Table 1).

Eyelid color in Bali cattle is 100.00% pigmented, while in Limbal cattle, 15.00% do not have pigment. Horn color in Limbal cattle is more diverse than in Bali cattle, with three horn colors identified: black (62.50%), brown (2.50%), and brown-black (35.00%). Meanwhile, Bali cattle have 100.00% black horn color. The white color on the legs differs between Bali cattle and Bali cattle crosses, in this case, Limbal cattle. All Bali cattle studied have white on their legs with clearly distinct boundaries. However, 15.00% of Limbal cattle have legs with indistinct boundaries white, and 85.00% of Limbal cattle have legs that match their body color.

The white color on the buttocks of Limbal cattle is also different from that of Bali cattle, with 60.00% having white buttocks with indistinct boundaries and 40.00% having buttocks that are not white or mirror-shaped. Meanwhile, Bali cattle exhibit white buttocks with firm boundaries (62.50%) and white color without firm boundaries (37.50%). The tip tail color of Bali cattle, compared to Limbal cattle, was not significantly different, with the dominant color being black (60.00% vs. 57.50%), followed by brown (40.00% vs. 42.50%). The black color of the dorsal line between the two breeds differed; it was identified that 57.50% of Limbal cattle had a thin black dorsal line, and 35.00% had no dorsal line. Meanwhile, 100.00% of Bali cattle exhibited a thick black dorsal line color. Regarding vulva color, there was also a difference between Limbal and Bali cattle. Bali cattle have 100% black vulva color, while Limbal cattle have 77.50% black, 15.00% brown, and 7.50% a combination of black and brown vulva colors.

Table 1. Color characteristics between Bali cattle and Limbal crossed cattle

Variable	Bali (40)		Limbal (40)		X^2-Value	P-Value
	N	%	N	%		
Body color (%)					10.168	0.017
Dark Red	21	52.50	17	42.50		
Dark brown	2	5.00	7	17.50		
Light brown	14	35.00	6	15.00		
Fawn	3	7.50	10	25.00		
Muzzle color					7.671	0.006
Pigmented	40	100.00	33	82.50		
Not pigmented	-	-	7	17.50		
Eyelid color					6.486	0.011
Pigmented	40	100.00	34	85.00		
Not pigmented	-	-	6	15.00		
Horn color					18.462	0.000
Black	40	100.00	25	62.50		
Brown	-	-	1	2.50		
Brown-Black	-	-	14	35.00		
Legs color (%)					80.000	0.000
White with distinct boundaries	40	100.00	-	-		
White with indistinct boundaries	-	-	6	15.00		
Same as body color	-	-	34	85.00		
Buttock color (%)					43.077	0.000
White with distinct boundaries	25	62.50	-	-		
White with indistinct boundaries	15	37.50	24	60.00		
Same as body color	-	-	16	40.00		
Tail tip color (%)					0.052	0.820
Black	24	60.00	23	57.50		
Brown	16	40.00	17	42.50		
Dorsal line (%)					80.000	0.000
Thick Black	40	100.00	-	-		
Medium Black	-	-	3	7.50		
Thin Black	-	-	23	57.50		
Absence	-	-	14	35.00		
Vulva color					10.141	0.006
Black	40	100.00	31	77.50		
Brown	-	-	6	15.00		
Combination	-	-	3	7.50		

Note: N: Number of observations; %: Percentage of observations; X^2-Value: Chi-square value

Table 2. Physical characteristics between Bali cattle and Limbal crossed cattle

Variable	Bali (40)		Limbal (40)		X^2-Value	P-Value
	N	%	N	%		
Facial (head) profile					30.345	0.000
Straight	40	100.00	18	45.00		
Concave	-	-	22	55.00		
Backline Profile (%)					8.455	0.004
Straight	13	32.50	26	65.00		
Slopes down from withers	27	67.50	14	35.00		
Ear orientation					42.288	0.000
Erect	36	90.00	7	17.50		
Lateral	4	10.00	33	82.50		
Horn orientation					68.518	0.000
Upward	1	2.50	33	82.50		
Laterally	-	-	5	12.50		
Backward	38	95.00	2	5.00		
Downward	1	2.50	-	-		

Note: N: Number of observations; %: Percentage of observations; X^2-Value: Chi-square value

Physical characteristics

The physical characteristics of the female Bali and Limbal cattle are presented in Table 2. Bali and Limbal cattle face profiles, backline profiles, ear orientation, and horn orientation are significantly different ($p < 0.01$). The face profile of Bali cattle is 100.00% straight, while in Limbal cattle, the dominant face profile is concave (55.00%), followed by a straight face profile (45.00%). Concerning the backline profile, Bali cattle exhibit dominant slopes down from withers (67.50%), whereas, in Limbal cattle, the dominant backline profile is straight (65.00%). The ear orientation in Bali cattle is dominantly erect (90.00%), while in Limbal cattle, the ear orientation is dominantly lateral (82.50%). Furthermore, Bali cattle have dominant horns pointing backward (95.00%), while in Limbal cattle, the dominant horns point upwards (82.50%).

Discussion

The reddish-brown body color is the predominant color observed in local Indonesian cattle breeds especially Madura cattle (Kurniati et al. 2022), Aceh cattle (Widyaningrum et al. 2021), Katingan cattle (Utomo and Widjaja 2021), Pesisir cattle (Putra et al. 2018), and Pasundan cattle (Said et al. 2017). The increased yellowish-brown color in Limousin-Bali crossbred cattle is a characteristic inherited from Limousin, considering that Limousin belongs to the yellow-brown (chestnut) group of cattle, generally exhibiting yellow, red, and brown colors (Alderson 1992). Body color indicates genetic purity and is valuable for branding a cattle breed (Kimura et al. 2022; Kunene et al. 2022). Additionally, body color is a factor that influences an animal's ability to withstand heat stress and resist fly and tick attacks (Islam et al. 2022). Cattle with brighter colors demonstrate higher adaptability to heat stress than those with black fur, making them more suitable for extensive systems in hot climates (Anzures-Olvera et al. 2019; Isola et al. 2020). In addition to adaptability, cattle with lighter coat colors exhibit better weight gain than dark-colored cattle, as observed in Tharparkar cattle (*Bos indicus* Linnaeus, 1758) in India (Rashid et al. 2019).

Ongole Grade and Madura cattle are local Indonesian breeds with a black muzzle color, similar to Bali cattle (Hartatik et al. 2018; Kurniati et al. 2022). This characteristic is also evident in the crossbreeding of Limousin cattle with Madura cattle, resulting in a black and red muzzle color (Hartatik 2014), consistent with the muzzle color observed in Limbal cattle in this study. The melanocyte process influences the diversity in muzzle color, which melanocortin receptors regulate. This process involves the distribution of pheomelanin and eumelanin as color determinants in the fur and snout (Kim et al. 2014). Apart from serving as a means of livestock identification, muzzle color is now utilized in biometrics for identification purposes, analogous to fingerprints in humans (Li et al. 2022; Lee et al. 2023).

The black eyelid pigment in Bali cattle is also found in local Indonesian Pasundan cattle (Said et al. 2017). Then, the unpigmented eyelid color in Limousin-Bali cattle is also found in several cattle breeds in taurine in West Africa, namely N'Dama, Lagunaire, Lobi, and Somba (Grema et al. 2017). Similarly, Rarámuri Criollo cattle developed in the United States have unpigmented eyelids that account for 19% of the total population (McIntosh et al. 2020). The production of melanin pigment from melanocytes in the skin influences the pigmentation of the eyelids. Non-genetic factors such as environmental and physiological conditions cause differences in skin pigmentation in each cow (Jara et al. 2022). Low pigmentation of the eyelids can cause several eye diseases, such as squamous cell carcinoma and keratoconjunctivitis, which can affect cattle production (Jara et al. 2020).

The horn is a bony core surrounded by a sheath of cornified epithelium. It is present in livestock belonging to the Bovidae family, including buffalo (*Bubalus bubalis*), cattle (*Bos taurus* Linnaeus, 1758, *B. indicus*, and *B. javanicus*), goats (*Capra hircus* Linnaeus, 1758), and sheep (*Ovis aries* Linnaeus, 1758) (Knierim et al. 2015). The shape and length of horns are specific to each species and breed, exhibiting high variation between individuals (Grobler et al. 2021). Horn variation is evident in Bali and

Limbal cattle in Indonesia. The black color of horns in Bali cattle is also observed in Aceh cattle (Hartatik 2014), Madura cattle, and Jabres cattle (Adinata et al. 2023). The diversity of horn color in Limbal cattle is also found in Hungarian Grey cattle, albeit with different variants of horn color. In Hungarian Grey cattle, horns come in white, green, and cardy (a mixture of green and white) (Zsolnai et al. 2021). Regarding the orientation of horns, the dominant upward orientation observed in Limousin cattle crosses with Bali cattle is also found in Limousin cattle crosses with Madura cattle (Limura) (Hartatik 2014). While horns are not a trait directly impacting productivity, they hold significance as a physical trait employed as a selection criterion in Ankole cattle in Uganda (Kugonza et al. 2012) and Taccek (display) cattle on Madura Island, Indonesia (Herviyanto et al. 2020).

The white coloration on the legs and buttocks in Bali cattle is also observed in Madura and Pasundan cattle, where the white color exhibits indistinct boundaries (Maylinda et al. 2017; Said et al. 2017). Similarly, the black dorsal stripe identified in Bali cattle is found in the local Indonesian breed of Galekan cattle (Kuswati et al. 2022). Despite sharing some characteristics, a genetic distance exists between local Indonesian cattle breeds. There is a higher genetic similarity between local breeds such as Madura, Galekan, and Bali cattle. Still, Aceh, Ongole Grade, and Pesisir cattle have a genetic similarity closer to Indian zebu cattle (Mohamad et al. 2009). Cattle breeding in Indonesia has developed unique and adaptable genetic resources by merging the zebu ability to endure tropical and arid climates with the native Banteng adaptation to local environments and farms (Mohamad et al. 2012).

The characteristics observed in Limousin-Bali crossbred cattle are also evident in Simmental crossbred cattle with Bali cattle. These characteristics include legs sharing the same color as the body, buttocks color following the body color, and a white border on the buttocks with indistinct boundaries. However, Simmental crosses with Bali cattle still exhibit a thick black dorsal line (Chusna et al. 2022). In contrast, the crossbreeding of Limousin cattle with Madura cattle results in similar body, rump/buttock, and leg color as observed in the cross of Limousin cattle with Bali cattle. Notably, a distinction is found in the dorsal line, where Limousin crossbred Madura cattle lack a dorsal line (Hartatik 2014), while in Limousin crossbred Bali cattle, a thin to medium black dorsal line is still present.

The facial morphology characterized by a straight face, as seen in Bali cattle, corresponds to the results reported by Gelaye et al. (2022) in indigenous cattle from Southwestern Ethiopia and Getaneh et al. (2019) in Malle cattle. In contrast, Limbal cattle's predominantly concave facial profile reflects the facial shape inherited from their Limousin ancestors (Alderson 1992). Additionally, the predominantly straight-back profile of Limbal cattle is a physical characteristic shared with several taurine cattle breeds in Africa, such as Kuri, N'Dama, Lagunaire, Lobi, and Somba (Grema et al. 2017; Edouard et al. 2018).

The dominant upward ear orientation in Bali cattle is in line with the research of Karnuah et al. (2018) found in beef cattle in Liberia, West Africa, namely N'Dama and Muturu. The lateral ear orientation in Limbal cattle is similar to the results of research by Gelaye et al. (2022) on local cattle in Southwestern Ethiopia. The laterally oriented ear is composed of well-developed muscles that allow the ear to be moved even to listen to faint sounds from distant locations (Woldeyohannes et al. 2019).

These phenotypic characteristics facilitate the easy identification of cattle breeds due to the unique attributes inherent in each breed. Phenotypic variations within local livestock genetic resources signify the presence of genetic diversity that merits conservation efforts. A comprehensive understanding of phenotypic characteristics in local livestock is crucial for formulating conservation policies to preserve these valuable resources (Yakubu et al. 2022). In addition to phenotypic changes, crossbred cattle are anticipated to manifest heterosis effects in the subsequent generation, enhancing productivity and influencing the economic value generated (Chusna et al. 2022).

Crossbreeding is a process that aims to create new cattle breeds to meet the market's demands. However, crossbreeding should not be done carelessly, as it may endanger the purity of local livestock (Sutarno and Setyawan 2015). Studies have shown that the crossbreeding program in Indonesia has failed because it is solely based on body weight selection, while other productive and adaptive traits are overlooked (Widyas et al. 2022). Therefore, it is crucial to formulate a crossbreeding and purification plan that will lead to genetic improvement.

Strategies that can be applied to achieve sustainable livestock breeding are at the policy, environmental, and farms level. The policy and ecological level includes the implications of government policies in agriculture, infrastructure, farmer involvement, setting breeding goals and production systems that take place based on the region and market targets. At the farm level includes breeding by purification or crossbreeding, livestock recording and data processing, reproduction methods, genetic analysis and estimation of breeding values, and selection and monitoring of genetic progress (Philipsson et al. 2006; Leroy et al. 2016). The strategy applied for crossbreeding Limousin cattle with Bali cattle certainly refers to the principles described above. The goal is for crossbreeding to continue at the breeder level with regular monitoring and evaluation by the local government and research institutions and to ensure that Indonesia's indigenous genetic resources are preserved.

The phenotypic characterization of Bali and Limousin-Bali cattle revealed significant differences between the two breeds in terms of body color, eyelid color, legs color, buttocks color, dorsal line color, vulva color, muzzle color, horn color, face profile, backline profile, horn orientation, and ear orientation. These findings conclude that crossbreeding induces changes in phenotypic characteristics in the subsequent generation. Consequently, it is imperative to conduct phenotypic characterization in the next generation of this crossbred and establish selection criteria to attain sustainable breeding goals. The results of

this study are expected to be a basic reference in genetic improvement, conservation efforts, the development of new breeds, and in setting selection criteria for crossbred cattle in the future. Further research related to phenotypic adaptation and genotype testing needs to be conducted to obtain more comprehensive information on the development of crossbred cattle in the future.

ACKNOWLEDGEMENTS

The researchers wish to acknowledge the Ministry of Education, Culture, Research, and Technology of the Republic of Indonesia for their financial support for this study through the PMDSU (*Pendidikan Magister menuju Doktor untuk Sarjana Unggul*) research program. The contract with 2209/UN1/DITLIT/Dit-Lit/PT.01.03/20 is linked to the grant number 0217/E5/PG.02.00/2023. The authors express their gratitude to the farmers who participated in the research, as well as the Faculty of Animal Science at Universitas Gadjah Mada, Indonesia and the Agriculture Office of Lombok Tengah District, Indonesia for their valuable help in this study.

REFERENCES

Adinata Y, Noor RR, Priyanto R, Cyrilla L, Sudrajad P. 2023. Morphometric and physical characteristics of Indonesian beef cattle. Arch Anim Breed 66: 153-161. DOI: 10.5194/aab-66-153-2023.

Alderson L. 1992. The categorisation of types and breeds of cattle in Europe. Arch Zootec 41: 325-334.

Anzures-Olvera F, Véliz FG, de Santiago A, García JE, Mellado J, Macías-Cruz U, Avendaño-Reyes L, Mellado M. 2019. The impact of hair coat color on physiological variables, reproductive performance and milk yield of Holstein cows in a hot environment. J Therm Biol 81: 82-88. DOI: 10.1016/j.jtherbio.2019.02.020.

Badan Pusat Statistik (BPS). 2023. Lombok Tengah Regency in Figures. Badan Pusat Statistik, Praya. [Indonesian]

Baliarti E, Rozzaq MA, Warman AT, Bintara S, Widi TSM, Widayati DT, Atmoko BA, Nugroho T. 2023. Body morphometric characterization in conjunction with reproductive performance of Bali and Bali cross cattle in Indonesia. Adv Anim Vet Sci 11: 977-986. DOI: 10.17582/journal.aavs/2023/11.6.977.986.

Bhinchhar BK, Paswan VK, Yadav SP, Saroj, Singh P. 2017. Physical and morphometric characteristics of Gangatiri cattle. Indian J Anim Res 51: 1101-1104. DOI: 10.18805/ijar.11329.

Bila L, Malatji DP, Tyasi TL. 2023. Morphological characterization of Sussex cattle at Huntersvlei farm, Free State Province, South Africa. Plos ONE 18: e0292088. DOI: 10.1371/journal.pone.0292088.

Chusna RQ, Ramadhan YF, Fadhilah GT, Warman AT, Maharani D, Atmoko BA, Baliarti E. 2022. The difference in qualitative characteristics between Simmental-Bali (SIMBAL) crossed cows and Bali cows in West Nusa Tenggara, Indonesia. IOP Conf Ser: Earth Environ Sci 1114: 012059. DOI: 10.1088/1755-1315/1114/1/012059.

Edouard NK, Lacine BK, Cyrille KN, Etienne LN, Guiguigbaza-Kossigan D, Mamadou S, Valentine YGC. 2018. Multivariate analysis for morphological characteristics of N'Dama cattle breed in two agro-ecological zones of Côte d'Ivoire. Eur Sci J 14: 602-621. DOI: 10.19044/esj.2018.v14n3p602.

FAO. 2012. Phenotypic Characterization of Animal Genetic Resources. FAO Animal Production and Health Guidelines, Roma.

Gelaye G, Baye M, Masho W, Begna R, Admasu Z. 2022. Morphometric traits and structural indices of indigenous cattle reared in Bench Sheko zone, southwestern Ethiopia. Heliyon 8: e10188. DOI: 10.1016/j.heliyon.2022.e10188.

Getaneh D, Banerjee S, Taye M. 2019. Morphometrical traits and structural indices of Malle Cattle reared in the South Omo Zone of Southwest Ethiopia. Intl J Vet Sci Res 5: 32-47. DOI: 10.18488/journal.110.2019.52.32.47.

Grema M, Traoré A, Issa A, Hamani M, Abdou M, Fernández I, Soudré A, Álvarez I, Sanou M, Tamboura HH, Alhassane Y, Goyache F. 2017. Morphological assessment of Niger Kuri cattle using multivariate methods. S A J Anim Sci 47: 505-515. DOI: 10.4314/sajas.v47i4.9.

Grobler R, van Marle-Koster E, Visser C. 2021. Challenges in selection and breeding of polled and scur phenotypes in beef cattle. Livest Sci 247: 104479. DOI: 10.1016/j.livsci.2021.104479.

Habaora F, Fuah AM, Abdullah L, Priyanto R, Yani A, Purwanto BP. 2020. Importance-performance analysis toward productivity of Bali cattle based on agroecosystem in Timor Island. J Anim Vet Adv 19: 57-66. DOI: 10.36478/javaa.2020.57.66.

Hartatik T, Maharani D, Sidadolog JHP, Fathoni A, Sumadi. 2018. Haplotype diversity of partial cytochrome b gene in Kebumen Ongole Grade Cattle. Trop Anim Sci J 41: 8-14. DOI: 10.5398/tasj.2018.41.1.8.

Hartatik T. 2014. Analisis Genetik Ternak Lokal. Universitas Gadjah Mada Press, Yogyakarta. [Indonesian]

Herviyanto D, Kuswati, Ciptadi G. 2020. Identification characteristic Madura cattle female taccek type. J Trop Anim Prod 21: 83-92. DOI: 10.21776/ub.jtapro.2020.021.02.1. [Indonesian]

Heryani LGSS, Wandia IN, Suarna IW, Puja IK. 2016. Morphometric characteristics of the Taro White cattle in Bali. Glob Vet 16: 215-218. DOI: 10.5829/idosi.gv.2016.16.03.102116.

Islam MS, Yimer N, Haron AW, Abdullah FFJ, Han MHW, Mamat-Hamidi K, Zawawi HBM. 2022. First study on phenotypic and morphological characteristics of Malaysian Kedah-Kelantan cattle (*Bos indicus*) and method of estimating their body weight. Vet World 15: 728-736. DOI: 10.14202/vetworld.2022.728-736.

Isola JVV, Menegazzi G, Busanello M, dos Santos SB, Agner HSS, Sarubbi J. 2020. Differences in body temperature between black-and-white and red-and-white Holstein cows reared on a hot climate using infrared thermography. J Therm Biol 94: 102775. DOI: 10.1016/j.jtherbio.2020.102775.

Jara E, Peñagaricano F, Armstrong E, Ciappesoni G, Iriarte A, Navajas EA. 2022. Revealing the genetic basis of eyelid pigmentation in Hereford cattle. J Anim Sci 100: skac110. DOI: 10.1093/jas/skac110.

Jara E, Peñagaricano F, Menezes C, Tardiz L, Rodons G, Iriarte A, Armstrong E. 2020. Transcriptomic analysis of eyelid pigmentation in Hereford cattle. Anim Genet 51: 935-939. DOI: 10.1111/age.13004.

Karnuah AB, Dunga G, Wennah A, Wiles WT, Greaves E, Varkpeh R, Osei-Amponsah R, Boettcher P. 2018. Phenotypic characterization of beef cattle breeds and production practices in Liberia. Trop Anim Health Prod 50: 1287-1294. DOI: 10.1007/s11250-018-1557-z.

Kim SH, Hwang SY, Yoon JT. 2014. Microarray-based analysis of the differential expression of melanin synthesis genes in dark and light-muzzle Korean cattle. PLoS ONE 9: e96453. DOI: 10.1371/journal.pone.0096453.

Kimura S, Hatakeyama T, Koutaka T, Kubo K, Morita S, Eguchi K, Saitoh K, Yamauchi K, Imai S, Kashimura A, Inenaga T, Matsumoto H. 2022. PMEL p.Leu18del dilutes coat color of Kumamoto sub-breed of Japanese Brown cattle. BMC Genom 23: 694. DOI: 10.1186/s12864-022-08916-8.

King FJM, Banga C, Visser C. 2022. Morphological characterisation of three indigenous Mozambican cattle populations. J Agr Rural Dev Trop Subtrop 123: 225-234. DOI: 10.17170/kobra-202212057192.

Knierim U, Irrgang N, Roth BA. 2015. To be or not to be horned—Consequences in cattle. Livest Sci 179: 29-37. DOI: 10.1016/j.livsci.2015.05.014.

Kugonza DR, Nabasirye M, Hanotte O, Mpairwe D, Okeyo AM. 2012. Pastoralists' indigenous selection criteria and other breeding practices of the long-horned Ankole cattle in Uganda. Trop Anim Health Prod 44: 557-565. DOI: 10.1007/s11250-011-9935-9.

Kunene LM, Muchadeyi FC, Hadebe K, Mészáros G, Sölkner J, Dugmore T, Dzomba EF. 2022. Genetics of base coat colour variations and coat colour-patterns of the South African Nguni cattle investigated using high-density SNP genotypes. Front Genet 13: 832702. DOI: 10.3389/fgene.2022.832702.

Kurniati AD, Nugiartiningsih VMA, Kuswati, Suyadi S. 2022. Study of the physical and physiological response of the Madura as a breeding source (case study in Waru Sub-District, Pamekasan District). KnE Life Sci 2022: 292-299. DOI: 10.18502/kls.v0i0.11811.

Kuswati K, Ali MI, Wahyuni RD. 2022. Morphometric characteristics of Galekan cattle breed base on Principle Component Analysis (PCA). J

Ilmu-Ilmu Peternakan (Indonesian Journal of Animal Science) 32: 1-12. DOI: 10.21776/ub.jiip.2022.032.01.01.

Lee T, Na Y, Kim BG, Lee S, Choi Y. 2023. Identification of individual Hanwoo cattle by muzzle pattern images through deep learning. Animals 13: 2856. DOI: 10.3390/ani13182856.

Lembaga Ilmu Pengetahuan Indonesia (LIPI). 2015. Panduan Pengisian Form Penampilan Fisik. LIPI, Bogor. [Indonesian]

Leroy G, Baumung R, Boettcher P, Scherf B, Hoffman I. 2016. Review: Sustainability of crossbreeding in developing countries; definitely not like crossing a meadow. Animal 10: 262-273. DOI: 10.1017/S175173111500213X.

Li G, Erickson GE, Xiong Y. 2022. Individual beef cattle identification using muzzle images and deep learning techniques. Animals 12 (11): 1453. DOI: 10.3390/ani12111453.

Maylinda S, Nugroho H, Busono W. 2017. Phenotypic characteristics of local cattle in Madura Island. AIP Conf Proc 1844: 060002 DOI: 10.1063/1.4983442.

McIntosh MM, Gonzalez AL, Cibils AF, Estell RE, Nyamuryekung'e S, Almeida FAR, Spiegal SA. 2020. A phenotypic characterization of Rarámuri Criollo Cattle introduced into the Southwestern United States. Arch Latinoam Prod Anim 28: 111-119. DOI: 10.53588/alpa283406.

Mekonnen T, Meseret S. 2020. Characterization of Begait cattle using morphometric and qualitative traits in Western Zone of Tigray, Ethiopia. Intl J Livest Prod 11: 21-33. DOI: 10.5897/IJLP2019.0637.

Mohamad K, Olsson M, Andersson, Purwantara B, van Tol HTA, Rodriquez-Martinez H, Colenbrander B, Lenstra JA. 2012. The origin of Indonesian cattle and conservation genetics of the Bali cattle breed. Reprod Domest Anim 47: 18-20. DOI: 10.1111/j.1439-0531.2011.01960.x.

Mohamad K, Olsson M, van Tol HTA, Mikko S, Vlamings BH, Andersson G, Rodrı´guez-Martı´nez H, Purwantara B, Paling RW, Colenbrander B, Lenstra JA. 2009. On the origin of Indonesian cattle. PloS ONE 4: e5490. DOI: 10.1371/journal.pone.0005490.

Muhtadi A, Yulianda F, Boer M, Krisanti M, Desrita. 2023. Ichthyofauna diversity and its distribution in a Low-Saline Lake of Indonesia. Hayati J Biosci 30: 421-431. DOI: 10.4308/hjb.30.3.421-431.

Philipsson J, Rege JEO, Okeyo AM. 2006. Sustainable breeding programmes for tropical farming systems. Anim Genet Train Resour 2: 1-25.

Putra DE, Paul RC, Thu LNA, Okuda Y, Yurnalis, Ibi T, Kunieda T. 2018. Genetic characterization of Indonesian Pesisir cattle using mitochondrial DNA and Y-chromosomal haplotypes and loci associated with economical traits and coat color. J Anim Genet 46: 17-23. DOI: 10.5924/abgri.46.17.

Rashid SA, Tomar AKS, Verma MR, Mehrotra S, Bharti PK. 2019. Effect of skin and coat characteristics on growth and milk production traits in Tharparkar cattle. Indian J Anim Sci 89: 1251-1254. DOI: 10.56093/ijans.v89i11.95882.

Said S, Putra WPB, Anwar S, Agung PP, Yuhani H. 2017. Phenotypic, morphometric characterization and population structure of Pasundan cattle at West Java, Indonesia. Biodiversitas 18: 1638-1645. DOI: 10.13057/biodiv/d180443.

Sumantri I, Chang HSC, Widi TSM, Hadi NH, Rohaeni ES. 2022. Gross margin comparison of Bali and crossbred cattle in small holder beef cattle farming in South Kalimantan, Indonesia. Proceedings of the 9th International Seminar on Tropical Animal Production. Universitas Gadjah Mada, Yogyakarta, 21-22 September 2021. DOI: 10.2991/absr.k.220207.071.

Sutarno, Setyawan AD. 2015. Review: Genetic diversity of local and exotic cattle and their crossbreeding impact on the quality of Indonesian cattle. Biodiversitas 16: 327-354. DOI: 10.13057/biodiv/d160230.

Tahuk PK, Budhi SPS, Panjono, Baliarti E. 2018. Carcass and meat characteristics of male Bali cattle in Indonesian smallholder farms fed ration with different protein levels. Trop Anim Sci J 41: 215-223. DOI: 10.5398/tasj.2018.41.3.215.

Traoré A, Koudandé DO, Fernández I, Soudré A, Granda V, Álvarez I, Diarra S, Diarra F, Kaboré A, Sanou M, Tamboura HH, Goyache F. 2015. Geographical assessment of body measurements and qualitative traits in West African cattle. Trop Anim Health Prod 47: 1505-1513. DOI: 10.1007/s11250-015-0891-7.

Utomo BN, Widjaja E. 2021. Genetic resources of Katingan cattle and effort to conserve at the time in Katingan District, Central Kalimantan. Proceedings of the 3rd KOBI Congress, International and National Conferences (KOBICINC 2020). Universitas Bengkulu, Bengkulu, 24-25 November 2020. DOI: 10.2991/absr.k.210621.018.

Widyaningrum R, Budisatria IGS, Fathoni A, Maharani D. 2021. Profile and population dynamics of Aceh cattle in livestock breeding and forage centre, Indrapuri. IOP Conf Ser: Earth Environ Sci 667: 012033. DOI: 10.1088/1755-1315/667/1/012033.

Widyas N, Widi TSM, Prastowo S, Sumantri I, Hayes BJ, Burrow HM. 2022. Promoting sustainable utilization and genetic improvement of Indonesian local beef cattle breeds: A review. Agriculture 12 (10): 1566. DOI: 10.3390/agriculture12101566.

Woldeyohannes T, Hankamo A, Banerjee S. 2019. Morphological characterization and structural indices of indigenous cattle in Hadiya Zone, Southern Ethiopia. Glob J Anim Sci Res 7: 23-38.

Yakubu A, Jegede P, Wheto M, Shoyombo AJ, Adebambo AO, Popoola MA, Osaiyuwu OH, Olafadehan OA, Alabi OO, Ukim CI, Vincent ST, Mundi HL, Olayanju A, Adebambo OA. 2022. Multivariate characterisation of morphobiometric traits of indigenous helmeted Guinea fowl (*Numida meleagris*) in Nigeria. PLoS ONE 17: e0261048. DOI: 10.1371/journal. pone.0261048.

Zsolnai A, Kovács A, Kaltenecker E, Anton I. 2021. Identification of markers associated with estimated breeding value and horn colour in Hungarian Grey cattle. Anim Biosci 34: 482-488. DOI: 10.5713/ajas.19.0881.

Zulkharnaim, Jakaria, Noor RR. 2010. Identification of Genetic Diversity of Growth Hormone Receptor (GHR|AluI) Gene in Bali. Media Peternakan 33: 81-87. DOI: 10.5398/medpet.2010.33.2.81.

NUSANTARA BIOSCIENCE
Vol. 16, No. 1, pp. 111-118
May 2024

ISSN: 2087-3948
E-ISSN: 2087-3956
DOI: 10.13057/nusbiosci/n160114

Molecular identification of *Scopellaria marginata* from East Java, Indonesia, based on *trn*L-UAA and *trn*L-*trn*F intergenic spacer regions

TURHADI♥, BRILIYAN NATALINA SUDARJAYANTI, FIFI MAR'ATUN SOLIHAH, RODIYATI AZRIANINGSIH, MUFIDAH AFIYANTI, ESTRI LARAS ARUMINGTYAS

Department of Biology, Faculty of Mathematics and Natural Sciences, Universitas Brawijaya. Jl. Veteran, Malang 65415, East Java, Indonesia.
Tel.: +62-341-575841, ♥email: turhadibiologi@ub.ac.id

Manuscript received: 3 January 2024. Revision accepted: 18 March 2024.

Abstract. *Turhadi, Sudarjayanti BN, Solihah FM, Azrianingsih R, Afiyanti M, Arumingtyas EL. 2024. Molecular identification of* Scopellaria marginata *from East Java, Indonesia, based on* trn*L-UAA and* trn*L*-trn*F intergenic spacer regions. Nusantara Bioscience 16: 111-118. Scopellaria marginata* (Blume) W.J.de Wilde & Duyfjes is a wild species in Cucurbitaceae, which was recorded as new expanding their distribution in East Java, Indonesia. The *trn*L-UAA and *trn*L-*trn*F intergenic spacer (IGS) sequences of *Scopellaria* are still limited in publicly accessible databases. This study aimed to evaluate the *trn*L-UAA and *trn*L-*trn*F IGS sequences of *S. marginata* from Malang, East Java. Total DNA of *S. marginata* was used to amplify the *trn*L-UAA and *trn*L-*trn*F IGS region. Then, the PCR products are sequenced using bi-directional Sanger dideoxy sequencing to obtain the DNA sequence of those two regions. The results showed that the partial sequences of *S. marginata* for *trn*L-UAA ranged from 528 to 571 bp, while the sequence for *trn*F-*trn*L IGS ranged from 434 to 445 bp. The *S. marginata* samples are similar to *S. marginata* in the database with similarity levels of 97.14-97.50% and 98.36-98.61%, respectively, based on the *trn*L-UAA and *trn*L-*trn*F IGS. Both *trn*L-UAA and *trn*L-*trn*F IGS showed a Correct Assignment Rate (CAR) of 100% for *S. marginata*. Two-dimensional DNA barcoding with lengths 505 and 417 bp for *trn*L-UAA and *trn*L-*trn*F IGS proposed as specific barcodes for *S. marginata*. These results prove that Malang, East Java was an additional distribution area for *S. marginata* in Indonesia.

Keywords: Cucurbitaceae, DNA barcoding, *Scopellaria marginata*, *trn*L-*trn*F intergenic spacer, *trn*L-UAA intron

INTRODUCTION

Cucurbitaceae is a plant family with 101 genera and about 1000 species with a wide distribution, especially in tropical regions (Simpson 2019; POWO 2024) and a group with diverse economic use. As a member of Cucurbitaceae, *Scopellaria* consists of two species, namely *S. diversiflora* and *S. marginata*. The *S. diversiflora* and *S marginata* are grow wild and not popular in the community. Only *S. marginata* is found in Indonesia because of its wide distribution, while *S. diversifolia* is only found in the central and eastern parts of Borneo (Sabah). According to de Wilde and Duyfjes (2010), *Timun tikus* (*S. marginata*) is divided into two varieties, including *S. marginata* var. *marginata* and var. *penangense* which is differentiated based on the characteristics of their leaf blade, leaf base, and seed size. A previous study showed the presence of *S. marginata* in Malang, East Java, Indonesia, based on the morphological characterization (Arumingtyas et al. 2023).

As a expanding their distribution, *S. marginata* must be characterized molecularly to strengthen evidence that it matches the DNA barcodes in the database. The availability of DNA sequences helps the morphological characterization approach to identify a species. Providing a DNA barcode for *S. marginata* is very important because the morphological characters, especially during the early vegetative stage are similar between several species of the Cucurbitaceae members, such as cucumber, melon, etc. Several characters are very variable and do not correlate with phylogenetic relationships between species of Cucurbitaceae based on chloroplast-based DNA barcode sequences, including petals, fruit characters, and karyotypes (Kocyan et al. 2007). Moreover, morphological characters are also greatly influenced by environmental factors (Kwon et al. 2017; Nadeem et al. 2018), so it takes longer for identification to be carried out until the generative phase is achieved. Therefore, to resolve this problem, a molecular approach such as DNA barcoding can speed up species identification, such as Cucurbitaceae.

DNA barcoding is a molecular biology technique using short standardized sequences that help identify plant species and support conservation and further utilization strategies (Kress 2017). DNA barcodes can be quickly, accurately, and effectively used in species identification, when morphological characteristics difficult to determine the sample (Taberlet et al. 2007; Trivedi et al. 2020). Several types of gene loci are commonly used as plant DNA barcodes, for example, *trn*L-UAA and *trn*L-*trn*F intergenic spacer (IGS). The *trn*L is the chloroplasts genome with a very conservative secondary structure and widely used as a marker for plant phylogenetic analyses (Yulita 2013; Kishor and Sharma 2018). Furthermore, the number of *trn*L-UAA sequences available in databases is already very high, by far the most numerous among non-coding chloroplast DNA sequences (Taberlet et al. 2007). The *trn*L-UAA and *trn*L-*trn*F IGS have been effectively used to identify Cucurbitaceae (Kocyan et al. 2007; Schaefer and Nee 2012), *Taxus* (Taxaceae) (Coughlan et al.

2020), *Prunus* (Rosaceae) (Sevindik et al. 2020), and *Eurycoma longifolia* (Simaroubaceae) (Yulita et al. 2022). Furthermore, the availability of DNA sequences in publicly accessible databases is also crucial in species identification using DNA barcoding (Roslim 2018).

DNA barcode, especially for *Scopellaria* are still very limited in publicly accessible databases. This study aimed to evaluate the *trn*L-UAA and *trn*L-*trn*F IGS sequences from *S. marginata* from Malang, East Java, Indonesia. The availability of those DNA barcodes for *S. marginata* is useful as basic information in conservation strategies. This study is also useful as additional information on new expanding distribution of *S. marginata* in Indonesia, especially in East Java. Based on our findings, it opens up opportunities for further studies, especially exploring the potential of *S. marginata* which has not yet been widely reported.

MATERIALS AND METHODS

Sample collection

All plant material used in this research was wild *S. marginata* collected from Malang, East Java, Indonesia (7°57'7.01420" S; 112°36'41.29880" E) (Figure 1.A). The herbarium specimens (Figure 1.B) were identified by Turhadi and deposited at the Herbarium Universitas Brawijaya (MUBR), Laboratory of Plant Taxonomy, Structure, and Development, Department of Biology, Faculty of Mathematics and Natural Sciences, Universitas Brawijaya, Malang, East Java, Indonesia with collection number SM 08 (Sm_UB1), SM 09 (Sm_UB2), and SM 10 (Sm_UB3).

Procedures

Total DNA extraction

A total of 40 mg of fresh leaf tissues of *S. marginata* were used for total DNA extraction. The total DNA extraction using Wizard® Genomic DNA Purification Kit (Promega, USA) and followed the manufacturer's extraction protocol. The extracted DNA was checked for quality on gel electrophoresis with 0.8% agarose and run using 1X TBE (Tris-Borate EDTA) buffer (Promega, USA) at 100 V for 30 minutes. Subsequently, the extracted DNA was also checked for its concentration and purity level using a NanoPhotometer® NPOS 6.6c (Implen, Inc., USA) at the wavelength (λ) of 260 and 280 nm. The extracted DNA was diluted in TE buffer pH 8.0 (Promega, USA) and stored at -30°C for further analysis.

DNA amplification and sequencing

A Polymerase Chain Reaction (PCR) final volume of 25 µL was used in target region amplification. It consisted of the following components: 12.5 µL GoTaq® Green Master Mixes (Promega, USA), 0.5 µL each forward and reverse primers (10 pmol/µL), 10.5 µL nuclease-free water (Promega, USA), and 1 µL (100 ng/uL) genomic DNA. Amplification of the target region was carried out using the Takara PCR Thermal Cycles Dice Gradient (Takara Bio Inc., USA). The amplification of the target regions using two specific primer pairs which consisted of *trn*L-UAA and *trn*L-*trn*F IGS (Taberlet et al. 1991) (Table 1). The amplification process was carried out in 35 cycles with the following PCR program: pre-denaturation at 95°C for 1 minute, denaturation at 95°C for 15 seconds, annealing at 55°C for 15 seconds, extension at 72°C for 10 seconds, and post-extension at 72°C for 10 minutes. The electrophoresis of the PCR product was 80 V for 35 minutes using 1X TBE (Tris-Borate EDTA) buffer and then visualized on a 1% agarose gel and the nucleic acids stained using Diamond™ Nucleic Acid Dye (Promega, USA). Electrophoresis results were documented using a Gel Documentation tool, UV Transilluminator (Major Science Co. Ltd., USA). Subsequently, the PCR products obtained were used for bi-directional Sanger dideoxy sequencing using Genetic Analyzer 3730XL instrument (Thermo Fisher Scientific Inc, USA) at the Macrogen Company, Singapore.

Data analysis

Moreover, the sequence data of multiple individuals in a studied species is very important as it allows comparisons between sequences. The sequencing results obtained were prepared for further analysis using BioEdit Sequence Alignment Editor software ver.7.0.9.0. Then, each sequence was manually edited and verified by examining the sample's placement within the phylogenetic tree (de Vere et al. 2015). The DNA sequences were matched to the database using the Basic Local Alignment Search Tool (BLAST) (https://blast.ncbi.nlm.nih.gov/Blast.cgi). Phylogenetic tree construction using the Maximum Parsimony (MP) algorithm with 1000 replicates was carried out in MEGA X version 10.0.5 using the default parameters by comparing the *S. marginata* samples of this study with its relatives in the Cucurbitaceae family (Kumar et al. 2018) (Table 2). Additionally, *Begonia oxyloba* (Begoniaceae) was determined as the outgroup in the phylogenetic tree construction.

Table 1. Primers used in this study

Region	Sequence (5'→ 3')	Amplicon (bp)
*trn*L-UAA	CGAAATCGGTAGACGCTACG	~500
	GGGGATAGAGGGACTTGAAC	
*trn*L-*trn*F IGS	GGTTCAAGTCCCTCTATCCC	~400
	ATTTGAACTGGTGACACGAG	

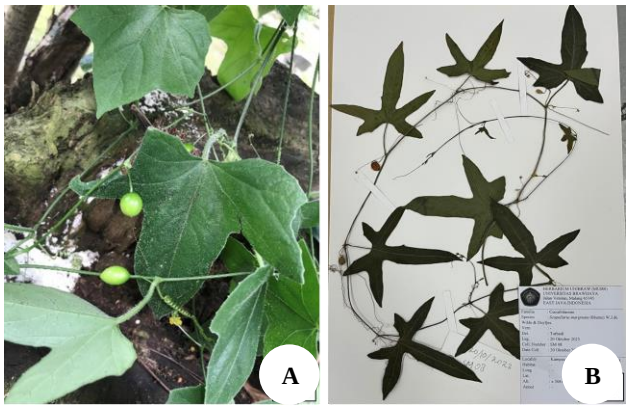

Figure 1. A. Living *Scopellaria marginata* and B. Herbarium specimen

Table 2. The *trn*L-UAA and *trn*L-*trn*F IGS sequences used for analysis in this study

Region	Species	GenBank Accession Number	Note
*trn*L-UAA	*Coccinia grandiflora* Cogn.	HQ608407	Ingroup
	Citrullus lanatus (Thunb.) Matsum. & Nakai	DQ536761	Ingroup
	Zehneria bodinieri (H.Lév.) W.J.de Wilde & Duyfjes	KY523355	Ingroup
	Zehneria perpusilla (Blume) Bole & M.R.Almeida	KY523367	Ingroup
	Zehneria maysorensis (Wight & Arn.) Arn.	KY523373	Ingroup
	Trochomeriopsis diversifolia Cogn.	DQ536878	Ingroup
	Eureiandra formosa Hook.f.	DQ641905	Ingroup
	Citrullus rehmii De Winter	KP036545	Ingroup
	Citrullus colocynthis (L.) Schrad.	KY613619	Ingroup
	Raphidiocystis phyllocalyx C.Jeffrey & Keraudren	DQ536855	Ingroup
	Peponium caledonicum (Sond.) Engl.	DQ536774	Ingroup
	Blastania cerasiformis (Stocks) A.Meeuse	DQ536803	Ingroup
	Scopellaria marginata (Blume) W.J.de Wilde & Duyfjes	DQ536882	Ingroup
	Sm_UB1	OR703797	*This study*
	Sm_UB2	OR703798	*This study*
	Sm_UB3	OR703799	*This study*
	Begonia oxyloba Welw. ex Hook.f.	AY968563	Outgroup
*trn*L-*trn*F IGS	*Neoachmandra cunninghamii* (F.Muell.) W.J.de Wilde & Duyfjes	KY523360	Ingroup
	Bambekea racemosa Cogn.	DQ536788	Ingroup
	Zehneria guamensis (Merr.) Fosberg	KY523363	Ingroup
	Zehneria polycarpa (Cogn.) Keraudren	KY523381	Ingroup
	Seyrigia humbertii Keraudren	AY973010	Ingroup
	Dieterlea fusiformis (E.J.Lott)	KJ531878	Ingroup
	Ibervillea hypoleuca (Standl.) C.Jeffrey	DQ536829	Ingroup
	Scopellaria marginata (Blume) W.J.de Wilde & Duyfjes	DQ536882	Ingroup
	Ceratosanthes palmata (L.) Urb.	DQ536795	Ingroup
	Neoachmandra japonica (Thunb.) W.J.de Wilde & Duyfjes	DQ536884	Ingroup
	Sm_UB1	OR703800	*This study*
	Sm_UB2	OR703801	*This study*
	Sm_UB3	OR703802	*This study*
	Begonia oxyloba Welw. ex Hook.f.	AY968378	Outgroup

The nucleotide sequences of the candidate barcode markers for *S. marginata* were converted to two-dimensional DNA barcode images using an open-source DNA Barcode and QR code generator (Yu et al. 2016; Khan et al. 2017). Mobile terminals (such as Android and iPhone devices) can read the information as QR code scanners (Ma et al. 2017).

RESULTS AND DISCUSSION

The *trn*L-UAA and *trn*L-*trn*F intergenic spacer characteristics

The Polymerase Chain Reaction (PCR) technique successfully amplified the *trn*L-UAA and *trn*L-*trn*F IGS regions in all *S. marginata* samples with a single band (Figure 2). The PCR products of those two regions were ~500 bp and ~400 bp, respectively. Our results correspond with previous studies that the length of whole chloroplast *trn*L-UAA is ranged from 254 to 767 bp (Taberlet et al. 2007), and *trn*L-*trn*F IGS on various monocots and dicots groups are ranged from 206 to 756 bp (Tsai et al. 2006). DNA sequencing for the *trn*L-UAA and *trn*F-*trn*L IGS in *S. marginata* samples was also successfully carried out using bi-directional Sanger dideoxy sequencing. Furthermore, our results also showed clean calls of chromatograms for those two target regions (Figure 3). The good sequencing chromatogram indicates no overlapping peaks, indicating the potential simultaneous sequencing of two DNA molecules (Aguirre-Dugua et al. 2019). These profiles are also shown in our results.

Contig DNA sequences from pre-processing showed that the sequence length was relatively similar for surveyed samples. The sequence length for the *trn*L-UAA ranged from 528 to 571 bp, while the sequence length for the *trn*F-*trn*L IGS ranged from 434 to 445 bp. Similar results also showed in various studies, for instance the sequence length of *trn*L-UAA ranged from 582 to 602 bp in *Oxytropis* (Fabaceae) (Tekpinar et al. 2016), 525 to 528 bp in *Melothria domingensis* (Cucurbitaceae) and 527 bp in *Cionosicyos excisus* (Cucurbitaceae) (Schaefer and Nee 2012), 555 to 559 bp in *Nepenthes* (Nepenthaceae) (Bunawan et al. 2017), 464 to 465 bp in *Cinnamomum osmophloeum* (Hsu et al. 2019), 519 to 528 in *Laurus nobilis* (Lauraceae) (Sevindik and Okan 2020). While the *trn*L-*trn*F IGS in some previous studies showed 381 to 395 bp in *M. domingensis* (Cucurbitaceae) and 410 bp in *C. excisus* (Cucurbitaceae) (Schaefer and Nee 2012), 372 to 376 bp in *L. nobilis* (Lauraceae) (Sevindik and Okan 2020), 449 bp and 179 bp in *Pisum vera* (Fabaceae) and *Pisum*

sativum (Fabaceae), respectively (Sen et al. 2020), 455 bp in *Gossypium hirsutum* (Malvaceae) (Hocaoglu-Ozyigit et al. 2022), 444 to 473 bp in species of Gramineae (Wang et al. 2022), and 298 to 306 bp in *Salvia miltiorrhiza* (Labiate) (Feng et al. 2022).

The average nucleotide composition of *trn*L-UAA of *S. marginata* was 38.5% A, 28.3% T, 17.5% G, and 15.7% C. The highest A+T content (67.0%) and the lowest G+C content (33.0%) were observed in Sm_UB3, while the lowest A+T content (66.5%) and the highest G+C content (33.5%) were shown in Sm_UB1 (Table 3). While, the *trn*F-*trn*L IGS of *S. marginata* was 30.8% A, 32.3% T, 16.4% G, and 20.5% C. The highest A+T content (63.5%) and the lowest G+C content (36.5%) were observed in Sm_UB1, while the lowest A+T content (62.8%) and the highest G+C content (37.2%) were shown in Sm_UB3 (Table 3). These nucleotide profiles were similar to the previous study in *L. nobilis* (Lauraceae) (Sevindik and Okan 2020). The low proportion of G+C than A+T content in *trn*L-UAA is also found in various taxa, such as *Pistacia vera* (Sarra et al. 2015), *Citrus* (Rutaceae) (Sevindik and Yalçin 2018), and *Dittrichia viscosa* (Asteraceae) (Sevindik et al. 2023). Like *trn*L-UAA, the lower proporsion of G+C than A+T content also showed in *trn*F-*trn*L IGS of *S. marginata*. In *Pennisetum glaucum* (Poaceae) (Almutairi 2022) showed a lower proportion of G+C than A+T content. According to Ismail et al. (2020), higher A+T contents than G+C in a barcode indicate high nucleotide composition variability and higher nucleotide substitution rate in that region.

Identification of *Scopellaria marginata*

The matching results with the GenBank (NCBI) database using BLASTn showed that the samples were identified as *S. marginata* based on the *trn*L-UAA and *trn*F-*trn*L IGS with similarity level of 97.14-97.50% and 98.36-98.61% respectively (Table 4). Furthermore, our samples of *S. marginata* showed similar with *S. marginata* voucher code A. Kocyan AK187 (BKF), which originates from Thailand (Kocyan et al. 2007). A sample is a similar species if the similarity value >97% (Mukhopadhyay et al. 2018). There were 468 and 369 positions in the final dataset for phylogenetic tree construction based on *trn*L-UAA and *trn*L-*trn*F IGS, respectively. Construction of a phylogenetic tree based on both the *trn*L-UAA (Figure 4) and *trn*L-*trn*F IGS (Figure 5) shows that the three samples (Sm_UB1, Sm_UB2, and Sm_UB3) were in the same clade with *S. marginata*. This result indicated that the three specimens identified as *S. marginata*.

Table 3. Nucleotide composition of *trn*L-UAA and *trn*L-*trn*F IGS of *Scopellaria marginata* samples

Region	*Scopellaria marginata*	A (%) Content	T (%) Content	G (%) Content	C (%) Content	A + T (%) Content	G + C (%) Content
*trn*L-UAA	Sm_UB1	38.4	28.1	17.7	15.8	66.5	33.5
	Sm_UB2	38.3	28.6	17.4	15.6	66.9	33.1
	Sm_UB3	38.8	28.2	17.4	15.5	67.0	33.0
	Average	38.5	28.3	17.5	15.7	66.8	33.2
*trn*F-*trn*L IGS	Sm_UB1	31.2	32.3	16.2	20.3	63.5	36.5
	Sm_UB2	30.7	32.3	16.5	20.5	63.0	37.0
	Sm_UB3	30.4	32.4	16.6	20.6	62.8	37.2
	Average	30.8	32.3	16.4	20.5	63.1	36.9

Note: G: Guanin, A: Adenin, C: Cytosin, T: Thymin

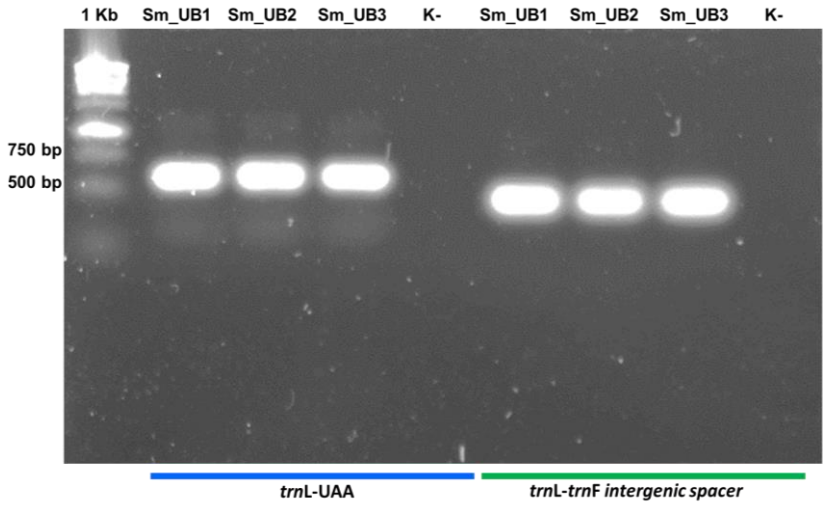

Figure 2. Electrophoregram of PCR results of *Scopellaria marginata* samples using primer *trn*L-UAA and *trn*F-*trn*L. K-: nuclease-free water

Table 4. Results of highest BLASTn pairwise identity (%) for *trn*L-UAA and *trn*L-*trn*F IGS

Region	Sample ID	GenBank/BLAST	Max. ID (%)	Accession No.
*trn*L-UAA	Sm_UB1	*Scopellaria marginata*	97.14	DQ536882
	Sm_UB2	*Scopellaria marginata*	97.50	DQ536882
	Sm_UB3	*Scopellaria marginata*	97.33	DQ536882
*trn*F-*trn*L IGS	Sm_UB1	*Scopellaria marginata*	98.36	DQ536882
	Sm_UB2	*Scopellaria marginata*	98.61	DQ536882
	Sm_UB3	*Scopellaria marginata*	98.39	DQ536882

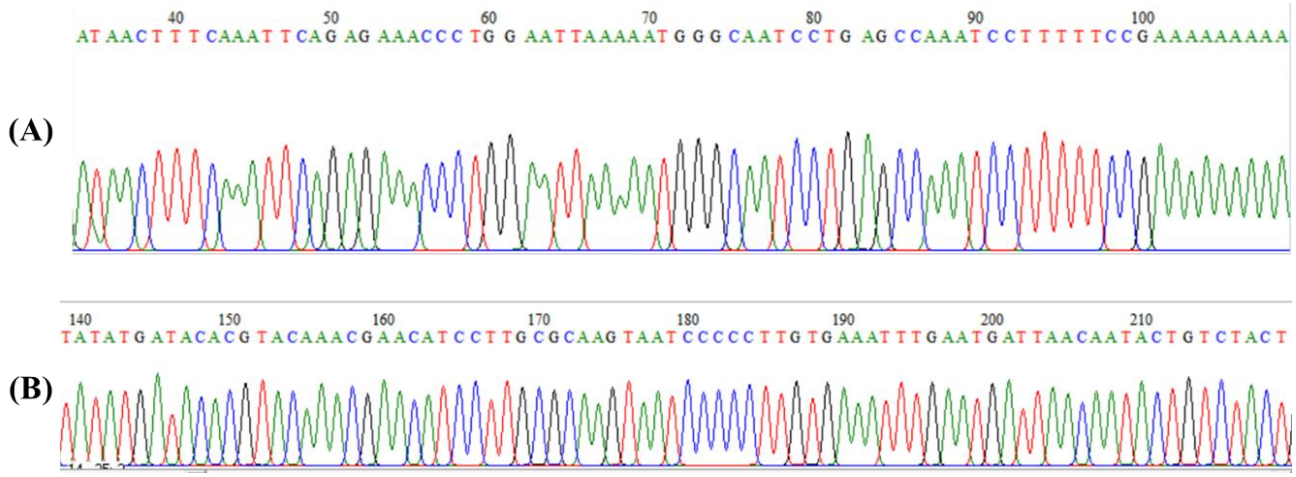

Figure 3. Representative sequencing chromatogram of *Scopellaria marginata* samples using primer *trn*L-UAA (A) and *trn*F-*trn*L (B)

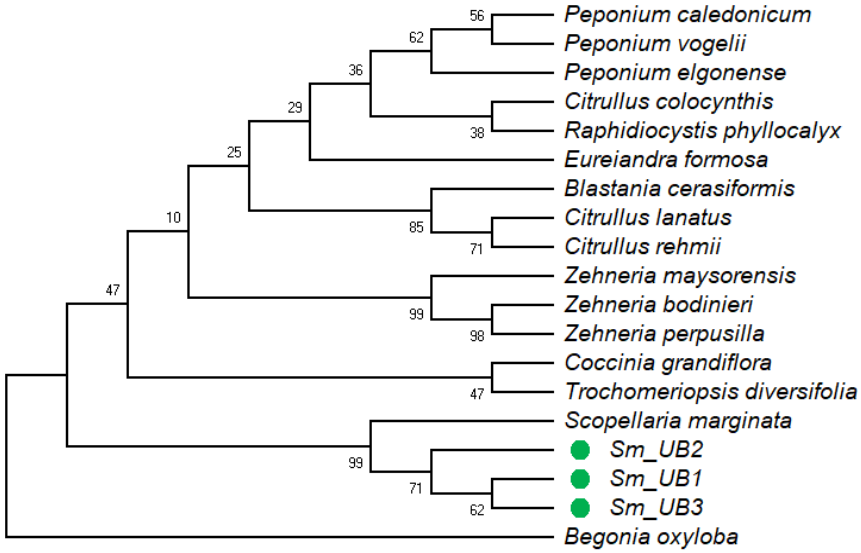

Figure 4. Phylogenetic tree of *Scopellaria marginata* from Malang, East Java, Indonesia (Sm_UB1, Sm_UB2, and Sm_UB3) based on the *trn*L-UAA

The *trn*L-UAA and *trn*L-*trn*F IGS produced in this study were the first sequences obtained from *S. marginata* originating from Indonesia. The *trn*L-*trn*F IGS is a barcode region in the chloroplast genome consisting of two transfer RNA regions, namely *trn*L-UAA and *trn*F-GAA. A non-coding spacer region separates these two regions. The *trn*L region consists of two exons and an intron where the 3'-end joins the exon of the *trn*F gene, which is separated by a spacer, and during the transcription process, these two genes are transcribed simultaneously (Yulita 2013).

Specific DNA barcode of *Scopellaria marginata*

Both *trn*L-UAA and *trn*L-*trn*F IGS showed a correct assignment rate (CAR) of 100% for *S. marginata* samples (Table 5). This result means both *trn*L-UAA and *trn*L-*trn*F IGS are good candidates for DNA barcoding to identify *S.*

marginata. The correct assignment rate at the species level also showed a high result (87.5%) in species of Gramineae, including *Agropyron*, *Bromus*, *Elymus*, *Elytrigia*, *Festuca*, *Leymus*, and *Lolium* (Wang et al. 2022). The good discrimination is also shown by the *trn*L-*trn*F intergenic spacer, which significantly separates the genus *Hedysarum* (Fabaceae) into two sections, *Hedysarum* and *Multicaulia* (Nuzhdina et al. 2018).

This study also successfully generated specific DNA barcodes for *S. marginata* using *trn*L-UAA and *trn*L-*trn*F IGS. DNA sequence with lengths of 505 and 417 bp for *trn*L-UAA and *trn*L-*trn*F IGS proposed as specific barcodes for *S. marginata* (Figure 6.A-B). Two-dimensional DNA barcoding produced in our study is useful for converting the information of *S. marginata* identity. According to Yu et al. (2016), this barcode can be applied to species identification and provide a new clinical safety protection technique. We can apply those barcodes by scanning them using a mobile phone equipped with a barcode scanning device. Subsequently, specific DNA sequence information will be displayed and can be used to identify a species accurately (Khan et al. 2017). Various studies also generated specific barcode markers which transformed into QR codes to benefit the diverse researchers. QR codes were also produced for family level in plants, such as Apocynaceae (Lv et al. 2020), Orchidaceae (Li et al. 2021), Theaceae (Jiang et al. 2022), Apiaceae (Jiang et al. 2023); genera level in plants, such as *Syringa* (Yao et al. 2022), *Clerodendrum* (Gogoi et al. 2020); and species level in plants, such as *Trachelospermum jasminoides* (Yu et al. 2016), *Panax ginseng* (Cai et al. 2016); and also plant-derived product level, such as Shi-Liang tea which made from the processed leaves of *Chimonanthus salicifolius* and *Chimonanthus zhejiangensis* (Ma et al. 2017).

Our results also confirmed that the samples analyzed were *S. marginata* based on morphological data evidence (Arumingtyas et al. 2023) and molecular data obtained from this study. This result also proves that the *S. marginata* found in Malang is a expanding the distribution, especially for the East Java region, and an additional record of the distribution area of *S. marginata* in Indonesia. The existence of *S. marginata* in Indonesia, especially Java, has been reported to be found in West Java (de Wilde and Duyfjes 2006). Based on our study on the digital herbarium collection of Royal Botanic Garden Edinburgh's (RBGE); Rijksherbarium, Leiden (Herb. Ludg. Bat.); and Herbarium Universitas Andalas (ANDA), *S. marginata* was found in Indonesia, including West Java (Purwakarta; Padalarang, Bandung; and Bogor), Southeast Sulawesi (Rantapao Toraja), North Sumatera, West Sumatera (Padang, Payakumbuh, and Bukittinggi). Furthermore, *S. marginata* was also found in several locations in Sumatera, namely Mt. Koeta Boeloer, H.van Tromon, Simeloengoen-Batak landen, Padang, and Sibolangit (Sitorus et al. 2019). Moreover, the distribution of *S. marginata* is based on the description in the Flora Malesiana book, including East Myanmar, China (Yunnan), Thailand, Laos, Cambodia, Vietnam, Philippines, the Malaysian Peninsula, Borneo (Sabah), Sumatera, West Java, and Sulawesi (Schaefer and Renner 2011).

The study concluded that the *Scopellaria* samples found in Malang, East Java, Indonesia, identified as *S. marginata* based on the *trn*L-UAA and *trn*L-*trn*F IGS. The similarity level of *Scopellaria* samples with *S. marginata* in the database showed 97.14-97.50% and 98.36-98.61%, respectively, for the *trn*L-UAA and *trn*L-*trn*F IGS.

Table 5. Correct Assignment Rate (CAR) of species level in *Scopellaria marginata* samples based on *trn*L-UAA and *trn*L-*trn*F IGS

Region	Correct Assignment Rate (CAR) (%)
*trn*L-UAA	100
*trn*F-*trn*L IGS	100

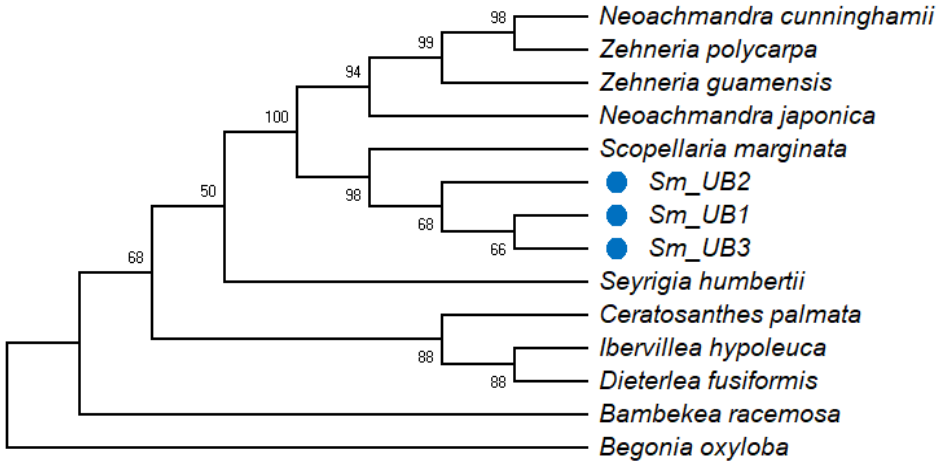

Figure 5. Phylogenetic tree of *Scopellaria marginata* from Malang, East Java, Indonesia (Sm_UB1, Sm_UB2, and Sm_UB3) based on the *trn*F-*trn*L IGS

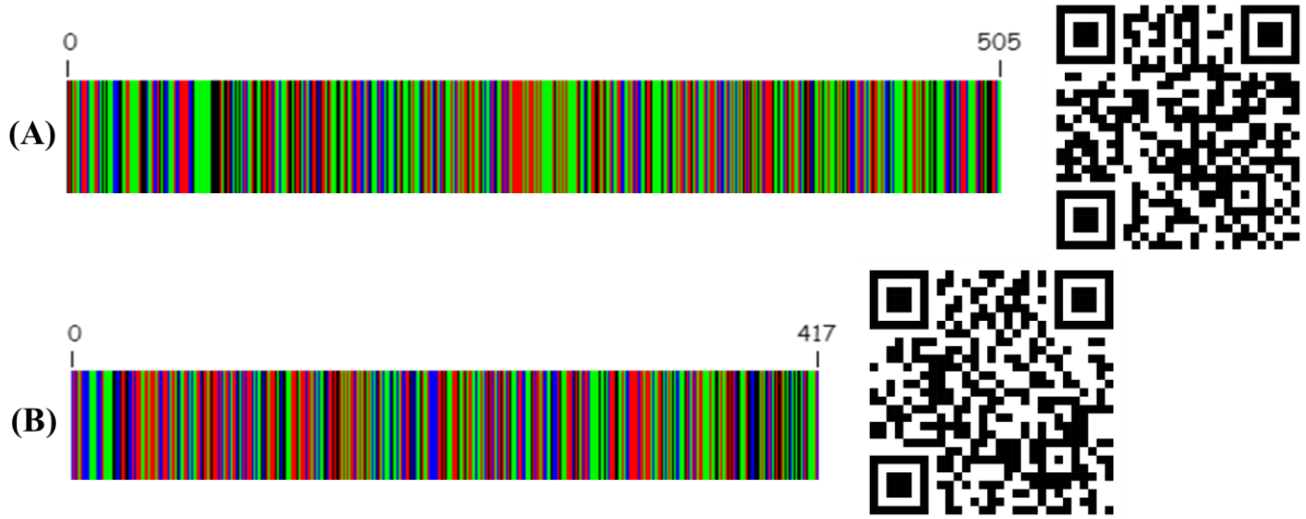

Figure 6. DNA barcodes and two-dimensional DNA barcodes of: A. *trn*L-UAA and B. *trn*L-*trn*F IGS for *Scopellaria marginata* Sm_UB3. Green, red, black, and blue represent base A, T, G, and C, respectively.

ACKNOWLEDGEMENTS

The authors thank Universitas Brawijaya, Malang, Indonesia for funding this research through the FMIPA Internal Fund scheme Year 2023 (Contract no. 2824.22/UN10.F09/PN/2023).

REFERENCES

Aguirre-Dugua X, Castellanos-Morales G, Paredes-Torres LM, Hernández-Rosales HS, Barrera-Redondo J, Sánchez-de la Vega G, Tapia-Aguirre F, Ruiz-Mondragón KY, Scheinvar E, Hernández P, Aguirre-Planter E, Montes-Hernández S, Lira-Saade R, Eguiarte LE. 2019. Evolutionary dynamics of transferred sequences between organellar genomes in *Cucurbita*. J Mol Evol 87 (9-10): 327-342. DOI: 10.1007/s00239-019-09916-1.

Almutairi ZM. 2022. Genetic diversity and phylogeny of pearl millets [*Pennisetum glaucum* (L.) R. Br.] based on chloroplast *trn*L-F region. Genet Resour Crop Evol 69: 2849-2859. DOI: 10.1007/s10722-022-01404-8.

Arumingtyas EL, Turhadi, Azrianingsih R, Afiyanti M, Pratami MP, Sudarjayanti BN, Solihah FM. 2023. Rekaman baru *Scopellaria marginata* (Cucurbitaceae) dari Malang, Jawa Timur, Indonesia. J Bio Unud 27(2): 183-190. DOI: 10.24843/JBIOUNUD.2023.v27.i02.p06. [Indonesian]

Bunawan H, Yen CC, Yaakop S, Noor NM. 2017. Phylogenetic inferences of Nepenthes species in Peninsular Malaysia revealed by chloroplast (*trn*L intron) and nuclear (*ITS*) DNA sequences. BMC Res Notes 10 (1): 67. DOI: 10.1186/s13104-017-2379-1.

Cai Y, Li P, Li X, Zhao J, Chen H, Yang Q, Hu H. 2016. Converting *Panax ginseng* DNA and chemical fingerprints into two-dimensional barcode. J Ginseng Res 41: 339-346. DOI: 10.1016/j.jgr.2016.06.006.

Coughlan P, Carolan JC, Hook ILI, Kilmartin L, Hodkinson TR. 2020. Phylogenetics of *Taxus* using the internal transcribed spacers of nuclear ribosomal DNA and plastid *trn*L-F Regions. Horticulturae 6 (1): 19. DOI: 10.3390/horticulturae6010019.

de Vere N, Rich TCG, Trinder SA, Long C. 2015. DNA barcoding for plants. In: Batley J (eds). Plant Genotyping. Methods in Molecular Biology. Humana Press, New York. DOI: 10.1007/978-1-4939-1966-6_8.

de Wilde WJJO, Duyfjes BEE. 2006. *Scopellaria*, a new genus name in Cucurbitaceae. Blumea 51 (2): 297-298. DOI: 10.3767/000651906X622238.

de Wilde WJJO, Duyfjes BEE. 2010. Flora Malesiana Cucurbitaceae Series 1 Vol. 19. Netherlands Centre for Biodiversity Naturalis (NHN). Leiden University, Leiden.

Feng J, Liao F, Kong D, Ren R, Sun T, Liu W, Yin Y, Ma H, Tang J, Li G. 2022. Genetic diversity of the cultivated *Salvia miltiorrhiza* populations revealed by four intergenic spacers. PLoS ONE 17 (4): e0266536. DOI: 10.1371/journal.pone.0266536.

Gogoi B, Wann SB, Saikia SP. 2020. DNA barcodes for delineating *Clerodendrum* species of North East India. Sci Rep 10: 13490. DOI: 10.1038/s41598-020-70405-3.

Hocaoglu-Ozyigit A, Ucar B, Altay V, Ozyigit II. 2022. Genetic diversity and phylogenetic analyses of turkish cotton (*Gossypium hirsutum* L.) lines using ISSR markers and chloroplast *trn*L-F regions. J Nat Fibers 19 (5): 1837-1850. DOI: 10.1080/15440478.2020.1788493.

Hsu W-K, Lee S-C, Lu P-L. 2019. A useful technical application of the identification of nucleotide sequence polymorphisms and gene resources for *Cinnamomum osmophloeum* Kaneh. (Lauraceae). Forests 10 (4): 306. DOI: 10.3390/f10040306.

Ismail M, Ahmad A, Nadeem M, Javed MA, Khan SH, Khawaish I, Sthanadar AA, Qari SH, Alghanem SM, Khan KA, Khan MF, Qamer S. 2020. Development of DNA barcodes for selected Acacia species by using *rbc*L and *mat*K DNA markers. Saudi J Biol Sci 27 (12): 3735-3742. DOI: 10.1016/j.sjbs.2020.08.020.

Jiang S, Chen F, Qin P, Xie H, Peng G, Li Y, Guo X. 2022. The specific DNA barcodes based on chloroplast genes for species identification of Theaceae plants. Physiol Mol Biol Plants 28(4): 837-848. DOI: 10.1007/s12298-022-01175-7.

Jiang Z, Zhang M, Kong L, Bao Y, Ren W, Li H, Liu X, Wang Z, Ma W. 2023. Identification of Apiaceae using *ITS*, *ITS2* and *psb*A-*trn*H barcodes. Mol Biol Rep 50 (1): 245-253. DOI: 10.1007/s11033-022-07909-w.

Khan SA, Baeshen MN, Ramadan HA, Baeshen NA. 2017. Emergence of plastidial intergenic spacers as suitable DNA barcodes for arid medicinal plant *Rhazya stricta*. Am J Plant Sci 8: 1774-1789. DOI: 10.4236/ajps.2017.88121.

Kishor R, Sharma GJ. 2018. The use of the hypervariable P8 region of *trn*L (UAA) intron for identification of orchid species: evidence from restriction site polymorphism analysis. PLoS ONE 13 (5): 1-20. DOI: 10.1371/journal.pone.0196680.

Kocyan A, Zhang LB, Schaefer H, Renner SS. 2007. A multi-locus chloroplast phylogeny for the Cucurbitaceae and its implications for character evolution and classification. Mol Phylogenet Evol 44(2): 553-577. DOI: 10.1016/j.ympev.2006.12.022.

Kress WJ. 2017. Plant DNA barcodes: Applications today and in the future. J Syst Evol 55 (4): 291-307. DOI: 10.1111/jse.12254.

Kumar S, Stecher G, Li M, Knyaz C, Tamura K. 2018. MEGA X: Molecular evolutionary genetics analysis across computing platforms. Mol Biol Evol 35: 1547-1549. DOI: 10.1093/molbev/msy096.

Kwon YE, Yu HJ, Baek S, Kim GB, Lim KB, Mun JH. 2017. Development of gene-based identification markers for Phalaenopsis' KS Little Gem' based on comparative genome analysis. Hortic Environ Biotechnol 58 (2): 162-169. DOI: 10.1007/s13580-017-0189-y.

Li H, Xiao W, Tong T, Li Y, Zhang M, Lin X, Zou X, Wu Q, Guo X. 2021. The specific DNA barcodes based on chloroplast genes for species identification of Orchidaceae plants. Sci Rep 11: 1424. DOI: 10.1038/s41598-021-81087-w.

Lv YN, Yang CY, Shi LC, Zhang ZL, Xu AS, Zhang LX, Li XL, Li HT. 2020. Identification of medicinal plants within the Apocynaceae family using *ITS2* and *psb*A-*trn*H barcodes. Chin J Nat Med 18 (8): 594-605. DOI: 10.1016/S1875-5364(20)30071-6.

Ma S, Lv Q, Zhou H, Fang J, Cheng W, Jiang C, Cheng K, Yao H. 2017. Identification of traditional she medicine shi-liang tea species and closely related species using the *ITS*2 barcode. Appl Sci 7 (3): 195. DOI: 10.3390/app7030195.

Mukhopadhyay CS, Choudhary RK, Iquebal MA. 2018. Basic Applied Bioinformatics. John Wiley & Sons, Inc, Hoboken.

Nadeem MA, Nawaz MA, Shahid MQ, Doğan Y, Comertpay G, Yıldız M, Hatipoğlu R, Ahmad F, Alsaleh A, Labhane N, Özkan H, Chung G, Baloch FS. 2018. DNA molecular markers in plant breeding: Current status and recent advancements in genomic selection and genome editing. Biotechnol Biotechnol Equip 32 (2): 261-285. DOI: 10.1080/13102818.2017.1400401.

Nuzhdina NS, Bondar AA, Dorogina OV. 2018. New data on taxonomic and geographic distribution of the *trn*L-UAA intron deletion of chloroplast DNA in *Hedysarum* L. (Fabaceae L.). Russ J Genet 54: 1282-1292. DOI: 10.1134/S1022795418110108.

Plant of the World Online (POWO). 2024. Cucurbitaceae Juss. https://powo.science.kew.org/taxon/urn:lsid:ipni.org:names:30000781-2.

Roslim DI. 2018. Pandan (*Pandanus* sp.), rotan (*Calamus* sp.), and rengas (*Gluta* sp) from Kajuik Lake, Riau Province, Indonesia. Braz Arch Biol Technol 61: e18160419. DOI: 10.1590/1678-4324-2018160419.

Sarra C, Soumaya R-C, Zined M, Khaled S, Noureddine C, Khaled C. 2015. Chloroplast DNA analysis of Tunisian pistachio (*Pistacia vera* L.): sequence variations of the intron *trn*L (UAA). Sci Hortic 191: 57-64. DOI: 10.1016/j.scienta.2015.04.037.

Schaefer H, Nee MH. 2012. *Melothria domingensis* (Cucurbitaceae), an endangered Caribbean endemic, is a *Cayaponia*. PhytoKeys 18: 45-60. DOI: 10.3897/phytokeys.18.3914.

Schaefer H, Renner SS. 2011. Phylogenetic relationships in the order Cucurbitales and a new classification of the gourd family (Cucurbitaceae). Taxon 60 (1): 122-138. DOI: 10.1002/tax.601011.

Sen F, Uncu AO, Uncu AT, Erdeger SN. 2020. The *trn*L (UAA)-*trn*F (GAA) intergenic spacer is a robust marker of green pea (*Pisum sativum* L.) adulteration in economically valuable pistachio nuts (*Pistacia vera* L.). J Sci Food Agric 100 (7): 3056-3061. DOI: 10.1002/jsfa.10336.

Sevindik E, Bozkurt M, Yilmaz M, Şenyüz E, Paksoy MY. 2023. Molecular characterization of *Dittrichia viscosa* (L.) greuter (Asteraceae) populations revealed by ISSR markers and chloroplast (CpDNA) *trn*L intron sequences. Genetika 55 (1): 217-228. DOI: 10.2298/GENSR23010217S.

Sevindik E, Murathan ZT, Sevindik M. 2020. Molecular genetic diversity of *Prunus armeniaca* L. (Rosaceae) genotypes by RAPD, ISSR-PCR, and chloroplast DNA (cpDNA) *trn*L-F sequences. Intl J Fruit Sci 20 (S3): S1652-S1661. DOI: 10.1080/15538362.2020.1828223.

Sevindik E, Okan K. 2020. Genetic diversity and phylogenetic analyses of *Laurus nobilis* L. (Lauraceae) populations revealed chloroplast (cpDNA) *trn*L intron and *trn*L-F region. Intl J Fruit Sci 20 (S2): S82-S93. DOI: 10.1080/15538362.2019.1707745.

Sevindik E, Yalçin K. 2018. Phylogenetic analysis of some *Citrus* L. (Rutaceae) taxa in Turkey based on chloroplast (cpDNA) *trn*L intron and *trn*l-f DNA sequences. Genetika 50 (3): 1035-1044. DOI: 10.2298/GENSR1803035S.

Simpson MG. 2019. Plant Systematics, 3rd edition. Academic Press, Oxford. DOI: 10.1016/B978-0-12-812628-8.50001-8.

Sitorus RE, Rugayah, Navia ZI. 2019. Manajemen herbarium dan pengenalan jenis-jenis Cucurbitaceae yang jarang ditemukan di Sumatra. Biologica Samudra 1 (2): 48-55. [Indonesian]

Taberlet P, Coissac E, Pompanon F, Gielly L, Miquel C, Valentini A, Vermat T, Corthier G, Brochmann C, Willerslev E. 2007. Power and limitations of the chloroplast *trn*L (UAA) intron for plant DNA barcoding. Nucleic Acids Res 35 (3): e14. DOI: 10.1093/nar/gkl938.

Taberlet P, Gielly L, Pautou G, Bouvet J. 1991. Universal primers for amplification of three non-coding regions of chloroplast DNA. Plant Mol Biol 17: 1105-1109. DOI: 10.1007/BF00037152.

Tekpinar AD, Erkul SK, Aytaç Z, Kaya Z. 2016. Phylogenetic relationships among native *Oxytropis* species in Turkey using the *trn*L intron, *trn*L-F IGS, and *trn*V intron cpDNA regions. Turkish J Bot 40: 472-479. DOI: 10.3906/bot-1506-45.

Trivedi S, Rehman H, Saggu S, Panneerselvam C, Ghosh SK. 2020. DNA Barcoding and Molecular Phylogeny, 2nd edition. Springer, New York. DOI: 10.1007/978-3-030-50075-7.

Tsai LC, Yu YC, Hsieh HM, Wang JC, Linacre A, Lee JC. 2006. Species identification using sequences of the *trn*L intron and the *trn*L-*trn*F IGS of chloroplast genome among popular plants in Taiwan. Forensic Sci Int 164 (2-3): 193-200. DOI: 10.1016/j.forsciint.2006.01.007.

Wang J, Yan Z, Zhong P, Shen Z, Yang G, Ma L. 2022. Screening of universal DNA barcodes for identifying grass species of Gramineae. Front Plant Sci 13: 998863. DOI: 10.3389/fpls.2022.998863.

Yao R, Guo R, Liu Y, Kou Z, Shi B. 2022. Identification and phylogenetic analysis of the genus *Syringa* based on chloroplast genomic DNA barcoding. PLoS ONE 17 (7): e0271633. DOI: 10.1371/journal.pone.0271633.

Yu N, Gu H, Wei Y, Zhu N, Wang Y, Zhang H, Zhu Y, Zhang X, Ma C, Sun A. 2016. Suitable DNA barcoding for identification and supervision of *Piper kadsura* in chinese medicine markets. Molecules 21 (9): 1221. DOI: 10.3390/molecules21091221.

Yu N, Wei YL, Zhang X, Zhu N, Wang YL, Zhu Y, Zhang HP, Li FM, Yang L, Sun JQ, Sun AD. 2017. Barcode *ITS*2: A useful tool for identifying *Trachelospermum jasminoides* and a good monitor for medicine market. Sci Rep 7 (1): 5037. DOI: 10.1038/s41598-017-04674-w.

Yulita KS, Susilowati A, Rachmat HH, Susila, Hidayat A, Dwiyanti FG. 2022. Molecular identification of *Eurycoma longifolia* Jack from Sumatra, Indonesia using *trn*L-F region. Biodiversitas 23 (3): 1374-1382. DOI: 10.13057/biodiv/d230323.

Yulita KS. 2013. Secondary structures of chloroplast *trn*L intron in Dipterocarpaceae and its implication for the phylogenetic reconstruction. Hayati J Biosci 20 (1): 31-39. DOI: 10.4308/hjb.20.1.31.

NUSANTARA BIOSCIENCE
Vol. 16, No. 1, pp. 119-129
May 2024

ISSN: 2087-3948
E-ISSN: 2087-3956
DOI: 10.13057/nusbiosci/n160115

Incidence of methicillin-resistant *Staphylococcus aureus* in wastewater and its survival after discharge from two hospitals in Akure, Nigeria

TOLULOPE EMORUWA♥, OLUFUMILOLA OMOYA
Federal University of Technology Akure. P.M.B. 704 Akure, Ondo State, Nigeria. Tel.: +234-906 670-7545, ♥email: emoruwatolu09@gmail.com

Manuscript received: 1 December 2023. Revision accepted: 25 March 2024.

Abstract. *Emoruwa T, Omoya O. 2024. Incidence of methicillin-resistant* Staphylococcus aureus *in wastewater and its survival after discharge from two hospitals in Akure, Nigeria. Nusantara Bioscience 16: 119-129.* The prevalence of Methicillin-Resistant *Staphylococcus aureus* (MRSA), a silent infection-causing bacteria that is resistant to several antibiotics is rising in the population, increasing morbidity and mortality rates. The goal of this study was to find MRSA in hospital wastewater from the University of Medical Science Teaching Hospital and University Health Center, The Federal University of Technology Akure, Nigeria. Wastewater were collected from outlets in different wards, and pipe-borne water was collected as a control. The wastewater underwent bacteriological analysis using membrane filtration, identifying all the bacteria isolates. Zones of inhibition were interpreted to screen *S. aureus* isolates for antibiotic susceptibility. The *mecA* gene was molecularly identified in *S. aureus* isolates using bacterial DNA extraction and polymerase chain reaction. The plasmid profile and MRSA survivability at various pH, temperature, and salt concentrations were examined as well. The total bacterial counts in wastewater collected from UNIMEDTH and FUTA Health Center ranged from 49.72±0.86 CFU/100 mL (pipe-borne water) to 877.91±1.55 CFU/100 mL (Accident and Emergency ward) and 73.71±0.72 CFU/100 mL (pipe-borne water) to 422.05±1.55 CFU/100 mL (Wound treatment ward) respectively, while the total staphylococcal counts in UNIMEDTH and FUTA Health Center ranged from 0.00±0.00 CFU/100 mL (pipe-borne water) to 220.14±1.06 CFU/100 mL (Medical Laboratory Science Laboratory) and 1.02±0.11 CFU/100ml (pipe-borne water) to 60.11±0.11 CFU/100 mL (doctors' station) respectively. Isolates of *S. aureus* were more resistant to ampiclox 10 (62.50%), oxacillin 7 (43.75%), zinnacef 10 (62.50%), and amoxicillin 8 (50.00%). The incidence of MRSA in hospital wastewater and its survival under different environmental conditions could present a public health challenge as the discharge of untreated wastewater could contaminate different water bodies.

Keywords: Antimicrobial resistance, *Staphylococcus aureus*, wastewater

INTRODUCTION

Staphylococcus aureus (*S. aureus*) is a Gram-positive bacterium that can be normal flora in the upper respiratory tract and the skin. It has been implicated in causing infection of the skin and various tissues as well as toxin-mediated diseases like food poisoning and toxic shock syndrome (Tong et al. 2015). It can cause both community- and hospital-acquired infections, and it can easily acquire antibiotic-resistant genes by horizontal gene transfer (Haaber et al. 2017).

Water is necessary for hospital operations and hygiene. Due to the nature and significance of the compounds they contain, hospital wastewater discharge poses threats to human health and the environment. Because there aren't enough wastewater treatment and purification facilities in developing nations, managing hospital wastewater is a serious issue.

Hospitals are one of the sectors in the world with the greatest pollution emissions (Achak et al. 2021). Reusing treated water presents a health risk to the public since wastewater treatment plants, and hospital wastewater treatment plants in particular, are believed to be hotspots for the emergence of antibiotic resistance (Rizzo et al. 2013; Yuan and Pia 2023).

Previous investigations have detected significant quantities of drugs and residual microorganisms in Hospital Wastewater (HWW). These results may exert a selective pressure on the growth of microorganisms resistant to antibiotics (Rowe et al. 2017). Because of this, HWWs have a higher chance of spreading Antibiotic Resistant Genes (ARGs) than other wastewater systems, like urban wastewater systems (Verlicchi et al. 2015; Zheng et al. 2018). Hospitals utilize antibiotics such as carbapenems, glycopeptides, and others more often than in other settings.

This divergence raises the possibility of an increase in ARGs associated with hospitals. Since the 1980s, restrictions for sludge and wastewater emission limitations have been put into place globally to reduce the harm caused by post-discharge effluent (Meng et al. 2016).

Only a few nations, like France and Italy, have raised legal concerns about pre-release HWW therapy (Verlicchi et al. 2010; Al Aukidy et al. 2017; Mehanni et al. 2023). Antibiotic resistance levels in hospital wastewater may differ from those in other aquatic ecosystems due to variations in antibiotic application patterns. Hospitals are the primary settings for the use of certain antibiotics, including cefotiam, piperacillin, and vancomycin (Mehanni et al. 2023).

The ability of *S. aureus* to outwit the immune system, above and beyond its Multidrug-Resistance (MDR) phenotype, makes it one of the most intractable pathogenic bacteria in the history of antibiotic chemotherapy (Rowe et al. 2017). The spread of methicillin-resistant *S. aureus* (MRSA) has become a significant concern for both animal and human health worldwide (Rowe et al. 2017; Zheng et al. 2018; Mehanni et al. 2023). MRSA is predominantly mediated by the expression of the *mecA* gene, which is located on a mobile genetic element; the Staphylococcal Cassette Chromosome mec (SCCmec), encoding an altered Penicillin-Binding Protein (PBP2a) with an exceedingly low susceptibility to beta-lactam antibiotics. Thus, *S. aureus* will be practically resistant to most beta-lactam antibiotics (Al Aukidy et al. 2017; Mehanni et al. 2023). On the other hand, resistance to vancomycin is accomplished by horizontal transfer of a plasmid-born transposon carrying the *vanA* gene from vancomycin-resistant Enterococcus to *S. aureus* across the genus barrier (Mehanni et al. 2023).

The *S. aureus* has been used as an indicator microorganism in wastewater and river water (López et al. 2019). Antibiotic-resistant *S. aureus* itself is considered an opportunistic organism, but it is spreading to a wider spectrum of society due to the difficulty of treating it with antimicrobials and disinfectants in medical facilities (Garcia et al. 2017). Therefore, this research aimed to clarify the status of *S. aureus* in hospital wastewater in two selected hospitals in Akure, Nigeria.

The objectives of this study are to determine the antibiotic susceptibility profile of *S. aureus* isolated from hospital wastewater in Akure. Investigate the presence of Methicillin-Resistant *S. aureus* (MRSA) in hospital wastewater. Evaluate the survival of MRSA isolates in hospital wastewater under different environmental conditions. The plasmid profile of Methicillin-Resistant *S. aureus* (MRSA) isolated from hospital wastewater in Akure.

MATERIALS AND METHODS

Study design and area

This case-control study was carried out in selected hospitals in Akure, and microbiological analysis was conducted at the Department of Microbiology, The Federal University of Technology, Akure (FUTA), Nigeria. Wastewater (200 mL) was collected from the University of Medical Science (UNIMED) teaching hospital and University Health Center FUTA. These two hospitals were selected because they are the only hospitals affiliated with tertiary institutions in Akure, the state capital. A letter of introduction (Ethical approval) was collected from the Head of the Department of Microbiology, FUTA, and was used as a valid means of identification at the hospitals where samples were collected in Akure.

Isolation of bacteria from wastewater

Samples were randomly collected from twelve (12) different locations at UNIMED and seven (7) different locations from FUTA two times daily for three weeks. Microbiological examinations of wastewater were carried out using the membrane filtration method as described by WHO (2016), on nutrient agar, some selective and differential media (Salmonella Shigella agar, Eosin Methylene Blue agar, MacConkey agar and Mannitol Salt agar). One hundred (100 mL) milliliters of wastewater was gently shaken and filtered with a 0.45 µm membrane filter and the filter was aseptically placed on molten agar and incubated at 37°C for 24 hours. A colony count was performed and the average of all the tests for each sample location was considered as the colony-forming unit per 100 milliliters (CFU/100 mL) of hospital wastewater. Morphological and biochemical characterization of bacterial isolates were used for identification (Fawole and Oso 2004; Cheesbrough 2014). Bacterial colonies showing typical characteristics of *S. aureus* including golden yellow color colonies on MSA were subjected to gram staining, catalase test, and DNase test (Olutiola et al. 2018).

Antimicrobial susceptibility testing

CLSI (5th edition) guidelines recommend the Kirby–Bauer disk diffusion method, which involves using Muller–Hinton Agar (MHA) to inoculate bacterial suspensions (CLSI 2017). The method is standardized and incubated at 37°C for 18 hours. After incubation, the diameter of clear zones around the disk was measured in millimeters and recorded as the zones of inhibition and then compared with Clinical and Laboratory Standards Institute (CLSI) standard interpretative charts for their sensitivity, intermediate, or resistance. The *S. aureus* ATCC strain 25923 was used for quality control. The isolates were defined as Multidrug-Resistance (MDR) strains by lack of susceptibility to at least three classes of antibiotics (Akya et al. 2020).

Determination of physicochemical parameters of water

The American Public Health Association (APHA, 5th edition) standard procedures were used to determine several physicochemical properties of hospital wastewater samples that were collected in their raw state. According to Oladipo et al. (2019), these factors include pH, dissolved oxygen, Chemical Oxygen Demand (COD), and Biochemical Oxygen Demand (BOD). Detection of the *mecA* Gene in Multiple Antibiotic Resistance *S. Aureus*.

Genomic DNA extraction

Multidrug-resistance bacterial broth culture of 1.5 mL was taken in the centrifuge tube, centrifuged at 10,000 rpm for 2 minutes, and the supernatant was discarded. To the pellet, 1 mL of distilled water was added, which dissolved the pellet completely. Again, after centrifuging at 10,000 rpm for 2 minutes, the procedure was repeated two times. The supernatant was discarded, and to the pellet, 100 µL of Tris-EDTA buffer was added, which dissolved the pellet completely in the buffer. The supernatants containing the DNA were transferred to another tube and stored at -20°C. The concentration and purity of the extracted DNA were estimated using a Nanodrop spectrophotometer (Model 752) (Natàlia et al. 2019).

PCR amplification of the *mecA* gene in multidrug-resistance *S. aureus*

The *mecA* gene, which in *S. aureus* species encodes for methicillin resistance, was amplified by PCR. For every PCR reaction, the following ingredients were added: 12.5 µL of 2x PCR Master Mix (Thermos Scientific Technologies, Waltham, MA, USA), 50 ng of DNA template, 5 µM of both forward and reverse primers, and 25 µL of nuclease-free water. Table 4 provides specific information on the primers and PCR conditions. The C1000 thermocycler (Bio-Rad, Hercules, USA) was used to amplify DNA. GelRed staining was used to visualize the amplicons after they were electrophoresed on 1% w/v agarose gel under a UV transilluminator.

Sequencing of amplified 16S rRNA Gene

The BigDye terminator V. 3.1 cycle sequencing kit (Applied Biosystems, Warrington, UK) was used to sequence the purified PCR products on an Applied Biosystems/Hitachi 3130 genetic analyzer (Tokyo, Japan). After utilizing Finch TV for inspection, the produced sequence electropherograms were manually modified. MUSCLE, which was integrated into MEGA V. 7.0, was used to perform multiple sequence alignment (Kumar et al. 2017). The Neighbor-Joining tree method was utilized to generate phylogenetic sequence dendrograms from closely related sequences found in GenBank, utilizing the substitution model.

Plasmid DNA extraction and profiling of MRSA

Plasmid DNA extraction was carried out as stated by Zyppy™ Plasmid Miniprep Kit Catalog Nos. D4019's manufacturer's procedure. Overnight growth of bacteria in broth culture was used for the plasmid isolation using Zyppy™ Plasmid Miniprep Kit Catalog Nos. D4019.

A 600 µL of bacterial culture grown in LB medium was added to a 1.5 mL microcentrifuge tube and centrifuged for 30 seconds at 14,000 rpm. The supernatant was discarded, and 100 µL of 7X Lysis Buffer (Blue) 1 was added and mixed by inverting the tube 4-6 times. After the addition of 7X Lysis Buffer, the solution changed from opaque to clear blue, indicating complete lysis. Then 350 µL of cold Neutralization Buffer (Yellow) was added and mixed thoroughly. The sample then turned yellow with a yellowish precipitate. Centrifuge at 11,000-16,000 x g for 2-4 minutes and transfer the supernatant (~900 µL) into the provided Zymo-Spin™ IIN column. The flow-through in the column was discarded after centrifugation for 15 seconds. After which, 200 µL of Endo-Wash Buffer was added and centrifuged for 30 seconds. Elution Buffer 2 was added directly to the column matrix, left for one minute at room temperature, and centrifuged for 30 seconds to elute the plasmid DNA. The extracted plasmid was examined on 0.8% agarose gel, 1 kbp DNA ladder (NEB) was used as control, 1 and 5 µL of loading dye (bromophenol blue) and plasmid DNA respectively were mixed and loaded on solidified agarose gel and 1X TAE buffer was used for the electrophoresis.

Survival of MR *Staphylococcus aureus* Isolates

The survival of MR *S. aureus* subjected to different environmental conditions (pH, temperature, and salt concentration) was examined as described by Marwan et al. (2014). For the influence of pH on the survival of MRSA, each isolate was inoculated into sterile test tubes with 9 mL of Nutrient broth (with the following pH adjusted to 3, 4, 5, 6, 7, 8, 9, 10, and 11) and incubated at 37°C for 24 hours, the influence of temperature on the survival of MRSA was carried out by inoculating the tubes with 9 mL of nutrient broth, and the tubes were incubated at different temperatures (ranging from 4 to 40°C) for 24 hours. Also, salt concentrations ranging from 0 to 30% v/v were prepared in test tubes and inoculated at 37°C for 24 hours to determine the survival of MRSA at different salt concentrations. The microbial growth was observed after 24 hours using a spectrophotometer at an absorbance of 600 nm, and 0.1 mL of each preparation was poured on nutrient agar and incubated at 37°C for 24 hours, after which the colonies were counted.

Statistical analysis of data

Data obtained was expressed as mean ± standard error of mean. The new Duncan Multiple Range test was used to compare means. A p-value of < 0.05 was considered statistically significant

RESULTS AND DISCUSSION

Bacterial counts of wastewater collected from selected hospitals in Akure

Bacterial counts of hospital wastewater are shown in Table 1 (UNIMED) and Table 2 (FUTA). All the wastewater samples were contaminated with bacteria, and the total viable bacterial counts of the tap water (source) used as a control were significantly ($p<0.05$) lower than those in other water sources. All the wastewater samples were also contaminated with *Staphylococcus*, except those from the community clinic, blood bank, and water source at UNIMED that had zero staphylococcal counts. The highest staphylococcal counts were observed in wastewater samples collected from the MLS laboratory (220.14±1.06 CFU/100 mL) and the doctor's station (60.11±0.11 CFU/100 mL) at UNIMED and FUTA, respectively.

Physicochemical parameters of hospital wastewaters

The physicochemical parameters of the wastewaters are shown in Table 5. The pH, DO, COD, and BOD of the wastewaters ranged from 5.31±0.62 (postnatal ward, H) to 8.93±0.74 (Children's ward, N), 2.01±0.02 mg/L (UNIMED Laundry, K) to 8.31±0.11 mg/L (UNIMED Water Source, L), 5.11±0.05 mg/L (UNIMED Water Source, L) to 931.44±5.06 mg/L (UNIMED Laundry, K) and 3.68±0.07 mg/L (FUTA Water Source, T) to 11.73±0.93 mg/L (UNIMED Laundry, K), respectively. The ratio of BOD and COD in some samples was less than 0.03.

Antibiotic susceptibility profiles of *Staphylococcus aureus* isolated from hospital wastewater

Antibiotic susceptibility profiles of all the *S. aureus* isolates are shown in Figures 1 and 2. In wastewater collected from UNIMED (Fiure 1), the isolates from all sample locations were more susceptible to gentamicin (3.06±0.21 to 20.41±0.03 mm), pefloxacin (7.06±0.02 to 20.11±0.01 mm), ciprofloxacin (20.06±0.11 to 25.72±0.04 mm), streptomycin (11.42±0.10 to 20.21±0.22 mm), septrin (10.41±0.04 to 18.21±0.31 mm) and erythromycin (12.01±0.05 to 20.02±0.21 mm). On the other hand, *Staphylococcus aureus* isolates from wastewater collected in FUTA (Figure 2) were more susceptible to ciprofloxacin (18.21±0.10 to 25.03±0.06 mm) and streptomycin (12.03±0.04 to 23.00±0.05 mm), while those from the wound treatment ward showed lesser susceptibility to all the antibiotics tested, and those isolated from water sources were not susceptible to ampiclox, zinnacef, and amoxicillin. Also, those isolated from children's wards and doctor's stations were not susceptible to amoxicillin.

Multiple antibiotic resistant patterns of *Staphylococcus aureus* isolated from wastewater

Multiple antibiotic resistance patterns of isolated *S. aureus* are shown in Table 6. Generally, the *S. aureus* isolates showed varying proportions of resistance to ampiclox (62.50%), amoxicillin (50%), oxacillin (43.75%), rocephin (31.25%), gentamicin (31.25%), pefloxacin (18.75%), erythromycin (12.50%), and septrin (6.25%). The multiple antibiotic resistant index (MARi) of the isolates from FUTA had a MARi of greater than 0.3 except for the water source and laundry While in UNIMED, isolates from the eye clinic, postnatal, and laundry have a MARi greater than 0.

Molecular detection of the *MecA* gene in antibiotic resistant *Staphylococcus aureus* from hospital wastewaters in Akure

Molecular detection of the *mecA* gene in the isolate of *S. aureus* is shown in Figure 3. It was noted that of all thirteen (13) multidrug-resistance isolates examined, six (6) were positive for the *mecA* gene, which was amplified at approximately 300 bp. The isolates were from the eye clinic, postnatal ward, nurses' station, children's ward, doctor's station, and wound treatment ward.

Effects of temperature on MRSA isolated from different wastewater sources in selected hospitals in Akure

The effects of temperature on MRSA from hospital wastewater are shown in Figure 4. All the MRSA isolates were able to survive in the temperature range of 4°C to 40°C except those that were isolated from postnatal ward and survived the temperature range 30°C to 40°C. Generally, there were variations in the staphylococcal counts at different temperatures, with 35°C being the optimum temperature for growth.

Effects of pH on MRSA isolated from different wastewater sources in selected hospitals in Akure

The effects of pH on MRSA isolated from different wastewater sources in selected hospitals in Akure are shown in Figure 5. The result showed that MRSA isolates survived a wide range of pH; the isolates from the children's ward and eye clinic survived in the pH range of 3 to 11, while others survived in the pH range of 4 to 11, with optimum growth pH at 7.0.

Effects of salt concentration on MRSA isolated from different wastewater sources in selected hospitals in Akure

The effects of salt concentration on MRSA isolated from different wastewater sources in selected hospitals in Akure are shown in Figure 6. It was noted that all the MRSA survived the salt concentrations between 0 and 30%; however, the isolates from the eye clinic survived better than other isolates within these ranges of salt concentrations.

Table 1. Bacterial Counts of wastewater collected from UNIMED Teaching Hospital Akure, Nigeria

Wastewater sampling points	Total bacterial counts (cfu/ 100 mL)	Total staphylococcal counts (cfu/100 mL)
Chemical Laboratory	421.08±1.41^{c}	1.65±0.10^{b}
Microbiology Laboratory	873.08±1.32^{f}	10.02±0.43^{c}
Eye Clinic	672.08±1.19^{e}	21.04±0.59^{d}
Community Clinic	471.38±0.55^{d}	0.00±0.00^{a}
Blood bank	743.09±0.08^{e}	0.00±0.00^{a}
MLS Laboratory	743.44±0.60^{e}	220.14±1.06^{g}
Antenatal	721.07±0.42^{e}	20.07±0.21^{d}
Post natal	801.47±1.30^{ef}	39.22±0.62^{e}
Accident and Emergency	877.91±1.55^{ef}	77.61±0.50^{f}
Pharmacy	516.03±0.70^{d}	11.14±0.31^{c}
Laundry	293.06±1.09^{b}	11.06±0.51^{c}
Water source	49.72±0.86^{a}	0.00±0.00^{a}

Note: Values are presented as mean ± standard error, values in the same column carrying the same superscript are not significantly different at $p<0.05$ using the new Duncan Multiple Range test

Table 2. Bacterial counts of wastewater collected from FUTA Health Center Akure, Nigeria

Wastewater sampling points	Total bacterial counts (cfu/ 100 mL)	Total staphylococcal counts (cfu/100 mL)
Nurses' station	81.66±0.08^{b}	7.14±0.08^{c}
Children's ward	94.43±1.31^{c}	17.05±0.50^{d}
Doctor's station	241.58+1.44^{d}	60.11±0.11^{e}
Laundry	62.11±1.58^{a}	15.041±0.55^{d}
Health center entrance	291.17±1.83^{e}	4.53±0.14^{b}
Wound treatment ward	422.05±1.55^{f}	1.23±0.07^{a}
Water source	73.71±0.72^{a}	1.02±0.11^{a}

Note: Values are presented as mean ± standard error, values in the same column carrying the same superscript are not significantly different at $p<0.05$ using the new Duncan Multiple Range test

Table 3. Occurrence of Bacteria in Wastewater from UNIMED Teaching Hospital and FUTA Health Center Akure, Nigeria

Wastewater Sampling Points	*Aeromonas hydrophila*	*Bacillus cereus*	*Bacillus subtilis*	*Citrobacter freundii*	*Enterobacter aerogenes*	*Escherichia coli*	*Klebsiella pneumonia*	*Proteus mirabilis*	*Pseudomonas aeruginosa*	*Salmonella typhi*	*Staphylococcus aureus*
UNIMED											
Chemical Laboratory	-	+	-	-	-	+	-	-	+	-	+
Microbiology Laboratory	-	+	-	+	-	+	-	+	-	+	+
Eye clinic	-	+	+	-	-	+	+	-	-	-	+
Community clinic	-	-	+	+	-	+	+	-	-	-	+
Blood bank	-	-	+	+	-	-	-	-	-	-	-
MLS laboratory	-	+	-	-	+	+	+	-	-	-	+
Antenatal	-	+	+	+	-	+	-	-	-	-	+
Post natal	-	+	-	-	-	+	-	+	+	+	+
Accident and Emergency	-	-	+	-	-	+	-	-	-	-	+
Pharmacy	-	-	-	-	+	-	+	-	-	-	+
Laundry	-	-	-	-	-	+	-	-	-	-	+
Water source	-	-	-	-	-	+	-	-	-	-	-
Total = 47	0(0)	6(12.77)	5(10.64)	4(8.51)	2(4.26)	10(21.28)	4(8.51)	2(4.26)	2(4.26)	2(4.26)	10(21.28)
FUTA Health Center`											
Nurses' station	-	-	-	+	-	+	-	-	-	-	+
Children's ward	-	-	-	-	-	-	-	-	+	-	+
Doctor's station	-	-	-	-	+	-	-	-	-	-	+
Laundry	-	-	-	+	-	-	-	-	-	-	+
Health center entrance	-	+	-	-	+	-	-	-	-	-	-
Wound treatment ward	+	+	+	-	-	-	-	-	-	-	+
Water source	-	-	-	-	-	+	-	-	+	-	+
Total = 18	1(5.56)	2(11.11)	1(5.56)	2(11.11)	2(11.11)	2(11.11)	0(0)	0(0)	2(11.11)	0(0)	6(33.33)

Note: +: Present in the sample, -: Absent in the sample

Table 4. Primers used for the identification of *Staphylococcus* species and the detection of antibiotic resistant marker genes

Primers	Primer Sequence (5′–3′)	PCR Conditions	Size (bp)
Staphylococcus spp.	27F - 5′GAGTTTGATCATGGCTCAG3′ 1492R - 5′GGTTACCTTGTTACGACTT3′	1 cycle of 2min at 95°C; 35 cycles of 30 sec at 94°C; 30sec at 53°C for, 1 min at 72°C; 1 cycle 10 min at 72°C	1500
mecA gene	F - 5′AACGATTGTGACACGATAGCC3′ R - 5′GGGATCATAGCGTCATTATC3	1 cycle of 5min at 94°C; 30 cycles of 30s at 94°C; 30sec at 55oC; 1 min at 72°C; 1 cycle of 10 min at 72°C	527

Table 5. Physicochemical Parameters of Wastewater from UNIMED Teaching Hospital and FUTA Health Center Akure, Nigeria

Sample source	pH	DO (mg/L)	COD (mg/L)	BOD (mg/L)	BOD:COD
A	5.41±0.41^{ab}	5.13±0.43^{b}	280.03±2.32^{d}	8.92±0.82^{b}	0.03
B	7.38±0.31^{b}	6.04±1.83^{bc}	170.11±3.07^{d}	4.86±0.11^{a}	0.03
C	8.42±0.03^{b}	4.02±0.04^{b}	123.31±3.41^{d}	9.07±0.08^{b}	0.07
D	5.53±0.46^{ab}	3.10±0.55^{a}	143.06±1.03^{d}	11.06±0.26^{b}	0.08
E	8.26±0.12^{b}	5.06±0.07^{b}	219.04±5.07^{d}	9.02±0.33^{b}	0.04
F	8.42±0.22^{b}	8.11±0.64^{d}	280.33±4.03^{d}	5.01±0.39^{a}	0.02
G	7.11±0.05^{b}	6.82±1.32^{c}	7.86±0.82^{a}	4.29±0.06^{a}	0.55
H	5.31±0.62^{a}	7.53±0.32^{d}	8.31±1.02^{a}	4.88±0.05^{a}	0.59
I	6.48±0.01^{b}	4.16±0.07^{b}	155.39±4.06^{d}	8.63±0.51^{b}	0.06
J	6.77±0.01^{b}	5.62±0.41^{b}	293.06±2.22^{d}	7.03±0.04^{b}	0.02
K	7.03±0.03^{b}	2.01±0.02^{a}	931.44±5.06^{e}	11.73±0.93^{b}	0.01
L	7.41±0.48^{b}	8.31±0.11^{d}	5.11±0.05^{a}	4.81±0.22^{a}	0.94
M	8.29±1.32^{b}	6.54±0.71^{c}	9.42±0.31^{b}	5.22±1.28^{a}	0.55
N	8.93±0.74^{b}	6.93±0.07^{c}	6.17±0.71^{a}	4.82±0.93^{a}	0.78
O	7.16±0.86^{b}	7.32±0.61^{d}	10.32±0.42^{b}	5.02±0.11^{a}	0.49
P	5.93±0.12^{b}	6.34±0.73^{c}	11.63±1.06^{b}	5.38±0.08^{a}	0.46
Q	9.82±1.33^{c}	2.04±0.61^{a}	34.16±2.65^{b}	14.57±0.55^{c}	0.43
R	6.83±0.06^{b}	5.72±0.54^{b}	43.26±1.32^{bc}	10.31±0.03^{b}	0.24
S	6.59±0.05^{b}	5.32±1.03^{b}	721.05±0.63^{e}	9.42±0.52^{b}	0.01
T	7.31±0.22^{b}	8.22±0.55^{d}	5.32±0.07^{a}	3.68±0.07^{a}	0.69
EPA	7.0 - 8.5	6 - 9.5	3.0 - 900	<5.0	

Note: Values are means ± SE for samples. Values in the same column carrying the same superscript are not significantly different at ($p \leq 0.05$) using the Duncan's New Multiple Range test. A: Chemical Laboratory, B: Microbiology Laboratory C: Eye clinic, D: Community clinic E: Blood bank, F: MLS laboratory, G: Antenatal, H: Post natal, I: Accident and Emergency, J: Pharmacy, K: Laundry (UNIMED), L: Water source (UNIMD), M: Nurses' station, N: Children's ward, O: Doctor's station, P: Oda Road, Q: Laundry (FUTA), R: Health center entrance, S: Wound treatment ward, T: Water source (FUTA), EPA: environmental protection agency Standards. DO: Dissolved Oxygen, COD: Chemical Oxygen Demand, BOD: Biochemical Oxygen Demand

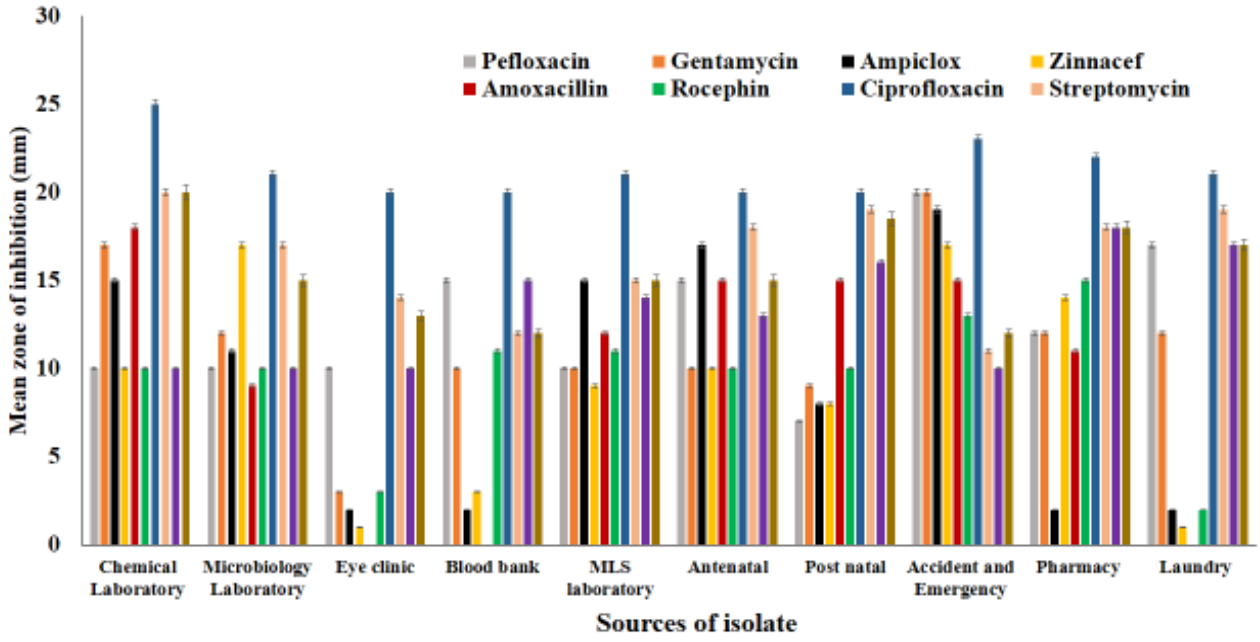

Figure 1. Antibiotic susceptibility profiles of *Staphylococcus aureus* isolated from wastewater in UNIMED Teaching Hospital Akure, Nigeria

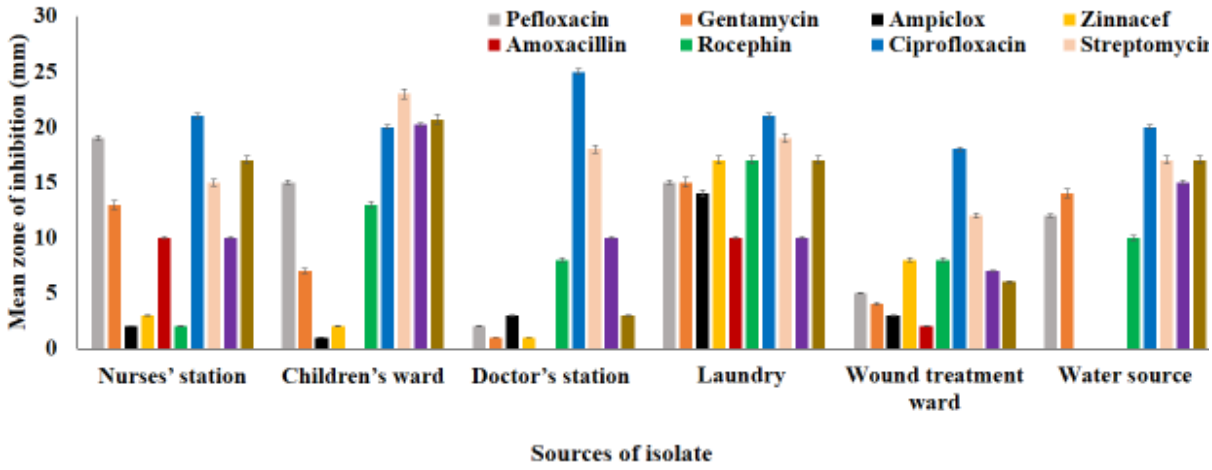

Figure 2. Antibiotic susceptibility profiles of *Staphylococcus aureus* isolated from wastewater in FUTA Health Center Akure, Nigeria

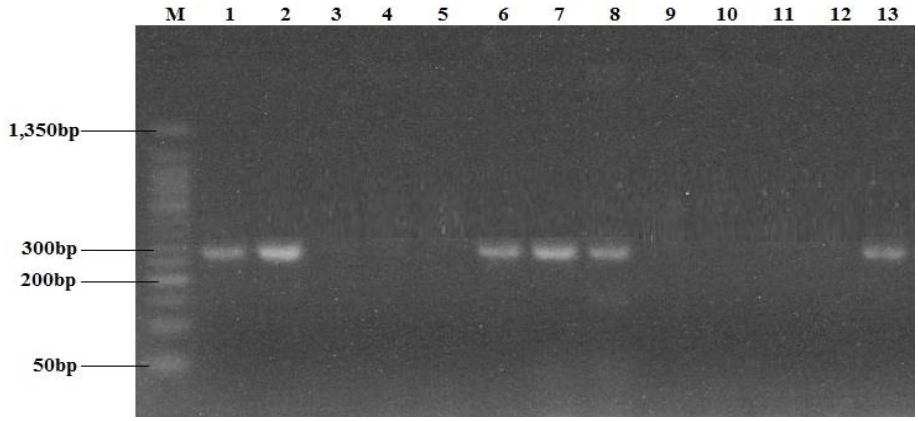

Figure 3. Agarose gel electrophoresis of amplified *MecA* gene (300 bp) in antibiotic resistant *Staphylococus aureus* from hospital wastewaters in Akure, Nigeria. M: 50 bp ladder, Wells 1 (Eye clinic), 2 (Post natal), 6 (Nurses' station), 7 (Children's ward), 8 (Doctor's station) and 13 (Wound treatment ward) showed positive amplification of *MecA* gene

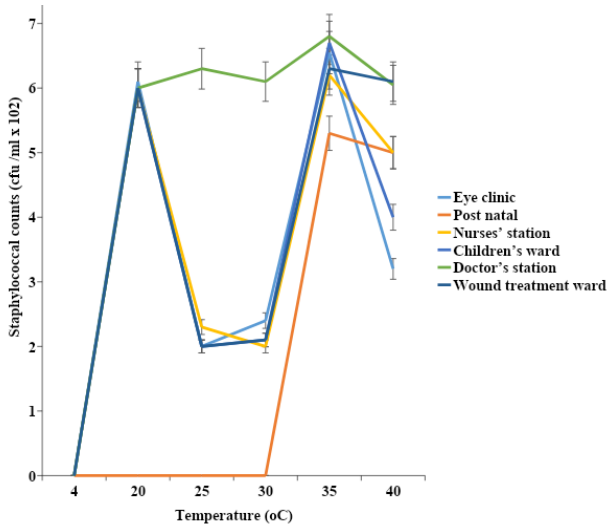

Figure 4. Effects of temperature on MRSA isolated from different wastewater sources in selected hospitals in Akure, Nigeria

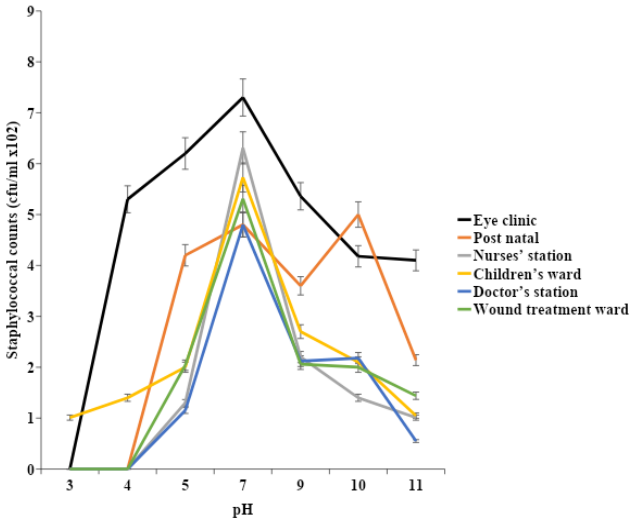

Figure 5. Effects of pH on MRSA isolated from different wastewater sources in selected hospitals in Akure, Nigeria

Agarose gel electrophoresis of plasmids in MRSA isolated from different wastewater sources in selected hospitals in Akure, Nigeria

Agarose gel electrophoresis of plasmids in MRSA isolated from different wastewater sources in selected hospitals in Akure is shown in Figure 7. It was noted that all the MRSA isolates had one (1) to three (3) plasmids of different molecular weights. Plasmids with the highest molecular weight were observed in the children's ward (80 kbp), while those with the lowest molecular weight were observed in the eye clinic (3 kbp).

The plasmid size and post plasmid curing resistance patterns of MRSA isolated from different wastewater sources in selected hospitals in Akure

The plasmid size and post-plasmid curing resistance patterns of MRSA isolated from different wastewater sources in selected hospitals in Akure are shown in Table 7. The number of plasmids did not correlate to the phenotypic antibiotic-resistant patterns; the resistance observed in isolates from the postnatal ward with plasmid size 4.5 kbp was plasmid-mediated; also, after plasmid curing, it was noted that the resistance to oxacillin, gentamicin, ampiclox, amoxicillin, pefloxacin, erythromycin, and septrin by MRSA was plasmid-mediated.

Table 6. Multiple antibiotic resistant patterns of *Staphylococcus aureus* isolated from wastewater in UNIMED Teaching Hospital and FUTA Health Center Akure, Nigeria

Wastewater sampling points	Antibiotics Used											Multiple Antibiotic-Resistant Index
	Oxacillin	Septrin	Erythromycin	Perfloxzcin	Gentamicin	Ampiclox	Zinnacef	Amoxicillin	Rocephin	Ciprofloxacin	Streptomycin	
UNIMED												
Chemical Laboratory	S	I	S	I	S	S	I	S	I	I	S	-
Microbiology Laboratory	I	I	I	I	I	I	I	R	I	S	I	0.10
Eye clinic	R	I	I	I	R	R	R	R	R	S	I	0.55
Blood bank	I	S	S	S	S	R	R	R	S	S	S	0.27
MLS laboratory	I	S	S	I	S	S	R	S	I	S	S	0.10
Antenatal	S	I	S	S	I	S	I	S	I	S	S	-
Post natal	S	S	S	R	R	R	R	I	S	S	S	0.36
Accident and Emergency	S	I	I	S	S	S	S	S	I	S	I	-
Pharmacy	R	S	S	I	I	R	I	I	I	S	S	0.18
Laundry	R	S	S	S	I	R	R	R	R	S	S	0.45
FUTA Health Center												
Nurses' station	R	I	S	S	I	R	R	I	R	S	S	0.36
Children's ward	R	S	S	S	R	R	R	R	S	S	S	0.45
Doctor's station	R	I	R	R	R	R	R	R	R	S	S	0.73
Laundry	S	I	S	S	S	S	S	I	S	S	S	-
Wound treatment ward	R	R	R	R	R	R	R	R	R	S	I	0.82
Water source	I	S	S	I	S	R	R	R	I	S	S	0.27
Percentage resistance	7 (43.75)	1 (6.25)	2 (12.50)	3 (18.75)	5 (31.25)	10 (62.50)	10 (62.50)	8 (50.00)	5 (31.25)	0	0	

Note: R: Resistance, I: Intermediate, S: Susceptible

Table 7. The plasmid size and post plasmid curing resistance patterns of MRSA isolated from different wastewater sources in selected hospitals in Akure, Nigeria

Bacterial strain	Plasmid size (kbp)	Phenotypic resistance patterns	
		Resistance patterns before plasmid curing	Post plasmid curing resistance patterns
Staphylococcus aureus	3, 10, 50	OX GEN AMP AMX Z R	Z R
Staphylococcus aureus	4.5	PFX GEN AMP Z	-
Staphylococcus aureus	25	OX AMP Z R	Z R
Staphylococcus aureus	50, 80	OX GEN AMP Z AMX	GEN Z
Staphylococcus aureus	4	OX ERY PFX GEN AMP Z AMX R	OX AMP AMX R
Staphylococcus aureus	25	OX S ERY PFX GEN AMP Z AMX R	S ERY Z R

Note: 1**.** Eye clinic, 2. Post natal, 3. Nurses' station, 4. Children's ward, 5. Doctor's station, and 6. Wound treatment ward**,** OX: Oxacillin, GEN: Gentamicin, AMP: Ampiclox, AMX: Amoxicillin, R: Rocephin, Z: Zinnacef, PFX: Pefloxacin, ERY: Erythromycin, S: Septrin, kbp: kilobase pair

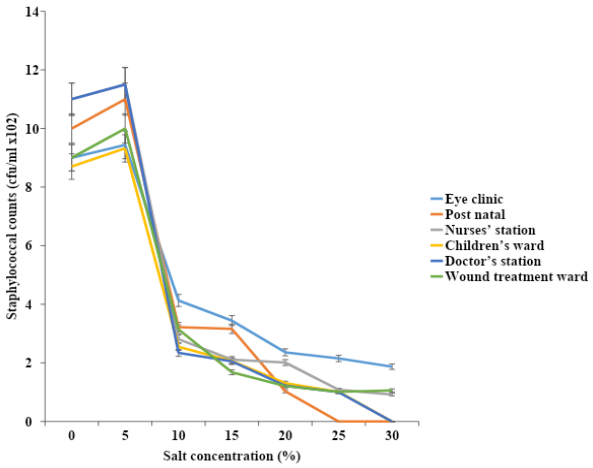

Figure 6. Effects of salt concentration on MRSA isolated from different wastewater sources in selected hospitals in Akure, NIgeria

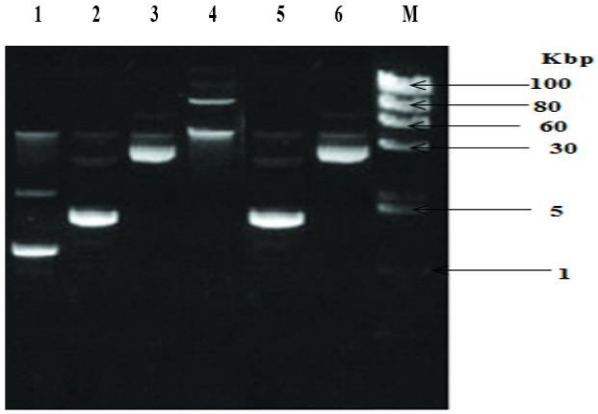

Figure 7. Agarose gel electrophoresis of plasmid in MRSA isolated from different wastewater sources in selected hospitals in Akure, Nigeria. M: 100 bp ladder, Wells 1. Eye clinic, 2. Post natal, 3. Nurses' station, 4. Children's ward, 5. Doctor's station, and 6. Wound treatment ward showed the plasmid

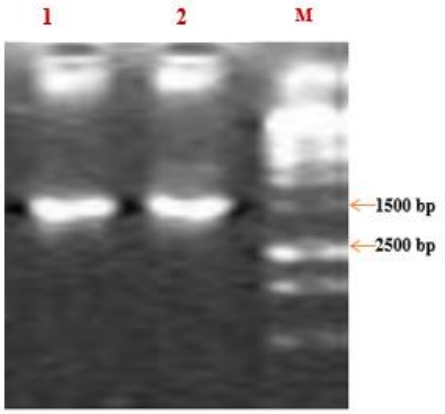

Figure 8. Agarose gel electropherogram of 16S rRNA gene of *Staphylococcus aureus* isolated from wastewater in UNIMED Teaching Hospital and FUTA Health Center Akure, NIgeria. Note: Line 1-2: Bacterial isolates, M: Molecular marker 1kb DNA ladder

Molecular detection of *Staphylococcus aureus* isolated from wastewater in UNIMED Teaching Hospital and FUTA Health Center Akure

The agarose gel electrophoretogram of the 16S rRNA gene of *Staphylococcus aureus* isolated from wastewater at UNIMED teaching hospital and FUTA health center Akure is shown in Figure 8. The 16S rRNA of MRSA was amplified at 1500 bp.

Discussion

To evaluate the risk to human health, it is imperative to ascertain the present state of *S. aureus* in the aquatic environment. Wastewaters, including the tap water used as a control, that was collected in this study from different locations in hospitals were contaminated with bacteria. The presence of bacteria in hospital wastewater was reported in previous research, stating that there is a presence of residual bacteria in hospital wastewater (Rowe et al. 2017; Mehanni et al. 2023). There was a presence of *S. aureus* in hospital wastewater, and higher staphylococcal counts were observed in samples collected from the MLS laboratory and doctor's station at UNIMED and FUTA, respectively. Although the counts were less than what was reported by Rice et al. (2012), who reported bacterial counts of 67 x 10^7 CFU in the untreated wastewater outlet pipe of Beni-Suef University Hospital, The presence of bacteria, especially *S. aureus*, in hospital wastewater justified the statement that hospital wastewaters are hot spots for the dissemination of bacteria that could pose a threat to public health (Rizzo et al. 2013; Yuan and Pia 2023).

Different bacterial species were present in the wastewater examined in this study, *Bacillus subtilis*, *Escherichia coli*, and *S. aureus* dominated in UNIMEDTH wastewater while *S. aureus* dominated the wastewater from FUTA (Table 3) and this could be as a result of the source of the water used at both hospitals.

In this study, the MLS laboratory and doctor's station could be the major hotspots for the dissemination of bacteria into the environment. The differences in microbial diversity of these wastewaters could be due to the degree of pollutant, type of pharmaceutical, chemical disinfectant, hospital general practices, and antibiotic-resistant patterns of the bacteria in the wastewater (Kumar et al. 2017; Azuma et al. 2022). Also, differences in the bacterial composition of wastewater have been reported to vary from region to region and country to country (Adachi et al. 2016; Mackul'ak et al. 2021; Azuma et al. 2022).

The findings of this study support the need for further research by considering different hospital practices and chemical or pharmaceutical pollutants that are present in the wastewater. In most hospitals, the BOD and COD concentrations of wastewater are almost equal to domestic wastewater values. In another study, the averages of BOD and COD in the wastewater of Tehran hospitals were 444.3 mg/L and 792 mg/L, respectively (Tchobanoglous et al. 2004). In this study, the pH, DO, COD, and BOD of the wastewaters ranged from 5.31±0.62 to 8.93±0.74, 2.01±0.02 mg/L to 8.31±0.11 mg/L, 5.11±0.05 mg/L to 931.44±5.06 mg/L and 3.68±0.07 mg/L to 11.73±0.93 mg/L respectively. The ratio of BOD and COD in some

samples was less than 0.03. The lower BOD-to-COD ratio seen in some wastewater samples could be because the sample contains non-biodegradable substances. The high biodegradability of organic matter is very desirable from the viewpoint of wastewater treatment and promotes the efficiency of wastewater treatment plants (Mesdaghinia et al. 2009). Hospital wastewater effluents contain pathogenic microorganisms, partially metabolized pharmaceuticals, radioactive elements, heavy metals, and toxic chemicals (Mehanni et al. 2023), which may have influenced the physicochemical parameters of the wastewater. The *S. aureus* isolates showed varying proportions of resistance to ampiclox, amoxicillin, oxacillin, rocephin, gentamicin, pefloxacin, erythromycin, and septrin. The abundance of antimicrobial-resistant *S. aureus* in hospital wastewater has been reported (Azuma et al. 2022; Mehanni et al. 2023); their resistance to these antibiotics could be because the antibiotics were mostly used in these hospital settings. Antibiotic-Resistant *S. aureus* (ARSA) is classified as a high-priority bacterium in hospital wastewater; however, all ARSA should be screened for the presence of the methicillin-resistant gene (Azuma et al. 2022). Therefore, there is a need for further study to determine if the *S. aureus* isolates are Methicillin-resistant.

The majority of the antibiotic-resistant *S. aureus* isolates from the two hospitals had a Multiple Antibiotic Resistance index (MARi) greater than 0.3. MARi greater than 0.3 has been attributed to the overuse of antibiotics (Sharkir et al. 2021). Therefore, the resistance shown by the *S. aureus* isolates in this study could be a result of the use of antibiotics in hospital environments. In this study, 37.5% of *S. aureus* isolates harbored the *mecA* gene. The presence of *mecA* genes in *S. aureus* indicates the resistance of the isolates to methicillin. A higher presence of MRSA has been reported by Hiramatsu et al. (2002), in wastewater generated from industry, hospitals, and domestic activities, respectively.

In this study, MRSA isolates were able to survive different ranges of temperature, pH, and salt concentrations. The staphylococcal cell membrane is rich in Fatty Acids (FAs) and lipid content, which are essential to its adaptive functions and acclimatization to environmental fluctuations. The survival of MRSA isolates in different environmental conditions is a public health challenge, as this could aid the fast dissemination of the isolates beyond the hospital environment. All the MRSA isolates in this study had plasmids. Possession of a plasmid by *Staphylococcus* could enhance its virulence and antibiotic-resistant ability (Akindolire et al. 2015). Also, resistance to oxacillin, gentamicin, ampiclox, amoxicillin, pefloxacin, erythromycin, and septrin by MRSA was plasmid-mediated, and this could pose an additional serious threat to public health as the plasmid could transfer the resistance to other non-antibiotic-resistant *S. aureus* in the environment.

ACKNOWLEDGEMENTS

The Federal University of Technology Akure Health Center's (FUTAHC), Nigeria, technical personnel provided support to the authors during the sample collection for this study, which is greatly appreciated.

REFERENCES

Achak M, Bakri SA, Chhiti Y, Alaoui FEM, Barka N, Boumy W. 2021. SARS-CoV-2 in hospital wastewater during outbreak of COVID-19: A review on detection, survival and disinfection technologies. Sci Total Environ 761: 143192. DOI: 10.1016/j.scitotenv.2020.143192.

Adachi F, Sekizuka T, Yamato M, Fukuoka K, Yamaguchi N, Kuroda M, Kawahara R. 2016. Characterization of fricarbapenemase-producing enterobacter spp. Isolated from a hospital and the environment in Osaka, Japan. J Antimicrob Chemother 76: 3061-3062. DOI: 10.1093/jac/dkab284.

Akindolire MA Babalola OO, Ateba CN. 2015. Detection of antibiotic resistant *Staphylococcus aureus* from milk: A public health implication. Intl J Environ Res Public Health 12 (9): 10254-10275. DOI: 10.3390/ijerph120910254.

Akya A, Chegenelorestani R, Shahvaisi-Zadeh J, Bozorgomid A. 2020. Antimicrobial resistance of *Staphylococcus aureus* isolated from hospital wastewater in Kermanshah, Iran. Risk Manag Health Policy 13: 1035-1042. DOI: 10.2147/RMHP.S261311.

Al Aukidy M, Al Chalabi S, Verlicchi P. 2017. Hospital wastewater treatments adopted in Asia, Africa, and Australia. In: Verlicchi P (eds). Hospital Wastewaters. The Handbook of Environmental Chemistry, vol 60. Springer, Cham. DOI: 10.1007/698_2017_5.

Azuma T, Murakami M, Sonoda Y, Ozaki A, Hayashi T. 2022. Occurrence and quantitative microbial risk assessment of Methicillin-Resistant *Staphylococcus aureus* (MRSA) in a Sub-Catchment of the Yodo River Basin, Japan. Antibiotics 11: 1355. DOI: 10.3390/antibiotics11101355.

Cheesbrough M. 2014. District Laboratory Practice in Tropical Countries. 2nd Ed. Cambridge University Press, Cambridge, UK. DOI: 10.1017/CBO9780511543470.

Committee for Clinical Laboratory Standards (CLSI). 2017. Performance Standards for Antimicrobial Susceptibility Testing; Twenty-Seventh Informational Supplement. CLSI document M100-S27 Wayne, PA.

Fawole, M. O. and Oso, B. A. 2004. Characterization of Bacteria: Laboratory Manual of Microbiology. 4th Edition, Spectrum Book Ltd., Ibadan, Nigeria, 24-33. DOI. 10.1007/0-387-30741-9_4.

Garcia AB, Vinuela-Prieto JM, Lopez-Gonzalez L, Candel FJ. 2017. Correlation between resistance mechanisms in *Staphylococcus aureus* and cell wall and septum thickening. Infect Drug Resist 10: 353-356. DOI. 10.2147/IDR.S146748.

Haaber J, Penadés JR, Ingmer H. 2017. Transfer of antibiotic resistance in *Staphylococcus aureus*. Trends Microbiol 25 (11): 893-890 DOI: 10.1016/j.tim.2017.05.011.

Hiramatsu K, Katayama Y, Yuzawa H, Ito T. 2002. Molecular genetics of methicillin-resistant *Staphylococcus aureus*. Intl J Med Microbiol 292 (2): 67-74. DOI: 10.1078/1438-4221-00192.

Kumar S, Lekshmi M, Parvathi A, Nayak BB, Varela MF. 2017. Antibiotic resistance in seafood-borne pathogens. In: Singh OV (eds). Foodborne Pathogens and Antibiotic Resistance, First Edition. John Wiley & Sons, Hoboken, New Jersey. DOI: 10.1002/9781119139188.ch17.

López A, Rodríguez-Chueca J, Mosteo R, Gómez J, Rubio E, Goñi P, Ormad MP. 2019. How does urban wastewater treatment affect the microbial quality of treated wastewater? Proc Safe Environ Protec 130: 22-30. DOI: 10.1016/j.psep.2019.07.016.

Mackul'ak T, Cverenkárová K, Vojs Staˇnová A, Fehér M, Tamáš M, Škulcová AB, Gál M, Naumowicz M, Špalková V, Bírošová L. 2021. Hospital wastewater—Source of specific micropollutants, antibiotic-resistant microorganisms, viruses, and their elimination. Antibiotics 10: 1070. DOI.10.3390/antibiotics10091070.

Marwan AB, Gabrielle CH, Pauline FT, Corinne BL, Djamel DR. 2014. Effects of growth, temperature, surface type, and incubation time on resistance of Staphylococcus aureus biofilms to disinfectants. Appl

Microb Cell Physiol 98: 2597-2607. DOI: 10.1007/s00253-013-5479-4.

Mehanni MM, Gadow SI, Alshammari, FA, Modafer Y, Ghanem KZ, El-Tahtawi NF, Homosy RF, Hesham AEL. 2023. Antibiotic-resistant bacteria in hospital wastewater treatment plant effluent and the possible consequences of its reuse in agricultural irrigation. Front Microbiol 14: 1141383. DOI: 10.3389/fmicb.2023.1141383.

Meng XZ, Venkatesan AK, Ni YL, Steele JC, Wu LL, Bignert A. 2016. Organic contaminants in Chinese sewage sludge: a meta-analysis of the literature of the past 30 years. Environ Sci Technol 50: 5454-5466. DOI: 10.1021/acs.est.5b05583.

Mesdaghinia A, Nadafi K, Nabizadeh NR, Saeidi R, Zamanzade M. 2009. Wastewater characteristics and appropriate method for wastewater management in the hospitals. Iran J Public Health 38: 34-40.

Natàlia C, Tobias O, Lucas S, Alexander E. 2019. Comparison of four DNA extraction methods for comprehensive assessment of 16S rRNA bacterial diversity in marine biofilms using high-throughput sequencing. FEMS Microbiol Lett 364: 14. DOI: 10.1093/femsle/fnx139.

Oladipo AO, Oladipo OG, Cornelius C. 2019. Multi-drug resistance traits of methicillin-resistant *Staphylococcus aureus* and other Staphylococcal species from clinical and environmental sources. J Water Health 17 (6): 930-943. DOI: 10.2166/wh.2019.177.

Olutiola PO, Famurewa O, Sonntag HG. 2018. An Introduction to General Microbiology, A Practical Approach. Heidelberger Verlagsanstalt und Druckerei GmbH, Heidelberg. DOI: 10.1007/978-3-662-00449-4.

Rice EW, Baird RB, Eaton AD, Clesceri LS. 2012. Standard Methods for the Examination of Water and Wastewater. American Public Health Association, Washington DC.

Rizzo L, Manaia C, Merlin C, Schwartz T, Dagot C, Ploy MC, Michael I, Fatta-Kassinos D. 2013. Urban wastewater treatment plants as hotspots for antibiotic resistant bacteria and genes spread into the environment. Sci Total Environ 447: 345-360. DOI: 10.1007/978-3-662-00449-4.

Rowe WP, Baker-Austin C, Verner-Jeffreys DW, Ryan JJ, Micallef C, Maskell DJ, Pearce GP. 2017. Overexpression of antibiotic resistance genes in hospital effluents over time. J Antimicrob Chemother 72: 1617-1623. DOI.10.1093/jac/dkx017.

Sharkir ZM, Alhatami AO, Khudhair YI, Abdulwahab HM. 2021. Antibiotic resistance profile and multiple antibiotic resistance index of Campylobacter species isolated from poultry. Arch Razi Inst 76 (6): 1677-1686. DOI: 10.22092/ARI.2021.356400.1837.

Tchobanoglous G, Burton F, Stensel H. 2004. Wastewater Engineering-Treatment and Reuse. McGraw-Hill Education, New York.

Tong SY, Davis JS, Eichenberger E, Holland TL, Fowler Jr VG. 2015. *Staphylococcus aureus* infections: Epidemiology, Pathophysiology, Clinical Manifestations, and Management. Clin Microbiol Rev 28 (3): 603-661. DOI: 10.1128/cmr.00134-14.

Verlicchi P, Al Aukidy M, Zambello E. 2015. What have we learned from worldwide experiences on the management and treatment of hospital effluent? An overview and a discussion on perspectives. Sci Total Environ 514: 467-491. DOI: 10.1016/j.scitotenv.2015.02.020.

Verlicchi P, Galletti A, Petrovic M, Barcelo D. 2010. Hospital effluents as a source of emerging pollutants: An overview of micropollutants and sustainable treatment options. J Hydrol 389: 416-428. DOI: 10.1016/j.jhydrol.2010.06.005.

World Health Organization (WHO). 2016. Guidelines for Drinking-Water Quality 9th Ed. Vol. Geneva Pp. 1-16una. DOI: 10.3390/healthcare11020242.

Yuan T, Pia Y. 2023. Hospital wastewater as hotspots for pathogenic microorganisms spread into aquatic environment. Front Environ Sci 10: 1734. DOI: 10.3389/fenvs.2022.1091734.

Zheng HS, Guo WQ, Wu QL, Ren NQ, Chang JS. 2018. Electroperoxone pretreatment for enhanced simulated hospital wastewater treatment and antibiotic resistance genes reduction. Environ Intl 115: 70-78. DOI: 10.1016/j.envint.2018.02.043.

NUSANTARA BIOSCIENCE
Vol. 16, No. 1, pp. 130-138
May 2024

ISSN: 2087-3948
E-ISSN: 2087-3956
DOI: 10.13057/nusbiosci/n160116

First metagenome report of *Haemaphysalis bispinosa* ticks of Moa buffalo from Southwest Maluku District, Indonesia

PRASETYARTI UTAMI[1], RONY MARSYAL KUNDA[2,♥], YOFIAN ANAKTOTOTY[3]

[1]Program of Biology, Faculty of Sciences and Technology, Universitas Terbuka. Jl. Cabe Raya, Pondok Cabe, South Tangerang 15437, Banten, Indonesia

[2]Program of Biotechnology, Faculty of Mathematics and Natural Sciences, Universitas Pattimura. Jl. Ir. Putuhena, Poka, Ambon 97233, Maluku, Indonesia. Tel./fax.: +62-911-322626, ♥email: ronykunda14@gmail.com

[3]Graduate Program in Animal Biosciences, Department of Biology, Faculty of Mathematics and Natural Sciences, Institut Pertanian Bogor. Jl. Raya Dramaga, Bogor 16680, West Java, Indonesia

Manuscript received: 6 February 2024. Revision accepted: 14 April 2024.

Abstract. *Utami P, Kunda RM, Anaktototy Y. 2024. First metagenome report of* Haemaphysalis bispinosa *ticks of Moa buffalo from Southwest Maluku District, Indonesia. Nusantara Bioscience 16: 130-138.* Ticks are vectors of pathogenic organisms such as bacteria, protozoa, and viruses, which are potentially fatal to humans and livestock. *Haemaphysalis bispinosa* Neumann, 1897 is a tick species with three mammalian hosts in Asia and Australia, including Indonesia, with the highest infestation in cattle (*Bos taurus* Linnaeus, 1758) and sheep (*Ovis aries* Linnaeus, 1758). *H. bispinosa* is known to transmit many pathogens, but studies on the profile and structure of the microbiota are still very limited. This study aims to investigate the abundance and diversity of microbiota in *H. bispinosa* to evaluate the bacterial community's structure and to identify and examine potential zoonotic agents from Moa buffalo (*Bubalus bubalis* (Linnaeus, 1758). Amplification in this study used primers from the region (V1-V9) of the 16S rRNA gene. Metagenomic analysis shows that the microbiota community structure is dominated by non-zoonotic bacteria (96.83%), and zoonotic bacteria are found in the percentage (3.17%). Zoonotic agents were dominated by members of the genus *Rickettsia* (71.82%), *Ehrlichia* (19.19%), *Romboutsia* (3.16%), *Anaplasma* (2.43%), *Coxiella* (2.24%), *Staphylococcus* (0, 48%) and *Streptococcus* (0.43%). Overall, 16 species were found in *H. bispinosa*, i.e., 11 species belonging to the genus *Rickettsia*, 2 species from the genus *Ehrlichia* (i.e., *E. canis* and *E. minasensis*), and 1 species each belonging to the genera *Anaplasma*, *Coxiella*, and *Romboutsia.* It was concluded that the abundance of the microbial community in *H. bispinosa* based on metagenome analysis using the 16S rRNA gene from Moa buffalo in the Southwest Maluku District was classified as having a diverse abundance of species.

Keywords: *Haemaphysalis bispinosa*, microbiome, Moa buffalo, tick, vector-borne disease

INTRODUCTION

Ticks are vectors for pathogenic organisms such as bacteria, protozoa, and viruses that cause great suffering and potentially fatal human diseases (Khoo et al. 2016; Utami et al. 2021). Ticks also cause considerable losses to the livestock industry as they cause skin irritation and blood loss to the host (Muhammad et al. 2021). This reduces the elasticity of the skin epidermis and, at the same time, acts as a vector for many pathogens (Roy et al. 2018; Kim et al. 2021). *Haemaphysalis bispinosa* Neumann, 1897 is a tick species with three mammalian hosts found on the continents of Asia and Australia, with the highest infestation in cattle (*Bos taurus* Linnaeus, 1758) and sheep (*Ovis aries* Linnaeus, 1758). Petney et al. (2019) reported that in South Asia, there are about 97 tick species dominated by members of *Haemaphysalis*. Several field studies have shown that members of *Haemaphysalis* are commonly found on cattle (*B. taurus*) (Sahara et al. 2023) and recently reported on Moa buffalo (*Bubalus bubalis* (Linnaeus, 1758), Southwest Maluku District (Utami and Kunda 2023). *Haemaphysalis* is the second largest genus of the Ixodidae family, distributed in Australia, China, Indonesia, Japan, Malaysia, Nepal, New Zealand, Pakistan, Sri Lanka, Thailand, Myanmar, and Vietnam (Sahara et al. 2019; Utami and Kunda 2023). Sahara et al. (2019) reported that *H. bispinosa* were mostly reported in Java Island, while in other parts of Indonesia, they were rarely reported, including buffalo.

Several studies reported that tick species that most frequently infest Asian buffalo in Pakistan, i.e., *Rhipicephalus* (Boophilus) *microplus*, *R. turanicus*, *R. haemaphysaloides*, *R. annulatus*, *R. sanguineus* (Sensu Lato), *Hyalomma anatolicum, H. hussaini, H. isaaci, H. scupense, H. dromedarii, H. bispinosa, H. montgomeryi, H. cornupunctata, H. kashmirensis*, and *H. sulcata* (Karim et al. 2017; Ali et al. 2019; Rehman et al. 2019; Ghafar et al. 2020; Aiman et al. 2022). Corrêa et al. (2012) found 19 species of ticks that are parasitic on buffalo in India, i.e., *Amblyomma testudinarium, Nosomma monstrosum*, five species from the genus *Hyalomma*, nine species from the genus *Haemaphysalis* and three species from the genus *Rhipicephalus*.

Pathogenic bacteria transmitted by members of *Haemaphysalis* spp. were found in 946 bacterial genera with the highest abundance, i.e., *Lactobacillus, Coxiella, Rickettsia*, and *Muribaculum.* Moreover, *Rickettsia rickettsii, Rickettsia japonica, Candidatus Rickettsia jingxinensis, Anaplasma bovis, Ehrlichia ewingii, Ehrlichia chaffeensis, Coxiella* spp. and *Coxiella*-like endosymbiont

were detected in *Haemaphysalis* spp. (Zhao et al. 2021; Zeng et al. 2022a). These pathogens cause diseases, i.e., Rocky Mountain spotted fever, Siberian or North Asian typhus, Japanese spotted fever, and Australian spotted fever, human monocytic ehrlichiosis and canine ehrlichiosis; human granulocytic anaplasmosis, and bovine anaplasmosis; tularemia; Q fever, rabbit fever, Taylor disease, Crimean Congo hemorrhagic fever, and Lyme disease and tick-borne relapsing fever (Wu et al. 2013; Fang et al. 2015; Zhao et al. 2021). Besides carrying various disease-causing pathogenic bacteria, members of *Haemaphysalis* spp. also transmit several pathogenic parasites, i.e., *Theileria* spp, *Babesia* spp, and *Hepatozoon* spp. that cause tropical theileriosis, babesiosis in cattle, dogs, and sheep; and hepatozoonosis (Chen et al. 2019).

Currently, research results on the microbiome in Indonesia are rarely reported from various samples, including from ticks, even though the potential for ticks as a vector for transmitting various zoonotic agents in humans is very high (Levytska and Mushynskyi 2020). Although it is known that *H. bispinosa* ticks play an important role as pathogen vectors of various microbes, there is very little information about the profile and composition of the microbiota contained in these ticks. Studying the profile and composition of the microbiota found in *H. bispinosa* is interesting. In this study, we used high-throughput sequencing of the intact regions V1-V9 of the 16S rRNA gene to investigate the abundance and diversity of microbiome in *H. bispinosa* to evaluate the structure of the bacterial community to the identification and potential discovery of zoonotic pathogenic bacteria in Moa buffalo. This metagenomic data will be very helpful in mapping and tracing the potential pathology that these zoonotic agents will cause.

MATERIALS AND METHODS

Ethical approval

This study received approval from the Animal Ethics Committee at the Faculty of Veterinary Medicine, Universitas Gadjah Mada, Yogyakarta, Indonesia, following the procedures for using animal models for research purposes.

Study area

Tick specimens were collected from 50 local Moa buffalo (20 male and 30 female) in four different locations, i.e., Werwaru, Tounwawan, Klis, and Moain villages of Southwest Maluku District, Maluku Province, Indonesia (Figure 1). The buffalo were selected based on age and categorized as adults (3-4 years), which were found in local farmers. The sampling process was carried out from March until October 2023. Tick collection activities are carried out in the morning (07.00-08.30 WIT) and afternoon (17.30-18.30 WIT) following the time buffalo entered and left *Lutur* (stone cage). Farmers assist the sampling process because it avoids aggressive activities from buffalo.

Procedures

Sample collection, DNA preparation and extraction

A total of 85 Moa buffalo ticks (52 females and 33 males) were collected between March, May, and October 2023 (3 seasons of tick activity) using the flagging method in the afternoon during summer. Each tick was preserved in 70% alcohol solution in the Eppendorf tube, and samples were brought to the laboratory under cold conditions. The humidity and air temperature were measured in the morning and afternoon by using the temperature and humidity meter HTC-2. The ground surface was measured using GPS Garmin 11. Each tick was examined with a stereomicroscope (Olympus, Germany) using a dichotomous key and character matrix containing growth phase and sex by Anastos (1950).

Pre-PCR (Polymerase chain reaction) and PCR procedures are prepared with sterile equipment and sterile laboratory to avoid cross-contamination. Ticks were cleaned up for one minute in 70% ethanol to remove all microorganisms from the tick body surface. Then, the next process is homogenization by grinding each tick with phosphate-buffered PBS saline (without Ca2+ and Mg2+, pH=7.4). In the next step, samples were centrifuged, and the supernatant (300 µL) was used for DNA extraction. DNA Extraction was done with a spin column kit (EURx, Poland), according to the manufacturer's protocol with modifications. The quality and quantity of DNA were checked using a WPA UV1101 spectrophotometer (WPA The Old Station, Linton, Cambridge, UK) to ensure the presence of a minimum standard DNA concentration (10 ng/µL DNA). The further step was the DNA extract sample (100 µL) has been stored at -20°C.

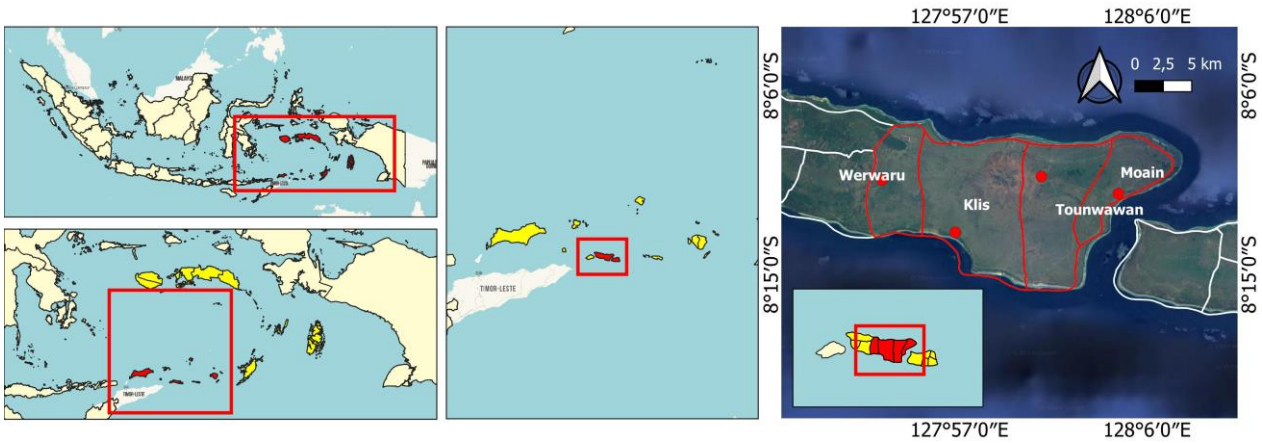

Figure 1. Map of tick sample collection in Southwest Maluku District, Maluku Province, Indonesia

Molecular analysis (PCR) for metagenomics uses 16S rRNA

Amplification of the 16S rRNA gene sequence was performed with Start-Warm HS-PCR Mix (A&A Biotechnology, Gdynia, Poland), ddWater (aseptic, free from nuclease-free water). The primer sequence used for amplifying the 16S rRNA gene is based on primer sequence 16S, full length (Nanopore). The primer sequence is the most suitable primer pair for NGS (27F: 5'- AGA GTT TGA TCM TGG CTC AG -3'; 1492R: 5'- GGT TAC CTT GTT ACG ACT T- 3'). The PCR protocol used in NGS analysis is as follows: pre-denaturation 95°C for 3 minutes, denaturation 25 x (95°C for 30 seconds, annealing 55°C for 30 seconds, elongation 72°C for 30 seconds), and post elongation 72°C for 5 minutes), then electrophoresed in a 2% agarose gel (Sigma-Aldrich, Germany) stained by using Midori Green (Nippon Genetics Europe GmbH, Germany) with electrophoresis at 90 volts for 45 minutes. The results of PCR amplicons were visualized using UV light in a 100 Gel Logic System (Kodak Imaging System, Inc., USA). The amplification product, which is 1500 bp in size, was selected for further metagenomic investigation (Nanopore MySeq).

NGS-metagenomic library preparation and sequencing

The NGS process was followed by using the Nanopore 16S metagenomic protocol (Nanopore MySeq, Inc., San Diego, California, USA). A DNA paired with the end library was created with an insert size (± 1500 bp) using a series primer for the variables V1 to V9 in the 16S rRNA region. The quantity and quality of the metagenomic libraries were evaluated by electrophoresis on 2200 Agilent TapeStation Instrument with Genomic DNA ScreenTape Assay (Agilent Technologies Inc., St Clara, CA, USA). Samples were pooled in equal proportions and sequenced for 600 cycles using the MiSeq Platform (Macrogen, Seoul, Korea) with v3 reagent (2 × 300 bp paired-end reads). 10% PhiX bacterial meta biome DNA was added to the sample as an internal control. Paired-end reads, recorded in FASTQ format. The FASTQ data was automatically demultiplexed and Macrogen conducted Nanopore adapters.

Data analysis

Data were analyzed using QIIME with high-throughput community sequencing data (Caparaso et al. 2010). The obtained Nanopore MySeq 16S rRNA sequences were clustered at 97% sequence similarity and analyzed with the Quantitative Insights into Microbial Ecology 2 (QIIME2) software package version 3.5.3 (Swei and Kwan 2017). The zoonotic profile was classified according to the etiological agent and divided into zoonotic and non-zoonotic microbe groups (Rahman et al. 2020).

RESULTS AND DISCUSSION

Metagenomic profile of *H. bispinosa* tick

A total of 85 adult *H. bispinosa* ticks were found in four villages, i.e., Werwaru (n=21), Tounwawan (n=22), Klis (n=21), and Moain (n=21) individuals. Molecular analysis showed that the relative abundance of the *Rickettsia* group reached ≥ 50% (very high) (Figure 4), which infested the bodies of *H. bispinosa* ticks. The *Paenibacillus* group has a lower relative abundance percentage than *Rickettsia*, i.e. ≤ 10%. The *Ehrlichia* and other microbial groups have a relatively small abundance percentage ≥ 1% (Figure 2).

Heatmap analysis

A total of 34 species of microbes were found in the results of this study based on heatmap analysis (Figure 3). Based on the heatmap results, three categories of microbial groups were found with high, medium and low abundance (Table 1). The abundance of microbial species that are categorized as high has a heatmap score > 15. The results of the heatmap analysis show that there are two microbes with a high heatmap category, i.e., *Ehrlichia minasensis* and *Rickettsia prowazekii*. The abundance of medium-category microbial species was found in species with a score of 5-10, i.e. *Coxiella burnetii*, *Ehrlichia canis*, *Rickettsia akari*, *Rickettsia australis*, *Rickettsia conorii*, *Rickettsia hoogstraalli*, *Rickettsia hulinii*, *Rickettsia tamurae*, and *Romboutsia timonensis*. The low scores (≤ 5) microbial groups were *Bacillus anthracis*, *Bacillus capparidis*, *Bacillus cytotoxicus*, *Bacillus licheniformis*, *Bacillus marcorestinctum*, *Bacillus oleivorans*, *Bacillus pseudoflexus*, *Bacillus pseudomycoides*, *Bacillus rhizoplanae*, *Bacillus tianmuensis*, *Bacillus laterosporus*, *Rickettsia asiatica*, *Rickettsia monacensis*, and *Rickettsia slovaca* (Figure 3; Table 1).

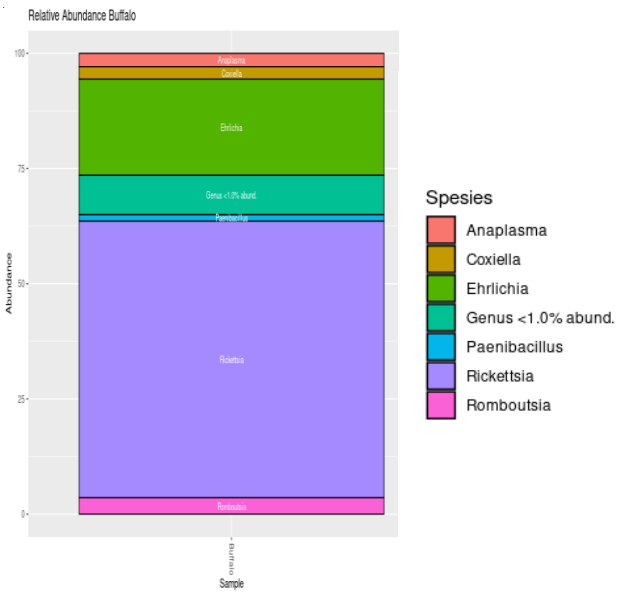

Figure 2. Relative abundance of potential pathogens at genus level

Table 1. Microbiome communities found in *H. bispinosa* (General explanation of microbiome characters and heatmap scoring)

Species name	Microbiome characters	Heatmap analysis range based on *present study*
Anaplasma phagocytophillum (Dixon and Bedenice 2019)	Human granulocytic anaplasmosis, tick-borne fever, equine ehrlichiosis.	< 5
Bacillus anthracis (Carlson et al. 2019)	Cutaneous, Inhalation, Gastrointestinal disease in animal and human	< 5
Bacillus capparidis (Wang et al. 2017)	Isolated from the surface-sterilized roots of a medicinal plant	< 5
Bacillus cytotoxicus (Cairo et al. 2021)	Member of the *Bacillus cereus* group with bacterial abilities to grow in high temperatures (> 52°C)	< 5
Bacillus licheniformis (Zeng et al. 2022b)	Found in the soil, on bird feathers, especially chest and back plumage, and most often in ground-dwelling birds and aquatic animal	< 5
Bacillus marcorestinctum (Zhong et al. 2022)	A Gram-positive, facultatively anaerobic, endospore-forming, and rod-shaped bacterium was found in soil.	< 5
Bacillus oleivorans (Azmatunnisa et al. 2015)	Two Gram-stain-positive, diesel oil-degrading, solvent-tolerant, aerobic, endospore-forming, rod-shaped bacteria were isolated from a contaminated laboratory plate.	< 5
Bacillus pseudoflexus (Chandna et al. 2016)	A Gram-stain-positive, motile, rod-shaped, endospore-forming moderately halophilic bacterium was isolated from compost.	< 5
Bacillus pseudomycoides (Elsharawy et al. 2023)	Members of the *Bacillus cereus* group species include *B. cereus*, *B. anthracis*, *B. thuringiensis*, *B. mycoides*, *B. pseudomycoides*, and *B. eihenstephanensis*	< 5
Bacillus rhizoplanae (Kampfer et al. 2022)	Isolated from the wheat rhizoplane, including aquatic bacteria.	< 5
Bacillus tianmuensis (Théatre et al. 2021)	Isolated from a soil sample, a gram-negative, endospore-forming, rod-shaped strain	< 5
Brevibacillus laterosporus (Ruiu 2013)	A unique canoe-shaped lamellar body attached to one side of the spore is a natural inhabitant of water, soil, and insects.	< 5
Coxiella burnetii (Mobarez et al. 2014)	An obligate intracellular, pleomorphic gram-negative rod-shaped bacteria that causes Q fever	5-10
Ehrlichia canis (Hmoon et al. 2021)	An obligate intracellular bacterium that acts as the causative agent of ehrlichiosis	5-10
Ehrlichia minasensis (Moura et al. 2019)	Tick-borne obligate intracellular gram-negative alphaproteobacteria of the family Anaplasmataceae	>15
Rickettsia akari (Szakacs et al. 2020)	An intracellular, gram-negative pathogen is the etiologic agent of rickettsialpox.	5-10
Rickettsia asiatica (Thu et al. 2019)	A tick-borne pathogenic species borne by *Ixodes ovatus*	< 5
Rickettsia australis (Stewart et al. 2017)	The etiologic agent of Queensland tick typhus (QTT)	5-10
Rickettsia conorii (Kamani et al. 2017)	Group of endotheliotropic infectious diseases caused by different species of genera *Rickettsia*	5-10
Rickettsia montanensis (Snellgrove et al. 2021)	Members of the genera *Rickettsia* range from nonpathogenic endosymbionts	< 5
Rickettsia honei (Parte et al. 2020)	A unique spotted fever group (SFG) agent that is pathogenic for humans	5-10
Rickettsia hoogstraalli (Reeves et al. 2020)	Substantial risks to both human and animal well-being	5-10
Rickettsia hulinii	A rickettsia pathogenic in humans	5-10
Rickettsia monacensis (Burkhardt et al. 2022)	Arthropod-associated gram-negative prokaryotes that reside within the cytoplasm and sometimes nuclei of eukaryotic host cells	< 5
Rickettsia parkeri (Lackman et al. 1965)	*R. parkeri* is closely related to *R. rickettsii*, the causative agent of Rocky Mountain spotted fever (RMSF)	< 5
Rickettsia prowazekii (Khan et al. 2023)	An obligate, intracellular, gram-negative coccobacillus belonging to the genera Rickettsia	>15
Rickettsia rhipicephali (ex Burgdorfer et al. 1978) Weiss and Moulder 1988	Obligate intracellular bacteria belonging to the spotted fever group of the genera *Rickettsia*	< 5
Rickettsia ricketsii (Brumpt 1922)	Rocky Mountain spotted fever (RMSF) is an acute febrile tick-borne illness caused by *Rickettsia rickettsii*	< 5
Rickettsia sibirica (Li et al. 2017)	The causative agent of Siberian tick typhus	< 5
Rickettsia slovaca (Sekeyová et al. 1998)	A pathogenic, tick-borne, spotted fever group (SFG) rickettsiae.	< 5
Rickettsia tamurae (Seo et al. 2021)	Registered spotted fever group rickettsiae.	5-10
Rickettsia tillamookensis (Gauthier et al. 2021)	Recognized typhus and spotted fever group *Rickettsia* species.	< 5
Romboutsia timonensis (Ricaboni et al. 2016)	A new bacterium isolated from the right human colon	5-10

Note: Heatmap score < 5: Low, 5-10: Moderate, > 15: High

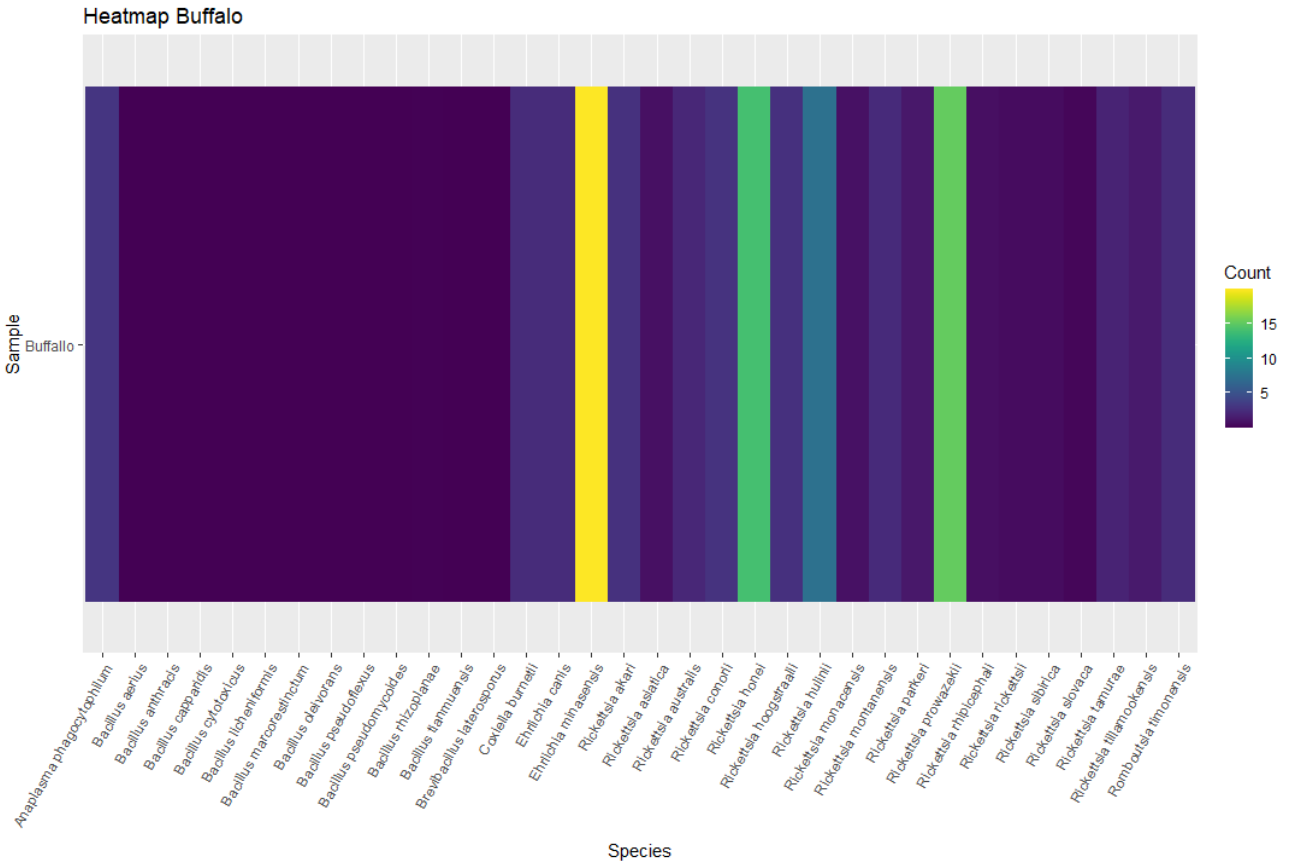

Figure 3. Heatmap of bacterial meta biome at the species level in Moa buffalo tick samples

Zoonotic profile in *H. bispinosa* tick

Analysis of zoonotic potential using the 16S rRNA gene shows that the highest percentage is found in the group of non-zoonotic bacteria. The group of bacteria classified as non-zoonotic reached 96.83%, while the group of zoonotic bacteria was 3.17% (Figure 5). Non-zoonotic microbial populations are quite high compared to the zoonotic microbial group. Zoonotic microbial population figures are dominated by the genus *Rickettsia* (71.82%), *Ehrlichia* (19.19%), *Romboutsia* (3.17%), *Anaplasma* (2.43%), *Coxiella* (2.24%), *Staphylococcus* (0 .48%) and *Streptococcus* (0.43%) (Figure 6). The results of this study indicate that members of the genus *Rickettsia* are the most dominant group of microbes found in *H. bispinosa* and have a high abundance.

Discussion

Utami and Kunda (2023) reported that the ticks found on Moa buffalo were dominated by the species *Dermacentor (Indocentor) auratus* (Supino, 1897) and *H. bispinosa* (Neumann, 1897). Research conducted by Jiao et al. (2021) shows that the genera *Rickettsia*, *Anaplasma*, and *Coxiella* are most commonly found compared to the species *Dermacentor nuttalli* and *Ixodes persulcatus*, which attack the bodies of cattle in Mongolia. These scientific findings are a preliminary study of metagenome community analysis of ticks that attack livestock in ecosystems with limited rainfall and green food sources, such as in the Moa buffalo habitat, and the sample identification in this study found only *H. bispinosa* ticks and no *D. auratus*. It is strongly suspected that the sampling period in the field was during the life cycle phase of *H. bispinosa*, so this species was often found.

The results of analysis at the species level showed that around 16 species of bacteria were found in Moa buffalo ticks, including 11 species from the genus *Rickettsia*, 2 species from the genus *Ehrlichia* (i.e., *E. canis* and *E. minasensis*), 1 species from the genus *Anaplasma* (*Anaplasma phagocytophilum*), 1 species belonging to the genus *Coxiella* (*C. burnetii*), and 1 species of the genus *Romboutsia* (*R. timonensis*). The relative abundance of *E. minasensis* species in Moa buffalo ticks indicates a high population. The relative abundance for the three species (*Rickettsia hoonei*, *R. hulinii*, and *R. prowazekii*) shows that the population figures for these three microbes are quite high after *E. minasensis* (Figure 4). The microbiota group that infests *H. bispinosa* ticks consists of various microbial genera and is non-zoonotic, while zoonotic ones are found in small numbers. Relative abundance values that vary in each genus and species of microorganisms are caused by climate and environmental factors, as well as interaction patterns of microbes with the environment (Cabezas-Cruz 2021).

Metagenome-based molecular analysis of the zoonotic potential of microbial communities will provide comprehensive basic data regarding the profile of the tick

H. bispinosa (Neumann 1897) as an ectoparasite of the Moa buffalo. The results obtained from this research are very useful for analyzing and investigating the potential of the Moa buffalo tick as a vector for carrying zoonotic agents. In addition, precautions need to be taken to identify potential risks of cross-infection. This cross-infection occurs from *Coxiella*, *Rickettsia*, *Anaplasma*, *Staphylococcus*, and *Streptococcus* members. The zoonotic agents can spread from ticks to humans or other animals. Molecular approaches to the microbial ecology of livestock origin provide a broad perspective on the application of epidemiological science (Riley and Blanton 2018). Metagenome analysis of the Moa buffalo tick identified it at the species level. The results of this research are very useful in studying epidemiological approaches, especially strategies for controlling microbial manifestations carried by Moa buffalo ticks (*H. bispinosa*). The results of metagenome analysis have identified the bacterial species *A. phagocytophilum* as a pathogen that weakens host cells immune system, especially the antimicrobial mechanism of neutrophils (Rikihisa 2011), granulocytic anaplasmosis fever in humans, and ehrlichiosis in horses (*Equus caballus* Linnaeus, 1758). The presence of *Bacillus* groups, including *Bacillus aerius, B. anthracis, B. capparidis, B. cytotoxicus, B. licheniformis, B. marcorestinctum, B. oleivorans, B. pseudoflexus, B. pseudomycoides, B. rhizoplanae*, and *B. tianmuensis* were classified into metabolically diverse groups. The *B. licheniformis* is a hematogenous bacterium that infects after entering the tick body from the digestive tract (Ramirez-Olea et al. 2022). The mechanism for microbial *entry* through the tick body starts from the opening of the mouth, which is accompanied by bleed feeding into the midgut. The virus or bacteria multiply and move to the ovaries and salivary glands and settle at the anus opening (Maqbool et al. 2022).

The *Bacillus* genus member in this study's results is *B. anthracis*. The results of this study show that the *B. anthracis* species can be found in *H. bispinosa*. Generally, *B. anthracis* is a pathogenic microbe that can damage the skin or enter through the mucosa (gastrointestinal anthrax) in livestock. The *B. anthracis* can carry out extracellular multiplication with simultaneous production of capsules and toxins (Spencer 2003). Generally, buffalo is one of the opportunistic hosts of *B. anthracis* (Bakhteeva and Timofeev 2022). There has never been any reported incidence of anthrax in Moa buffalo in Southwest Maluku District and in Maluku Province at large, but the results of metagenomic analysis prove the presence of *B. anthracis*, which was detected in *H. bispinosa*.

Members of *Bacillus* spp. i.e., *Bacillus cereus, Bacillus subtilis*, and *B. licheniformis* are associated with septicemia, endocarditis, meningitis, and infections of wounds, ears, eyes, respiratory tract, urinary tract, and gastrointestinal tract. *B. cereus* can also cause two different food poisoning syndromes, including vomiting syndrome with rapid symptoms characterized by nausea and vomiting and diarrhea syndrome with slow symptoms (Senesi and Ghelardi 2010).

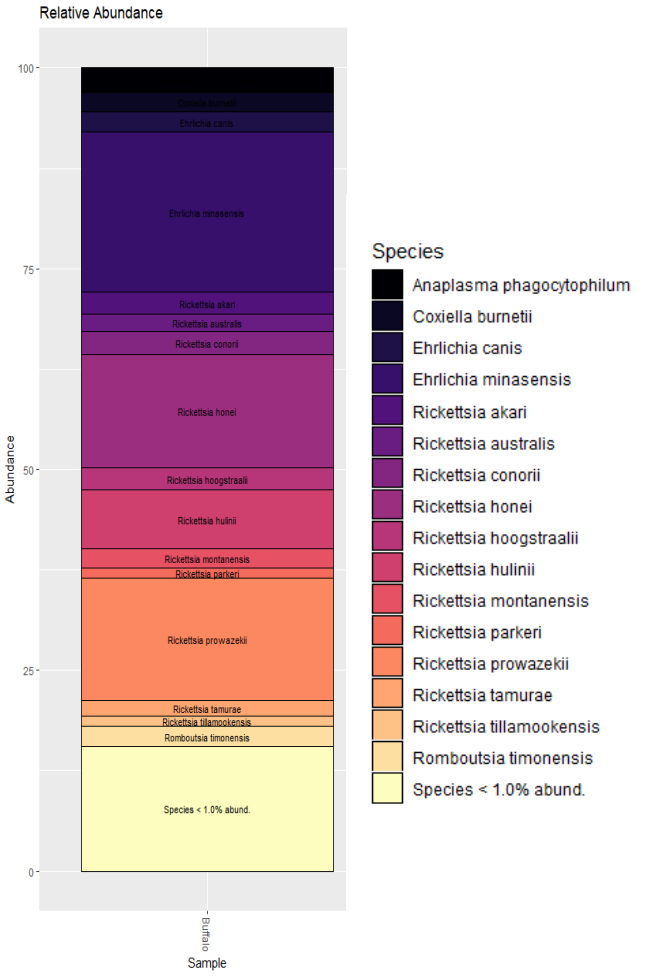

Figure 4. Relative abundance of meta biome bacteria at the species level

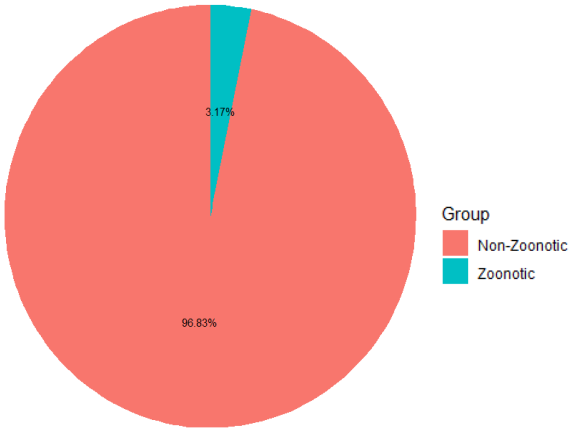

Figure 5. Percentage of the microbiome population zoonotic and non-zoonotic

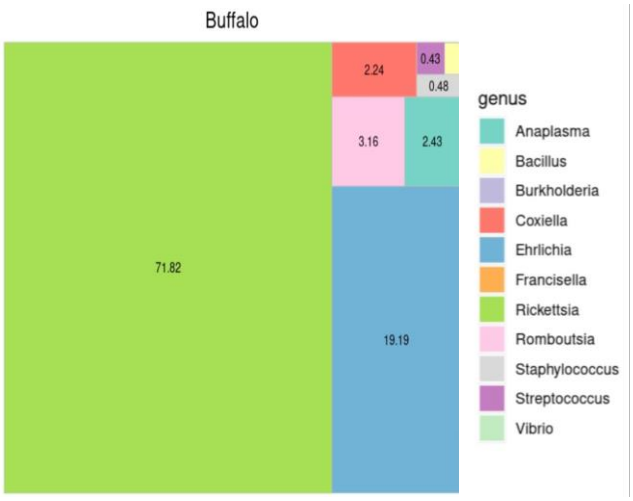

Figure 6. Profile of zoonotic agents of *H. bispinosa*

The *R. prowazekii* and *E. minasensis* are 2 species found in high percentages of *H. bispinosa* from buffalo farms on Moa Island, Southwest Maluku District. The species *E. minasensis* is a new pathogen that causes fever, lethargy, thrombocytopenia, and depression in cattle (Aguiar et al. 2014), while little is known about the biology of the rickettsial disease vector. Research by Kazimirova and Stibraniova (2013) reported that 100% of ticks infected with *R. prowazekii* will die from rickettsiae. The bacterial species *R. rickettsii* was found in less than 0.1%, with the dominant vector found in the tick *Dermacentor variabilis* compared to *Rickettsia africae* and *Rickettsia amblyommatis* (Kazimirova and Stibraniova 2013).

This study revealed that *H. bispinosa*'s role in microbial transmission is very important. Pathogen-host interactions are established through coevolution of microbes with arthropods. These interactions also include the process of pathogen replication, maintenance of persistent infections, and cross-transmission (Ravindran et al. 2023). It has been well documented that several species of ticks belonging to the Ixodidae act as vectors for carrying pathogenic agents, i.e., *Rickettsia* spp., *Anaplasma* spp., and *Ehrlichia* spp. (Barbieri et al. 2023).

The microbial groups Proteobacteria, Firmicutes, Bacteroidetes, and Actinobacteria are the three groups of bacteria that most often live on the bodies of *Haemaphysalis* spp. ticks (Zeng et al. 2022a). It was found in another study on species related to the tick *H. bispinosa*, including *Haemaphysalis longicornis* and *Haemaphysalis flava,* which are living hosts for 946 genera of microbes (Zeng et al. 2022a). High abundance was found in the genera *Lactobacillus*, *Coxiella*, *Rickettsia* and *Muribaculaceae* (Zeng et al. 2022a). Other species not found in this study but found in *Haemaphysalis* spp. from Shanghai, i.e., *Rickettsia japonica*, *Candidatus Rickettsia jingxinensis*, *Anaplasma bovis*, *Ehrlichia ewingii*, *Ehrlichia chaffeensis*, and *Coxiella*-like endosymbionts (Zeng et al. 2022a).

The results of this study show the high diversity of rickettsial organisms in *H. bispinosa*. They are the first report on metagenomic data on *H. bispinosa* in Moa buffalo from the Southwest Maluku District. This research contributes to a better understanding of the distribution of microbes of the genus *Rickettsia*, *Ehrlichia*, *Anaplasma*, *Coxiella*, and *Romboutsia* in Moa buffalo. The results of this study have implications for scientific aspects, i.e., knowing the profile of the microbiota community in Moa buffalo ticks, as well as the division of zoonotic and non-zoonotic bacterial groups as a scientific reference in anticipating zoonotic events in buffalo. In addition, this metagenomic analysis produced a specific molecular database for microbiota collected from ticks that had never been reported before.

In conclusion, the microbial community structure in *H. bispinosa* from Moa buffalo is dominated by non-zoonotic (96.83%) and zoonotic (3.17%) microbes. Zoonotic microbes are dominated by members of the genus *Rickettsia* (71.82%), *Ehrlichia* (19.19%), *Romboutsia* (3.16%), *Anaplasma* (2.43%), *Coxiella* (2.24%), *Staphylococcus* (0.48%) and *Streptococcus* (0.43%) respectively. Overall, 16 species of microbes were found on *H. bispinosa*, i.e., 11 species belonging to the genus *Rickettsia*, 2 species from the genus *Ehrlichia* (i.e., *E. canis* and *E. minasensis*), and 1 species each belonging to the genus *Anaplasma*, *Coxiella*, and *Romboutsia*. It was concluded that the abundance of the microbial community in *H. bispinosa* based on metagenome analysis using the 16S rRNA gene from Moa buffalo in the Southwest Maluku District was reported.

ACKNOWLEDGEMENTS

The authors are grateful to the authorities of the agriculture office of Southwest Maluku District, Laboratory of Parasitology, Faculty of Biology Universitas Jenderal Soedirman, Purwokerto, and LPPT-UGM Yogyakarta, Indonesia for the assistance in the permit process for field sample collection and the identification of ultrastructure surfaces and *Genomik Solidaritas Indonesia* (GSI) laboratory for metagenomic analysis. The authors are also grateful to Albertus Sairudy for helping collect tick samples on Moa Island, Southwest Maluku District, Indonesia. This study received funding support or grants from the Universitas Terbuka, Indonesia, through the Institute for Research and Community Service in 2022.

REFERENCES

Aguiar DM, Ziliani TF, Zhang X, Melo AL, Braga ÍA, Witter R, Freitas LD, Rondelli A, Luis MÂ, Sorte ED, Jaune FW, Santarém VA, Horta MC, Pescador CA, Colodel EM, Soares HS, Pacheco RD, Onuma SS, Labruna MB, McBride JW. 2014. A novel *Ehrlichia* genotype strain distinguished by the TRP36 gene naturally infects cattle in Brazil and causes clinical manifestations associated with ehrlichiosis. Ticks Tick Borne Dis 5 (5): 537-44. DOI: 10.1016/j.ttbdis.2014.03.010.

Aiman O, Ullah S, Chitimia-Dobler L, Nijhof AM, Ali A. 2022. First report of *Nosomma monstrosum* ticks infesting Asian water buffaloes (*Bubalus bubalis*) in Pakistan. Ticks Tick Borne Dis 13 (2): 101899. DOI: 10.1016/j.ttbdis.2022.101899.

Ali A, Khan MA, Zahid H, Yaseen PM, Qayash Khan M, Nawab J, Ur Rehman Z, Ateeq M, Khan S, Ibrahim M. 2019. Seasonal dynamics, record of ticks infesting humans, wild and domestic animals and

molecular phylogeny of *Rhipicephalus microplus* in Khyber Pakhtunkhwa Pakistan. Front Physiol 10: 793. DOI: 10.3389/fphys.2019.00793.

Anastos G. 1950. The Scutate Tick, or Ixodidae, of Indonesia. Entomologica Americana. New York Entomological Society, New York.

Azmatunnisa M, Rahul K, Subhash Y, Sasikala C, Ramana CV. 2015. *Bacillus oleivorans* sp. nov., a diesel oil-degrading and solvent-tolerant bacterium. Intl J Syst Evol Microbiol 65 (Pt 4): 1310-1315. DOI: 10.1099/ijs.0.000103.

Bakhteeva I, Timofeev V. 2022. Some peculiarities of anthrax epidemiology in herbivorous and carnivorous animals. Life 12 (6): 870. DOI: 10.3390/life12060870.

Barbieri AR, Suzin A, Rezende LM, Tognolli MH, Vogliotti A, Nunes PH, Pascoli GV, Ramos VD, Yokosawa J, Azevedo Serpa MC, Adami SF, Labruna MB, Szabó MP. 2023. *Rickettsia* communities and their relationship with tick species within and around the national park of Iguaçu, Brazil. Exp Appl Acarol 91: 339-358. DOI: 10.1007/s10493-023-00839-7.

Burkhardt NY, Price LD, Wang XR, Heu CC, Baldridge GD, Munderloh UG, Kurtti TJ. 2022. Examination of Rickettsial host range for shuttle vectors based on dnaA and par A genes from the pRM plasmid of *Rickettsia monacensis*. Appl Environ Microbiol 88 (7): e0021022. DOI: 10.1128/aem.00210-22.

Cabezas-Cruz A. 2021. Can the impact of climate change on the tick microbiome bring a new epidemiological landscape to tick-borne diseases? In: Nuttal P (eds). Climate, Ticks and Disease. CABI, Oxfordshire. DOI: 10.1079/9781789249637.0007.

Cairo J, Gherman I, Day A, Cook PE. 2021. *Bacillus cytotoxicus* A potentially virulent food-associated microbe. J Appl Microbiol 132: 31-40. DOI: 10.1111/jam.15214.

Caparaso JG, Kuczynski J, Stombaugh J, Bittinger K, Bushman FD, Costello EK, Fierer N, Peña AG, Goodrich JK, Gordon JI, Huttley GA, Kelley ST, Knights D, Koenig JE, Ley RE, Lozupone CA, McDonald D, Muegge BD, Pirrung M, Reeder J, Sevinsky JR, Turnbaugh PJ, Walters WA, Widmann J, Yatsunenko T, Zaneveld J, Knight R. 2010. QIIME allows analysis of high-throughput community sequencing data. Nat Methods 7: 335-336. DOI: 10.1038/nmeth.f.303.

Carlson CJ, Kracalik I, Ross N, Alexander KA, Hugh-Jones ME, Fegan M, Elkin BT, Epp T, Shury TK, Bagirova M, Getz WM, Blackburn JK. 2019. The global distribution of *Bacillus anthracis* and associated anthrax risk to humans, livestock and wildlife. Nat Microbiol 4: 1337-1343. DOI: 10.1038/s41564-019-0435-4.

Chandna P, Mayilraj S, Kuhad RC. 2016. *Bacillus pseudoflexus* sp. nov., a moderately halophilic bacterium isolated from compost. Ann Microbiol 66: 895-905. DOI: 10.1007/s13213-015-1174-2.

Chen Z, Li H, Gao X, Bian A, Yan H, Kong D, Liu X. 2019. Human Babesiosis in China: A systematic review. Parasitol Res 118: 1103-1112. DOI: 10.1007/s00436-019-06250-9.

Corrêa FD, Da Cunha NC, Rangel CP, da Fonseca AH. 2012. Ticks on buffaloes (*Bubalus bubalis*) in the state of Rio de Janeiro, Brazil. Rev Bras Parasitol Vet 21 (3): 313-314. DOI: 10.1590/s1984-29612012000300026.

Dixon CE, Bedenice D. 2019. Transplacental infection of a foal with *Anaplasma phagocytophilum*. Equine Vet Educ 33 (3): e62-e66. DOI: 10.1111/eve.13233.

Elsharawy AA, Eid NA, Ebrahiem AM. 2023. Effectiveness of *Bacillus pseudomycoides* strain for biocontrol of Early Blight on tomato plants. Intl J Phytopathol 12 (3): 313-326. DOI: 10.33687/phytopath.012.03.4632.

Fang LQ, Liu K, Li XL, Liang S, Yang Y, Yao HW, Sun RX, Sun Y, Chen WJ, Zuo SQ, Ma MJ, Li H, Jiang JF, Liu W, Yang XF, Gray GC, Krause PJ, Cao WC. 2015. Emerging tick-borne infections in mainland China: An increasing public health threat. Lancet Infect Dis 15: 1467-1479. DOI: 10.1016/S1473-3099(15)00177-2.

Gauthier DT, Karpathy SE, Grizzard SL, Batra D, Rowe LA, Paddock CD. 2021. Characterization of a novel transitional group *Rickettsia* species (*Rickettsia tillamookensis* sp. nov.) from the western black-legged tick, *Ixodes pacificus*. Intl J Syst Evol Microbiol 71 (7): 004880. DOI 10.1099/ijsem.0.004880.

Ghafar A, Gasser RB, Rashid I, Ghafoor A, Jabbar A. 2020. Exploring the prevalence and diversity of bovine ticks in five agro-ecological zones of Pakistan using phenetic and genetic tools. Ticks Tick Borne Dis 11: 101472. DOI: 10.1016/j.ttbdis.2020.101472.

Hmoon MM, Htun LL, Thu MJ, Chel HM, Thaw YN, Win SY, Chan SN, Khaing Y, Thein SS, Bawm S. 2021. Molecular prevalence and identification of *Ehrlichia canis* and *Anaplasma platys* from dogs in Nay Pyi Taw Area, Myanmar. Vet Med Intl 2021: 8827206. DOI: 10.1155/2021/8827206.

Jiao J, Lu Z, Yu Y, Ou Y, Fu M, Zhao Y, Wu N, Zhao M, Liu Y, Sun Y, Wen B, Zhou D, Yuan Q, Xiong X. 2021. Identification of tick-borne pathogens by metagenomic next-generation sequencing in *Dermacentor nuttalli* and *Ixodes persulcatus* in Inner Mongolia, China. Parasit Vectors 14 (2021): 287. DOI: 10.1186/s13071-021-04740-3.

Kamani J, Baneth G, Gutierrez R, Nachum-Biala Y, Mumcuoglu KY, Harrus. 2017. *Coxiella burnetii* and *Rickettsia conorii*: Two zoonotic pathogens in peridomestic rodents and their ectoparasites in Nigeria. Ticks Tick Borne Dis 9 (1): 86-92. DOI: 10.1016/j.ttbdis.2017.10.004.

Kampfer P, Lipski A, McInroy JA, Clermont D, Criscuolo A, Glaeser SP. 2022. *Bacillus rhizoplanae* sp. nov. from maize roots. Intl J Syst Evol Microbiol vol 72 (7). DOI: 10.1099/ijsem.0.005450.

Karim S, Budachetri K, Mukherjee N, Williams J, Kausar A, Hassan MJ, Adamson S, Dowd SE, Apanskevich D, Arijo A, Sindhu ZU, Kakar MA, Khan RMD, Ullah S, Sajid MS, Ali A, Iqbal Z. 2017. A study of ticks and tick-borne livestock pathogens in Pakistan. PLoS Neglect Trop Dis 11: e0005681. DOI: 10.1371/journal.pntd.0005681.

Kazimirova M, Stibraniova I. 2013. Tick salivary compounds: Their role in modulation of host defences and pathogen transmission. Front Cell Infect Microbiol 3: 43. DOI: 10.3389/fcimb.2013.00043.

Khan A, Khanzada MH, Khan K, Jalal K, Uddin R. 2023. Integrating core subtractive proteomics and reverse vaccinology for multi-epitope vaccine design against *Rickettsia prowazekii* endemic typhus. Immunol Res 72: 82-95. DOI: 10.1007/s12026-023-09415-y.

Khoo JJ, Chen F, Kho KL, Shanizza AIA, Lim FS, Tan KK, Chang L, Abubakar S. 2016. Bacterial community in *Haemaphysalis* ticks of domesticated animals from the Orang Asli communities in Malaysia. Ticks Tick Borne Dis 7 (5): 929-937. DOI: 10.1007/s00436-019-06250-9.

Kim M, Kim JY, Yi M, Lee I, Yong D, Jeon B, Yong T. 2021. Microbiome of *Haemaphysalis longicornis* tick in Korea. Kor J Parasitol 59: 489-496. DOI: 10.3347/kjp.2021.59.5.489.

Levytska V, Mushynskyi A. 2020. Diagnosis and treatment of Tick-Borne diseases of pets. Podilian Bull 32: 175-183. DOI: 10.37406/2706-9052-2020-1-20.

Li H, Fu X, Jiang J, Liu R, Li R, Zheng Y, Qi W, Liu W, Cao W. 2017. Severe illness caused by *Rickettsia sibirica* subspecies sibirica BJ-90 infection, China. Emerg Microbes Infect 6 (11): e107. DOI: 10.1038/emi.2017.95.

Maqbool M, Sajid MS, Saqib M, Anjum FR, Tayyab MH, Rizwan HM, Rashid MI, Rashid I, Iqbal A, Siddique RM, Shamim A, Hassan MA, Atif FA, Razzaq A, Zeeshan M, Hussain K, Nisar RH, Tanveer A, Younas S, Kamran K, Rahman SU. 2022. Potential mechanisms of transmission of tick-borne viruses at the virus-tick interface. Front Microbiol 13: 846884. DOI: 10.3389/fmicb.2022.846884.

Mobarez AM, Khalili MA, Mostafavi E, Esmaeili S. 2021. Molecular detection of *Coxiella burnetii* infection in aborted samples of domestic ruminants in Iran. PLoS ONE 16 (4): e0250116. DOI: 10.1371/journal.pone.0250116.

Moura DAD, Pessoa Araujo Junior J, Nakazato L, Bard E, Aguilar-Bultet L, Vorimore F, Leonidovich Popov V, Moleta Colodel E, Cabezas-Cruz A. 2019. Isolation and characterization of a novel pathogenic strain of *Ehrlichia minasensis*. Microorganisms 7 (11): 528. DOI 10.3390/microorganisms7110528.

Muhammad A, Bashir R, Mahmood MM, Afzal MS, Şimşek S, Awan UA, Khan MR, Ahmed H, Cao J. 2021. Epidemiology of ectoparasites (ticks, lice, and mites) in the livestock of Pakistan: A review. Front Vet Sci 8: 780738. DOI: 10.3389/fvets.2021.780738.

Parte AC, Sardà Carbasse J, Meier-Kolthoff JP, Reimer LC, Göker M. 2020. List of prokaryotic names with standing in nomenclature (LPSN) moves to the DSMZ. Intl J Syst Evol Microbiol 70: 5607-5612. DOI: 10.1099/ijsem.0.004332.

Petney TN, Saijuntha W, Boulanger N, Chitimia-Dobler L, Pfeffer M, Eamudomkarn C, Andrews RH, Ahamad M, Putthasorn N, Muders SV, Petney DA, Robbins RG. 2019. Ticks (Argasidae, Ixodidae) and tick-borne diseases of continental Southeast Asia. Zootaxa 4558 (1): 1-89. DOI: 10.11646/zootaxa.4558.1.1.

Rahman MT, Sobur MA, Islam MS, Ievy S, Hossain MJ, El Zowalaty ME, Rahman AT, Ashour HM. 2020. Zoonotic diseases: Etiology,

impact, and control. Microorganisms 8 (9): 1405. DOI: 10.3390/microorganisms8091405.
Ramirez-Olea H, Reyes-Ballesteros B, Chávez-Santoscoy RA. 2022. Potential application of the probiotic *Bacillus licheniformis* as an adjuvant in the treatment of diseases in humans and animals: A systematic review. Front Microbiol 13: 993451. DOI: 10.3389/fmicb.2022.993451.
Ravindran R, Hembram PK, Kumar GS, Kumar KG, Deepa CK, Varghese A. 2023. Transovarial transmission of pathogenic protozoa and rickettsial organisms in ticks. Parasitol Res 122: 691-704. DOI: 10.1007/s00436-023-07792-9.
Reeves WK, Mans BJ, Durden LA, Miller MM, Gratton EM, Laverty TM. 2020. *Rickettsia hoogstraalii* and a Rickettsiella from the Bat Tick *Argas transgariepinus*, in Namibia. J Parasitol 106 (5): 663-669. DOI: 10.1645/20-46.
Rehman A, Conraths FJ, Sauter-Louis C, Krücken J, Nijhof AM. 2019. Epidemiology of tick-borne pathogens in the semi-arid and the arid agroecological zones of Punjab province, Pakistan. Transbound Emerg Dis 66: 526-536. DOI: 10.1111/tbed.13059.
Rikihisa Y. 2011. Mechanisms of obligatory intracellular infection with *Anaplasma phagocytophilum*. Clin Microbiol Rev 24: 469-489. DOI: 10.1128/cmr.00064-10.
Riley LW, Blanton RE. 2018. Advances in molecular epidemiology of infectious diseases: Definitions, approaches, and scope of the field. Microbiol Spect 6 (6): 10.1128/microbiolspec.AME-0001-2018.. DOI: 10.1128/microbiolspec.AME-0001.
Roy BC, Estrada-Peña A, Krücken J, Rehman A, Ard Menzo Nijhof AM. 2018. Morphological and phylogenetic analyses of *Rhipicephalus microplus* ticks from Bangladesh, Pakistan and Myanmar. Ticks Tick Borne Dis 9: 1069-1079. DOI: 10.1016/j.ttbdis.2018.03.035.
Ruiu L. 2013. *Brevibacillus laterosporus*, a pathogen of invertebrates and a broad-spectrum antimicrobial species. Insects 4 (3): 476-492. DOI: 10.3390/insects4030476.
Sahara A, Budianto BH, Kunda RM, Firdausy LW. 2023. Tick (Acari: Ixodidae) infestation in cattle from Sleman, Yogyakarta Province, Indonesia. Biodiversitas 24 (7): 4087-4094. DOI: 10.13057/biodiv/d240747.
Sahara A, Nugraheni YR, Patra G, Prastowo J, Priyowidodo D. 2019. Ticks (Acari: Ixodidae) infestation on cattle in various regions in Indonesia. Vet World 12 (11): 1755-1759. DOI: 10.14202/vetworld.2019.1755-1759.
Senesi S, Ghelardi E. 2010. Production, secretion and biological activity of *Bacillus cereus* enterotoxins. Toxins (Basel) 2 (7): 1690-703. DOI: 10.3390/toxins2071690.
Seo M, Kwon O, Kwak D. 2021. Molecular detection of *Rickettsia raoultii*, *Rickettsia tamurae*, and associated pathogens from ticks parasitizing water deer (*Hydropotes inermis argyropus*) in South Korea. Ticks Tick Borne Dis 12 (4): 101712. DOI: 10.1016/j.ttbdis.2021.101712.
Snellgrove AN, Krapiunaya I, Scott P, Levin ML. 2021. Assessment of the pathogenicity of *Rickettsia amblyommatis*, *Rickettsia bellii*, and *Rickettsia montanensis* in a Guinea Pig model. Vector Borne Zoonotic Dis 21 (4): 232-241. DOI: 10.1089/vbz.2020.2695.
Spencer RC. 2003. *Bacillus anthracis*. J Clin Pathol 56 (3):182-7. DOI: 10.1136/jcp.56.3.182.
Stewart A, Armstrong M, Graves S, Hajkowicz K. 2017. *Rickettsia australis* and Queensland tick typhus: A rickettsial spotted fever group infection in Australia. Am J Trop Med Hyg 97 (1): 24-29. DOI: 10.4269/ajtmh.16-0915.
Swei A, Kwan JY. 2017. Tick microbiome and pathogen acquisition altered by host blood meal. Intl Soc Microbiol Ecol J 11 (3): 813-816. DOI: 10.1038/ismej.2016.152.
Szakacs TA, Wood H, Russell C, Nelder MP, Patel SN. 2020. An apparent, locally acquired case of rickettsialpox (*Rickettsia akari*) in Ontario, Canada. J Assoc Med Microbiol Infect Dis Can 5 (2): 115-119. DOI: 10.3138/jammi-2019-0028.
Théatre A, Cano-Prieto C, Bartolini M, Laurin Y, Deleu M, Niehren J, Fida T, Gerbinet S, Alanjary M, Medema MH, Léonard A, Lins L, Arabolaza A, Gramajo H, Gross H, Jacques P. 2021. The Surfactin-like lipopeptides from *Bacillus* spp.: Natural biodiversity and synthetic biology for a broader application range. Front Bioeng Biotechnol 9: 623701. DOI: 10.3389/fbioe.2021.623701.
Thu MJ, Qiu Y, Yamagishi J, Kusakisako K, Ogata S, Moustafa MA, Isoda N, Sugimoto C, Katakura K, Nonaka N, Nakao R. 2019. Complete genome sequence of *Rickettsia asiatica* strain Maytaro1284, a member of spotted fever group rickettsiae isolated from an *Ixodes ovatus* tick in Japan. Microbiol Resour Announc 8 (37): e00886-19. DOI: 10.1128/MRA.00886-19.
Utami P, Budianto BH, Sahara A. 2021. Tick (Acari: Ixodidae) infestation of cuscuses from Maluku Province, Indonesia. Vet World 14: 1465-1471. DOI: 10.14202/vetworld.2021.1465-1471.
Utami P, Kunda RM. 2023. Surface ultrastructure of tick (Acari: Ixodidae) on Moa buffalo from Southwest Maluku District, Indonesia. Biodiversitas 24 (6): 3230-3235. DOI: 10.13057/biodiv/d240617.
Wang HF, Li QL, Zhang YG, Xiao M, Zhou XK, Guo JW, Duan YQ, Li WJ. 2017. *Bacillus capparidis* sp. nov., an endophytic bacterium isolated from roots of *Capparis spinosa* L. Intl J Syst Evol Microbiol 67 (2): 282-287. DOI 10.1099/ijsem.0.001616.
Wu XB, Na RH, Wei SS, Zhu JS, Peng HJ. 2013. Distribution of tick-borne diseases in China. Parasit Vectors 6: 119. DOI: 10.1186/1756-3305-6-119.
Zeng W, Li Z, Jiang T, Cheng D, Yang L, Hang T, Duan L, Zhu D, Fang Y, Zhang Y. 2022a. Identification of bacterial communities and tick-borne pathogens in *Haemaphysalis* spp. collected from Shanghai, China. Trop Med Infect Dis 7 (12): 413. DOI: 10.3390/tropicalmed7120413.
Zeng Z, Zhang J, Li Y, Li K, Gong S, Li F, Wang P, Iqbal M, Kulyar MF, Li J. 2022b. Probiotic potential of *Bacillus licheniformis* and *Bacillus pumilus* Isolated from Tibetan Yaks, China. Probiotics Antimicrob Proteins 14: 579-594. DOI: 10.1007/s12602-022-09939-z.
Zhao GP, Wang YX, Fan ZW, Ji Y, Liu MJ, Zhang WH, Li XL, Zhou SX, Li H, Liang S. 2021. Mapping ticks and tick-borne pathogens in China. Nat Commun 12: 1075. DOI: 10.1038/s41467-021-21375-1.
Zhong Y, Zou Y, Zheng Z, Chen Q, Xu W, Wu Y, Gao J, Zhong K, Gao H. 2022. Impact of inoculating with indigenous *Bacillus marcorestinctum* YC-1 on quality and microbial communities of Yibin Yacai (fermented mustard) during the fermentation process. Foods 11: 3593. DOI: 10.3390/foods11223593.

NUSANTARA BIOSCIENCE
Vol. 16, No. 1, pp. 139-147
May 2024

ISSN: 2087-3948
E-ISSN: 2087-3956
DOI: 10.13057/nusbiosci/n160117

Diversity and conservation status of dragonflies (Odonata) at three streams in Donomulyo Sub-district, Malang District, Indonesia

MUHAMAD AZMI DWI SUSANTO[1,♥], FATHURRAHMAN SIDIQ[2], SUFRAHA ISLAMIA[3], MUHAMMAD IQBAL PRATAMA[4]

[1]Department of Biology, Faculty of Mathematics and Natural Sciences, Universitas Brawijaya. Jl. Veteran, Malang 65145, East Java, Indonesia. Tel.: +62-341-554403, ♥email: muhammadazmidwi@gmail.com

[2]Green Community, Department of Biology, Faculty of Mathematics and Natural Sciences, Universitas Negeri Semarang. Sekaran, Gunung Pati, Semarang 50229, Central Java, Indonesia

[3]Perhimpunan Kebun Binatang Se-Indonesia-Global Species Management Plan. Jakarta, Indonesia

[4]Department of Biology, Faculty of Science and Technology, UIN Sunan Ampel Surabaya. Jl. Dr. Ir. H. Soekarno No.682, Gn. Anyar, Surabaya 60294, East Java, Indonesia

Manuscript received: 12 November 2023. Revision accepted: 20 April 2024.

Abstract. *Susanto MAD, Sidiq F, Islamia S, Pratama MI. 2024. Diversity and conservation status of dragonflies (Odonata) at three streams in Donomulyo Sub-district, Malang District, Indonesia. Nusantara Bioscience 16: 139-147.* The aquatic environment is currently experiencing massive threats, especially from anthropogenic activities. Polluted effluent discarded in streams damages the existing ecosystems and negatively impacts various organisms. Donomulyo, a sub-district in Malang District of East Java Province, Indonesia, has many rivers and streams that are pivotal for local people and wildlife. Water quality in these aquatic bodies can be monitored using bioindicators. Odonata (dragonflies and damselflies) are bioindicators indicating environmental change in rivers and streams. Unfortunately, there has been no data regarding Odonata in the Donomulyo streams. Hence, this research aims to determine the diversity of dragonfly species at three streams in Donomulyo and its meaning for the environmental status. The research was conducted at Sengik, Kedungceleng, and Kedungsalam streams using a Visual Encounter Survey (VES) to count individuals of each dragonfly species. This study recorded 258 individuals identified into 25 species of 4 families. Aside from *Copera vittata javana* (Lieftinck, 1940) which International Union for Conservation of Nature (IUCN) Red List status is Not Evaluated, all other dragonflies are Least Concern evaluated. The three streams studied in this research generally had moderate Odonata diversity ($2.02 < H' < 2.41$), indicating good habitat conditions.

Keywords: Habitat, insect, microclimate, river, wildlife

INTRODUCTION

Dragonflies are flying insects included in the order Odonata, with two suborders, Anisoptera (common dragonflies) and Zygoptera (damselflies) (Orr and Kalkman 2015). Dragonflies undergo incomplete metamorphosis with three cycles: egg, nymph, and adult (Paulson 2009). In general, eggs are laid by female dragonflies on the water's surface or in water close to aquatic plants and will hatch into nymphs in 1–21 days (Setiyono et al. 2017). The nymphs will molt up to 15 times and take up to several months before emerging as adult dragonflies (Setiyono et al. 2017). The egg and nymph phases require aquatic bodies (Orr and Kalkman 2015; Choong et al. 2020), while adults live terrestrially and aerially. Dragonflies highly depend on waterbodies to accomplish their life cycle. Adult dragonflies can generally be found around aquatic ecosystems such as rivers (Zaman et al. 2020), waterfalls (Koneri et al. 2020; Susanto and Arianti 2021), reservoirs or ponds (Susanto et al. 2023), and lakes (Potapov et al. 2020); either in lowlands or highlands (Leksono et al. 2017).

As they associate with and depend highly on water quality, dragonflies are sensitive to disturbances and changes in aquatic environmental quality (Dolný et al. 2012), thus leading to the use of dragonflies as bioindicators to determine water quality (Buczyński et al. 2020). In addition, dragonflies also indicate the quality of the terrestrial environment as they react to the changes in habitat components' quality, such as landscape conditions (Perez and Bautista 2020), vegetation (Briggs et al. 2019; Oliveira-Junior et al. 2017), and canopy cover (Susanto et al. 2023). Most dragonflies require a specific natural habitat, which determines their disappearance whenever their habitat changes. This situation is practically the reason for using dragonflies as bioindicators in indicating the quality of aquatic environments.

Dragonflies also play an important role in terrestrial and aquatic ecosystems as predators of small insects (Orr and Kalkman 2015). Dragonflies are carnivorous insects that can control insects that are potential vectors of diseases that can harm humans, such as mosquitoes (Samways 2008; Vatandoost 2021; Ramlee and Mohd 2022). In addition, dragonflies are also predators of insect pests in agricultural areas and rice fields (Suroto et al. 2021; Sharma and Oli 2022; Raut et al. 2023). Therefore, the presence of dragonflies in an ecosystem is very important for humans. Population decline and the loss of dragonfly species in a location due to environmental damage can have a negative impact on humans. Research on dragonflies is very important as an early indicator for analyzing terrestrial and

aquatic environmental quality changes.

Streams are lotic aquatic habitats that become natural habitats for dragonflies due to their vegetated banks. Several previous studies in Indonesia confirmed it, such as at Brantas River in Batu-Malang of East Java, with 10 species recorded (Virgiawan et al. 2015), at Kalibendo River in Banyuwangi, East Java with 13 species (Nugrahani et al. 2022), at Gajah Wong River in urban Yogyakarta with 25 species observed (Zaman et al. 2022), at the stream in Ujung Kulon National Park with 17 species found (Sugiman et al. 2020), at Mahaka River in South Sulawesi with 12 species (Nuraeni et al. 2019), and at Batubolong River, in West Lombok with 11 species (Zulhariadi et al. 2022). Despite having a considerable intact lowland forest with a vast riverine area, the data on Odonata from Malang District is still lacking. Donomulyo, a prominent sub-district in this area, is a good representative for studying its dragonflies, as it has never been conducted before. Hence, this study intended to analyze the diversity of dragonflies in Donomulyo, which is expected to provide basic data for future study and conservation of this insect group.

MATERIALS AND METHODS

Time and location of research

This research was conducted between August–September 2021 at Donomulyo Sub-district (8°16'49.39"S, 112°25'47.13"E), Malang District, East Java Province, Indonesia. Fieldwork occurred at three streams in this sub-district, i.e.: Sengik, Kedungceleng, and Kedungsalam (Figure 1). These three research sites were selected based on the similarity of habitat types, namely streams in the Donomulyo sub-district. The detail on the three streams is provided in Table 1. This research was conducted for six days, with details of each research location being repeated twice on different days. Field sampling occurred during active dragonfly hours, from 07.00 to 13.00 hours, along the transect erected following the stream embankment.

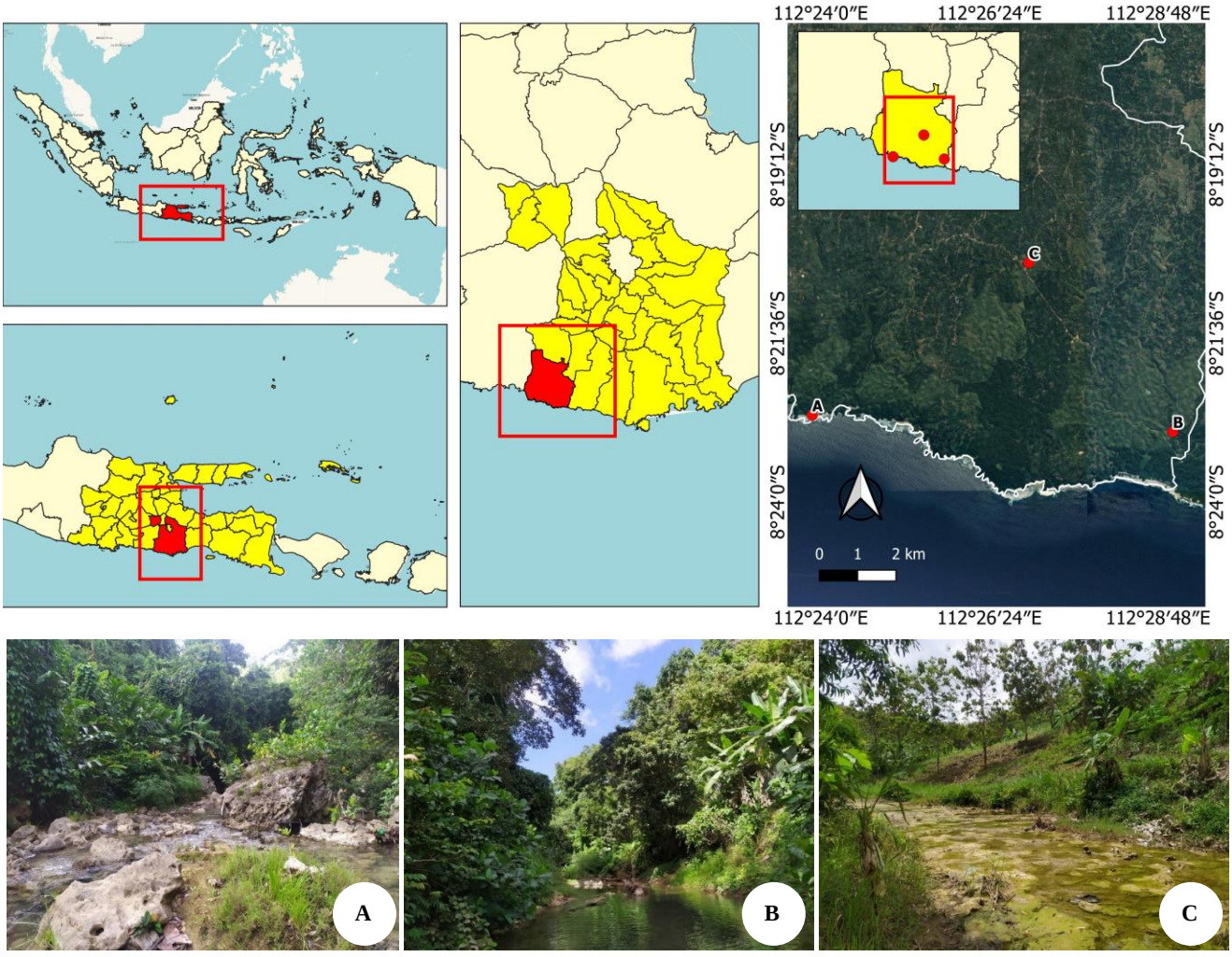

Figure 1. Map and physical appearance of sampling sites in Donomulyo, Malang, Indonesia. A. Sengik, B. Kedungceleng, C. Kedungsalam

Table 1. Coordinate point and description of research sites in Donomulyo, Malang, Indonesia

Stream	Coordinate points		Description
	Latitude	Longitude	
Sengik	8° 22' 45.9"S	112° 23' 52.8"E	Flows through secondary forest and plantation, flanked with ponds
Kedungceleng	8° 22' 59.9"S	112° 29' 0.7"E	Flows through secondary forests and plantations
Kedungsalam	8° 20' 35.7"S	112° 26' 57.8"E	Flows through plantations and in adjacency with settlements

Sampling method

Field data was collected along a 200 m length and 5 m width line transect erected following the stream pathways. Adult dragonflies were recorded using the Visual Encounter Survey (VES) method, equipped with a sweeping net and photography. The individual number from each adult species was counted, while pictorial documentation was used for species identification purposes. Species identification used morphological aspects, including shape, pattern, and color of the body and wings. The identification process was guided with proper references (Rahadi et al. 2013; Setiyono et al. 2017). In addition, environmental factors (air temperature, air humidity, and light intensity) were measured using a thermo-hygrometer and light meter. Air temperature, humidity, and light intensity measurements were observed at each study site's on the beginning of data collection.

Data analysis

Odonata diversity was calculated using some ecological indices (Shannon-Wiener Diversity Index, Evennes Index, and dominance index) ran with PAST (paleontological statistics) 4.03 software. This software also commenced a Principal Component Analysis (PCA) test to determine the correlation between sampling sites and environmental factors. Other factors, such as analysis of taxa numbers and the abundance of dragonfly species, were displayed using graphs generated through Microsoft Excel 2021.

RESULTS AND DISCUSSION

Diversity of species

The fieldwork conducted at three streams in the Donomulyo Sub-district recorded 25 Odonata species of four families identified from 285 observed individuals. Suborder Anisoptera was represented by two families, Aeshnidae and Libellulidae, with a total of 15 species of 118 individuals recorded, while suborder Coenagrionidae and Platycnemididae represented Zygoptera with a total of 10 species of 167 individuals. Libellulidae became a family with the most recorded species, 14 species of 117 individuals, while Aeshnidae, with one species and one individual, was the most scarce. In addition, Libellulidae also had the highest percentage of family composition based on the number of species (Figure 2) and abundance (Figures 3 and 4) at all study sites.

The observation results showed that at the Sengik stream, there were 10 species with 46 individuals; the Kedungceleng stream was with 13 species of 66 individuals; and the Kedungsalam stream was observed with 15 species and 173 individuals (Figure 5). Kedungceleng stream had the highest Odonata diversity (H' = 2.41), followed by Kedungsalam stream (H' = 2.26) and Sengik stream (H' = 2.02) (Figure 6). Furthermore, Kedungceleng had the most evenly distributed species among the other two streams (E = 0.86), while the Sengik stream indicated the existence of the most dominant species (D = 0.17) (Figure 7).

Conservation status

According to the International Union for Conservation of Nature (IUCN) 2023 assessment, only *Copera vittata javana* possessed discernible status as Not Evaluated (NE), which is considerably higher than the other 24 species that are Least Concern (LC) (Table 2). Moreover, 9 species are categorized as stable populations as indicated in the IUCN database, including *Gynacantha subinterrupta, Agrionoptera insignis, Neurothemis ramburii, Neurothemis terminata, Orthetrum sabina, Pantala flavescens, Pseudagrion microcephalum, Pseudagrion pruinosum,* and *Prodasineura autumnalis.* Meanwhile, 13 species which comprise of *Camacinia gigantea, Orthetrum glaucum, Orthetrum pruinosum, Potamarcha congener, Rhodothemis rufa, Trithemis aurora, Trithemis festiva, Agriocnemis femina, Agriocnemis pygmaea, Heliocypha fenestrata, Pseudagrion rubriceps, Copera marginipes,* and *Nosoticta insignis* are with unknown population trend. Only *Crocothemis servilia* and *Orthetrum testaceum* were assessed to have an increased population trend.

Correlation between sampling sites and environmental factors

The measuring of environmental factors hints that the Kedungsalam stream has the highest temperature and light intensity site among other locations (T = 32.1°C, Ev 30,272 lx; Table 3), while the Sengik stream recorded the highest humidity (AH = 72%). The analysis tested the relation between three variables of environmental factors and five factors of dragonfly diversity, showing that the total variance of PC1= 69.397% and PC2= 30.603% (Figure 8). PCA analysis shows that the Kedungsalam stream positively correlates with air temperature, while the Sengik stream positively correlates with air humidity.

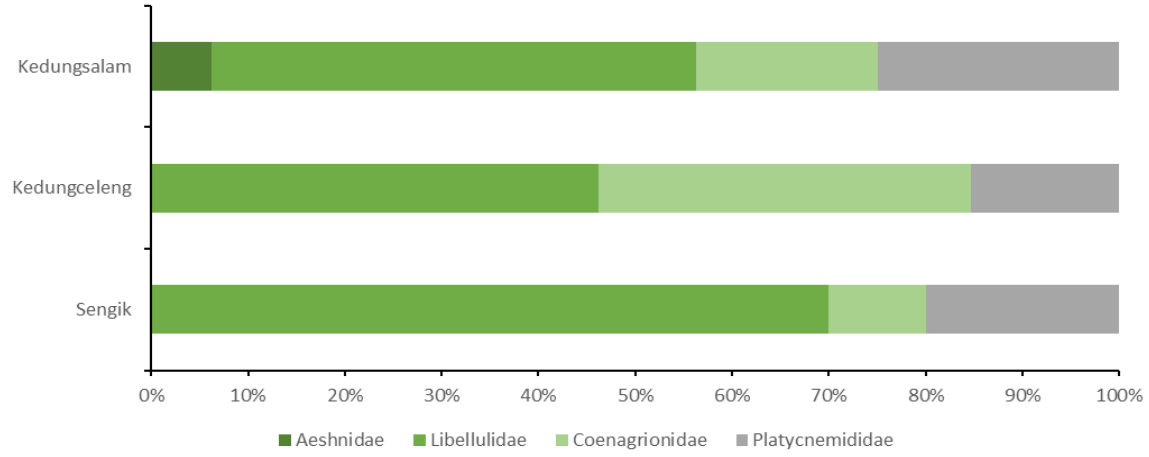

Figure 2. Composition of Odonata families according to its species members at three streams in Donomulyo, Malang, Indonesia

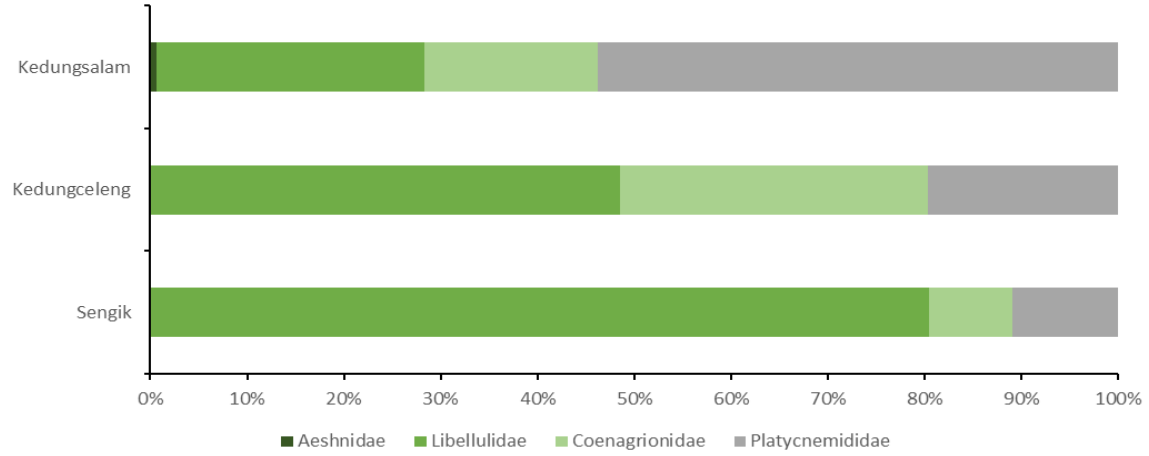

Figure 3. Composition of Odonata families according to abundance at three streams in Donomulyo, Malang, Indonesia

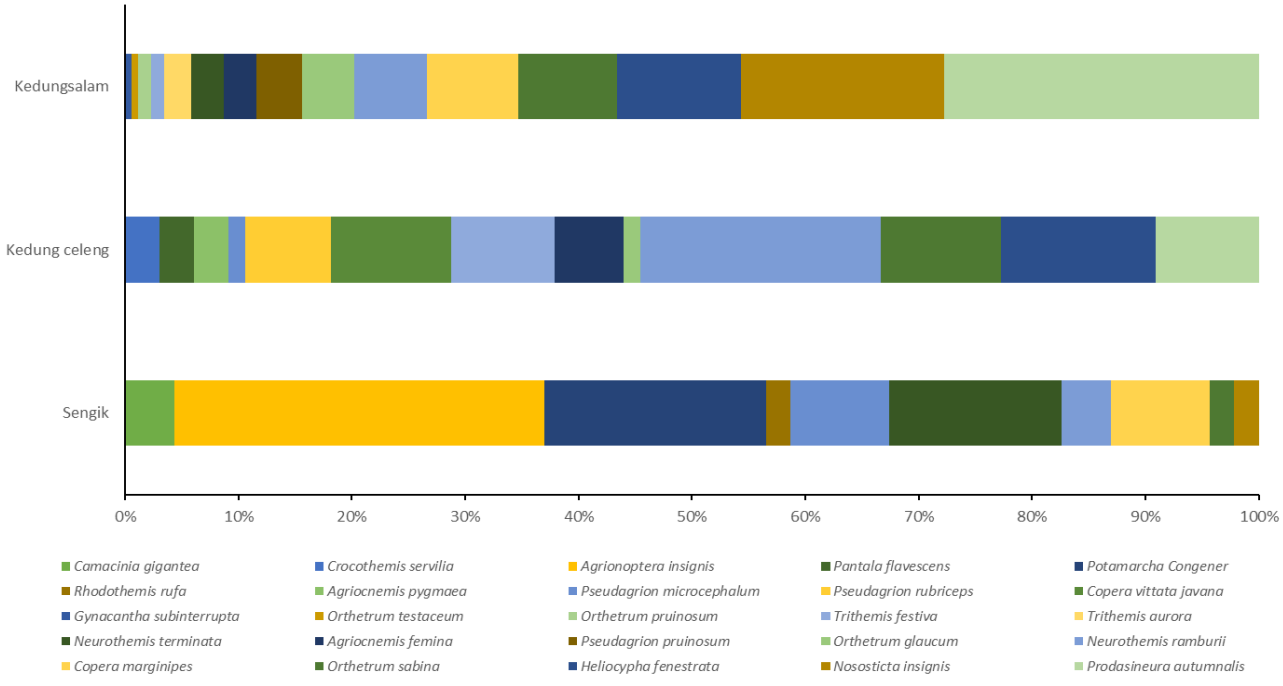

Figure 4. Relative abundance of Odonata species at three streams in Donomulyo, Malang, Indonesia

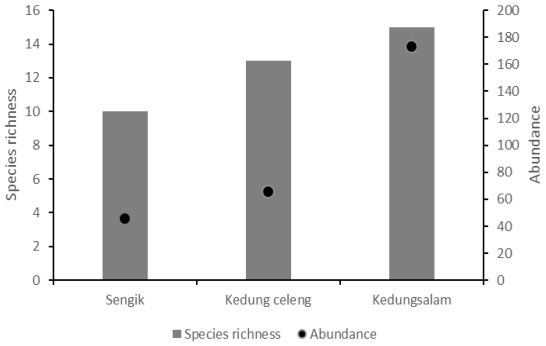

Figure 5. The richness and abundance of Odonata species at three streams in Donomulyo, Malang, Indonesia

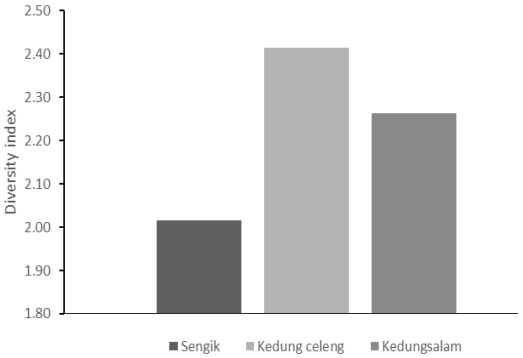

Figure 6. Odonata diversity at three streams in Donomulyo, Malang, Indonesia

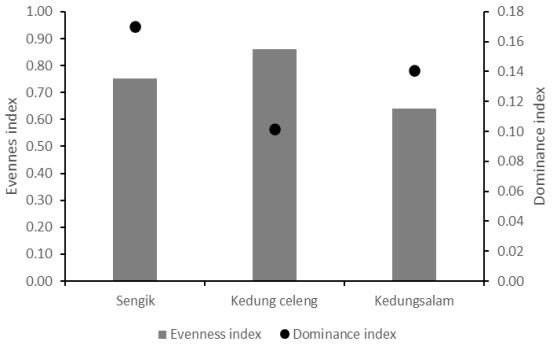

Figure 7. The distribution and dominance of Odonata species at three streams in Donomulyo, Malang, Indonesia

Discussion

Analysis of family composition based on the number of members of the species shows that Libellulidae is the Odonata family that has the highest number of species in this study, namely 14 species, at the three research sites and also has the highest percentage of 46.15% to 70% of all species recorded during the study (Figure 2). Therefore, Libellulidae also had the highest number of individuals of all individuals in this study, namely 117 individuals, and the three research sites also had the highest percentage of 48.48% to 80.43% of all individuals recorded during the study (Figure 3). As a family with the most members within the Order Odonata, Libellulidae is commonly found in various habitats (Setiyono et al. 2017). In addition, its members generally have good flight ability and wide mobility.

Table 2. List of species and conservation status of Odonata at streams in Donomulyo, Malang, Indonesia

Suborder & family	Species	Locations			Conservation Status
		Sengik	Kedungceleng	Kedungsalam	
Anisoptera					
Aeshnidae	*Gynacantha subinterrupta* (Rambur, 1842)	-	-	+	LC
Libellulidae	*Agrionoptera insignis* (Rambur, 1842)	+	-	-	LC
	Camacinia gigantea (Brauer, 1867)	+	-	-	LC
	Crocothemis servilia (Drury, 1770)	-	+	-	LC
	Neurothemis ramburii (Brauer, 1866)	+	+	+	LC
	Neurothemis terminata (Ris, 1911)	+	-	+	LC
	Orthetrum glaucum (Brauer, 1865)	-	+	+	LC
	Orthetrum pruinosum (Burmeister, 1839)	-	-	+	LC
	Orthetrum sabina (Drury, 1770)	+	+	+	LC
	Orthetrum testaceum (Burmeister, 1839)	-	-	+	LC
	Pantala flavescens (Fabricus, 1798)	-	+	-	LC
	Potamarcha congener (Rambur, 1842)	+	-	-	LC
	Rhodothemis rufa (Rambur, 1842)	+	-	-	LC
	Trithemis aurora (Burmeister, 1839)	-	-	+	LC
	Trithemis festiva (Rambur, 1842)	-	+	+	LC
Zygoptera					
Coenagrionidae	*Agriocnemis femina* (Brauer, 1868)	-	+	+	LC
	Agriocnemis pygmaea (Rambur, 1842)	-	+	-	LC
	Heliocypha fenestrata (Burmister, 1839)	-	+	+	LC
	Pseudagrion microcephalum (Rambur, 1842)	+	+	-	LC
	Pseudagrion pruinosum (Burmeister, 1839)	-	-	+	LC
	Pseudagrion rubriceps (Selys, 1876)	-	+	-	LC
Platycnemididae	*Copera marginipes* (Rambur, 1842)	+	-	+	LC
	Copera vittata javana (Lieftinck, 1940)	-	+	-	NE
	Nosoticta insignis (Selys, 1886)	+	-	+	LC
	Prodasineura autumnalis (Fraser, 1922)	-	+	+	LC

Note: (+) present and (-) absent. LC: Least Concern & NE: Not Evaluated (IUCN 2023)

Table 3. Environmental factors during field time at three streams in Donomulyo, Malang, Indonesia

Location	Temperature (°C)	Humidity (%)	Light intensity (lx)
Sengik	30.6	72	14,786
Kedungceleng	31.0	69	25,643
Kedungsalam	32.1	67	30,272

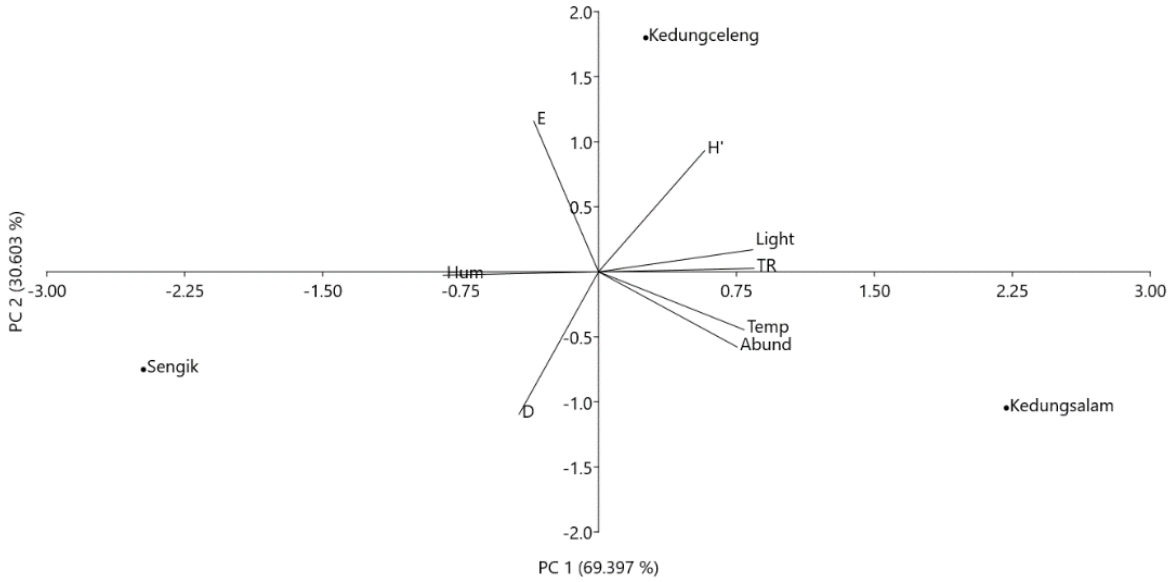

Figure 8. Correlation between sampling sites and environmental factors at three streams in Donomulyo, Malang, Indonesia

Figure 9. Odonata representatives from Donomulyo, Malang, Indonesia: A. *Agrionoptera insignis*, B. *Neurothemis ramburii*, C. *Prodasineura autumnalis*, D. *Camacinia gigantea*, E. *Heliocypha fenestrata*, F. *Copera vittata javana*

The dominance of the Libellulidae family has been confirmed through previous studies from various locations in Indonesia, such as at Batubolong River in West Lombok, with 7 species and 17 individuals out of a total of 11 species and 33 individuals (Zulhariadi et al. 2022), at Gajahwong River in Yogyakarta with 13 species recorded out of total 25 species (Zaman et al. 2020), at Kuningan Resort of Mount Ciremai National Park in West Java Province with 14 species and 342 individuals out of total 24 species and 591 individuals (Hastomo et al. 2022), at lowland forest in Central Kalimantan with 18 species out of total 22 species (Hendriks et al. 2023), at Mount Bromo's Forest Area in East Java with 13 species out of total 23 species (Astuti et al. 2022), and at protected forests in Bengkulu with 22 species out of total 52 species (Janra et al. 2022).

The only member of the Aeshnidae family recorded in this study was with a single individual, hence contributing 6.25% and 0.58%, respectively, toward family and species composition. During observation, *G. subinterrupta* was spotted at the Kedungsalam stream and, at the same time, perched by hanging among dense shrubs and bushes within the stream embankment. The members of Aeshnidae are always scantily recorded in many studies. Observations at Gajahwong River and Nglanggeran Ancient Volcano Area in Yogyakarta recorded only *G. subinterrupta* (Zaman et al. 2020; Setyawati and Triatmanto 2022). One at Ujung Kulon National Park in West Java observed only *G. basigutatta* (Sugiman et al. 2020). A study in Bengkulu Province listed 4 species, *Anax panybeus, Anaeschna jaspidea, Gynacantha dohrni,* and *Gynacantha basiguttata* (Janra et al. 2022), similar to one conducted in Nusakambangan Island of Central Java which observed *Anax guttatus, Gynacantha musa, G. subinterrupta* and *Tetracanthagyna plagiata* (Nu'manuddin et al. 2021).

Further analysis showed that each site in the current study had different species with the highest relative abundance, i.e., *A. insignis* in Sengik stream, *N. ramburii* in Kedungceleng stream, and *P. autumnalis* in Kedungsalam stream (Figure 9. A-C). In this study, *A. insignis* perched on branches around stagnant water on the streamside, considerably shaded by a canopy. This species prefers perching on vegetation in the nearby stagnant waters under a fairly closed canopy (Kosterin 2014; Setiyono et al. 2017). This species ranges stream habitats (Kosterin 2014; Pratama and Rosalini 2016; Setiyono et al. 2017; Kartini et al. 2022; Zulhariadi et al. 2022;) and ponds (Saefullah et al. 2021) in the lowlands, with an altitude range of 0 to 365 m (Dow 2020a).

The *N. ramburii* was found perched on dry twigs and vegetation on streambanks with open canopy. This species was reported to abundantly inhabit irrigated areas with open canopy (Ilhamdi et al. 2021). It has a high tolerance to disturbance (Dow 2019; Potapov et al. 2020) and is adaptable to various environmental conditions, which explains its observation in all sites of the current study. In addition, it also inhabits flowing waters (Ilhamdi et al. 2021; Astuti et al. 2022) or stagnant waters (Potapov et al. 2020; Susanto and Arianti 2021), between 0-800 meters above sea level (Dow 2019).

The *P. autumnalis* was observed perched on vegetation and woody branches on the streambanks with open to closed canopy conditions in this study. Susanto and Arianti (2021) reported that *P. autumnalis* was found in small streams with fairly open canopy. It prefers perching on wooden branches (Astuti et al. 2022) within forested habitats (Koneri et al. 2022), rivers, ponds, and rice fields (Setiyono et al. 2017). It is known as a damselfly species with a fairly high tolerance toward disturbance (Dow 2020b), including water locations with poor environmental conditions.

The three sites in this study had moderate Odonata diversity (2.02> H'> 2.41; Figure 6). Kedungceleng stream had the highest Odonata diversity, with 13 species and 66 individuals recorded, opposite to the Sengik stream, where the diversity was lowest (10 species and 46 individuals) (Figure 5). Differences in Odonate diversity among locations are thought to be due to various factors such as ecological conditions and microclimate (Table 3). Previous studies indicated the difference in diversity in Odonata is caused by habitat conditions (Susanto and Zulaikha 2021), vegetation (Simaika et al. 2016; Maldonado-Benítez et al. 2022), canopy cover (Paulson 2009), food availability, water quality, temperature (Schalkwyk et al. 2014; Simaika et al. 2016), and light intensity (Monteiro-Júnior et al. 2013).

The three stream locations have different species compositions, with only two species found in all three streams, i.e., *N. ramburii* and *O. sabina.* Some species are typical in one certain location, such as Sengik stream with *A. insignis, C. gigantea, P. congener,* and *R. rufa*; Kedungceleng stream with *C. servilia, P. flavescens, A. pygmaea, P. rubriceps,* and *C. v. javana*; and Kedungsalam stream with *G. subinterrupta, O. pruinosum, O. testaceum, T. aurora,* and *P. pruinosum.* Despite having streams as a common feature in all locations, unique microhabitats, and certain ecological conditions, they have greatly affected the diversity of dragonfly species. Many Odonata species also require specific habitat preferences, creating species composition differences among studied locations.

The PCA analysis indicated the differences in microclimates among the three streams. Sengik stream, characterized by high humidity, was observed to have low Odonata diversity, taxa richness, and abundance. On the other hand, the Kedungsalam stream with high temperature seemed favorable for having high taxa richness and abundance. The analysis further showed a correlation between air humidity with species dominance. Air humidity is believed to affect the flight of dragonflies; hence, the higher it is, the fewer dragonfly individuals or species flying in that area. On the contrary, light intensity positively correlates with dragonfly diversity, as it is needed for sunbathing, mating, and foraging (Goforth 2010).

All dragonfly species found in this study have low conservation status. As many as 24 species retain the Least Concern (LC) status as having a very low extinction threat and wide-range distribution (IUCN 2023). Conservation status is an indicator applied to animals or plants to show the threat level that affects the distribution and abundance

of their populations in an area (Laikre et al. 2009). Despite having low conservation status, it is necessary to assess the local population status for each species as it is likely to differ from the comforting global status. There is always the possibility that species with LC conservation status face regional or local threats that are not detected globally. In addition to this concern, there are 13 Odonata species in this study whose current population trend is unknown, including *C. gigantea* and *H. fenestrata.*

The *C. gigantea* (Figure 9. D) was spotted perching at a plant stem atop a small pond near the beach of the stream. Its main habitat is near shallow, stagnant waters, such as ponds near mangroves and beaches (Sharma 2010) and natural freshwater ponds (Sugiman et al. 2020). This is also supported by Leksono et al. (2017), who reported that *C. gigantea* was reported to have slight tolerance to habitat disturbance and was confined in low altitudes. Coastal areas are currently experiencing tremendous anthropogenic disturbances, threatening the existence of habitat for *C. gigantea* (Sharma 2010).

The *H. fenestrata* (Figure 9. E) was found perching and basking on rocks in the middle of a stream or at vegetation on the stream banks. The *H. fenestrata* is an exclusive inhabitant in shaded, clean, rocky forest streams (Günther 2019, Sugiman et al. 2020). Its range includes streams in natural forests down to the rivers in agricultural areas and aquatic tourism (Astuti et al. 2022, Nafisah and Soesilohadi 2021). Land conversion and forest alteration create huge changes in the landscape, which later threaten the life of *H. fenestrata* (Günther 2019).

Among other species recorded in this study, only *C. v. javana* (Figure 9. F), whose conservation status is slightly higher as Not Evaluated (NE). This conservation status implies that despite a species not being assessed for its extinction risk, it still requires being conserved and cared for (IUCN 2022). This member of the Platycnemididae family prefers stream banks with dense canopy, which in this study recorded only from the Kedungceleng stream. Damselfly *C. v. javana* was historically only recorded from the southern coast of West Java and Central Java which then its distribution included Nusakambangan Island, off-south of Central Java, based on a recent study (Nu'manuddin et al. 2021).

This study's results show that differences in dragonfly richness and diversity were found in locations with the same habitat type (stream) but different habitat conditions. Diversity analysis showed that the value of dragonfly diversity in the three research locations was H' = 2.41–2.02, with the Kedungceleng stream being the location with the highest value. All dragonfly species found in this study are non-threatened except one species, *C. v. javana*, whose conservation status has not been evaluated.

ACKNOWLEDGEMENTS

We thank all those who have helped with this research. Thanks also to friends who have helped with data analysis and writing. We thank Muhammad Nazri Janra and Magdalena Putri Nugrahani for their review and improvement of the manuscript.

REFERENCES

Astuti A, Nayasilana IN, Sugiyarto S, Budiharjo A. 2022. Community structure of dragonflies (Odonata) in Gunung Bromo's Forest Area with Special Purpose (FASP), Karanganyar, Central Java, Indonesia. Biodiversitas 23 (5): 2493-2501. DOI: 10.13057/biodiv/d230529.

Briggs A, Pryke JS, Samways MJ, Conlong DE. 2019. Macrophytes promote aquatic insect conservation in artificial ponds. Aquat Conserv 29 (8): 1190-1201. DOI: 10.1002/aqc.3157.

Buczyński P, Buczyńska E, Baranowska M, Lewniewski Ł, Góral N, Kozak J, Tarkowski A, Szykut KA. 2020. Dragonflies (Odonata) of the city of Lublin (Eastern Poland). Pol J Entomol 89 (3): 153-180. DOI: 10.5604/01.3001.0014.4239.

Choong CY, AD DF, AA MAA, Chung AYC, Maryati M. 2020. Diversity of Odonata Species at Kangkawat, Imbak Canyon, Sabah. J Trop Biol Conserv 17: 1-10. DOI: 10.51200/jtbc.v17i.2644.

Dolný A, Harabiš F, Bárta D, Lhota S, Drozd P. 2012. Aquatic insects indicate terrestrial habitat degradation: changes in taxonomical structure and functional diversity of dragonflies in tropical rainforest of East Kalimantan. Trop Zool 25 (3): 141-157. DOI: 10.1080/03946975.2012.717480.

Dow RA. 2019. *Neurothemis ramburii*. The IUCN Red List of Threatened Species 2019: e.T163690A83302471. DOI: 10.2305/IUCN.UK.2019-3.RLTS.T163690A83302471.en.

Dow RA. 2020a. *Agrionoptera insignis*. The IUCN Red List of Threatened Species 2020: e.T167298A83373853. DOI: 10.2305/IUCN.UK.2020-1.RLTS.T167298A83373853.en.

Dow RA. 2020b. *Prodasineura autumnalis*. The IUCN Red List of Threatened Species 2020: e.T167139A138284262. DOI: 10.2305/IUCN.UK.2020-1.RLTS.T167139A138284262.en.

Goforth CL. 2010. Behavioural responses of Enallagma to changes in weather (Zygoptera: Coenagrionidae). Odonatologica 39 (3): 225-234.

Günther A. 2019. *Heliocypha fenestrata*. The IUCN Red List of Threatened Species 2019: e.T122798694A122799250. DOI: 10.2305/IUCN.UK.2019-3.RLTS.T122798694A122799250.en.

Hastomo SOE, Muttaqin Z, Cita KD. 2022. Inventory and diversity of dragonflies (Odonata) at Kuningan Resort of Mount Ciremai National Park, West Java Province. IOP Conf Ser: Earth Environ Sci 959 (1): 012019. DOI: 10.1088/1755-1315/959/1/012019.

Hendriks JA, Mariaty, Maimunah S, Anirudh NB, Holly BA, Erkens RH, Harrison ME. 2023. Odonata (Insecta) Communities in a Lowland Mixed Mosaic Forest in Central Kalimantan, Indonesia. Ecologies 4 (1): 55-73. DOI: 10.3390/ecologies4010006.

Ilhamdi ML, Idrus AA, Santoso D, Hadiprayitno G, Syazali M. 2021. The species richness and conservation priority of dragonflies in the Suranadi Ecotourism Area, Lombok, Indonesia. Biodiversitas 22 (4): 1846-1852. DOI: 10.13057/biodiv/d220430.

IUCN. 2022. Guidelines for Using the IUCN Red List Categories and Criteria. Version 15.1. Prepared by the Standards and Petitions Committee. https://www.iucnredlist.org/documents/RedListGuidelines.pdf.

IUCN. 2023. The IUCN Red List of Threatened Species. https://www.iucnredlist.org/en.

Janra MN, Gusman D, Singkam AR, Susanto A, Yatap H, Fahrudin A, Andriyansyah F, Prameswara A, Melian M, Herwina H. 2022. Into the database of Bencoolen Odonata: Synthesis of two years dragonfly survey in Bengkulu Province. IOP Conf Ser: Earth Environ Sci 1097 (1): 012056). DOI: 10.1088/1755-1315/1097/1/012056.

Kartini J, Syachruddin S, Ilhamdi ML. 2022. The diversity of dragonflies (Odonata) in the Joben Resort Area, East Lombok. Jurnal Biologi Tropis 22 (2): 675-688. DOI: 10.29303/jbt.v22i2.3458.

Koneri R, Nangoy M, Maabuat PV. 2020. Composition and diversity of dragonflies (Insecta: Odonata) in Tunan waterfall area, North Minahasa, North Sulawesi, Indonesia. Pak J Zool 52 (6): 2091-2100. DOI: 10.17582/journal.pjz/20181214071225.

Koneri R, Nangoy MJ, Siahaan P. 2022. Species diversity of dragonflies on The Sangihe Islands, North Sulawesi, Indonesia. Appl Ecol Environ Res 20 (2): 1763-1780. DOI: 10.15666/aeer/2002_17631780.

Kosterin OE. 2014. Odonata briefly observed on the islands of Bali and Lombok, Lesser Sundas, Indonesia, in the late February 2014. J Intl Dragonfly Fund 74: 1-48.

Laikre L, Nilsson T, Primmer CR, Ryman N, Allendorf FW. 2009. Importance of genetics in the interpretation of favourable conservation status. Conserv Biol 23 (6): 1378-1381. DOI: 10.1111/j.1523-1739.2009.01360.x.

Leksono AS, Feriwibisono B, Arifianto T, Pratama AF. 2017. The abundance and diversity of Odonata along an altitudinal gradient in East Java, Indonesia. Entomol Res 47 (4): 248-255. DOI: 10.1111/1748-5967.12216.

Lieftinck MA. 1940. Revisional notes on some species of *Copera* Kirby. With notes on habits and larvae (Odon., Platycnemididae). Treubia 17 (4): 281-306. DOI: 10.14203/treubia.v17i4.2577.

Maldonado-Benítez N, Mariani-Ríos A, Ramírez A, 2022. Effects of urbanization on Odonata assemblages in tropical island streams in San Juan, Puerto Rico. Intl J Odonatol 25: 31-42. DOI: 10.48156/1388.2022.1917163.

Monteiro-Júnior CDS, Couceiro SRM, Hamada N, Juen L. 2013. Effect of vegetation removal for road building on richness and composition of Odonata communities in Amazonia, Brazil. Intl J Odonatol 16 (2): 135-144. DOI: 10.1080/13887890.2013.764798.

Nafisah NA, Soesilohadi RH. 2021. Community structure of dragonfly (Ordo: Odonata) in natural forest and tourist sites petungkriyono Forest, Central Java, Indonesia. J Trop Biodivers Biotechnol 6 (3): 1-9. DOI: 10.22146/jtbb.67328.

Nugrahani MP, Firmansyah RD, Susintowati, S. 2022. Keanekaragaman dan kemelimpahan Odonata di Kawasan Hulu Aliran Sungai Kalibendo, Banyuwangi. Jurnal Biosense 5 (1): 175-186. DOI: 10.36526/biosense.v5i01.2160.

Nu'manuddin M, Rachman HT, Rahadi WS, Pamungkas DW, Kamaludin N, Irawan F, Wardhana PK, Nugrahaningrum A, Soesilohadi RH. 2021. Keanekaragaman Capung (Ordo Odonata) Di Pulau Nusakambangan, Kabupaten Cilacap, Jawa Tengah. Bioma 17 (2): 57-64. DOI: 10.21009/Bioma17(2).2.

Nuraeni S, Budiaman, Yaspeta S. 2019. Identification of dragonfly and damselfly species around Mahaka river, Hasanuddin university teaching forest. IOP Conf Ser: Earth Environ Sci 343 (1): 012052. DOI: 10.1088/1755-1315/343/1/012052.

Oliveira-Junior JMB, Junior PDM, Dias-Silva K, Leitão RP, Leal CG, Pompeu PS, Gardnerj TA, Hughesl RM, Juen L. 2017. Effects of human disturbance and riparian conditions on Odonata (Insecta) assemblages in eastern Amazon basin streams. Limnologica 66: 31-39. DOI: 10.1016/j.limno.2017.04.007.

Orr AG, Kalkman VJ. 2015. Field guide to the dragonflies of New Guinea. Nederlandse Vereniging voor Libellenstudie, Gelderlandfabriek.

Paulson D. 2009. Dragonflies and Damselflies of the West. Princeton University Press, Princeton, New Jersey. DOI: 10.1515/9781400832941.

Perez ESN, Bautista MG. 2020. Dragonflies in the city: Diversity of odonates in urban Davao, Philippines. J Agric Sci Technol A 10 (1): 12-19. DOI: 10.17265/2161-6256/2020.01.002.

Potapov GS, Kolosova YS, Gofarov MY, Bolotov IN. 2020. Dragonflies and damselflies (Odonata) from Flores Island, Lesser Sunda Archipelago: New occurrences in extreme environments and an island-level checklist of this group. Ecol Montenegrina 35: 5-25. DOI: 10.37828/em.2020.35.2.

Pratama R, Rosalini RA. 2016. Dragonflies inventory (Odonata) in Kota Waringin Village, Puding Besar District–Bangka Island. Biovalentia 2 (2): 94-103. DOI: 10.24233/BIOV.2.2.2016.43.

Rahadi WS, Feriwibisono B, Nugrahani MP, Dalia BPI, Makitan T. 2013. Naga Terbang Wendit: Keanekaragaman Capung Perairan Wendit, Malang, Jawa Timur. Indonesia Dragonfly Society, Yogyakarta. [Indonesian]

Ramlee S, Mohd SA. 2022. Odonata nymphs as potential biocontrol agent of mosquito larvae in Malaysia. Southeast Asian J Trop Med Public Health 53 (4): 426-435.

Raut AM, Banu AN, Akram W, Nain RS, Singh K, Wahengabam J, Shankar C, Shah MA. 2023. Impact of pesticides on diversity and abundance of predatory arthropods in rice ecosystem. Appl Environ Soil Sci 2023: 1-10. DOI: 10.1155/2023/8891070.

Saefullah AA, Latifah L, Sa'adah M, Salsabila N, Muslimah S. 2021. The inventory of dragonfly species in Kedung Kopong and Banyak Angkrem Areas in Kalirejo Village, Salaman-Magelang. Proc Intl Conf Sci Eng 4: 41-47.

Samways MJ. 2008. Dragonflies and damselflies of South Africa. Pensoft Publishers, Sofia. [Bulgaria]

Schalkwyk JV, Samways MJ, Pryke JS. 2014. Winter survival by dragonfly adults in the Cape Floristic Region. Intl J Odonatol 17 (1): 17-30. DOI: 10.1080/13887890.2014.880382.

Setiyono J, Diniarsih S, Oscilata ENR, Budi NS. 2017. Dragonflies of Yogyakarta. Jenis Capung Daerah Istimewa Yogyakarta, Indonesia Dragonnfly Society, Yogyakarta. [Indonesian]

Setyawati M, Triatmanto T. 2022. Keanekaragaman Capung (Odonata) di Kawasan Gunung Api Purba Nglanggeran Kabupaten Gunungkidul. Bioscientist 10 (2): 809-817. DOI: 10.33394/bioscientist.v10i2.5872. [Indonesian]

Sharma G. 2010. *Camacinia gigantea*. The IUCN Red List of Threatened Species 2010: e.T167427A6346507. DOI: 10.2305/IUCN.UK.2010-4.RLTS.T167427A6346507.en.

Sharma, M, Oli BR. 2022. Odonates (Insecta: Odonata) associated with rice ecosystems in Sunwal municipality, central Nepal. J Nat Hist Museum 32 (22): 35-48. DOI: 10.3126/jnhm.v32i1.49951.

Simaika JP, Samways MJ, Frenzel PP. 2016. Artificial ponds increase local dragonfly diversity in a global biodiversity hotspot. Biodivers Conserv 25: 1921-1935. DOI: 10.1007/s10531-016-1168-9.

Sugiman U, Atmowidi T, Priawandiputra W. 2020. Diversity of dragonflies (Insecta: Odonata) in Ujung Kulon National Park. IOP Conf Ser: Earth Environ Sci 457 (1): 012031. DOI: 10.1088/1755-1315/457/1/012031.

Suroto A, Istiqomah D, Syarifah RNK. 2021. Composition of pests and predators in the early generative phase of rice cultivation in two different conditions. IOP Conf Ser: Earth Environ Sci 653 (1): 012088. DOI: 10.1088/1755-1315/653/1/012088.

Susanto MAD, Arianti OF. 2021. Diversity and abundance of dragonfly (Anisoptera) and damselfly (Zygoptera) at Sabo Dam Complang, Kediri, East Java, Indonesia. Biosfer 12 (2): 110-122. DOI: 10.24042/biosfer.v12i2.9883.

Susanto MAD, Firdhausi NF, Bahri S. 2023. Diversity and community structure of dragonflies (Odonata) in various types of habitat at Lakarsantri District, Surabaya, Indonesia. J Trop Biodivers Biotechnol 8 (2): 76690. DOI: 10.22146/jtbb.76690.

Susanto MAD, Zulaikha S. 2021. Diversity and community structure of dragonfly and damselfly (Odonata) at the Selorejo Waterfall Area, Ponorogo Regency, East Java Indonesia. Jurnal Riset Biologi dan Aplikasinya 3 (1): 30-37. DOI: 10.26740/jrba.v3n1.p30-37.

Vatandoost H. 2021. Dragonflies as an important aquatic predator insect and their potential for control of vectors of different diseases. J Mar Sci 3 (3): 13-20. DOI: 10.30564/jms.v3i3.3121.

Virgiawan C. 2015. Studi keanekaragaman capung (Odonata) sebagai bioindikator kualitas air Sungai Brantas Batu-Malang dan sumber belajar biologi. JPBI 1 (2): 188-196. DOI: 10.22219/jpbi.v1i2.3330. [Indonesian]

Zaman MN, Fuadi BF, Luthfika M. 2022. Struktur komunitas capung dan capung jarum di Sungai Gajah Wong Segmen Perkotaan Daerah Istimewa Yogyakarta. Bioveritas J Biol 1 (1): 31-36. [Indonesian]

Zaman MN, Purwanto PB, Iman DI, Sari AM, Maulany SL, Luthfika M, Rofiah N, Halimah GS, Cahya. 2020. Dragonfly and damselflies at Gajahwong River in Yogyakarta Urban District. Proc Intl Conf Sci Eng 3: 73-76. DOI: 10.14421/icse.v3.471.

Zulhariadi M, Irawan RD, Zulfaeda A, Hidayani N. 2022. Dragonflies diversity and land cover changes in The Batubolong River, West Lombok District. Biotropia 29 (2): 112-123. DOI: 10.11598/btb.2022.29.2.1637.